QC
851
.G73
V.9

Air Ministry
Meteorological Research Committee
MRP 908-951 (non-inclusive)

MRP No.	Title	Author
908 AD 223085	Transportable Anemometer for Use With Mobile Meteorological Unit.	G.E.W. Hartley
912 AD 143190	Radiation Fog: Investigations at Cardington, 1951-54.	K.H. Stewart
913 AD 079754	The Nocturnal Dissipation of Strato-cumulus Cloud.	D.G. James
914 AD 223092	Measurements of the Flux of long Wave Radiation in the Upper Air 1953-54.	J.T. Houghton A.W. Brewer
915 AD 131895	The Representation of the Annual Temperature Variation Over Central and Northern Europe by a Two Term Harmonic Form.	J.M. Craddock
916 AD 223087	A Refrigerated Disc Icing Meter.	G.J. Day
917 AD 079753	The Variation of the Normal Air Temperature Over the Northern Hemisphere During the Year.	J.M. Craddock
918 AD 079752	Average Height of the Standard isobaric Surfaces Over the Area From the North Pole to 55 degrees N. in January.	H. Heastie
919 AD 117798	Atmospheric Turbulence in Aviation.	G.A. Corby
922 AD 223091	Wind Finding Trials of Radar A.A. No. 3 Mk. VII (Second Series).	C.V. Else
923 AD 223090	Five Year Means of Meteorological Observations Made at the Ocean Weather Stations Item and India, Jig and Juliett 1948-52.	R.F.M. Hay
924 AD 143191	The Sub-tropical Jet-stream of the Eastern North Pacific in January and April, 1952.	H.D. Hoyle
925 AD 117796	The Mean Wind at 60 mb.	J.K. Bannon R.A. Jones
928 AD 223089	Radar Wind Comparisons on the Ocean Weather Ships (Second Series).	D.N. Harrison

MRP No.	Title	Author
929 AD 146236	The Energy Balance of Surface and Atmosphere at Kew, May 1953 to April 1954.	G.D. Robinson
930 AD 223088	Some Further Determinations Made by the M.R.F. of the Speed Correction Coefficients of Aircraft Thermometers.	W.G. Durbin
931 AD 223104	Some Statistical Aspects of a Rain-making Experiment.	A.F. Jenkinson
933 AD 143192	Investigations Relating to Cirrus Cloud.	D.G. James
935 AD 143193	Dynamical Similarity in an Incompressible Fluid Model of Two-dimensional Airflow Over a Ridge.	J.S. Sawyer
936 AD 223101	Measurements of Atmospheric Radiation and the Heat Balance at the Ground at Kew, May, 1953 - May, 1954.	W.T. Roach
939 AD 223100	Airflow Over Mountains - the Lee Wave Amplitude.	G.A. Corby C.E. Wallington
941 AD 117797	An Experimental Pulsed-light Cloud-base Meter.	R. Almond
943 AD 223086	Fog Density Indicator.	J.R. Bibby
946 AD 117800	Ozone Concentration Measurements From an Aircraft in N. Norway.	A.W. Brewer
949 AD 145681	Some Aspects of Variations of Air and Sea Surface Temperature in Short Periods at Ocean Weather Stations I and J of Significance to the Synoptic Climatologist.	R.F.M. Hay
951	Index of M.R.P.'s Approved for General Distribution.	

has not been published. Any author desiring to quote this paper should refer to it as "A paper of the Meteorological Research Committee (London).
M.R.P. No. 908 by Mr. G.E.W. Hartley
A copy is available in the Library of the Meteorological Office."

M.R.P. 908
S.C.I/98
8th February, 1955

AD 223085

AIR MINISTRY

METEOROLOGICAL RESEARCH COMMITTEE

Transportable Anemometer for use with Mobile Meteorological Unit

by

G. E. W. Hartley (Meteorological Office)

Mobile meteorological units require a remote indicating anemometer and wind vane which can be carried on a 30 foot support erected, if need be, at some distance from the mobile "Caravan". The support when packed for transport must be light enough and compact enough to be carried in the "Caravan"; it must be capable of being easily erected by not more than 5 men.

It was considered, and this has been confirmed by experience, that the standard cup generator anemometer Mk. Ib, and Wind Vane Mk.IIIa would be quite suitable for use with a mobile meteorological unit provided that a suitable support could be devised.

Four kinds of support were tried; first a standard R.A.F. aerial mast 30 ft. high made from 3 ft. 6 in. sections of 2 in. diameter steel tube, with push in spigot joints. This was very easy to put up by itself, but when a weight equivalent to the wind vane and anemometer was fastened to the top, the bending load on the mast while hauled up from the horizontal position was too great, and the mast buckled.

Next a telescopic steel tubular mast was designed and made in M.O.16. This consists of four lengths of steel tube of decreasing diameters which in the retracted position telescope inside each other. Each length can be extended from inside the next larger section by pulling on three wires passing over pulley blocks at the top of the section; when the section which is being extended has been pulled up as far as it will go (against a stop), the three wires are used as guy wires, besides holding up their particular section of the mast. The largest section has three extra guy wires to hold it upright while the second section is being pulled up and has a spiked base plate; a special fitting is provided to carry the anemometer with the wind vane above it on the top of the mast. The retracted length is $9\frac{1}{2}$ ft. and the weight about 120 lb.

To put it up, three guy wire anchoring posts are driven into the ground on a 30 ft. diameter circle about the position of the foot of the mast; anemometer, wind vane and electric wires are fastened to the top section, and the retracted mast is then raised to the vertical position and held there by the three fixed guy wires. Then the next three guy wires are pulled by three men, to raise the second section of the mast, and fastened to the posts. This process is repeated with the other two sets of three guy wires to raise the third and top sections of the mast.

On trial, omitting wiring up the instruments, erection took about 30 minutes, 5 of which were spent freeing a stuck pulley; and about the same time was taken to lower the mast and coil up the various wires. The chief disadvantages are (a) the whole mast when retracted is clumsy to handle because of all the guy wires hanging about and because of its weight; (b) it will be difficult to prevent rust, because pulling up and retracting will scrape off any form of rust-proof finish in time; steel tubing is necessary to give the required strength and the mast must be kept all in one for transport; (c) it is expensive in time to make. Four men are required to erect the mast.

The third support tried is a light alloy ladder, illustrated in Fig.1. It is made of 3 in. by 1¼ in. box section alloy sides and tubular rungs. It is in four sections each 8 ft. long, and jointed by channel section light alloy fish plates with long bolts passing right through the hollow rungs. This is a standard ladder obtained commercially, and weighs 91 lb; if desired, only one, two or three sections need be used. The fittings made in M.O.16 to go with it are a hinged base, top fittings to hold the anemometer and wind vane, and two sets of four guy wires with fittings and anchor posts.

The ladder is assembled on the ground, its foot attached to the hinged base and the instrument fittings attached to the top. The anemometer without its cups is fastened to its fittings. The anchor posts are driven into the ground at the corners of a square, each post 24 ft. from the foot of the ladder, and the guy wires are bolted to the ladder at the top and half way up. Five men are required to pull up the mast. Two pull on, say, the N.E. and S.E. guy wires while two men "walk up" the ladder, the fifth man steadying the N.W. and S.W. guy wires until the N.E. and S.E. guy wires can take the weight of the ladder; this is then manoeuvred into a vertical position by adjustment of the guy wires which are then made fast. The ladder is now quite firm and may be safely climbed.

The anemometer cups are carried up and put on their spindle and the wind vane is bolted to its tubular support. The anemometer is put on before pulling up the mast because it is on a side bracket where it is not so easy to get at when the mast is erected, whereas the wind vane support is directly over one leg of the ladder; also, the wind vane is rather heavy and would make it more difficult to pull up the ladder. Assembly and erection take about 40 minutes, and lowering and dismantling rather less. Handling is easy because each section weighs only about 20 lb., and the wires can be unbolted from the mast and coiled up separately. The ladder has been adopted as the most suitable and convenient support.

The remainder of the anemograph consists of standard cup generator anemometer and dial, Mk.III(a) wind vane and dial, two drums of cable; and a 12 V. D.C. supply is needed for the wind vane, either by trickle charger if mains are available or from batteries.

A fourth type of support has recently been obtained and tried; this is a 30 ft. sectional tower made from lengths of 1¾ x 1¾ x 3/16 inch light alloy angle. It was obtained from a firm who make servicing stages for aircraft, and is built up from standard parts. It weighs about 2 cwt. and can be packed up into a space approximately 3 ft. 6 in. cube.

It takes much longer to erect and dismantle than the ladder, but has the advantage that it can be built up from the ground by one man without any help, given enough time, and can be taken down from the top by the reverse process; and it provides a platform to stand on, with a hand rail, which makes for easier attention to the instruments, without using a safety belt. The tower is shown in Fig.2.

The ladder formed part of the equipment of a mobile meteorological vehicle recently tried by 2nd T.A.F. No difficulty was found in putting it up and taking it down.

Some criticisms were made on matters of detail but these can easily be put right.

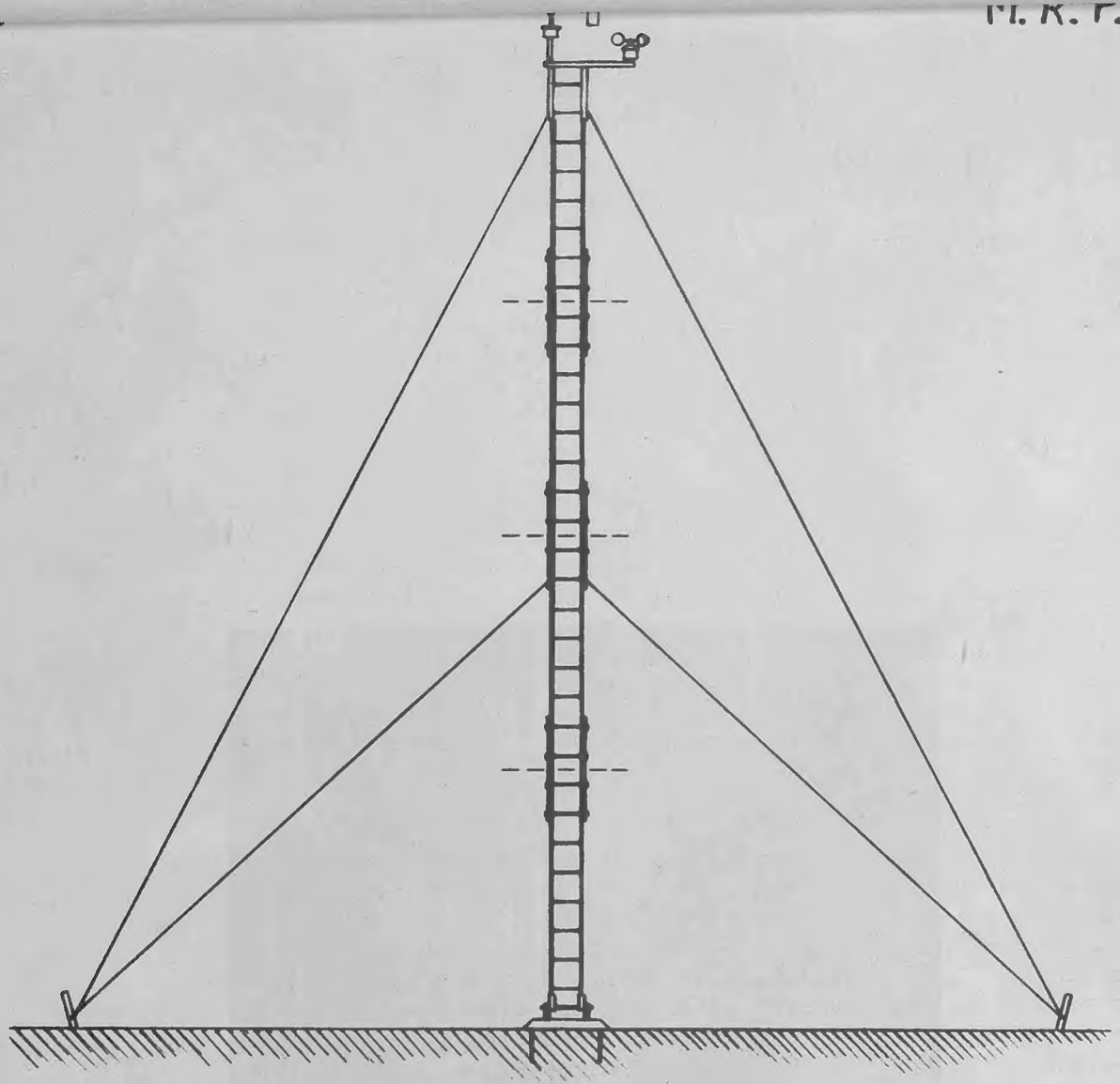

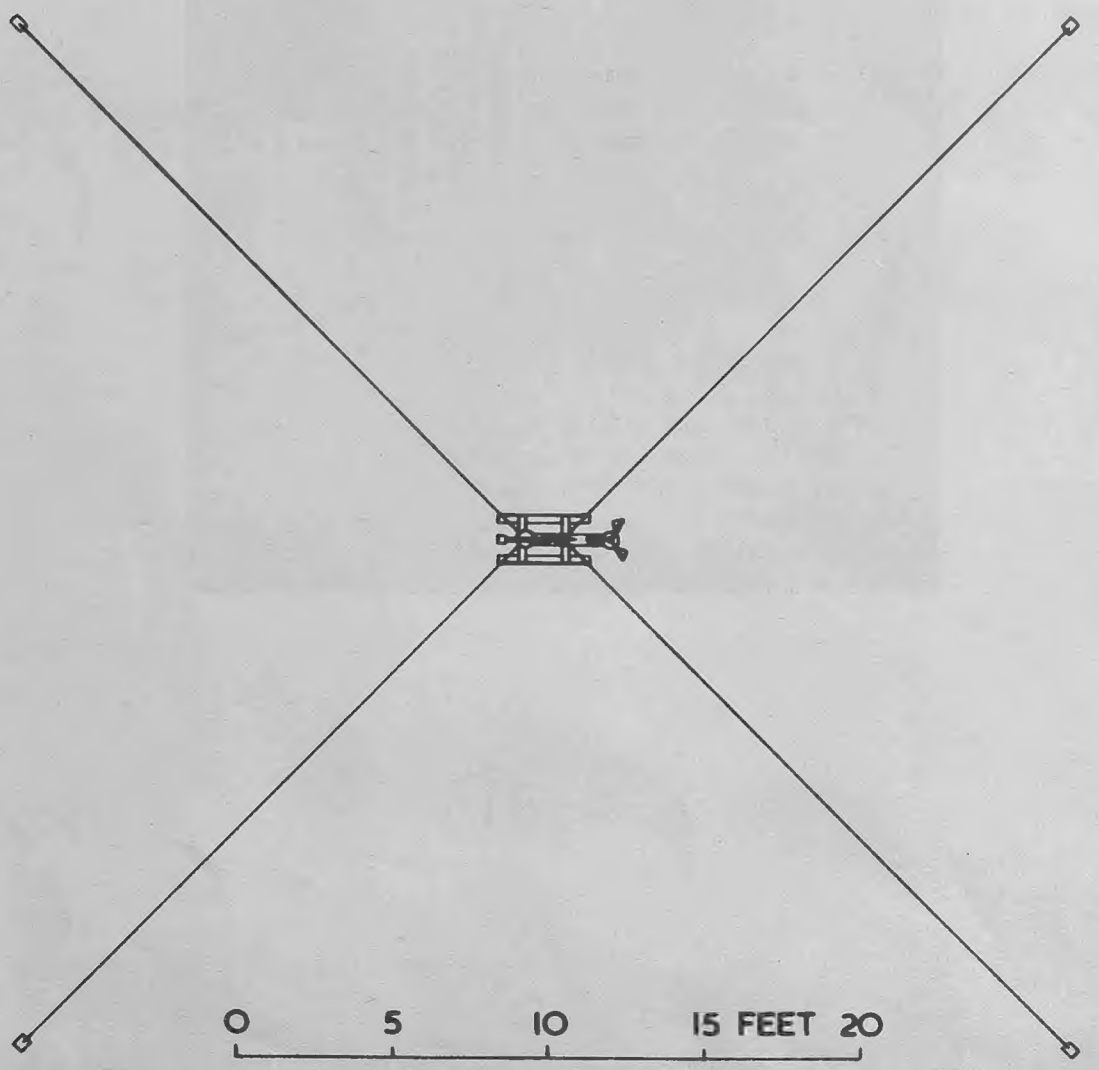
0
5
10
15 FEET 20

M.R.P. 908

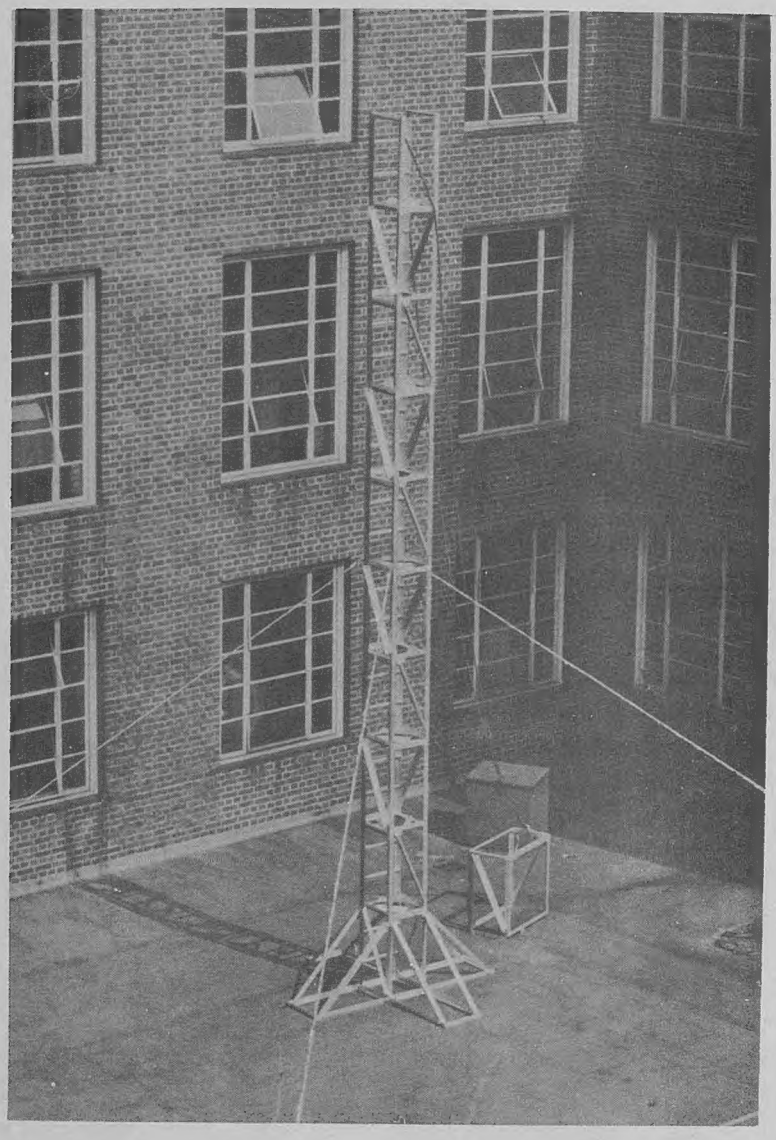

FIG. 2

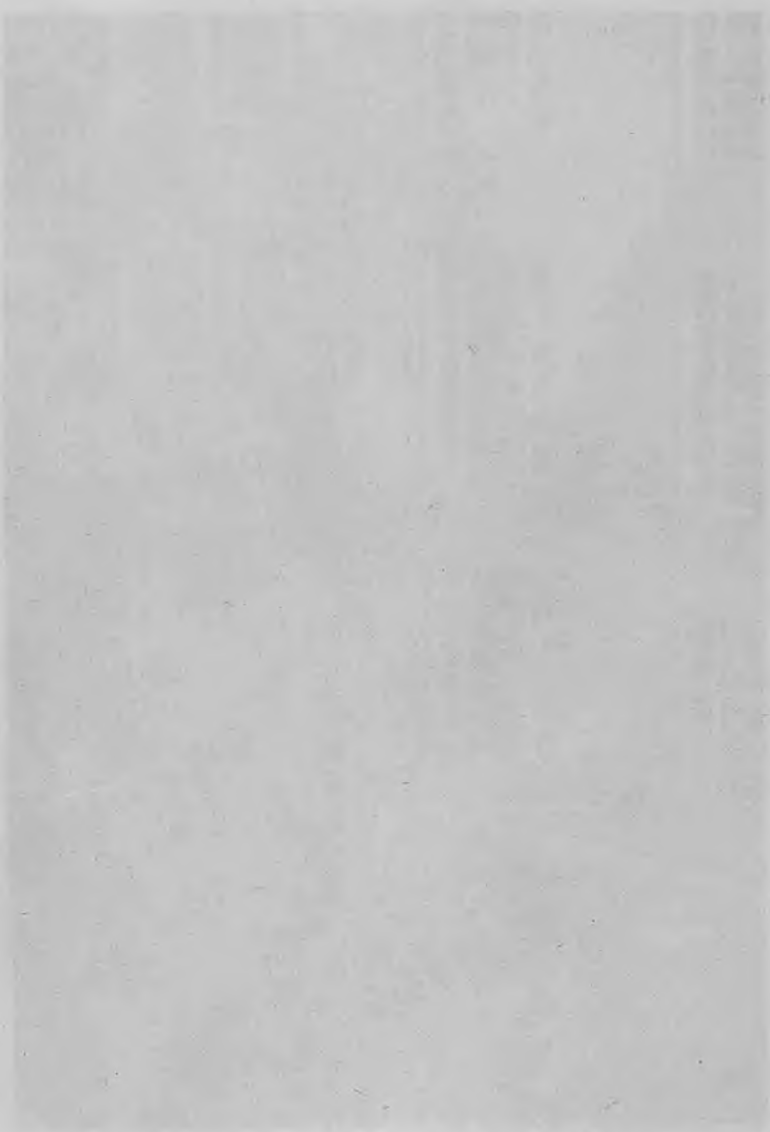

M.R.P. 912.
S.C. III/183.
27th MAY, 1955.

AD143190

AD-143190

RADIATION FOG.
INVESTIGATIONS AT CARDINGTON, 1951-54

by

K. H. STEWART.
(METEOROLOGICAL OFFICE)

AWSSS
ROUTING SLIP

FILE	INFO	ACTION			
			DIRECTOR		
			DD/S		
			TO DIRECTOR		
		1	CONSULTANTS CRJ JM		
		2	TI	CHF	
				TSS	
				EDB	
				SEC	
		3	EDD	CHF	CRS
				HLFB	
				STB	
				SPFB	
				CU	
				SEC	
		4	TIPD	CHF	
				EDE	
				TECH INFO	
				SEC	

13 OCT 1955

METEOROLOGICAL RESEARCH COMMITTEE.
AIR MINISTRY

At the time of issue this report has not been published. Any author desiring to quote this paper should refer to it as "A paper of the Meteorological Research Committee (London), M.R.P. No. 912 by Dr. K.H. Stewart
A copy is available in the Library of the Meteorological Office."

M.R.P. 912
S.C.III/183.
27th May, 1955.

AIR MINISTRY

METEOROLOGICAL RESEARCH COMMITTEE

Radiation fog: investigations at Cardington, 1951-54

by

K. H. Stewart (Meteorological Office)

Contents

1. Introduction

.1 Observations and apparatus

.2 Occasions on which observations have been made

.3 Discussion of results; plan of the report

2. General qualitative description and discussion of results on clear and foggy nights

.1 Brief description of typical cases

.2 Advective effects

.3 Fuller description of typical cases

.1 The simplest type of foggy night

(a) Late afternoon - the changing balance

(b) Early evening - the end of rapid changes

(c) Early night - the quasi-equilibrium period

(d) The small hours - fog formation

(e) Late night - the growth of fog

(f) Morning - dispersal of fog

.2 Other types of night

.1 Fog under subsidence inversion

.2 Radiation nights without fog

.4 Wind structure

.5 Horizontal and oblique visibility in fog

.6 Summary of qualitative results

/3.

3. Quantitative discussion of physical processes

.1 Heat balance

.2 Heat exchange within the cooling layer

.3 Water exchanges

.4 Measurements required for the investigation of physical processes

.1 Radiation

.2 Heat from the ground

.3 Convection processes

.4 Fog formation

.5 Fog density and structure

4. Empirical fog-forecasting methods

.1 Tests of suggested methods

.2 Development of forecasting methods

5. General conclusions - future programme

.1 Results of the investigation

.2 Future programme

.1 Theoretical work

.2 General study of behaviour of wind, temperature and humidity

.1 Peculiarities of wind profiles

.2 Erratic variations of humidity

.3 Representativeness of data from one station

.3 Study of transfer of heat and water vapour (and momentum) near the ground

.1 Radiation

.2 Convection

.4 Investigations of fog structure and mode of formation

.1 Measurement of size, number and composition of fog droplets

.2 Variation of visibility with time and height in a fog, and its relation to drop size and number

.3 Final stages of fog formation

.5 Empirical forecasting methods

.1 Use of existing data

.2 Collection and use of new data

/Appendices

Appendices
I Details of site and apparatus
II Estimation of radiation effects
III Heat flow in freezing ground
IV Effect of convection on relative humidity
V Effects of radiation on growth of fog droplets
VI Variation of visibility with height

References

Figures 1 - 18

(f) Atmospheric pollution, by filter-paper gauge.

(g) Wind speed, by sensitive cup anemometers } at height of 4ft., 20ft. and 55ft. on a steel tower

(h) Temperature } by aspirated thermocouple psychrometers } (continuous recordings)

(j) Humidity }

(k) Size and number of water drops in fog, by impactor technique.

(l) Specific heat of soil samples.

(m) "Slant visibility" from the ground to various heights.

Details of the apparatus used in these measurements are given in Appendix I. It has, unfortunately, proved impossible to carry out all the measurements planned; many of the instruments have been difficult to instal and maintain, and the limited staff available (1 E.O. or S.E.O. with 2 or 3 assistants) have not had time to keep them all in working order. First priority has been given to the routine daily balloon soundings and to making frequent soundings on occasions when fog was forecast. In addition, measurements (a) - (g) have been made with fair regularity, as will be seen from the results given below, but (h) and (j) have not yet given reliable results and (k) and (l) have not been attempted at all. (m) was not added to the programme till 1953; measurements have since been made on several nights, but not on all nights, because they interrupt the other observations.

1.2. Occasions on which observations were made

Detailed observations (i.e. hourly synoptic observations, balloon

.1 Theoretical work

.2 General study of behaviour of wind, temperature and humidity

.1 Peculiarities of wind profiles

.2 Erratic variations of humidity

.3 Representativeness of data from one station

.3 Study of transfer of heat and water vapour (and momentum) near the ground

.1 Radiation

.2 Convection

.4 Investigations of fog structure and mode of formation

.1 Measurement of size, number and composition of fog droplets

.2 Variation of visibility with time and height in a fog, and its relation to drop size and number

.3 Final stages of fog formation

.5 Empirical forecasting methods

.1 Use of existing data

.2 Collection and use of new data

/Appendices

Radiation fog: investigations at Cardington, 1951 - 54

1. Introduction

Measurements of temperature, humidity and wind speed in the lowest 4000 ft. of the atmosphere have been made at Cardington since 1944, using the balloon-borne thermocouple psychrometer and cup anemometer described by Swinbank (1946). Routine measurements have been made with fair regularity three times a day (0700, 1200, 1800 hr.) except in strong winds. In the autumn of 1951 these balloon soundings were made the basis of a considerably expanded programme of observations at Cardington, in the hope of learning more about the processes of fog formation. This report reviews the results of the expanded programme and the contribution they make to fog problems; it does not attempt to deal with the great body of data available from the ten years of routine observations.

1.1. Observations and apparatus

The general plan of the investigation was to make regular measurements of as many as possible of the quantities that might be important in fog formation on as many as possible of the occasions when radiation fog was to be expected. In addition to the balloon soundings mentioned above and the usual hourly observations of a synoptic reporting station, it was planned to make the following measurements:-

(a) Continuous recordings of "visibility" (atmospheric attenuation coefficient for visible light) by photoelectric meters at 4ft. and 55ft. above ground level.

(b) Height of top of fog, by a photoelectric instrument carried on the balloon.

(c) Earth temperatures at several depths down to 40 cm.

(d) "Surface temperature" as indicated by a spirit thermometer.

(e) Dewfall, by weighing methods.

(f) Atmospheric pollution, by filter-paper gauge.

(g) Wind speed, by sensitive cup anemometers } at height of 4ft., 20ft. and 55ft. on a steel tower

(h) Temperature } by aspirated thermocouple psychrometers } (continuous recordings)

(j) Humidity } by aspirated thermocouple psychrometers } (continuous recordings)

(k) Size and number of water drops in fog, by impactor technique.

(l) Specific heat of soil samples.

(m) "Slant visibility" from the ground to various heights.

Details of the apparatus used in these measurements are given in Appendix I. It has, unfortunately, proved impossible to carry out all the measurements planned; many of the instruments have been difficult to instal and maintain, and the limited staff available (1 E.O. or S.E.O. with 2 or 3 assistants) have not had time to keep them all in working order. First priority has been given to the routine daily balloon soundings and to making frequent soundings on occasions when fog was forecast. In addition, measurements (a) - (g) have been made with fair regularity, as will be seen from the results given below, but (h) and (j) have not yet given reliable results and (k) and (l) have not been attempted at all. (m) was not added to the programme till 1953; measurements have since been made on several nights, but not on all nights, because they interrupt the other observations.

1.2. Occasions on which observations were made

Detailed observations (i.e. hourly synoptic observations, balloon

/soundings

soundings at 2 - 3 hr. intervals and as many as possible of the measurements (a) - (m) mentioned above) were begun at midday on any day when the Central Forecast Office forecast the possibility of fog or clear skies at night and were continued until the fog cleared, until the temperature began to rise after dawn, if no fog had formed, or until it became clear that the forecast was incorrect. Observations were made in the winter months only (Sept. - Mar. inclusive). They have been made on a total of 60 nights in the past three seasons. About 30 suitable nights have been missed, chiefly because of unserviceability of the balloon or lack of a balloon crew. Many of the nights worked had, in fact, considerable amounts of cloud; for simplicity, they are not considered in this report (they include 9 nights with low stratus cloud, which might well repay separate investigation). The remaining nights are made up as follows: 18 with thick fog; 5 with thin fog (visibility $\leq$ 1100 yd. but $>$ 220 yd.); 11 clear nights (average cloud less than 2/8 medium and low or 4/8 high).

1.3. Discussion of results; plan of the report

The results of the investigation are discussed below under three headings. First there is the general picture of events on a foggy night given by the Cardington observations; this is not, in essentials, different from pictures based on previous work, such as the Leafield and Rye observations, but it is in some respects more detailed, and an attempt has been made to interpret the picture as fully as possible in terms of physical processes. The second heading is the detailed quantitative discussion of these physical processes in the light of the data available. Finally the new data can be used in attempts to find or test semi-empirical rules or formulae for fog forecasting.

The new Cardington data appear to be reasonably satisfactory for work under the first heading - in fact it is suggested that further collection of general data of the same type is likely to yield rapidly diminishing returns. For work under the second and third headings, however, the new data seem inadequate; for the study of physical processes the need is for more detailed, accurate and carefully planned measurements, while for the proper testing of forecasting procedures it is essential to have data for many more occasions. The report therefore ends with recommendations for changes in the plan of the research intended to produce more useful results.

It is clearly almost impossible to be certain that all possible information has been extracted from a large quantity of measurements such as is available from Cardington. It is hoped that the present report has covered the most profitable lines of inquiry and, perhaps more important, that it will give a good idea of the scope and limitations of the results obtained and thus serve as a basis for discussion of possible further analysis or fuller presentation of the data.

2. General qualitative description and discussion of results on clear and foggy nights

The behaviour of temperature and humidity varies so much from night to night that much of the value of the observations is lost by attempting to summarize them in the form of statistics. It seems better to present and discuss observations made on a few selected nights, with references to mean values observed on other occasions as appropriate.

Figs. 1 - 6 show the results obtained on 6 nights selected, as far as possible, to illustrate the main types of behaviour observed. The diagrams show, in their lower parts, the profiles of temperature, dew point and wind speed obtained from the balloon soundings; the temperature profiles have been extended below ground level by using earth thermometer readings. Above these profiles is shown the time-variation of elements observed at screen and ground level. In most cases the graphs are drawn through points representing average values observed over a few minutes at each hour. The

/original

original records - from visibility meters or anemometers for example- often give much greater detail.

2.1. Brief description of typical cases

The main features of figs. 1 - 6 and the occasions they represent will be described briefly, as a preliminary to a discussion of some general characteristics of the results; a more detailed description and discussion of the individual cases follows in section 2.3.

Figs. 1 and 2 represent the commonest and simplest type of behaviour resulting in fog formation. The temperature profiles in the early evening show a small but steep inversion below 50 ft. with a lapse tending towards the dry adiabatic value at greater heights. During the night the air cools rapidly near the ground but more slowly higher up, so that the inversion near the ground becomes steeper and extends to greater heights. When the temperature near the ground has fallen far enough, fog forms in a somewhat thin, shallow and patchy layer; at this stage the fog appears to have little effect on the temperature structure, but after some time the fog becomes denser and deeper, the ground surface temperature rises sharply and the temperature gradient within the fog layer becomes zero or negative. Above the fog there is a steep inversion, similar to the one near the ground before fog formed, changing gradually to a lapse at greater heights.

Rather more than half the foggy nights studied follow the pattern of events shown in figs. 1 and 2 fairly closely. The remainder show a wide variety from which it is difficult to pick out recognizable types of behaviour of frequent occurrence, but figs. 3 and 4 have been selected to show patterns that are followed, at least approximately, on a number of occasions, particularly during prolonged spells of fog. Their common feature is that cooling in the lowest few hundred feet is more or less uniform instead of being greatest near the ground, as in figs. 1 and 2. In fig 3 this is clearly connected with the fact that fog formed early in the night - in fact the chief interest in this example is in showing how a fog grows and changes during the night. In fig. 4 the obvious point of difference from earlier examples is the marked inversion, with dry air above, at about 1500 ft. which is to be attributed to subsidence. Such an inversion is almost always accompanied by relatively uniform cooling in the lower layers and by rapid increase in depth of the fog, once it has formed, as shown in fig. 4. Figs. 5 and 6 show two occasions typical of those on which fog did not form. In fig. 5 there is considerable cooling similar to that shown in figs. 1 and 2, but, presumably because of the rather low initial relative humidity, no fog formed. Fig. 6 is typical of many occasions in winter with temperatures in the region of freezing point, when the total amount of cooling is small and no fog, or at most only very thin fog, forms.

2.2. Advective effects

In the above brief summary the diagrams have been classified chiefly by reference to the temperature profiles. Although there are many minor irregularities, these profiles do follow a fairly regular pattern, with maximum cooling near the ground and less marked cooling aloft. The dew point profiles are very different; it is true that there is a general tendency for dew point to decrease with time below about 500 ft. but above that height no regular pattern is discernible. This general impression from figs. 1 - 6 is confirmed by the summary of changes observed on all foggy or clear nights in fig. 7. Temperature changes (from 1800 - 0600 hr.) at 3000 ft. are relatively small and show no significant bias to positive or negative values. At all lower heights there is a definite tendency for temperature to decrease during the night; the magnitude of the decrease increases steadily towards the ground and is decidedly greater on "foggy" than on "non-foggy" nights. Humidity changes, on the other hand, cover a wide range at all levels and it is only below 1000 ft. that a systematic

/tendency

tendency to decrease in humidity appears to exceed the random variations. The true systematic change in total water content near the ground is even smaller than is suggested by fig. 7(b), because the diagram is derived from observations of water vapour (dew point), neglecting water present as liquid droplets; the open squares of the diagram should therefore all be moved some distance to the right if changes in total water content are to be indicated.

This irregular behaviour of the humidity profiles is disappointing because the detailed observation of humidity structure was one of the chief novel features of the Cardington work and it had been hoped that some simple pattern would emerge from the results. It seems clear that the greater part of the humidity variation above about 1000 ft. is to be accounted for by the horizontal movement of air with non-uniform humidity; the only alternative is to assume that vertical transport of water vapour occurs to a considerable extent by some mechanism quite unrelated to the humidity gradient and frequently working against the gradient. There is a clear example in fig. 2; the considerable increase in humidity in the region of 1000 ft. from 1800 - 0450 hr. implies either the advection of much wetter air or the vertical transport of water vapour to that region against fairly steep humidity gradients. Similar, though sometimes less clear-cut, arguments can be applied to many of the other large changes in humidity shown in figs. 1 - 6.

It would not be particularly surprising that humidity variations due to horizontal movements should turn out to be greater than those due to vertical movements if the relative simplicity of the temperature profiles did not encourage the belief that advective temperature changes form a small part of the total; the big difference between the temperature and humidity profiles requires some explanation. The humidity fluctuations are far too large to be accounted for by errors in the psychrometer; sampling errors are more serious, as mentioned in Appendix I, but even so the mean deviation of a long series of dew point readings at a fixed height from the smoothed curve drawn through them was only about 0.5°F, corresponding to a change in specific humidity of the order of 0.1 gm./Kg., which would be almost negligible on the scale of fig. 7(b). The most natural explanation lies in the fact that vertical transport of heat can occur by radiation as well as by eddy diffusion, while the only mechanism for transport of water vapour is the eddy diffusion one. We may suppose that as air from different sources, with various temperatures and humidities, moves towards Cardington, the temperature and humidity are modified towards profiles characteristic of the terrain around Cardington. Eddy diffusion usually suffices to modify the profiles up to heights of the order of 500 ft. but above that height the humidity remains characteristic of the original air rather than of the local conditions; the temperature profiles are similarly modified by eddy diffusion but in addition they can be changed by radiative transfer of heat so that they lose evidence of their origin and become representative of local conditions more quickly and to greater heights than the humidity profiles.

A general survey of the profiles thus suggests that it may be useful to discuss the temperature changes up to 3000 ft. in terms of processes going on at one site, i.e. in terms of a simple one-dimensional model, (making allowance for advective effects in individual cases, where necessary) but that it is only in the lowest few hundred feet that humidity changes will conform, even approximately, to such a model. The profiles indicate that 500 ft. is about the height to which the humidity is appreciably affected by local conditions, but it is obvious that there is no sharp boundary between an upper region where advective effects predominate and a lower one where local conditions exercise control. The upper limit for a precise one-dimensional treatment of humidity changes must be well below 500 ft. even for values averaged over many nights and may be lower still when individual occasions are considered and non-uniformity of the immediate surroundings of the instruments becomes important.

If fig. 7 is accepted as showing that humidity changes associated with nocturnal cooling do not usually extend much above 500 ft. it is reasonable

/to

to infer that the changes in humidity at ground level are not directly affected, to any appreciable extent, by the humidity structure above this level. There will, of course, be individual cases, particularly when a deep fog layer is formed, in which humidity at higher levels is of direct importance, and it may exert indirect effects, by affecting the infra-red emissivity, in other cases.

2.3. Fuller description of typical cases

Despite the difficulties in interpretation caused by advection, it is interesting to see how far the results of figs. 1 - 6 fit a simple qualitative account of the processes at work on a "radiation night".

2.3.1. The simplest type of foggy night (figs. 1 and 2)

(a) Late afternoon - the changing balance

During the afternoon the temperature lapse reaches or slightly exceeds the dry adiabatic value and the specific humidity is constant or decreasing with height (the afternoon ascents would only increase the confusion of figs. 1 - 6 and have been omitted). This corresponds to an excess of incoming over outgoing radiation at the ground, with the balance of heat serving to warm the earth, to evaporate water from it and to heat up the air near the ground. As the sun sinks and the incoming radiation diminishes, the earth's surface cools rapidly to maintain the balance of heat-flow and by 1800 hr. it is several degrees colder than the air above or the soil below. The air near the ground is thus losing heat to the surface both by eddy transfer and by long wave radiation; its fall in temperature is most rapid close to the ground but is noticeable up to 1000 ft. or more. The changes in humidity (as measured by the dew point) are less marked up to 1800 hr. In general there is a small fall in dew point at screen level, presumably because the supply of water by evaporation from the ground is cut off as the heat supply decreases but the upward movement of water vapour by eddy transfer in the direction of lowest specific humidity continues.

(b) Early evening - the end of rapid changes

After sunset the temperature near the ground begins to fall less rapidly, but the dew point, on the whole, falls more rapidly than before. A change in the rate of fall of temperature is to be expected, because before sunset the incoming radiation decreases rapidly and the surface temperature must adjust itself to maintain the balance of heat, but after sunset the incoming radiation (which now contains only a long-wave component) is much smaller and changes much more slowly, so that slow changes of surface temperature suffice to maintain heat balance. (More detailed investigations of this change in rate of fall of temperature, with more elaborate explanations of it, have been reported by Saunders (1949) and by Pedlow (1952); it seems unnecessary to introduce such explanations until the simple mechanism just outlined is shown to be quantitatively inadequate). A change in the rate of fall of dew point is to be expected as soon as the surface temperature falls below the dew point near ground level and dew begins to be deposited; the air near the ground will lose water and its dew point will fall. Fig. 1 and most of the other results shown support the idea that dew begins to form as soon as surface temperature falls below screen level dew point, but fig. 2 shows evaporation continuing even when the surface temperature is recorded as being 7 - 8°F below the screen dew point. "Surface temperature", however, was that measured by a "grass minimum" thermometer with the standard exposure; this is known to give a good approximation to the effective radiating temperature of the surface, which is presumably the temperature of the foliage, but the temperature of the soil surface itself may well be higher, permitting evaporation from the soil even when dew is forming on the grass. This possibility seems to be confirmed by the recent dew measurements of Jennings and Monteith (1954).

/(c)

(c) Early night - the quasi-equilibrium period

After these changes near the time of sunset, the general form of the profiles changes little for some hours. Temperature is low at the ground, rises to a maximum at a height of several hundred feet then falls off again, but at a rate less than the adiabatic lapse rate. There is no abrupt change in temperature gradient at any level and there is therefore little significance in the "height of the inversion"; if this is defined as the height with maximum temperature, it rises, rapidly at first, then more slowly. At sunset the level of most rapid fall of temperature is close to the ground but a few hours later it appears to be higher up, near the level of maximum temperature; the temperature gradient near the ground (below about 100 ft.) thus increases fairly sharply to a maximum soon after sunset then tends to decrease slowly. This is, of course, the sort of behaviour that would be expected to result from the fairly abrupt cutting off of a supply of heat to the surface, with processes such as radiation and eddy transfer acting to spread the cooling upwards at a relatively slow rate. The temperature profiles in the ground are similar, with the vertical scale reversed and much reduced because the thermal diffusivity of the soil is much less than that of the air.

The dew point changes during the same period are, as usual, smaller and more confused by advective effects but the general trend, illustrated in figs. 1 and 2, is for the dew point close to the ground to fall nearly as rapidly as the temperature, while the rate of fall higher up, even as low as 100 ft. on some occasions, is a good deal less rapid. If we consider the difference between temperature and dew point at any level resulting from these changes we see that the first rapid fall of temperature near the ground brings the air there close to saturation, but the subsequent slower cooling and the accompanying fall in dew point following the deposition of dew make further approach to saturation very slow; at higher levels the fall in temperature is later and less abrupt in its beginning, so that the approach to saturation is steadier.

A close association between temperature changes and humidity changes is to be expected if the mechanism responsible for the changes is the upward transfer and mixing of eddies of air cooled by contact with the ground. It has indeed been suggested (Emmons and Montgomery, 1947) that saturation can never be reached by this mechanism alone because water vapour will be transported downwards too rapidly in relation to the heat transfer; this overstates the argument, by neglecting the non-linearity of the temperature-saturation vapour pressure relation, but it is certainly true that eddy transport in nearly saturated conditions will bring about changes in dew point which are, to a first approximation, equal to the temperature changes. Cooling of the air, however, can be caused by radiation (from water vapour and carbon dioxide) as well as by eddy transfer; this type of cooling does not involve any loss of water vapour and can thus help to narrow the gap between temperature and dew point.

(d) The small hours - fog formation

The period with rather slowly changing conditions that has just been considered ends, in figs. 1 and 2, with the formation of fog an hour or two after midnight. Towards the end of the period, in the hours about midnight, conditions at screen level become erratic, with occasional increases of temperature or dew point superimposed on their general slow decrease. These fluctuations are probably connected with small changes in the speed, direction or turbulence of the airflow, but there is no obvious connection with any of the quantities recorded so far. It is very difficult to say what finally determines the time at which fog forms. In both fig. 1 and fig. 2 the screen measurement indicates 100 per cent relative humidity some time before fog is reported. This is particularly noticeable in fig. 2, where there is a period of three or four hours (2100-2400 hr.) during which the screen temperature and dew point are equal and fall by several degrees, yet no general fog forms (though patches of fog were reported in particular directions). It is often suggested that fog formation is brought about by small increases in wind speed and turbulence, but there is little evidence

/for

for this in the Cardington records. No observations of turbulence were made near the ground, but the pressure-tube anemometer at 140 ft. does not reveal any tendency for turbulence to increase just before fog forms and the sensitive cup anemometers at lower heights show no increase in wind speed. When fog does finally form the detailed visibility records (of which an example is given in fig. 10) show that it usually does so rather abruptly, sometimes in two or more steps. The fact that thick fog often forms quickly (visibility falling from 2500 yd. to 50 yd. in 10 minutes in fig. 10) may be an important clue to the processes involved. Unless it contains a high proportion of very small drops, a fog with visibility 50 yd. must have a liquid water content of at least 0.5 gm./m^3. It seems very unlikely that such a thick fog could be formed by mixing air saturated at different temperatures, as is often suggested, because to produce 0.5 gm./m^3 of liquid water the temperature difference would have to be over 20°F (if the cooler air was at 32°F). On the other hand if 0.5 gm./m^3 is condensed by cooling in a time of the order of 10 minutes, the rate of loss of heat is far greater than the average rate observed before and after fog formation. The simplest explanation (considered in more detail in Appendix V) is that sudden cooling of the air is brought about through loss of heat by radiation from the water drops; it can be shown that as the relative humidity is increased and the size of hygroscopic nuclei grows, a critical size is reached beyond which the loss of heat by radiation from the nuclei leads to unlimited growth - the droplets will stop growing only when they have become large enough to shield each other from further radiative loss.

(e) Late night - the growth of fog

Fog formation is followed by marked changes in the temperature structure near the ground. The screen-level temperature usually shows a fall of a few degrees in the hour covering the period of fog formation but the fall is not always noticeably greater than the fluctuations of temperature normally occurring in the middle-night period; if continuous, short-lag temperature records were available, a closer correlation of temperature change with fog formation might be possible. It is above and below screen level that the most marked changes occur; at the ground surface, the temperature rises sharply to about the screen-level value, presumably as a consequence of the increased back-radiation from the fog, while at greater heights, up to the top of the fog, there is a considerable fall in temperature to values at or below the screen temperature. The result of these changes is to replace the inversion in the lowest layers by an isothermal or lapse region; the fogs of figs. 1 and 2 are too shallow for the precise observed value of the lapse rate to have much significance, but in deeper fogs such as those of figs. 3 and 4 the lapse rate usually seems close to the saturated adiabatic value (3.3°F/1000 ft.). The upper boundary of the lapse region is formed by a steep inversion very similar to the ground-level inversion present before fog formed. The dew point values indicate saturation within the lapse region, sometimes extending a little way into the inversion above, but at greater heights the dew point continues its slow fall, apparently little affected by the formation of fog below, and remains below the air temperature. The few soundings that have been made with the "fog density indicator", combined with visual estimates of fog top height and the results of the humidity measurements, show that the top of the fog is normally close to the level at which the temperature begins to increase steeply with increasing height, i.e. to the base of the inversion.

The fogs of figs. 1 and 2 appear to have reached heights of about 100 ft. shortly after their formation but to have grown very little deeper in the next two or three hours. Fig. 2 shows that after dawn the temperature in the fog layer increased and the height of the fog top rose to at least 250 ft., no doubt because of an increase in turbulence. The growth of fogs can be followed more closely in figs. 3 and 4. Here again a rapid initial growth (much more rapid and extensive than in figs. 1 and 2) is followed, for the rest of the night, by a period of slow change. Fig. 3 shows steady cooling both inside and above the fog layer, with very little change in height of fog top after 2200 hr. Fig. 4 seems to show similar behaviour (though the data are less complete) with the addition of slight warming and upward growth of the fog after dawn.

/A

A more complete picture of variations in the depths of fog is given in fig. 8. This shows the changes in height of fog top for all occasions on which the height was determined with reasonable certainty, either directly, by the fog density indicator, or indirectly, from the temperature and humidity profiles. It will be seen that there is apparently little tendency for fogs to grow deeper steadily throughout the night; the more typical behaviour is a fairly rapid growth at first, followed by a more or less static period and a final brief period of upward growth as a preliminary to the dispersal of the fog by rising wind and temperature. The sequence of rapid initial change followed by a quasi-equilibrium state is similar to that in figs. 1 and 2 before fog formed, with the difference that in fig. 3 and the other similar cases included in fig. 8 fog formed before conditions had settled down after the change from day to night. The height of the fog top during the quasi-equilibrium period may well be fixed by the need to balance heat exchange there.

(f) Morning - dispersal of fog

The Cardington observations were not planned to study conditions while fog was dispersing. Nevertheless it might be interesting to use them, where possible, for such a study; this has not been done in the present report.

2.3.2. Other types of night

Figs. 1 and 2 were selected for fairly full description and discussion as representing the simplest and most easily explicable type of behaviour. The remaining examples can be discussed more briefly, emphasizing only the points of difference from the description just given.

2.3.2.1. Fog under subsidence inversion

Examination of all the Cardington results gives the impression that there is a second general type of behaviour, less well defined than that represented in figs. 1 and 2, but with certain characteristics worth describing. The important characteristics are that the air temperature falls at roughly the same rate at all heights up to several hundred or even 1000 ft. and that when fog forms it does so in a fairly deep layer, sometimes, in fact, appearing as low cloud which quickly extends down to the surface. These characteristics are most marked when the wind is fairly strong, particularly when it blows from the North Sea (in which case the fog should usually be classed as advection fog not radiation fog) but they are also noticeable in light wind conditions whenever there is an appreciable subsidence inversion in the layer reached by the balloon soundings. Such an inversion usually occurs in prolonged anticyclonic spells so that this type of fog formation is characteristic of the later days of a spell of fog whereas the type of figs. 1 and 2 is characteristic of isolated foggy nights or of the first night of a spell. It is difficult to find an example not complicated by advection effects or by the formation of fog early in the night; fig. 4 is the best that can be found. The effects of subsidence are shown by the warmth and dryness of the air at 1500 ft. and above. It will be seen that the temperature fall (1835-0310 hr.) is about equal at 500 ft. and at screen level, whereas in fig. 2 the fall at 500 ft. was only about half that at screen level.

A possible explanation of the more uniform temperature fall lies in the radiative properties of the air. The air under the subsidence inversion of fig. 4 probably contained fairly large quantities of smoke and other suspended matter (the visibility in mid-afternoon was only three miles for fig. 4 against ten miles for fig. 2) and cooling of the air by radiation from the suspended particles may well have been very appreciable.

The fall in dew point, too, is more uniform with height in fig. 4 than in figs. 1 and 2, and there seems to be a significant loss of water vapour up to nearly 500 ft.; the total amount of water lost from this layer is much greater than in figs. 1 and 2 and is too great to be accounted for by the measured

/deposition .

deposition of frost. It seems likely that in this case, with a steep lapse of humidity above 1000 ft., an appreciable amount of water was lost by upward eddy diffusion.

2.3.2.2. Radiation nights without fog

Fig. 5 represents an occasion similar to those of figs. 1 and 2 but one on which fog did not form. There is no important qualitative difference from fig. 2, but presumably a combination of several quantitative factors - the higher initial gap between temperature and dew point, the greater warmth of the ground and the shorter night period available for cooling - were responsible for the fact that the temperature did not fall as low as the dew point and no fog formed.

Fig. 6 is characteristic of several nights with low temperatures when the total amount of cooling of the air (represented by the area between the temperature profiles for 1800 hr. and 0600 hr.) was much less than on the other nights already considered. It is not obvious why the cooling should be so much less; it is true that radiation from a cold ground surface is less than from a warm one, but the back radiation from the atmosphere is also less and the net change in radiative flow is small. The wind was light and the temperature lapse somewhat less than adiabatic, so it seems unlikely that heat was lost by convection to heights above those studied. It is possible that the main reason for the small net heat loss from the air was the liberation of latent heat in the ground as freezing penetrated downwards from the surface. It is impossible to check this hypothesis fully without more detailed measurements in the ground, but it can be shown to be qualitatively plausible (see Appendix III).

The dew point behaviour on this occasion was not significantly different from that on other nights.

2.4. Wind structure

The balloon can only be used when the surface wind is less than 15 kt. and the wind aloft less than about 30 kt. There are thus no observations for occasions of strong winds. However, the fact that observations were made only when fog or radiation conditions were forecast would in any case have excluded occasions with strong winds; there are results for roughly equal numbers of occasions with winds of 0 - 10 and 10 - 20 kt. (at 2-3000 ft.), but for many fewer occasions with winds over 20 kt. The (2000 ft.) wind speed, below about 20 kt., appears to have little effect on the general course of events; there is no obvious difference between the group of results with speeds 0-10 kt. and that with speeds 10-20 kt. The few cases with speeds over 20 kt., however, were all ones when fog did not form, apparently because the fall of temperature near the ground (though not the mean fall in the lowest 1000 ft.) was much less than usual, as would be expected if turbulent mixing was occurring.

The wind profiles shown in figs. 1-6 are typical of all the results obtained. It will be seen that individual points are somewhat erratic, probably because the wind was measured over only fairly short time intervals ($\sim$1 min.) at each height. Mean profiles for 1800 hr. on ten nights which remained clear and ten which subsequently became foggy are shown in fig. 9. The most interesting feature is the decrease in speed with increasing height above about 750 ft. on fog nights. Even in the mean profiles this decrease amounts to some 30 per cent of the maximum speed; in the individual profiles (e.g. 2200 hr. in fig. 1) it is often much greater, and occurs with great regularity, particularly in the period just before fog forms. Indeed, examining the last ascent before fog formed in each case, we find that on 19 out of 21 occasions with complete enough wind data the wind at 3000 ft. was less than that at some level below 2000 ft. On the other hand, on non-foggy nights this decrease with increasing height occurred on only about half the occasions, and when it occurred was less marked than on foggy nights.

/The

The simplest explanation of the decrease in wind speed with increasing height is that it is a "thermal wind" effect. A decrease should occur if there is a horizontal temperature gradient in the opposite direction to the pressure gradient. Such conditions should exist in the anticyclonic situations typical of foggy weather, either because the air temperature is lowest near the high pressure centre or because the subsidence inversion is highest there, giving the greatest depth of cold air. The winds are so light that quite small gradients would produce the observed effects - gradients of the order of 2°F in 100 mi., equivalent to a 10°F inversion with a slope of 1 in 500 - and the observations available are not exact enough to test the explanation just given.

Below about 1000 ft. the mean profiles of fig. 9 show the effect of friction at the ground in reducing the wind speed near the surface, but it seems clear that the layer in which this friction is the chief factor determining the profiles is only 500 or at most 1000 ft. deep. The wind profiles thus resemble the humidity profiles rather than the temperature ones and tend to confirm the idea that so far as eddy diffusion is concerned the effects of the surface do not usually extend much above 500 ft.; the changes in temperature at greater heights can be attributed to radiative effects (or, possibly, to a greater effectiveness of eddies in transporting heat).

The changes in wind speed during the night show little regularity, though, as can be seen in figs. 1 - 6, they may be large. Close to the ground the wind usually drops in the late afternoon, but after 1800 hr. there is little systematic change until fog forms, when the speed often drops below the range of the anemometers (1 ft./sec.). This calm often extends through the whole depth of the fog, so that there may be a very noticeable drop in wind speed at levels of a few hundred feet when the fog reaches the level concerned. At greater heights large changes in wind speed are common, with decreases on the whole more common than increases. This may well be because rising winds are often associated with approaching fronts and cloudy conditions, whereas falling winds are common in ridges of high pressure, with their clear skies. The practice of making observations only on clear nights (or ones becoming foggy later) thus introduces a bias against occasions with increasing winds.

The wind profiles seem to be rather little affected by the vertical temperature structure. In fig. 2, for example, the wind profile changes little in the lowest 1000 ft. despite the growth and intensification of a considerable temperature inversion.

2.5. Horizontal and oblique visibility in fog

We have so far discussed fog in terms of its presence or absence, without mentioning its intensity, which is conveniently measured by the "visibility" in the fog. It will be seen that in all the examples given there was, in fact, a rather abrupt change from a state of no fog, with visibility of the order of 1500 yd., to one of thick fog, with visibility between 50 and 200 yd. Examination of all the records from Cardington shows that visibilities between about 200 and 1000 yd. are rare, except when fog forms at temperatures well below freezing point. This suggests that most thin fogs are in some way unstable; it is possible that this instability is produced by radiative cooling of the fog droplets, in the way discussed in Appendix V.

The final values reached by the visibility all lie within a rather narrow range (50-200 yd. except for very cold fogs) and the visibility usually remains fairly constant for most of the life of the fog. It might be thought that the visibility should be related to the extent to which the temperature falls below the temperature at which the air becomes saturated, but no such relation can be seen in the Cardington data; in particular it can be seen in fig. 3 that the temperature throughout the depth of the fog fell by some 3°F between 2030 and 0730 hr. while the visibility fluctuated about a constant value of 50 yd.

/The

The variation of visibility with height is of considerable importance to aircraft operators. Measurements to investigate this have been made on a few occasions since 1953 and the results are shown in fig. 11. The quantity measured and plotted is the one of direct interest to aircraft, the slant visual range of a lamp at various heights to an observer at ground level; it represents the integrated effect of the fog in the layers between the observer and the lamp and therefore varies much less abruptly with height than the fog density itself. Readings from the "fog density indicator" agree qualitatively with the slant visibility observations but are thought to be less accurate because of difficulties in calibration, and are not used in fig. 11. It will be seen that the observations are too few to allow general conclusions to be drawn (they were nearly all made in one foggy spell) but their indication is that slant visibility commonly decreases with increasing height, the decrease being most marked in relatively thin fogs. A theoretical interpretation of these results is given in Appendix VI.

2.6. Summary of qualitative results

General study of the Cardington results, as indicated in the last few sections, shows that there is little difficulty in giving a satisfactory qualitative account of events on a foggy night in terms of physical processes. For a fuller understanding of these processes we must turn to a more exact quantitative treatment of the data. Before doing so, it is well to review the main features of the general picture we have outlined. The dominating process is obviously the loss of heat by radiation from the ground and the balancing of this loss by downward radiation, by heat convected from the air or conducted through the soil and by latent heat released near the surface. Transport of water vapour is also important, but there is good evidence that in many cases only transport in the lowest 500-1000 ft. need be considered and that this transport is largely balanced, as far as the approach to saturation is concerned, by the simultaneous transport of heat. It appears that large-scale advective changes of temperature are usually small compared with the time-change during a night, so that one-dimensional treatment of heat flow may be practicable, but that advective humidity changes are much larger than the time-changes, except quite close to the ground, and make a one-dimensional treatment of very doubtful validity. The wind structure appears to affect and be affected by the temperature structure rather less than might be expected, which may permit some simplification in theoretical treatments. For the formation of fog at Cardington, the attainment of a relative humidity of at least 99 per cent is a necessary condition for fog formation (at least, at temperatures above freezing point) but it is not a sufficient condition. Certain additional conditions must, apparently, be fulfilled before fog forms, but the present data are insufficient to decide what they are; they may well be connected with the detailed humidity structure and radiative properties of the atmosphere over the site, but small horizontal movements of inhomogeneous air may also be essential.

Before attempting a more quantitative examination of the processes discussed, it is worth pointing out the few features of the general picture of events that might be clarified if a longer series of observations were available (and assuming that the complete plan of observations set out in 1.1. had been carried out). The most important, and probably the most complicated, is the effect of wind and cloud on the cooling process. Observations have so far been deliberately restricted to more or less cloudless nights and most of them have been made in relatively calm conditions. The effect of wind and cloud are already known approximately, but it is possible that observations on windy and cloudy nights would bring some new facts to light. Another subject on which more data might be valuable is the vertical extent and growth of fog, particularly when combined with information about the visibility (i.e. the density of the fog at various levels). The present data do give a general idea of typical behaviour at Cardington, but are not extensive enough to give accurate averages, which may well be required in aircraft or atmospheric pollution problems.

/3.

3. Quantitative discussion of physical processes

Although the physics of the various component processes leading to fog formation is fairly well understood and it is possible to calculate the results of each process in simple conditions, the interactions between the different processes lead to such complexities that there has so far been little success in calculating the important features of the final state on a foggy night from observable initial conditions. The first step in disentangling the problem is to find out the relative importance of the various processes at work; we can then try to estimate whether or not the current theory for each process fits the facts with sufficient accuracy, and seek to make improvements in the theory or empirical approximations to the required results where necessary.

3.1. Heat balance

It is clear from fig. 7 and the temperature profiles shown in figs. 1 - 6 that the main temperature changes on a radiation night are usually confined to the lowest 3000 ft. or less. The heat balance of this "cooling layer" has the heat lost by radiation through the top of the layer on one side and on the other side the heat given up by cooling of the air, by cooling of the earth and by condensation or freezing of water. In addition we may have to allow for heat flowing through the top of the cooling layer by convection and for heat transferred horizontally by advection. The components of the heat balance on a number of occasions already discussed (figs. 1 - 6) are set out in Table I. The methods of finding the various components from the observations are indicated below.

Table I

Rate of loss of heat from cooling layer. Units mW/cm^2

Date	29/9/51	29/9/51	27/9/53	5/12/52	31/10/53	18 foggy nights	13 clear nights
Time	0001	0400	0100	0001	0001	18 - 06	18 - 06
Level of top of cooling layer	2000ft.	3000ft.	3000ft.	1000ft.	1500ft.	2500ft.	2000ft.
Observed loss of heat							
(a) from air	5.0	11.7	7.8	1.8	1.6	5.9	3.0
(b) from earth	5.0	4.5	3.9	1.0	3.6	4.5	3.0
(c) from condensing water vapour	0.7	0.7	0.4	0.4	0.7	1.0	0.5
Total observed loss	10.7	16.9	12.1	3.2	5.9	11.4	6.5
Loss by radiation through top of cooling layer (calculated from "Kew chart")	9.3	9.0	9.5	7.6	8.8	9.0	8.2

In all columns there is a large difference between the figures in the last two rows, indicating a serious lack of balance between the components considered. The most uncertain of the components is the heat lost by the earth. This was estimated from temperature profiles drawn through earth thermometer readings at 2 in., 4 in. and 8 in. in the ground, by taking

/the

the area between profiles at two-hour intervals and multiplying by a mean capacity of 0.7 cal.cm^{-3} °C^{-1} measured at Cardington some years ago by Swinbank. The temperature profiles are not determined very closely by the three temperature readings and the heat capacity may well have varied with the condition of the soil, so that the figures in Table I may be in error by as much as 50 per cent. On 5/12/52 and 31/10/53 there is another source of error in the earth-heat estimates because the surface temperature was below freezing point and any water present in the soil was presumably freezing and giving up latent heat. The freezing of 1 mm. of water per hour (i.e. of 2-3 mm. of damp soil per hour) would release about 8mW/cm^2 of heat, so this latent heat component can easily be an important one.

It is thus possible to explain the discrepancies in all but the second case of Table I in terms of errors in the estimates of the heat contribution from the earth. There may, of course, be other errors in the table; the loss of heat from the air and the loss by radiation are probably correct to 10 per cent but the latent heat of condensation of water depends on the measurement of dewfall, which is only accurate to about 30 per cent. As far as convective transport of heat through the top of the "cooling layer" is concerned, we may note that in all cases the lapse rate was less than the dry adiabatic one, so that convection would convey heat downwards and would thus increase the discrepancy in the first three cases of Table I but reduce it in the fourth and fifth. In the fourth case the wind speed was low and convection through the 1000 ft. level probably small, but in the fifth case the wind was fairly strong and it seems better to attribute the unbalance shown in Table I to the downward transport of heat than to latent heat of freezing in the earth (the surface temperature fell only 3°F below freezing point).

In the second case of Table I none of the errors so far invoked can explain the discrepancy, and we are forced to attribute it to an advective change in air temperature.

The last two columns of the table give averaged estimates of the heat balance components for 18 foggy nights and 13 clear ones (the nights for which data were given in figs. 7(a) and 7(b)). The air and earth losses should have the same accuracy as in the individual cases of Table I, but the condensation and radiation components are rougher estimates, because the necessary measurements and calculations were not made on all occasions. The heat of condensation for the foggy occasions assumes that, in addition to an average amount of dew, water condensed to form the fog to an extent of 0.5 gm./m^3 in a layer 200 metres deep.

There is a striking difference between corresponding heat components on foggy and non-foggy nights. The explanation probably lies in the high proportion of the non-foggy nights which had freezing ground, and release of latent heat (as on 5/12/52), or strong winds, and downward transport of heat from above (as on 31/10/53).

These results in Table I are very similar to the longer series obtained by Swinbank (1946) from earlier observations at Cardington. Both sets of results show that the outward flux of radiation (as calculated from a radiation chart) is relatively constant from night to night but that the observed losses of heat from air and earth (and also their sum) are considerably more variable. Some of this variability may be due to errors in measurement, but advective changes also seem to play a significant part and it is quite possible that the "chart" estimates of radiation may be inaccurate on some occasions. Swinbank, indeed, suggested that his results demonstrated a systematic error in the radiation chart (Elsasser's) he used, but the general scatter of his results (as of the present ones) appears too great to justify such a conclusion. On the other hand, it cannot be said that the results provide any serious check on the accuracy of radiation charts - this is done far better by direct measurements of radiation.

/3.2.

3.2. Heat exchange within the cooling layer

Though the study of the heat balance of the cooling layer as a whole casts doubt on the accuracy with which the various components can be estimated from the Cardington data, it is interesting to carry the analysis a stage further and try to find the components of heat flow at a series of levels within the cooling layer. This has been done for a few cases, and results are given in Table II. We again start by finding the flux of radiation, using the observed temperatures and humidities in conjunction with a radiation chart. The first three columns of Table II show the upward, downward and net fluxes calculated in this way for various levels, including the ground surface. The difference in net flux at any two levels (col. 4) gives the loss of heat by radiation from the intervening air-layer. The observed loss of heat from the layer (col. 5) can be found by multiplying its heat capacity by its mean rate of change of temperature, and the difference between this loss and the radiative loss measures the loss of heat in the layer by convection (col. 6). Col. 6 thus gives the difference in convective flow between each pair of levels; in order to find the actual magnitude of the flow, some boundary condition is needed. This could be provided by the balance condition at the earth's surface, if all the other components there were known, but we have seen that the value of heat flux from the earth is not known precisely from the measurements, and it has seemed better to assume the condition that the heat flow through the top of the cooling layer was zero (in the first three cases analysed in Table II; in the last case, as noted in discussing Table I, this assumption seems unreasonable and the alternative boundary condition provided by the balance equation at the earth's surface has been used). With these conditions, we can use col. 6 of Table I as a set of differences to build up col. 7, giving the convective flow through each level. To complete the list of heat flow components at the surface, the latent heat of condensation of dew (the product of the latent heat and the measured dewfall) and the heat lost by the earth are given in cols. 8 and 9. For balance, the sum of the ground-level values in cols. 7, 8 and 9 should be equal to the value of net outward radiation in col. 3. The obvious lack of balance has already been discussed in connection with Table I and attributed mainly to errors in heat flow from the earth (col. 9) - but the possibility of systematic error in the convection components (col. 7) must also be borne in mind.

The first interesting feature of Table II is the broad equality between cols. 4 and 6, the radiative and convective cooling of the air, within the "cooling layer".

The main analysis into radiation and convection components in Table II is independent of errors in the heat flow from the earth, but, as will be obvious from the table, it is very sensitive to errors in the estimation of the upward and downward fluxes of radiation, particularly when shallow air layers are involved. It is shown in Appendix II how the usual process of estimation from a radiation chart can be rearranged to give changes in net flux directly (i.e. col. 5 of Table II, rather than cols. 1 and 2) and thus allow greater precision, provided the observations and the data on the radiative properties of the atmosphere are accurate enough. It is easy to show, however, that the radiative properties of a hazy or misty atmosphere are very different from those of the clear air to which radiation charts refer, and that quite small amounts of liquid or solid particles can seriously upset the sort of calculations on which Table II is based.

Even when radiation from particles is ignored, as in Table II, we find that radiation is, broadly speaking, as important as convection in cooling the air. Radiative cooling is seen to be greatest near the ground but to fall off rather slowly with increasing height; even at 2-3000 ft. it is usually of the order of 1 mW/cm^2 per 1000 ft. layer, equivalent to a rate of fall of temperature of about $0.2^{\circ}F/hr$. In most cases, as we have seen, no appreciable fall in temperature is observed above about 2500 ft. and we must assume that the air at these heights usually gains heat in some way to compensate for the loss by radiation. It seems likely that this heat is frequently provided by anticyclonic

/subsidence.

subsidence.

As far as can be seen from Table II, convective cooling is usually a maximum at heights of a few hundred feet; it certainly falls off at greater heights, but the analysis is not exact enough to be certain of the behaviour near the ground. It is likely that the radiative cooling becomes very large (and the convective component correspondingly small) at heights of a few feet, while at heights of a few inches where the air is close to the surface temperature of the ground, with considerably warmer air above, radiation must warm rather than cool the air. The heat economy of these low levels is interesting but cannot be studied with the present observations.

It can be seen that the convective flux normally changes by an amount of the order of 10 per cent in the lowest 100 ft. setting a limit to the height to which the assumption of approximately non-divergent flux is valid. The convective fluxes in col. 7 of Table II can be combined with the observed gradients of potential temperature (col. 10) to obtain values for the "eddy conductivity", K_H, given in col. 11. (The values given at heights of 0 ft. were calculated from the flux at 0 ft. and the gradient at 50 ft.; they thus represent the eddy conductivity at 50 ft., assuming that the flux there is the same as that at the surface). The zero values of K_H at certain heights are, of course, a direct consequence of the assumption that the convective flux there was zero; in view of the smallness of the temperature gradients at these heights a quite small flux would correspond to a large value of K_H, and little reliance can be placed on the values in the table for heights of 1000 ft. and over. At lower heights the values of K_H should be correct as to order of magnitude but are obviously by no means exact. It would be unjustifiable to use the figures to deduce a law for the variation of K_H with height, but there is some indication that changes in K_H in the layers between 50 and 500 ft. are small compared with changes in temperature gradient. To illustrate the relation between the observed values of K_H and the stability, values of the Richardson number for the 50 ft. level are given in col. 12 of the table and values of K calculated from Rossby and Montgomery's formula ($K = \kappa^2 z^2 (\partial u/\partial z)(1+\sigma Ri)^{-1}$ with $k = 0.4$, z = height, u = velocity, σ = const. = 8, Ri = Richardson number) in col. 13. It will be noticed that the values of Richardson number are a good deal higher than in most previous studies of eddy diffusion, partly because of the great stability, but partly because they refer to a relatively great height. There appears to be very little connection between the values of K_H given in col. 11 and either the Richardson number or the calculated values in col. 13, but it must be pointed out that the gradients of temperature and wind speed, on which these calculations depend, are not at all well defined by the observations.

Table II is interesting as indicating orders of magnitude of certain quantities on typical radiation nights but is clearly unsuccessful as an attempt to apply to the Cardington data the type of analysis which has been used successfully in detailed investigations of the lowest few metres. Unfortunately it does not seem possible to say whether the failure is due to lack of precise observations or to the more fundamental reason that a one-dimensional treatment of events is inadequate.

3.3. Water exchanges

We can attempt to build up a table indicating the movement of water in the way Table II indicated the movement of heat. The process is simpler, because radiation plays no part; the basic data are the flux of water at the surface (the dewfall) and the changes in water content of each layer of air. Satisfactory dew measurements were made on relatively few occasions and Table III includes all cases for which an analysis can be made. (Water transport after fog formed cannot be studied because no measurements were made of the water content of the fogs).

It will be seen from Table III that although the measured amounts of dewfall are of the same order of magnitude as the changes in water content of the

/lowest

TABLE III

Analysis of flow of water vapour on selected occasions

Units: micrograms / cm^2/sec. (gradients in μgm./gm./cm.)

Date		18-19/9/53	26-27/9/53	30-31/10/53	28/2/53	1/3/53	6-7/3/53	8-9/3/53	10-11/3/53	Mean	Mean deviation
Period		2108-0310	2155-0100	1800-0001	1800-2400	1800-2100	1800-0600	1800-0600	1800-0200		
Measured dewfall		0.28	0(< .05)	0.30	0	0.20	0.18	-0.02	0.17	0.14	± 0.11
Change in water-vapour content of layer	0-100'	-0.20	0.32	-0.02	-0.01	-0.15	-0.05	0.04	+0.07		
	100-250'	-0.18	-0.32	0.03	0	0.30	-0.08	+0.05	+0.10		
	250-1000'	-0.95	+0.63	+0.29	-0.10	-0.32	+0.10	+0.09	+0.04		
Flux of water (+ = downwards)	0	0.28	0	0.30	0	0.20	0.18	-0.02	0.17	0.14	± 0.11
	100'	0.08	-0.32	0.28	-0.01	0.05	0.13	-0.06	0.24	+0.05	± 0.13
	250'	-0.10	-0.64	0.25	-0.01	-0.25	0.05	-0.01	0.34	-0.05	± 0.21
	1000'	-1.05	-0.01	0.54	-0.11	-0.57	0.15	+0.08	0.38	-0.07	± 0.38
Specific humidity gradient (+ = incr. upwards)	0	-	-	-							
	100'	0.13	0.23	0.092							
	250'	0.002	0.08	0.033	-0.01	-	0.023	-0.09	< 0.02		
	1000'	0.006	0.006	-0.015							

lowest few hundred feet of air, there is very little correlation between the water lost from the air on any occasion and that deposited on the earth. The table includes estimates of the gradients of specific humidity at each level. These are not very accurate, because of the irregularity of the profiles, but they do show clearly that there is practically no correlation between the gradient and the flow through any level; in fact, in six cases out of twelve the flow is apparently against the gradient. This result seems to indicate that advective changes are swamping the effects of vertical transport even at heights as low as 100 ft. The "advection" involved is not necessarily on a large scale; it may be that the horizontal movement of quite small patches ($\sim$ 100 yd.) of damp or dry air makes the "spot" humidity readings on which Table III is based unrepresentative of mean conditions over the site.

Although Table III suggests that water diffusion coefficients calculated from the Cardington data will have little significance, there is some interest in comparing them with the values of K_H in Table II. This can be done in only two cases, 27/9/53 and 31/10/53. Following the procedure used in Table II we estimate the diffusion coefficient, K_w, at 50 ft. by using the flux at the surface (dewfall) and the humidity gradient at 50 ft. In this way we find, for 0100 hr. on 27/9/53, K_w = 200 cm^2/sec. (K_H was 2,000 cm^2/sec.) and for 0001 hr. on 31/10/53, K_w = 1700 cm^2/sec. (K_H was 2,800 cm^2/sec.). Errors in the measurement of dew and of humidity gradient can easily account for the discrepancy between K_H and K_w in the second case; in the first case the discrepancy suggests that K_H has been overestimated as well as K_w underestimated, or else that there is a genuine difference between K_H and K_w, defined in the way implied by the method used for calculating them.

We can attempt to overcome the irregularity of the humidity results on individual occasions by taking averages. Table III therefore includes mean values (with mean deviations) for the flow through each level. There appears to be a significant downward flow at the surface and at 100 ft., but at 250 ft. and even more at 1000 ft. the spread of individual values is so wide that the mean flow cannot be determined accurately. The most that can be said is that the results do not contradict the simple hypothesis that the mean flow several hundred feet above the surface is zero, i.e. that the normal loss of water from the lower layers on a radiation night can be wholly attributed to the deposition of dew.

3.4. Measurements required for the investigation of physical processes

The last few sections have shown the order of magnitude of the various terms in the heat and water budgets on a radiation night. It turns out that the three most obvious components of heat flow at the earth's surface - radiation, conduction from the earth and convection - are of roughly equal importance. Slightly less obvious results are that direct radiation from the air contributes at least as much to its cooling as does convection and that latent heat of freezing of water in the earth can provide a significant amount of heat on some occasions. As far as water is concerned, the outstanding result is the frequent occurrence of large changes in water content which, since they are apparently uncorrelated with vertical humidity gradient, must be attributed to horizontal advection. On average, the amount of dew deposited is comparable with the amount of water lost from the air.

More detailed examination of the results given in Tables I - II showed that they could not be used to check or develop theories of the various processes going on. On radiation no measurements at all were made, on conduction in the earth the measurements were too incomplete and for convective processes the measurements of gradients showed considerable observational uncertainty, while the estimates of flux were very sensitive to small errors in the radiation or conduction terms. It is important to try to decide what accuracy is needed in any future measurements if they are to contribute

/effectively

effectively to our understanding of the physical processes of fog formation. This involves rough theoretical treatments of various processes, which are set out in Appendices II - IV. Only the main results will be mentioned here.

3.4.1. Radiation

It is shown in Appendix II that for calculating heat balance at the surface an accuracy of the order of 2 per cent is required in estimating the "back radiation" from the sky. This is about the limit of accuracy obtainable from a radiation chart (Robinson, 1947) provided the estimate is not upset by the "additional radiation" tentatively attributed by Robinson to haze particles. It seems essential to find by direct measurement how large this additional radiation can become on a hazy night. When we come to calculate the direct radiative cooling of the air, the effects of haze seem even more important; Appendix II suggests that if the visibility is as low as 2500 yd. cooling by radiation from the haze or mist may equal that by radiation from water vapour. Direct measurement to test this conclusion seems very desirable. The accuracy of measurement required for both back radiation and radiative cooling measurements is probably just within the capacity of ordinary radiometers, if used with care.

Another point which requires attention is the variability of ground surface temperature from place to place. "Surface temperature" in the Cardington work has been given by the readings of a thermometer resting just above the ground, as recommended by Robinson (1947). This is probably representative of the immediate surroundings of the site, but if we are concerned with the equilibrium of a 3000 ft. layer of air, variations over a wider area, including hedges and ploughland as well as grass, may be important. It might be possible to measure a mean radiating temperature by a downward-directed radiometer from a balloon.

3.4.2. Heat from the ground

For heat balance calculations such as those giving Table I and for acceptable accuracy in predicting the course of temperature changes it is probably sufficient to know the heat flow from the earth to about 10 per cent. This is impossible with the present earth temperature measurements and without measurements of the specific heat of the soil, but it has always been planned to increase the number of depths at which earth temperatures are measured and to make specific heat determinations, and these extra observations should give the required accuracy. The use of "flux plates" as developed at Kew, might simplify the measurements.

As far as the theory of heat transfer in the earth is concerned, there is little to suggest that ordinary heat conduction theory is inadequate, though when more detailed temperature profiles are available it is possible that difficulties will be revealed. As with radiation, the question of the representativeness of the site and the possible effects of variation in heat flow from place to place must be borne in mind.

Complications in the calculation of heat flow occur when the ground is freezing, as considered in Appendix III. In order to measure the heat flow from the ground, special measurements would be necessary in these conditions.

3.4.3. Convection processes

Convection is the most difficult transfer process to deal with, as there is no fully worked out theoretical treatment available and no generally accepted method of measuring it directly. In Table II we

/tried

tried to estimate the convective heat flow by the usual indirect method, but found that the data on which we relied were not accurate enough to give good estimates. If measurements of radiation and more accurate measurements of earth flux were made, as just suggested, reasonably accurate estimates of convective flux should become possible, so long as advective effects are not too large. There is evidence that they will probably be large enough to upset the results on a fairly large proportion of occasions, even when synoptic charts show no obvious signs of advection.

Given satisfactory estimates of convective flux, we shall require to relate them to the gradients of wind and temperature. The profiles obtained by the present procedure are too erratic to give good estimates of gradient, as can be seen from the examples in figs. 1 - 6. This is not surprising since, even in work in the lowest few metres, it is usually found necessary to average over periods of the order of half an hour in order to get smooth profiles, and it is unlikely that any much shorter time of averaging will suffice at greater heights.

The most that can reasonably be hoped for from a study of convection processes is that it may be possible to find empirical expressions relating the eddy diffusion coefficients to wind and stability parameters. This has been done (e.g. Rider, 1954) in near-neutral conditions of stability and for the lowest layers of the atmosphere, where the divergence of the convective flux is negligible. To extend this type of treatment to extremely stable conditions and to deep layers where the product of diffusion coefficient and gradient is known to vary with height is clearly a big undertaking. There would be little hope of predicting fog formation by physical methods if the result depended on calculating from a convection theory the rate of cooling of air at a given height or the loss of water vapour from the air. The chief reason for thinking that some sort of success may be possible is that we are interested in obtaining saturated air, and with nearly saturated air the rates of change of temperature and of dew point by convection should be nearly equal, provided the eddy diffusion coefficients for heat and for water vapour are the same. The question of the combined eddy diffusion of heat and water is considered in Appendix IV and it is shown that a relatively rough value of the diffusion coefficient and its variation with height is all that is required, so long as the coefficient is the same for heat and for water. The question of the equality or otherwise of "K_H" and "K_W" is thus one of great importance. It is suggested that the first aim of future experiments should be to settle this question for the conditions of a radiation night. The very erratic nature of dew point variations above about 100 ft. suggests that the experiments will have to be confined to the lower layers, in the first place, if they are to have any chance of success.

3.4.4. Fog formation

It was mentioned in section 2.6 that there is some doubt about the conditions necessary for the actual formation of fog. It seems impossible that fog could form as suddenly as it often does by the mere continuing of the cooling processes considered in the last few sections. Two other mechanisms can be suggested, the effects of horizontal air movements in mixing air at different temperatures and the effects of radiative cooling in promoting the growth of fog drops once they have formed. The Cardington observations do not allow any detailed investigation of either mechanism, but a preliminary theoretical examination of the radiation mechanism is made in Appendix V and it is concluded that it may well be important. Experimental study of these questions requires measurements of radiation while fog is forming and a study of local temperature and humidity fluctuations.

3.4.5. Fog density and structure

The density or "visibility" of a fog may vary widely, as may its height and the way in which density varies with height. The fog problem will not

be solved until all these quantities can be predicted, but the observations made so far do not suggest any obvious ways of doing so. It seems unlikely that much progress will be made on the experimental side without measurements of the size and number of the water drops of the fog and possibly also of the nuclei around which they are formed. On the theoretical side studies such as those of Best (1953) on the growth of water drops should lead to useful results, though the radiation factor mentioned in the last section should probably be taken into account. For the variation of fog density with height (measurements of which were mentioned in 2.5) a provisional explanation is given in Appendix VI, but it cannot be tested quantitatively without measurements on the water drops.

4. Empirical fog-forecasting methods

In view of the difficulties of a full physical treatment of the processes leading to fog formation, one of the most attractive approaches to the practical problems of forecasting fog is by constructing semi-empirical formulae or graphical methods. The method is to choose certain parameters which seem likely to be important and arrange them in some plausible formula whose coefficients can then be obtained by appeal to experience through statistical or graphical methods. Forecasting procedures of this type have been suggested, among others, by Briggs (1950), Craddock and Pritchard (1951), Saunders (1950, 1954) and Swinbank (1949). The Cardington data can be used to test these procedures and to study possible extensions of them.

4.1. Tests of suggested methods

Briggs, Craddock and Pritchard, and Saunders all suggest methods for predicting the "fog-point", i.e. the temperature at which fog is expected to form. Fog points (T_f) have been calculated by each of these methods for every suitable night at Cardington, and compared with the actual temperature at which fog formed. (This work was done by Mr. D.B.B. Powell). The results are shown in figs. 12 - 14. It will be seen that the forecasting errors are large and are about the same, on average, with each of the methods (in each case the standard deviation of forecast minus actual fog points is about 5°F).

Swinbank's "fog prediction diagrams" give a different form of result. Points representing the initial conditions are plotted on the diagram (fig. 15) and it is found that lines can be drawn separating the points corresponding to fog formation from those corresponding to clear nights; the diagram can thus be used to predict whether fog will form or not, but not to predict the actual temperature at which it will form. The Cardington results are plotted on a diagram of this type in fig. 15. The diagram is rather confusing to interpret but the results are summarized in Table IV.

Table IV

Number of cases

	Predicted		
Actual	Widespread fog	Patchy or local fog	No fog
Widespread fog	6	8	1
Patchy or local fog	3	4	2
No fog	1	5	0

/Figs. 12 - 15

Figs. 12 - 15 suggest that the four methods tested are all rather inaccurate, but it should be pointed out that the data have been treated in a mechanical manner, without making allowance for special effects such as those of wet ground, frost or advection (though cases with obvious changes of air mass have, of course, been excluded) as recommended by the various authors. In addition, the methods have been applied to a different place from the ones for which they were designed (and in the case of Swinbank's method, which was intended for use in October and November only, to other times as well). In view of the small number of cases for which data were available, it seems impossible to allow for these effects without risking a tendency to force the observations to fit the theory in mind. For objective statistical testing of the empirical type of forecasting formula it seems essential to have of the order of a hundred cases, rather than the twenty so far available from Cardington.

4.2. Development of forecasting methods

The simplest of the forecasting formulae considered is that of Craddock and Pritchard, whose initial parameters are simply the screen level temperature and dew point (with an allowance for cloud amount and wind speed when these are not small). It is interesting that this formula seems about as successful as the others, which introduce additional, upper air parameters. As suggested by Craddock and Pritchard, their formula provides a useful starting point for the study of the importance of other parameters. It has been used in examining the Cardington results, by finding, for each case, the error (forecast - actual T_f) of the Craddock-Pritchard formula and plotting this error against various parameters - "hydrolapse" (average vertical gradient of specific humidity in the lowest 1000 ft.), wind shear and earth temperatures. No correlation was found with any of these quantities; this is surprising, in view of the importance given to hydrolapse in other forecasting formulae, but it may well be that a genuine effect of hydrolapse is being masked by large random variations due to other parameters, in the small sample of occasions from Cardington. It seems unlikely from these results that neglect of any one factor is responsible for the "errors" in current forecasting formulae. If there are several independent sources of error, the need for a reasonably large sample of occasions for study is clear.

A less systematic study has been made of various other parameters - humidity and temperature gradients at different levels, wind shear in various layers and heights of inversion levels - but no significant results have been obtained. The only interesting relationship found is one between the formation of fog and a parameter not observable at the beginning of a night, the "grass minimum" temperature. The basis for this relation was pointed out many years ago by Taylor (1917); if the air above the ground is cooled by mixing with air actually at the surface (which is assumed to have temperature and dew point equal to the surface temperature) the mixture cannot be saturated unless the surface temperature is lower than a certain value, determined by the temperature and humidity of the air above the surface and the curvature of the temperature - saturation vapour pressure relation. This suggests that, with given initial (screen level) temperature and dew point, fog cannot form unless the surface ("grass minimum") temperature falls below a certain, calculable value. We have seen that cooling of the air by radiation is also important and will upset this argument, but we have also seen (Appendix II) that radiative cooling near the ground is largely controlled by the difference between air and ground surface temperatures, so that it is possible that an empirical modification to the calculated surface temperature required for fog formation may allow for the radiation effect.

Fig. 16 illustrates a search for this hypothetical relationship. The initial temperature (T) and dew point (D) are represented by co-ordinates in the plane of the diagram and the observed grass minimum temperatures (T_m) by the co-ordinate perpendicular to this plane. (The values of T_m, in degrees Fahrenheit, are written at the appropriate places in the diagram). If the hypothetical relation between T, D, T_m and fog formation exists, there must

/be

be a surface (which can be represented by contours of T_m) separating the points of fig. 16 which correspond to foggy nights from those which correspond to clear nights. The T_m figures in fig. 16 corresponding to clear nights have been ringed and it will be seen that contours can, in fact, be drawn so that all ringed values of T_m are above the corresponding contour values and all unringed values below (with three or four exceptions in twenty-four cases). The 35°F contour to be expected on Taylor's theory (i.e. with radiation playing no direct part in cooling the air) is shown as a broken line; as might be expected, it has the same trend as the empirical contours, but is displaced upwards.

Fig. 16 thus appears to afford a fairly satisfactory way of forecasting fog at Cardington, provided the grass minimum temperature can be forecast to within a degree or two. This is, of course, a useful datum to take because it summarizes the effects of cloud, wind, stability and earth temperature, but the problem of predicting it is correspondingly hard.

5. General conclusions; future programme

5.1. Results of the investigation

The Cardington results have been discussed under three headings. Under the first it was shown that the results provided a fairly detailed general picture of events on a foggy night, which could readily be given a qualitative interpretation in terms of physical processes. The two most unexpected features of the general picture are the great variability of dew point (compared with that of temperature) at heights between, say, 300 and 3000 ft. and the form of the wind profiles, which almost always show a maximum speed in the layer 1 - 2000 ft. with lighter winds above, in the period before fog forms. It seems unlikely that much will be added to the general picture by continuing the present programme of observations at Cardington. Even the two unexpected features mentioned above could best be studied, in the first place, by observations at some other site, to make certain that they are not due to local peculiarities. It is suggested, then, that no further observations should be made for the sole purpose of gaining general information about fog. If the proposals made below for the study of specific points are carried out, it should be possible gradually to fill in the detail of the general picture.

Under the second heading, quantitative study of the results showed that they could give order-of-magnitude estimates of the physical quantities involved but were not accurate or detailed enough to test or suggest hypotheses about the relations between these quantities. General proposals for more elaborate experimental study of certain points were made in section 3.4 and they are set out more precisely below. These experiments would investigate individual processes which are thought to be important, and should give interesting results, but the experimental study of the conditions leading to the formation of fog could be planned much more effectively if it was guided by a general quantitative theory - however tentative - relating the various factors involved and suggesting what combinations of parameters should be observed. The work of Groen (1947) on night cooling might provide a good starting point for the development of this theoretical background; this work deals only with ground surface conditions and would have to be considerably extended if it was to include changes in the temperature and humidity of the air and so be relevant to fog problems.

Under the third heading, various empirical methods for fog forecasting were examined, using the Cardington data. None of the methods seemed very satisfactory, but it was clear that the data covered too few occasions to afford a reliable test and certainly too few to permit the incorporation of additional parameters into forecasting formulae in the hope of making them more accurate. The data required for this type of investigation are quite different from those required for the study of physical processes; there is no need for detailed data, since it is impracticable to include more than a very few parameters in a statistical treatment, but regularity and uniformity

/in

in the method of observing are prime requirements, and in order to obtain sufficient data in a reasonable time, it is desirable to have observations made at several different stations. The results of the small-scale tests of existing formulae suggest, however, that it might be well to make sure that the best use has been made of existing data (including radio-sonde data) before embarking on a further programme of observation.

5.2. Future programme

Various suggestions for future work have been made in the course of this report. It is obviously beyond the present resources of the Cardington station to carry them all out, and some selection will have to be made. Many of the items have the nature of fundamental rather than applied research and should presumably be considered in relation to the general programme of research in micrometeorology more than in relation to any programme for improving fog forecasts. Even in considering the items directly connected with fog, it must be remembered that they may not contribute very much to the accuracy of forecasting; the major sources of error in fog forecasts are in the forecasting of wind and cloud (see M.R.P. 664, 674 and 718) and will not be affected by the type of work under discussion.

The suggested lines of research are as follows:-

5.2.1. Theoretical work

Attempts should be made to set up equations describing the various processes at work on a radiation night and to produce approximate solutions in typical cases, the aim being to show the effects of interactions between different processes and to suggest important combinations of parameters to be observed. A subsection of this work would be the study of conditions controlling drop growth while a fog is forming, taking account of radiation effects, if necessary.

5.2.2. General study of behaviour of wind, temperature and humidity

5.2.2.1. Peculiarities of wind profiles. The tendency for wind speed to be a maximum at some fairly low height might be worth investigating further. This could best be done through wind and temperature observations at one or two other stations besides Cardington, which should show (a) whether the phenomenon is a local peculiarity and (b) whether it is connected with horizontal temperature gradients.

5.2.2.2. Erratic variations of humidity. It is desirable to make quite certain that the tendency for dew point to vary much more irregularly than temperature (at heights of, say, 300-3000 ft.) is not due to instrumental defects and, if it is not, to decide whether the variations are due to advection. This could be done by a careful study of the instruments and method of using them, at Cardington, and by making "Balthum" ascents at a small network of stations 20 - 50 miles apart.

5.2.2.3. Representativeness of data from one station. In any consideration of the use of data from a single station (particularly for "one dimensional" treatments of physical problems) it is important to know how far the data are typical of wide areas. Direct evidence on this, such as could be obtained from a set of stations at various distances apart, would be valuable.

5.2.3. Study of transfer of heat and water vapour (and momentum) near the ground

This is the central problem in any physical treatment of fog formation. It is obviously closely linked to existing studies (Kew, Cambridge) and is probably best regarded as an extension of them to very stable conditions and to greater heights. There is evidence that extension to heights much above

/100 ft.

100 ft. will be difficult because of advective effects (which may turn out to be serious at smaller heights too) and it is suggested that work should be confined to the lower layers, to start with. In this work it is more important to have complete and accurate data for a few periods of, say, half an hour, than to have data throughout the night on a large number of occasions, which has hitherto been the object of the Cardington programme. The processes needing study are radiation and convection - it can probably be assumed that heat conduction in the ground is well enough understood.

5.2.3.1. Radiation

There is a certain amount of experimental data and fairly convincing theoretical reasons to suggest that estimates of radiation from the usual charts may be seriously in error in typical fog-producing conditions, particularly where the direct cooling of the air by radiation is concerned. This could be investigated by making measurements of (a) total downward radiation at the ground surface and (b) change in net radiative flux between two or more levels.

5.2.3.2. Convection

The aim, in studying convection, is to find relations between the eddy transfer coefficients, K_H and K_W, and the wind and temperature structure and, in particular, to establish how far K_H is equal to K_W. This could probably be achieved by the method attempted in section 3.2 if more accurate data were available. The data required are (a) radiation measurements (as in 5.2.3.1), (b) measurements of heat flow from the earth, (c) measurements of dewfall, (d) measurements of wind, temperature and humidity profiles and rates of change. These data should be obtainable up to heights of 60 ft. with just sufficient accuracy from apparatus already at Cardington (except for (a)). Data could probably also be obtained at one higher level, by using the ballon borne apparatus at a fixed height (150 ft.?) but results obtained, as hitherto, by "spot" measurements at a series of heights are almost certainly not accurate enough for the type of work suggested.

The investigation would be greatly strengthened if, in addition to measurements (a) - (d), measurements could be made of wind drag on the surface and of detailed wind, temperature and humidity profiles in the lowest few feet. The apparatus at present used for such measurements (Cambridge) might need modification for use in nearly calm conditions.

5.2.4. Investigations of fog structure and mode of formation

There are several important problems connected with the properties and behaviour of a fog once it has formed, and study of these problems leads backwards to questions about the details of the way in which fogs form once the relative humidity has reached values near to 100 per cent. The experimental study of these problems requires the measurement of the sizes and other properties of fog droplets, for which no standard apparatus or techniques are available. The first step in the investigation of these problems must therefore be the development of apparatus.

5.2.4.1. Measurement of size, number and composition of fog droplets

Recent interest in the effects of fog, particularly town fog, on health has shown that a knowledge of the size distribution of droplets in typical fogs and, if possible, of their chemical composition, is important in deciding what steps can be taken to safeguard health. This knowledge does not exist, but it should be fairly simple to measure size distribution, once apparatus is developed and tested. These measurements seem likely to lead on to many other investigations into differences between town and country fog, the importance of condensation nuclei, factors affecting stability of fogs and so on, which cannot be clearly foreseen at present.

/5.2.4.2.

5.2.4.2. Variation of visibility with time and height in a fog, and its relation to drop size and number

There appears to be a tendency for visibility in a fog to fall rapidly as the fog forms, then to remain relatively steady, despite considerable fluctuations in temperature. Simultaneous measurements of drop size distribution, liquid water content and visibility should throw light on these changes and perhaps lead towards methods of predicting the value to which visibility will fall.

Variation of visibility with height is discussed in Appendix VI and a tentative explanation of the observations is put forward. This explanation could be tested by measurements of drop size distribution at various heights. If the explanation is correct, it should be possible to determine the height-variation of visibility from ground observations alone, which would be valuable in aircraft operations.

5.2.4.3. Final stages of fog formation

As pointed out in section 3.4 the detailed conditions required for fog formation are not known. Two factors that might be important are radiative cooling of droplets (nuclei) and the mixing of different parcels of air. The matter could be investigated by measuring (a) local variations of temperature, humidity and wind, (b) drop size and number just after fog formation, (c) drop temperature (by radiation measurements or by using fine thermocouples).

5.2.5. Empirical forecasting methods

5.2.5.1. Use of existing data

The rough tests of existing forecasting methods described in section 4.1 suggest that these methods do not make the best use of existing (radio-sonde) data. Adequate statistical tests of the methods should reveal the essential features of each and perhaps show how they could be combined to give an improved method.

5.2.5.2. Collection and use of new data

Although the Cardington results have contributed little to the development of forecasting formulae, it still seems likely that an adequate quantity of data on conditions in the lowest few thousand feet would enable additional parameters to be included in the formulae. These data will only accumulate slowly from a single station particularly if, like Cardington, it is preoccupied with other work, but could be obtained relatively quickly (in a few years) from a network of 4 - 6 stations making simple observations once daily (1800 hr.?).

APPENDIX I

by

R. H. Pedlow (Meteorological Office)

Site and Instruments

1. Site

The site, at 52° 7' N., 00° 25' W., is on level ground in the valley of the Great Ouse at an altitude of 85 ft. above sea level. To the south-east lies a low ridge running NE. - SW., the land rising a little over a mile from the site to nearly 300 ft. at a distance of 2 miles. From south-west to north-east through north, it is at least 5 miles before the land rises above 150 ft., but between NNW. and NNE. only 300 yd. away are two airship sheds 180 ft. high which considerably affect any flow of air from that quarter.

The semi-industrial town of Bedford lies three miles to the north-east, the nearest housing estate being only 1 mile from the site. In open country to the west and south-west there is a large number of brick kilns between 2 and 6 mi. distant.

The immediate surroundings of the site are mostly pasture land on clay soil. A stream runs from west to east in a drainage ditch 6 ft. deep by the north side of the enclosure. In addition to standard instruments with normal exposure, certain other instruments were mounted on two towers and on the cable of a kite-balloon.

2. Instruments

2.1. Standard Met. Office instruments

The following standard instruments were used:-

Dry-bulb, wet-bulb, maximum and minimum thermometers in a large screen.

Grass minimum thermometer.

2-in., 4-in. and 8-in. bent-stem earth thermometers exposed under close-cut grass, not under a bare earth surface.

5-in. raingauge and tilting-siphon rain recorder.

Cup contact anemometer on 20-ft. mast.

Assmann psychrometer.

Pressure-tube anemograph at effective height 135 ft. above ground but 200 ft. above the rain gauge on a 50-ft. rise 1100 yd. to the north-west.

Gold visibility meter with lamps at 800 and 280 yd.

2.2. Balloon-borne instruments

All balloon-borne instruments were fixed by clamps to the flying cable of a kite-balloon. Various balloons have been used but the most commonly used was an HZ-C balloon of 38,000 cu. ft. capacity, capable of lifting the instruments and cables to over 4,000 ft. in light winds. The instruments were fixed about 25 ft. below the belly of the balloon at which distance the airflow suffers little distortion. A 6-volt accumulator supplied current to lamps and to the aspirating motor of the psychrometer. For normal temperature-humidity-windspeed soundings the currents from the instruments to the ground were carried in a steel cable with insulated copper cores (the auxiliary cable) while the balloon was flown on a plain steel cable. When visibility measurements were also required, the balloon was flown on a similiar four-cored cable which was used for the transmission of anemometer

/contacts

contacts and of the high-voltage pulses used in remotely operating switches for the balloon-borne lamps, while the auxiliary cable was then used for thermo-electric and photo-electric currents.

The height of measurements was recorded as length of flying cable paid out; only in a calm is this the true height. When there is any wind the relation between true height and cable length is affected by many variables so that no simple working rule can be established. The ascent was brought to an end if it appeared that the discrepancy between nominal and true height was becoming excessive. Comparison with simple cases and measurement from sketches of the shape of the cable indicate that when this decision was reached the maximum error was probably about 10 per cent. For measurements within the strata of light winds on radiation nights the error was almost certainly less than 5 per cent.

2.2.1. Balloon-borne psychrometer

The balloon-borne psychrometer differed in two important particulars from that described by Swinbank (1946(1)), viz., it was not a quick-response instrument and consequently was not normally adapted for automatic recording. The thermocouples were made of 22 S.W.G. wire giving a 90 per cent response to sudden temperature change in about 3 minutes. As the e.m.f's generated were transmitted down the auxiliary instead of the flying cable, the copper-mercury contacts of Swinbank's circuit were avoided.

Calibration was carried out at intervals of several months with the junctions in water. The e.m.f. was about 0.08 mV per 1°F, and could be read to an accuracy of ±0.01 mV. Measurements taken on two occasions when the balloon was left stationary at fixed heights of 2000 and 500 ft. in radiation conditions indicated that despite the smoothing effect of the slow-response thermocouples, sampling errors were not negligible. Dry-bulb changes of the order of 1°F in 5 to 10 minutes were noted, and wet-bulb depressions were even more erratic in fairly dry air, one depression, averaging about 3.5°F, changing by 1.7°F in 5 minutes. There was nothing to indicate that this was due to faulty irrigation or aspiration of the wet-bulb and it is probable that sampling errors of 25 per cent in wet-bulb depressions are not uncommon, though further investigation is required.

2.2.2. Balloon-borne anemometer

The balloon-borne anemometer during the 1951-2 and 1952-3 seasons was a cup contact anemometer Mk. I with a stopping speed of about 2 kt. and an accuracy of ±1 kt. throughout its range. In the 1953-4 season this was most frequently replaced by a small sensitive cup anemometer made by Casella with a stopping speed of 1 ft./sec. and accuracy (limited by the reading period) of 0.2 ft./sec. In order to keep the duration of an ascent within reasonable limits windspeeds were read over one minute at each height. It was established that the probable error of a one-minute sample was less than 1 kt. The increase in windspeed due to the proximity of the balloon is of the order of 2 per cent.

2.2.3. Fog-density indicator

The fog-density indicator consists of 24 selenium photo-electric cells, each 2 sq. in. in area, connected in parallel and sandwiched between rectangular Perspex sheets with half the cells facing each way. In a rectangular space in the middle of the instrument three 6v. 12w. lamps are mounted in the same plane as the cells which are protected from the direct light of the lamps by a metal strip. When the lamps are lit in a turbid atmosphere, the light is reflected from suspended particles on to the cells and the resultant photoelectric current is a measure of the scattered light. The indicator can, of course, be used only in darkness. Calibration was carried out against the photo-electric visibility

/meter

meter described in para. 2.3.3 below, with both instruments at 55 ft. to avoid reflection from the ground to the indicator. A relationship:-

$$iV = 284$$

was found for the range 300 - 1200 yd., where i is the photo-electric current in microamps and V is the visibility in yards. As currents of the order of 0.5 microamp are caused in clear air by bright moonlight and at times (apparently) by stray loops of leads, the instrument is best regarded at present as an indicator of the presence of fog with visibility less than about 440 yd., though a cleaning up of the wiring may make possible the doubling of this distance.

2.2.4. Slant visibility

Measurements of slant visibility were made by walking away from the balloon to the extinction point of a 6v. 12w. (13 c.p.) lamp hanging below the other balloon-borne instruments.

2.3. Tower instruments

Variations in the vertical of temperature, humidity, windspeed and visibility were measured using two 55-ft. towers of tubular steel scaffolding built 160 yd. apart in a N.-S. line. The N. tower is about 5 ft. square at the base tapering to 3 ft. square at the top and has wooden platforms within the tower at about 17 and 51 ft. The S. tower has so far been used only as a support for lamps at 4 and 55 ft. (see para. 2.3.3 below).

2.3.1. Tower psychrometers

At 4, 20 and 55 ft. on the N. tower were aspirated wet- and dry-bulb thermocouples, each consisting of copper and constantan wires soldered to a cylindrical copper 'bulb' 1.0 in. long and 0.2 in. diameter, the bulb being fixed to the end of a hollow 3 in. rod of Tufnol supported in a half-inch-square air duct. Each pair of ducts (wet- and dry-bulb) was aspirated through a common orifice by a centrifugal air-pump driven by a 24 v. motor. The circuit was wired so that three such pairs of thermocouples plus a single junction in a vacuum flask of crushed ice and water provided measurements of all required temperatures, the effect of the electrically more remote thermocouples on the various galvanometers having been shown to be negligible. All the galvanometers recorded on the same sheet of bromide paper and time-marks were made automatically every 20 minutes. Calibration was carried out with the thermocouples in water and the galvanometers adjusted so that that which measured the temperature difference between the 4-ft. dry-bulb and ice had a deflexion of 0.5 cm/1°F, while those measuring the 4-ft. to 20-ft. and 20-ft. to 60-ft. dry-bulbs and all the dry- to wet-bulb differences gave deflexions of 1.0 cm/1°F. With this arrangement, temperature differences correct to 0.1°F should be measurable.

Accurate measurement, however, was made impossible by leakage from the aspirating motors and other 12- and 24-v. D.C. circuits on the tower into the thermocouple circuits, introducing errors of the order of 1°F which were aggravated in fog conditions. It has proved impossible to isolate the surface leaks and the trouble is now being obviated by the use of A.C. in all such circuits.

2.3.2. Tower anemometers

Three Casella sensitive anemometers, at 4, 20 and 55 ft., were used, each at the SW. corner of the N. tower, the two lower instruments being set out 3 ft. from the tower. Such small interference as the tower has on airflow thus affected the anemometers only when the wind came from the northerly quarter where it is already affected by the airship sheds. The

/recorder

recorder was essentially three recorders of the type described by Bibby (1944), with the impulse motors mounted one above the other, the three pens recording on one drum which was continuously driven by clockwork instead of being moved at intervals by another impulse motor. The pens were returned to zero at 20-min. intervals. The scale varied according to the anemometer in use between 6 and 8 ft./sec. per inch of trace. The stopping speed of the anemometers was 0.5 ft./sec., and the traces were read to the nearest 0.5 ft./sec., well within the accuracy of the instruments.

2.3.3. Photo-electric visibility meter

Photo-electric visibility meters were in use at 4 and 55 ft. The beam from a 24v. 250w. signal lamp in a parabolic reflector was directed over a 160-yd. range and the lamp image focussed by a 5 in. diameter lens of focal length 36 in. on to a selenium cell. Baffles within the tube of the instrument restricted the stray light which could reach the cell, and the field of view was so small that the meter could be used in full daylight except that the scatter of bright sunshine on dispersing fog caused fluctuations of photo-electric current so rapid that no useful measurements could then be made of the photographic trace from the galvanometers. The lamps were switched off for 40 seconds every 15 minutes, giving a measure of the deflexion due to daylight. A heater inside the meter lens prevented condensation from forming on the outer surface.

Since the brightness of a lamp varies with the third power of the applied voltage, the mains supply was transformed down, rectified and passed through a shunted galvanometer so that it could be monitored on the same bromide as the record from the meters, and the photo-electric current corrected accordingly.

Where

i_0 = galvo. deflexion for standard voltage and infinite visibility,
i = " " " " " " visibility V,
and d = distance between lamp and cell,

$$V \log_e (i_0/i) = 3.91 d.$$

The galvanometer was so arranged that i_0 was approximately 8 cm. The uncertainty in the measurement of the mains-monitor trace of about 1 per cent and in the measurement of the photoelectric deflexions of about 1 mm. combined to give an uncertainty of about ± 10 per cent at 1100 yd. visibility, ± 7 per cent between 900 and 400 yd., ± 5 per cent at 300 yd. and ± 11 per cent at 225 yd. During observations, whenever other work permitted, the 160-yd. lamp was switched off and replaced by a 230v. 300w. lamp at 30 yd. from the meter when the visibility fell below 250 yd., the galvanometer being simultaneously changed for one which maintained i_0 at about 8 cm. (This arrangement was only possible with the 4-ft. meter). The accuracy was still no better than ± 10 per cent above 170 yd., but was about ± 5 per cent for lower visibilities, down to about 30 yd.

Comparison of two cells working from the same lamp showed that small variations in the contacts at the cells introduced an uncertainty of about ±2 per cent into the value of i_0, which implies a further uncertainty of about ± 3 per cent in a visibility of 1100 yd., decreasing to ± 1 per cent at 250 yd. using the 160-yd. lamp, and about ± 3 or 4 per cent below 250 yd. using the 30-yd. lamp. Thus the total uncertainty was of the order of ± 150 yd. at 1100 yd. decreasing to ± 15 yd. at 250 yd.; or, using the 30-yd. lamp, ± 35 yd. at 250 yd. and ± 8 yd. at 100 yd. Considerably larger departures from eye observations occurred when the visibility was patchy and/or steeply stratified, and occasional gross errors arose when shifting contacts at either the cell or the lamp altered the value of i_0.

/2.3.4.

2.3.4. Wind direction recorder

A distant-reading wind-direction recorder was exposed at 56 ft. on the N. tower.

2.4. Earth thermocouples

Occasional readings were made with thermocouple earth thermometers with junctions at $\frac{1}{2}$, 1, 2, 4, 8 and 16 in. below ground level, visual measurements of temperature difference from a junction in ice being made by potentiometer at hourly intervals. Temperatures correct to 0.1°F could be read. The electrical insulation of the thermocouples from the ground presented difficulty and the failure of several types of insulation interrupted the readings.

2.5. Dew measurements

After preliminary experiment with a recording dew-balance and Duvdevani dew gauges, both of which were discarded as unreliable, dew measurements were made using the technique employed by Pasquill (1949) except that the evaporimeter pans and outer containers were, during the 1953-4 season, fitted with bottoms of thin sheet brass instead of Tufnol, so that the heat exchange with the ground beneath should more nearly resemble that in the surrounding soil. Originally six, but in the last season four, pans were weighed, at first irregularly but ultimately at hourly intervals, differences being measured to ± 0.05 gm.

There was the same sort of scatter between the differences shown by the various evaporimeter pans as experienced by Pasquill (loc. cit.) and Rider (1954). The standard error of the mean difference was found for fifty separate hourly periods covering four different occasions. The average value of these standard errors was equivalent to 0.010mm. dewfall, but this was aggravated by a few exceedingly high values (the highest 0.085 mm.). The median value was 0.006 mm., the interquartile range being 0.004 to 0.011 mm.

APPENDIX II

Accuracy required in estimates of radiation

If we try to predict the phenomena of cooling and fog formation on a clear night by calculation of the physical processes involved, radiation enters the calculation in two ways. In the first place it is an important factor determining the temperature of the ground surface - the boundary condition for heat flow in earth and air. In the second place, we have seen that direct radiative cooling of the air is at least as important as convective cooling in determining the air temperature.

The surface temperature is fixed by the condition that the net heat flux must be zero; if we assume that the conductive and convective fluxes and the downward flow of radiation are fixed, the surface temperature will adjust itself until the outward radiation (equal to the radiation from a black body at the temperature of the surface) has the value required to balance the heat budget. This outward radiation changes by about 0.5 mW/cm^2 for each degree centigrade, in the range of temperature we are concerned with, so that if we wish to determine the surface temperature to 1°C, we must know each flux component, including the downward flux of radiation from the atmosphere, to 0.5 mW/cm^2. We have seen (Table II) that the downward radiation is usually of the order of 25 mW/cm^2, so that it is required to estimate it to about 2 per cent (assuming that the standard of accuracy implied by 1°C error in surface temperature is reasonable - some evidence for this is provided by fig. 16, section 4.2).

Robinson (1947) has shown that results of the required order of accuracy can be obtained from radiation charts on many occasions, though the presence of "additional radiation" may sometimes cause larger errors, and his simple treatment of carbon dioxide may be inaccurate in conditions with large temperature gradients. It is not difficult, using the Kew chart, to replace the simple assumption that infinitely thin layers of CO_2 are "black" within their absorption band by a more realistic estimate of the variation of emissivity with path length, provided it is assumed that the absorption regions of CO_2 and water vapour do not overlap. This was done for the estimates of radiation on 27.9.53 (see Table II); downward radiation was found to be 0.3 mW/cm^2 greater with the more exact treatment of CO_2 than with the simple treatment. The effects of radiation from suspended particles may well be more serious, but are difficult to estimate exactly; a rough treatment can be given, as follows.

To estimate downward radiation, using the Kew chart, (see fig. 17) we plot the percentage (of black body) emissivity of the layer of atmosphere up to a given height against the black body radiation corresponding to the temperature at that height. The emissivity is assumed to be a function of the total amount of water in the layer (modified by a pressure correction) only. If the atmosphere contains smoke or mist particles, assumed to radiate as black bodies,* the emissivity will be modified, If the particles in a given layer are sufficient to obscure a fraction A of the sky, we may suppose that the emissivity of the layer is made up of two parts, a fraction A

/representing

* It is by no means certain that all aerosol particles are "black", or that a very small particle, even of black material, will radiate as a black body at wavelengths large compared with its own size. In the absence of any full theoretical discussion of these points or of relevant experimental evidence, this Appendix makes the simplest assumption, that all the particles radiate as perfect black bodies. The estimates obtained for the effects of radiation from particles thus represent an upper limit.

representing the black body radiation from the particles and a fraction $(1 - A)(E(u) + E(CO_2))$ representing radiation from water vapour in the parts not screened by particles ($E(u)$ being the emissivity of the water vapour, with path length in the layer considered and $E(CO_2)$ the emissivity of the carbon dioxide). The total emissivity of the layer is therefore $E(u) + E(CO_2) + A(1 - E(u) - E(CO_2))$. On the Kew chart $E(u) + (E(CO_2)$ is represented by the distance between the base-line and the plotted curve (assuming $E(CO_2)$ to have a constant value of 0.185, whatever the thickness of the layer in this rough treatment) and $(1 - E(u) - E(CO_2))$ by the distance from the curve to the top of the diagram. The modification produced by particle radiation is therefore to move each point on the curve towards the top of the diagram by the fraction A of its original distance from the top, the result being shown by the uppermost curve of fig. 17.

The fraction A can be estimated from the visibility. If the attenuation coefficient for visible light is β, then the "visibility" is approximately $4/\beta$ (Koschmieder's formula) and the fraction A is $1-\exp(-\beta z)$ for a layer of height z, assuming that β is independent of height. On 29.9.51 (fig. 1) the visibility at ground level was about 2500 yd. If we assume that the visibility was constant up to 500 ft. (the height of the inversion) and that the air above was clear, we get values of A increasing from 0.005 at 100 ft. to 0.22 at 500 ft. and remaining constant for greater heights. These values were used to produce the modified curve of fig. 17 and so to calculate the extra downward radiation to be expected from the smoke or mist particles that were restricting the visibility. The area between the two curves of fig. 17 corresponds to extra downward radiation of about 2 mW/cm^2 - a very significant amount. On an occasion such as 5.12.52, when visibility was less and water vapour concentration smaller, the particle radiation must have been still more important. If particle radiation is as important as these rough estimates suggest, it should be measurable by ordinary radiation instruments, in suitable conditions, and it seems desirable to make such measurements before trying to develop the theoretical treatment further.

Turning to the calculation of the rate of cooling of the air by direct radiation, it is clear from the figures of Table II that the radiative cooling term is very sensitive to errors in the calculation of radiative fluxes. The cooling is, in fact, measured by long thin areas on a radiation chart (as explained by Robinson, 1950) which are sensitive to errors in the chart co-ordinates (or in the actual plotting of points) and are difficult to measure accurately. Some of these difficulties can be avoided by using a "flux divergence chart" in which, effectively, the heights of the long thin areas on the ordinary radiation chart are plotted against their horizontal co-ordinate, to give better shaped areas to measure. However, the co-ordinates of such a chart (in the simplest case dE/du and σT^4, E being fractional emissivity of a layer with water path u and σT^4 the black body radiation at temperature T) depend on the rate of change of emissivity with thickness of air-layer instead of on the emissivity itself, as in the more usual charts, and since this rate of change is known much less accurately than the emissivity, a good deal of the apparent gain in precision is illusory. Nevertheless, the plotting of data on a flux divergence chart (fig. 18) does help to show more clearly some of the factors controlling radiative cooling. Fig. 18 represents conditions at 100 ft. height at 0100 hr. on 27.9.53. The area to the left of the central vertical line represents the net exchange of the layer at 100 ft. with the ground and the air up to 100 ft.; the area to the right represents the exchange with layers above 100 ft. The temperature gradient is positive upwards at 100 ft. so the left hand area of fig. 18 represents cooling, the right hand area heating, and the difference of the two areas represents the net cooling effect. Near the central line (representing the 100 ft. level in this case) the curves rise to very high values, corresponding to the large value of dE/du for short water paths; the curves are not well determined in this region because the temperature observations were not close enough and because the values of dE/du are uncertain. If there were any marked discontinuities in temperature gradient near 100 ft., areas near the central line in fig. 18 might contribute very large amounts to the area

/representing

representing net heating or cooling, but if we assume that short-range radiative exchange is such an efficient transfer mechanism that it smooths out such discontinuities, it is reasonable to assume that areas to the right and left of the central line cancel each other out in the immediate neighbourhood of the line, leaving only the areas below the (arbitrarily drawn) broken horizontal line to be taken into account.

Areas on fig. 18 actually represent the radiative heating or cooling of a layer containing unit mass (per unit area) of water vapour, but this can, of course, be expressed as the rate of change of temperature by radiation, knowing the water vapour content and specific heat of the air at the height in question. The result, from fig. 18, is that radiative exchange with the layers below 100 ft. produces a cooling of 2.4×10^{-4} °F/sec. and exchange with the layers above a heating of 0.8×10^{-4} °F/sec. giving a net cooling rate of 1.6×10^{-4} °F/sec. Fig. 18 suggests that a rough approximation to the radiative cooling at levels not far below the level of maximum temperature, in inversion conditions, could be obtained by multiplying the difference between air temperature and surface temperature by a function of the water path from the surface to the level in question; it is clear that the surface temperature is one of the most important factors determining the cooling rate.

Although the emissivity data for water vapour are inadequate to determine the vertical co-ordinate scale of charts such as fig. 18 at all precisely, the biggest source of error in radiative cooling estimates is probably the presence of radiation from suspended particles. Modification of fig. 18 to take account of this is possible but rather complicated and a simpler procedure will serve to show the importance of the effect.

We consider again the conditions at 0001 hr. on 29.9.51 (figs. 1 and 17), supposing that a hazy layer with visibility 2500 yd. extended up to 500 ft., and will calculate the cooling due to radiation from the particles in the layer from the ground to 100 ft. (which can be compared with the figures in Table II - particularly the cooling of 0.3 mW/cm^2 by radiation from water vapour and carbon dioxide). If visibility was 2500 yd. the attenuation coefficient (the projected area of scattering particles per unit volume) must have been of the order of 4/2500 yd. or 1/2000 ft. The particles in a 1 cm^2 column of the lowest 100 ft. therefore had a projected area of 1/20 cm^2 and emitted 1/20 of the black body radiation (per cm^2) appropriate to their temperature in each direction (1/20 upwards, 1/20 downwards). However, they also absorbed 1/20 of the upward flux of radiation and 1/20 of the downward flux. The mean temperature between 0 and 100 ft. was 8.5°C, the black body radiation appropriate to this temperature is 35.5 mW/cm^2, the upward flux was 34.0 mW/cm^2 and the downward flux 27.2 mW/cm^2 (from Table II). These fluxes were calculated neglecting the presence of the particles; we have already shown that the particles would increase the downward flux at the surface by about 2 mW/cm^2, and for this rough calculation we shall assume that this applies to the whole of the lowest 100 ft. and is the only correction that need be made. The net radiation from the particles in a 1 cm^2 column 100 ft. high is, therefore,

$$\frac{1}{20}\left(2 \times 35.5 - 34.0 - 27.2 - 2\right) \text{mW} \approx 0.4 \text{ mW}$$

which is actually greater than the net radiation from water vapour and carbon dioxide in the same layer. (We may note that a cooling of 0.4 mW/cm^2 in a 100 ft. layer corresponds to a rate of fall of temperature of about 0.6 °F/hr).

APPENDIX III

Heat flow from freezing ground

The purpose of this appendix is not to give exact solutions (for which reference may be made to Ingersoll, Zobell and Ingersoll, 1948) but to estimate orders of magnitude in typical cases. We investigate the quantity of heat flowing to the surface when the surface temperature is held at a fixed amount (ΔT) below the initial earth temperature (supposed uniform with depth) in two cases, first with the surface temperature above freezing point, secondly with the surface temperature below freezing point. In the first case the well-known solution for the heat flow, H, at time t is

$$H = \Delta T \left(\frac{K \rho C}{\pi t} \right)^{\frac{1}{2}}$$

where K, ρ , C are the thermal conductivity, density and specific heat, respectively for the soil. If we use the typical values ΔT = 5°C, K = 0.002 cal.cm^{-1}soc.$^{-1}$ °C^{-1}; ρ = 1.5 gm.cm^{-3}. C = 0.5 cal.°C^{-1}gm.$^{-1}$

we find $H = 7 \times 10^{-4}$ cal.cm^{-2}sec.$^{-1}$

$\equiv 2.9$ mW/cm^2

for t = 3 hr., agreeing roughly with the heat fluxes found in Tables I and II.

In the second case we simplify matters by assuming the earth to be just above freezing point initially. Then a sudden fall in temperature, ΔT , at the surface will freeze the earth from the surface downwards. We suppose that at time t freezing has penetrated to a depth f. Then the temperature gradient in the upper layers will be approximately $\Delta T/f$ and the heat flow $K.\Delta T/f$ (neglecting the heat lost by these layers in comparison with the heat flowing through them). This heat flow can be equated to the rate of release of latent heat as the freezing level falls;

$$H = K.\Delta T/f = w L \, df/dt$$

where w is the water content of the soil (gm./cm^3) and L the latent heat of fusion of ice. We thus obtain

$$f = \left(\frac{2K.\Delta T.t}{wL} \right)^{\frac{1}{2}}$$

$$H = \left(\frac{KwL.\Delta T}{2t} \right)^{\frac{1}{2}}$$

Taking K = 0.002, ΔT = 5, t = 3 hr. as before, with w = 0.5 gm./cm^3 and L = 80 cal./gm. we find

$f = 2.2$ cm

$\frac{df}{dt} = 1.1 \times 10^{-4}$ cm /sec. (approximately 1 cm./3 hr.)

$H = 45.5 \times 10^{-4}$ cal.cm $^{-2}$ sec.$^{-1}$

$\equiv 19$ mW/cm^2

In our hypothetical conditions, therefore, the heat flow is some six times greater in the freezing than in the non-freezing case, for a given fall in

/surface

surface temperature. In practice, of course, the greater heat flow serves to increase the surface temperature, so that a state of balance is reached on freezing nights, other things being equal, with a smaller earth-air temperature difference than on non-freezing nights.

We may note that, in the conditions considered, the rate of loss of heat from the earth above the freezing level (2.2 cm. at t = 3 hr.) is about 0.8 mW/cm^2 so that its neglect in comparison with the flow of 19 mW/cm^2 was justified for a first approximation. If the earth is initially above freezing point, the above treatment will still be roughly correct, if ΔT is taken to be the amount by which the surface temperature falls below freezing point; there will be an extra contribution to the heat reaching the surface, from the layers below the freezing level, but this will be comparable to the heat flow in the "non-freezing" case and will be small compared with the latent heat contribution unless ΔT is very small.

APPENDIX IV

Effect of convection on relative humidity

The equation for the rate of change of temperature at any level by convection is

$$\frac{d\theta}{dt} = K_H \frac{\partial^2\theta}{\partial h^2} + \frac{\partial K_H}{\partial h}\frac{\partial\theta}{\partial h} \qquad (1)$$

where θ is potential temperature, t time, h height and K_H the eddy diffusion coefficient for heat. A similar equation governs the rate of change of specific humidity

$$\frac{dw}{dt} = K_w \frac{\partial^2 w}{\partial h^2} + \frac{\partial K_w}{\partial h}\frac{\partial w}{\partial h} \qquad (2)$$

where w is the specific humidity (mass of water vapour per unit mass of air) and K_W the eddy diffusion coefficient for water vapour. On a radiation night, convection leads to a fall in temperature and a fall in water content near the ground. There seems little prospect of predicting these falls with any accuracy from (1) and (2) because in most cases the terms on the right of the equations are nearly equal and of opposite sign, so that very accurate knowledge of the K's and their variation with height would be required to find the left-hand terms precisely. Thus, in a typical case from Table II (27.9.53) we have, at 100 ft.,

$$\frac{d\theta}{dt} = -1\times10^{-4} \ ^\circ\text{C sec}^{-1}$$

$$K_H\frac{\partial^2\theta}{\partial h^2} = -8\times10^{-4} \ ^\circ\text{C sec}^{-1}$$

$$\frac{\partial K_H}{\partial h}\frac{\partial\theta}{\partial h} = 7\times10^{-4} \ ^\circ\text{C sec}^{-1}$$

However, in the problem of fog formation we are not primarily interested in the temperature or the water content separately; the quantity of interest is the nearness to saturation, conveniently expressed by the difference between the saturation and actual specific humidities and written $\Delta\ (=w_s - w)$. It is reasonable to hope that $d\Delta/dt$ may be expressible in a form which depends less critically on the exact values of the K's, provided there is some simple relation between K_H and K_W. We assume the simplest relation $K_H = K_W$ (= K, say) and try to find an expression for $d\Delta/dt$. We have

$$\frac{d\Delta}{dt} = \frac{dw_s}{dt} - \frac{dw}{dt}$$

$$= \left(\frac{\partial w_s}{\partial\theta}\right)_h \frac{\partial\theta}{\partial t} - \frac{dw}{dt}$$

$$= \left(\frac{\partial w_s}{\partial\theta}\right)_h \left(K\frac{\partial^2\theta}{\partial h^2} + \frac{\partial K}{\partial h}\frac{\partial\theta}{\partial h}\right) - \left(K\frac{\partial^2 w}{\partial h^2} + \frac{\partial K}{\partial h}\frac{\partial w}{\partial h}\right)$$

which can be rearranged by using the relations

$$\frac{\partial w_s}{\partial h} = \left(\frac{\partial w_s}{\partial h}\right)_\theta + \left(\frac{\partial w_s}{\partial \theta}\right)_h \frac{\partial \theta}{\partial h}$$

$$\frac{\partial^2 w_s}{\partial h^2} = \left(\frac{\partial^2 w_s}{\partial h^2}\right)_\theta + \left(\frac{\partial^2 w_s}{\partial \theta^2}\right)_h \left(\frac{\partial \theta}{\partial h}\right)^2 + \left(\frac{\partial w_s}{\partial \theta}\right)_h \frac{\partial^2 \theta}{\partial h^2} + 2\frac{\partial^2 w_s}{\partial \theta \partial h} \cdot \frac{\partial \theta}{\partial h}$$

to give

$$\frac{d\Delta}{dt} = K\frac{\partial^2 \Delta}{\partial h^2} + \frac{\partial K}{\partial h}\frac{\partial \Delta}{\partial h} - K\left(\frac{\partial^2 w_s}{\partial h^2}\right)_\theta - \frac{\partial K}{\partial h}\left(\frac{\partial w_s}{\partial h}\right)_\theta$$

$$- K\frac{\partial \theta}{\partial h}\left[\left(\frac{\partial^2 w_s}{\partial \theta^2}\right)_h \frac{\partial \theta}{\partial h} + 2\frac{\partial^2 w_s}{\partial \theta \partial h}\right] \qquad (3)$$

which expresses the rate of change of Δ by an ordinary diffusion equation, modified by correcting terms for the variation of saturation specific humidity with height (at constant temperature) and for the curvature of the relation between saturation specific humidity and temperature. If it turns out that the individual terms of (3) are not large compared with their algebraic sum, then (3) will give a more accurate value of Δ than would be obtained by using (1) and (2) separately.

In particular we may be able, without introducing too much error, to eliminate $\partial K/\partial h$ from (3) by using the approximate relation

$$\frac{\partial \theta}{\partial h}\frac{\partial K}{\partial h} = -K\frac{\partial^2 \theta}{\partial h^2} \qquad (4)$$

Using this relation, (3) becomes

$$\frac{d\Delta}{dt} = K\left[\frac{\partial^2 \Delta}{\partial h^2} - \frac{\partial^2 \theta/\partial h^2}{\partial \theta/\partial h}\frac{\partial \Delta}{\partial h}\right]$$

$$- K\left[\left(\frac{\partial^2 w_s}{\partial h^2}\right)_\theta - \frac{\partial^2 \theta/\partial h^2}{\partial \theta/\partial h}\left(\frac{\partial w_s}{\partial h}\right)_\theta\right]$$

$$- \frac{\partial \theta}{\partial h} K\left[\left(\frac{\partial^2 w_s}{\partial \theta^2}\right)_h \frac{\partial \theta}{\partial h} + 2\frac{\partial^2 w_s}{\partial \theta . \partial h}\right] \qquad (5)$$

Equation (5) can be used to find $d\Delta/dt$ provided we know K and have sufficiently accurate profiles of temperature and humidity. Although

/the

the Cardington data are far from accurate enough it is interesting to use them in (5) to illustrate the magnitude of the various terms.

From fig. 2 and Table II we obtain, for 0100 hr. on 27.9.53 at 100 ft.,

$$K = 3800 \text{ cm}^2 \text{ sec}^{-1}, \quad \partial\theta/\partial h = 5.2 \times 10^{-4} \text{ °C cm}^{-1},$$
$$\partial^2\theta/\partial h^2 = -1.9 \times 10^{-7} \text{ °C. cm}^{-2}, \quad \partial\Delta/\partial h = 9.1 \times 10^{-8} \text{ cm}^{-1},$$
$$\partial^2\Delta/\partial h^2 = -9.0 \times 10^{-12} \text{ cm}^{-2}$$

(The variation of Δ with h given by the balloon ascents is very irregular, and drastically smoothed curves have been used to obtain the above values). The values of the constants in eq. (5) are as follows (at 10°C):

$$\left(\frac{\partial^2 w_s}{\partial h^2}\right)_\theta = +2.1 \times 10^{-13} \text{ cm}^{-2}; \quad \left(\frac{\partial w_s}{\partial h}\right)_\theta = -3.8 \times 10^{-8} \text{ cm}^{-1};$$

$$\left(\frac{\partial^2 w_s}{\partial \theta^2}\right)_h = +3.2 \times 10^{-5} \text{ °C}^{-2}; \quad \frac{\partial^2 w_s}{\partial\theta.\partial h} = -2.3 \times 10^{-9} \text{ cm}^{-1} \text{ °C}^{-1}.$$

Putting these values in eq. 5 we obtain

$$\frac{10^{12}}{3800}\cdot\frac{d\Delta}{dt} = \left.\begin{array}{rrr} -9.0 & + & 33.2 \\ -0.21 & + & 13.9 \\ -8.7 & + & 2.4 \end{array}\right\} \text{ the terms are arranged in the same order as in eq. (5).}$$

$$= 31.6 \text{ cm}^{-2}$$

$$\frac{d\Delta}{dt} = 1.2 \times 10^{-7} \text{ sec.}^{-1}$$

$$\equiv 1.2 \text{ gm./Kg. in } 10^4 \text{ seconds.}$$

We notice that the second term is numerically a good deal greater than the first and the fourth considerably greater than the third, so that the effects of the approximation made by using (4) will not be too serious. However, the final result does not agree at all well with the observations; the actual value of $d\Delta/dt$ should be the sum of the part due to convection, which we have just calculated, and a part due to radiative cooling (if the air is cooled by radiation the saturation specific humidity, w_s, will fall and Δ will therefore decrease), but the values in the case we are considering were

Convection contribution to $d\Delta/dt$	=	1.2×10^{-7} sec.$^{-1}$
Radiation " " $d\Delta/dt$	=	-0.3×10^{-7} sec.$^{-1}$
Observed value of $d\Delta/dt$	=	-0.2×10^{-7} sec.$^{-1}$

Equation (5) thus appears to overestimate the effects of convection very considerably, but the possible errors in the quantities we have had to use are so large that they could easily account for the discrepancy, and we must conclude that it is impossible to test the validity of (5) without much more accurate observations. The chief sources of error are in the estimates of radiation, which we have already discussed, and in the profiles of humidity.

/In

In order to test (5) to an accuracy of the order of 20 per cent we should require radiation measurements or estimates to about 0.1 mW/cm^2 and smooth humidity profiles defined to about 0.2°F in dew point - if the humidity profiles turn out to be irregular even at small heights and when averaged over reasonable periods, it is clear that there will be little possibility of dealing with humidity changes in the way attempted here.

Just before fog forms, the air is often very close to saturation for some distance above the ground, and it is interesting to apply eq. (5) to the ideal case with $\Delta = 0$. If $d\Delta/dt$ is found to be negative it would indicate the onset of supersaturation, and we should expect fog to form; if it is positive the air would be becoming drier (unless radiation counteracted this effect) and no fog should form. From (5) we see that with $\Delta = 0$ the limiting case $d\Delta/dt = 0$ occurs when

$$\frac{\partial^2\theta/\partial h^2}{\partial\theta/\partial h}\left(\frac{\partial w_s}{\partial h}\right)_\theta = \left(\frac{\partial^2 w_s}{\partial h^2}\right)_\theta + \left(\frac{\partial^2 w_s}{\partial\theta^2}\right)_h \left(\frac{\partial\theta}{\partial h}\right)^2 + 2\,\frac{\partial^2 w_s}{\partial\theta\,\partial h}\,\frac{\partial\theta}{\partial h} \qquad (6)$$

independently of K. Putting in the values of constants used before, (6) becomes

$$-3{\cdot}8\times10^{-8}\,\frac{\partial^2\theta}{\partial h^2} = 3{\cdot}2\times10^{-5}\left(\frac{\partial\theta}{\partial h}\right)^3 - 4{\cdot}6\times10^{-9}\left(\frac{\partial\theta}{\partial h}\right)^2 + 2{\cdot}1\times10^{-13}\left(\frac{\partial\theta}{\partial h}\right) \qquad (7)$$

If, as an illustration, we put $\partial^2\theta/\partial h^2 = -1{\cdot}9\times10^{-7}$ °C.cm^{-2} (as at 0100 on 27.9.53) we can solve (7) approximately for $\partial\theta/\partial h$ and find

$$\partial\theta/\partial h \simeq 0{\cdot}7\times10^{-3}\ ^\circ\text{C.cm}^{-1}$$

This implies that, with the postulated value of $\partial^2\theta/\partial h^2$ and at a temperature of about 50°F, the relative humidity of an already practically saturated atmosphere should increase if there is an inversion steeper than 0.7 x 10^{-3} °C/cm., or about 4°F/100 ft., and decrease if the inversion is less steep, unless radiation or other effects outweigh the convection process.

APPENDIX V

Effects of radiation on growth of fog droplets

It is well known (eg. Best, 1954) that the size of a droplet of salt solution varies in a characteristic way with the relative humidity of the surrounding air. As the humidity is increased the equilibrium size of droplet increases, slowly at first then more rapidly until, for some value of relative humidity in excess of 100 per cent, the size will increase without limit, if the humidity is held constant. It is tempting to identify this phase of unlimited growth with the rather sudden transition which we have seen often occurs from mists with visibilities of the order of a mile to fogs with visibility of the order of 100 yd. It must be borne in mind, however, that the theoretical unlimited growth can only occur if the relative humidity of the atmosphere remains constant, and that the growth of a cloud of drops will tend to reduce the relative humidity both by removing water vapour and by raising the temperature, through the release of latent heat. We find, in fact, that if we replace the condition of a fixed relative humidity by the more realistic one of a fixed temperature and take reasonable values for the size and concentration of droplet nuclei, there is no stage where unlimited growth is possible. As the temperature is lowered the drops will grow, but the total amount of water condensed is always fixed by the temperature, being, to a close approximation, equal to the difference between the original vapour density ($gm./m^3$) and the saturation vapour density at the temperature reached.

It seems possible to account for the sudden growth of droplets by allowing for the effects of radiation. As we saw in Appendix II, a particle 100 ft. above the ground on a typical radiation night would lose heat by radiation at a rate of the order of 8 mW/cm^2 of its area projected on a horizontal plane. As a consequence the particle will be at a slightly lower temperature than its surroundings, so that the loss of heat by radiation is compensated by heat conducted from the surrounding air. In the case of a droplet, its lower temperature will mean that it will be in equilibrium with air of a slightly lower humidity than a droplet of the same size not subject to radiative cooling. This effect is quite small, as is shown by Table V, calculated for a droplet formed on a sodium chloride nucleus of mass 6×10^{-14} gm.

Table V

Equilibrium radius of droplet (microns)	1.0	1.2	1.5	1.9	2.5	3.1
Relative humidity, without cooling per cent	99.99	100.04	100.04	100.05	100.04	100.04
Relative humidity, with cooling at 8 mW/cm^2 per cent	99.98	100.02	100.03	100.03	100.01	100.01

Table V suggests that radiative cooling will have little direct effect on the early stages of drop growth. When the critical size (corresponding to the underlined values of R.H. in Table V) is reached, radiation effects become important. Condensation will occur freely so long as the relative humidity remains at or above the values in the table (i.e. for most practical purposes at 100 per cent), but, as already pointed out, condensation tends to lower the relative humidity. When the drops are radiating, the rate of condensation can be found by equating the loss of heat by radiation to the sum of the latent heat of condensation and the heat that must be removed from the air (via the drop) to keep it saturated in spite of the loss of water vapour. For a drop of radius r we can write the radiative loss of heat as $\pi r^2 R$,

/the

the latent heat of condensation as $4\pi r^2 L\, dr/dt$ and the heat to be extracted from the air in order to maintain saturation as

$$\frac{4\pi r^2 dr/dt}{dw/dT}\,\rho c_p$$

where dw/dT is the rate of change of saturation vapour density with temperature and ρc_p the thermal capacity of unit volume of air. Equating these quantities, we obtain

$$\frac{dr}{dt} = \frac{R}{4(L + \rho c_p/(dw/dT))}$$

With R = 8 mW cm^{-2}, L= 600 cal.cm^{-3}, ρ = 1/800 gm.cm^{-3}, C_p = 0.24 cal. $gm.^{-1}$ $^oC^{-1}$ and $dw/dT = 0.5 \times 10^{-6}$ gm.cm^{-3} $^oC^{-1}$. We find

$$dr/dt \simeq 0.4 \times 10^{-7} \text{ cm./sec.}$$

i.e. a rate of growth of 1 micron in about 4 minutes. The visibility in fog is roughly inversely proportional to the square of the drop radius, so that once the radius has reached the critical value of about 1.5μ a ten-fold fall in visibility (i.e. drop growth to about 5 μ) should occur in 14 minutes, in the postulated conditions. The radiative cooling mechanism thus seems quite capable of explaining the sudden increase in density of fogs so often observed.

The only obvious limit to the growth of fog drops by this method is set by the cutting off of radiation by the drops themselves. Presumably the fog should appear throughout the layer in which the relative humidity is high enough. As soon as the fog is dense enough to obscure the sky from the ground and the drops near it, the ground surface temperature will rise and the loss of heat by radiation from the drops near the ground will become very small. The final value of visibility reached near the ground will probably depend on a balance between the rate of growth of the individual drops and the rate of growth upwards of the fog as a whole. These rates depend on the size of the drop nuclei and on the temperature and humidity structure of the lower layers, respectively, so that the problem of predicting visibility is likely to be complicated.

APPENDIX VI

Variation of visibility with height

The observations plotted in fig. 11 suggest that fog is commonly thicker above the ground than at ground level. This appendix suggests a possible interpretation.

The upper surface of a well-established fog loses heat by radiation in much the same way as the ground surface on a clear night. This cooling will tend to make fog convectively unstable and thus set up convection currents conveying heat upwards. This is confirmed by the Cardington observations (figs. 3 and 4) which usually show a lapse rate close to the saturated adiabatic, in a deep fog. Within a fog, then, we must imagine that there are individual parcels of air ascending and descending, with condensation occurring in the ascending parcels and evaporation in the descending ones. It is reasonable to suppose that this condensation occurs on drops already in existence, so that the number of drops per unit volume should be much the same throughout the depth of the fog, but their size should be greater near the top, and the visibility should be less there than at ground level. If we make the further simplifying assumption that all the drops are of the same size at any given height, we can calculate the change in size with height and estimate the effect on fog density.

For a fixed number of drops per unit volume the visibility, V, is approximately inversely proportional to their cross-sectional area, i.e. to $m^{-2/3}$, where m is the mass of liquid water per unit volume of air, so that if V_o and m_o are the visibility and liquid water content at ground level and δm is the extra water condensed by adiabatic ascent to a height h, the visibility at h, V_h, is given by

$$V_h = V_o \left(\frac{m_o}{m_o + \delta m} \right)^{2/3}$$

$$= V_o \left(\frac{m_o}{m_o + \Gamma_w h \, dw/dT} \right)^{2/3}$$

since $\delta m = \Gamma_w h \, dw/dT$ where Γ_w is the saturated adiabatic lapse rate and dw/dT the rate of change of vapour density with temperature. Table VI shows values of V_h/V_o calculated from this formula for various values of h and m_o assuming $\Gamma_w = 0.004^\circ F/ft.$ and $dw/dT = 0.2$ gm./m^3/$^\circ F$ (the value appropriate to $40^\circ F$).

Table VI

V_h/V_o

H (ft.) \ m_o	0.1	0.2	0.5	1.0 g./m^3
0	1.00	1.00	1.00	1.00
100	0.68	0.80	0.91	0.95
200	0.53	0.68	0.83	0.93
500	0.35	0.47	0.68	0.80
1000	0.23	0.37	0.53	0.68

According to the table, visibility should decrease with increasing height, rapidly near the ground, more slowly higher up; the decrease is least marked when the water content is high, i.e. broadly speaking, when the fog is thick. This behaviour accords quite well, qualitatively and as to order of magnitude, with the observations of slant visibility plotted in fig. 11. It is impossible to make a quantitative comparison, because no measurements of liquid water content (m_o) were made.

REFERENCES

Best, A. C.	1953 1954	Tellus, 5, 32 Quart. J.R. Met.Soc., 80, 89
Bibby, J. R.	1944	Quart. J.R. Met.Soc., 70, 277
Briggs, J.	1950	Met. Mag., 79, 243
Craddock, J. M. and Pritchard, D.	1951	M.R.P. 624
Emmons, G. and Montgomery, R. B.	1947	J. Met., 4, 206
Groen, P.	1947	J. Met., 4, 63
Ingersoll, Zobell and Ingersoll	1948	"Heat Conduction". McGraw-Hill
Jennings, E. G. and Monteith, J. L.	1954	Quart. J.R. Met.Soc., 80, 222
Pasquill, F.	1949	Proc.Roy.Soc., A.198, 116
Pedlow, R. H.	1952	M.R.P. 742
Rider, N. E.	1954	Phil.Trans., A.246, 481
Robinson, G. D.	1947 1950	Quart. J.R. Met.Soc., 73, 127 Quart. J.R. Met.Soc., 76, 37
Saunders, W.E.	1949 1950 1954	Quart. J.R. Met.Soc., 75, 154 Met. Mag., 79, 213 Met. Mag., 83
Swinbank, W.C.	1946(1) 1946(2) 1949	M.R.P. 270 M.R.P. 307 Prof. Notes, 6, No. 100
Taylor, G. I.	1917	Quart. J.R. Met.Soc., 43, 241

/TABLE II

TABLE II

Analysis of heat flow on selected occasions Units for columns (1) - (9) are milliwatts per square centimetre

Date and time	Height (ft.)	(1) Flux of radiation Up	(2) Flux of radiation Down	(3) Net (Up)	(4) Radiative cooling of layer	(5) Observed cooling of layer	(6) Convective cooling of layer	(7) Convective flux (down)	(8) Latent heat of dew	(9) Flux of heat from earth	(10) Gradient of potl. temp. (°C /Km.)	(11) Eddy diffusivity (cm^2/sec.)	(12) Ri	(13) K_{RM} (cm^2/sec.)
27. 9.53	3000	35.7	26.2	9.5				0			5.5	0		
					2.3	2.7	0.4							
0100 hr.	1000	35.9	28.7	7.2				0.4			8.0	4,000		
					1.7	3.4	1.7							
	250	34.5	29.0	5.5				2.1			40.8	4,100		
					0.4	0.9	0.5							
	100	33.8	28.7	5.1				2.6			51.8	3,800		
					0.2	0.6	0.4							
	0	32.7	27.8	4.9				3.0	0.4	3.9	122+	1,900+	3.6+	370+
5.12.52	2250	30.4	21.6	8.8				0.9			1.1	66,000		
					1.2	0.3	-0.9							
0001 hr.	1000	30.5	22.9	7.6				0			3.6	0		
					0.5	0.6	0.1							
	500	30.3	23.2	7.1				0.1			17.9	450		
					0.2	0.9	0.7							
	100	29.5	22.6	6.9				0.8			67	930		
					0.2	0.2	0.0							
	30	29.2	22.5	6.7				0.8			69	920	0.24	13,000
					0.2	0.1	-0.1							
	0	28.9	22.4	6.5				0.7	0.4*	1.0				
28. 9.51	3000	35.0	25.0	10.0				0.5			3.5	11,000		
					0.7	0.2	-0.5							
0001 hr.	2000	35.5	26.2	9.3				0			2.6	0		
					2.3	4.4	2.1							
	100	34.4	27.4	7.0				2.1			51	3,300		
					0.3	0.6	0.3							
	0	33.6	26.9	6.7				2.4	0.7*	5.0	55+	3,000+	0.50+	4,500
31.10.53	3000	32.5	21.9	10.6				5.3			1.8	233,000		
					2.2	-0.4	-2.6							
0001 hr.	1000	33.3	24.9	8.4				2.7			6.2	35,000		
					2.0	1.4	-0.6							
	0	31.0	24.6	6.4				2.1	0.7	3.6	60+	2,800+	0.20+	14,000+

*Estimated from eye observations of dew +Values for 50 ft. level

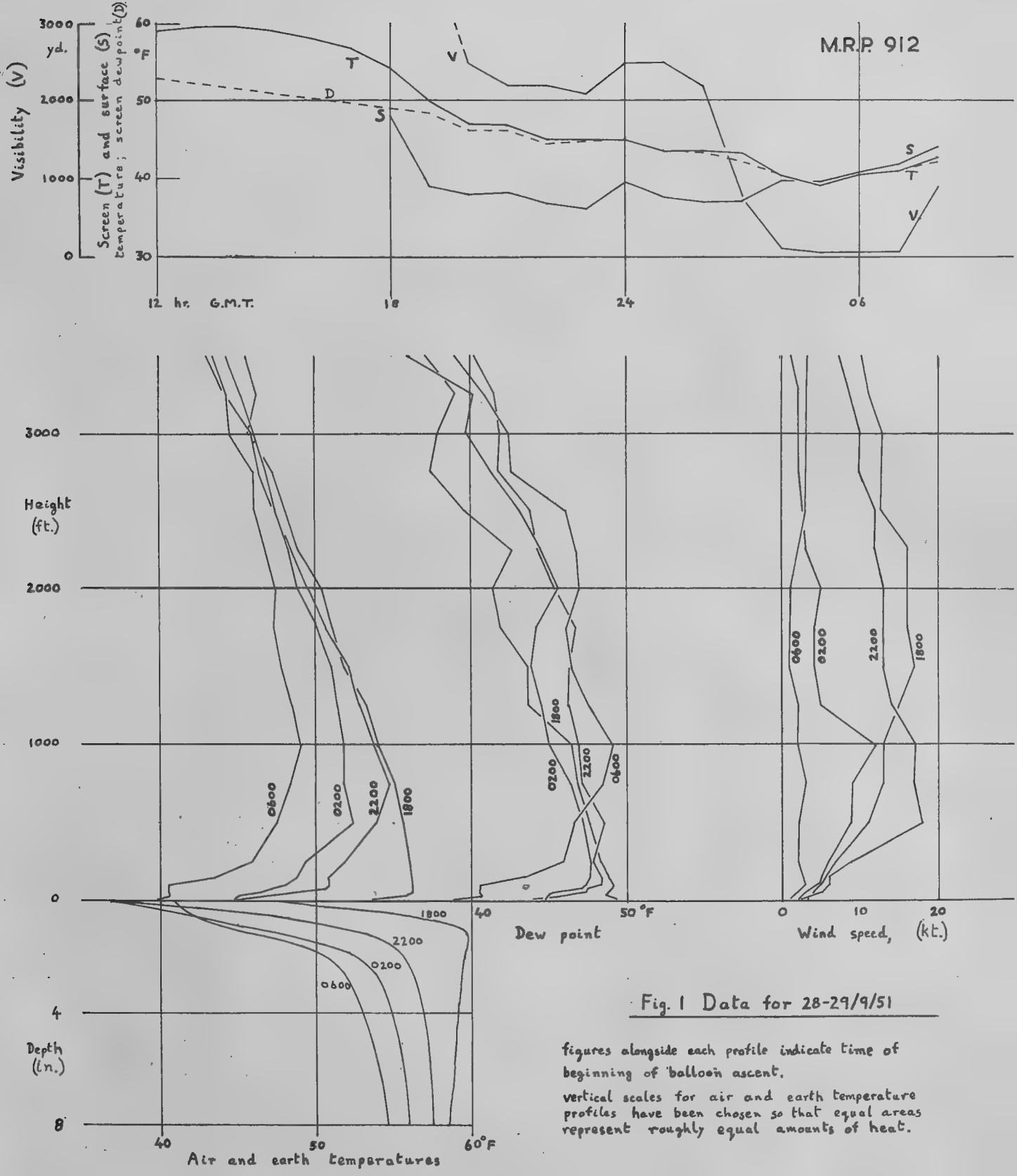

Fig. 1 Data for 28-29/9/51

figures alongside each profile indicate time of beginning of balloon ascent.

vertical scales for air and earth temperature profiles have been chosen so that equal areas represent roughly equal amounts of heat.

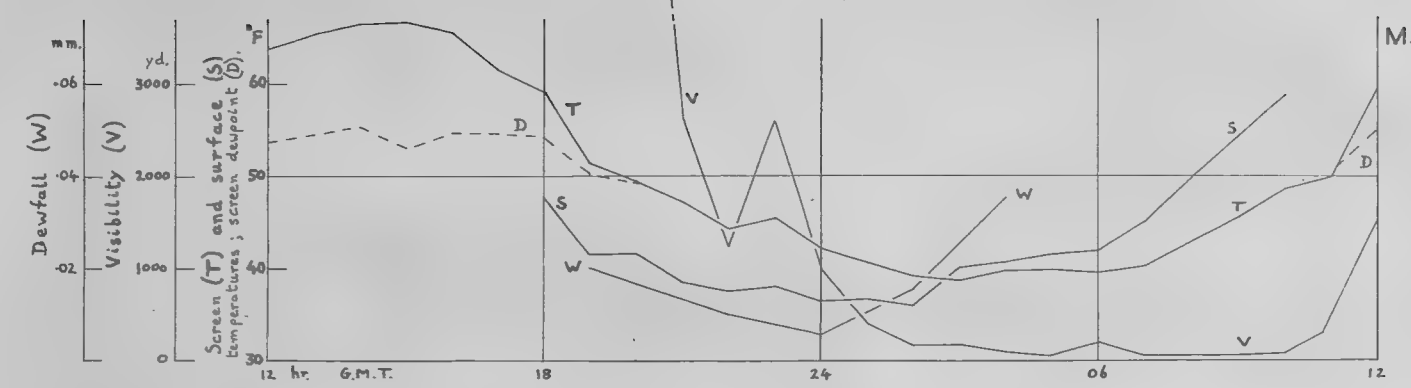

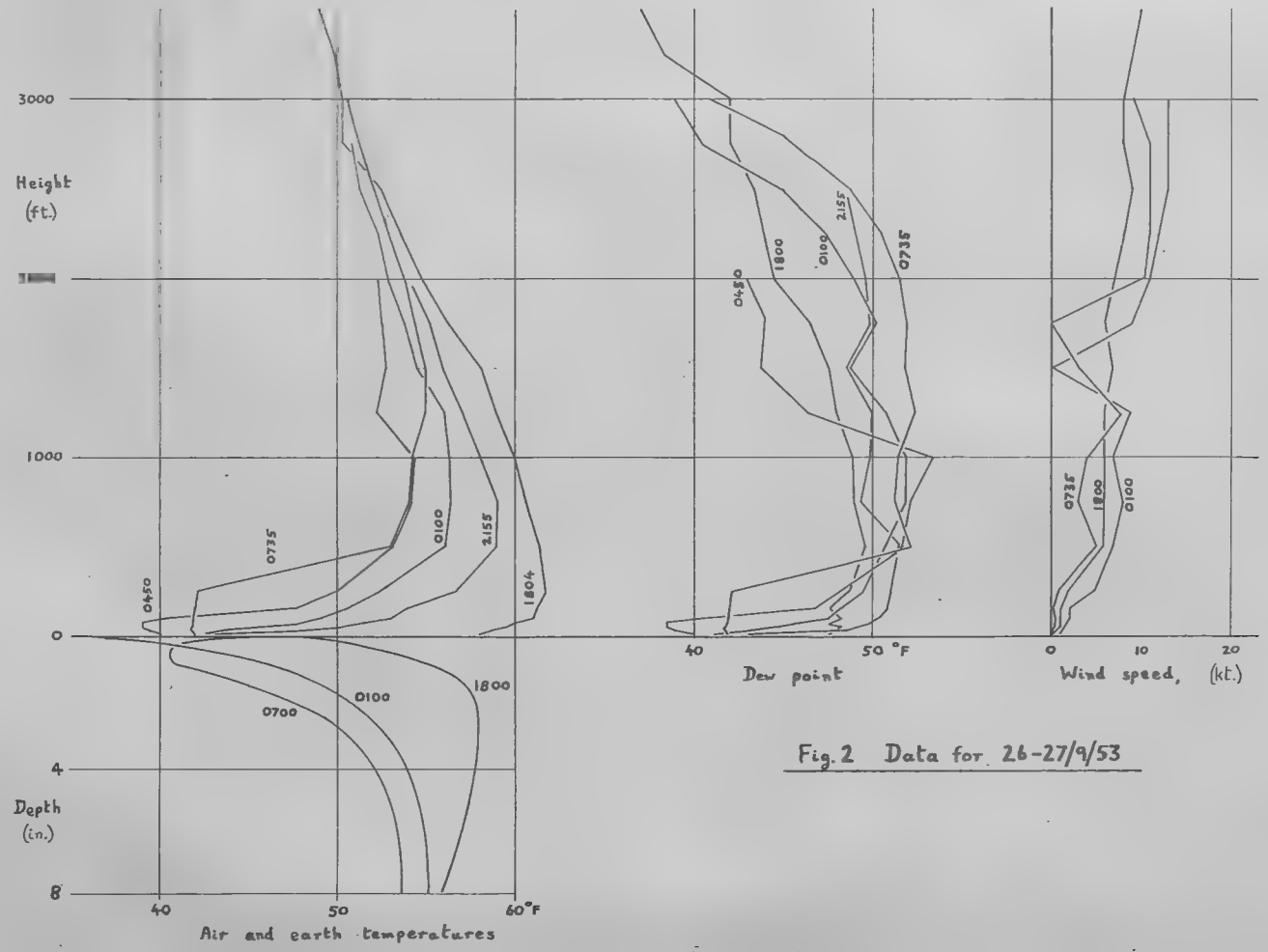

Fig. 2 Data for 26-27/9/53

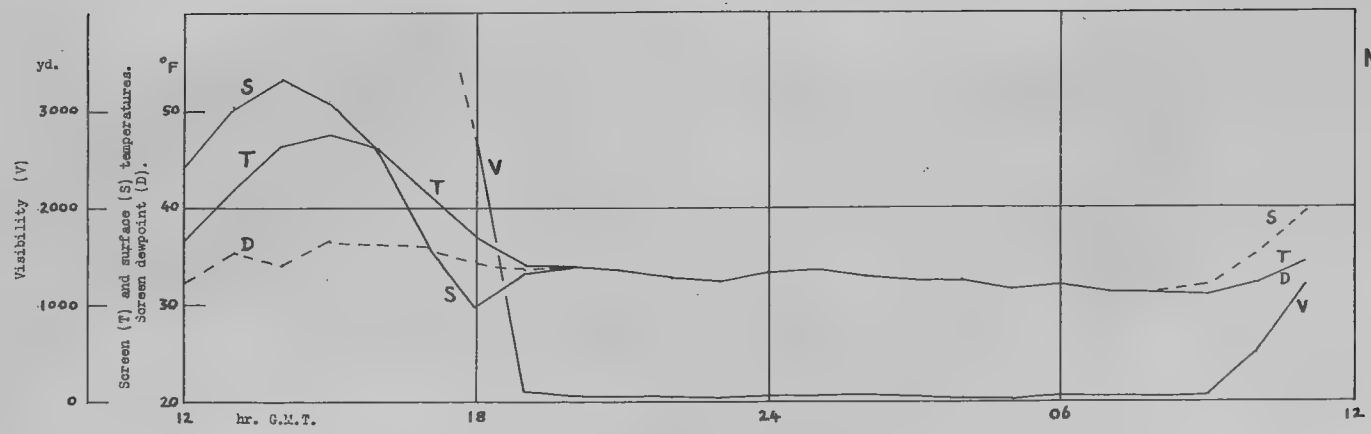

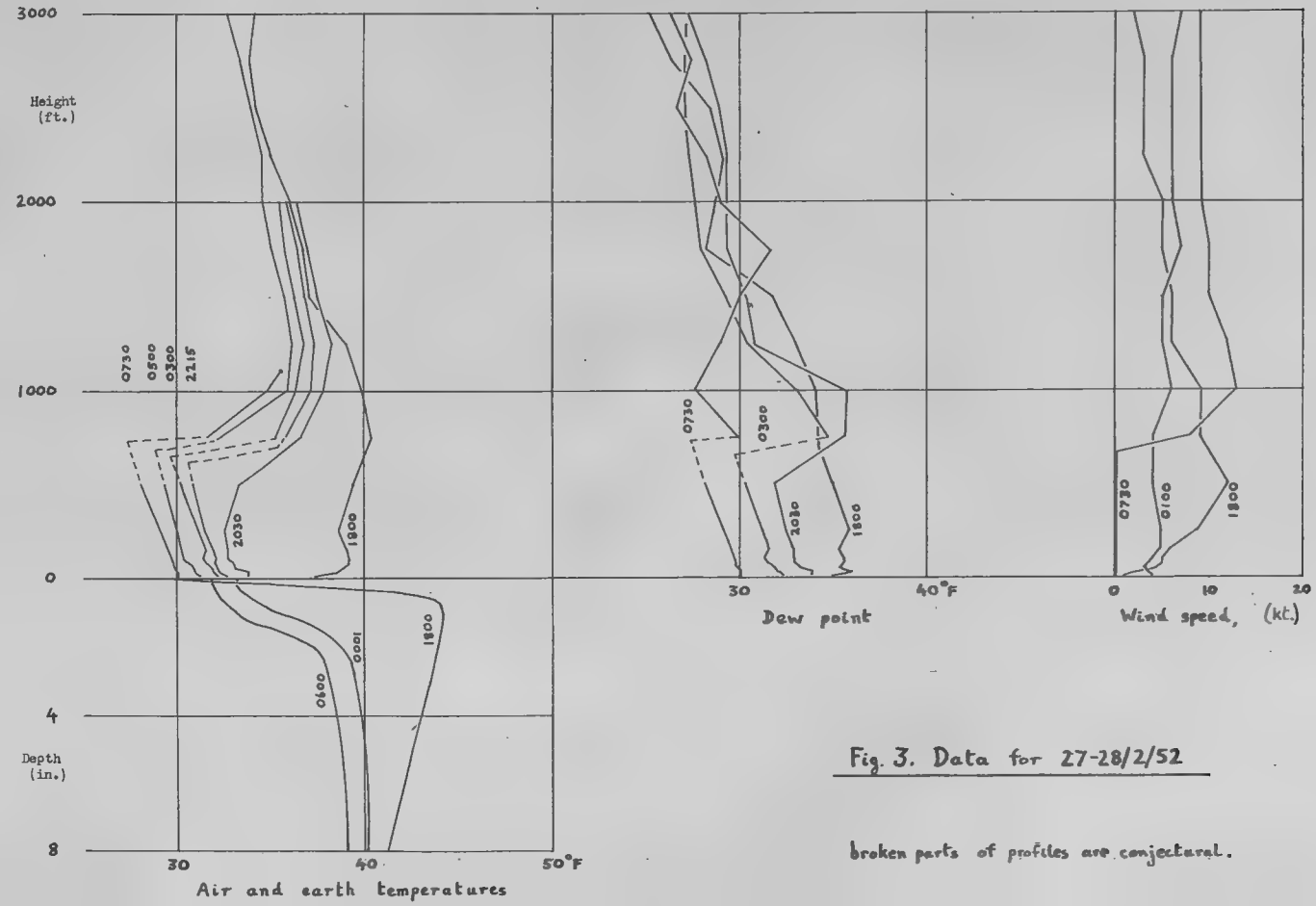

Fig. 3. Data for 27-28/2/52

broken parts of profiles are conjectural.

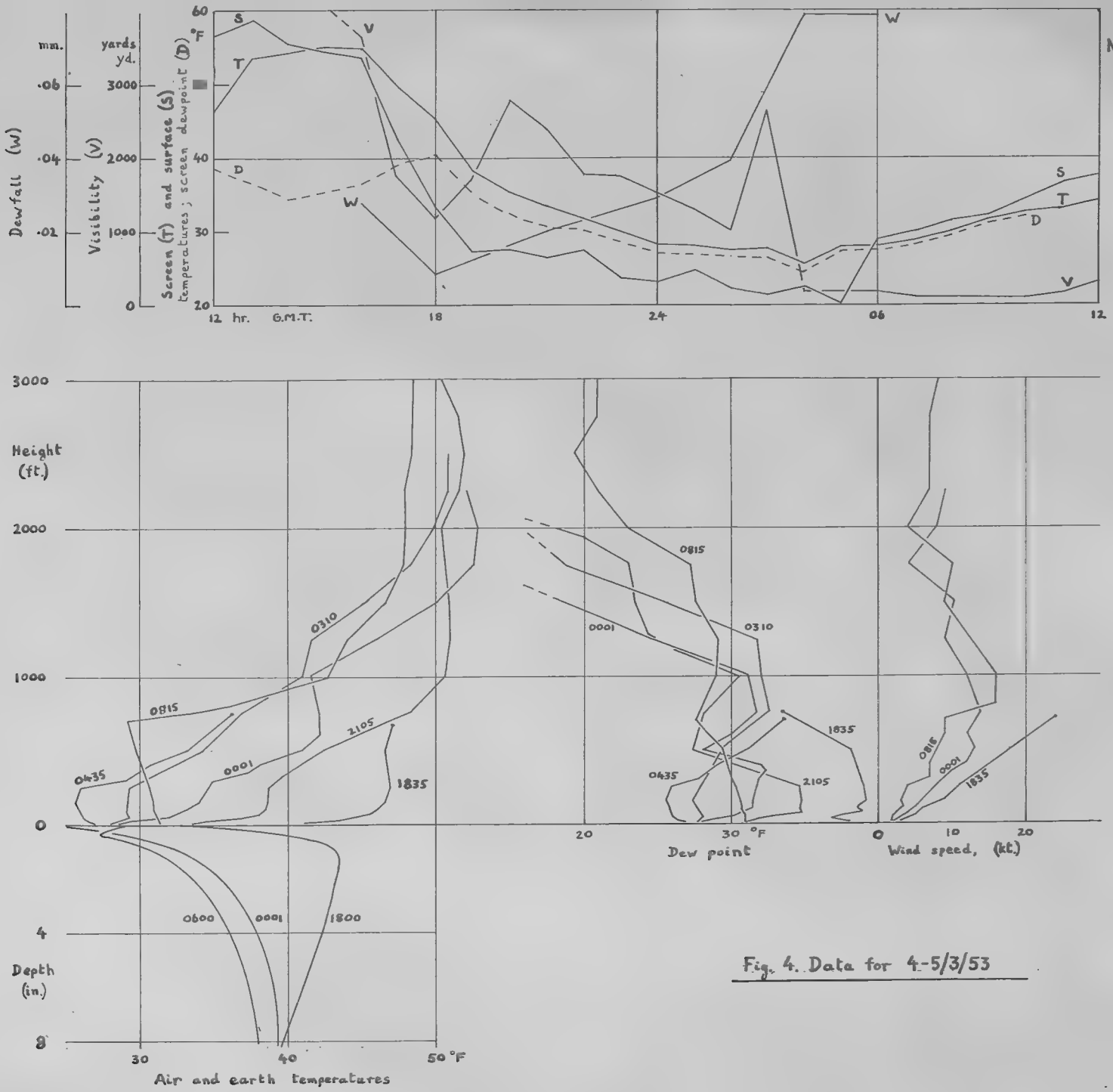

Fig. 4. Data for 4-5/3/53

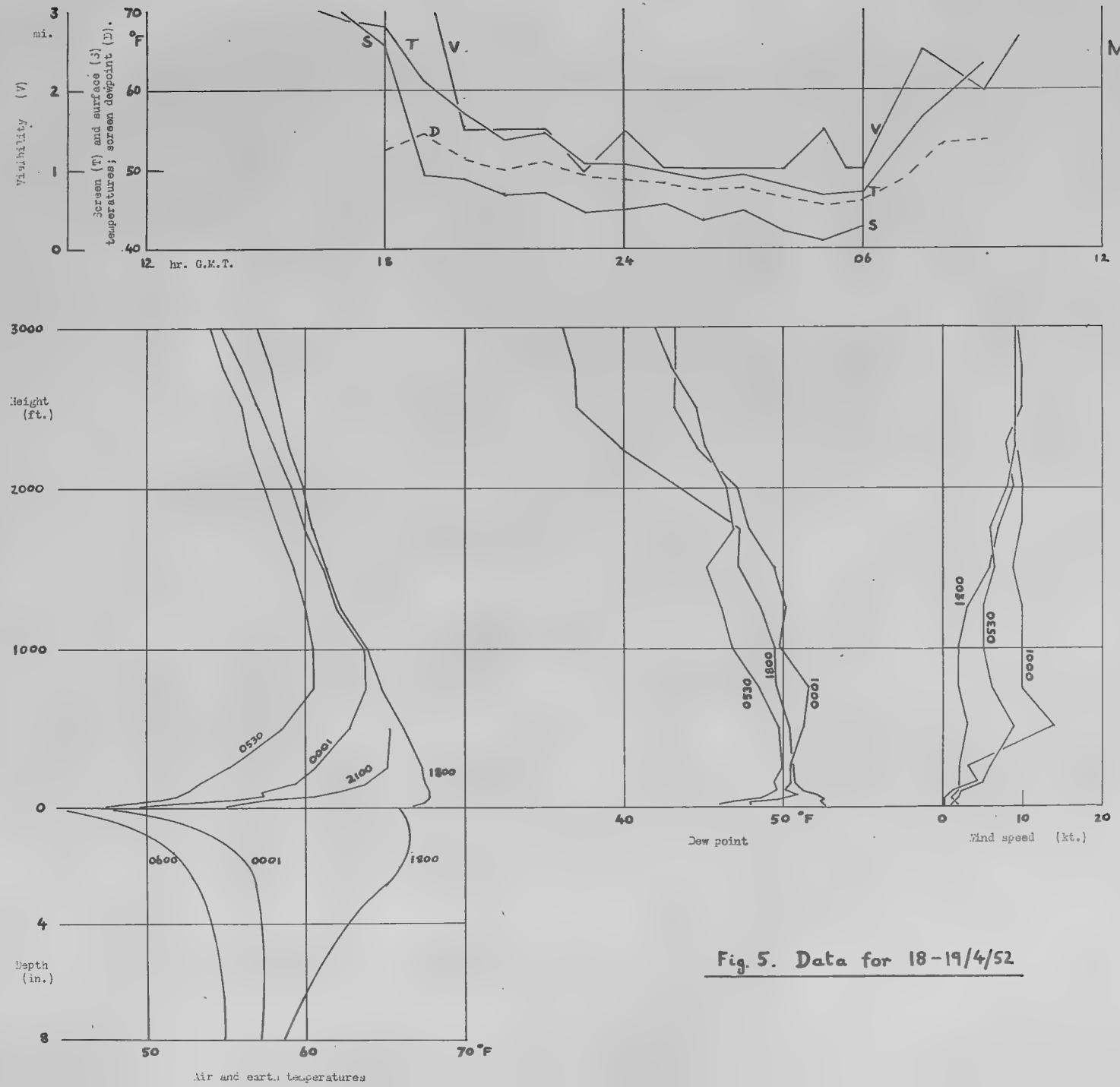

Fig. 5. Data for 18-19/4/52

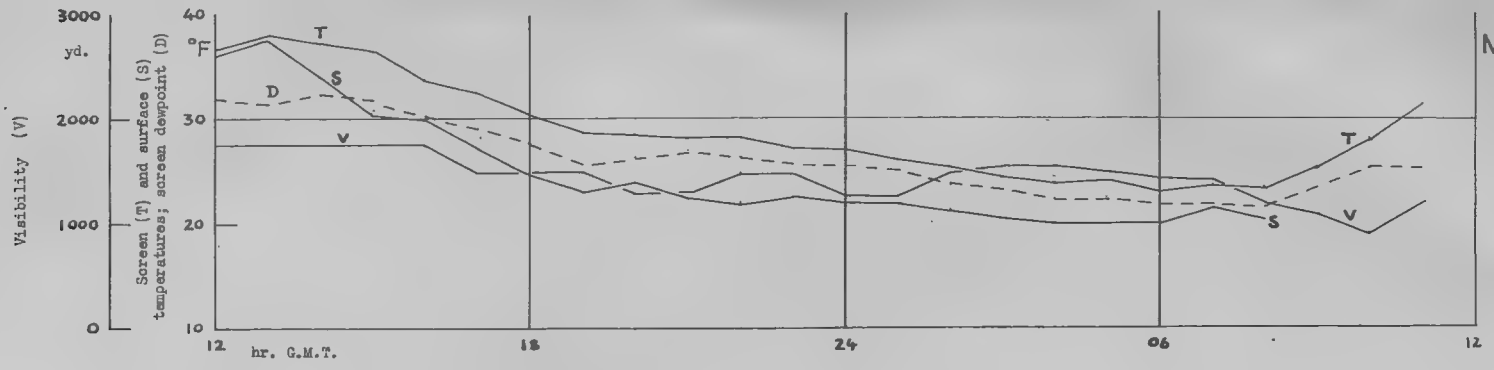

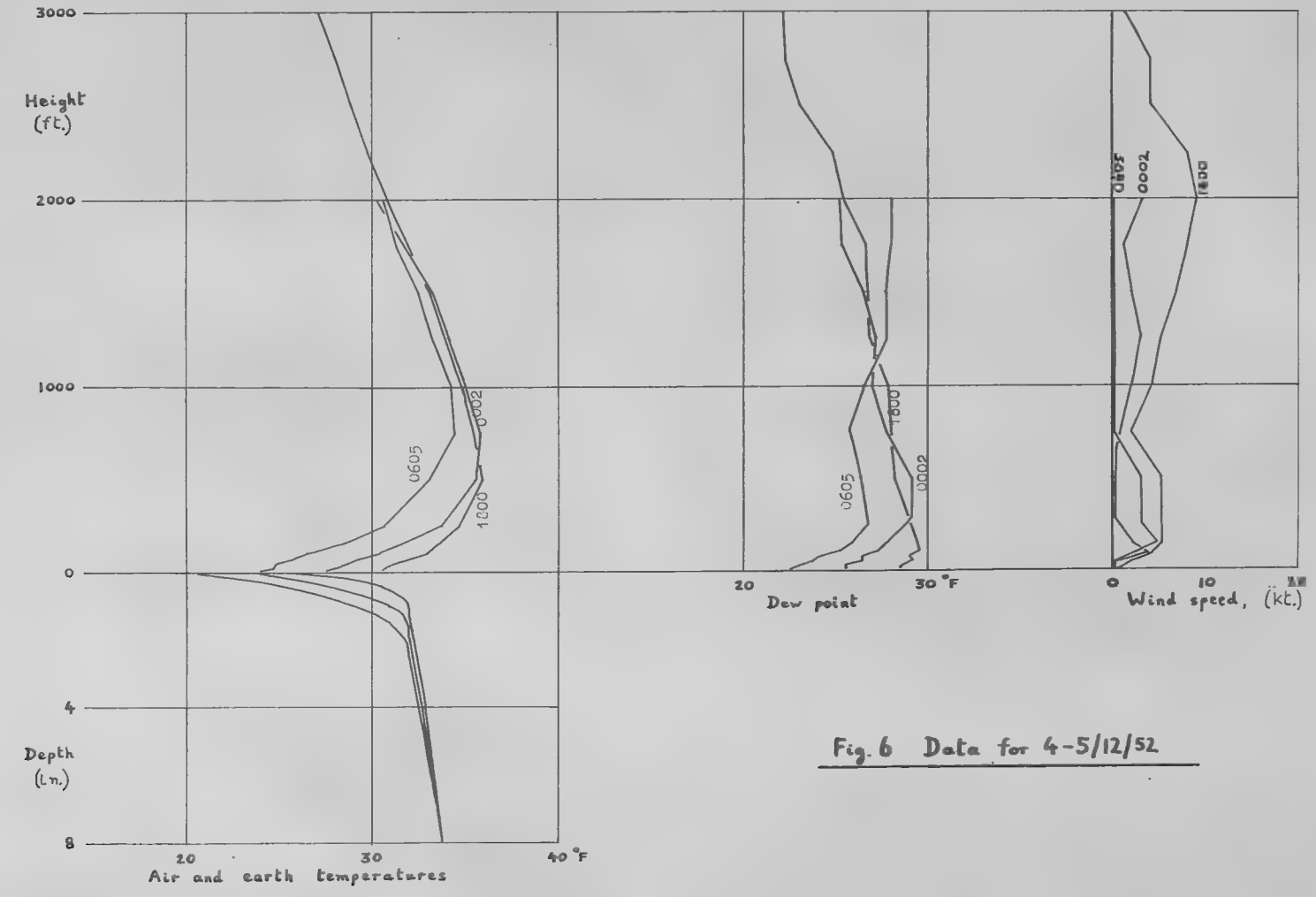

Fig. 6 Data for 4-5/12/52

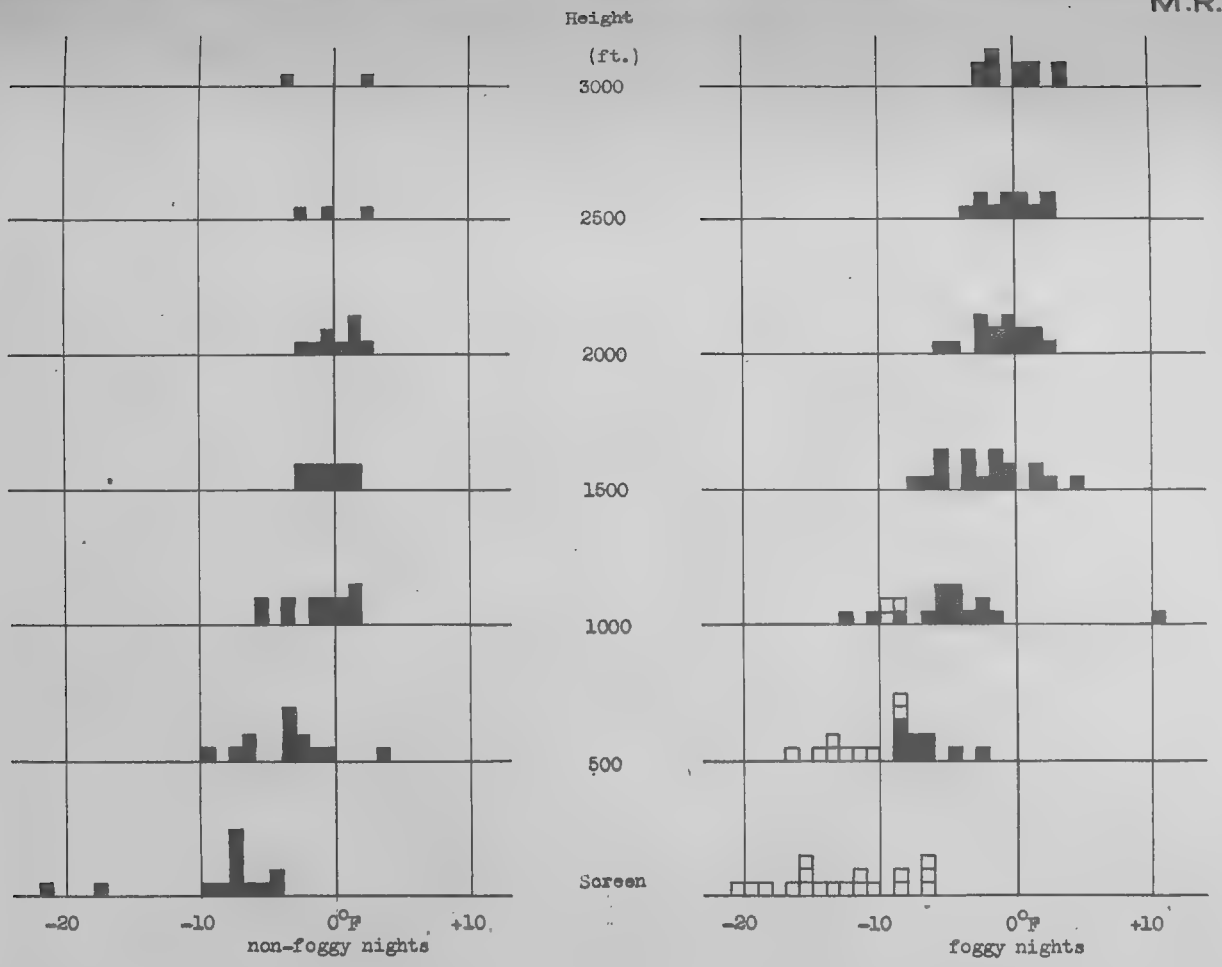

Fig. 7(a) Temperature changes 1800 - 0600 hr. Each square represents one occasion.
Open squares indicate observations within fog layer.

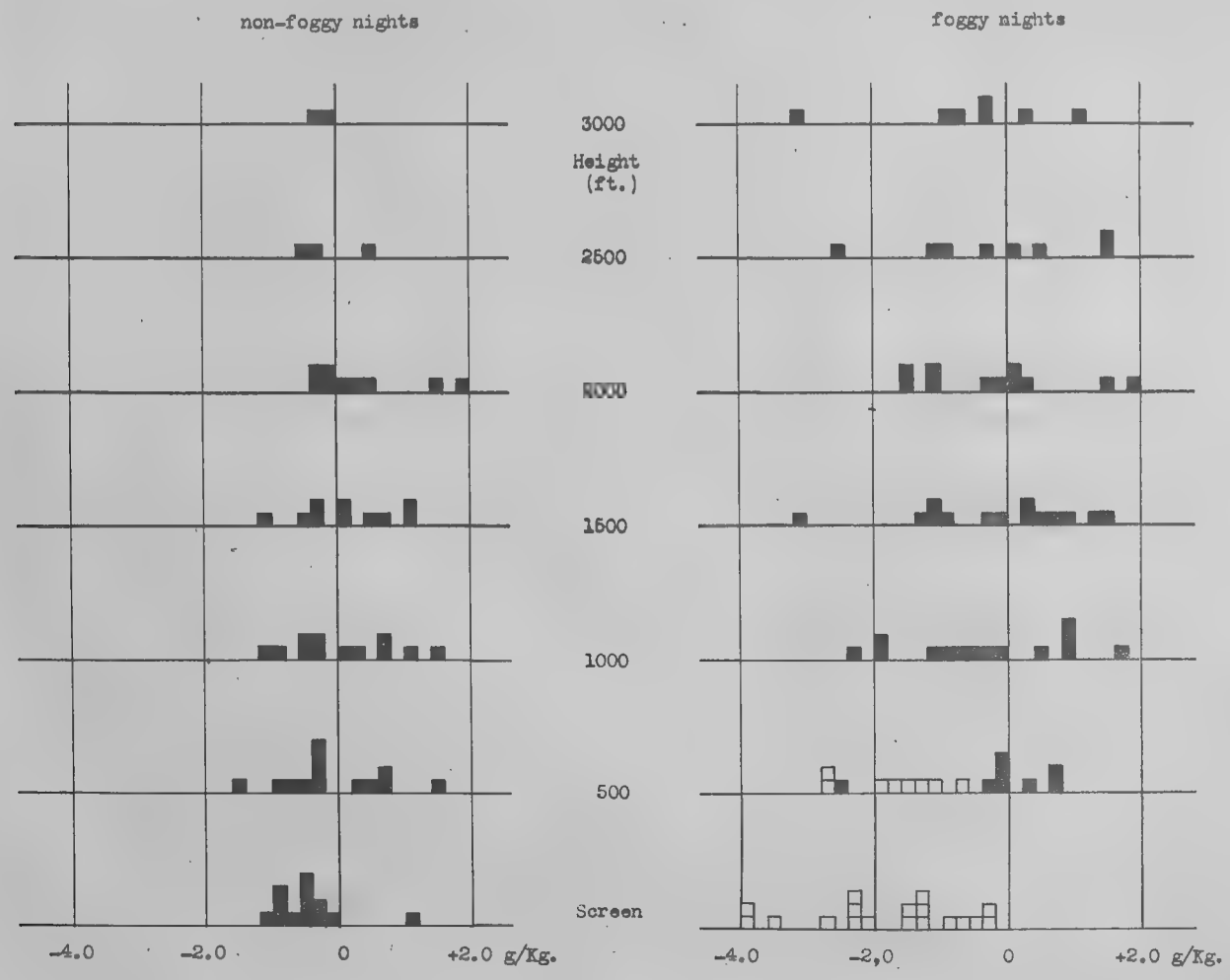

Fig. 7(b) Changes in specific humidity, 1800 - 0600 hr. Each square represents one occasion.
Open squares indicate observations in fog layer.

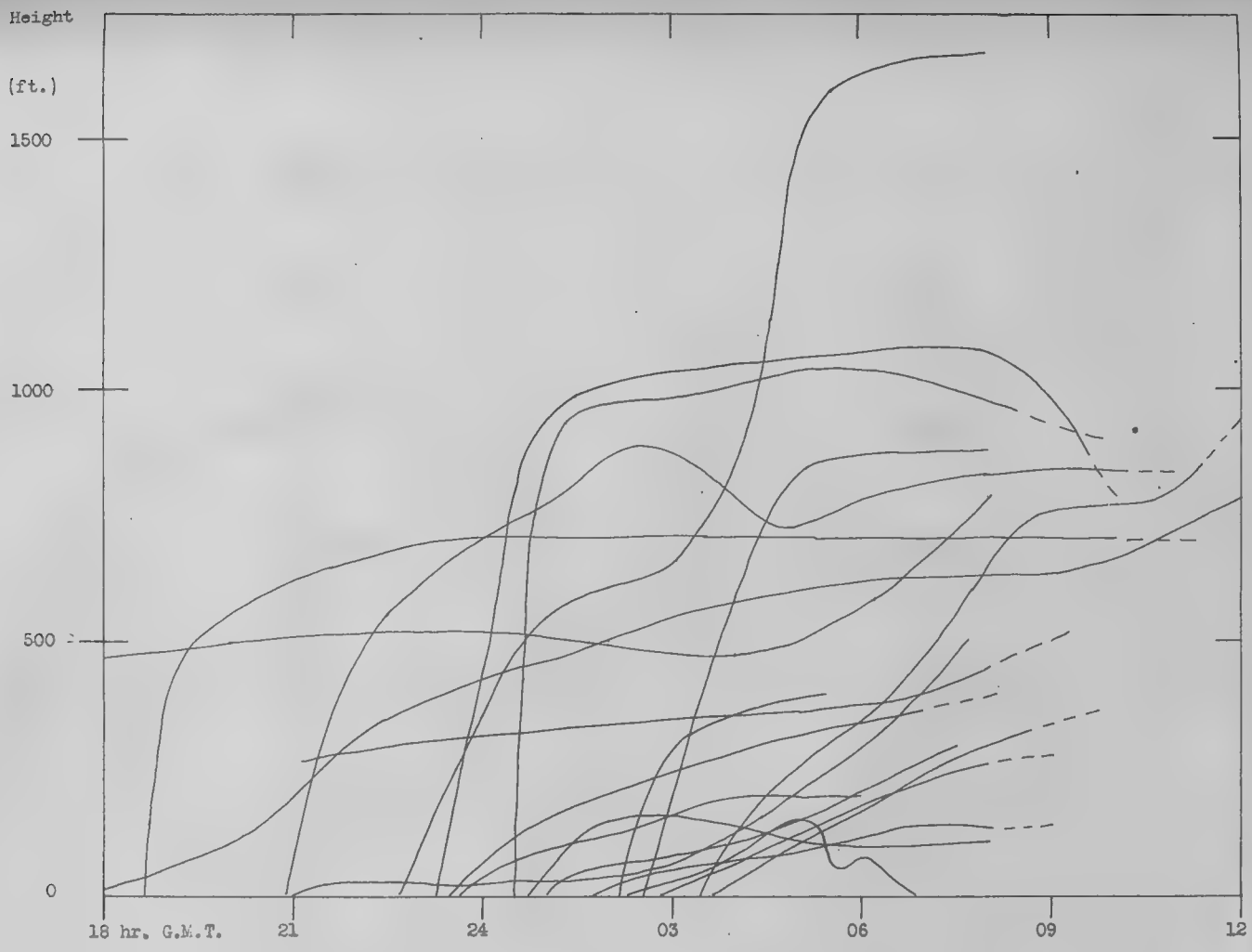

Fig. 8 Height of top of fog vs. time . Each line represents one night. Observations were mostly made at 2-3 hr. intervals and at standard heights, so curves are not very precise. Broken lines indicate dispersal of fog.

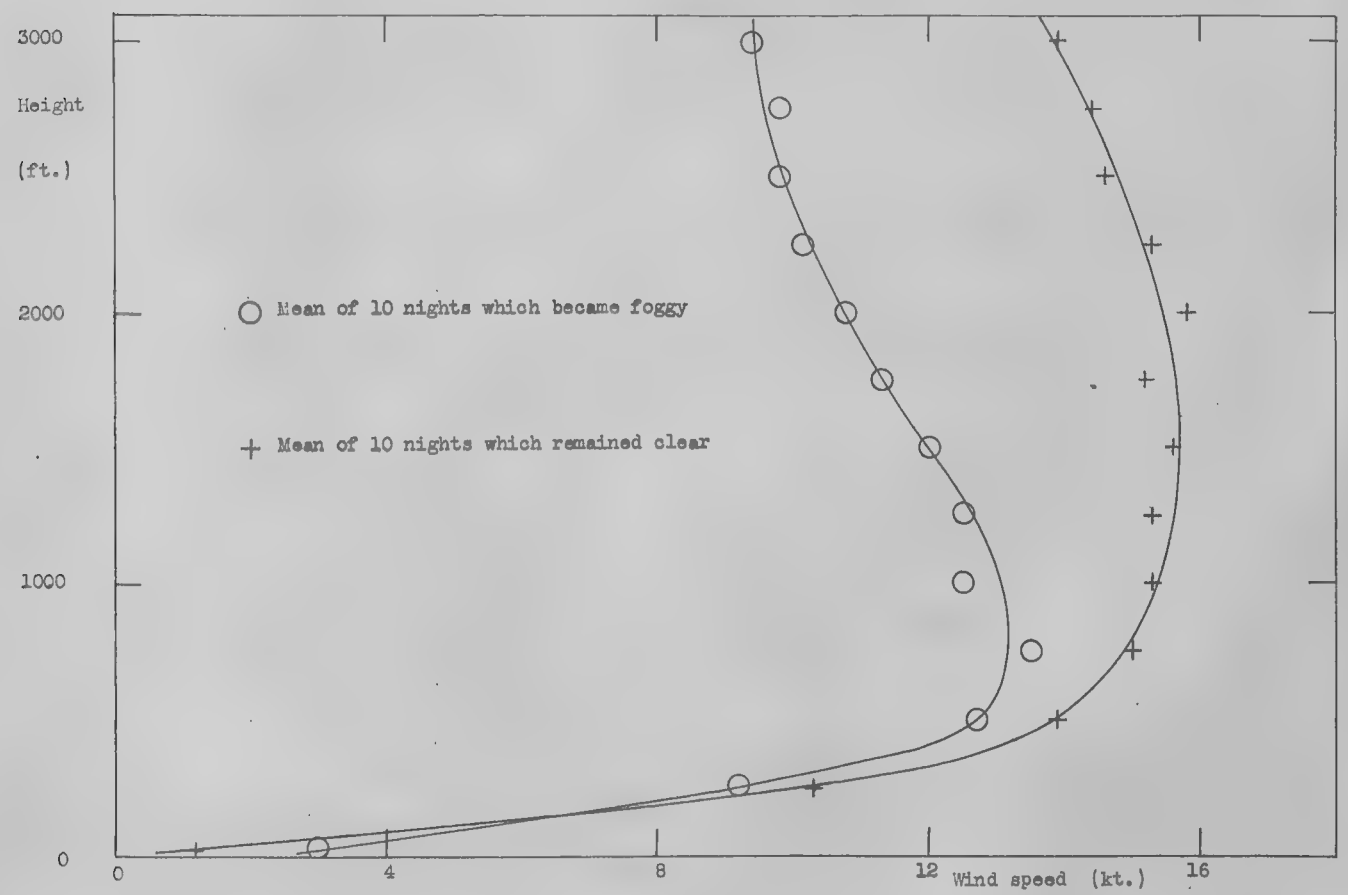

Fig. 9 Profiles of wind speed at Cardington at 1800 hr. on clear evenings

FIG. 10 Visibility meter record for 18-19/9/54

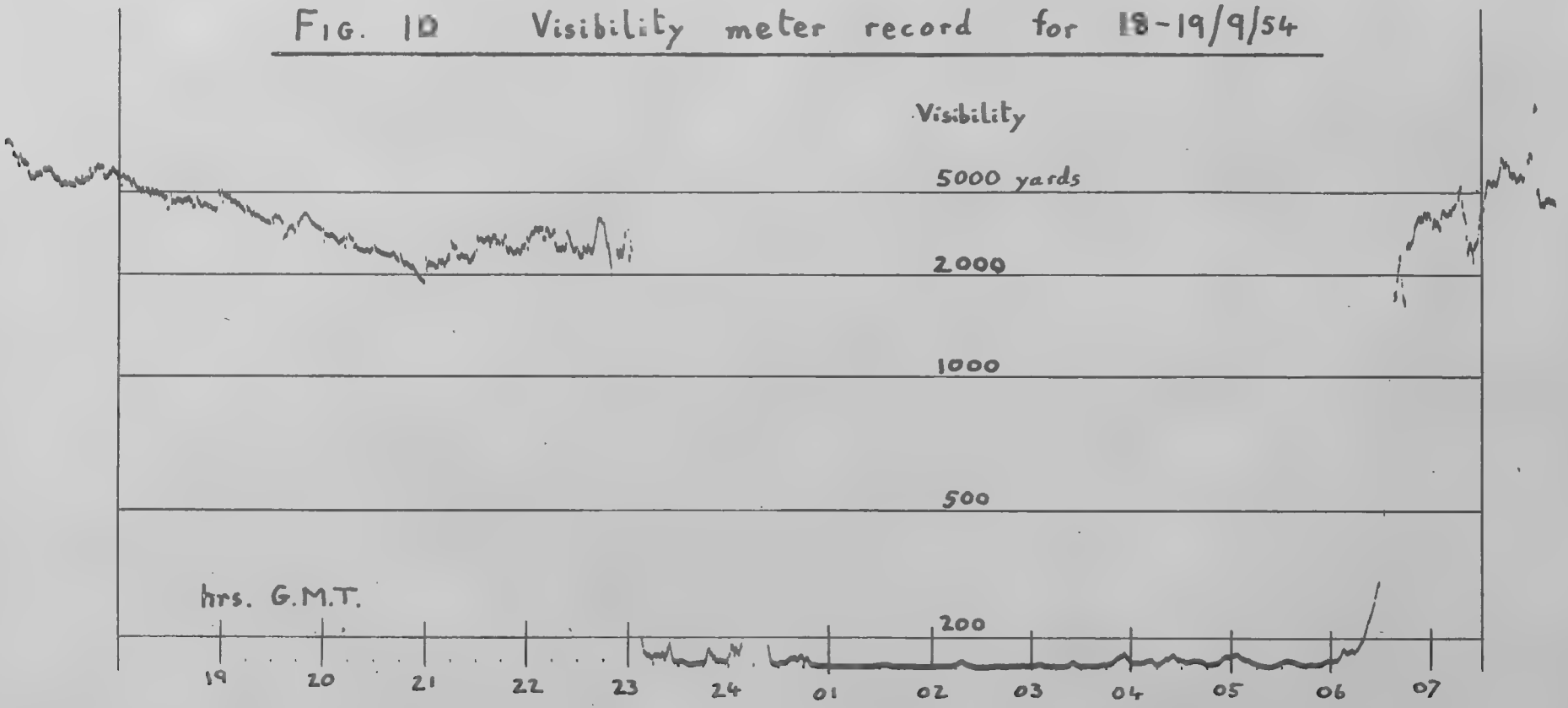

M.R.P. 912

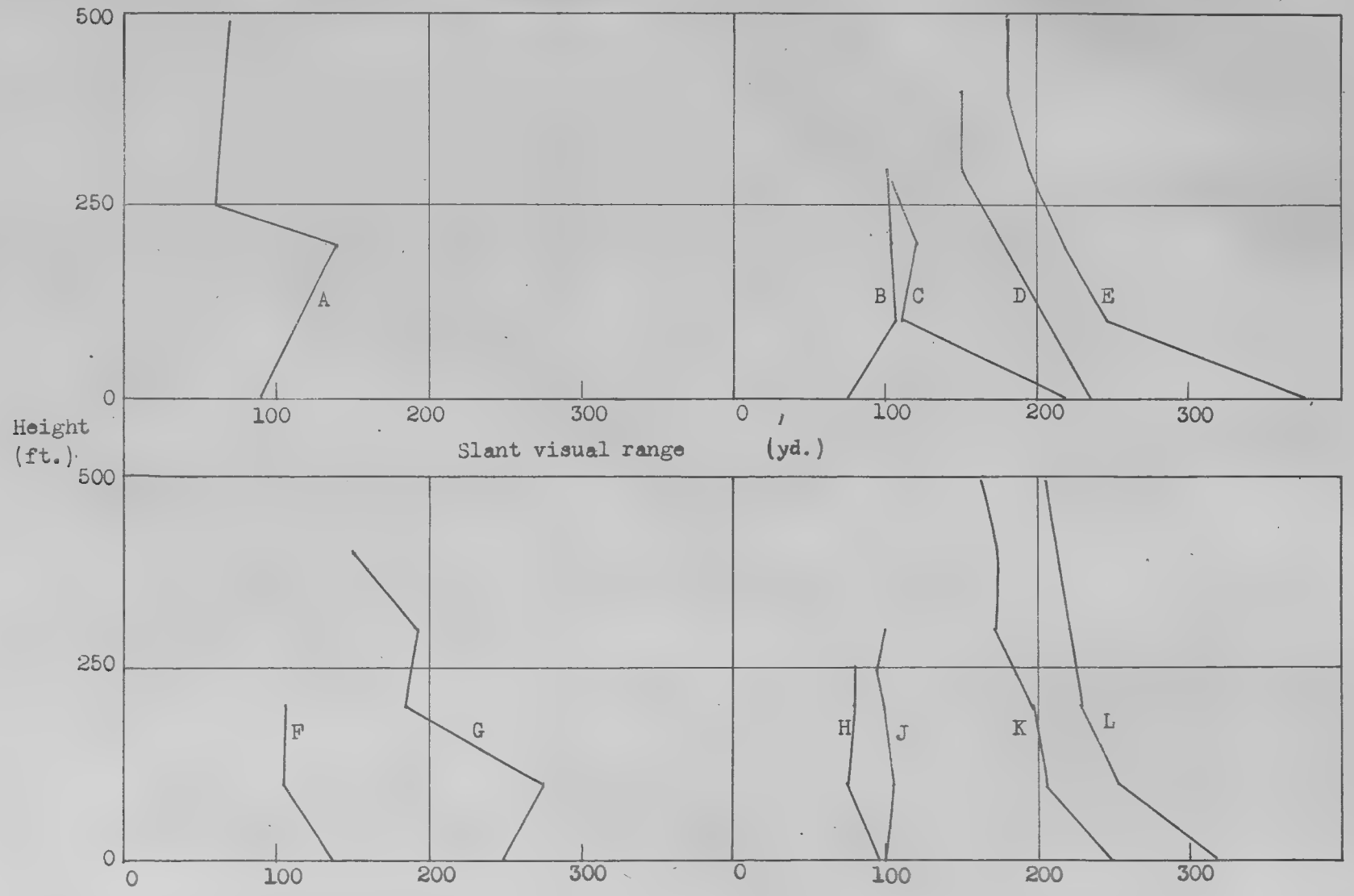

Fig. 11 Slant visual range of a 12 watt lamp vs. height for various occasions.

A 28/2/53 0130 B 3/3/53 0020 C 2/3/53 2140 D 1/3/53 2300 E 2/3/53 0500 F 3/3/53 0210
G 3/3/53 0500 H 4/3/53 0030 J 4/3/53 0245 K 21/3/53 0200 L 21/3/53 0400

Fig. 12

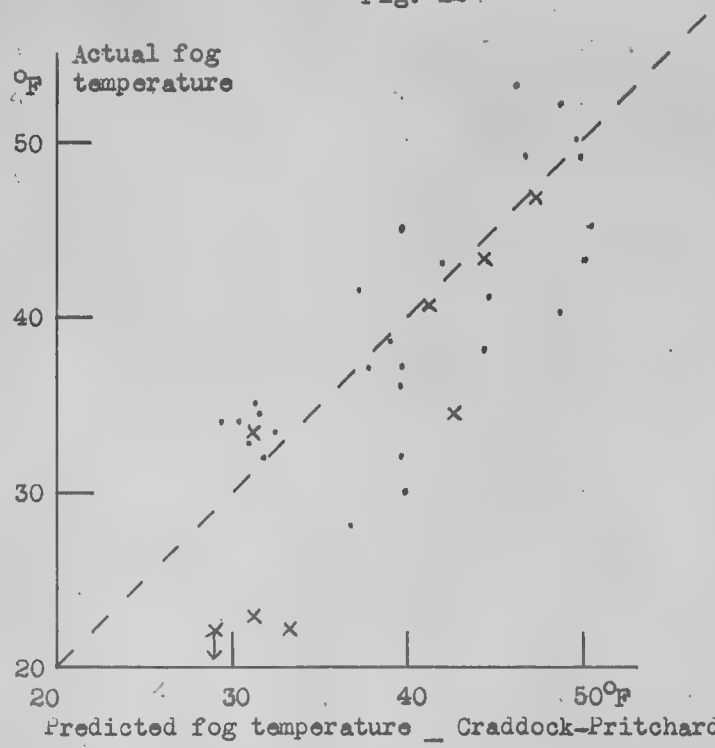

Fig. 13

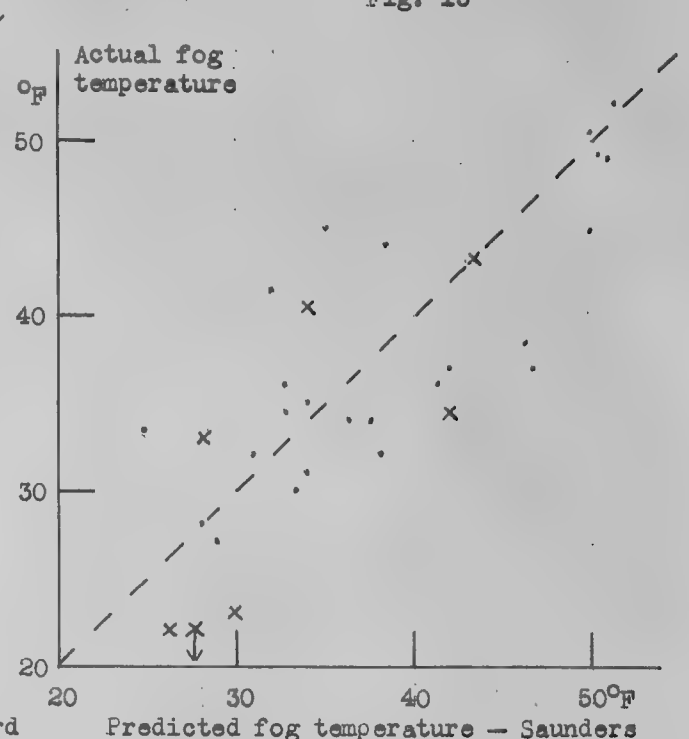

Crosses represent cases where fog did not form; minimum temperature is plotted in place of "actual fog temperature".

Fig. 14

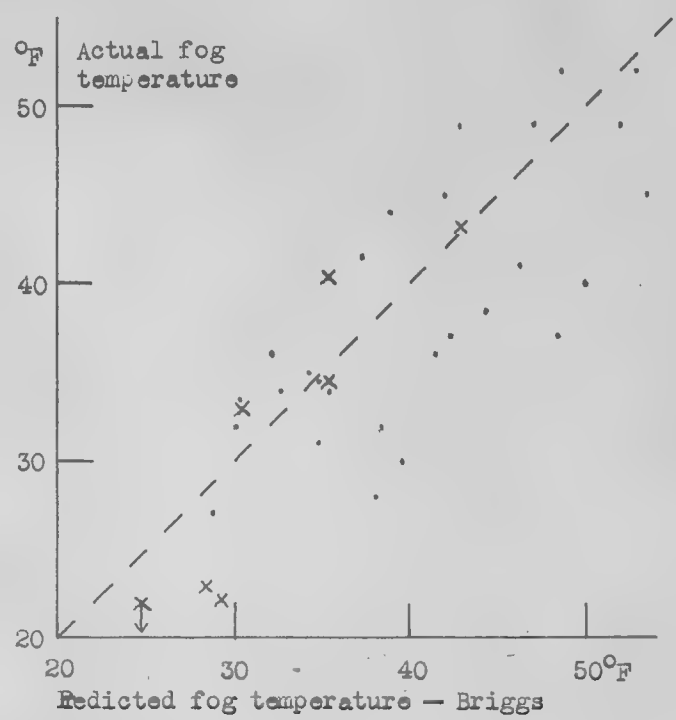

Fig. 15

Swinbank's fog-prediction diagram

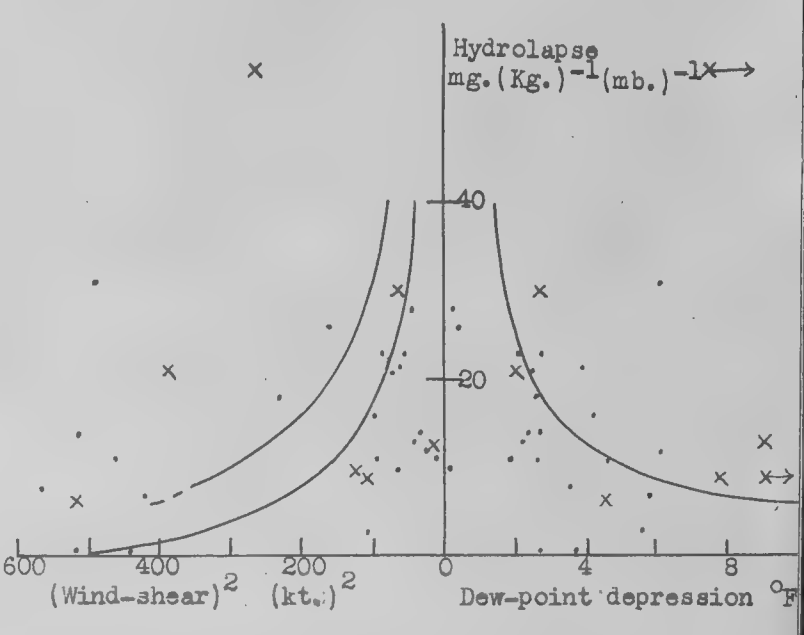

If representative points lie closer to the origin than the curves, fog should form.

Fig. 16 Relation between fog formation and minimum surface temperature, T_m.

Figures give values of T_m in °F and are ringed for nights on which no fog formed.

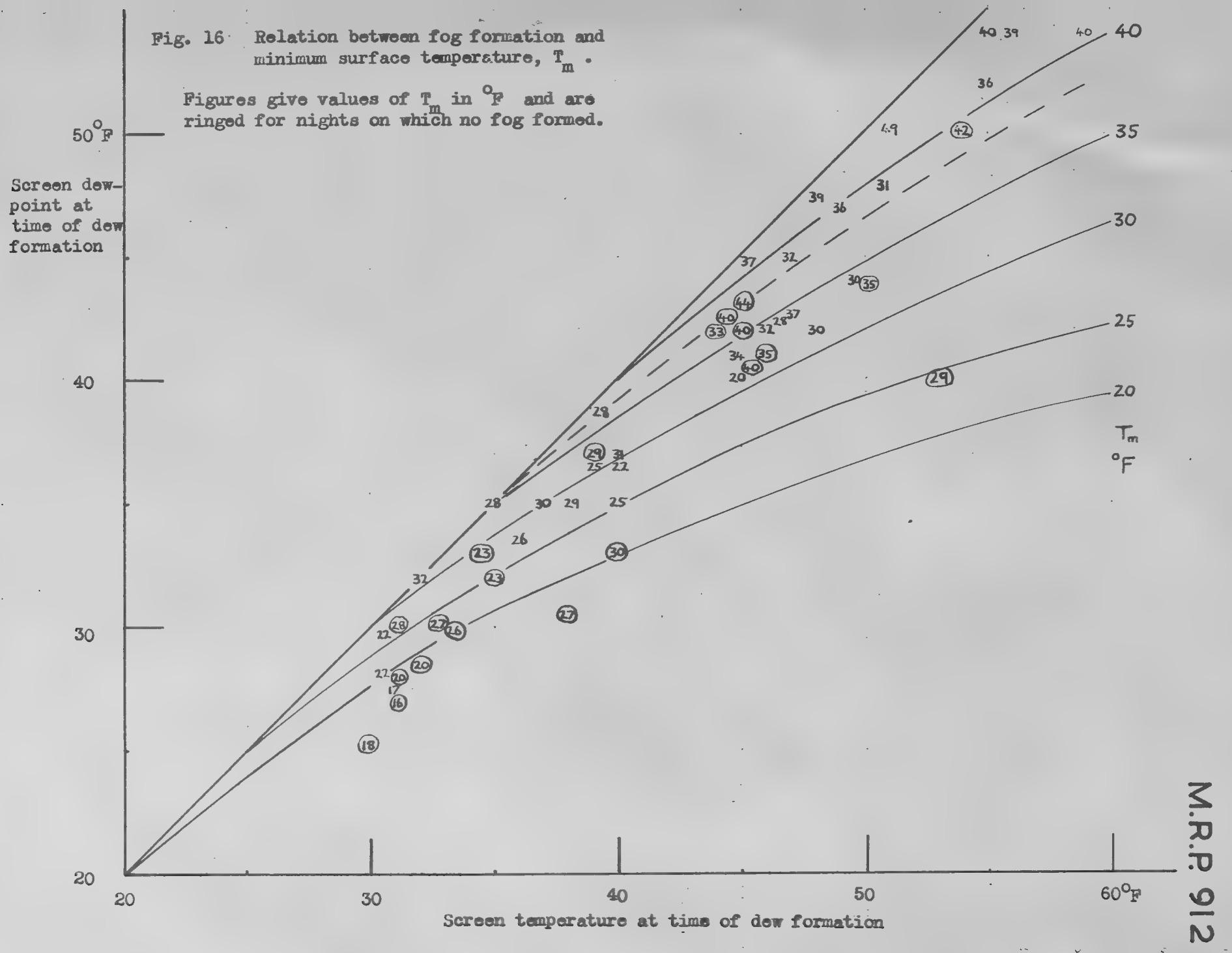

M.R.P. 912

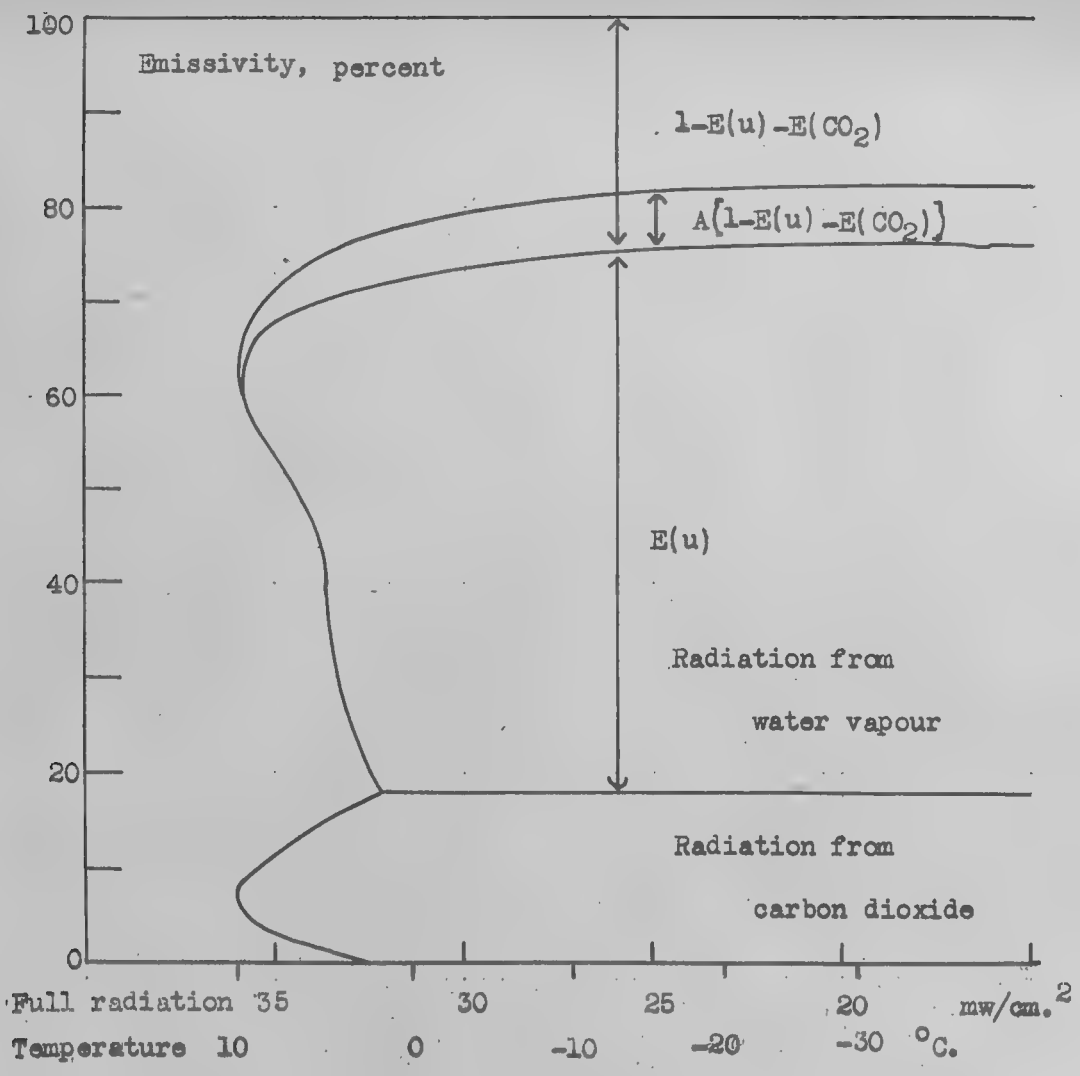

Fig. 17. "Kew" radiation chart for 0001hr. on 29/9/51, showing methods of estimating radiation from CO_2 and from particles.

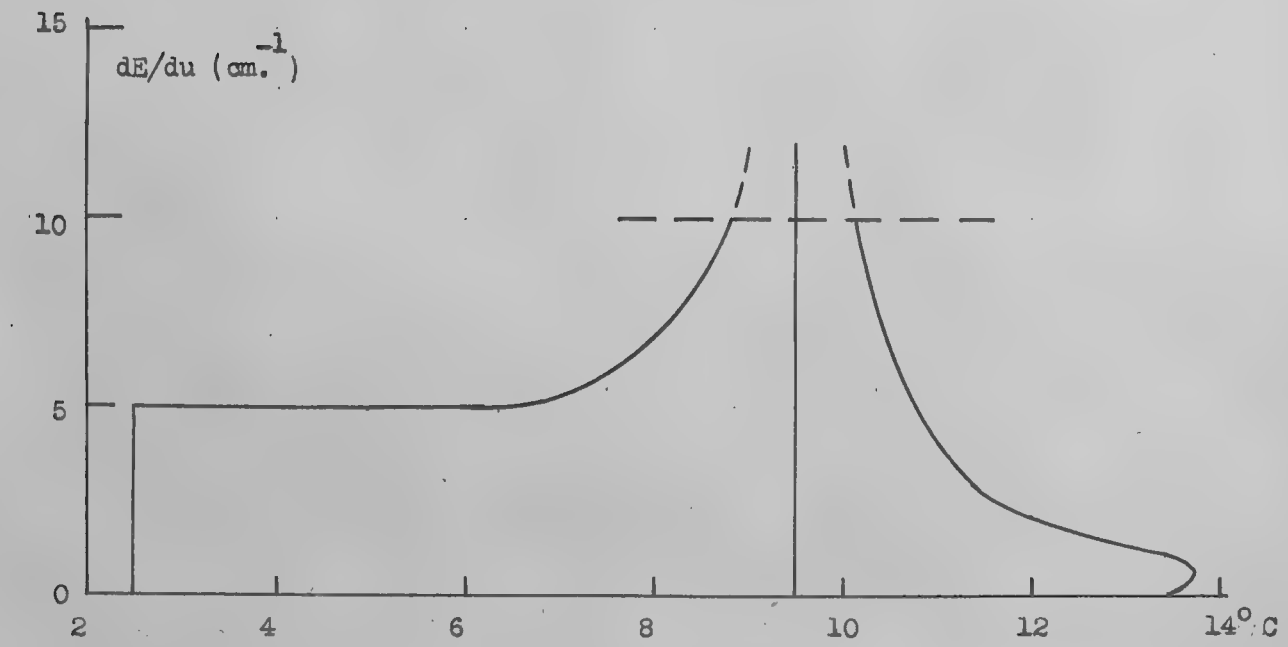

Fig. 18 Flux divergence chart for 100ft level at 0100 hr on 27/9/53. T is plotted as abscissa rather than σT^4 because σT^4 is roughly proportional to T over a limited range of temperature.

M.R.P. 913.
S.C. II/187.
S.C. III/184.
12th APRIL, 1955.

THE NOCTURNAL DISSIPATION OF STRATO-CUMULUS CLOUD.

by

D. G. JAMES.
(METEOROLOGICAL OFFICE)

AWSS
ROUTING SLIP

FILE	INFO	ACTION		
	1			
	2		TRSD	PRB EDB SEC CHF ALFB FLB SEFB SO SEC
	3		EDD	
	4			TECH INFO SEC

04 OCT 1955

METEOROLOGICAL RESEARCH COMMITTEE.
AIR MINISTRY

At the time of issue this report has not been published. Any author desiring to quote this paper should refer to it as "A paper of the Meteorological Research Committee (London).
M.R.P.No. 913 by Dr. D. G. James
A copy is available in the Library of the Meteorological Office."

M.R.P. 913
S.C.II/187
S.C.III/184
12th April, 1955

AIR MINISTRY

METEOROLOGICAL RESEARCH COMMITTEE

The nocturnal dissipation of strato-cumulus cloud

by
D.G. James (Meteorological Office)

(1) Introduction

The difficulty encountered in forecasting the dissipation or persistence of a sheet of strato-cumulus cloud suggests that the cloud layer is in a delicate state of balance with its environment.

Subsidence or ascent within the air mass at cloud heights can dissipate or reinforce the cloud sheet, whilst advective changes might transfer the layer from one locality to another. Radiation from the cloud layer produces a net flux of heat outwards and cools the cloud sheet, and mixing by eddy diffusion occurs at cloud base and top with the air below and above the layer; in addition the radiative cooling of the cloud may be sufficient to produce mixing by convective turbulence at cloud base. Generally, analysis of surface synoptic charts and radio-sonde observations gives little indication as to which processes dominate the behaviour of the cloud sheet, though instances of considerable vertical motion or advection at cloud levels would be at once evident. Thus it seemed desirable to select a number of cases and examine them statistically for significant differences between the means of the parameters (or combination of the parameters) involved, for the two classes of dissipating and non-dissipating cloud.

(2) Selection of cases

The choice of examples for statistical analysis was made from 1952-1954, and was governed by the following simple criteria.

(i) The strato-cumulus sheet was bounded at its top by a dry type inversion, i.e. a rapid decrease of humidity with height through the region of temperature increase. (This was realised in almost all cases of non-frontal strato-cumulus.)

(ii) There was no surface front within 400 miles of the locality of the cloud sheet.

(iii) The cloud base was above the condensation level of any convection from the sea, all cases being taken over land.

(iv) The cloud sheet was extensive covering perhaps several hundred square miles, and gave almost complete cover, i.e. greater than 6/8 for at least two consecutive hours. The cloud was considered to have dissipated if the sheet had reduced to 2/8 or less for at least two consecutive hours.

(v) Only nocturnal dissipation or persistence was considered because there was then no continuous maintenance of the cloud by convection from the surface.

/In general

In general, cloud bases were determined from surface observations and cloud tops from the vertical temperature profiles obtained by radio-sonde ascents at the same time. In some cases, when the cloud bases reported from the ground were not fully consistent with the vertical temperature profiles indicated by the ascents, the values of the cloud bases used were obtained by the use of the temperatures and dewpoints given by the soundings. Several cases were rejected since the cloud bases so obtained were completely at variance with those reported from the ground.

(3) Advection and vertical motion

Advective changes were rarely responsible for the dissipation of sheets of strato-cumulus cloud of the type considered. This was concluded from examination of hourly surface charts in cases when the strato-cumulus dispersed, when extensive areas of cloud present at one hour had almost completely vanished by the next. The process of dispersal when it occurred was usually quite sudden, and no cases were observed in which the edge of the cloud sheet retreated steadily with the wind as would be expected with advective clearance. It did appear, however, that local fluctuations in cloud height were often due to minor advective changes.

Consideration of the potential temperatures, humidity mixing ratios and wet-bulb potential temperatures of soundings through the air masses relevant to the cloud sheets showed little evidence that vertical motion in the atmosphere was the chief cause of the persistence or dissipation of the cloud. Although, on occasions, subsidence of the order of 4-5 mb. per hour could be detected at 700 mb. and above, little direct evidence of the influence of subsidence could be observed at cloud heights. Thus it was thought that for the cases selected, advective changes and vertical motions in the air masses were not primarily responsible for the behaviour of the cloud sheet.

(4) Radiation from the cloud

The net radiative flux from a cloud sheet was calculated for several cases by use of the Elsasser radiation charts. The loss of heat flux was of the order of 20 cal/cm^{-2} in 3 hr and varied little from case to case, being almost independent of cloud thickness. Thus the variation of radiative flux did not seem to be a principal factor in determining persistence or dissipation of the cloud sheet. To calculate the cooling of the cloud layer, the cloud was regarded as a black body, and the cooling depended greatly upon cloud thickness. Hewson (1948) has demonstrated how such cooling could be responsible for the dissipation of scattered fragments of cloud. In this process, the cloud fragments cool by radiation and sink relative to the environment, so ultimately dispersing. In considering such a mechanism, Hewson neglects any compensating up-currents in the environmental air. This is quite legitimate if the cloud comprises only isolated fragments. If, however, the cloud amount is substantial, or indeed the cloud is continuous, we cannot neglect the up-currents in such a way. They would almost certainly have the effect of continuously reforming the cloud. Thus Hewson's process cannot be invoked to explain the dissipation of a continuous sheet of strato-cumulus cloud. In this case the effect of the radiational cooling of the cloud is to establish an adiabatic lapse rate below cloud and thus convective mixing between cloud and the air below. Such convective mixing could in theory result in the dispersal of the cloud provided the sub-cloud air were sufficiently dry not to reach saturation at cloud height. It was found that the extreme dryness necessary did not occur; in fact, convective mixing with the air below cloud would in general retard rather than assist dissipation of the cloud.

In the course of carrying out the radiation calculations it was noted that the calculated amount of cooling of the cloud was considerably greater than that suggested by successive radio-sonde ascents, even after allowing for the latent heat released by additional condensation. This fact supports the idea that continuous mixing with the air above and/or below cloud must be important processes in maintaining the temperature of the cloud and these are, therefore, considered further.

(5) Turbulent mixing with air above cloud top

Turbulent mixing caused by eddy diffusion at the cloud-inversion interface would cause much warmer and drier air to enter the cloud. Consequently it was thought that there might be a significant difference between the warmth and dryness of the air above cloud for the two classes of dissipation and persistence.

The depression of the dewpoint below dry bulb temperature in °F at a given pressure level was used as a simple parameter, and Table 1 was constructed relating the persistence or dissipation of the cloud (within 12 hours of the radio-sonde ascent used) with the maximum depression up to 50 mb. above cloud top. It was thought that the standard error in estimating cloud top was such that the parameter used would be more representative than if a much smaller or much greater depth of air above cloud was taken. This was shown to be the case when tables similar to Table 1 were prepared for the dewpoint depression within 25 mb. and 100 mb. of cloud top.

Table 1

Maximum value of depression of dewpoint below temperature in °F taken over 50 mb. above cloud top

	Breaks ($\leq$ 12 hours)	No breaks
Mean (°F)	24	18
Standard deviation	13	14
Standard error of mean	2.6	2.7
No. of cases	26	27

Student's 't' evaluated for the difference between the means in Table 1 gave t = 1.60 which showed that the means were significantly different at about the 10% level. The dryness of the air above cloud must, therefore, be relevant to the problem of dissipation.

(6) Turbulent mixing with air below cloud base

In all of the cases examined the air below cloud was not sufficiently dry for any mixing at cloud base to produce dissipation of the cloud. The radiative cooling of the cloud was usually great enough for the establishment of a dry adiabatic layer directly below cloud, so that mixing by convective turbulence as well as eddy diffusion took place at these levels. Hence these processes probably acted as a retarding factor on any dissipating mechanism produced by mixing through the inversion.

Table 2 presents the means and standard deviations of the hydrolapses averaged over 50 mb. below cloud base for cases of "Breaks" and "No breaks" of the strato-cumulus sheets.

Table 2

Hydrolapses over 50 mb. below cloud in 10^{-2} gm/Kg per mb.

	Breaks ($\leq$ 12 hours)	No breaks
Mean ($\times 10^{-2}$ gm/Kg per mb.)	1.1	1.5
Standard deviation	0.8	0.8
Standard error of mean	0.16	0.16
No. of cases	26	27

Evaluation of Student's 't' for the means above gave t = 1.77 which indicated that the means were significantly different at about the 10% level.

/(7).

(7) Effect of cloud thickness

Table 3 presents the means and standard deviations of the observations of cloud thickness in mb. for the two classes of "Breaks" and "No breaks".

Table 3

Cloud thickness in mb.

	Breaks ($\leq$ 12 hours)	No breaks
Mean (mb.)	33.5	43.5
Standard deviation	20.0	19.0
Standard error of the mean	3.9	3.9
No. of cases	26	27

For the above means, Student's 't' = 1.86, which showed that the difference between the means was significantly different from zero at about the 10% level.

(8) Combination of the parameters

Tables 1, 2, and 3 suggested that it would be worth devising a new parameter by a combination of the three variables used in the preparation of the tables. The new parameter was defined as $\xi = x + \alpha y + \beta z$ where x, y, z, were the three variables used above, and α and β were constants, to be determined by the condition that the departure from zero of the difference between the means of ξ for cases of "Breaks" and "No breaks" should have maximum significance. The conditions were determined by maximising Student's 't' for the difference between the two means of ξ, and the final parameter obtained as:-

$$\xi = x - 9.15\, y - 0.77\, z .$$

where x = Maximum depression in °F of dewpoint below temperature at any pressure level up to 50 mb. above cloud top,

y = Average hydrolapse in 10^{-2} gm/Kg per mb. over 50 mb. below cloud base,

and z = Cloud thickness in mb.

Table 4 presents the means and standard deviations of ξ for the two classes of cloud behaviour.

Table 4. $\xi = x - 9.15\, y - 0.77\, z$

	Breaks ($\leq$ 12 hours)	No breaks
Mean	-12.1	-28.4
Standard deviation	18.9	16.4
Standard error of the mean	3.71	3.35
No. of cases	26	27

Student's 't' now gives t = 3.36, which indicates that the means are significantly different at about the 0.2% level; the form of ξ is the best relationship that can be obtained by a linear combination of the three parameters used.

Fig. 1 shows the distribution of values of ξ for cases of "Breaks" and "No breaks". 74% of the cases of "No breaks" have values of ξ less than - 20, whilst 76% of the cases of "Breaks" have values of ξ greater than - 20.

These figures would be somewhat better were it not for two cases of each type which fall well to the wrong side of the dividing line at ξ = -20. These cases are perhaps worthy of some discussion if only to illustrate the difficulties encountered.

/(a)

(a) One case of dissipating cloud gives ξ = -65.8 which is well to the wrong side of the dividing line at ξ = -20. This large value is given mainly by an assessed cloud thickness of 90 mb., which was consistent with the observations of cloud base (2,500 to 3,000 ft.). However, a thickness of 30 mb. is easily possible from the ascent, but this would require a cloud base of 4,500 ft.

(b) A second case of dissipating cloud gives ξ = -60.2 which is again to the wrong side of the dividing line. The cloud thickness used in this case was 30 mb., although any value up to 70 mb. was possible, and hence uncertainties in the cloud thickness alone could not have been responsible for the excessively large value of ξ. The hydrolapse above cloud had a shallow slope, but was verified by comparison with other soundings in the same air mass.

(c) One case of persisting cloud gives ξ = 14.1, well to the wrong side of ξ = -20. This discrepancy is again attributed to lack of definite information regarding cloud base and top. A thickness of 10 mb. was used in the statistical study implying a cloud base of 4,000 ft. This was a case when the surface reports of cloud base were rejected in favour of assessment from the ascent. Had the surface observations been accepted (2,000 to 3,000 ft.), a value for cloud thickness of from 120 to 70 mb. would have been indicated. It is possible, of course, that there were two layers in this case.

(d) The final point well to the wrong side of ξ = -20 is given by ξ = 19.6 for persisting cloud. The cloud was assumed to be 35 mb. thick with a base of 4,000 ft., although surface observations were reporting the base as 2,000-3,000 ft. It is possible that there could have been two cloud layers, the first as already assumed, and the second base 2,000 ft. and thickness 35 mb. The air above this lower layer was not very dry, and it is also possible that the layer was being reinforced by convection from sea surface.

It is concluded from the above that the most glaring discrepancies in the indication provided by the combined parameter ξ almost certainly arise owing to the difficulties and uncertainties of assessing cloud thicknesses in the absence of positive information.

(9) Conclusions

(i) In the cases examined, there was little evidence to show that vertical motion in the atmosphere was responsible for the dispersal or persistence of strato-cumulus cloud.

(ii) Hewson's processes for the dissipation of broken and scattered cloud by differential radiation could not explain the dispersal of a continuous sheet of cloud. Although mixing at cloud base with air below was always present, exceedingly dry air below cloud would have been required for dissipation.

(iii) Radiative cooling of the cloud sheet caused an intensification of the mixing process at cloud base, and could not produce dissipation of the cloud.

(iv) Turbulent mixing of the cloud with the dry air above seemed to be significant in the subsequent behaviour of the cloud.

(v) A combination of three parameters expressing the warmth and dryness of the air above cloud, the hydrolapse below cloud, and cloud thickness gave means, the difference between which differed significantly from zero for cases of "Breaks" and "No breaks". This result may be of some value for forecasting.

/(vi)

(vi) If mixing with the air above and below a strato-cumulus layer is the main controlling process determining whether the cloud layer will persist or dissipate, it is doubtful whether any more specific criteria for the dispersal of the cloud can be developed on the basis of synoptic observations because of their limitations for determining the essential parameters, - cloud thickness and humidity distribution above and below cloud.

Before any more detailed routine observations are recommended a better physical understanding of the mixing process is required, and it is suggested that the next stage in research on the behaviour of strato-cumulus should be a study of this process based on temperature, humidity and accelerometer readings by aircraft immediately above and below the cloud layer. In addition observations of liquid water content in such cloud would be useful.

References:

Hewson, E. W. Quart. J.R. met. Soc., 74, p.243, 1948.

Fig. 1 Frequency of Cases with Values of $\xi = x - 9{\cdot}15y - 0{\cdot}77z$

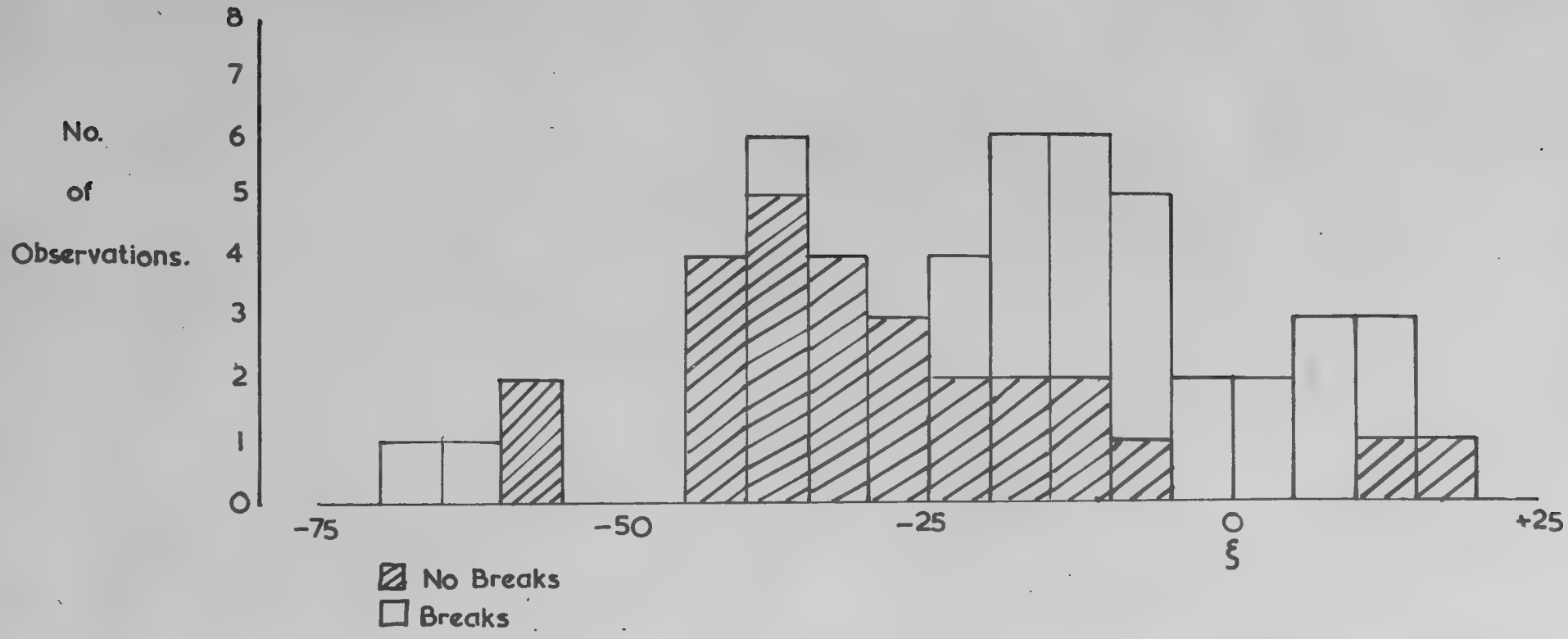

M.R.P. 913

M.R.P. 914
S.C. 111/185
28th April, 1955

Measurements of the flux of long wave radiation in the upper air 1953 - 1954

by

J. T. Houghton and A. W. Brewer.

AIR MINISTRY
METEOROLOGICAL RESEARCH COMMITTEE

At the time of issue this report has not been published. Any author desiring to quote this paper should refer to it as "A paper of the Meteorological Research Committee (London), M.R.P. No.914 by Drs. J.T. Houghton and A.W. Brewer.
A copy is available in the Library of the Meteorological Office."

M.R.P. 914
S.C. III/185
28th April, 1955

AIR MINISTRY
METEOROLOGICAL RESEARCH COMMITTEE

Measurements of the flux of long wave radiation in the upper air 1953-54

by

J. T. Houghton and A. W. Brewer

As part of the programme of the M.R.C. and of the Gassiot Committee of the Royal Society a new radiometer has been made suitable for use from an aircraft, and measurements of the upward and downward flux of long wave radiation have been made at levels up to 40,000 ft. in night flights during the period 1953-54. It was necessary to fly at night as the radiometer used is also partly sensitive to short wave (solar) radiation.

Instruments.

(a) Radiometer.

The radiometer used has been described by Houghton and Brewer (1954). It was designed with the present measurements specifically in mind, and the radiometers were mounted in a M.R.F. Mosquito aircraft at places indicated in the photograph (Fig. 1(a)). For the later flights two radiometers using windows of different sizes and of different origin were mounted side by side in the upward facing position. This was done as a check on the errors involved.

The instrument indicates by a resistance measurement on a resistance bridge. This is an a.c. bridge with an electronic detector which was mounted in the cabin and the measurements were made by the meteorological observer. The different radiometers are selected in turn by a switch (Fig. 1(e)). The observation is not difficult but rather more care is needed than in the ordinary air temperature measurement by the standard balanced bridge thermometer. The temperature of the radiometer must also be measured in order to apply corrections to the radiometer readings. This was done with an auxiliary resistance thermometer and an ordinary balanced bridge indicator.

(b) Other meteorological observations.

Air temperature and humidity, upon which the radiation fluxes depend, were observed in the usual way by a standard M.O. balanced bridge thermometer and a Dobson-Brewer frost-point hygrometer. The cloud details were also noted by the observer as clouds have a very great effect on the fluxes. Normal variations in temperature and humidity which exist in the atmosphere set a serious limit to the accuracy of possible interpretation of any measurements of this kind and several flights were marred by complex cloud structures.

All observations were made at 3,000 ft. intervals.

Ozone concentrations were not measured during the flights. When the work was originally planned it was thought that this might be necessary and a simultaneous programme was undertaken by Dr. Kay to permit this.

/Dr. Kay's

Dr. Kay's results (M.R.P. 817) have, however, shown that the concentration of atmospheric ozone remains small up to levels well above 40,000 ft. and showed that simultaneous ozone measurements would not be necessary. We were glad to take advantage of this simplification of flight procedure.

The flights.

In addition to a preliminary flight in a Hastings aircraft nine ascents were made in the Mosquito aircraft. The nine ascents are listed in Table 1 which gives a brief statement of the results obtained from each flight. The results of ascent 8 are given graphically in Fig. 2.

It will be seen that teething troubles continued till ascent 6 and to some extent reduced the value of results up to that stage. Ascents 2 and 5 reached unusually cold tropopauses and in each case two of the rubber sealing rings in the radiometers froze and air leaked in. For ascent 6 silicone rubber sealing rings were used. These certainly remained soft down to low temperatures but appeared to be porous, for after the flight some air was found to have leaked into the radiometer. For later flights we reverted to standard rings without any further trouble as such low temperatures were not encountered.

The results.

The flux of radiation being a very complex function of the atmospheric structure the results can most simply be described by comparison with the flux which would be calculated using one of the standard radiation charts. "Elsasser's" chart is that described by him in his paper, Elsasser (1942), and "Yamamoto's" chart is described in Yamamoto (1952). Elsasser's chart makes no provision for the diminishing path length of CO_2 with height, but this becomes important at high levels. For this reason, above 1 Km. the CO_2 radiation has always been calculated according to Yamamoto's chart. It will be noted that for the purposes of comparison of observed and computed fluxes, we had the advantage not enjoyed by any other workers of having a simultaneous frost-point hygrometer ascent.

(a) The downward flux of radiation at low levels.

Below about 1 Km. Elsasser's chart can be used without modification and Robinson's (1950) results can be readily checked over a rather wider range of temperature and radiation flux than he obtained. We do not observe the systematic difference between the calculated (after Elsasser) and the observed flux at the low fluxes which Robinson described. Our observed points and Robinson's curve are shown in Fig. 3.

(b) The downward flux at various levels below 30,000 ft.

We have compared the measured flux with those calculated in various ways and the best agreement over the widest range of conditions below 30,000 ft. has been obtained by using Elsasser's chart to compute the water vapour radiation but with a pressure correction directly proportional to p, Yamamoto's chart for the radiation from the carbon dioxide, and multiplying the result by 1.2 (a factor which arises, in part at least, from different allowances for overlap between the two spectral bands of water vapour and CO_2). The accuracy of the result calculated in this way will depend chiefly upon the accuracy of the humidity data. Our results are shown plotted in Fig.4 as the difference between the observed radiation and that calculated in the above way, but without the application of the factor 1.2.

The upward radiation stream.

Patches of low cloud affect the upward radiation stream at all levels above the cloud, and all ascents except Nos. 5, 8 and 9 were affected in this way. Even on these there may have been a few patches of dispersing low cloud. The various pressure effects cannot be separated for the upward stream since most of the radiation originates at low levels, but the indications are that the

/chart

chart values are too small and that areas on the chart when multiplied by about 1.2 will give substantially the correct answer.

Clouds.

Dense clouds have always appeared to have emissivities of 100%. The emissivity of visible cirrus clouds is, however, very variable. For example, a very tenuous cirrus cloud present in a very deep layer - possibly 9,000 ft.- radiated very little more than would be expected from its water vapour - the additional grey emissivity certainly being less than 10%.

The emissivity of the ground.

On five of the ascents when successful measurements of the upward radiation were made, the values observed were consistently less than that to be expected if the earth's surface were a perfect black-body. The results indicated an emissivity for the ground of 90-95%. It would be valuable to make further measurements to confirm this, and also to find its variation with type of surface; in particular, measurements on snow-cover would provide interesting results.

The divergence of the radiation fluxes.

The cooling of the atmosphere by radiation is the main meteorological interest. To the sort of accuracy we are prepared to accept, calculated and observed divergences agree. The main feature of a general cooling of the clear atmosphere of 1 or 2°C/day is clearly shown, and also its fluctuations due to varying cloud and humidity patterns. Fig. 2 shows the calculated and observed divergences plotted as cooling rates in °C/day for 3,000 ft. layers as observed in ascent 8. The intense cooling of 9°C/day of the Sc at 3,000 ft. would occur near the ground if the cloud were absent, and the moist layer at 25,000 ft. has concentrated the divergence into itself which would otherwise have been spread out more uniformly.

If attempts are made to compute non-adiabatic cooling rates for introduction as correction terms in dynamic meteorology or numerical forecasting, the main errors will be due to the difficulty of prescribing the humidity and cloud patterns, - not due to errors in radiation charts - to which the divergence is far less sensitive.

The stratosphere.

The value of the observations in the stratosphere is unfortunately less than we had hoped. Since the radiation from ozone and CO_2 in the stratosphere is known with some confidence, and since the emissivities of small quantities of water have been measured it should be possible to determine the water content of the stratosphere from the downward flux at the tropopause. We would of course measure the "spectroscopic amount of water vapour." This is the quantity which would have the observed emissivity if it were at a pressure of 1000 mb.

Our observations are, however, very weak because at low temperatures and for small amounts of water vapour the emission is in the rotation band at wavelengths beyond 25μ , and our KRS5 window is opaque beyond about 40μ . Nevertheless using Cowling's (1950) data our observations suggest a spectroscopic water vapour content for the stratosphere which is less than 10μ , with a large probable error. Any value up to say 12μ would be possible.

For comparison we have actual measurements of the water content published by Barrett, Herndon & Carter (1950), who made three ascents to 30 Km., and Murgatroyd's (1954) results are available up to 50,000 ft. These last are regarded as entirely reliable, though, of course, the height range is limited. If we use a $\sqrt{p}$ correction to the water vapour contents, which Cowling (1950) suggests is better for the small quantities of water vapour concerned, the Barrett, Herndon & Carter data give a value of 20-40μ as the spectroscopic

/amount

amount of water in the stratosphere and Murgatroyd's results suggest 1 or 2μ -to be compared with our value which, as mentioned above, is from 0 - 12μ .

Acknowledgements.

All the fitting of the equipment into the aircraft was done by M.R.F. ground personnel and all the flights were carried out by M.R.F. air crew and observers. We are very grateful to the Director, Meteorological Office, for permitting this work to be carried out, and for the very pleasant and willing assistance which we received from Mr. R.J. Murgatroyd and every member of the flight, without which the work would not have been possible.

References.

Barrett, E.W., Herndon, O.R. and Carter, H.J., 1950, Tellus, 2, 302.
Cowling, T.G., 1950, Phil. Mag., 41, 109.

Elsasser, W.M., 1942, Harvard Met. Studies, No. 6.

Houghton, J.H. and Brewer, A.W., 1954, J.Sci.Inst., 31, 184.
Murgatroyd, R.J., 1954, M.R.P. 877.
Robinson, G.D., 1950, Quart. J.R. Met.Soc., 76, 37.

Yamamoto, G., 1952, Sci.Rep.Tohuka, Univ. Geophys., 4, 9.

Table 1

Flights		
Ascent 1.	13.8.53	One upward facing radiometer only. Calibration against a black-body changed after flight.
Ascent 2.	12.8.53	4-6/8 Sc clearing during flight, some Ac and 8/8 Cs. An intermittent fault in the electronics made some readings unreliable. Air leaked into both radiometers at 36,000 ft.
Ascent 3.	23.2.54	Small patches Sc and perhaps some thin Ci at 20,000 ft. Both radiometers changed their calibration against a black-body after flight.
Ascent 4.	6.4.54	4-5/8 Sc in large patches gradually dispersing. Interpretation of the upward flux measurements above 8,000 ft. impossible on account of patchiness in the cloud. Three radiometers carried, all worked satisfactorily.
Ascent 5.	13.4.54	A few patches of Sc dispersed during flight but did not seem to affect the upward flux measurements. Two of three radiometors developed leaks at 36,000 ft. Some trouble experienced with the hygrometry.
Ascent 6.	2.7.54	Patches of Sc around 3,000 ft. dispersing during flight. Thin Ac or As 12,000 - 18,000 ft. and perhaps little Ci around 30,000 ft. One radiometer calibration did not repeat accurately after flight. One radiometer using a silicone rubber seal developed a small leak which might have affected results.
Ascent 7.	7.7.54	4/8 medium cloud present which made all readings except those at highest level difficult to interpret. All instruments worked well.
Ascent 8.	20.7.54	8/8 Sc 2,000-4,000 ft. and tr very thin Ci. All instruments worked well. This ascent is illustrated (Fig. 2).
Ascent 9.	21.7.54	Tr Sc on horizon, none over Farnborough where ascent was made. All instruments worked well.

(a) MOSQUITO AIRCRAFT (POSITIONS OF RADIOMETERS INDICATED BY ARROWS

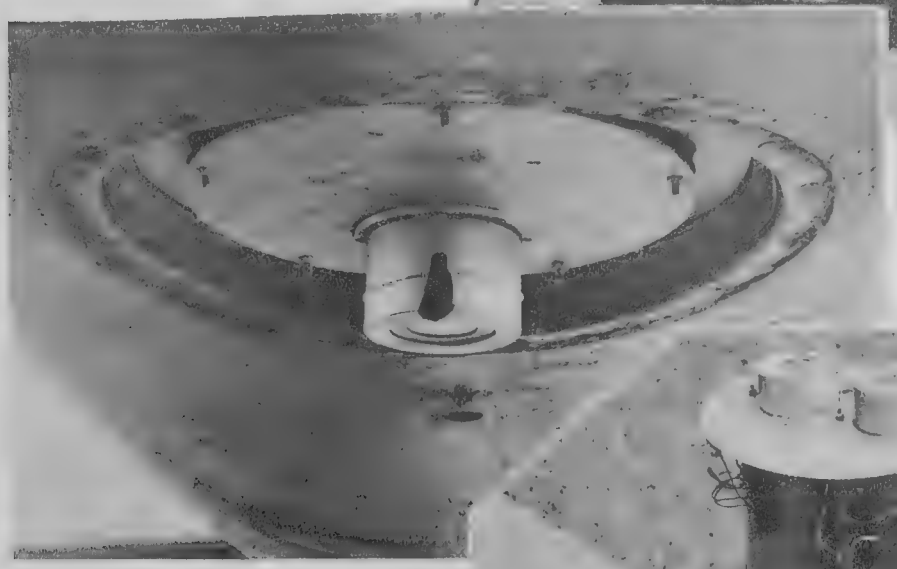

(b) DOWNWARD-FACING RADIOMETER

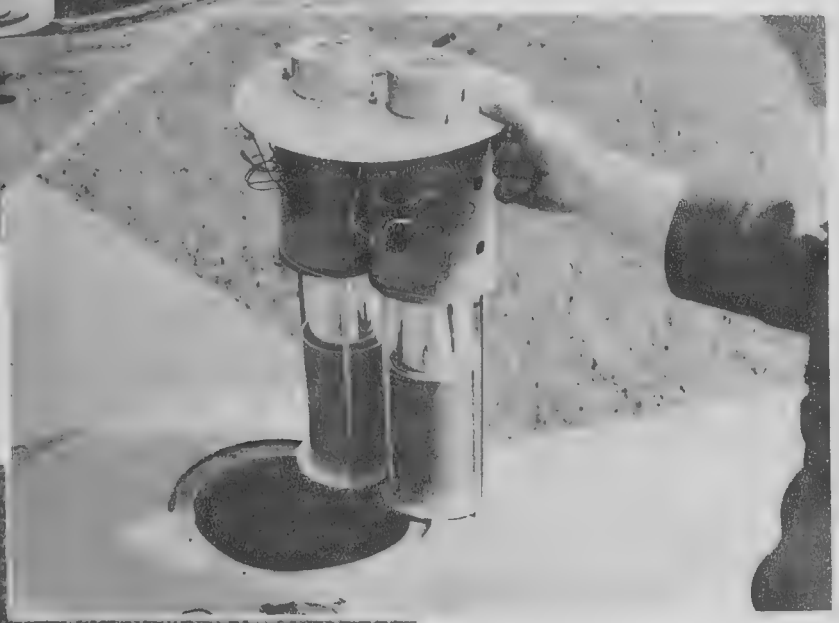

(c) UPWARD-FACING RADIOMETERS

(d) UPWARD-FACING RADIOMETERS

(e) MEASURING BRIDGE IN CABIN OF AIRCRAFT

FIG. 1

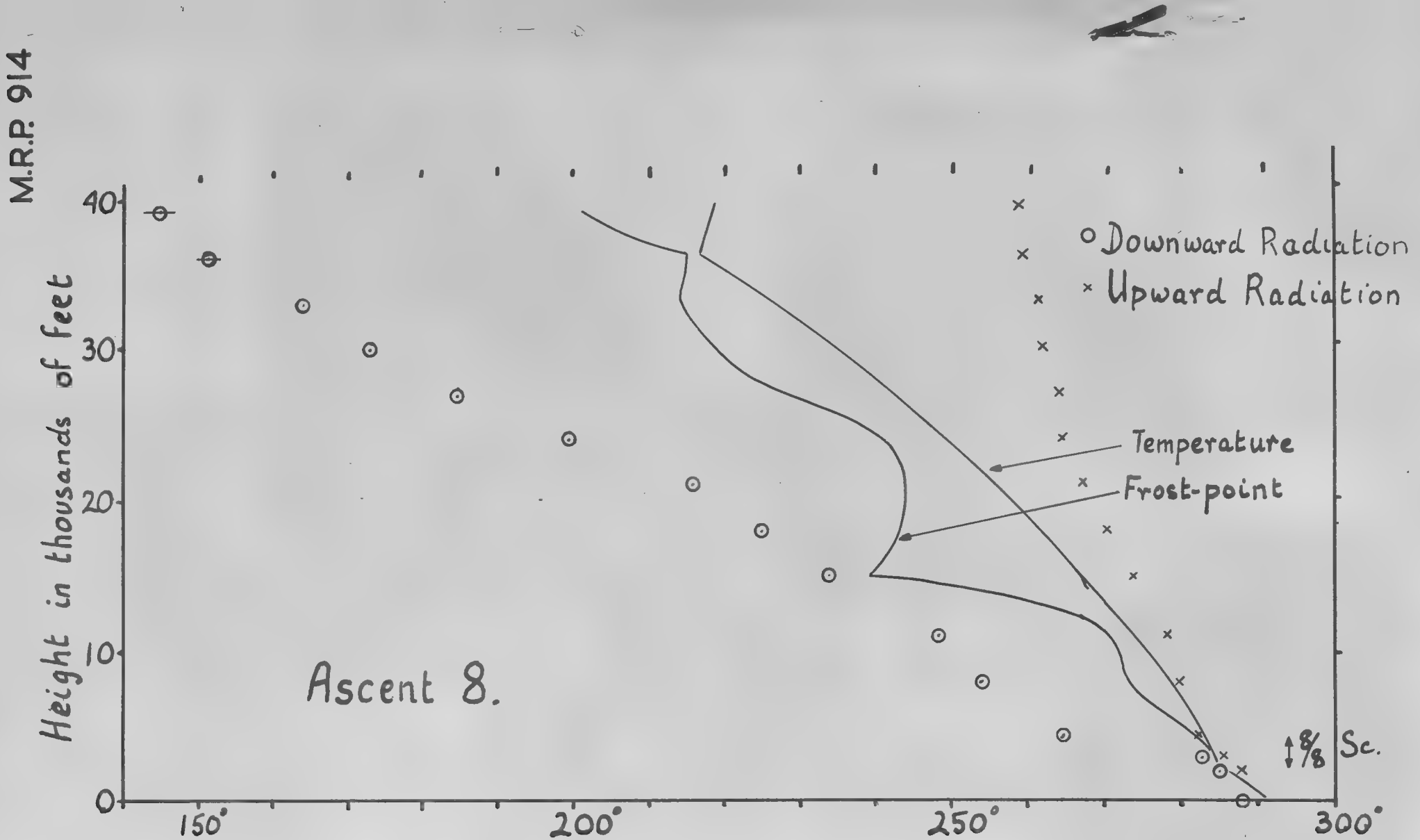
M.R.P. 914
Height in thousands of feet
40
30
20
10
0
150°
200°
250°
300°
Temperature °K.
Ascent 8.
Downward Radiation
Upward Radiation
Temperature
Frost-point
8/8 Sc.

Figure 2a

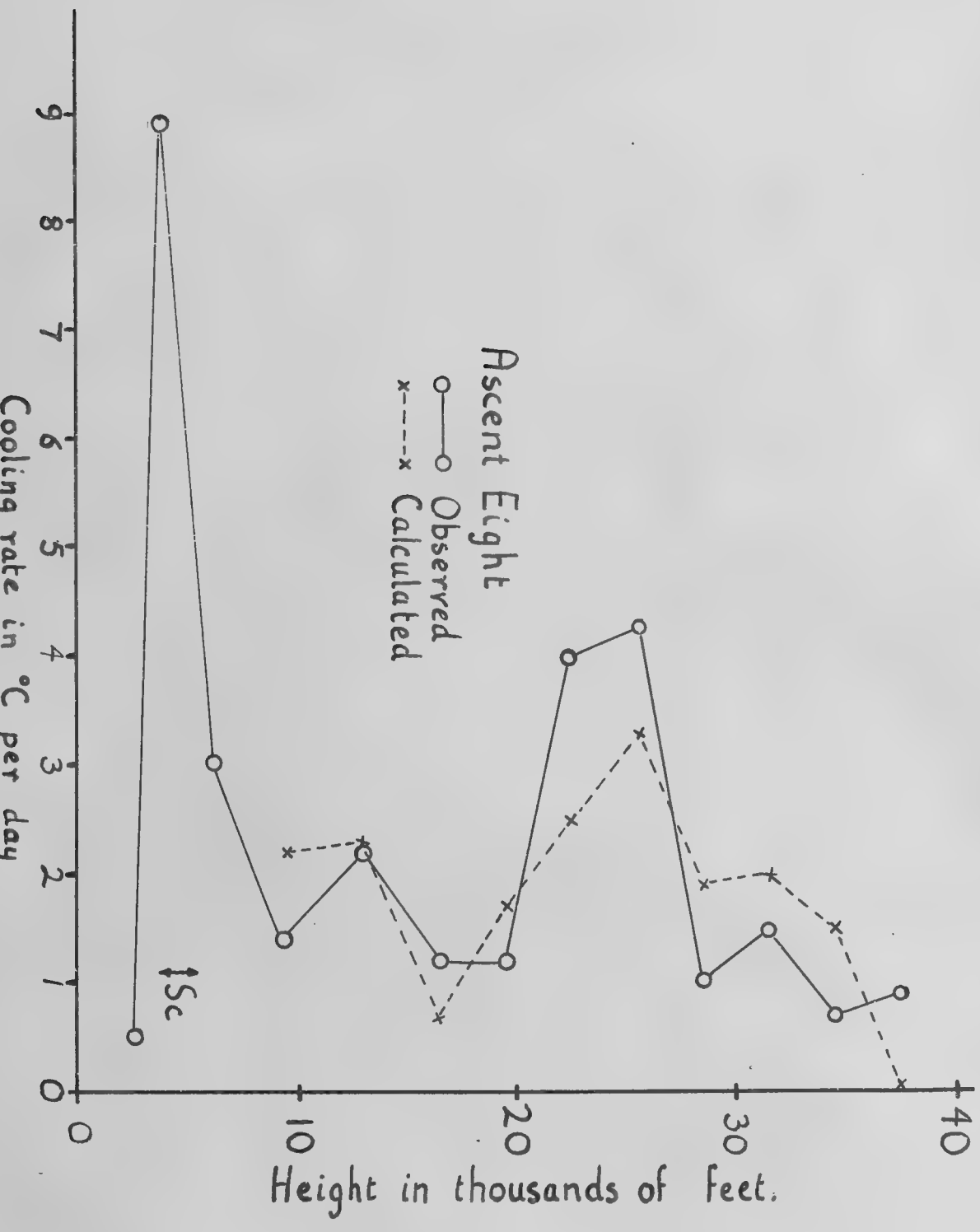
Ascent Eight
Observed
Calculated
15c
Cooling rate in °C per day
Height in thousands of Feet.
0
1
2
3
4
5
6
7
8
9
0
10
20
30
40

Figure 2 b.

M.R.P. 914

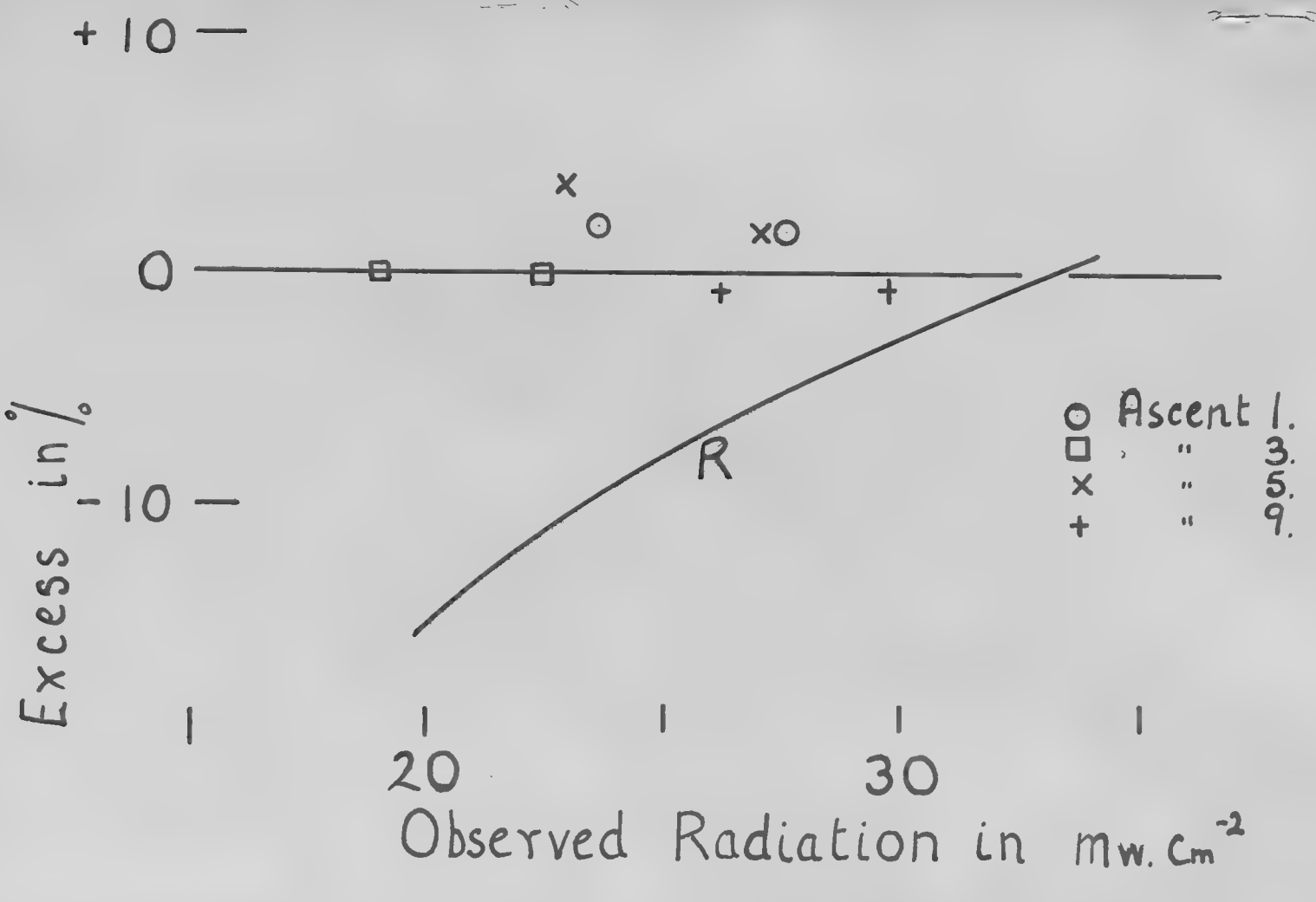

Excess of observed radiation over that calculated using Elsasser's chart. R shows Robinson's results.

Figure 3.

M.R.P. 914

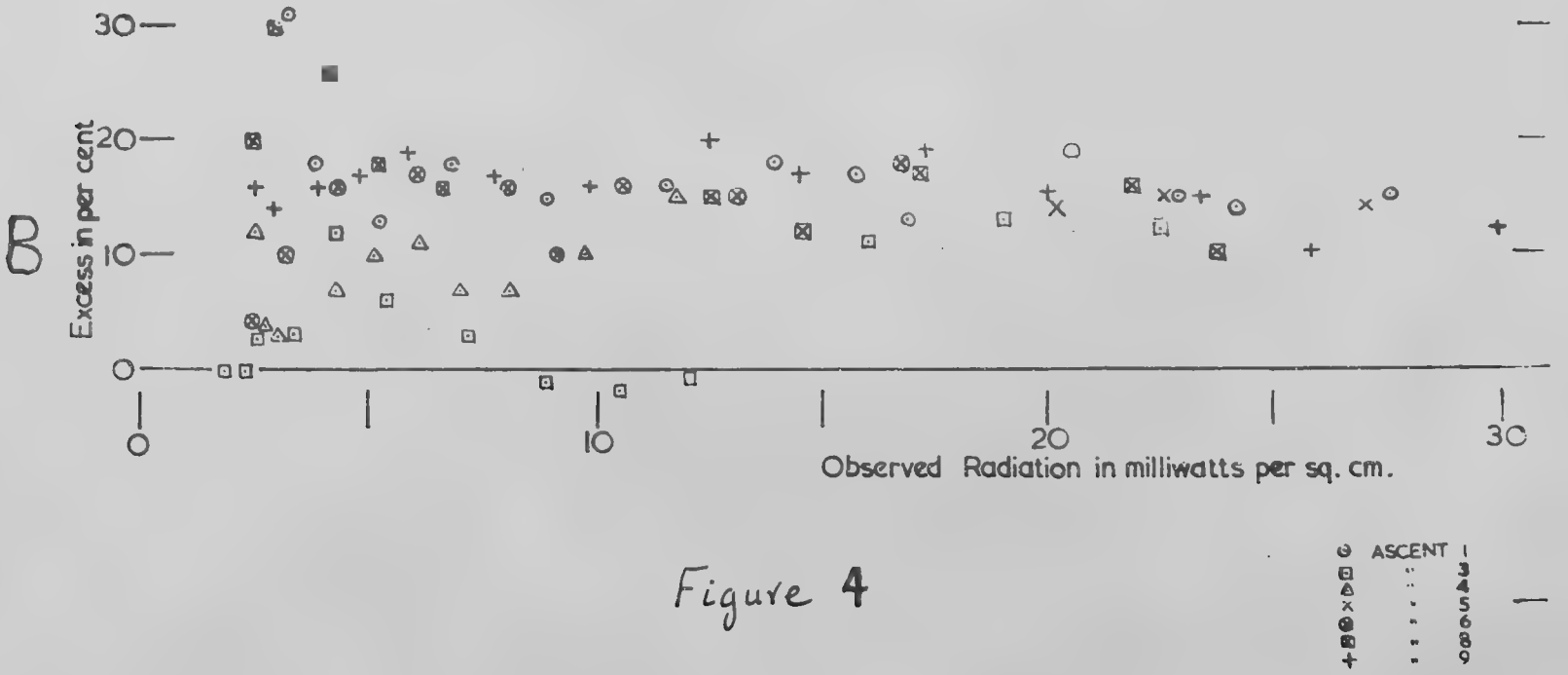

Figure 4

M.R.P. 915
S.C.11/188
29th April, 1955.

AD131

The representation of the annual temperature variation over Central and Northern Europe by a two term harmonic form.

by

J.M. Craddock
(Meteorological Office)

AWSSS
ROUTING SLIP

FILE	INFO	ACTION	
	1		NTS CRD WS JH.
	2		SEC
	3	EDD	CHF HLFB STB SPFB
	4		INFO SEC

AIR MINISTRY
METEOROLOGICAL RESEARCH COMMITTEE

At the time of issue this report has not been published. Any author desiring to quote this paper should refer to it as "A paper of the Meteorological Research Committee (London). M.R.P.No. 915 by Mr. J. M. Craddock A copy is available in the Library of the Meteorological Office."

M.R.P. 915
S.C.II/188
29th April, 1955.

AIR MINISTRY

METEOROLOGICAL RESEARCH COMMITTEE

The representation of the annual temperature variation over Central and Northern Europe by a two term harmonic form

by

J.M. Craddock (Meteorological Office)

Summary

A harmonic analysis is made of the annual temperature variation at 42 stations spread over Central and Northern Europe, using in each case 5-day mean temperature averaged over a considerable number of years. It is found that the first two harmonics account for nearly all the annual variance, the residual variance being usually less than 0.4 per cent of the total. Most of this residual variance seems to be random in origin, but a small part may be due to systematic departures from the two term harmonic form.

In about 10 of the 73 5-day periods which cover the year, it is found that departures from the two term harmonic form are in the same direction at nearly all the stations considered, and similar departures are found in the same periods in data for independent periods of years.

1. Introduction

The present paper covers some of the groundwork of Item II.5(b) of the Meteorological Research Programme "Studies of the variations of weather conditions over the British Isles with "periods" of up to about one month, and their relationships with the large scale circulation". A natural approach to this problem is to choose as many cases as possible in which some weather element takes an extreme value, for example, periods of unusually cold weather in the British Isles during spring and find as much as possible about them; how far does the cold weather extend, and how long does it last, and is it accompanied or preceded by abnormalities in the values of any other weather elements, especially in any element indicative of the state of the general circulation? To answer these questions we must know the normal values of the weather elements, not only for the British Isles, but for an area covering at least a large sector of the Northern Hemisphere, and for unit periods, not of calendar months, but of much shorter periods of only a few days. Finally, when we have prepared our anomaly charts, we may find, for example, that cold periods in spring in London are usually preceded by unusually high pressure in Greenland. Out of the myriad of such possible relations we have to select those which are statistically significant, and may be expected to recur in the future. The process of separating the significant relationships from the casual is a necessary and inescapable part of the research, and to do it we have to have representative normal values of the weather elements over the whole vast area which concerns us. For most of the area the only basic observations we have to go on are daily synoptic observations plotted on charts, and tabulated monthly mean values, and neither source will yield directly what we want, namely, mean values and standard deviations, (or other suitable measures of variability) for periods of less than one month for a network of stations covering a large part of the Northern Hemisphere. The weather elements which interest us include

/surface

surface pressure, surface temperature, rainfall, sunshine and upper air temperature and we have to estimate the normal value of any of these for periods of only a few days. Such estimates may be made subjectively, based on observed monthly means, but this introduces an avoidable source of error. Instead we propose to use harmonic analysis to find the normal form of the annual variation of each meteorological element, and hence the normal value for any day or period of days.

The problem can be dealt with in three stages, namely

(1) an investigation of daily values of the element concerned, to find how many harmonic terms must be taken to obtain an acceptable fit,

(2) a harmonic analysis to find the required number of terms from observed monthly mean values for each station we wish to use, and

(3) a harmonic synthesis to obtain the normal value for any period which interests us.

The present report covers the first stage of the investigation of the first element studied, namely, mean daily air temperature. The second and third stages will be covered in a later paper. The processes used can be applied to other weather elements with only slight modifications.

We propose to fit the annual temperature variation by an expression of the form

$$T = a_0 + \sum_{j=1}^{N} (a_j \cos j\theta + b_j \sin j\theta) \qquad \text{----------} \quad (1)$$

where θ increases by 2π during the year, and in this work is measured from zero at midnight on December 31st. (The year is regarded as having exactly 365 days, February 29th being ignored in leap years.) An expression of the form given can, of course, be made to fit any series of observed data by taking N large enough, but we have no justification for seeking an exact fit to any series obtained by averaging observed temperatures over a finite number of years. The mean of the temperatures observed during a finite number of years will differ from the hypothetical normal by a sampling error depending on the variation between one year and another, and the normal form of the annual temperature variation will be given as accurately as the data will allow by any function which does not differ from the observed averages at any time of year by amounts which singly or collectively exceed the limits fixed by the hazards of sampling.

If we do fit exactly a series of observations covering a year, and V(T) denotes the variance of temperature during the year, then a standard theorem states that

$$V(T) = \tfrac{1}{2}(a_1^2 + b_1^2 + a_2^2 + b_2^2 + \ldots\ldots) \qquad \text{----------} \quad (2)$$

Thus we can, by calculating expressions such as $V(T) - \tfrac{1}{2}(a_1^2 + b_1^2)$, decide how much of the total variance is due to the first harmonic, or due to whatever combination of harmonics we have chosen to calculate, and since these expressions are essentially positive, we can fix an upper limit on the amplitude of any harmonic we have not calculated so far. This relation is useful in showing us where to stop.

/2.

2. Data and method

For completeness, the investigation should start with daily mean temperatures for every day of the year. However, an investigation which started on these lines would be handicapped by the labour involved, and by the difficulty of finding enough suitable data. There are, however, many publications containing mean temperatures for the 73 non-overlapping 5-day periods which cover the year, and it is unlikely that any temperature anomaly which is smoothed out by averaging over a period as short as five days will recur on the same day from year to year. So the present investigation was based on 5-day mean temperatures, in the expectation that any significant and annually recurring feature of the sequence of daily mean temperatures would also be present in the 5-day means. Table 1 gives particulars of the stations used, and the sources from which the data were obtained.

3. The calculation

The calculation of harmonic coefficients from 73 equally spaced observations is not difficult, but it is laborious and hard to check. The formulae are,

$$a_k = 2/73 \sum_{j=1}^{73} T_j \cos \theta_j \quad \text{----------} \quad (3)$$

and

$$b_k = 2/73 \sum_{j=1}^{73} T_j \sin \theta_j \quad \text{----------} \quad (4)$$

where k=0,1 or 2 and T_j, θ_j are the observed mean temperature and the angle corresponding to the j^{th} 5-day period of the year. Here θ_1 is the angle corresponding to the middle of the first 5-day period, Jan. 1st to 5th. The values of $\cos \theta_j, \sin \theta_j$ are given by Pollak (1948) and these were multiplied by the factor 2/73 and incorporated in a special computing form prepared in M.O.22, of which a specimen is shown in Fig.1(a). The 5-day mean temperatures are written into another form shown in Fig.1(b) which also contains spaces for all numbers required in calculation. Corresponding columns on the two forms are brought together and the products are formed and summed on a desk machine. Experience shows that arranged in this way the calculation is reasonably easy to check. For about 8 stations the harmonic analysis was carried out in this way: later, data for 34 more stations were analysed by punched card methods, taking advantage of facilities for processing the cards offered by Rothamsted Experimental Station. In Table 2 are given the coefficients of the first two harmonics for each set of data, the total annual variance, and the residual variance after subtracting that due to the first two harmonics.

4. The geographical variation of the harmonic parameters

The semi amplitude and phase of the first and second harmonics are shown in Figs.2 (a) to 2(d). Besides the parameters calculated in the present work values have been obtained from two other sources. The parameters for 18 Norwegian stations are given by Birkeland (1936) while those for 160 stations in the British Isles have been calculated in M.O.22. These values which are computed from monthly mean temperatures are somewhat less reliable than those computed from 5-day mean temperatures. In Fig.2(e) are given the names and positions of the original stations and those used by Birkeland, together with their altitudes and mean annual temperatures. Fuller information about the stations used by Birkeland is given in Tables 1(a) and 2(a).

/Fig.2(a)

Fig.2(a) shows the semi amplitude of the first harmonic. The amplitude increases generally towards the east, but there is a striking difference between the rapid increase as the Norwegian mountains are crossed compared with the much slower increase across the North German plain. In Fig.2(b) the phase of the first harmonic is given by the calendar date on which the maximum is attained. The German data show with surprising consistency that the phase is earlier in the interior of the Continent than in coastal regions. This association is borne out by the dense network of stations over the British Isles, which shows, moreover, that the change of phase is most rapid in a belt of perhaps 20 or 30 miles inland from the coasts. The four German stations which are bracketed are mountain stations, and at these the amplitude is smaller and the phase later than at nearby stations at lower altitudes. In these respects the mountain stations seem to have a more maritime climate than their neighbours. Figs.2(c) and 2(d) give the semi-amplitude and phase of the second harmonic. The data are self consistent enough to suggest that the variations shown are not due to chance, but we can hardly from these data alone suggest what the cause or large scale character of the variation may be. The variations of the harmonic parameters with geographical situation and with altitude deserve further study, using more stations spread over a larger area.

5. The magnitude of the residual variance

The residual variance is given in Table 2 both in absolute units, ($^{o}C^{2}$) and expressed as a percentage of the total annual variance. It seems to be disproportionately large at three of the four mountain stations, and if we exclude these its value is never greater than 0.23 $^{o}C^{2}$, and in some places is as low as 0.05 $^{o}C^{2}$. Expressed as a percentage, the residual variance, except at the mountain stations, is generally less than 0.4 per cent. These figures give an upper limit to the order of magnitude of the errors we accept if we assume that the annual march of temperature is given by the best fitting two term harmonic form.* For some purposes these errors may be negligible, for example, in long range forecasting, the errors in predicting the future value of the temperature anomaly on a given day will probably far exceed the errors in predicting the normal temperature for that day. At any rate the investigator, knowing their probable magnitude, can decide whether to ignore them or not.

These results complete the main purpose of the paper, which is to give some idea what to expect if the annual temperature variation is assumed to follow the two term harmonic form. The rest of the paper sets out to find a little more about the way in which the residual variance is made up. The data are not very suitable for this purpose, and the work does not claim to be exhaustive, but simply to examine some of the more obvious indications which may be extended and confirmed by later more extensive and laborious investigation.

/6.

* The corresponding values in Fig.2(a) give for Birkeland's Norwegian data the corresponding errors involved in omitting the third to sixth harmonics - they are mostly lower than our estimates of the total residual variance, as is to be expected.

6. The dependence of the residual variance on the place and the period over which the data are averaged

Suppose we make a two term harmonic analysis of the 5-day mean temperatures for one station for each of a number of years, and then do the same for the same data averaged over, say, 30 years. The harmonic coefficients for the 30-year mean data would be the mean of those for the individual years, and while they will show some sampling variation, depending on which 30 years are chosen, this variation will probably be small. In any case, we cannot investigate it with our present data, which consist only of the mean values for long periods of years, and not the temperatures for 5-day periods of the individual years. The residual variance for each single year may be made up of two parts, A which measures the departure of the individual year from the true normal, and B, which measures the departure of the true normal from the best fitting two term harmonic form. Experience suggests that in an individual year A is far larger than the value found in Section 5 from the mean of many years, and also that the departures in one year do not bear any easily recognisable relation to those in any other year. It is a reasonable hypothesis that A is a random variable. If so, and if we write V(n) for the residual variance for data averaged over n years, then

$$V(n) = A/n + B \qquad (5)$$

or

$$nV(n) = A + Bn \qquad (6).$$

These equations suggest that V(n) should tend to decrease as n increases (and the values in Table 2 suggest this), while nV(n) should either be constant or should tend to increase with n. Except for Halle and Prague, we have only one value of nV(n) for each station, and these are plotted against n in Fig.3, while their geographical distribution is shown in Fig.4. The mountain stations (ringed) do not agree with the rest and if these are omitted, then Fig.3 does suggest some slight increase of nV(n) with n. The regression line giving the best estimate of nV(n) in terms of n is

$$nV(n) = 12.1 + 0.14n \qquad (7)$$

but the coefficient of n on the right hand side is not significantly different from zero. Turning now to Fig.4, there is a strong suggestion of a geographical variation of nV(n) with a maximum in central and north-western Germany. Most of the 80-year mean values on Fig.3 come from German stations, so this geographical variation accounts for some and perhaps all of the apparent increase of nV(n) with n. To sum up, the data are consistent with the residual variance in each individual year being an entirely random quantity, but they are also consistent with the existence of slight systematic departures of the true form of the annual temperature variation from the two term harmonic form. If such systematic departures exist, their contribution to the total annual variance averaged over these stations is probably less than 0.14 per cent. If in Equation (7) we put n equal to 50 or less, the first (random) component of the residual variance will outweigh the second, so that when we are estimating temperature normals from records covering less than 50 years, and in particular, if we are using data for the internationally agreed period of 30 years, the two term harmonic form will give as accurate an estimate of the normal temperature as the data themselves will justify.

7. Departures from the two term harmonic form at particular times of year

Even if departures from the two term harmonic form are not important on the average in estimating the normal temperature they may be important at particular times of year, and they are of interest in themselves, even if very small, provided they can be shown to be systematic and permanent, since they may focus attention on periods of the year when synoptic situations peculiar to the season are to be expected.

/The

The nature of these departures is shown in Fig.5 which shows superimposed curves of the observed mean temperature and the best fitting two term harmonic form for eight stations spread over the area covered by the observations. The horizontal scale, which is the same for all stations, gives the time, in 5-day units, numbered from the beginning of the year, while the vertical scales, which are in degrees Celsius, have been separated to avoid confusion. Thus anomalies for different stations for the same period appear in the same vertical line. It appears that the anomalies for any station for consecutive 5-day periods are serially correlated: in cases worked out later (Table 6) the first serial correlations are mostly between 0.5 and 0.7. There is also a suggestion of spatial correlation: that is, the anomaly at a particular period of the year tends to have the same sign over a large part or the whole of the area for which we have data. These temporal and spatial correlations are what we would expect if the anomalies are due, not to fortuitous or local effects, but to large scale features of the atmospheric circulation, and they must be allowed for when we decide on the statistical significance of the anomalies. For example, a single exceptional winter may produce a substantial negative contribution to the temperature anomalies for stations over a large area for several consecutive periods, and if we treat all these anomalies as independent we will arrive at a wholly unjustified degree of confidence that similar anomalies will repeat themselves in future. However, to start with, we will examine the eight records to see what they suggest, without at this stage trying to show whether these suggestions are significant. The features which deserve further investigation are given in Table 3.

Table 3. 5-day periods in which the temperature anomalies are remarkably consistent in sign at the 8 stations

Number of period	Direction of anomaly	Where present
No. 1	Warm	All except Tilsit
No. 2	Warm	All except Glasgow
No. 7	Warm	All 8 stations
No. 9	Cold	All except Kew and Glasgow
No. 15	Cold	All 8 stations
No. 19	Warm	All 8 stations
No. 24	Cold	All except Uppsala and Tilsit
No. 29	Warm	All except Vienna and Glasgow
No. 30	Warm	All 8 stations
No. 31	Warm	All except Uppsala
No. 33	Cold	All except Tilsit
Nos. 34	Cold	All except Glasgow
35	Cold	All 8 stations
No. 55	Warm	All 8 stations
No. 60	Cold	All except Tilsit and Uppsala
No. 62	Warm	All except Potsdam
No. 64	Cold	All except Uppsala
No. 65	Cold	All 8 stations
No. 73	Warm	All except Glasgow and Uppsala

If the anomalies at the eight stations were unrelated, then the expectation that all eight for a given period should agree in sign is 1/128, and the

/expectation

expectation that seven of the eight should agree is 1/16. Thus when we examine 73 periods we would expect to find perhaps one period in which all eight agree, and four or five periods in which seven of the eight agree. In fact there are seven periods in which all eight agree, and seven others in which seven of the eight agree, so there is a presumption that the agreements are not wholly due to chance. This presumption is increased when we note, from Table 3, that the exceptional stations, when seven of the eight agree, are nearly always stations on the edge of the area considered, namely, Glasgow, Uppsala or Tilsit. This feature is explicable if the weather processes which produce the anomalies are on a scale usually not quite big enough to affect the whole of this area in the same way.

If it is accepted that during the period to which most of these data relate (the 80 years 1851 to 1930) there are significant departures over this area from the two term harmonic form, we yet have to consider whether these are likely to be parmanent, or to arise from the peculiarities of that particular period. The features likely to be permanent at a place should be identifiable by comparing two records for that place for independent periods of years. Such records are not easy to find, but two have been found, namely, for Prague (Fig.6) and for Halle (Fig.7), while there are also mainly non-overlapping records for two pairs of stations which are sufficiently close for us to presume that they will be affected alike in any large scale process. These pairs are Edinburgh and Glasgow (Fig.8) and Brussels and Kleve (Fig.9).

When we compare the anomalies for the periods listed in Table 3 with those in Figs.6 to 9, we find that in most cases the anomalies are repeated in the records for independent periods of years. In particular it is hardly possible to doubt that for the periods listed in Table 4 the anomalies are systematic and permanent departures from the two term harmonic form.

Table 4

Number of 5-day period	Dates	Direction of anomaly	Remarks
No. 7	Jan. 31 - Feb. 4	Warm	Present in every record, though very small in one or two.
No.15	Mar. 12-16	Cold	Present in all except Edinburgh 1795-1850
No.19	Apr. 1-5	Warm	Present in all except Prague 1775-1839
No.29	May 21-25	Warm	Present in all except Vienna and Glasgow, where it is zero.
No.30	May 26-30	Warm	Present at all stations
No.31	May 31 - June 4	Warm	Present at all stations except Prague and Uppsala
No.35	June 20-24	Cold	Present at all except Brussels 1831-1860
No.55	Sept.28 - Oct.2	Warm	Present in all stations
No.64	Nov.12-16	Cold	Present at all except Uppsala
No.65	Nov.17-21	Cold	Present at all stations

One other deduction can be made from Figs.6 to 9. If these anomalies are partly non-random in origin, then there should be a positive correlation between the anomalies found from comparable records for non-overlapping periods of years. These correlations are given in Table 5.

/Table 5.

Table 5. Correlations between anomalies for wholly or mainly independent periods of years

First station	Second station	Correlation
Glasgow 1868-1912	Edinburgh 1795-1804 and 1821-1850	0.05
Brussels 1831-1860	Kleve 1851-1930	0.35
Prague 1775-1839	Prague 1840-1934	0.29
Halle 1851-1900	Halle 1901-1950	0.29

The correlation between the anomalies at Edinburgh and Glasgow is evidently not significant: the significance of the other three must be judged in the light of the auto-correlations which exist in the various series of anomalies, the first serial correlations of which are given in Table 6.

Table 6. Auto-correlations of multi year averages of 5-day mean temperatures

Station	Period	Correlation
Glasgow	1868 - 1912	0.15
Edinburgh	1795-1804 and 1821 - 1850	0.46
Kleve	1851 - 1930	0.56
Brussels	1831 - 1860	0.49
Prague	1775 - 1839	0.72
Prague	1840 - 1934	0.56
Halle	1851 - 1900	0.45
Halle	1901 - 1950	0.47

Clearly we cannot treat the correlations given in Table 5 as derived from 73 independent pairs of observations. An estimate following the lines of work by Lewis and McIntosh (1952) gives the "equivalent number of repetitions" as between 3 and 5, so that the correlations in Table 5 may be judged as based on from 15 to 25 independent pairs of observations. On this basis none of them is significant even at the 10 per cent level. However, the three values for the continental stations are large enough to be suggestive, particularly as the periods of the three comparisons are virtually independent. The absence of association between the anomalies for Edinburgh and Glasgow agrees with the conclusion of Brooks and Mirrlees (1930) who made a similar comparison between temperature anomalies at Kew for the periods 1870-1900 and 1901-1929, so there is a possibility that persistent temperature anomalies may occur over the Continent of Europe without extending to the British Isles.

8. The significant temperature anomalies

It would be premature to attempt a full scale discussion of the temperature singularities listed in Table 4. The network of stations was not chosen to show the significance of singularities and there is no guarantee that this list is complete. Nevertheless, it is worthwhile to consider what has been proved, and some possible directions of future investigation. In the first place, the

/hypothesis

hypothesis that the temperature anomalies are due to local causes independent for each station and period is decisively disproved. On this hypothesis the occurrence of an anomaly of given sign in corresponding periods in each of the 15 records shown in Figs. 5 to 9 should occur only once in 2^{15} investigations, and the number of cases of complete or near complete agreement among the 73 comparisons actually made is far greater than the chance expectation.

Looking now at Fig. 5, no one would have been surprised to find the amount of agreement between the anomalies which actually exists had the stations been spaced, say, within a 50-mile radius. What is interesting is that the anomalies should agree to the extent which they do over an area extending from London to the Baltic. It seems that the processes which produce these anomalies work on a scale rather larger than that of a European country, and approaching the size of the half waves in the general westerly circulation. Further, it appears as if most of the region considered has some kind of climatic homogeneity since when the anomaly in a given period has the same sign at all except one station, the exceptional station is usually one on the northern or eastern borders of the area. If we had to outline the area in which this homogeneity might be expected, we should exclude Glasgow, Edinburgh, Uppsala and Tilsit, but include Kew, Potsdam, Vienna, the whole of Germany, and an area to west of the Rhine not covered by present observations.

9. A particular singularity

The most obvious feature in the cycle is the occurrence of positive anomalies in late May and the first few days of June, followed by negative anomalies in late June. This succession is clearly seen on Fig.5, for example, in the records for Darmstadt and Potsdam, but it occurs in each of the records within the area described above, and is responsible for three of the widespread anomalies listed in Table 4. The magnitude of the temperature anomaly is largest in the German records, where the positive and succeeding negative anomalies may be nearly 1°C. At Kew the anomalies are similar but a good deal smaller, while they are very small at Edinburgh and Glasgow. At Tilsit and Uppsala the anomalies are smaller and the change from positive to negative anomalies is smoother and less abrupt than at the Central European stations.

This singularity is evidently a phenomenon primarily affecting Central Europe, and becoming less important as we go north and east.

In any part of the world, the climate at a given time of year is the result of several weather types, some warmer, and some colder than the average, and to get an average 5-day mean temperature anomaly of 1°C, which is the figure actually attained in Central Europe, must mean a considerable excess of warm weather types in May followed by an excess of cool types in June. Thus the singularity in Central Europe implies a tendency of features of the large-scale circulation to persist in fixed positions during the months of May and June, and if this happens in Central Europe, the weather conditions over the British Isles will be materially affected by it. Hence the weather during these months in the British Isles may be influenced by the processes producing a temperature singularity which is most strongly developed in Central Europe.

In this case it is easy to suggest a physical cause for the singularity, namely, a monsoonal effect arising from the solar heating of the European land mass, but if we are to forecast the character of the phenomenon from year to year, we should probably look at the area where it is most intense, namely, Central Europe, rather than a marginal region such as the British Isles, to find what makes it slight or vigorous, late or early.

10. Discussion

The first part of the investigation shows that over the large area examined the annual temperature variation can be represented for most purposes by two

/harmonic

harmonic terms. This conclusion has been used in a later paper in which normal temperatures at 5-day intervals throughout the year are given for a network of stations covering the entire Northern Hemisphere. The methods used have been programmed for electronic computation, so that the work can be repeated with slight modifications for every weather element we wish to investigate, and we intend to do this as time permits. Further work projected will deal with the variability of weather elements at any given time of year, and this should complete the statistical ground-work for the attack on the problem of weather anomalies.

The second part of the investigation, which suggests that the annual temperature variation shows small persistent departures from the two term harmonic form at particular times of the year, is an unexpected by-product of the first. The question whether these departures will recur in the future cannot be settled beyond doubt from the present evidence, but there is no doubt that during the period covered by the historical record some of the departures occurred at the same time over a very large area, on the same scale of the half waves of the planetary circulation. We cannot, of course, deduce that disturbances of the planetary circulation are prone to occur in particular areas at particular times of the year, but at least the evidence is consistent with the existence of such disturbances.

References

Birkeland	1936	Geofysiske Publikasjoner, Vol. XIV, No. 1: Utgitt av det Norske Videnskaps - Akademi i Oslo.
Brooks and Mirrlees	1930	Quart. J.R.Met.Soc., London, Vol. LVI, p. 375.
Forbes	1860	Trans. Roy. Soc., Edin., Vol. XXII, part II, p.327.
Hlavac	1937	Prager Geophysikalische Studien, Vol. VIII, Teil 1.
Lewis and McIntosh	1952	Met. Mag., London, Vol. 81, p. 242.
Pollak	1948	Harmonic analysis and synthesis schedules, Dublin Meteorological Service.
Quetelet	1867	Memoire de l'Academie Royale Belgique, 36.

Table 1. The stations used

Station	Latitude	Longitude	Altitude m.	Period over which data are averaged	Source of data
Augsberg	48°22'N	10°54'E	502	1851-1930	Deutsche Klimakünde
Bayreuth	49°57'N	11°34'E	364	1851-1930	Deutsche Klimakünde
Berlin	52°31'N	13°22'E	62	1851-1930	Deutsche Klimakünde
Breslau	51°07'N	17°02'E	147	1851-1930	Deutsche Klimakünde
Brussels	50°52'N	04°23'E	39	1831-1860	Quetelet (1867)
Brocken	51°48'N	10°37'E	1150	1896-1930	Deutsche Klimakünde
Darmstadt	49°53'N	08°40'E	150	1851-1930	Deutsche Klimakünde
Dresden	51°04'N	13°46'E	112	1851-1930	Deutsche Klimakünde
Edinburgh	55°57'N	03°15'W	76	(1795-1804 (1821-1850	Forbes (1860)*
Emden	53°22'N	07°12'E	8	1851-1930	Deutsche Klimakünde
Erfurt	50°58'N	11°04'E	218	1851-1930	Deutsche Klimakünde
Frankfurt a.O.	52°20'N	14°35'E	57	1851-1930	Deutsche Klimakünde
Friedrichshafn	49°39'N	09°29'E	408	1851-1930	Deutsche Klimakünde
Glasgow	55°52'N	04°17'W	56	1868-1912	M.O.M. Vol.III
Görlitz	51°10'N	15°00'E	217	1851-1930	Deutsche Klimakünde
Gütersloh	51°55'N	08°23'E	81	1851-1930	Deutsche Klimakünde
Halle	51°29'N	11°59'E	94	1851-1930	Deutsche Klimakünde
Halle	51°29'N	11°59'E	94	1851-1900	Met. Zeitschrift
Halle	51°29'N	11°59'E	94	1901-1950	Met. Zeitschrift
Hohenpeissenberg	47°48'N	11°01'E	994	(1851-1874 (1879-1930	Deutsche Klimakünde
Kew	51°28'N	00°19'W	8	1871-1950	M.O. Tabulation, 1951. Averaged in M.O.22
Kiel	54°19'N	10°08'E	47	1851-1930	Deutsche Klimakünde
Kleve	51°48'N	06°08'E	48	1851-1930	Deutsche Klimakünde
Köln	50°56'N	06°57'E	56	1851-1930	Deutsche Klimakünde
Königsberg	54°43'N	20°30'E	7	1851-1930	Deutsche Klimakünde
Konitz	53°42'N	17°34'E	175	1851-1930	Deutsche Klimakünde
Köslin	54°12'N	16°11'E	46	1851-1930	Deutsche Klimakünde
Lüneberg	53°15'N	10°24'E	20	1851-1930	Deutsche Klimakünde
Memel	55°43'N	21°08'E	18	1851-1930	Deutsche Klimakünde
München	48°10'N	11°30'E	531	1851-1930	Deutsche Klimakünde
Posen	52°25'N	16°56'E	66	1851-1930	Deutsche Klimakünde
Potsdam	52°23'N	13°04'E	80	1901-1950	Met. Zeitschrift
Prague	50°05'N	14°25'E	197	1775-1839	Hlavac (1937) worked in M.O.22
Prague	50°05'N	14°25'E	197	1840-1934	Hlavac (1937)
Ratibor	50°06'N	18°13'E	191	1851-1930	Deutsche Klimakünde
Schneekoppe	50°44'N	15°44'E	1618	1881-1930	Deutsche Klimakünde
Stettin	53°26'N	14°30'E	26	1851-1930	Deutsche Klimakünde
Stuttgart	48°47'N	09°10'E	267	1851-1930	Deutsche Klimakünde
Tilsit	55°04'N	21°54'E	18	1851-1930	Deutsche Klimakünde
Torgau	51°34'N	13°00'E	99	1851-1930	Deutsche Klimakünde
Treuberg	54°02'N	22°30'E	162	1851-1930	Deutsche Klimakünde
Trier	49°45'N	06°38'E	150	1851-1930	Deutsche Klimakünde
Uppsala	59°51'N	17°38'E	24	1871-1950	Year books, worked in M.O.22
Vienna	48°15'N	16°22'E	203	1873-1947	" "
Zugspitze	47°25'N	10°59'E	2962	1901-1930	Deutsche Klimakünde

* Observations made at three locations less than $1\frac{3}{4}$ mi. apart. Elevation from 70-79 m.

Table 1a. The Norwegian stations used (after Birkeland (1936))

Station	Latitude	Longitude	Altitude m.	Source of data
As	59°40'N	10°46'E	95	Geofysiske Publikasjoner Vol. XIV No. 1
Bodo I.	67°17'N	14°24'E	22	"
Dalen I.	59°27'N	07°58'E	103	"
Dombas	62°05'N	09°07'E	643	"
Hamar	60°48'N	11°04'E	139	"
Hattfjelldal	65°36'N	14°00'E	235	"
Kristiansand N.	63°07'N	07°45'E	18	"
Kristiansand S.	58°10'N	07°59'E	22	"
Nordfjordeid	61°55'N	06°00'E	5	"
Oslo	59°55'N	10°43'E	22	"
Skudenes	59°09'N	05°16'E	2	"
Sorvaranger	69°44'N	30°03'E	5	"
Tromso I.	69°39'N	18°58'E	45	"
Trondheim	63°26'N	10°25'E	58	"
Ullensvang	60°19'N	06°40'E	10	"
Vollen	61°06'N	08°58'E	403	"

Table 2. Harmonic coefficients, total and residual variances

Station	Annual mean temperature and harmonic coefficients in degrees Celsius a_0	a_1	b_1	a_2	b_2	Annual variance	Residual variance	Residual variance as percentage of total	No. of years
Augsberg	8.12	-9.54	-2.59	-0.33	0.45	49.21	0.16	0.33	80
Bayreuth	7.76	-9.42	-2.55	-0.22	0.28	47.81	0.12	0.25	80
Berlin	9.27	-9.35	-2.73	0.11	0.28	47.59	0.14	0.29	80
Breslau	8.58	-9.88	-2.94	-0.06	0.16	53.25	0.13	0.24	80
Brussels	10.28	-7.87	-2.66	-0.02	0.33	34.80	0.23	0.66	30
Brocken*	2.63	-6.83	-2.92	0.41	0.26	27.86	0.16	0.57	35
Darmstadt	9.61	-8.76	-2.22	-0.05	0.36	40.93	0.06	0.15	80
Dresden	9.14	-9.04	-2.71	0.00	0.29	44.71	0.18	0.40	80
Edinburgh	8.31	-5.68	-2.14	0.21	0.48	18.65	0.08	0.43	40
Emden	8.52	-7.65	-2.85	0.15	0.43	33.51	0.12	0.36	80
Erfurt	7.93	-8.94	-2.61	-0.07	0.24	43.58	0.19	0.44	80
Frankfurt a.O.	8.54	-9.50	-2.77	0.07	0.24	49.19	0.17	0.35	80
Friedrichshafn	8.84	-9.21	-2.65	-0.13	0.26	46.08	0.12	0.26	80
Glasgow	8.29	-5.10	-2.04	0.45	0.54	15.36	0.05	0.33	45
Görlitz	8.24	-9.43	-2.83	-0.41	0.21	48.70	0.18	0.37	80
Gütersloh	9.05	-8.11	-2.49	0.16	0.29	36.22	0.17	0.47	80
Halle (1851-1930)	9.07	-9.22	-2.63	0.07	0.30	46.12	0.15	0.33	80
Hohenpeissenberg*	6.00	-8.11	-2.91	0.12	0.43	37.49	0.23	0.61	76
Kew (1901-1950)	10.29	-6.23	-2.39	0.34	0.62	22.63	0.10	0.44	50
Kiel	8.47	-7.72	-3.04	0.43	0.36	34.69	0.10	0.29	80
Kleve	9.13	-7.75	-2.45	0.11	0.41	33.26	0.14	0.42	80
Köln	10.24	-8.00	-2.44	-0.02	0.38	35.19	0.15	0.43	80
Königsberg	7.06	-9.90	-3.47	0.22	0.16	55.20	0.15	0.27	80
Konitz	6.81	-9.85	-3.11	0.27	0.15	53.53	0.16	0.30	80
Köslin	7.22	-8.82	-3.21	0.26	0.30	44.21	0.14	0.32	80
Lüneberg	8.47	-8.51	-2.61	0.31	0.27	39.89	0.17	0.43	80
Memel	6.85	-9.51	-3.89	0.31	0.14	52.97	0.07	0.13	80
München	7.64	-9.53	-2.65	-0.36	0.36	49.18	0.12	0.24	80
Posen	8.29	-9.95	-2.89	0.17	0.12	53.86	0.16	0.30	80
Potsdam	8.54	-9.35	-2.65	-0.08	0.12	47.44	0.15	0.32	50
Prague (1775-1839)	9.57	-10.33	-3.01	-0.35	0.08	58.16	0.18	0.31	65
Prague (1840-1934)	9.04	-10.00	-2.83	-0.13	0.20	54.12	0.09	0.17	95
Ratibor	8.05	-9.97	-2.80	-0.22	-0.01	53.69	0.09	0.17	80
Schneekoppe*	0.24	-7.28	-3.07	0.36	0.19	31.60	0.28	0.89	50
Stettin	8.41	-9.37	-2.95	0.19	0.29	48.48	0.14	0.29	80
Stuttgart	10.00	-8.98	-2.35	-0.16	0.41	43.34	0.13	0.30	80
Tilsit	6.59	-10.53	-3.40	0.32	-0.05	61.41	0.14	0.23	80
Torgau	9.01	-9.35	-2.72	0.08	0.29	47.62	0.18	0.38	80
Treuberg	5.43	-10.83	-3.23	0.30	-0.37	64.22	0.21	0.33	80
Trier	9.17	-8.22	-2.27	-0.06	0.40	36.58	0.12	0.33	80
Uppsala	5.25	-9.96	-3.63	0.97	0.25	56.73	0.05	0.09	80
Vienna	9.38	-10.09	-2.77	-0.50	0.19	54.89	0.06	0.11	75
Zugspitze*	-4.92	-6.10	-3.19	0.22	0.16	24.12	0.39	1.62	30

* denotes mountain stations.

Table 2a. Harmonic coefficients, total and residual variances for Norwegian stations (after Birkeland (1936))

Station	Annual mean temperature and harmonic coefficients in degrees Celsius a_0	a_1	b_1	a_2	b_2	Annual variance	Residual variance*	Residual variance as percentage of total*	No. of years
As	4.96	-10.10	-3.24	0.65	0.18	56.44	0.04	0.07	60
Bodo I.	4.11	-6.85	-3.24	0.86	0.78	24.49	0.09	0.31	60
Dalen I.	5.07	-9.90	-2.98	0.75	0.32	53.75	0.06	0.11	40
Dombas	1.04	-10.23	-3.06	0.56	0.50	57.28	0.07	0.12	60
Hamar	3.44	-11.19	-3.56	0.48	-0.03	69.07	0.04	0.06	52
Hattfjelldal	0.91	-10.84	-3.63	0.53	0.62	65.83	0.17	0.26	52
Kristiansand N.	6.59	-5.39	-2.74	0.60	0.58	18.63	0.03	0.16	60
Kristiansand S.	6.88	-8.11	-3.12	0.83	0.25	38.09	0.04	0.11	44
Nordfjordeid	6.03	-7.25	-2.27	1.14	0.48	29.82	0.17	0.57	15
Oslo	5.84	-10.58	-3.18	0.68	0.17	61.21	0.02	0.03	60
Skudenes	7.51	-5.55	-3.21	0.45	0.40	20.77	0.04	0.19	60
Sorvaranger	-0.71	-10.92	-4.44	0.36	0.68	70.01	0.21	0.30	60
Tromso I.	2.40	-6.79	-3.15	1.09	0.90	29.02	0.05	0.17	60
Trondheim	4.78	-8.14	-2.86	0.63	0.58	37.57	0.06	0.16	51
Ullensvang	6.68	-7.50	-2.56	0.88	0.30	31.83	0.04	0.13	60
Vollen	1.89	-11.44	-3.56	0.08	-0.01	71.81	0.17	0.24	60

* This value for the residual variance is half the sum of the squares of Birkeland's values for the semi-amplitudes of harmonics 3, 4, 5 and 6, and therefore is less than the true value.

Fig 1(a) M.R.P. 915

Multipliers for evaluating Harmonic Co-efficients from 73 equally spaced values of a function

Term No.	$\frac{2}{73}\cos\theta$	$\frac{2}{73}\cos 2\theta$	$\frac{2}{73}\cos 3\theta$	$\frac{2}{73}\cos 4\theta$		$\frac{2}{73}\sin\theta$	$\frac{2}{73}\sin 2\theta$	$\frac{2}{73}\sin 3\theta$	$\frac{2}{73}\sin 4\theta$
1	274	273	272	270		012	024	035	047
2	272	265	254	238		035	070	103	135
3	268	249	219	179		059	114	165	208
4	262	226	170	098		081	155	215	256
5	254	196	109	006		103	192	251	274
6	244	160	041	-087		125	222	271	260
7	232	120	-029	-170		145	246	272	215
8	219	076	-098	-232		165	263	256	145
9	204	029	-160	-268		183	272	222	059
10	187	018	-212	-272		200	273	174	-035
11	170	-064	-249	-244		215	266	114	-125
12	150	-109	-270	-187		229	251	047	-200
13	130	-150	-273	-109		241	229	-024	-251
14	109	-187	-258	-018		251	200	-092	-273
15	087	-219	-226	076		260	165	-155	-263
16	064	-244	-179	160		266	125	-208	-222
17	041	-262	-120	226		271	081	-246	-155
18	018	-272	-053	265		273	035	-269	-070
19	-006	-274	018	273		274	-012	-273	024
20	-029	-268	087	249		272	-059	-260	114
21	-053	-254	150	196		269	-103	-229	192
22	-076	-232	204	120		263	-145	-183	246
23	-098	-204	244	029		256	-183	-125	272
24	-120	-170	268	-064		246	-215	-059	266
25	-140	-130	274	-150		235	-241	012	229
26	-160	-087	262	-219		222	-260	081	165
27	-179	-041	232	-262		208	-271	145	081
28	-196	006	187	-274		192	-274	200	-012
29	-212	053	130	-254		174	-269	241	-103
30	-226	098	064	-204		155	-256	266	-183
31	-238	140	-006	-130		135	-235	274	-241
32	-249	179	-076	-041		114	-208	263	-271
33	-258	212	-140	053		092	-174	235	-269
34	-265	238	-196	140		070	-135	192	-235
35	-270	258	-238	212		047	-092	135	-174
36	-273	270	-265	258		024	-047	070	-092
37	-274	274	-274	274					

Fig. 1(b) Form for Harmonic Analysis of function given by 73 equally spaced values

Term No.				sum	diff.
1	73				
2	72				
3	71				
4	70				
5	69				
6	68				
7	67				
8	66				
9	65				
10	64				
11	63				
12	62				
sums					
sums of squares					
13	61				
14	60				
15	59				
16	58				
17	57				
18	56				
19	55				
20	54				
21	53				
22	52				
23	51				
24	50				
sums					
sums of squares					
25	49				
26	48				
27	47				
28	46				
29	45				
30	44				
31	43				
32	42				
33	41				
34	40				
35	39				
36	38				
sums					
sums of squares					
37					

Mean & Variance

	Sum	Sum of squares
Block 1		
Block 2		
Block 3		
Term 37		
Total		

Mean =

Variance =

=

=

Cosine component

	$\frac{1}{10} a_1$	$\frac{1}{10} a_2$
Block 1		
Block 2		
Block 3		
Term 37		
Total		

a_1 =

a_2 =

Sine components

	$\frac{1}{10} b_1$	$\frac{1}{10} b_2$
Block 1		
Block 2		
Block 3		
Total		

b_1 =

b_2 =

Amplitudes & phases

$A_1 = \sqrt{a_1^2 + b_1^2} =$

$\phi_1 = \tan^{-1} b_1/a_1$

$A_2 = \sqrt{a_2^2 + b_2^2} =$

$\phi_2 = \tan^{-1} b_2/a_2$

Residual variances

$V_1 = V_0 - \frac{1}{2}(a_1^2 + b_1^2) =$

$V_2 = V_1 - \frac{1}{2}(a_2^2 + b_2^2) =$

$\frac{V_2}{V_0} =$

FIG 2ω SEMI-AMPLITUDE OF FIRST HARMONIC, IN DEGREES CELSIUS.

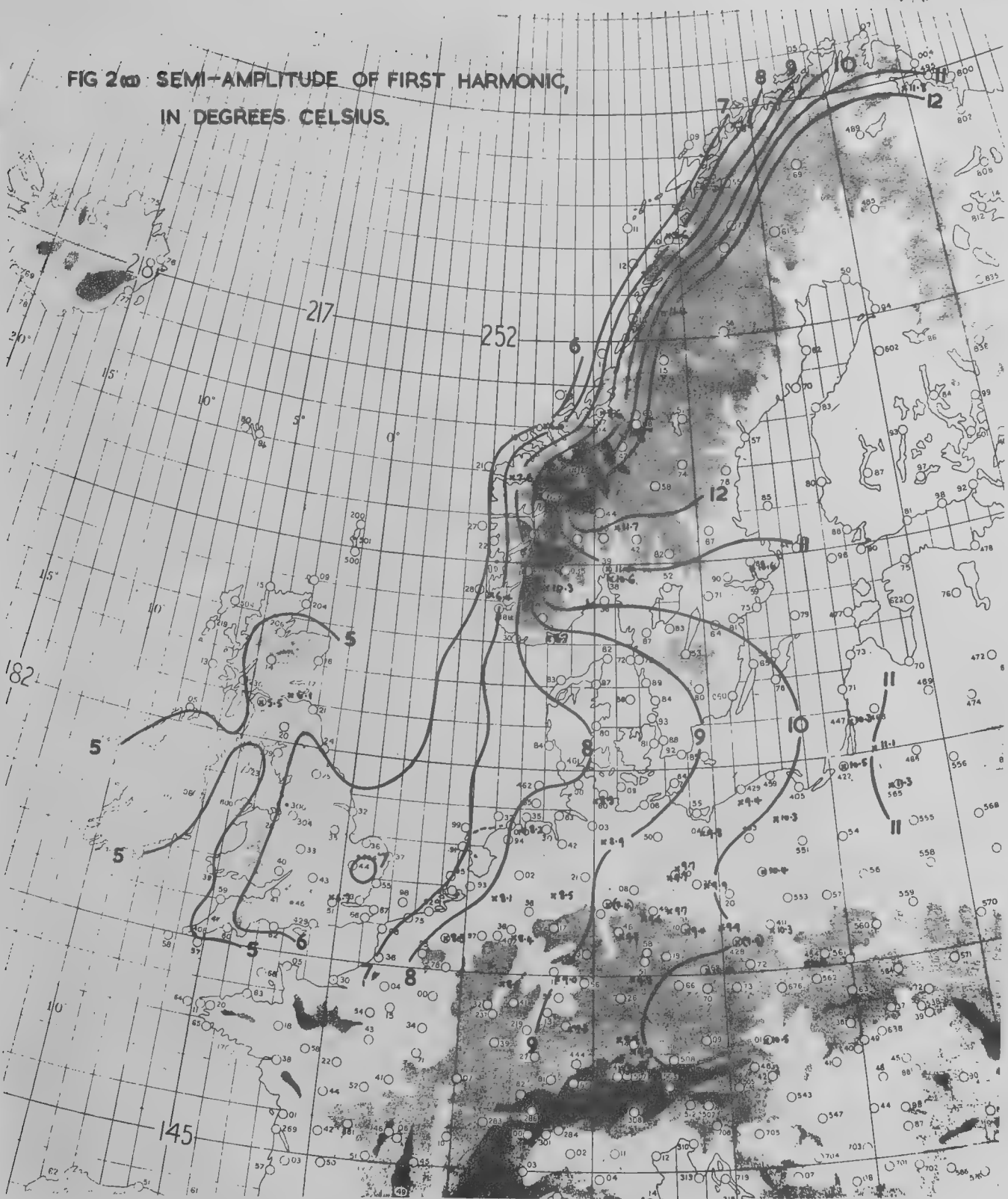

FIG 2 (b) PHASE OF FIRST HARMONIC, DATE OF MAXIMUM.

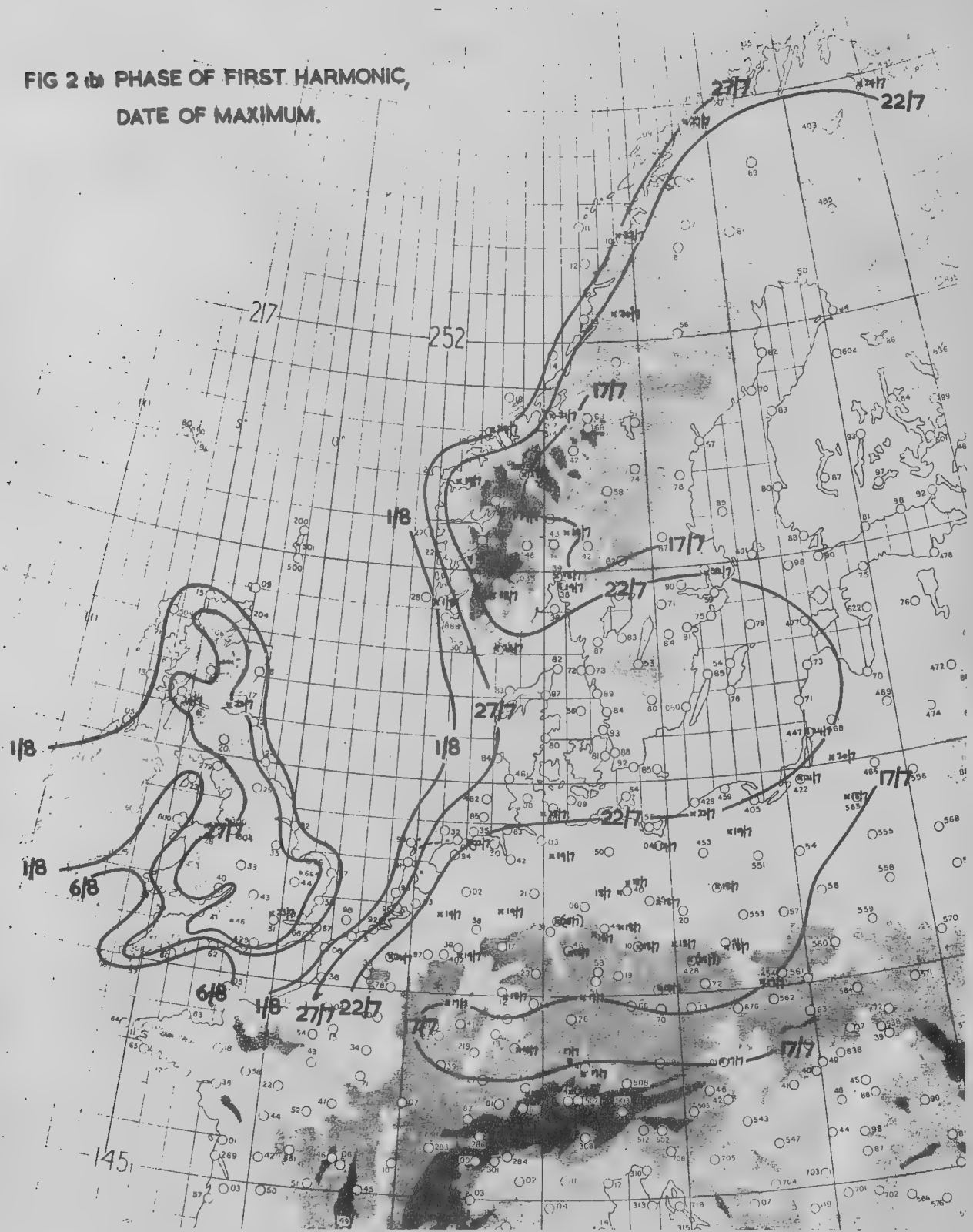

M.R.P. 915

FIG 2 — SEMI-AMPLITUDE OF SECOND HARMONIC, IN DEGREES CELSIUS

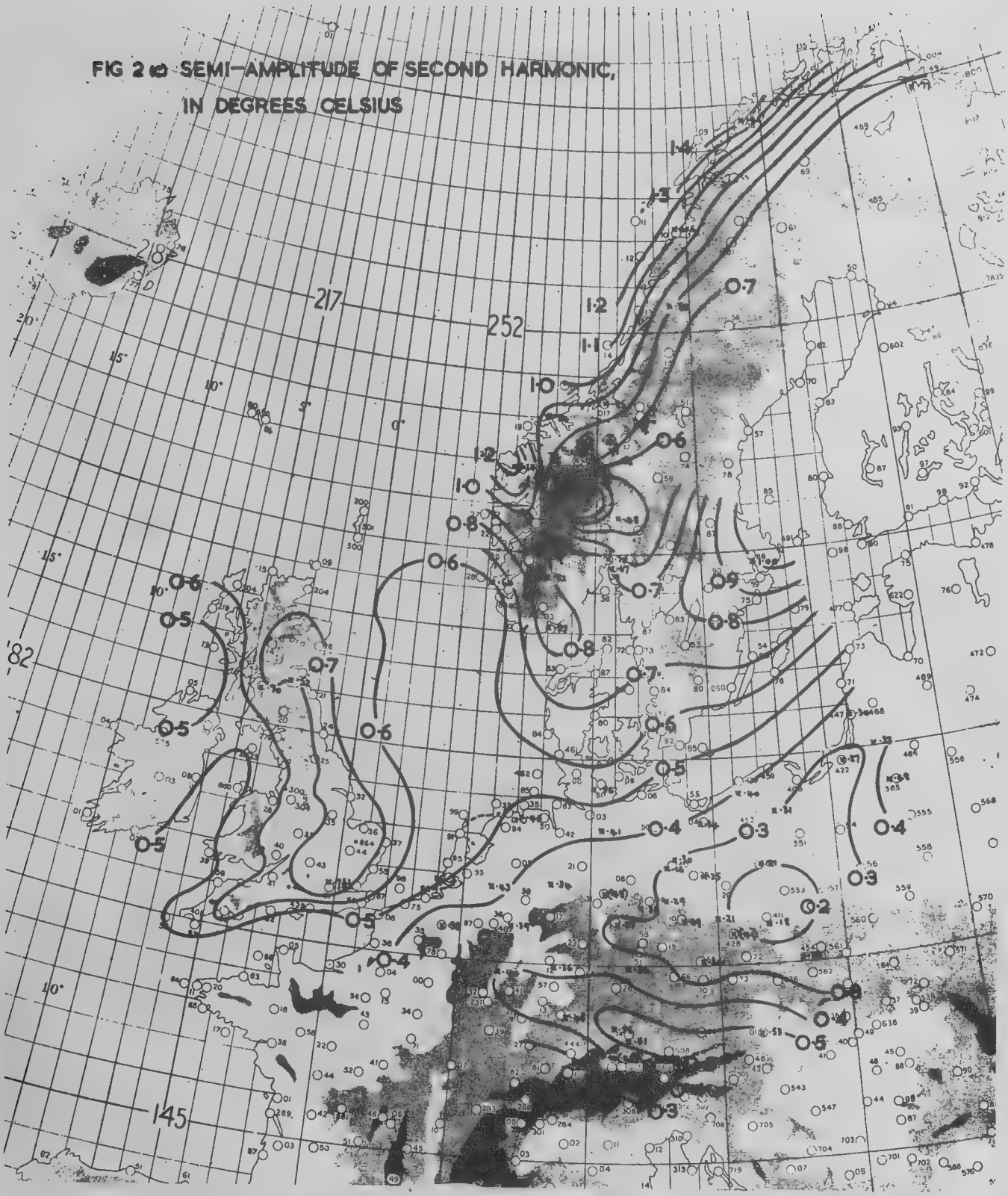

FIG 2(d) PHASE OF SECOND HARMONIC, DATE OF MAXIMUM.

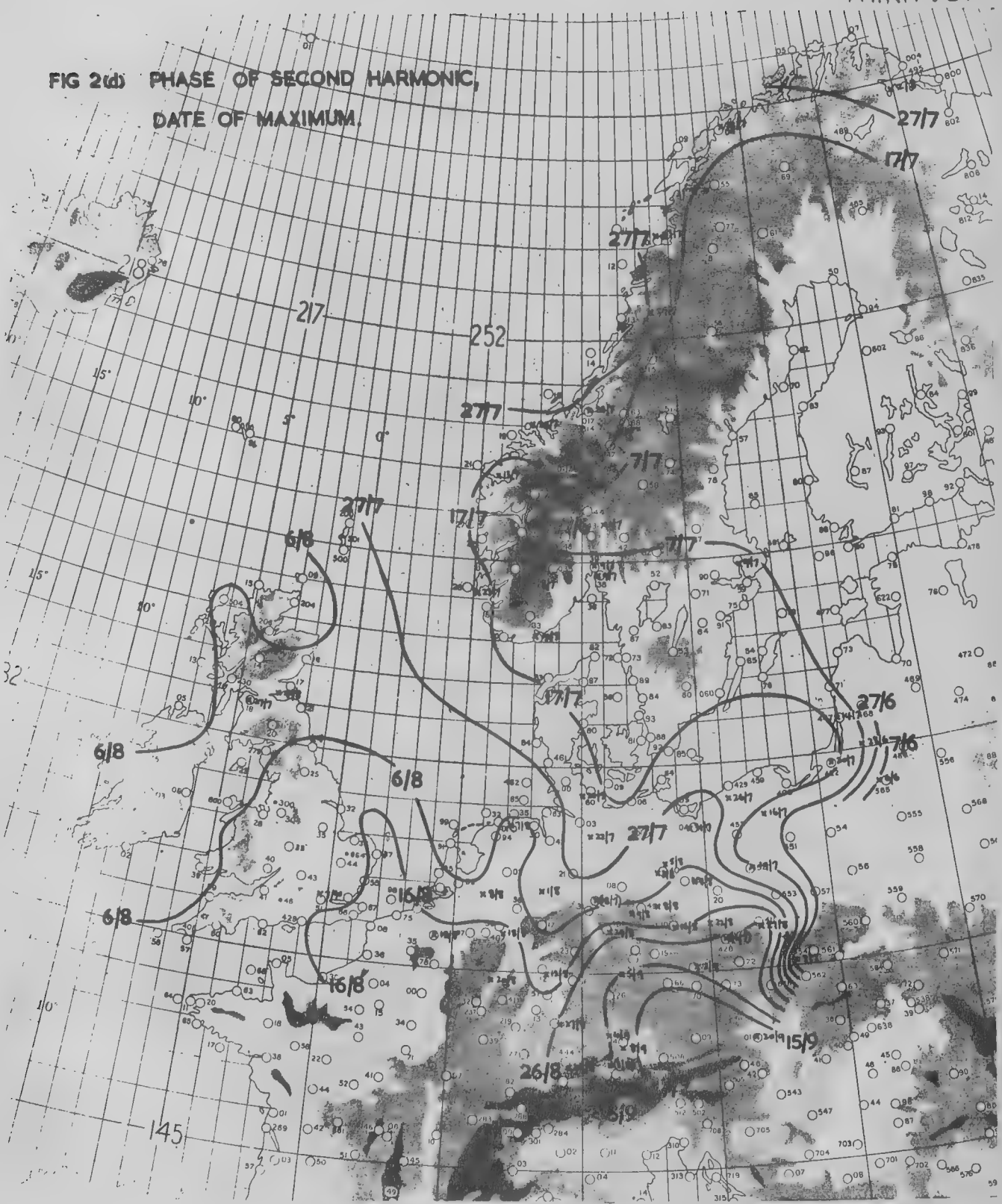

M.R.P. 915

FIG 2(a) POSITION, ALTITUDE & ANNUAL MEAN TEMPERATURE OF STATIONS.

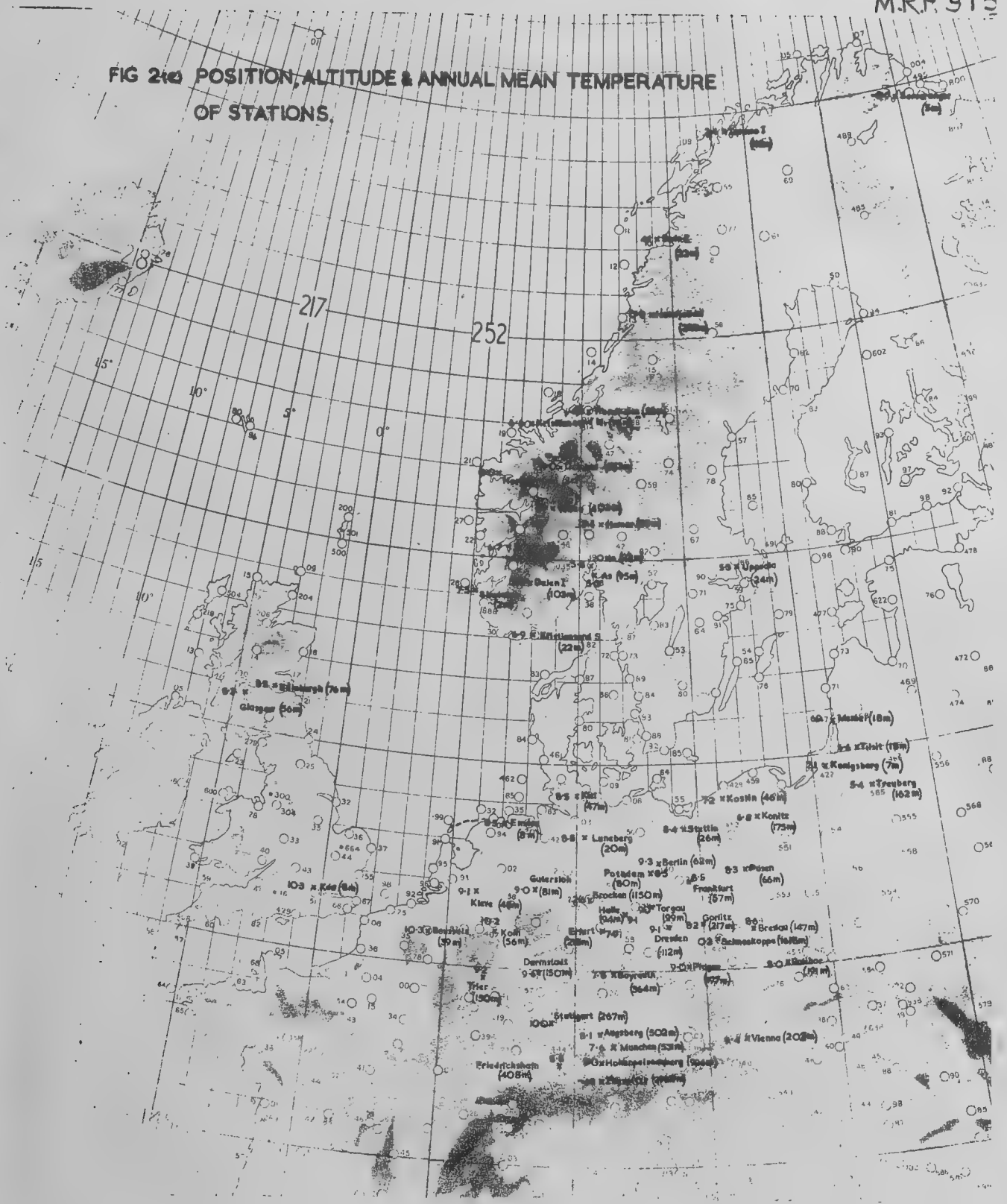

Fig. 3 The relation between nV and n

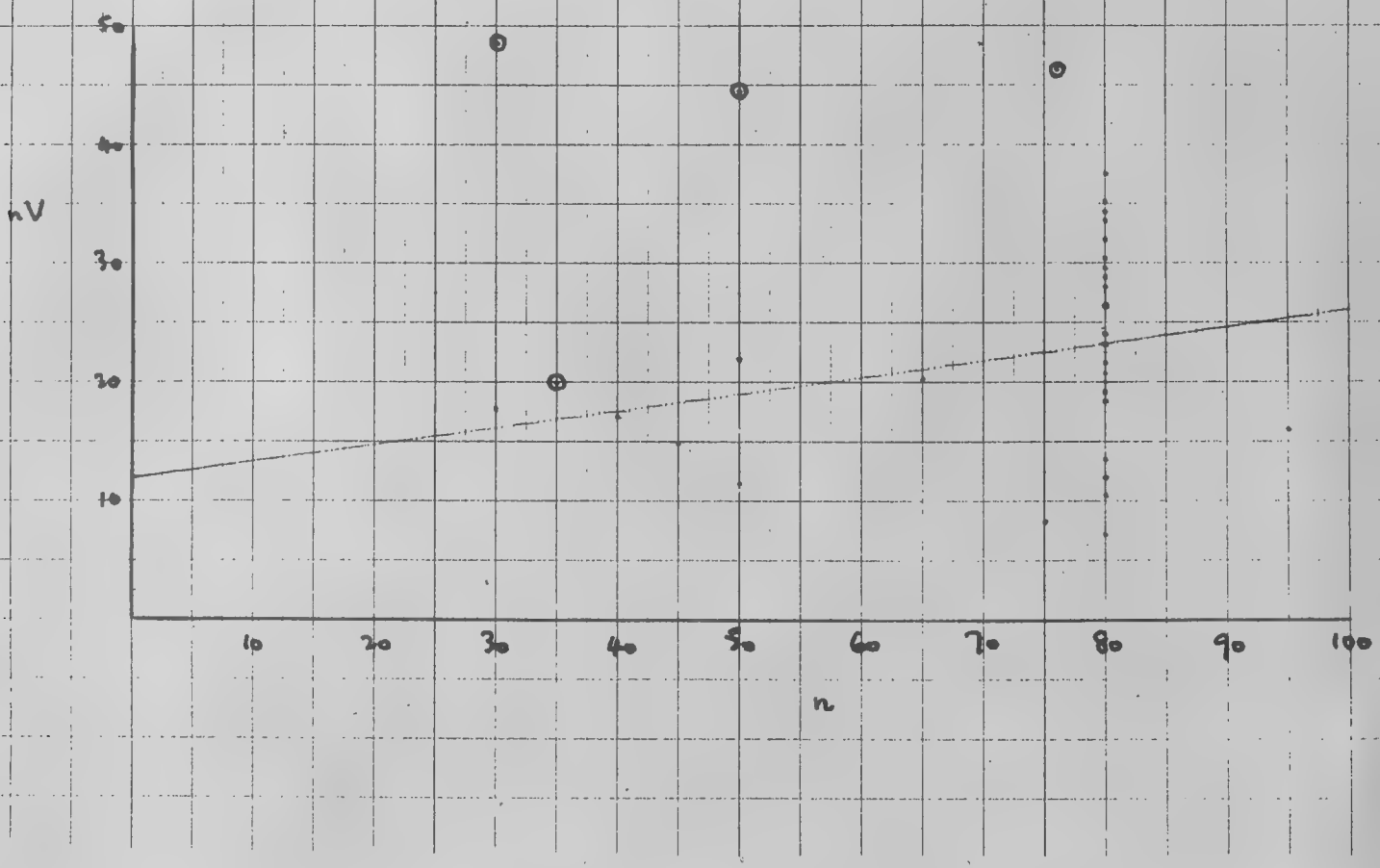

M.R.P. 915

FIG. 4 GEOGRAPHICAL DISTRIBUTION OF PERCENTAGE RESIDUAL VARIANCE x NUMBER OF YEARS.

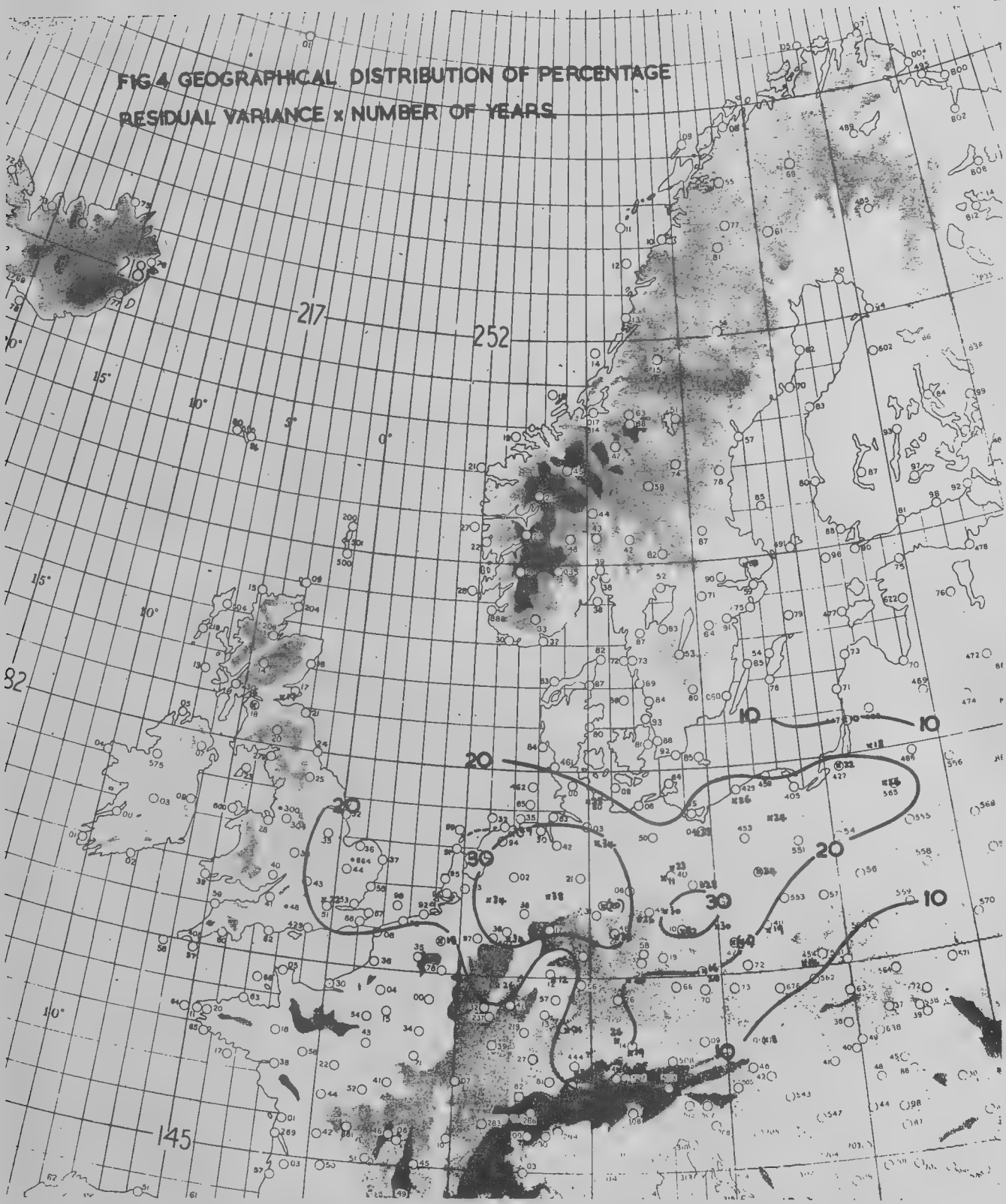

FIG 5

ANOMALIES OF 5 DAY MEAN TEMPERATURES FOR 8 STATIONS IN NORTH-WEST & CENTRAL EUROPE.

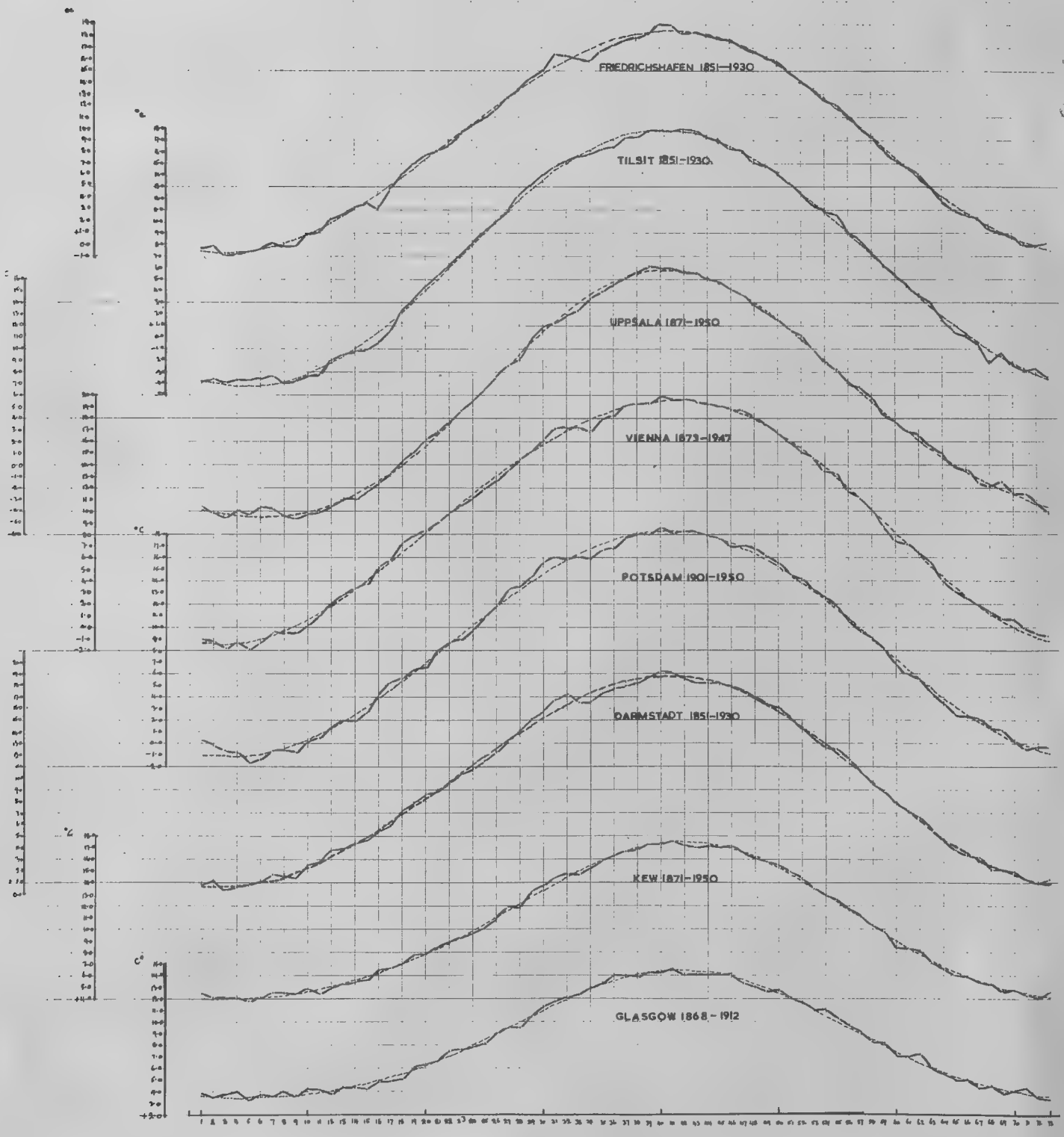

FIG 6

TEMPERATURE ANOMALIES AT PRAGUE (50°05'N, 14°25'E, 197·2 M. A.S.L.) 5 DAY MEAN TEMPERATURES COMPARED WITH THE TWO TERM HARMONIC NORMALS FOR THE PERIODS 1775–1839 & 1840–1934.

NORMAL FOR 1775–1839 $(9{\cdot}54 - 10{\cdot}33\cos\Theta - 3{\cdot}01\sin\Theta - 0{\cdot}35\cos 2\Theta + 0{\cdot}08\sin 2\Theta)^{\circ}C$

NORMAL FOR 1840–1934 $(9{\cdot}04 - 10{\cdot}00\cos\Theta - 2{\cdot}83\sin\Theta - 0{\cdot}13\cos 2\Theta + 0{\cdot}20\sin 2\Theta)^{\circ}C$

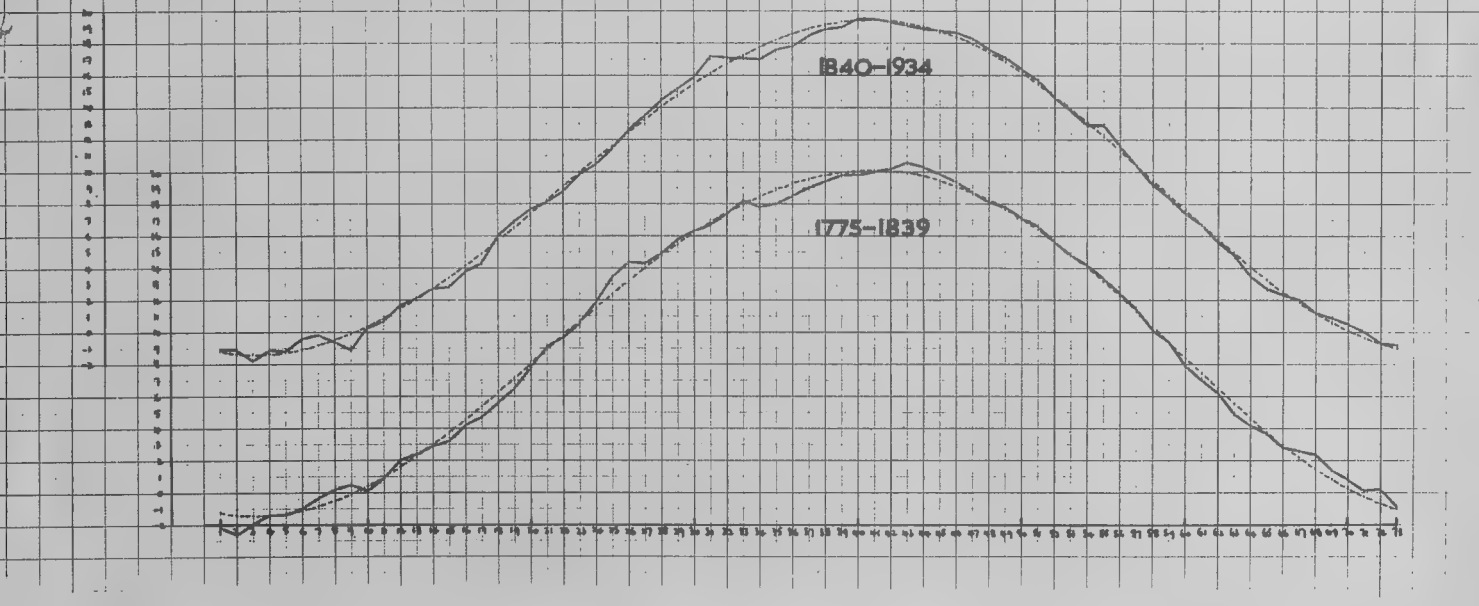

FIG 7

TEMPERATURE ANOMALIES AT HALLE S. (52°29'N 11°58'E. 90·8 M. A.S.L.) 50 YEAR 5 DAY MEAN TEMPERATURES COMPARED WITH THE TWO TERM HARMONIC NORMALS FOR THE PERIODS 1851–1900 & 1901–50.

NORMAL FOR 1851–1900 $(8{\cdot}95 - 9{\cdot}44\cos\Theta - 2{\cdot}79\sin\Theta + 0{\cdot}04\cos 2\Theta + 0{\cdot}36\sin 2\Theta)^{\circ}C$

NORMAL FOR 1901–50 $(9{\cdot}42 - 9{\cdot}13\cos\Theta - 2{\cdot}57\sin\Theta - 0{\cdot}05\cos 2\Theta + 0{\cdot}15\sin 2\Theta)^{\circ}C$

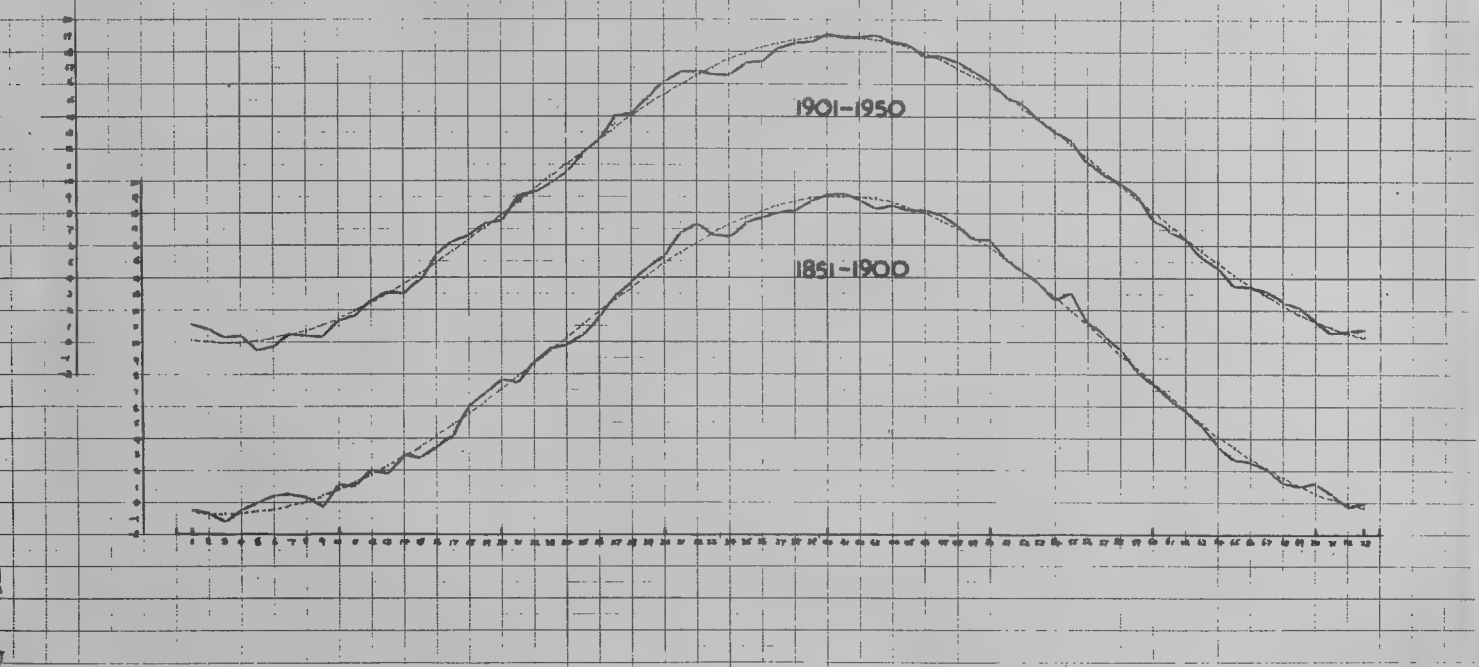

FIG 8

5 DAY MEAN TEMPERATURE ANOMALIES FOR EDINBURGH (55°57′N, 3°11′W) 1795–1804, 1821–1850 COMPARED WITH GLASGOW (55°51′N, 4°16′W) 1868–1912.

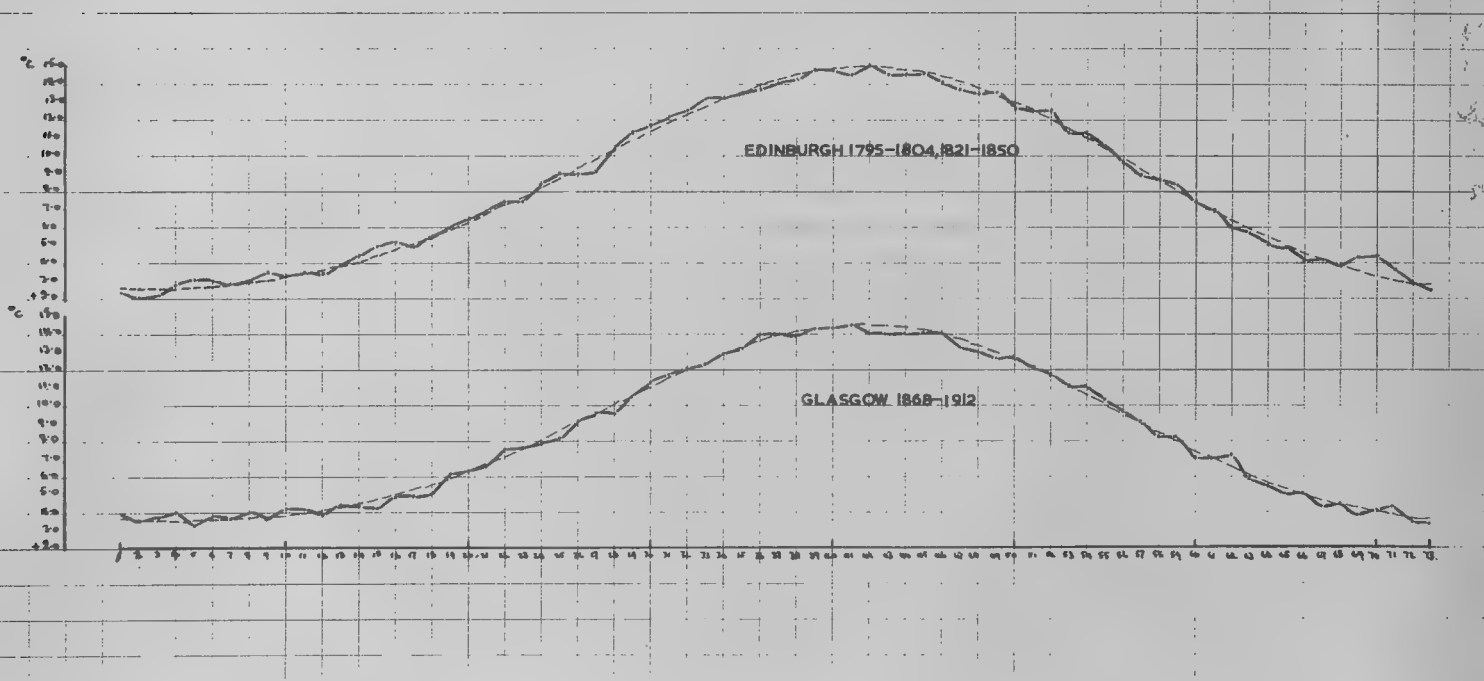

FIG 9.

5 DAY MEAN TEMPERATURE ANOMALIES FOR KLEVE (51°48′N, 6°8′E) 1851–1930 COMPARED WITH BRUSSELS (50°51′N, 4°22′E) 1831–1860.

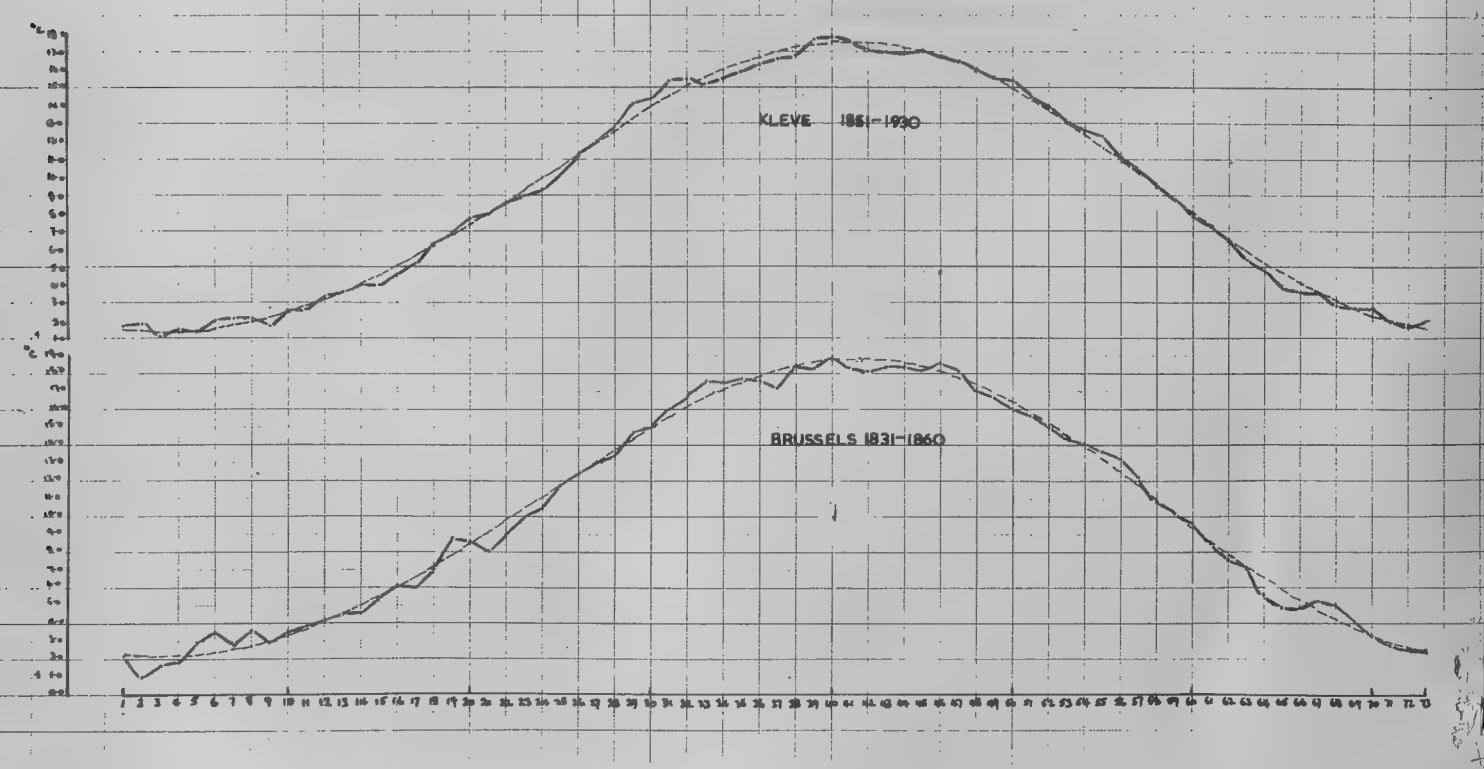

M.R.P. 916
S.C. 1/99
17th June, 1955

A.D.2-4.1.47

A refrigerated disc icing meter

by

G. J. Day
(Meteorological Office)

AIR MINISTRY
METEOROLOGICAL RESEARCH COMMITTEE

At the time of issue this report has not been published. Any author desiring to quote this paper should refer to it as "A paper of the Meteorological Research Committee (London).
M.R.P. No. 916 by Mr. G. J. Day
A copy is available in the Library of the Meteorological Office."

M.R.P. 916
S.C.I/99
17th June, 1955.

AIR MINISTRY

METEOROLOGICAL RESEARCH COMMITTEE

A refrigerated disc icing meter

by
G. J. Day (Meteorological Office)

1. Summary

The performance required from an instrument to measure rates of icing and water contents of cloud is considered and it is shown that the refrigerated rotating disc type meets most of the requirements. The design of this instrument is considered theoretically and constructional details of the model used in the Meteorological Research Flight are given. Results of wind tunnel and aircraft tests are presented.

2. Introduction

A knowledge of the supercooled water content of clouds is of importance both in the study of rainfall mechanisms and in the design of aircraft de-icing systems. In the past it has been customary to obtain values of this parameter by consideration of the rate of accretion of ice on slowly rotating cylinders or discs, of known dimensions and rate of rotation, in an air stream of known speed. Originally the weight or the thickness of ice of assumed density accumulated over a known period was measured directly but this practice proved both cumbersome and inaccurate particularly for the smaller water contents when the period of exposure was necessarily of the order of minutes. The current practice is to use a thin rotating disc continuously exposed and to measure continuously by an electrical method the thickness of ice accumulated on the edge of the disc.

A typical rotating disc design due to the Mechanical Engineering Department, R.A.E., and in use by M.R.F., is shown in Figs. 1a and b. A steel disc A, 5cm. in diameter and 2mm. thick rotates at 2 revolutions per minute, edge on to the local airstream. The thickness of ice accumulated on the edge of the disc is measured by a transducer, C, through the medium of a feeler, B; the transducer is embodied in an alternating current bridge circuit the magnitude of whose unbalanced output is a function of the supercooled water content and of the speed of the local airstream. A scraper, D, removes the ice after measurement.

Thermodynamic analysis of the heat balance of ice accretion instruments by Ludlam (1) and more recently by Fraser, Rush and Baxter (2) has shown that there is an upper limit to the accretion of ice on to a cylinder or disc at any particular ambient temperature. This limit - commonly referred to as the "Ludlam Limit" - is set by the amount of latent heat of fusion which can be transported away from the accretion surface and given to the local airstream and to the remainder of the disc. For a disc such as that described above and operating at an ambient temperature of about $-10^{\circ}C$ in an airstream of speed 180 ft. sec.$^{-1}$ the limit is about 2.0 gm. m.$^{-3}$, i.e. adequate for the majority of icing encounters.

Several authors (3), (4), (5) and (6) have recently suggested that water contents of the order of 5.0 gm. m.$^{-3}$ may be found in regions, limited in both time and space, of vigorous convective clouds of temperate latitudes, higher

/values

values being probable in tropical latitudes. It, therefore, becomes important to raise the limit of ice accretion instruments in order that they may be operated in these conditions.

3. Theoretical considerations

Adopting the symbols listed in the Appendix and applying the method of Fraser, Rush and Baxter (2) to the determination of the disc temperature appropriate to a Ludlam Limit of 6.0 gm. m.$^{-3}$, we may say that for a heat balance, i.e. equilibrium conditions at the disc edge,

$$q_v + q_k + q_f + q_i = q_w + q_c + q_e + q_s$$

but $q_v = \dfrac{hrV^2}{2JC_p}$

$q_k = \dfrac{WV^2}{2J}$

$q_f = L_f W$

$\theta_d = \theta_o + \dfrac{rV^2}{2JC_p}$ in the non-refrigerated case

$q_w = W(\theta_s - \theta_o)$

$q_c = h(\theta_s - \theta_o)$

$q_e = \dfrac{h\varepsilon L_v}{c_p p_o}(e_s - e_o)$

$q_s = k_i \dfrac{\theta_s - \theta_d}{y}$

$y = \dfrac{60mVE}{\pi n \rho_i}$

and, since at the Ludlam Limit

$q_i = 0$,

we may obtain

$$m = \frac{k_i(\theta_s - \theta_d)\pi n \rho_i}{60VE\left\{\frac{V^2}{2J}\left(\frac{hr}{c_p} + w\right) + L_f W - (\theta_s - \theta_o)(W+h) - \frac{h\varepsilon L_v}{c_p p_o}(e_s - e_o)\right\}}$$

and

$$\theta_s - \theta_d = \frac{60VEm\left\{\frac{V^2}{2J}\left(\frac{hr}{c_p} + w\right) + L_f w - (\theta_s - \theta_o)(W+h) - \frac{h\varepsilon L_v}{c_p p_o}(e_s - e_o)\right\}}{k_i \pi n \rho_i}$$

Hence in the case where

$k_i = 5 \times 10^{-3}$ cal. cm.$^{-1}$ sec. (deg.C)$^{-1}$

$n = 2$ revolutions min.$^{-1}$

/N

$V = 55 \times 10^2$ cm. sec.$^{-1}$

$h = \frac{k}{d_c} R_e^{0.5}$

$= 22.9 \times 10^3$ cal. sec.$^{-1}$ cm.$^{-2}$ deg.$^{-1}$

$C_p = 0.24$ cal. gm.$^{-1}$ (deg. C)$^{-1}$

$L_f = 76$ cal. gm.$^{-1}$

$d_e = 0.245$ cm.

$\rho_i = 0.92$ gm. cm.$^{-3}$

$E = 0.97$

$J = 4.18 \times 10^7$ dyne. cm. cal.$^{-1}$

$r = 0.85$

$W = 3.3 \times 10^{-2}$ gm. sec.$^{-1}$ cm.$^{-2}$

$m = 6.0 \times 10^{-6}$ gm. m.$^{-3}$

$p_o = 0.95 \times 10^6$ dyne. cm.$^{-2}$

we may say that since

$\theta_s = 0$ deg. C at the Ludlam Limit

and

$$\frac{hL_v}{p_o}(e_s - e_o) \ll 1$$

then

$\theta_d = -213^\circ C$ at $\theta_o = +10^\circ C$

$\theta_d = -174^\circ C$ at $\theta_o = 0^\circ C$

$\theta_d = -136^\circ C$ at $\theta_o = -10^\circ C$

Thus, in order that the rotating disc type of instrument shall accommodate those conditions considered probable, considerable refrigeration of the disc is necessary.

4. The new instrument

The new instrument is essentially a conventional rotating disc icing meter in which a hollow disc is refrigerated by the application of a stream of liquid nitrogen to its inner surface. Considering the instrument, shown broken down in Fig. 2a and assembled in Figs. 2b, c and d, in detail:-

(a) The hollow copper disc, A, mounted on a hollow steel driving shaft, B, is driven at 2 rev.min.$^{-1}$ by a 24 volt direct current motor through a chain drive contained within E. The shaft is carried in phosphor-bronze plain bearings in the casing, C.

/(b)

(b) Refrigeration of the disc is achieved by the flow of liquid nitrogen through the hollow driving shaft into the hollow disc via the feed pipe, F, and the liquid nitrogen trap, N; the latter is incorporated to prevent damage of neighbouring aircraft components by excess liquid nitrogen. The refrigerant is forced to the disc by pressure from an air bottle as indicated in Fig. 3, the rate of flow, and hence the degree of refrigeration, being governed by the air pressure used. Flow of the refrigerant is governed to obtain a nominated disc temperature as indicated by the spring loaded thermometer, G_1, bearing on the under-side of the disc. The thermometer is shown broken down as G_2 in Fig. 2a where 'a' is a copper core and shoe contained within an anodised aluminium former 'b' on which is wound a platinum wire resistance element, the whole being enclosed within a plastic insulating casing 'c' designed to reduce casual heat flow into the system. Although the temperature required is strictly that of the edge of the disc, it is considered that the surface temperature in the position adopted does not depart materially from that required; further, owing to the low rotational speed and the smoothness of the surfaces concerned, frictional heat input at the thermometer shoe may be neglected.

(c) Ice thickness is measured by the transducer, I, through the feeler, H, feeler tension being adjusted by the ratchet device, J, reached through the access panel, L, in the streamlined outer casing, K. The transducer is incorporated in an alternating current bridge circuit shown in Fig. 4 and the rectified output of the unbalanced bridge circuit displayed either on a micro-ammeter or a galvanometer recorder.

(d) After detection the ice accumulated is removed from the disc edge and adjacent top and bottom surfaces by the scraper system, M. Ice forming on the streamlined housing of the instrument is removed by the flow of de-icing fluid through a thick strip of felt, O, covered with fine copper gauze incorporated in the leading edge of the housing. A certain amount of fluid reaches the top decking of the instrument beneath the disc and assists in clearing the ice removed by the scraper. Of this fluid a small amount reaches the disc edge but since the de-icing properties result only on application to an ice-metal interface there is no effect on the amount of ice measured. Any fluid which reaches the edge of the disc does so only after the removal of the ice by the scraper system. This fluid is removed by the airstream before this part of the edge of the disc travels to the position where it again starts to collect ice. Fluid is forced to flow in an analogous manner to that used in the case of the refrigerant and the details are shown in Fig. 3.

5. Laboratory tests of the instrument

These were performed in the Icing Wind Tunnel of R.A.E. by courtesy of Mechanical Engineering Department, and were directed towards:-

(a) Ensuring that the instrument was reliable during protracted periods of operation under full refrigeration.

(b) Ensuring that de-icing fluid at normal rates of supply did not affect accretion of ice on to the disc edge.

(c) Verifying the efficient operation of the cutter system.

(d) Examining the theoretical calibration of the instrument under a variety of typical conditions.

(e) Determining the value of ρ_L under typical conditions.
Considering these tests - which were made with the rig shown in Fig. 5 - in turn:-

/(a)

(a) It proved very difficult to avoid bearing seizure under maximum refrigeration and it was necessary to use rather generous clearances and to provide forced lubrication of the bearings with de-icing fluid. As originally designed the instrument was fitted with a plain copper disc but it was apparent both from theoretical considerations and from experiment that there was serious heat input into the system from the local airstream through the disc surface. Whilst it was not possible to overcome this defect during tunnel tests it was afterwards found possible to coat the disc, save the accretion surface, with a sheath of polythene about 2 mm. thick. This modification permitted a considerable reduction in the flow of liquid nitrogen for the more extreme conditions and made the bearing operating conditions much more favourable, thereby greatly improving reliability.

An early difficulty arose in the use of light alloy gearwheels in transmission of the motor drive to the main shaft. The gearwheels used were of comparatively shallow tooth depth and under full refrigeration contracted out of mesh. It was finally found necessary to abandon the original gear box and to resort to chain drive which proved quite reliable.

(b) Tests were made under a variety of representative conditions and no difference was detected in the output of the instrument under steady conditions when de-icing fluid was switched on or off.

(c) The cutter system was found to be extremely efficient although it was found that it flaked off all ice up to a point about 10° ahead of the cutter; it was therefore necessary to reposition the feeler to avoid disturbance of the feeler system.

(d) The Icing Wind Tunnel at R.A.E. was designed to produce water contents of the order of 4.0 gm.m.$^{-3}$ at speeds of about 100 mi.hr.$^{-1}$ and at temperatures ranging from ambient to about -30°C. It was therefore not possible to check the theoretical calibration over the full range of anticipated conditions nor was it possible to establish the calibration of the instrument accurately over the available range since the calibration of the tunnel itself is not known with sufficient accuracy. Further, in the absence of an insulating covering of the disc the degree of refrigeration available prevented operation of the instrument beyond these limits save at the lower air temperatures and it was necessary to use the uncovered disc in order that the surface temperature measurements should be reasonably accurate during this stage.

Within the tunnel limits, therefore, the response of the instrument to variable water content was obtained at a steady airspeed of 100 mi.hr.$^{-1}$ and at a variety of ambient conditions; in all cases observations were made under equilibrium conditions - a much more stringent condition than those of normal operation. The results of these experiments are shown in Fig. 7 and from them was deduced a provisional empirical calibration and the variation of the Ludlam Limit of the instrument with the degree of refrigeration; these are shown in Figs. 6c and 8 respectively. It will be observed that there is a wide divergence between Figs. 6c and 6b.

Considerable extrapolation in Fig. 8 shows that the desired Ludlam Limit of 6.0 gm. m.$^{-3}$ may be achieved with a disc temperature of about -100 deg. C, in reasonable agreement with the theory when the degree of extrapolation and the known inaccuracy of the empirical calibration is considered.

(e) By flotation tests using a variety of organic liquids non miscible with water the value of ρ_i for ice formed on the edge of the disc under typical operating conditions was found to be 0.92 ± 0.02 gm.cm.$^{-3}$.

6. Air tests of the instrument

These were directed principally to confirmation of the laboratory tests and to obtaining preliminary information concerning the maximum water content to be found in natural clouds. Particular attention was paid to the operation of the instrument as a water content meter in "warm" clouds.

/Traverses

Traverses were made at various ambient temperatures through both convective and layer clouds and the maximum water contents encountered are shown in Table 1. The instrument was found to operate quite satisfactorily under all the conditions encountered and has been adopted for routine work at M.R.F.

7. Accuracy of the instrument

The calibration obtained from the expression

$$y = \frac{60 m V E}{\pi n \rho_i}$$

having been shown to be seriously in error resort was made to an empirical calibration and the accuracy of the instrument calibration became directly dependent on that of the tunnel in which it was tested. The Icing Wind Tunnel at Artington has been calibrated by exploring the working section with a heated intake having unity velocity-ratio connected to a Dobson-Brewer Frost-Point Hygrometer. The distribution of water contents so obtained was integrated and normalised with reference to the input of water into the tunnel, the final distribution of water contents being accepted as the calibration of the working section.

Extreme care was taken in the calibration of the working section and the effect of all the tunnel variables on the calibration examined. The view of the tunnel operators is that this calibration is probably accurate to ± 5% and the experience of the Mechanical Engineering Department, R.A.E. supports this view.

An empirical calibration obtained in the Artington tunnel and used to obtain the figures presented in Table 1 is shown in Fig. 6d.

Discrepancies between the values obtained from the expression above and those obtained practically arise from the interpretation of E since all the other factors are accurately known. Comparison of the two calibrations suggests an empirical value for E of 0.48.

It appears that the constant E should be replaced by one E' which represents the joint effect of the true aerodynamic collection efficiency, E, and a further factor, S, which one might term the "shape factor". The collection efficiency, E, is a function of the shape and dimensions of the instrument and can only be obtained by calculations such as those of Langmuir and Blodgett (7). It does not appear, however, that any great inaccuracy arises in the adoption of the value calculated thus.

The factor, S, arises from the fact that the ice forming on the disc edge does not do so in the rectangular section implied in the equation above but in a more rounded section and further that some of the water tends to flow back from the disc edge before freezing. This factor is not one amenable to calculation and not readily obtainable experimentally.

Both factors are implicit, however, in the empirical calibration.

The question of the departure of the in flight calibration from that obtained in the wind tunnel arises. Any departure arises from variations in E and S due to variations in ρ. It is not considered that any appreciable variation occurs in S and calculations based on Reference 7 indicate that variations in E do not exceed 1% within the altitude range normally used.

The accuracy of the instrument, then, is probably better than ± 10% in the conditions normally encountered.

/8.

8. Conclusion

A reasonably reliable research tool for the measurement of liquid water contents in natural clouds, both "warm" and supercooled, has been produced. Although crude in concept it is, so far as the author is aware, the first successful attempt to measure, continuously, water contents of the order of 4.0 $gm.m^{-3}$.

The preliminary measurements made with this instrument suggest that water contents rather higher than commonly supposed are to be found within convective clouds approaching maturity and that the full theoretical water contents may well be approached. A full investigation of this contention has been commenced and will be the subject of a further report.

9. Acknowledgements

(i) Acknowledgement is particularly due to Mr. F. A. Gordon who constructed the instrument and assisted in the wind tunnel testing. Much of the detail design is due to him and without his enthusiastic and skilful co-operation it is doubtful whether the project could have been carried to a successful conclusion.

(ii) Acknowledgement is due to Mechanical Engineering Department, R.A.E. who provided the wind tunnel facilities and to Mr. F. J. Bigg of that department, with whom the design was discussed from time to time.

10. References

1. Ludlam, F. H., 1951, Quart. J. Roy. Met. Soc., 77, p. 663.

2. Fraser, D., Rush, C. K. and Baxter, D., 1952, N.A.E. Laboratory Report LR 32.

3. Murgatroyd, R. J., 1954, Met. Mag., 83, p. 211.

4. Ludlam, F. H., 1951, Quart. J. Roy. Met. Soc., 77, p. 666.

5. Zaitsev, V. A., 1950, Tech. Trans. Nat. Res. Counc. Canada, No. TT-395.

6. Weickmann, H., 1953, Thunderstorm Electricity, Chapter V, p. 130.

7. Langmuir, I. and Blodgett, K. B., 1946, A.A.E. Tech. Report 5418.

APPENDIX I

q_f = heat of fusion of impinging water, cal.sec.$^{-1}$cm.$^{-2}$

q_k = kinetic heating of water droplets, cal.sec.$^{-1}$cm.$^{-2}$

q_i = heat lost as ice cools from 0 deg.C to θ_s deg.C, cal.sec.$^{-1}$cm.$^{-2}$

q_v = kinetic heating from the air, cal.sec.$^{-1}$cm.$^{-2}$

q_w = heat required to raise water temperature from θ_o deg.C to θ_s deg.C, cal.sec.$^{-1}$cm.$^{-2}$

q_c = convective heat losses, cal.sec.$^{-1}$cm.$^{-2}$

q_e = evaporative heat loss, cal.sec.$^{-1}$cm.$^{-2}$

q_s = conductive heat loss, cal.sec.$^{-1}$cm.$^{-2}$

θ_o = ambient air temperature, degrees centigrade

θ_s = icing surface temperature, degrees centigrade

θ_d = disc temperature, degrees centigrade

L_f = latent heat of fusion, cal.gm.$^{-1}$

L_v = latent heat of vaporisation, cal.gm.$^{-1}$

W = rate of water impingement, gm.sec.$^{-1}$cm.$^{-2}$

E = collection efficiency of disc

m = liquid water content of air sample, gm.cm.$^{-3}$

V = speed of local airstream, cm.sec.$^{-1}$

J = mechanical equivalent of heat, joules cal.$^{-1}$

r = recovery factor, in this case that for a cylinder whose diameter is the edge thickness of the disc

C_p = specific heat of air, cal.gm.$^{-1}$ (deg.C)$^{-1}$

h = coefficient of convective heat transfer, cal.sec.$^{-1}$cm.$^{-2}$(deg.C)$^{-1}$
$= \frac{k}{d_c} . R_e^{0.5}$

p_o = barometric pressure, dynes cm.$^{-2}$

e_s = vapour pressure of water at θ_s, dynes cm.$^{-2}$

e_o = vapour pressure of water at θ_o, dynes cm.$^{-2}$

k = thermal conductivity of air, cal.cm.$^{-1}$sec.$^{-1}$ (deg.C)$^{-1}$

k_i = thermal conductivity of ice, cal.cm.$^{-1}$sec.$^{-1}$(deg.C)$^{-1}$

ρ_i = density of ice, gm.cm.$^{-3}$

n = rate of rotation of disc, rev.min.$^{-1}$

y = thickness of ice on disc edge, cm.

d_e = thickness of edge of disc, cm.

R_e = Reynolds number for disc, using the edge thickness as the significant length

ρ = air density, gm.cm.$^{-3}$

ϵ = specific gravity of water vapour = 0.622

TABLE 1

Date	Time, hr. local	Place	Height ft.	Maximum water content gm.m.-3	Temperature deg. F.	Remarks
15. 6.54	15.00	Local	7000	1.18	39.8	Cumulus
27.10.54	16.30	Local	6000	a. 1.17 b. 1.14	41.0	Cumulus
28.10.54	15.00	Barra Head	3500	a. 0.54	31.0	Rain below Cumulonimbus
			4300	b. 0.25	29.5	Rain below Cumulonimbus
				c. 0.70		Base of Cumulonimbus
	15.30	Isle of Man	11500	d. 0.59	13.1	Altostratus
	16.00	North Wales	7500	e. 0.34	29.8	Stratocumulus
	16.40	Local	3700	f. 0.29	45.0	Stratocumulus
10.11.54	12.20	Boscombe Down	10000	a. 0.57 b. 1.71 c. 2.29 d. 3.55 e. 4.20	20.6	Thick deck of cold front cloud. Embedded Cumulonimbus to 30000 ft. also reported by Boscombe Down aircraft. Peak values for periods of 10 - 15 sec.
	12.40	Local	1800	f. 0.49	42.5	Stratocumulus
10.11.54	16.30	Local	8400	a. 1.30	20.7	Small cumulus
	16.45	Local	7600	b. 0.74	25.4	Small cumulus
12.11.54	15.40	Poole	6000	a. 0.28	23.0	Shallow cumulus entering decay stage
	15.45	Poole	5300	b. 0.44	23.5	
22.11.54	16.13	Swansea	5600	1.49	31.9	Frontal cloud, embedded Cumulonimbus
24.11.54	10.40	(10.m. South of	8200	a. 1.55	19.3	Cumulus over Channel approaching maturity
	10.50	(Brighton	7900	b. 1.30	19.7	
	10.55	(30 m. South	8300	c. 0.57	18.4	Cumulus just past maturity; these clouds produced showers at 11.18 when base dropped from 1600 ft. (38.5°F) to 1270 ft. (40.2°F)
	11.05	(of Brighton	8100	d. 1.98	19.4	
	11.10		7600	e. 1.09	19.1	
23.11.54	12.25	Local	6800	0.87	23.6	Cumulus, base 1900 ft.

/25.11.54

TABLE 1 continued

Date	Time, hr. local	Place	Height ft.	Maximum water content gm.m.$^{-3}$	Temperature deg. F.	Remarks
25.11.54	11.55	Isle of Wight	6000	a. 0.48	31.2	Cumulus, base 1900 ft., 47.0°F
	11.58	" "	6020	b. 0.36	27.4	
	12.05	" "	7050	c. 1.11	27.6	Cumulus, base 1900 ft., 47.0°F
	12.15	" "	7500	d. 1.17	28.0	at maturity. Peaks last 5 - 10 sec.
30.11.54	12.25	English Channel	12000	a. 3.20	4.0	Cumulus close to maturity and about to
	12.35	" "	12800	b. 2.61	- 1.1	glaciate
	12.40	" "	10900	c. 3.75	7.9	
1. 12.54	15.40	English Channel	9000	a. 0.34	17.0	Cumulus approaching maturity, visibility
	15.45	" "	9000	b. 0.68	17.0	occasionally 5 yd.
	16.00	" "	8500	c. 0.75	19.4	

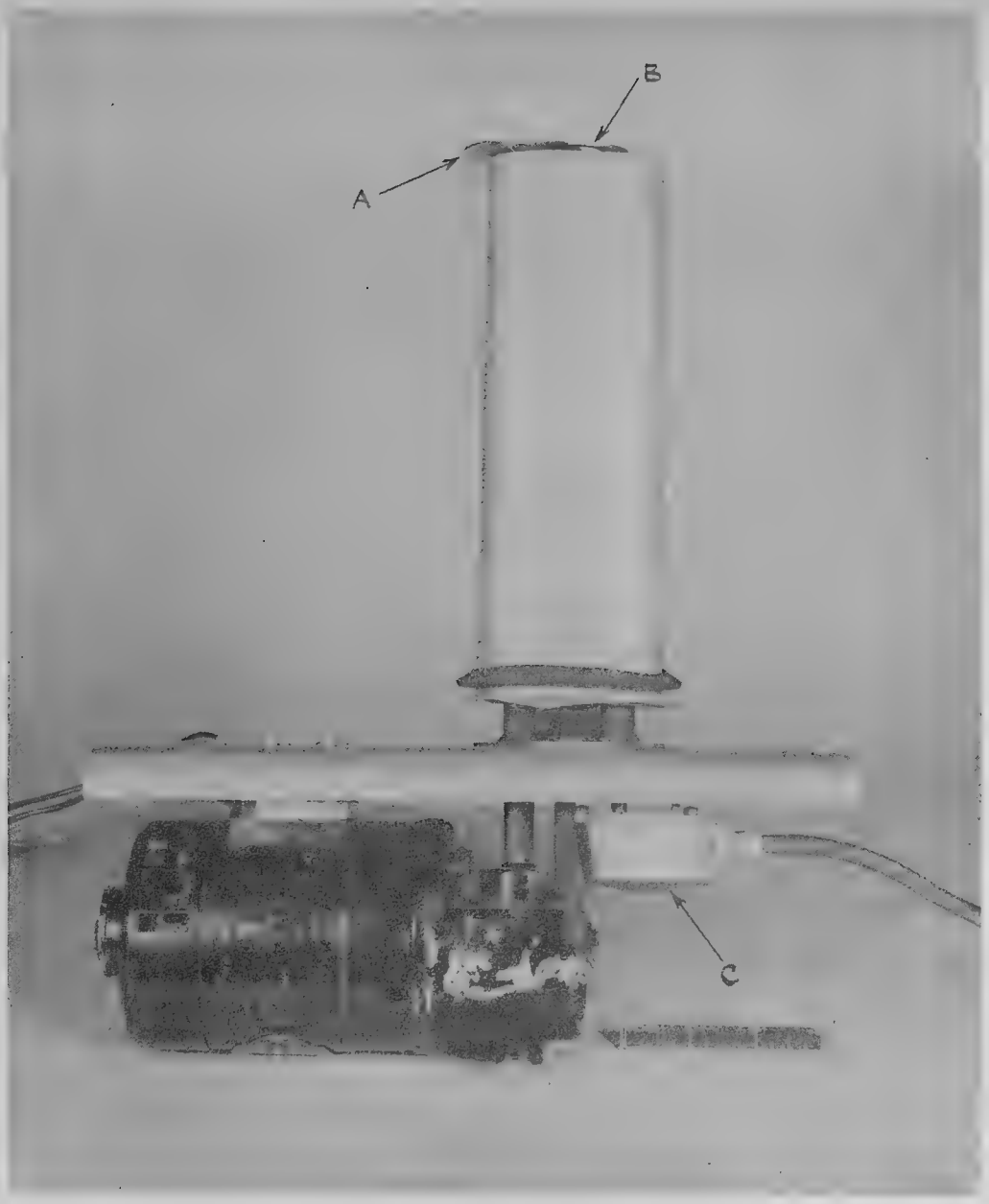

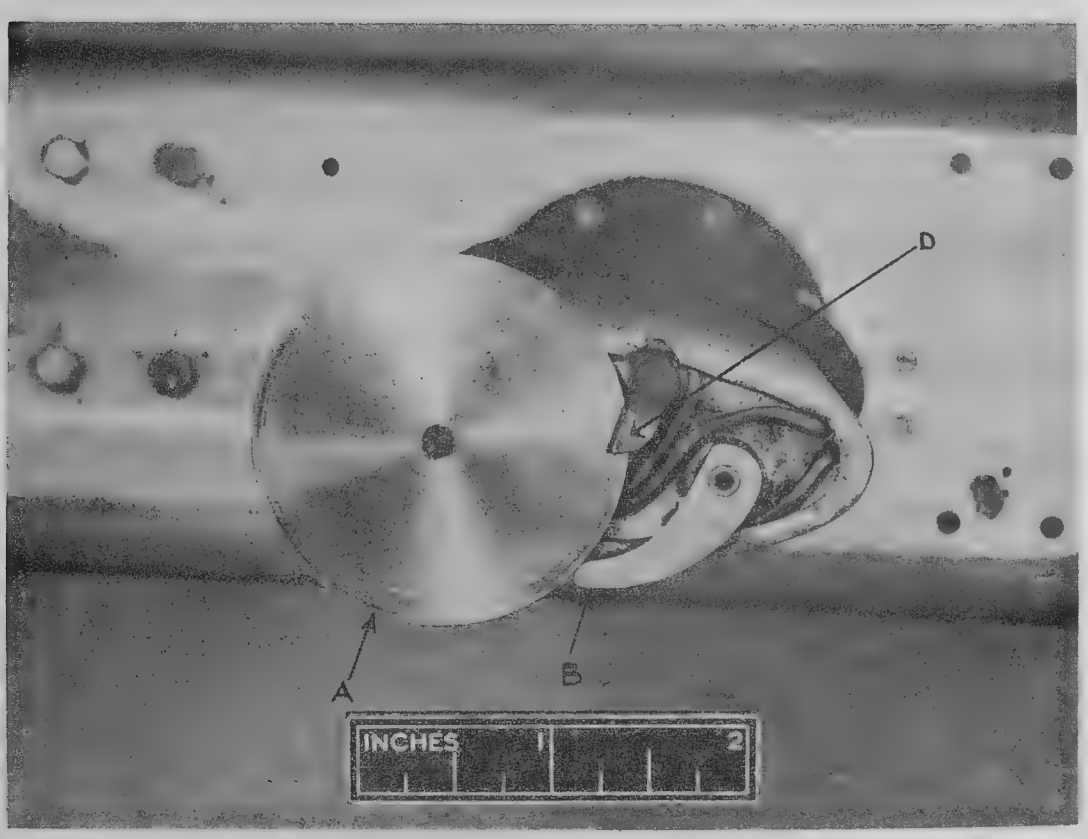

Figs. 1a. and b. Conventional Rotating Disc Icing Meter.

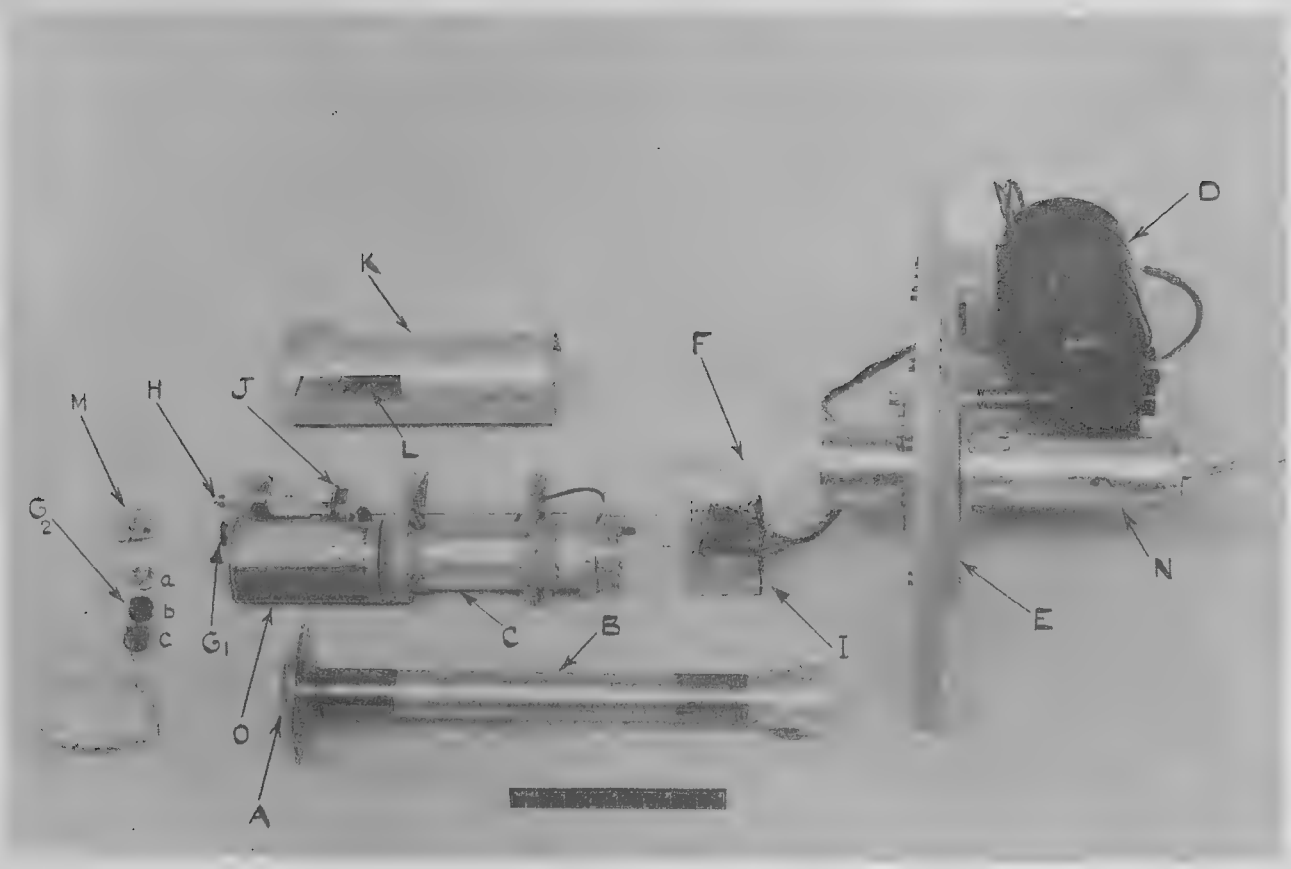

Fig. 2a. Refrigerated Rotating Disc Icing Meter Components.

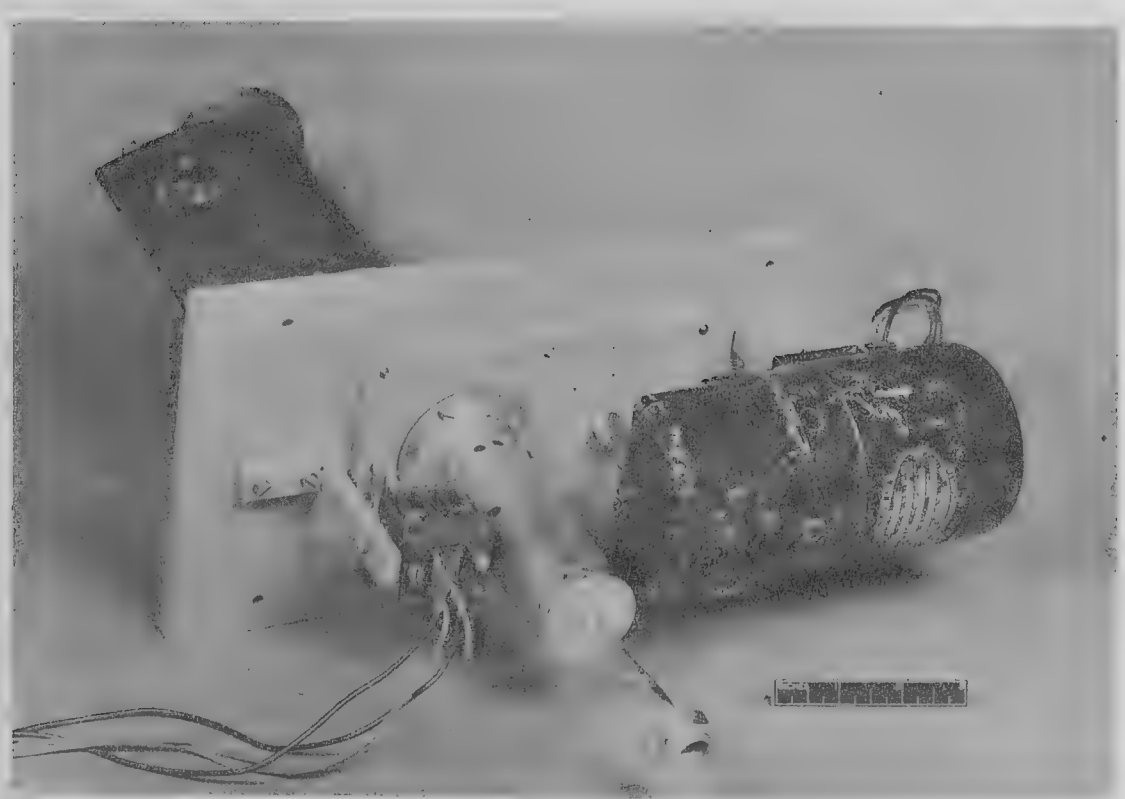

Fig. 2b. Refrigerated Rotating Disc Icing Meter – Bottom View

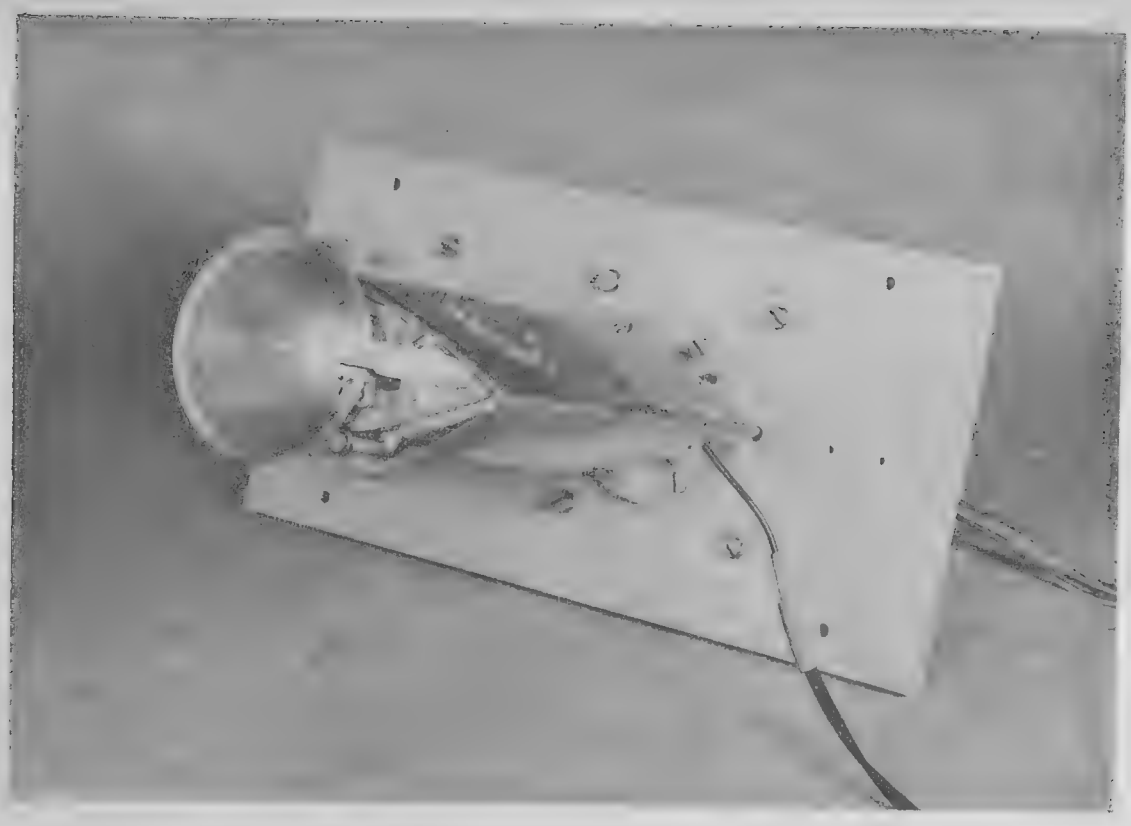

Fig. 2c. Refrigerated Rotating Disc Icing Meter - Top View.

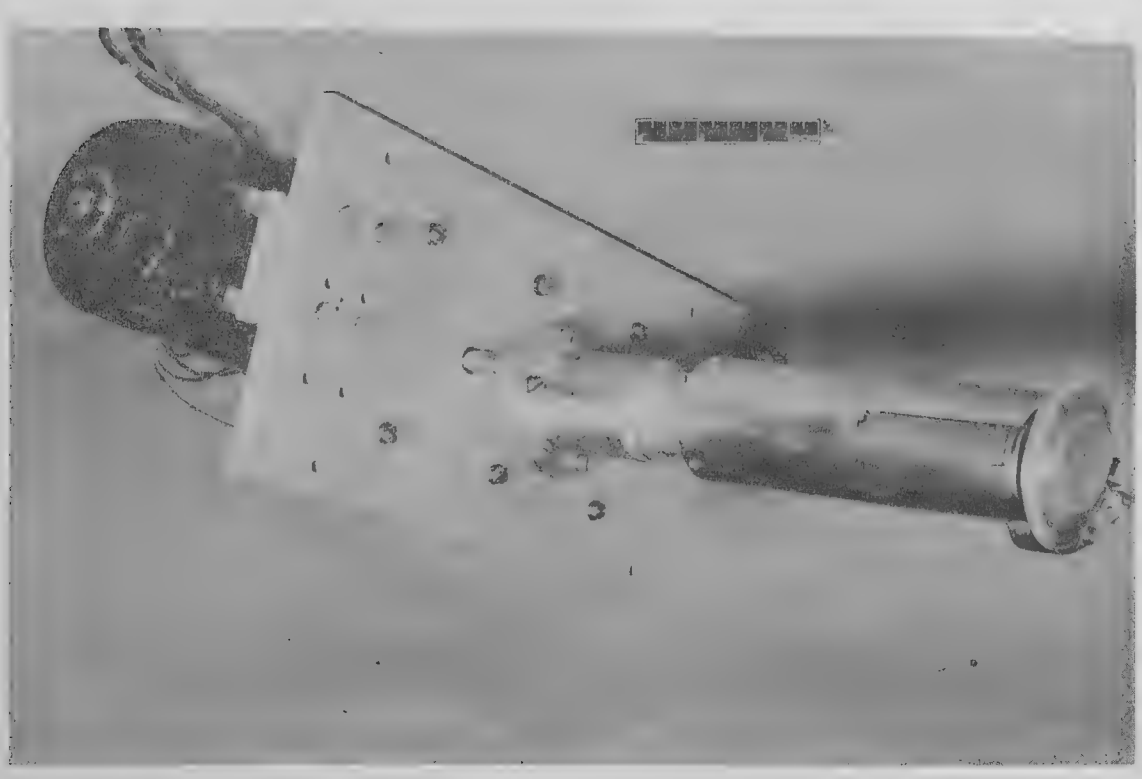

Fig. 2d. Refrigerated Rotating Disc Icing Meter - Front View

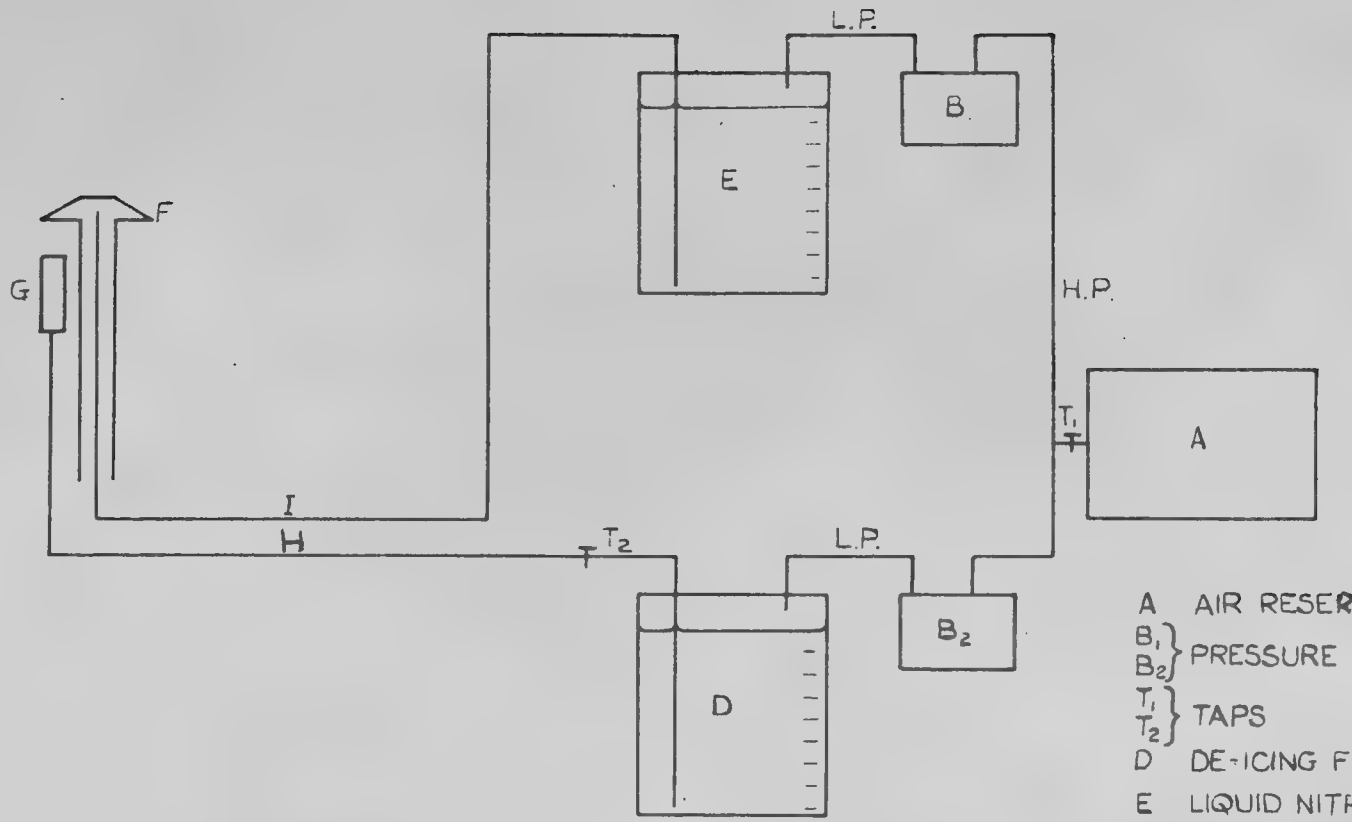

A AIR RESERVOIR
B1, B2 } PRESSURE REGULATORS
T1, T2 } TAPS
D DE-ICING FLUID RESERVOIR
E LIQUID NITROGEN RESERVOIR
F ROTATING DISC AND HOLLOW SHAFT
G DE-ICING STRIP
H.P. HIGH PRESSURE AIR
L.P LOW PRESSURE AIR
H DE - ICING FLUID
I LIQUID NITROGEN

FIG. 3. FLUID CIRCUITS - SCHEMATIC.

FIG. 3.

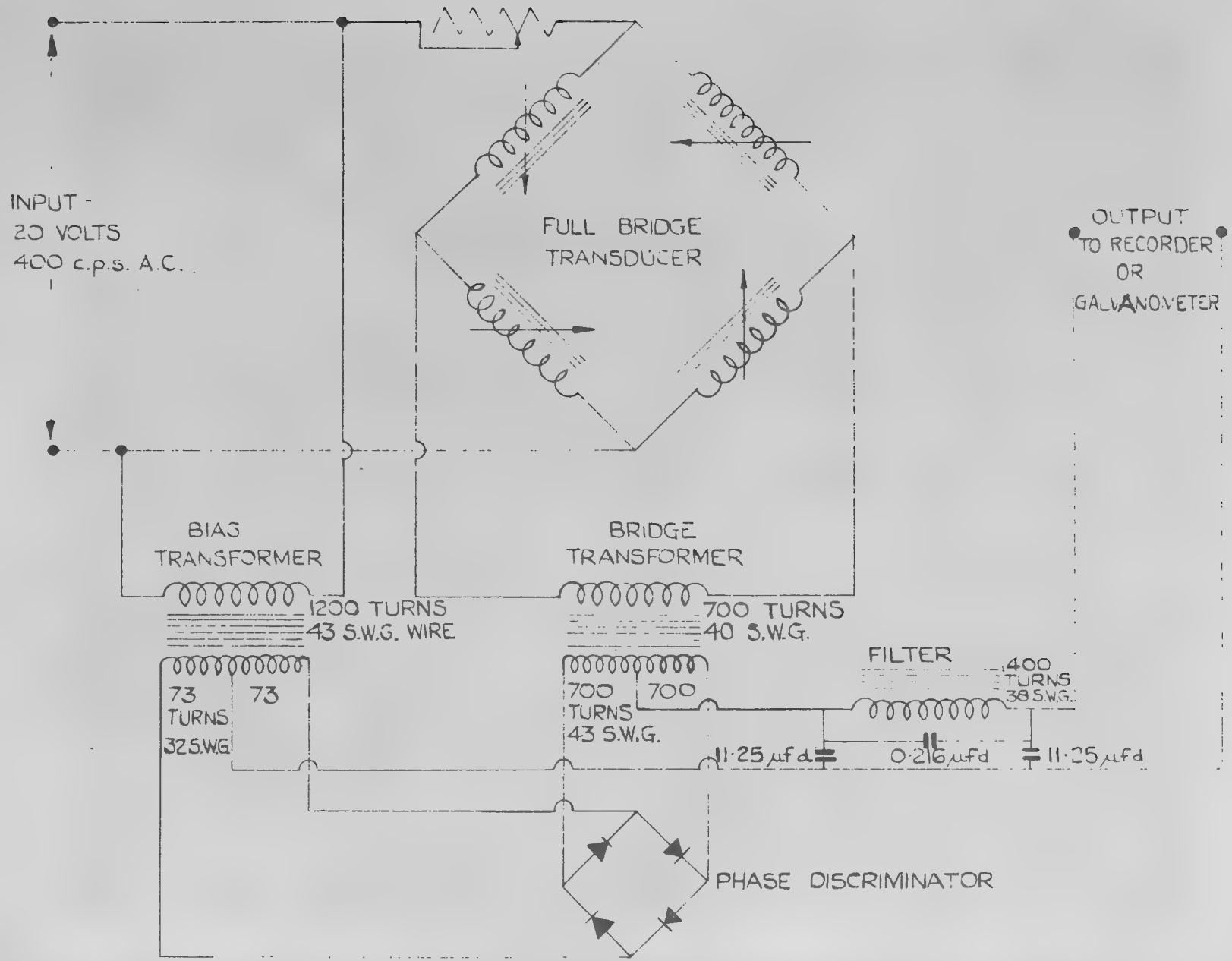

FIG. 4. ICE THICKNESS MEASUREMENT CIRCUIT

FIG. 4.

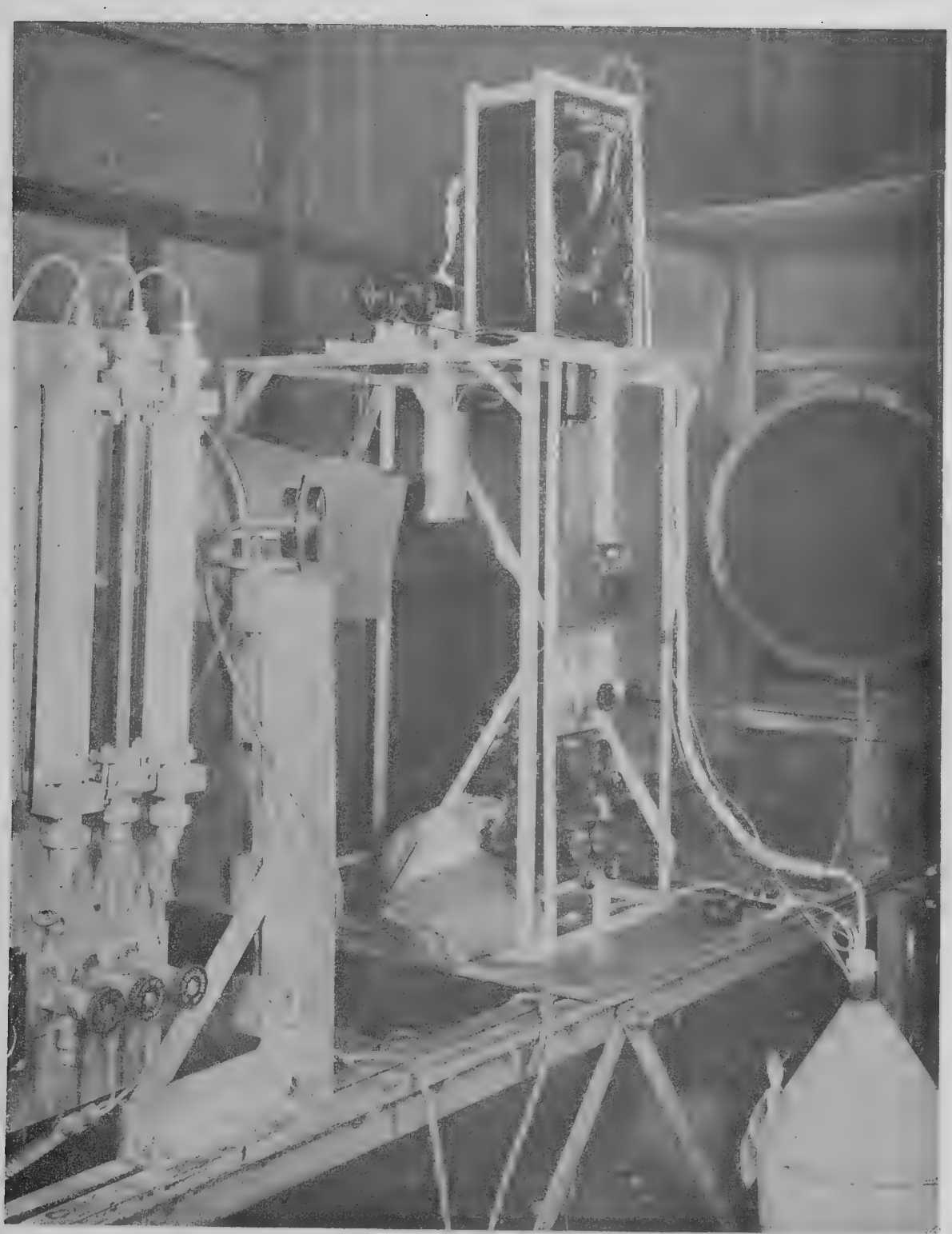

Fig. 5 Instrument under test in Icing Wind Tunnel.

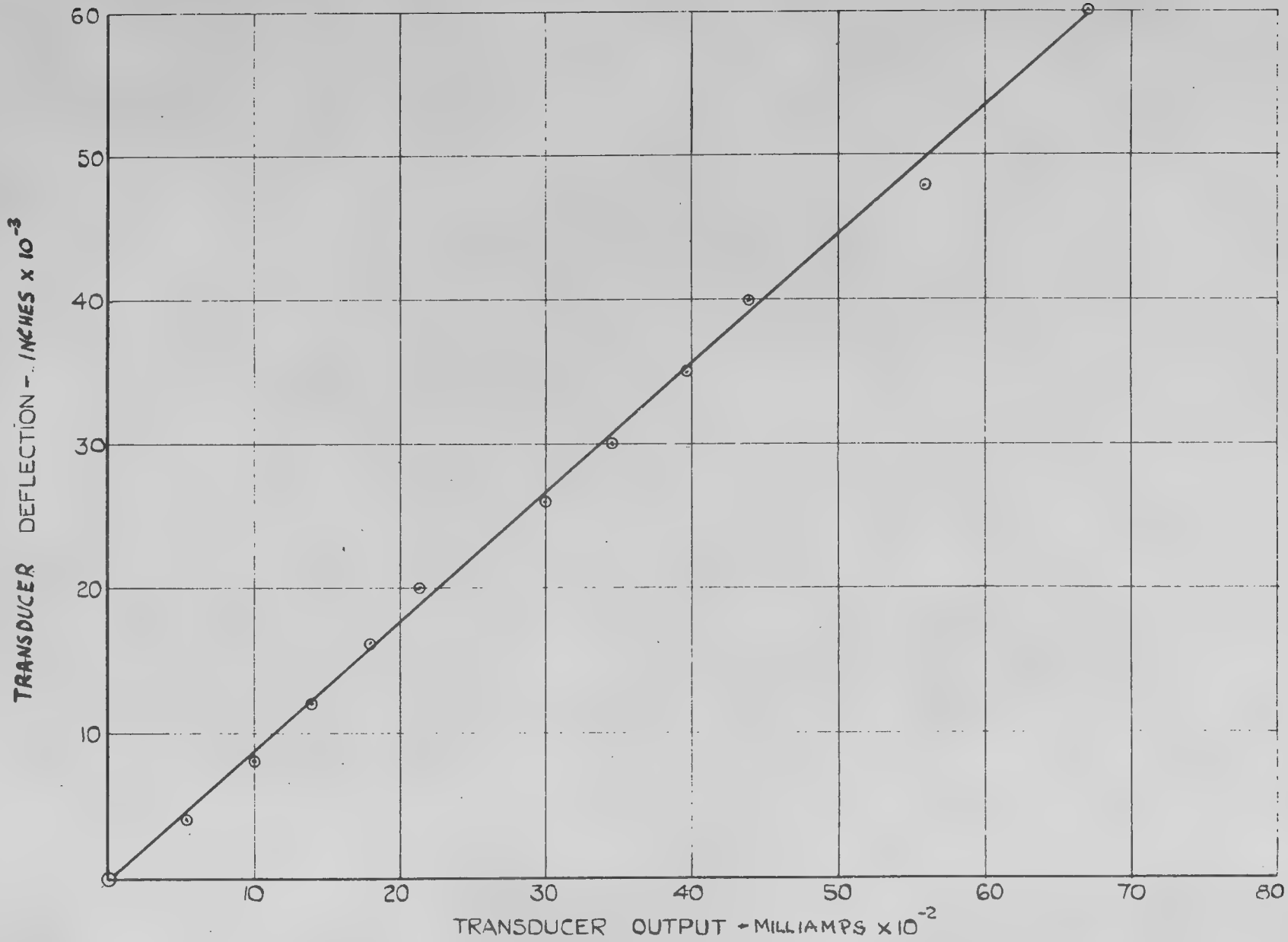

FIG. 6(a). TRANSDUCER PERFORMANCE.

FIG. 6(a).

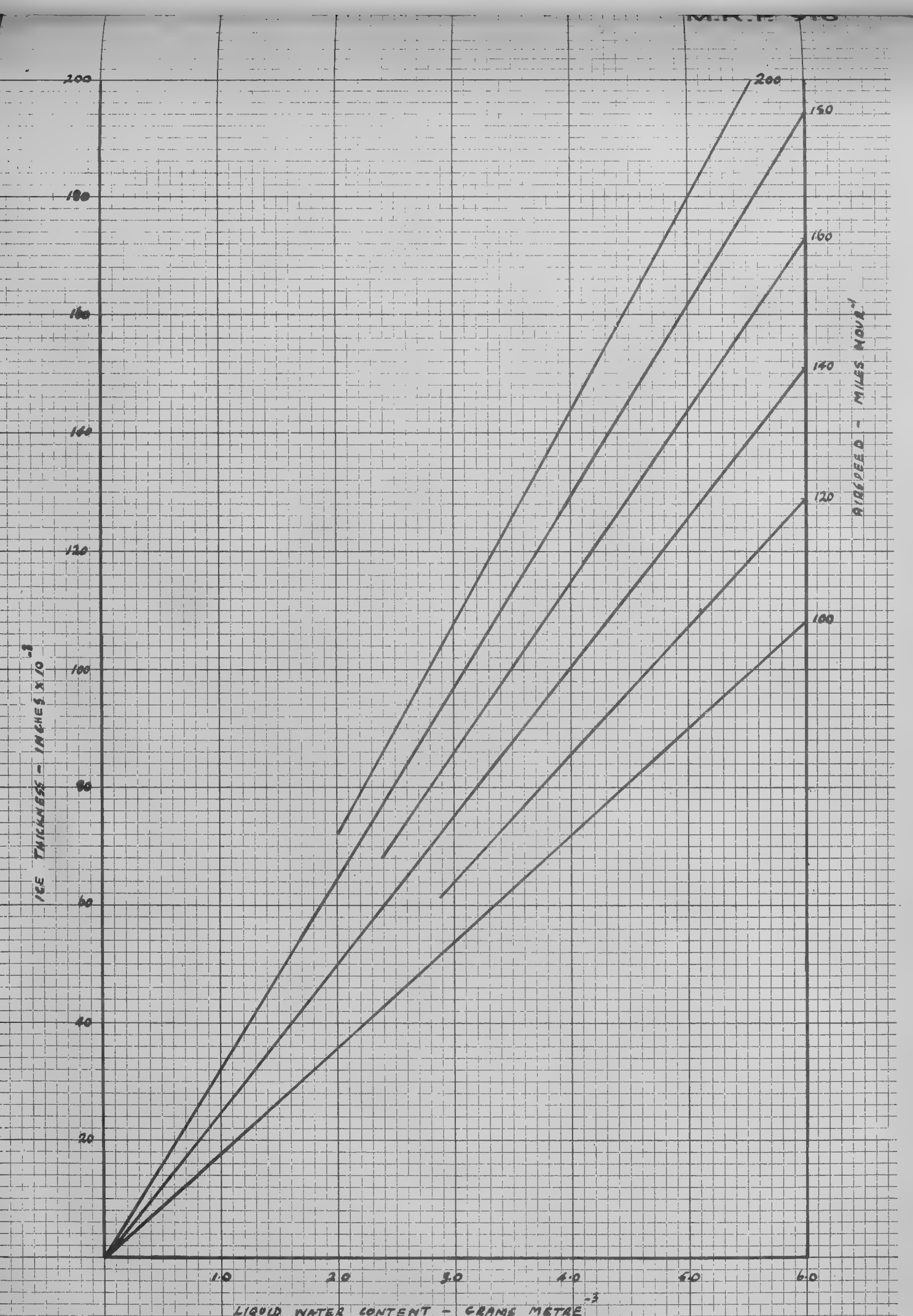

FIG. 6 b. THEORETICAL CALIBRATION BASED ON EQUATION $y = \frac{60\,m\,v\,\xi}{\pi r l i}$

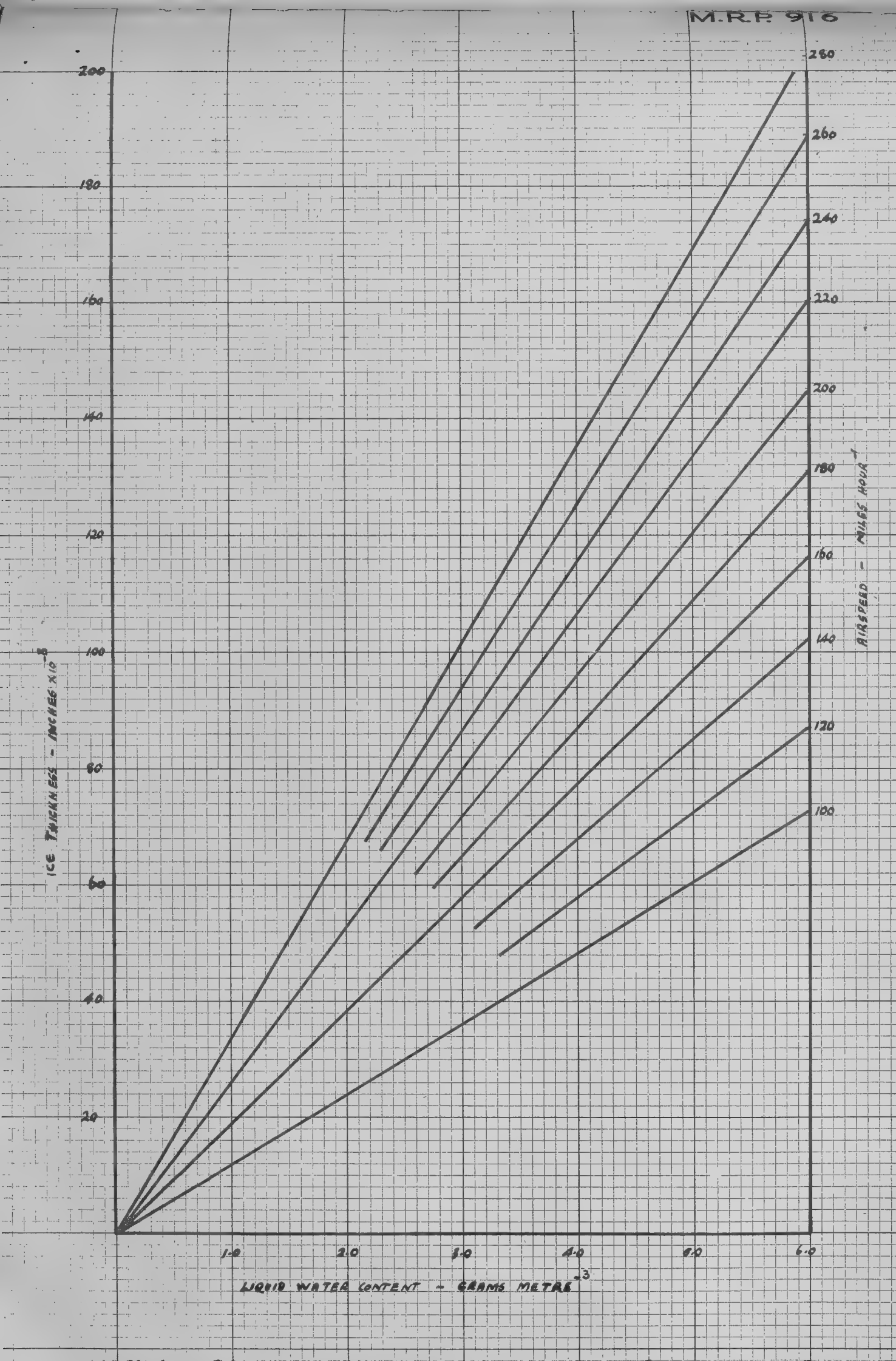

FIG. 6 c. PROVISIONAL EMPIRICAL CALIBRATION OBTAINED IN R.A.E. ICING WIND TUNNEL

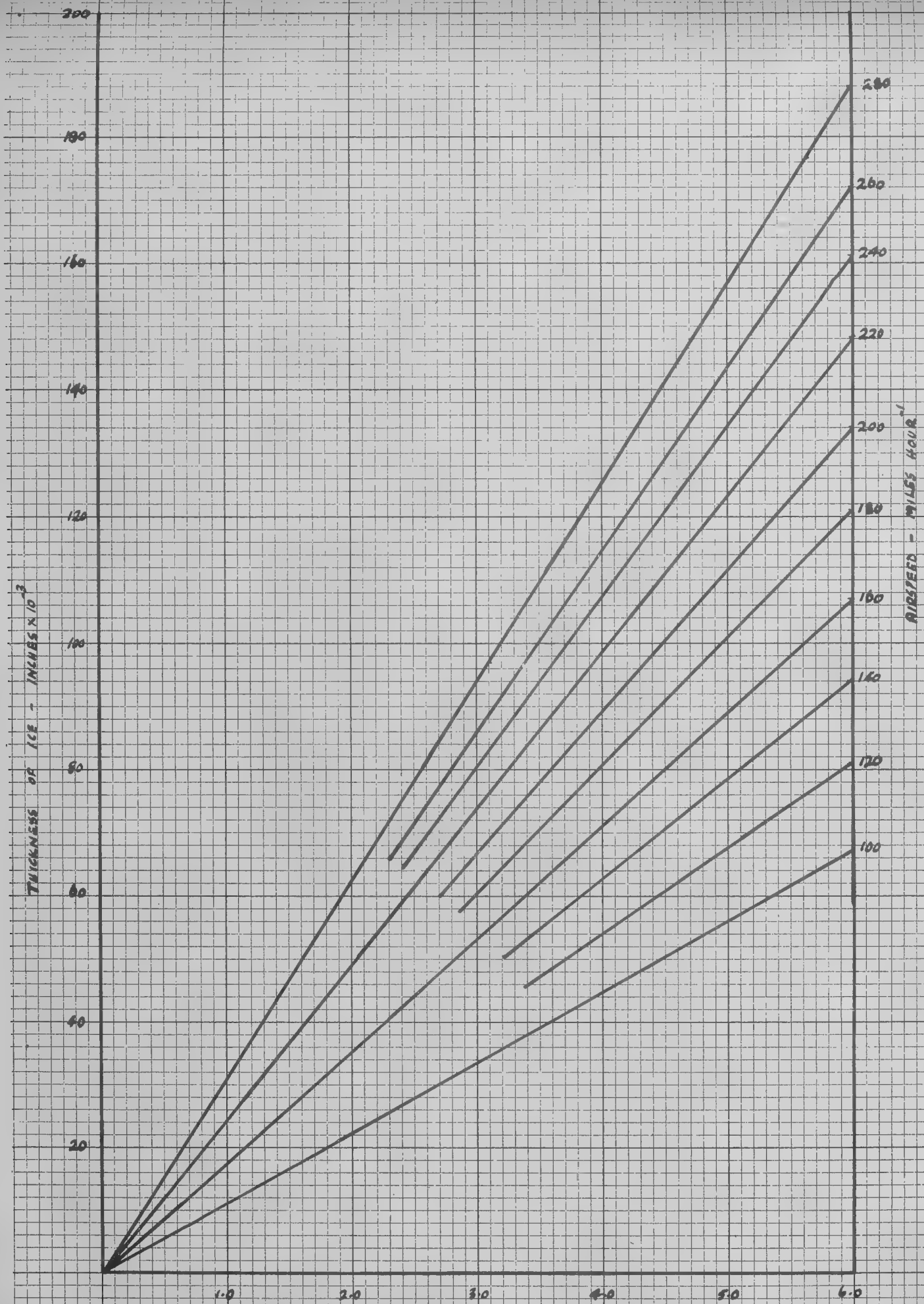

FIG. 6 d. FINAL EMPIRICAL CALIBRATION OBTAINED IN CALIBRATED ICING WIND TUNNEL AT ARTINGTON.

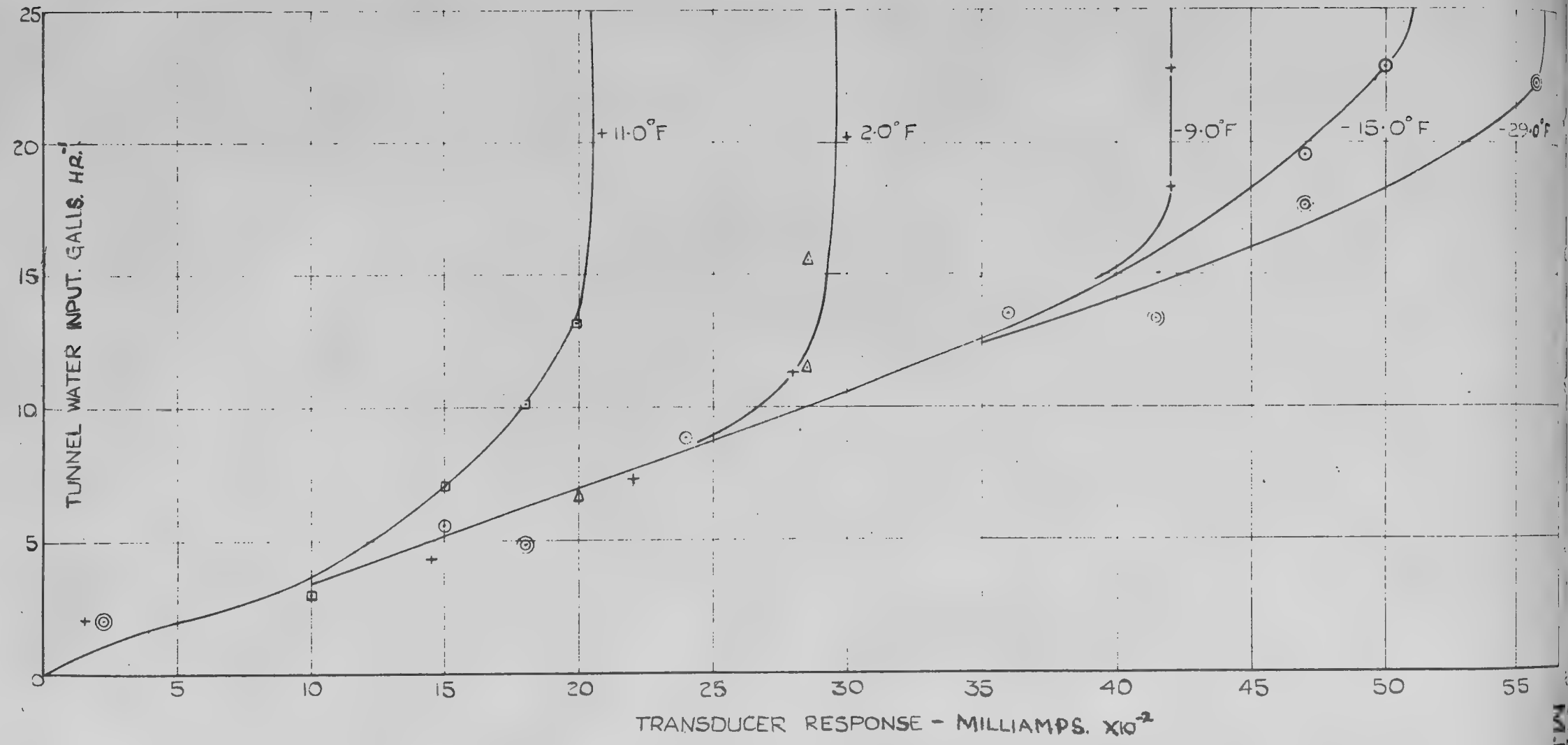

FIG. 7. TRANSDUCER CHARACTERISTICS AT VARIOUS DEGREES OF REFRIGERATION, FIGURES INDICATE DISC TEMPERATURE AT ZERO WATER CONTENT.

M.R.P. 916
FIG. 7.

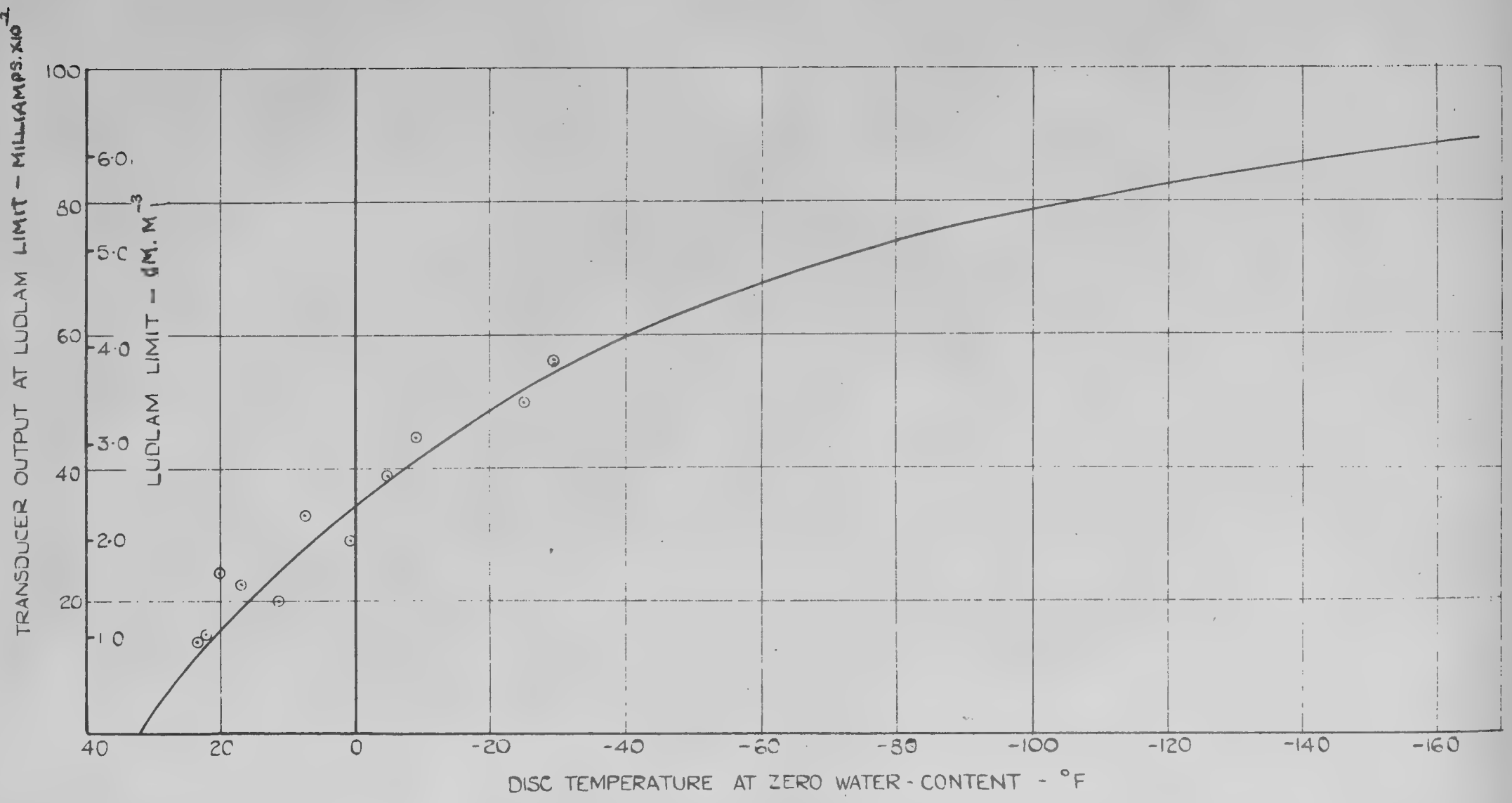

FIG. 8. VARIATION OF LUDLAM LIMIT WITH DEGREE OF REFRIGERATION OF DISC.

FIG. 8.

M.R.P. 917.
S.C. II/189.
8th JUNE, 1955.

The variation of the normal air temperature over the Northern Hemisphere during the year.

by

J. M. CRADDOCK.
(METEOROLOGICAL OFFICE)

AWSSS
ROUTING SLIP

FILE	INFO	ACTION	
			ASST TO DIRECTOR
	1		CONSULTANTS
	2		EDB
			SEC
			CHF
	3	EDD	HLFB
			STB
	4	TIPD	PUE
			SEC

AIR MINISTRY
METEOROLOGICAL RESEARCH COMMITTEE.

At the time of issue this report has not been published. Any author desiring to quote this paper should refer to it as "A paper of the Meteorological Research Committee (London).
M.R.P.No. 917 by Mr. J. M. Craddock
A copy is available in the Library of the Meteorological Office."

M.R.P. 917
S.C.II/189
8th June, 1955

AIR MINISTRY

METEOROLOGICAL RESEARCH COMMITTEE

The variation of the normal air temperature over the Northern Hemisphere during the year

by

J. M. Craddock (Meteorological Office)

Summary

Tables are given for calculating, on alternative hypotheses, the best fitting two term harmonic representation of 12 monthly mean values of a meteorological variable. One of these tables is used to estimate the harmonic parameters for the annual temperature variation for each of 305 stations covering the Northern Hemisphere, based on the monthly mean temperatures for the period 1921-1940. Charts showing the variation of the harmonic parameters over the hemisphere are described. A table is described giving the normal temperature, derived from the two term harmonic at 5-day intervals throughout the year for 280 of the 305 stations. The stability of normal temperatures computed in this way is discussed.

1. Introduction

This work arises directly from investigations under the Meteorological Research Programme, Part 2, 5(a) and (b) into the magnitude and persistence in time and space of temperature anomalies.

Weather anomalies are departures from a more or less well-defined normal state of the atmosphere, and our study of them is beset by two difficulties, depending on the time unit over which the data we look at are averaged. If the time unit is very short, an hour or a day, for example, it proves almost impossible to assemble the relevant data, or to assimilate their meaning when assembled. If the time unit is too long, important features will be obscured by the process of averaging. The optimum time unit for any purpose is the longest which shows all the important anomalies while smoothing those of shorter duration. To do this the time interval should last for only a fraction, perhaps not more than one half or one third of the lifetime of the important anomalies. The choice of the best, or at any rate a suitable time unit for use in long range forecasting is a fundamental question which does not seem to have been investigated fully. An investigation into this question is now in progress, but in the meantime we can be sure of one thing. General synoptic experience is that many significant anomalies last for much less than a month, so the time unit used in investigating them should also be less than a month. To study anomalies averaged over periods shorter than a month, we must have normals for the same shorter periods. Hence to examine the magnitude and geographical extent of significant temperature anomalies we must know the normal temperatures for periods less than a month, over the relevant area, which certainly covers a large part of the Northern Hemisphere. We are faced with the problem of preparing temperature normals for particular days, or periods of a few days, when generally the only data we have to go on are monthly mean temperatures.

/The

The present work seeks to solve the problem on the assumption, for which the justification lies in previous work, Craddock (1955), that the normal form of the annual temperature variation is given accurately enough by the two term harmonic form

$$T = a_0 + a_1 \cos\theta + b_1 \sin\theta + a_2 \cos 2\theta + b_2 \sin 2\theta \qquad \text{------ (1)}$$

The method is to find the values of the constants which best fit the observed monthly mean temperatures, and then find the normal for any individual day, or other period by harmonic synthesis. This may seem a roundabout way to estimate a quantity of which a crude estimate can be made by simple graphical interpolation between monthly mean values, but in fact it has a great deal to recommend it. The harmonic parameters are easy to manipulate, and to interpret, while it appears in the course of the investigation that they can be estimated very accurately. The fact that the estimation is quite objective means that it is possible and worthwhile to calculate statistics describing the anomalies of temperature in detail. Finally, now that the groundwork has been done, the whole process of calculation is efficient and reliable, and suitable for performance by either mechanical or electronic calculating machines.

2. The mathematical background

The harmonic analysis of monthly mean values has usually been carried out by treating all the months as of equal length, and the errors involved in doing this have been discussed by inter alia Forbes (1860) and Bilham (1918). The validity of this treatment may be open to argument and the present approach, which does not treat the months as of equal length, is thought to be more satisfactory theoretically, while being just as easy to use.

If it is assumed that the normal temperature variation at a station is of the two term harmonic form given by equation (1) in which θ is measured from zero at midnight on December 31st, and increases by 2π during the year then the problem is to find the parameters a_0, a_1, b_1, a_2, b_2, which give the best fit to the observed monthly mean temperatures.

When a Fourier analysis is carried out on a series of equally spaced observations covering the basic period, the successive harmonics are best fitting approximations to the observations by the criterion of least squares, and they are orthogonal in the sense that the omission of one harmonic or the inclusion of an extra one does not affect the values of the rest. If, however, the observations are at unequal intervals we must decide whether they should all be treated as of equal importance in fitting the harmonic form, and in general the harmonics will not be orthogonal. For this reason we cannot without further investigation use Weihrauch's solution (1890) quoted by Pollak (1948) which calculates six harmonics from monthly mean values (and therefore fits the data exactly) when we intend to use only two harmonics.

Assuming that the year has exactly 365 days, we can write down the value of θ corresponding to every day of the year, and by means of equation (1) express the temperature for that day as a linear function of a_0, a_1, b_1, a_2 and b_2. If this expression is written down for each day in a given calendar month, summed and divided by the number of days of the month, we obtain an estimate of the monthly mean temperature. If we denote by r_i the difference between this estimate and the observed temperature for the i^{th} month then r_i is a linear function of the parameters a_0, a_1, b_1, a_2 and b_2. We now seek the best fitting values of these parameters by minimising

$$S = \sum_{i=1}^{12} w_i r_i^2 \qquad \text{-------- (2)}$$

where w_i is a positive weighting coefficient which measures the importance we attach to a discrepancy between observed and estimated values in the i^{th} month. The solutions are

$$\frac{\partial S}{\partial a_0} = \frac{\partial S}{\partial a_1} = \frac{\partial S}{\partial b_1} = \frac{\partial S}{\partial a_2} = \frac{\partial S}{\partial b_2} = 0 \qquad \text{------- (3)}$$

giving 5 simultaneous equations from which the five parameters can be obtained as linear expressions of the twelve observed monthly mean temperatures.

Before solving these equations, we must decide on the weighting coefficients w_i. If the monthly mean temperatures were derived from a two term harmonic form, so that a perfect fit was possible, then all the residuals would be zero, and the choice of weighting coefficients would be a matter of indifference. Although a perfect fit is impossible, we do from our previous investigation expect a very good fit, so that the residuals should be very small. Hence if we choose weighting factors which are not quite the best, as we are compelled to in order to bring the calculation within the bounds of possibility, we may still get a fit which is not appreciably worse than the best. There are three obvious ways of choosing the weights:-

(1) We may make them all equal. This is simple, but not logically consistent, since we are trying to allow for the months being of unequal length. Moreover, it offers no advantages in time saving compared with the next alternative. On this hypothesis, a_o will be the mean of the 12 monthly means, and not the true annual mean. This case is not considered further.

(2) We may make the weights equal to the number of days in the respective months. This is logically correct if on all calendar days the temperature is equally variable, and if the serial correlations between temperatures on consecutive days are either all zero, or at least independent of the time of the year. These conditions are not satisfied strictly by any observed series of temperatures. Nevertheless, it is hard to suggest a better hypothesis for use when we have no prior knowledge of the variability to be expected at each station, and, as mentioned above, any resulting discrepancies are likely to be small, so this hypothesis was used in the practical work which follows.

(3) We may make the weights inversely proportional to the observed variances of the monthly mean temperatures for each station. This hypothesis, which includes the preceding one as a special case, ensures that a discrepancy in a month for which the temperature is very variable should be treated as of less account than an equal discrepancy in a more uniform month, which is just as it should be. However, to apply this hypothesis strictly it would be necessary, not only to calculate the variance of monthly mean temperature for each month for each station, but also to solve the equations (3) afresh for every station. It was quite impracticable to do this, but nevertheless it seemed desirable to provide some means of judging how the best fit would be altered because the monthly mean temperatures are more variable in some months than in others. So three typical weighting patterns were chosen, in the hope that any station for which the second hypothesis was inadequate might conform closely enough to one of these. The five linear simultaneous equations (3) can be solved by algebraic methods to give a_o, a_1, b_1, a_2, b_2 as linear functions of the monthly mean temperatures T_1, T_2 - - - T_{12}. Instead, however, the equations were solved numerically for twelve special cases, namely, those in which one monthly mean temperature was equal to unity, and all the rest were zero. The solutions on the second hypothesis (weights equal to the number of days in each month) were obtained by Mr. A. Gilchrist by relaxation methods and are given in Table 1 in the form suitable for practical use.

/Table 1

Table 1

Multipliers for finding the coefficients of the two term harmonic form $a_o + a_1 \cos\theta + b_1 \sin\theta + a_2 \cos 2\theta + b_2 \sin 2\theta$ from 12 monthly mean values of a meteorological variable

Monthly mean	Multipliers to give:-					
	a_o	a_1	b_1	a_2	b_2	Sum
T_1	.0849	.1655	.0455	.1526	.0904	.5389
T_2	.0767	.1111	.1088	.0034	.1621	.4621
T_3	.0849	.0490	.1646	-.1486	.0971	.2470
T_4	.0822	-.0389	.1616	-.1530	-.0786	-.0267
T_5	.0849	-.1185	.1242	-.0081	-.1776	-.0951
T_6	.0822	-.1598	.0467	.1453	-.0929	.0215
T_7	.0849	-.1669	-.0409	.1572	.0823	.1166
T_8	.0849	-.1227	-.1201	.0037	.1777	.0235
T_9	.0822	-.0444	-.1604	-.1476	.0891	-.1811
T_{10}	.0849	.0432	-.1664	-.1551	-.0864	-.2798
T_{11}	.0822	.1168	-.1184	-.0023	-.1726	-.0943
T_{12}	.0849	.1655	-.0455	.1526	-.0904	.2671

In use the 12 monthly mean temperatures are written in column and are multiplied in turn by the columns in Table 1 to give the respective harmonic coefficients. The final column provides a sum check (i.e. if the calculation is correct, the result of multiplication by this column will tally with the sum of the harmonic coefficients).

The solution on the other three hypotheses were obtained by electronic means under the direction of Mr. F. H. Bushby, and are given in Tables 2, 3 and 4.

Table 2

Monthly mean	Weighting coeff.	Multipliers to give:-					
		a_o	a_1	b_1	a_2	b_2	Sum
T_1	.1242	.0866	.1610	.0574	.0868	.0732	.4650
T_2	.0946	.0693	.0969	.0928	.0091	.0924	.3605
T_3	.1333	.0836	.0580	.1478	-.0700	.0953	.3147
T_4	.2188	.0932	-.0270	.1802	-.1471	.0081	.1074
T_5	.3731	.0851	-.1309	.1392	-.1012	-.1673	-.1751
T_6	.5780	.0637	-.1597	.0325	.1199	-.2107	-.1543
T_7	1.2195	.0994	-.1728	-.0631	.3291	.1017	.2943
T_8	.8772	.0913	-.1030	-.1005	-.0942	.2964	.0900
T_9	.4587	.0681	-.0544	-.1330	-.2048	.0364	-.2877
T_{10}	.3984	.0904	+.0325	-.2051	-.1186	-.1680	-.3688
T_{11}	.2227	.0810	.1239	-.1197	.0639	-.1325	.0166
T_{12}	.1621	.0882	.1756	-.0284	.1272	-.0249	.3377

/Table 3

Table 3

Monthly mean	Weighting coeff.	Multipliers to give:- a_o	a_1	b_1	a_2	b_2	Sum
T_1	.1136	.0839	.1538	.0490	.0941	.0717	.4525
T_2	.0926	.0672	.1035	.0807	.0280	.0966	.3760
T_3	.1563	.0875	.0730	.1553	-.0803	.1129	.3484
T_4	.2778	.1009	-.0379	.2067	-.1835	-.0152	.0710
T_5	.3125	.0716	-.1343	.1099	-.0562	-.1794	-.1884
T_6	.4000	.0730	-.1644	.0244	.1516	-.1662	-.0816
T_7	.5263	.0936	-.1510	-.0386	.2282	.0821	.2143
T_8	.5556	.0934	-.1212	-.1003	-.0269	.2633	.1083
T_9	.4167	.0699	-.0612	-.1522	-.2085	.0689	-.2831
T_{10}	.3571	.0844	.0409	-.1966	-.1344	-.1577	-.3634
T_{11}	.2222	.0892	.1373	-.1164	.0634	-.1497	.0238
T_{12}	.1409	.0855	.1615	-.0219	.1244	-.0274	.3221

Table 4

Monthly mean	Weighting coeff.	Multipliers to give:- a_o	a_1	b_1	a_2	b_2	Sum
T1	.1136	.0888	.1548	.0463	.1088	.0650	.4637
T2	.1111	.0793	.1149	.0933	.0233	.1163	.4271
T3	.1471	.0754	.0657	.1373	-.0822	.1090	.3052
T4	.3030	.0932	-.0337	.2111	-.2086	-.0159	.0461
T5	.3704	.0808	-.1508	.1215	-.0366	-.2130	-.1981
T6	.3333	.0796	-.1550	.0137	.1834	-.1230	-.0013
T7	.3030	.0838	-.1312	-.0374	.1752	.0838	.1742
T8	.3704	.0967	-.1416	-.1015	-.0122	.2329	.0743
T9	.2941	.0671	-.0661	-.1405	-.1753	.0791	-.2357
T10	.3333	.0916	.0550	-.2136	-.1548	-.1494	-.3712
T11	.1923	.0857	.1423	-.1097	.0596	-.1486	.0293
T12	.1177	.0781	.1457	-.0204	.1193	-.0362	.2865

In each case the weighting factors corresponding to the solution in question are given in the first column.

Comparison between the four solutions shows that the calculation of the first harmonic is much the same on any hypothesis, but that the evaluation of the second harmonic depends much more on the hypothesis used. The question how much difference this makes in the final results has not yet been investigated fully owing to the difficulty till recently of calculating the monthly variances and the harmonic coefficients on a scale large enough to enable a reliable comparison to be made. In what follows the second hypothesis, incorporated in Table 1, has been used throughout. The monthly mean values corresponding to any set of values of the harmonic parameters can be found by using Table 5 in a similar way.

Table 5

Multipliers for finding the monthly mean values corresponding to given values of the coefficients of the two term harmonic form $a_o + a_1 \cos\theta + b_1 \sin\theta + a_2 \cos 2\theta + b_2 \sin 2\theta$

	J	F	M	A	M	J	J	A	S	O	N	D	Sum
A_1	.9532	.7078	.2810	-.2319	-.6820	-.9493	-.9596	-.7062	-.2649	.2482	.6948	.9532	.0443
B_1	.2605	.6927	.9474	.9614	.7151	.2771	-.2359	-.6912	-.9528	-.9565	-.7038	-.2605	.0535
A_2	.8207	.0207	-.7991	-.8510	-.0451	.8060	.8447	.0205	-.8190	-.8330	-.0123	.8207	-.0262
B_2	.4849	.9615	.5197	-.4359	-.9522	-.5144	.4419	.9530	.4935	-.4635	-.9561	-.4849	.0475

3. The basic period and data

The basic period of years from which the normals are to be calculated must be long enough to reduce errors due to the peculiarities of individual years to an acceptable level, but not so long as to entail bias due to climatic change. Moreover, the period should be as recent as possible, since forecasting is the final objective, and should be as far as possible the same for all stations. The question of finding the period which represents the most satisfactory compromise between these requirements deserves an investigation to itself, but results were wanted quickly, and the 20 years 1921-1940 were chosen, largely because the World Weather Records published by the Smithsonian Institute provide a most convenient source of monthly mean temperature data for years up to 1940.

Synoptic arguments show that the area for which the normals are required must cover at any rate a large part of the Northern Hemisphere, and rather than fix an arbitrary and perhaps erroneous boundary, the analysis was extended to all Northern Hemisphere stations in the World Weather Records which gave enough data, and also to a good many additional stations for which data were obtained from other branches of the Meteorological Office, so as to form as complete a network as possible of stations covering all land areas of the Northern Hemisphere. To avoid having to break isopleths at the coastlines, the analysis was extended to the air temperature at enough points in the oceans to give the run of the isopleths, using data provided by the Marine Branch of the Meteorological Office. The stations used are shown in Fig. 1.

4. The practical calculation

The data were written in vertical columns, and the harmonic analysis carried out using Table 1. Rather over 300 stations were used, the summations of products being carried out on hand operated Friden multipliers. The whole calculation including checking, mostly by repetition, lasted over several months. The phase and amplitude of the first and second harmonics were found. The numerical values are given in Table 6 while Figs. 2 to 8 show the geographical variation of the parameters in a readily assimilable form.

5. The variation of the parameters of the normal temperatures over the Northern Hemisphere

The phase and amplitude of the first and second harmonics of the normal temperature were found from a_1, b_1, a_2, b_2 in the usual way, and charts showing variation over the northern hemisphere of the annual mean a_0 and of A_1, ϕ_1, A_2, ϕ_2 are shown in Figs. 2, 3, 4, 5 and 7. The second harmonic is in most parts of the hemisphere of much smaller amplitude than the first and it is generally better to consider it in relation to the first harmonic instead of by itself. Figs. 6 and 8 present this relation graphically. These figures will be discussed in turn. Only the main points will be mentioned here.

(a) Fig. 2. The yearly mean temperature

This chart is similar to others produced before e.g. in the Oxford Advanced Atlas and is included mainly to provide a basis for interpolation in conjunction with the other charts. The temperatures have not been corrected for altitude, so that due care should be taken in any interpolation between stations at different altitudes. The chart shows clearly the general decrease of annual mean temperature from the equator towards the pole and also the warming effect of proximity to the oceans. On any circle of latitude the lowest temperature occurs over land in the areas most shielded by orography from air blowing across open sea.

(b) Fig. 3. The semi-amplitude of the first harmonic

The semi-amplitude is seen to vary from less than a degree Centigrade in parts of the tropics to over 30 degrees Centigrade in North East Siberia.

/The

The moderating effect of proximity to the sea is seen clearly, particularly on the western borders of the continents. While a small semi-amplitude is characteristic of low latitudes and oceanic regimes, comparatively small values extend far north between Greenland and Norway to Spitzbergen and Nova Zemblya where the seas are ice covered for much of the year. In North America, the moderating influence of the Great Lakes is evident, whereas Hudson Bay seems to have less effect, at any rate on land immediately further west.

(c) Fig.4. The phase of the first harmonic

The isopleths here are at intervals of ten days, and separate stations for which the value of θ , converted into days of a yearly cycle, falls in different periods. That is, they effectively demarcate the hottest part of the summer. It appears that over the interior of the continents the time of highest mean temperature is very uniform, running from 2 to 3 weeks behind the sun. In oceanic stations and on sea coasts the maximum falls later, so that,for example, it is a whole month later in the Azores than in similar latitudes in Turkestan or the Middle West of America. In the subtropics the relative importance of the second harmonic is greater than elsewhere, and the values of ϕ_1 , which do not show much agreement between one region and another, are not readily explicable on the hemispherical scale.

(d) Fig. 5. The semi-amplitude of the second harmonic

The absolute magnitude of this is generally much less than that of the semi-amplitude of the first harmonic, and exceeds 3°C at only one of the stations examined. Most of the larger values occur in the subtropics, but fairly large values also occur in the interior of Russia and at stations bordering the Arctic basin.

(e) Fig. 6. The semi-amplitude of the second harmonic, expressed as a percentage of that of the first

When the relative importance of the second harmonic is expressed as a percentage, there is a sharp contrast between tropical regions, where the percentage amplitude exceeds 30 and temperate regions where it is usually below 20. If we take the 25 per cent value as the dividing line, we find that in Asia it generally lies to south of the main mountain barrier, crosses Egypt and the Sahara, and includes most of the West Indies on the temperate zone, but the mainland of Central America in the tropical. Looking further at the temperature zone, we find that in the interiors of continents, and on eastern seaboards, the ratio is nearly always less than 10 per cent, while in oceanic regions and western seaboards, it generally lies between 10 and 20 per cent.

(f) Fig. 7. The phase of the second harmonic

This is represented by the date of the maximum falling in the first half of the year. The variation of date is usually though not always consistent between adjacent stations: the maximum occurs earlier in certain regions bordering the North Atlantic and North Pacific than elsewhere, but the distribution is not easy to summarise. A more informative presentation is given by Fig. 8.

(g) Fig. 8. The phase of the second harmonic relative to that of the first

This chart shows the number of days up to 91 that the maximum of the second harmonic falls before or after the date of the maximum of the first. If the discrepancy is less than 45 days, the general effect of the second harmonic on the first is to shorten and intensify the maximum and to lengthen and reduce the minimum. That is, it tends to produce a short hot summer and a long rather uniform winter. Where the discrepancy exceeds 45 days these effects are reversed and the tendency is for a long uniform summer and a short cold winter. The one isopleth drawn divides the extratropical world into two regions: one including most of Europe, the Polar basin, Alaska and North Russia, where the

/climate

climate is of the first type and the other region, covering most of North America and Asia, where the climate is of the second type.

These divisions correspond fairly well with those shown on Fig. 6 between the regions where the second harmonic has greater or less relative importance, so that the extra-tropical world is roughly divisible into two regions, namely, one in which the annual temperature variation represented by a pure sine wave is modified considerably in the direction of a short summer and a long winter, and another in which the modification is in the opposite direction, but comparatively slight in amount.

6. The numerical values of the normal temperatures

The parametric form of the temperature normals used in Section 5 is convenient for trying to understand them, but not for showing, for example, how much the observed temperature in Austria on the 14th May is above or below normal. To do this we must have the numerical value on that day. There is no theoretical difficulty in finding the value for a particular day at one place by putting the appropriate values of θ and of the parameters into equation (1) but a table giving daily values for stations covering the Northern Hemisphere would take a long time to prepare, and would be bulky in use. Instead, the calculation was made for every fifth day, starting with January 3rd, for a network of 280 stations covering the hemisphere. For most purposes the normal for one day will be good enough to use for one or two days before or after, and where something better is needed a linear interpolation between normals at 5-day intervals will do. Even with this reduction, over 20,000 calculations are required, and to do these by hand would have absorbed more time and effort than could be spared. Instead the work was sent to the National Physical Laboratory, Teddington for completion by punched card methods, using the 602A calculating punch. The normal temperatures for each station are given in a vertical column with 73 entries to cover the year, 10 stations per page, and 28 pages to cover the 280 stations. In this table the normals for different stations for the same day lie horizontally, thus facilitating the preparation of charts of the normal air temperature for the whole hemisphere for any desired day.

This table has been reproduced photographically and copies can be provided for anyone who would find it useful.

7. The stability of the harmonic parameters

So far we have described the methods by which the normal temperatures were produced. In this section we consider their stability, that is, we examine the way in which the parameters depend on the choice of the period of years on which they are based. We are faced here by a fundamental difficulty, namely that all the quantities to be studied may show, besides the random, or comparatively short term fluctuations which we seek to minimise by choice of basic period, a slow secular variation, or trend. For some variables, for example, the annual mean temperature, such trends are known to be present, and we are certainly not justified in assuming that they do not exist when considering variables such as harmonic coefficients about which very little is known. The analysis of such series requires a detailed and careful investigation, which is already in progress. What are given here are simply some preliminary results, on the assumption that trends may be ignored in the cases considered.

Since each harmonic parameter is a linear function of the twelve monthly mean temperatures, it would be possible, if the latter were uncorrelated, to estimate the variance of the harmonic parameters directly from those of the monthly means. The numerical constants for doing this are given in Table 7, which is used in just the same way as Tables 2 to 5, the monthly mean variances taking the place of the monthly mean temperatures.

/Table 7

Table 7

Monthly mean variance	Multipliers to give variances of:-					
	a_o	a_1	b_1	a_2	b_2	Sum
$V(T_1)$	.0072	.0274	.0021	.0233	.0082	.0682
$V(T_2)$	.0059	.0123	.0118	.0000	.0263	.0563
$V(T_3)$	.0072	.0024	.0271	.0221	.0094	.0682
$V(T_4)$	.0068	.0015	.0261	.0234	.0062	.0640
$V(T_5)$	.0072	.0140	.0154	.0001	.0315	.0682
$V(T_6)$	.0068	.0255	.0022	.0211	.0086	.0642
$V(T_7)$	.0072	.0279	.0017	.0247	.0068	.0683
$V(T_8)$	.0072	.0151	.0144	.0000	.0316	.0683
$V(T_9)$	.0068	.0020	.0257	.0218	.0079	.0642
$V(T_{10})$	.0072	.0019	.0277	.0241	.0075	.0684
$V(T_{11})$	.0068	.0136	.0140	.0000	.0298	.0642
$V(T_{12})$	.0072	.0274	.0021	.0233	.0082	.0682

The practical value of the calculation is, however, reduced by two things, (1) for very few stations have we reliable estimates of the variances of the monthly mean temperatures, and in any case, such estimates may contain an element due to trend and (2) in fact the temperature anomalies in consecutive months are not unrelated, but show a positive correlation. However, for two stations, Kew and Prague, the variances have been calculated from many years data, and estimates of the variances of the harmonic parameters, using Table 7, are given in Table 8.

Table 8

	Variances of monthly mean temperatures	
	Kew 1871-1950 $^oF^2$	Prague 1775-1938 $^oC^2$
J	11.78	10.14
F	11.88	8.39
M	6.35	5.24
A	4.59	3.65
M	4.63	3.48
J	3.49	2.43
J	5.63	2.25
A	5.19	2.23
S	4.80	2.24
O	5.93	2.54
N	6.51	3.43
D	10.90	8.43
	Variances of harmonic coefficients for single years derived from the above	
a_o	0.56	0.38
a_1	1.29	0.89
b_1	1.02	0.65
a_2	1.24	0.85
b_2	1.24	0.80

It appears that the variance of any harmonic parameter is only 40 or 50 per cent of the variance in the most uniform month of the year, and less than 10 per cent of the variance in the most variable month. The existence of

serial correlations between the temperature anomalies in consecutive months means that these estimates have to be increased somewhat: if the correlations are about 0.3, a reasonable estimate, the increase will be about 10 per cent.

If the departures of the harmonic coefficients in a given year from their mean values are uncorrelated, then the values in Table 8 can be used to estimate the variance of the estimate of the normal temperature for a particular day or period obtained by harmonic synthesis. The estimate will be about twice the variance of the individual harmonic coefficients (since $\sin^2\theta + \cos^2\theta = 1$) or about 2.4 $^{\circ}F^2$ for Kew and 1.5 $^{\circ}C^2$ for Prague. To these have to be added the variance of a_o, giving totals of about 3 $^{\circ}F^2$ for Kew and 2 $^{\circ}C^2$ for Prague. The presence of serial correlations and trends will tend to increase these values, but even allowing for this the true values must be less than most of the monthly variances given in Table 8.

Thus the process of estimating normal temperatures by harmonic analysis followed by harmonic synthesis, if used to produce a monthly normal, appears to give a more accurate estimate than the mean temperatures for that month on which the calculation is based.

The above conclusions are only regarded as provisional, pending the completion of the investigation into the points on which reasonable assumptions have been made in the above argument. However, if we accept the numerical estimates as correct, we can make the following estimates of the uncertainty attaching to normal temperatures found in this way from data averaged over 20 or 30 years.

Table 9

	Variance	S.D.
For one year	3.0	1.73
For 20 year mean	0.15	0.38
For 30 year mean	0.10	0.32
For difference between 20 year mean, and mean for 30 years containing the first 20 years	0.05	0.23

Table 9 assumes the variance for a single year to have the value estimated for Kew. For stations where this is true, the normal temperature estimated from our 20 years basic period will generally (about 95 per cent of the time) be within 0.8°F of the true value, while the estimate based on our data will usually be within 0.5°F of a similar estimate based on data for the internationally agreed period 1921-1950. Elsewhere the confidence limits will be correspondingly greater or less, depending on the variance for the estimate based on a single year. These uncertainties are far less than the daily anomalies of temperature which are to be investigated, using these normals, so the results of this section, which are admittedly only provisional, suggest that the normals are quite accurate enough for the purpose for which they are intended.

References

Forbes 1860 Trans. Roy. Soc., Edin., Vol. XXII, part II, p.327.

Bilham 1918 Quart. J.R. Met. Soc., London, Vol. XLIV, p.41.

Weihrauch 1890 Schriften bei der Universität Dorpat. Bessel'sche Formel und deren Verwendung in der Meteorologie.

Pollak 1948 Harmonic analysis and synthesis schedules, Dublin Meteorological Service.

Table 6

Numerical values of harmonic coefficients at stations in Northern Hemisphere

No.	Station	a_0	a_1	b_1	A_1	ϕ_1	a_2	b_2	A_2	ϕ_2
1	Akureyri	4.76	-6.70	-2.40	7.12	21/7	1.03	0.31	1.08	9/1
2	Stykkisholm	4.51	-5.61	-2.17	6.01	23/7	0.82	0.65	1.05	20/1
3	Teigarhorn	5.08	-5.29	-1.83	5.60	21/7	0.75	0.72	1.04	23/1
4	Reykjavik	5.03	-5.27	-1.88	5.60	21/7	0.75	0.68	1.01	22/1
5	Vestmannaeyjar	5.83	-4.17	-1.69	4.50	24/7	0.66	0.69	0.95	24/1
6	Horta	17.47	-2.82	-2.93	4.07	17/8	0.12	0.79	0.80	11/2
7	Ponta Delgada	17.47	-2.54	-2.74	3.74	18/8	0.07	0.68	0.68	12/2
8	Funchal	18.80	-2.14	-2.52	3.31	21/8	-0.29	0.38	0.48	6/3
9	St. Vincent	23.82	-0.93	-2.26	2.44	8/9	-0.49	-0.08	0.50	6/4
10	Santiago	24.97	-1.17	-1.97	2.29	31/8	-0.42	-0.25	0.49	17/4
11	Freetown	26.37	0.61	0.79	1.00	23/2	-0.31	-0.42	0.52	29/4
12	Thorshavn	6.59	-2.87	-2.03	3.52	6/8	0.59	0.60	0.84	24/1
13	Bergen	7.60	-5.83	-2.55	6.36	25/7	0.55	0.53	0.76	23/1
14	Aberdeen	8.28	-4.52	-2.31	5.08	29/7	0.44	0.78	0.90	31/1
15	Edinburgh	8.67	-5.08	-2.32	5.59	26/7	0.50	0.79	0.93	30/1
16	Valentia	10.78	-3.67	-2.01	4.18	31/7	0.32	0.52	0.61	30/1
17	Greenwich	10.17	-6.13	-2.49	6.62	24/7	0.44	0.75	0.87	1/2
18	De Bilt	10.28	-8.15	-2.46	8.51	19/7	0.09	0.44	0.45	9/2
19	Frankfurt	10.08	-8.78	-2.23	9.06	16/7	-0.02	0.52	0.52	16/2
20	Paris	11.04	-7.45	-2.28	7.79	19/7	0.07	0.81	0.81	13/2
21	Nantes	11.63	-6.40	-2.45	6.85	23/7	-0.01	0.87	0.87	16/2
22	Lyon	11.31	-8.47	-2.82	8.93	20/7	-0.17	0.78	0.80	21/2
23	Zurich	8.82	-8.82	-2.43	9.15	17/7	-0.21	0.31	0.37	4/3
24	Milan	13.34	-10.70	-3.10	11.14	18/7	-0.38	0.65	0.75	2/3
25	Corunna	13.48	-4.02	-2.53	4.75	3/8	-0.35	0.64	0.73	2/3
26	Saragossa	14.26	-8.28	-2.98	8.80	22/7	-0.42	1.12	1.20	26/2
27	Barcelona	16.54	-6.52	-3.44	7.37	30/7	-0.24	0.92	0.95	23/2
28	Madrid	13.57	-8.83	-3.29	9.42	22/7	-0.18	1.59	1.60	18/2
29	Palma	16.46	-6.42	-3.84	7.48	2/8	-0.20	0.92	0.94	21/2
30	Lisbon	15.93	-4.86	-2.74	5.58	31/7	-0.41	0.92	1.01	27/2
31	Alicante	17.56	-5.87	-3.28	6.72	31/7	-0.39	0.93	1.01	27/2
32	Seville	18.31	-7.86	-3.58	8.64	26/7	-0.42	1.42	1.48	23/2
33	Gibraltar	17.37	-4.66	-3.00	5.54	4/8	-0.16	0.86	0.87	20/2
34	Bouzaréah	16.21	-5.85	-3.77	6.96	4/8	-0.22	0.87	0.90	22/2
35	Accra	26.63	0.98	1.16	1.52	20/2	-0.16	-0.68	0.70	10/5
36	Lagos	27.01	0.84	1.06	1.35	22/2	-0.42	-0.36	0.56	22/4
37	Calabar	25.16	0.29	0.71	0.77	10/3	-0.35	-0.42	0.55	27/4
38	Spitsbergen	-4.57	-7.63	-6.41	9.97	11/8	1.80	0.50	1.87	8/1
39	Stetnes	1.90	-6.08	-3.68	7.11	2/8	1.04	0.97	1.42	22/1
40	Bodo	5.09	-6.70	-3.23	7.44	28/7	1.06	0.91	1.40	21/1
41	Haparanda	1.81	-11.83	-4.85	12.79	24/7	1.62	0.21	1.63	4/1
42	Oslo	6.42	-9.78	-3.05	10.25	19/7	0.75	0.35	0.83	13/1
43	Uppsala	5.70	-9.80	-3.58	10.44	22/7	1.18	0.33	1.23	8/1
44	Helsinki	5.32	-10.40	-4.60	11.37	26/7	1.10	-0.04	1.10	11/5
45	Copenhagen	8.32	-7.96	-3.45	8.67	25/7	0.68	0.22	0.71	10/1
46	Konigsberg	7.36	-9.68	-3.64	10.34	22/7	0.22	-0.22	0.31	9/6
47	Vilna	6.48	-11.52	-3.44	12.02	18/7	0.09	-0.78	0.79	20/5
48	Berlin	9.41	-9.14	-2.70	9.53	18/7	0.08	0.30	0.32	8/2
49	Potsdam	8.73	-9.19	-2.77	9.60	18/7	0.06	0.27	0.28	9/2
50	Warsaw	8.16	-10.62	-3.11	11.07	18/7	0.00	-0.38	0.38	17/5

No.	Station	a_0	a_1	b_1	A_1	ϕ_1	a_2	b_2	A_2	ϕ_2
51	Breslau	8.74	-9.69	-2.80	10.08	18/7	-0.11	0.04	0.12	23/3
52	Cernauti	8.09	-11.97	-3.48	12.47	18/7	0.64	-0.79	1.02	6/6
53	Vienna	9.70	-9.88	-2.77	10.26	17/7	-0.21	0.09	0.23	21/3
54	Sonnblick	-5.98	-6.64	-3.53	7.52	30/7	0.34	0.17	0.38	14/1
55	Obir	0.74	-7.45	-3.74	8.34	29/7	0.28	0.35	0.45	27/1
56	Sibiu	9.02	-11.32	-3.01	11.71	17/7	-0.99	-0.49	1.11	15/4
57	Padua	12.83	-10.18	-3.14	10.65	19/7	-0.46	0.36	0.58	13/3
58	Modena	13.50	-11.27	-2.91	11.64	16/7	-0.73	0.78	1.07	9/3
59	Belgrade	11.74	-10.87	-3.21	11.33	18/7	-0.87	-0.27	0.91	10/4
60	Bucharest	11.10	-12.43	-3.79	13.00	19/7	-1.14	-0.50	1.25	14/4
61	Sulina	11.16	-10.95	-4.47	11.83	24/7	-0.09	-0.44	0.45	11/5
62	Sofia	10.59	-10.96	-3.42	11.48	19/7	-0.89	-0.11	0.90	4/4
63	Plovdiv	12.71	-11.08	-3.50	11.62	19/7	-0.56	0.08	0.57	29/3
64	Vigna di Valle	14.26	-7.69	-3.81	8.58	28/7	0.11	0.73	0.74	11/2
65	Naples	16.13	-7.27	-3.15	7.92	25/7	0.02	0.31	0.31	13/2
66	Corfu	18.43	-7.47	-3.91	8.43	30/7	0.06	0.60	0.60	12/2
67	Salonika	16.27	-9.70	-4.16	10.56	25/7	-0.17	0.26	0.31	4/3
68	Riposto	17.95	-6.38	-4.48	7.79	6/8	-0.54	1.00	1.14	2/3
69	Sparta	17.98	-9.15	-4.00	9.99	25/7	0.14	0.73	0.74	10/2
70	Heraklion	19.66	-6.44	-3.69	7.42	1/8	-0.06	0.14	0.15	27/2
71	Malta	18.39	-5.59	-4.36	7.09	9/8	0.60	0.47	0.76	20/1
72	Cyrene	15.83	-6.11	-3.53	7.06	1/8	-0.27	-0.61	0.67	5/5
73	Agedabia	21.00	-6.30	-2.54	6.79	24/7	-0.92	-0.92	1.30	24/4
74	Alexandria	20.90	-4.86	-3.70	6.11	8/8	-0.62	-0.25	0.67	13/4
75	Archangel	1.59	-12.97	-5.24	13.99	24/7	1.09	-0.03	1.09	11/5
76	Leningrad	4.84	-12.17	-4.52	12.98	22/7	0.81	-0.32	0.87	21/6
77	Moscow	4.37	-14.07	-4.27	14.70	19/7	0.15	-1.07	1.08	21/5
78	Kasan	4.24	-16.33	-4.67	16.99	18/7	0.02	-1.05	1.05	18/5
79	Nikolaevskoe	4.57	-16.98	-5.17	17.75	19/7	-0.02	-1.47	1.47	17/5
80	Astrachan U.S.S.R.	9.61	-15.83	-4.83	16.55	19/7	0.07	-1.11	1.11	19/5
81	Novorrossisk	13.03	-9.86	-4.88	11.00	28/7	0.33	0.05	0.34	5/1
82	Beirut	21.60	-6.30	-4.21	7.58	5/8	-0.58	0.01	0.58	1/4
83	Ramleh	21.56	-6.24	-3.84	7.33	3/8	-0.72	-0.72	1.02	24/4
84	Amman	18.71	-8.87	-4.02	9.74	26/7	-1.17	-0.67	1.35	17/4
85	Heliopolis	23.09	-7.60	-2.69	8.06	21/7	-0.76	-0.80	1.10	25/4
86	Helwan	21.83	-7.08	-2.81	7.62	23/7	-0.79	-0.76	1.10	24/4
87	Khartoum	29.56	-4.26	-0.52	4.29	9/7	-1.60	-2.00	2.56	28/4
88	Aden	28.75	-3.21	-0.80	3.31	16/7	-0.31	-0.68	0.75	5/5
89	Kampala	21.00	0.80	0.33	0.87	23/1	-0.04	0.07	0.08	2/3
90	Entebbe	21.47	0.51	0.31	0.60	1/2	-0.20	-0.07	0.21	11/4
91	Malye Karmakouly	-4.35	-8.13	-6.78	10.59	11/8	1.75	1.05	2.04	16/1
92	Waigatz	-5.60	-8.78	-8.00	11.88	13/8	0.99	0.30	1.03	9/1
93	Ust-Zylma	-1.31	-14.13	-5.20	15.06	22/7	0.75	0.24	0.79	9/1
94	Berezov	-3.08	-17.45	-6.03	18.46	21/7	0.00	0.72	0.72	15/2
95	Perm	2.09	-16.41	-4.33	16.97	16/7	-0.11	-0.68	0.69	12/5
96	Sverdlovsk	1.76	-16.34	-4.11	16.85	16/7	-0.28	-0.83	0.88	8/5
97	Tobolsk	0.63	-17.74	-4.60	18.32	16/7	-0.58	-0.50	0.77	22/4
98	Orenburg	4.35	-18.73	-5.48	19.51	18/7	-0.13	-1.65	1.65	15/5
99	Turgai	4.90	-20.54	-6.32	21.49	19/7	-0.18	-2.06	2.07	15/5
100	Fort Uritsky	11.49	-13.90	-5.33	14.89	23/7	0.05	-0.48	0.48	20/5

/101

No.	Station	a_0	a_1	b_1	A_1	ϕ_1	a_2	b_2	A_2	ϕ_2
101	Kasalinsk	8.18	-18.78	-4.54	19.32	15/7	-0.67	-1.54	1.68	5/5
102	Krasnovodsk	15.72	-12.54	-5.04	13.52	24/7	-0.25	0.36	0.44	5/3
103	Tashkent	13.37	-13.57	-2.78	13.85	13/7	-0.32	-0.06	0.33	7/4
104	Bushire	24.19	-8.28	-3.65	9.05	26/7	-1.03	-0.33	1.08	11/4
105	Quetta	14.87	-11.04	-2.37	11.29	14/7	-0.20	0.54	0.58	25/2
106	Kalat	13.42	-10.57	-2.49	10.86	15/7	0.18	0.16	0.24	22/1
107	Karachi	25.48	-4.70	-0.93	4.79	13/7	-0.87	-1.28	1.55	30/4
108	Dickson	-10.75	-13.53	-8.57	16.02	3/8	0.57	1.17	1.30	2/2
109	Turukhansk	-6.32	-20.01	-6.37	21.00	19/7	-0.55	2.21	2.28	22/2
110	Surgut	-2.48	-18.23	-5.79	19.12	19/7	-0.16	0.42	0.45	26/2
111	Omsk	0.85	-18.88	-5.58	19.69	18/7	-0.45	-1.50	1.57	9/5
112	Tomsk	-0.15	-18.26	-5.08	18.96	17/7	-0.52	-0.38	0.64	20/4
113	Barnard	1.55	-18.68	-5.28	19.41	18/7	-0.38	-1.21	1.27	8/5
114	Akmolinsk	1.70	-19.16	-5.51	19.93	18/7	-0.22	-1.46	1.48	13/5
115	Alma Ata	8.84	-15.00	-3.84	15.48	16/7	-1.17	-0.13	1.18	5/4
116	Naryn	2.69	-16.28	-4.28	16.83	16/7	-2.82	-1.29	3.10	14/4
117	Leh	5.72	-11.43	-3.73	12.02	20/7	-1.19	0.22	1.21	27/3
118	Lahore	24.51	-10.72	-1.45	10.82	9/7	-1.69	-1.11	2.02	18/4
119	Allahabad	26.08	-8.17	0.84	8.21	26/6	-2.16	-1.93	2.90	23/4
120	Nagpur	26.82	-5.02	2.48	5.60	5/6	-2.04	-1.89	2.78	23/4
121	Calcutta	26.59	-4.93	0.51	4.96	26/6	-2.46	-0.77	2.58	10/4
122	Bombay	27.31	-1.82	0.08	1.82	29/6	-0.81	-1.46	1.67	2/5
123	Vizagapatam	27.38	-3.34	0.17	3.34	29/6	-1.06	-0.62	1.23	17/4
124	Bangalore	24.01	-1.64	1.79	2.43	15/5	-1.58	-0.53	1.67	11/4
125	Hambantota	26.96	-0.88	0.10	0.89	25/6	-0.28	-0.09	0.31	11/4
126	Yenisseysk	-1.74	-19.51	-5.18	20.18	17/7	-0.94	-0.04	0.94	3/4
127	Kirensk	-3.18	-21.75	-5.09	22.34	15/7	-1.38	0.14	1.39	30/3
128	Minusinsk	0.40	-19.87	-5.41	20.59	17/7	-0.92	-1.32	1.61	29/4
129	Irkutsk	-0.88	-19.04	-4.57	19.58	15/7	-1.28	-0.38	1.33	10/4
130	Shillong	16.56	-5.68	-0.73	5.73	9/7	-1.57	-0.01	1.57	2/4
131	Yunnanfu	15.89	-5.92	-0.91	5.99	10/7	-0.92	-0.17	0.94	7/4
132	Mandalay	27.53	-4.40	0.44	4.42	26/6	-2.30	-0.94	2.49	13/4
133	Rangoon	27.56	-0.64	0.70	0.95	15/5	-1.28	-0.71	1.46	16/4
134	Port Blair	27.44	-0.42	0.53	0.68	11/5	-0.50	-0.46	0.68	23/4
135	Singapore	27.12	-0.62	0.05	0.62	27/6	0.14	0.00	0.14	2/7
136	Olekminsk	-5.83	-24.94	-5.96	25.64	15/7	-1.22	0.24	1.24	27/3
137	Yakutsk	-9.81	-30.27	-6.82	31.03	14/7	-2.26	-0.21	2.27	4/4
138	Tchita	-2.38	-21.82	-4.79	22.34	14/7	-1.90	-0.51	1.97	9/4
139	Nerchinsky Zavod	-3.17	-23.50	-5.11	24.05	14/7	-2.48	-0.54	2.54	8/4
140	Blagovyestchensk	0.33	-22.30	-5.40	22.94	15/7	-2.10	-0.04	2.10	2/4
141	Tientsin	12.18	-15.26	-3.81	15.73	16/7	-1.23	-0.17	1.24	5/4
142	Joshin	8.10	-11.56	-6.32	13.17	31/7	-1.56	0.68	1.70	21/3
143	Chempulo	10.80	-12.91	-5.89	14.19	26/7	-1.30	0.18	1.31	29/3
144	Hankow	17.46	-12.18	-4.34	12.93	16/7	-1.02	0.02	1.02	1/4
145	Nanking	15.53	-12.10	-4.62	12.95	23/7	-0.74	0.06	0.74	30/3
146	Shanghai	15.55	-10.89	-5.00	11.98	26/7	-0.42	0.22	0.47	19/3
147	Nagasaki	15.45	-9.23	-4.94	10.47	30/7	-0.36	0.41	0.55	8/3
148	Hong Kong	22.40	-5.95	-3.12	6.72	30/7	-0.34	-0.85	0.92	6/5
149	Naha	21.88	-5.20	-3.22	6.12	3/8	-0.08	-0.03	0.09	12/4
150	Legaspi	27.16	-0.99	0.13	1.00	24/6	-0.29	-0.46	0.54	1/5

/151

No.	Station	a_0	a_1	b_1	A_1	ϕ_1	a_2	b_2	A_2	ϕ_2
151	Sandakan	27.35	-0.51	-0.12	0.52	15/7	-0.19	-0.16	0.25	22/4
152	Verkhoyansk	-14.56	-31.94	-6.88	32.67	14/7	-1.32	0.09	1.32	31/3
153	Ust Mayskoe	-8.98	-29.40	-6.54	30.12	14/7	-2.92	-0.74	3.01	9/4
154	Okhotsk	-4.37	-16.49	-6.49	17.72	23/7	-1.96	1.20	2.30	17/3
155	Nikolaeyevsk-on-Amur	-2.05	-18.61	-7.64	20.12	24/7	-1.87	0.39	1.91	27/3
156	Ochiai	2.22	-12.96	-7.23	14.84	31/7	-1.48	-0.14	1.49	4/4
157	Nikolsk Ussuriysky	2.81	-19.01	-6.54	20.10	21/7	-3.40	-0.35	3.42	4/4
158	Nemuro	5.74	-8.43	-7.03	10.97	11/8	-1.15	-0.02	1.15	2/4
159	Vladivostok	4.25	-14.80	-6.78	16.28	26/7	-2.99	0.36	3.01	29/3
160	Miyako	10.13	-9.69	-5.75	11.27	2/8	-0.68	0.53	0.86	14/3
161	Kyoto	14.13	-10.74	-5.37	12.01	28/7	-0.15	0.60	0.62	22/2
162	Tokyo	14.21	-9.95	-5.24	11.24	30/7	-0.50	0.47	0.69	11/3
163	Omura	22.67	-3.97	-3.82	5.51	15/8	-0.49	-0.20	0.53	13/4
164	Guam	27.53	-0.56	0.03	0.56	29/6	-0.09	-0.44	0.45	11/5
165	Petropavlovsk	1.08	-8.82	-5.37	10.33	2/8	-0.73	1.07	1.30	5/3
166	34°N.162°E.	18.43	-3.10	-4.71	5.64	28/8	-0.43	1.02	1.11	27/2
167	Novo-Marinsky Post	-7.30	-14.69	-7.97	16.71	30/7	1.60	1.53	2.21	23/1
168	St. Paul Is.	1.99	-4.84	-4.26	6.45	12/8	0.34	0.31	0.46	22/1
169	32°N.178°E.	20.65	-3.38	-3.61	4.95	18/8	0.20	0.47	0.51	3/2
170	Midway Is.	21.99	-3.12	-2.61	4.07	11/8	-0.03	0.08	0.09	26/2
171	Barrow	-12.13	-14.90	-8.29	17.05	31/7	1.40	-0.17	1.41	28/6
172	Nome	-3.10	-12.12	-5.56	13.33	26/7	0.58	0.28	0.64	14/1
173	Tanana	-4.13	-19.33	-4.29	19.80	14/7	-0.07	-0.16	0.17	5/5
174	Kodiak	5.32	-5.86	-3.25	6.70	31/7	0.27	0.97	1.01	7/2
175	Dutch Harbour	4.79	-4.93	-3.18	5.87	4/8	0.19	1.06	1.08	10/2
176	Honolulu	23.92	-1.28	-1.42	1.91	19/8	-0.09	0.01	0.09	30/3
177	Aklavik	-9.35	-20.31	-7.52	21.66	22/7	0.83	0.84	1.18	23/1
178	Fairbanks	-3.47	-20.16	-3.86	20.53	12/7	-1.32	-0.52	1.42	12/4
179	Dawson	-4.82	-21.59	-4.72	22.10	14/7	-1.50	-1.12	1.87	20/4
180	Valdez	2.04	-8.92	-3.21	9.48	22/7	-0.35	0.11	0.37	24/3
181	Juneau	5.81	-7.30	-2.77	7.81	23/7	0.09	0.17	0.20	1/2
182	Sitka	6.98	-5.69	-2.85	6.36	28/7	-0.03	0.60	0.60	17/2
183	Massett	7.69	-5.19	-2.95	5.97	1/8	-0.04	0.64	0.64	17/2
184	Prince Rupert	7.69	-5.42	-2.60	6.01	27/7	-0.30	0.47	0.56	4/3
185	Ft.Good Hope	-8.01	-23.06	-6.74	24.02	18/7	0.43	-0.21	0.48	19/6
186	Coppermine	-11.43	-18.42	-8.85	20.43	28/7	1.06	1.42	1.77	27/1
187	Ft.Simpson	-3.62	-21.40	-6.07	22.25	18/7	-1.43	-0.98	1.73	19/4
188	Hay River	-4.34	-18.98	-7.70	20.48	24/7	-1.05	-0.37	1.11	11/4
189	Ft. Smith	-3.43	-20.28	-6.11	21.18	18/7	-1.19	-1.34	1.79	26/4
190	Ft. McMurray	-1.01	-18.86	-4.67	19.43	16/7	-2.29	-1.09	2.54	14/4
191	Bella Coola	7.58	-8.51	-2.51	8.87	18/7	-0.56	0.43	0.71	14/3
192	Prince George	4.13	-11.98	-3.23	12.41	17/7	-1.20	-0.37	1.26	10/4
193	Barkerville	1.77	-10.22	-2.88	10.61	17/7	-0.27	0.25	0.37	11/3
194	Edmonton	2.73	-14.82	-3.81	15.30	16/7	-1.27	-0.76	1.48	17/4
195	Calgary	4.05	-12.53	-3.81	13.10	19/7	-0.43	-0.16	0.46	12/4
196	Victoria	10.07	-5.33	-2.04	5.71	23/7	-0.40	0.34	0.53	12/3
197	Spokane	9.47	-11.39	-3.10	11.80	17/7	-0.40	1.05	1.12	26/2
198	Helena	7.14	-12.33	-3.76	12.89	19/7	-0.13	0.84	0.85	20/2
199	Portland	12.18	-7.33	-2.57	7.77	21/7	-0.61	0.74	0.96	7/3
200	Red Bluff	16.91	-9.30	-3.17	9.83	21/7	-0.25	1.06	1.09	22/2

/201

No.	Station	a_o	a_1	b_1	A_1	ϕ_1	a_2	b_2	A_2	ϕ_2
201	Salt Lake City	11.63	-12.83	-4.01	13.45	19/7	-0.21	1.23	1.25	20/2
202	San Francisco	13.59	-1.93	-1.42	2.40	7/8	-1.22	-0.34	1.27	9/4
203	Sacramento	16.42	-7.78	-2.74	8.25	21/7	-0.93	0.77	1.21	13/3
204	Modena (U.S.A.)	9.12	-11.87	-3.69	12.43	19/7	-0.53	1.26	1.37	27/2
205	San Diego	16.52	-3.01	-2.10	3.67	6/8	-0.33	0.52	0.62	4/3
206	Phoenix	21.66	-10.55	-3.38	11.08	20/7	-0.35	1.17	1.22	24/2
207	Chesterfield Inlet	-11.74	-19.09	-9.74	21.43	29/7	-0.09	0.36	0.37	22/2
208	Churchill	-7.42	-18.70	-8.93	20.72	27/7	-0.68	0.42	0.80	17/3
209	Prince Albert	1.47	-17.66	-5.13	18.39	18/7	-1.44	-1.03	1.77	20/4
210	The Pas	-0.18	-19.28	-5.89	20.16	19/7	-1.24	-0.87	1.51	19/4
211	Qu' Appelle	2.39	-16.50	-4.99	17.23	19/7	-1.15	-0.68	1.34	17/4
212	Winnipeg	2.76	-17.98	-5.83	18.90	20/7	-1.33	-0.88	1.59	18/4
213	Bismarck	5.90	-16.29	-4.90	17.01	18/7	-0.92	-0.18	0.94	7/4
214	Minneapolis	7.46	-15.81	-4.97	16.57	19/7	-1.00	-0.34	1.06	11/4
215	Cheyenne	7.46	-11.23	-4.42	12.06	23/7	0.50	0.98	1.10	1/2
216	Denver	10.66	-11.33	-3.97	12.00	21/7	0.31	1.02	1.07	7/2
217	North Platte	10.35	-13.84	-4.17	14.45	18/7	-0.38	0.90	0.98	27/2
218	Omaha	11.23	-14.64	-4.47	15.31	19/7	-0.87	0.17	0.89	27/3
219	St. Louis	13.99	-12.61	-4.16	13.28	20/7	-0.60	0.47	0.76	13/3
220	Sata Fe	9.56	-10.85	-3.41	11.37	19/7	-0.45	0.66	0.80	5/3
221	El Paso	17.92	-10.57	-2.53	10.86	15/7	-0.62	0.53	0.82	12/3
222	Abilene	18.30	-10.74	-3.03	11.16	17/7	-0.93	0.74	1.19	13/3
223	Little Rock	16.94	-10.69	-3.36	11.21	19/7	-0.77	0.68	1.03	12/3
224	Galveston	21.10	-7.65	-3.07	8.24	24/7	-0.78	0.23	0.81	24/3
225	Corpus Christi	22.00	-7.11	-2.56	7.56	22/7	-1.08	0.16	1.09	28/3
226	Monterrey	21.79	-6.63	-1.01	6.71	10/7	-1.04	0.28	1.08	25/3
227	Mazatlan	23.74	-3.45	-3.15	4.67	13/8	-0.25	-0.26	0.36	25/4
228	Leon	18.86	-3.32	0.64	3.38	21/6	-1.02	-0.84	1.32	22/4
229	Tacubaya	14.73	-2.27	0.67	2.37	15/6	-0.93	-0.29	0.97	10/4
230	Mexico City	16.51	-2.05	0.72	2.17	12/6	-0.86	-0.32	0.92	12/4
231	Puebla	16.25	-2.28	0.56	2.35	18/6	-1.01	-0.38	1.08	12/4
232	Oaxaca	20.21	-1.86	0.89	2.06	6/6	-0.92	-0.28	0.96	10/4
233	Nottingham Is.	-8.98	-14.29	-7.91	16.33	31/7	-0.52	-0.97	1.10	3/5
234	Moosonee	-1.72	-16.82	-7.47	18.40	26/7	-0.86	-0.62	1.06	20/4
235	Mistassini Post	-1.55	-16.30	-7.09	17.78	25/7	-0.95	-0.98	1.37	25/4
236	Chicoutimi	3.00	-16.16	-6.19	17.30	23/7	-1.31	-0.56	1.43	13/4
237	Marquette	5.50	-12.31	-5.69	13.56	27/7	-0.21	0.09	0.23	21/3
238	Toronto	8.30	-12.19	-5.20	13.25	25/7	0.23	-0.01	0.23	30/6
239	Montreal	6.42	-14.46	-5.53	15.48	23/7	-0.32	-0.69	0.76	5/5
240	Chicago	10.45	-12.35	-5.14	13.37	24/7	-0.54	0.40	0.67	14/3
241	Detroit	9.74	-12.57	-5.07	13.56	24/7	0.08	0.16	0.18	2/2
242	New York	11.49	-10.82	-4.73	11.81	25/7	-0.04	0.06	0.07	4/3
243	Albany	9.30	-12.57	-4.76	13.45	23/7	-0.12	-0.28	0.30	5/5
244	New Haven	10.44	-11.13	-4.69	12.08	25/7	-0.09	0.11	0.14	7/3
245	Cincinnati	13.20	-11.81	-4.09	12.50	21/7	-0.39	0.29	0.49	14/3
246	Washington D.C.	13.52	-11.13	-3.88	11.79	21/7	-0.15	0.30	0.34	1/3
247	Nashville	15.49	-10.74	-3.47	11.29	20/7	-0.52	0.56	0.76	9/3
248	Hatteras	17.08	-8.20	-3.83	9.05	27/7	-0.19	0.31	0.36	3/3
249	Charleston	18.95	-8.26	-2.83	8.73	21/7	-0.46	0.39	0.60	12/3
250	Mobile	19.67	-7.99	-2.57	8.39	20/7	-0.58	0.46	0.74	13/3
251	Key West	25.20	-3.54	-1.60	3.88	26/7	-0.40	0.21	0.45	19/3
252	Havana	24.87	-2.48	-1.14	2.73	27/7	-0.32	0.08	0.33	26/3
253	Merida	25.81	-2.45	-0.02	2.45	2/7	-0.70	-0.17	0.72	8/4
254	Negril Pt. Lighthouse	25.91	-1.07	-0.89	1.39	11/8	-0.02	-0.25	0.25	15/5
255	Kingston	26.22	-1.47	-0.54	1.57	22/7	0.11	-0.31	0.33	27/5

No.	Station	a_o	a_1	b_1	A_1	ϕ_1	a_2	b_2	A_2	ϕ_2
256	Port-au-Prince	26.48	-1.44	-0.53	1.53	22/7	-0.03	0.02	0.04	16/3
257	San Salvador	23.17	-0.62	0.42	0.75	28/5	-0.34	-0.10	0.35	10/4
258	Colon.	27.35	-0.30	0.21	0.37	28/5	-0.15	0.01	0.15	31/3
259	Uppernivik	-6.12	-10.66	-7.21	12.87	5/8	1.44	-1.41	2.01	9/6
260	Jacobshavn	-3.40	-10.09	-4.26	10.95	25/7	1.02	-0.24	1.05	25/6
261	Godthaab	-0.43	-7.71	-3.27	8.37	25/7	0.34	0.20	0.39	16/1
262	Resolution Is.	-6.16	-9.48	-6.09	11.27	4/8	-0.82	-1.49	1.70	3/5
263	Father Point	2.12	-12.10	-5.16	13.15	25/7	-0.78	-0.83	1.14	25/4
264	Anticosti	1.82	-10.41	-5.92	10.21	1/8	-0.45	-0.37	0.58	21/4
265	Natashquan	0.57	-12.94	-6.36	14.42	28/7	-0.92	-0.56	1.08	17/4
266	Eastport	5.52	-9.50	-5.06	10.76	30/7	-0.75	-0.21	0.78	9/4
267	Charlottetown	5.75	-11.82	-6.52	13.50	31/7	-0.11	-0.18	0.21	1/5
268	Cape Race	4.34	-6.98	-5.77	9.06	11/8	-0.38	0.31	0.49	13/3
269	St. Johns	4.97	-8.90	-5.90	10.68	4/8	0.17	0.21	0.27	26/1
270	Sable Island	7.11	-6.85	-6.53	9.46	15/8	-0.36	0.71	0.80	1/3
271	42°N. 62°W.	11.09	-7.46	-6.25	9.73	11/8	0.38	0.56	0.68	29/1
272	Bermuda (St. George)	21.43	-3.87	-3.36	5.13	12/8	0.18	0.46	0.49	4/2
273	32°N. 52°W.	22.16	-2.53	-3.26	4.13	23/8	0.20	0.44	0.48	3/2
274	San Juan	25.49	-1.23	-1.16	1.69	14/8	-0.10	-0.23	0.25	25/4
275	Trinidad	26.41	-0.68	-0.33	0.76	28/7	-0.26	-0.58	0.64	5/5
276	Georgetown	26.99	-0.15	-0.43	0.46	11/9	-0.41	-0.22	0.47	16/4
277	Ivigtut	1.54	-7.50	-2.62	7.95	21/7	0.38	-0.02	0.38	30/6
278	Angmagssalik	-0.66	-6.85	-2.42	7.27	21/7	1.10	0.46	1.19	12/1
279	55°N. 35°W.	7.74	-2.72	-1.69	3.20	3/8	-0.63	0.69	0.93	9/3
280	42°N. 42°W.	13.16	-4.93	-3.41	5.99	6/8	0.06	0.42	0.42	11/2
281	Peshawar	22.64	-11.11	-2.87	11.48	16/7	-0.44	-0.59	0.74	29/4
282	Simla	13.06	-6.81	-1.06	6.89	11/7	-0.80	-1.55	1.75	3/5
283	New Delhi	24.81	-9.37	-0.64	9.39	5/7	-1.79	-1.71	2.48	24/4
284	Jaipur	25.60	-7.94	0.25	7.95	30/6	-1.85	-1.93	2.67	25/4
285	Madras	28.47	-3.93	0.20	3.93	29/6	-0.32	-0.66	0.73	4/5
286	Amini Divi	28.11	-0.23	0.97	1.00	15/4	-0.58	-0.48	0.75	22/4
287	Minicoy	27.74	-4.68	0.69	4.73	24/6	-0.52	-0.41	0.66	21/4
288	Cochin	27.09	0.30	1.08	1.12	17/3	-0.67	-0.43	0.80	18/4
289	Kodaikanal	14.59	-1.32	0.85	1.57	30/5	-0.75	-0.35	0.83	14/4
290	Trincomalee	27.75	-2.25	-0.10	2.25	4/7	-0.36	-0.07	0.37	7/4
291	Nuwara Eliya	15.25	-0.89	-0.15	0.90	11/7	-0.22	-0.57	0.61	6/5
292	Colombo	26.86	-0.67	0.30	0.73	8/6	-0.28	-0.14	0.31	15/4
293	Akyab	25.62	-2.85	-0.28	2.86	7/7	-1.79	-1.18	2.14	18/4
294	Mergui	26.59	-0.39	0.69	0.79	2/5	-0.73	-0.44	0.85	17/4
295	Bangkok	28.13	-1.58	0.92	1.83	1/6	-1.08	-0.14	1.09	5/4
296	Medan	25.98	-0.60	0.34	0.69	2/6	-0.17	0.00	0.17	2/4
297	Fort Bayard	23.54	-6.13	-2.43	6.59	23/7	-0.56	-0.98	1.13	2/5
298	Aparri	26.11	-2.45	-0.46	2.49	12/7	-0.43	-0.46	0.63	25/4
299	Manila	26.59	-1.34	0.41	1.40	15/6	-0.61	-0.48	0.78	21/4
300	Iloilo	27.17	-0.92	0.22	0.95	18/6	-0.41	-0.45	0.61	26/4
301	Kolonie	27.23	-0.61	-0.20	0.64	20/7	0.17	0.09	0.20	15/1
302	Anna's Hope	26.06	-1.24	-1.00	1.59	10/8	0.04	-0.22	0.22	22/5
303	Fort de France	25.51	-0.94	-0.63	1.13	5/8	-0.24	-0.42	0.48	2/5
204	Richmond Hill, Grenada	26.35	-0.26	-0.19	0.32	7/8	-0.17	-0.09	0.19	16/4
305	Paramaribo	27.49	-0.10	-0.83	0.84	24/9	-0.66	-0.14	0.67	8/4

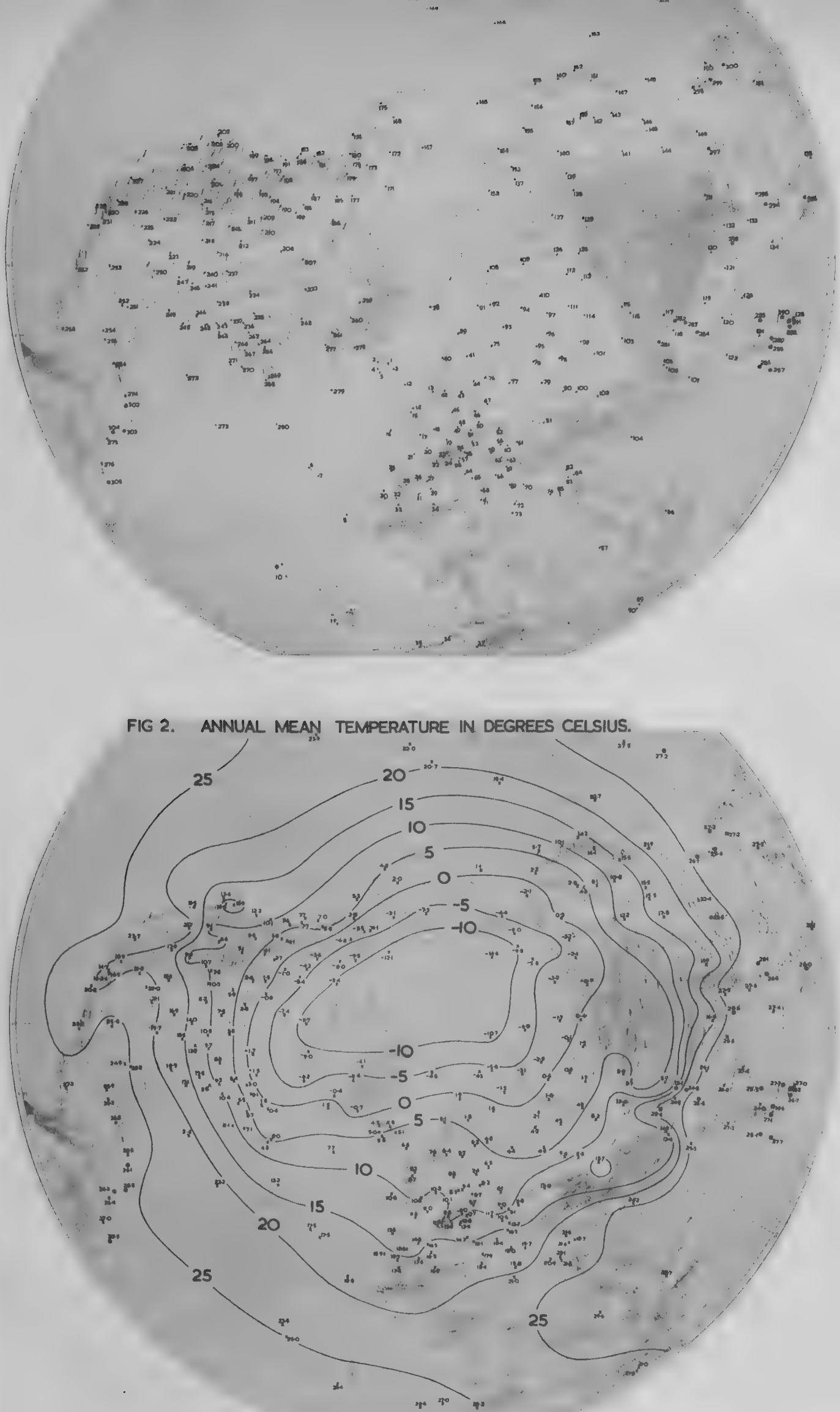

FIG 2. ANNUAL MEAN TEMPERATURE IN DEGREES CELSIUS.

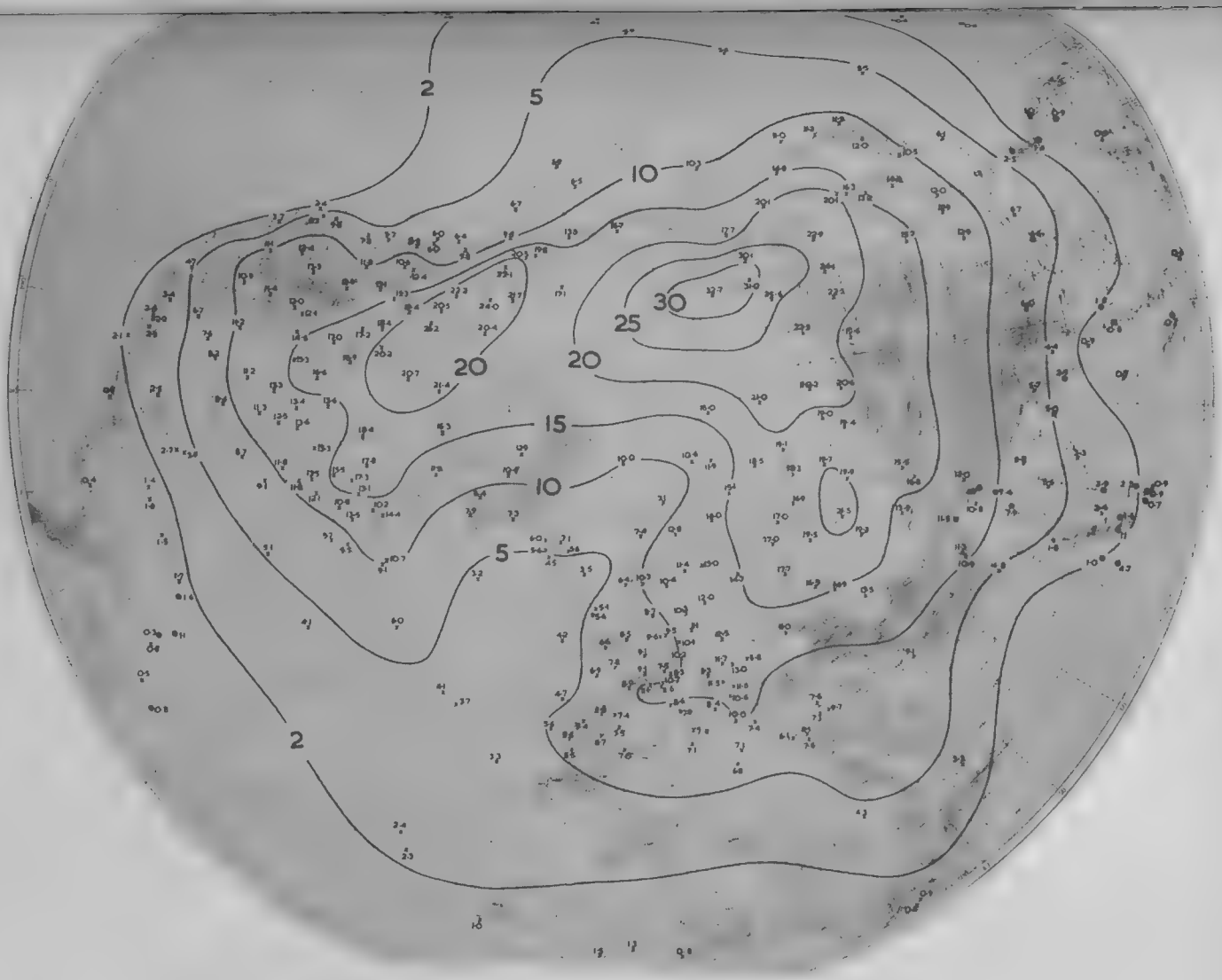

FIG 4. PHASE OF FIRST HARMONIC. DATE OF MAXIMUM.

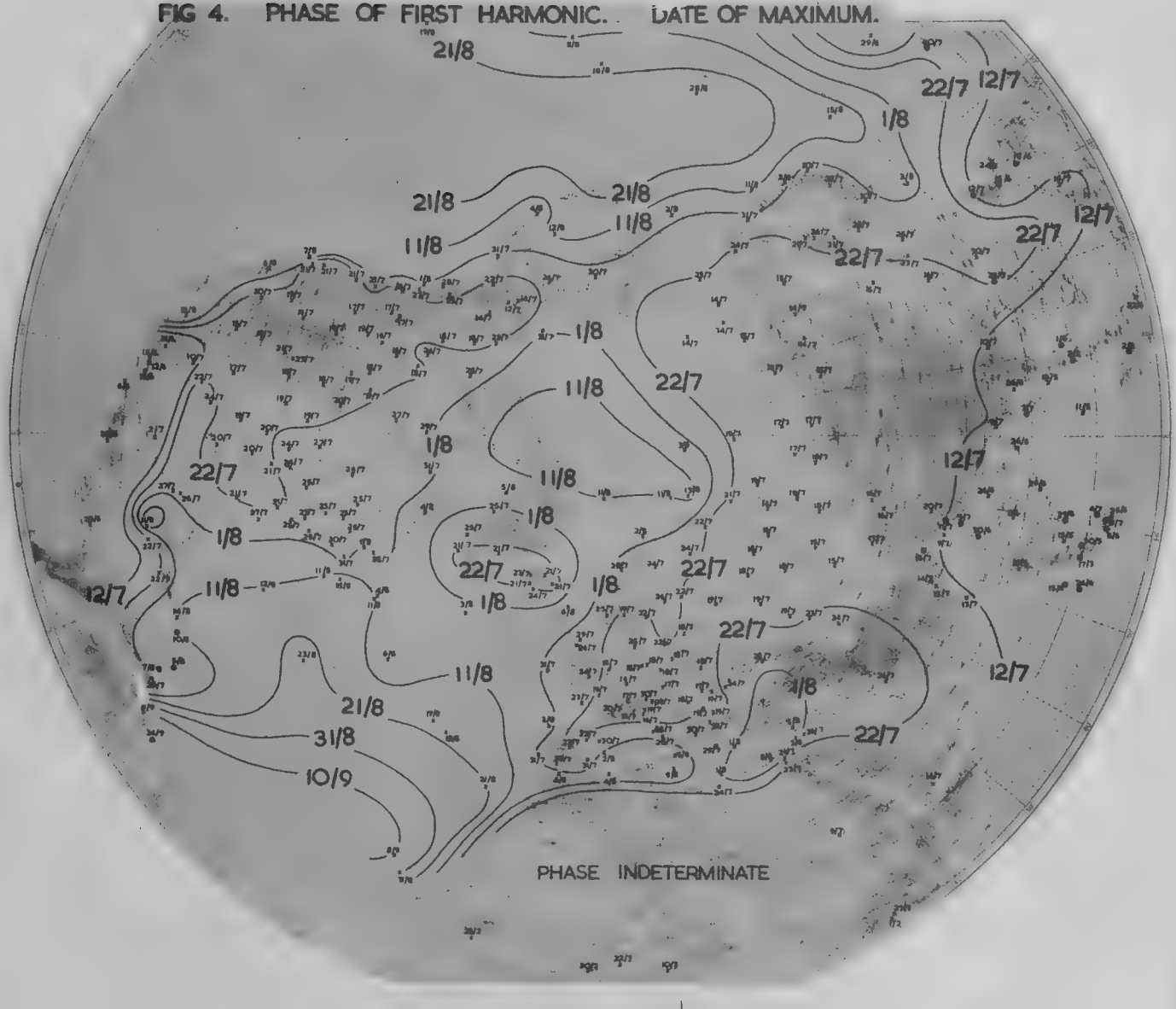

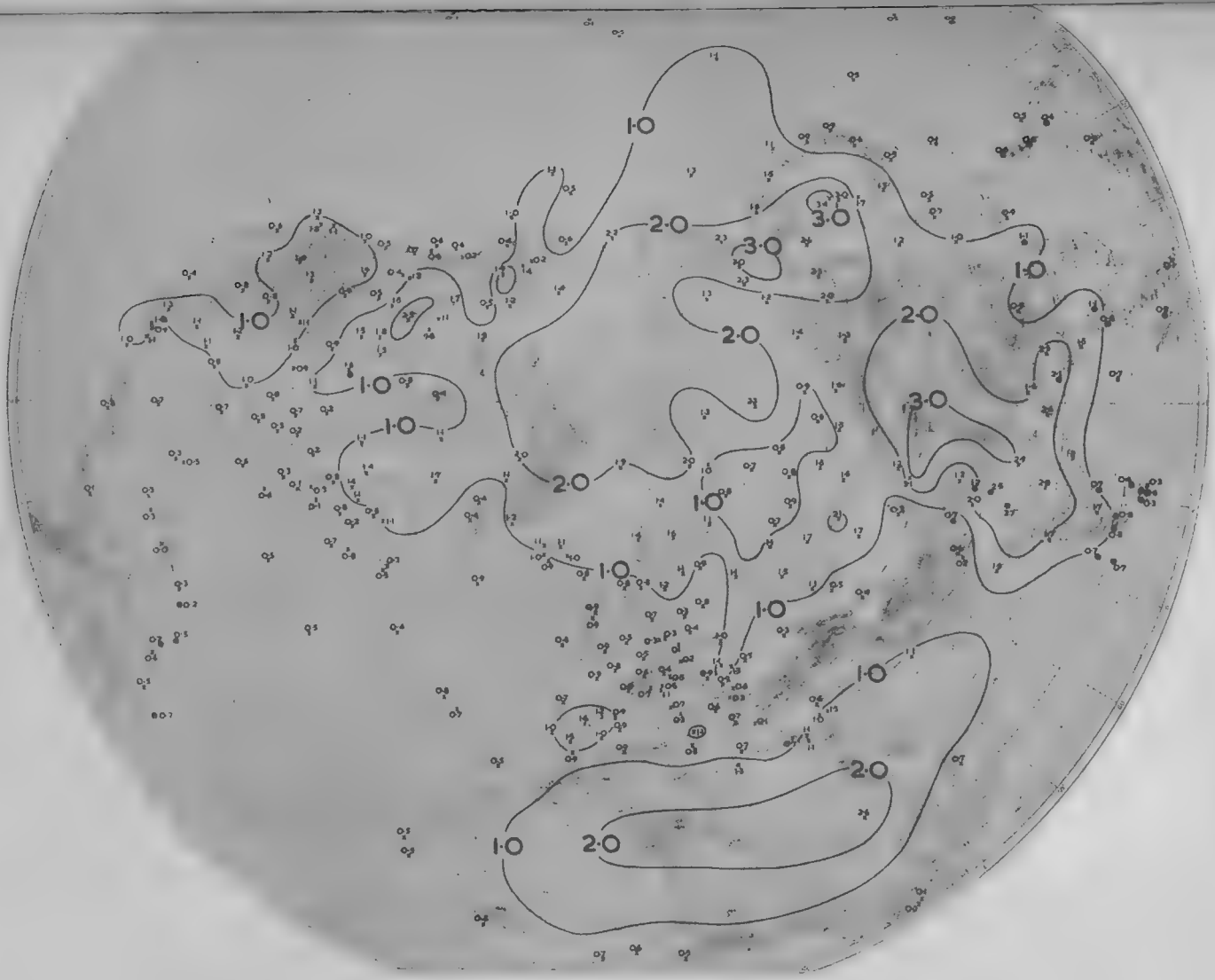

FIG 6. RATIO OF AMPLITUDES OF FIRST AND SECOND HARMONICS. ($A_2 / A_1 \times 100$)

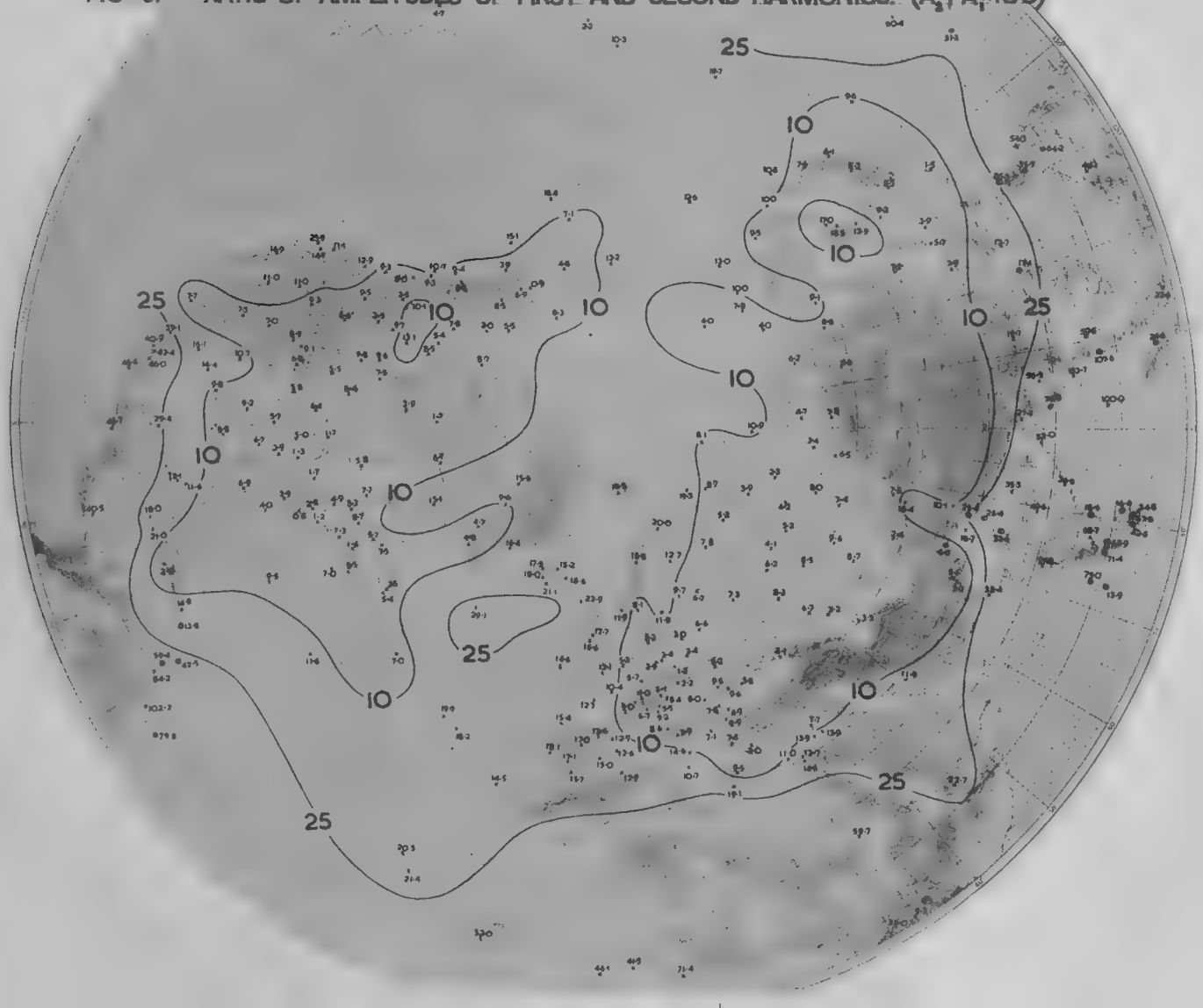

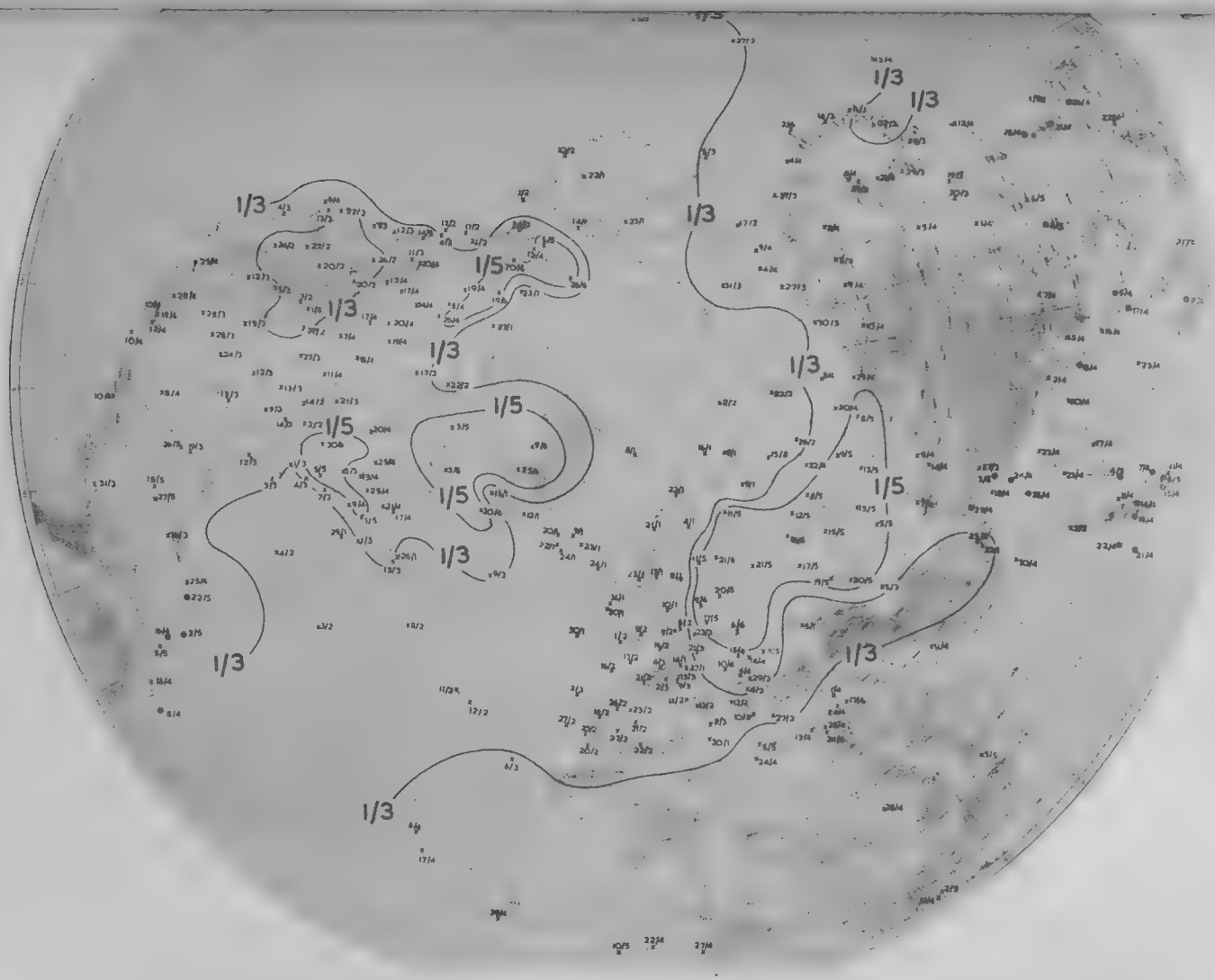

FIG 8. NUMBER OF DAYS BETWEEN DATES OF MAXIMUM OF FIRST AND SECOND HARMONICS.

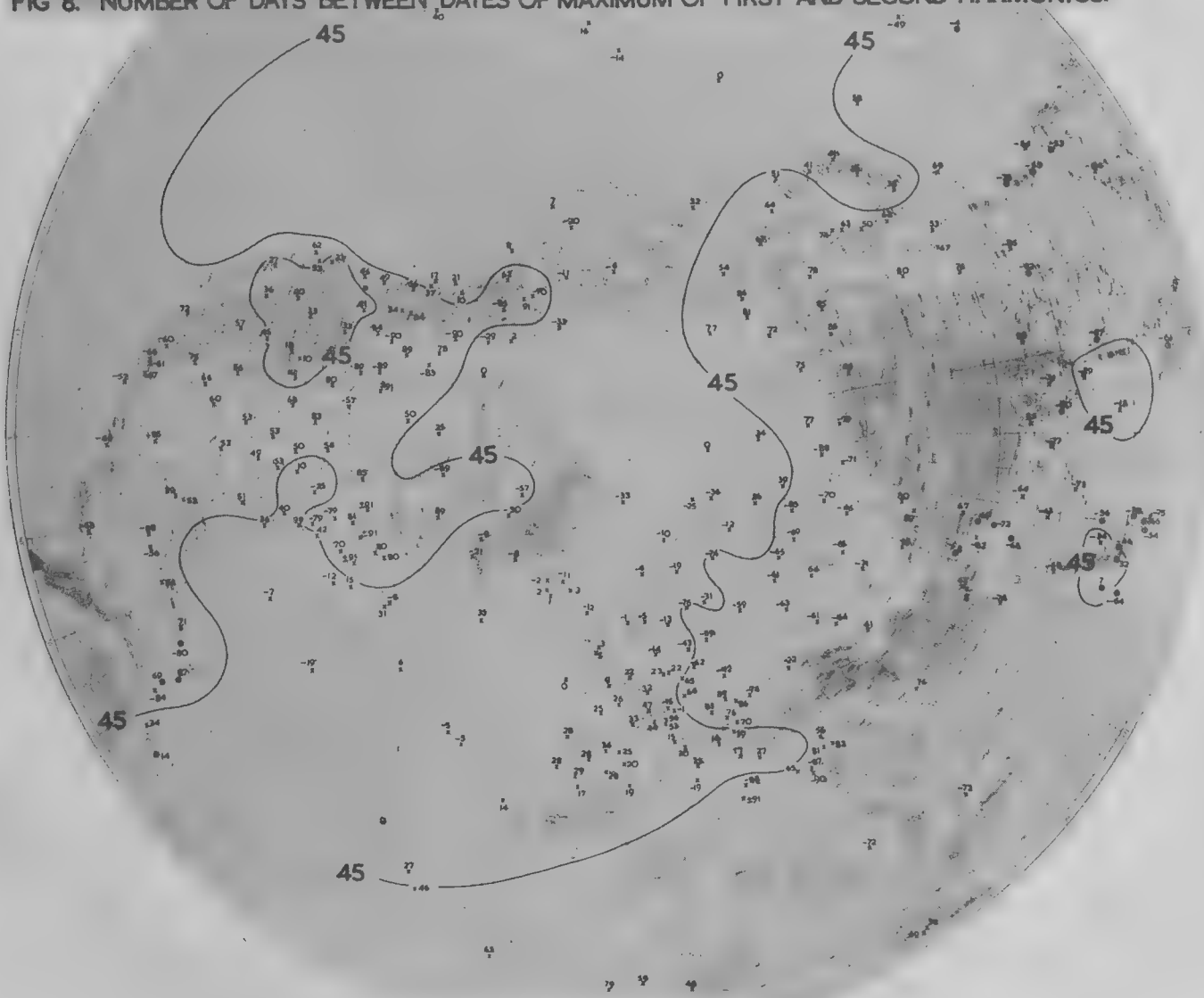

M.R.P. 918.
S.C. II/190
31st MAY, 1955.

Average height of the standard isobaric surfaces over the area from the North Pole to 55°N. in January.

by

H. HEASTIE.
(METEOROLOGICAL OFFICE)

AIR MINISTRY
METEOROLOGICAL RESEARCH COMMITTEE.

At the time of issue this report has not been published. Any author desiring to quote this paper should refer to it as "A paper of the Meteorological Research Committee (London). M.R.P. No. 918 by Mr. H. Heastie. A copy is available in the Library of the Meteorological Office."

M.R.P.918
S.C.II/190
31st May, 1955

AIR MINISTRY

METEOROLOGICAL RESEARCH COMMITTEE

Average height of the standard isobaric surfaces over the area from the North Pole to 55°N. in January

by
H. Heastie (Meteorological Office)

1. Introduction

Geophysical Memoir 85 - Upper Winds over the World - published in 1950, includes seasonal charts of the average heights of the isobaric surfaces 700, 500, 300, 200 and 130 mb. These charts were necessarily based on data for earlier years when the network of upper air stations was, in most parts of the world, extremely sparse. All available data were used irrespective of period, but the approach had still to be largely statistical. It was realised at the time of publication that these charts would need revision and, by about 1953, the increasing number of upper air data available made such a revision feasible.

The charts in G.M.85 are on a Mercator projection and do not extend beyond 75°N. In view, therefore, of the increasing importance of the polar regions for aviation, it was decided to start the revision by constructing circumpolar charts for the standard isobaric surfaces. The charts of the original memoir apply to the four seasons, each of three months. However, changes within a season can be very marked and to obviate the difficulty of maintaining equal weighting all over the chart for each month of the season, the charts were to be drawn for the mid-season months - January, April, July and October. Further, attention was to be confined to a fixed period rather than to one varied to include earlier years in particular areas. The five-year period 1949-53 was chosen mainly because January, 1949 marked the beginning of both regular CLIMAT TEMP data and publication by the meteorological service in western Germany (1) of monthly mean 500 mb. contour charts for a large part of the northern hemisphere. Finally it was decided to extend the range to 100 mb. and to include a chart for 150 mb.

This paper presents the circumpolar average contour charts for January and a discussion of the method used in their preparation.

2. The data

The sources of the data used in the preparation of the charts are given in the following list:-

(a) Climat temp reports.

Up to 200 mb. these give a reasonable network of data except over Russia and eastern Europe.

(b) Data tabulations from U.S.W.B. Daily Series Synoptic Weather Maps.

These publications give daily upper air reports from stations in the northern hemisphere. Daily values have been extracted to give monthly mean heights for:-

/(i)

(i) Climat stations at 200 and 100 mb.

(ii) Non-climat stations at all levels - in particular, Russia, Greenland and the Aleutians.

(iii) Certain climat stations at all levels, where the climat value seemed dubious.

(c) Micro-film.

Certain data for limited periods have been obtained from micro-film:-

(i) For Sola, Gardermoen, Tromso, Keflavik, Jan Mayen and weather ship "M" - from Norway.

(ii) For Stockholm - from Sweden.

(iii) For American weather ships "A", "B" and "C".

(d) Aerologiske Observationer i Danmark.

Data for limited periods for Thorshavn and Copenhagen.

(e) Hollerith tabulations in the Upper Air Climatology Branch.

Data for British stations and weather ships "I" and "J" were obtained from Hollerith tabulations.

(f) Manuscript data from U.S.A.

Data for Alaska at 200, 150 and 100 mb. were obtained from U.S.W.B.

The U.S.W.B Daily Series Synoptic Weather Maps for January, 1953 have not been received, so for this month additional sources of data were used.

(g) Dunstable synoptic charts.

Daily values were read off:-

(i) For eastern Europe, Russia in Europe and Greenland - all levels.

(ii) For climat stations in Europe - 200 and 100 mb. levels only.

(h) Teleprinter data from Dunstable.

All Russian data received at Dunstable were examined and data for stations in Russia in Asia were extracted.

(i) Russian data already extracted by Dunstable for use in drawing the climat charts were incorporated with (h) above.

(j) Manuscript data from Canada.

Data for Canadian stations at 200, 150 and 100 mb. were obtained from the Canadian Meteorological Service.

(k) German Daily Weather Report.

The daily weather report published by the meteorological service in western Germany (1) contains a 500 mb. contour chart covering a large part of the northern hemisphere. Daily values of 500 mb. height at a few stations in Siberia were extracted.

/3.

3. Method of constructing the charts

(1) General. It was found necessary to draw a separate set of charts for each year since:-

(a) The Russian data were very sparse; some of the monthly means were based on few observations and very few stations were available with equal reliability for all five years. Hence the only way to make use of all available data was to consider each year separately.

(b) Some of the climat data were obviously incorrect (possibly due to errors in transmission) and could most easily be checked on a yearly basis.

(c) At the upper levels, data were biased owing to loss of observations and, moreover, the number of data (particularly at 100 mb.) increased steadily through the period 1949 - 53.

Further, in drawing the individual charts, the area was divided into two sectors for which somewhat different procedures had to be adopted. For the first sector from 180°W. to 20°E., comprising the eastern Pacific, North America, the North Atlantic and western Europe, the data were reasonably adequate for the straightforward drawing of the charts. For the remaining sector from 20°E. to 180°E., comprising European and Asiatic Russia and the western Pacific, data were sparse and special procedures, described below, had to be adopted. These two sectors are referred to in the paper as the western and eastern sectors respectively.

(2) 700 mb., 500 mb. and 300 mb. charts. When all available data were plotted, it proved possible to draw the mean contours with some degree of confidence except over Russia in Asia. To assist in drawing this area of the chart, use was made of the monthly mean 500 mb. contour charts published in the monthly supplement to the German Daily Weather Report. These particular charts were used since reference to the corresponding daily charts suggested that more data from Russia in Asia were available in Germany than at Dunstable. Values of 500 mb. height were read off these charts for each of the five Januaries at a set of grid points covering the eastern sector and plotted on the working charts of 500 mb. contours. With the aid of these grid values and the Russian data available the drawing of the five 500 mb. contour charts was completed.

Unfortunately similar assistance at 700 mb. over Russia was not obtainable, so charts of 700-500 mb. thickness were next plotted for the available data for each January. It proved possible to draw these charts completely, though the isopleths over Russia were tentative. Values of 500 mb. height and of 700-500 mb. thickness were then read off at a set of grid points covering the eastern sector. By subtraction five sets of grid values of 700 mb. height were obtained and plotted on the working charts. The drawing of the five 700 mb. contour charts was then completed. Finally, for each year, the two contour charts and the thickness chart were examined together and minor adjustments made over Russia to produce the most plausible mutually consistent patterns.

The 300 mb. contour charts were then constructed in a similar manner, i.e. charts of 500-300 mb. thickness were drawn first and, over the eastern sector, grid values added to the 500 mb. height grid values to obtain five sets of 300 mb. height grid values. Again, for each year, the three contour charts and two thickness charts were examined together and minor adjustments made where necessary.

The average contour charts of the 700 mb., 500 mb. and 300 mb. surfaces for the period 1949-53 were then constructed by reading off values for the individual years at a set of grid points and meaning.

/(3)

(3) 200 mb. charts: effect of the tropopause. A new problem arose at the 200 mb. level, since no useful data were available over Russia. It was decided, therefore, to construct, for the eastern sector, a chart of average 300-200 mb. thickness, by making use of temperature lapse rates derived from the charts of average temperature of standard isobaric surfaces already drawn in the Upper Air Climatology Branch. A further complication arose because the average pressure at the tropopause was between 300 and 200 mb. almost everywhere over the area covered by the chart. However, by making use of the charts of average pressure and temperature at the tropopause, already constructed, a "correction for tropopause", to be applied to the thickness obtained from the mean temperature of the layer (assumed to be the mean of the temperatures at 200 and 300 mb.), was evaluated in the following manner. For any point on the chart let

T_T, p_T be the average temperature and pressure at the tropopause,

T_1, T_2 the average temperature at two standard isobaric surfaces p_1 and p_2, where $p_1 > p_T > p_2$,

$\Delta\phi$ the difference in geopotential between the two isobaric surfaces.

Then $\Delta\phi = R\, T'_m \log_e \frac{p_1}{p_2}$ in c.g.s. units

where R is the gas constant for dry air and T'_m is the mean virtual temperature (in degrees absolute) of the layer.

Writing $T'_m \simeq \frac{T_1 + T_2}{2}$, that is, ignoring the presence of the tropopause, a first approximation $\Delta\phi'$ to $\Delta\phi$ may be at once evaluated from standard tables, e.g. Smithsonian Meteorological Tables.

Taking into account the tropopause, a better approximation to $\Delta\phi$ is given by the expression

$$R \frac{T_1 + T_T}{2} \log_e p_1/p_T + R \frac{T_T + T_2}{2} \log_e p_T/p_2$$

and a "correction for tropopause", C, was defined as

$$C = -\Delta\phi' + \left(R \frac{T_1 + T_T}{2} \log_e p_1/p_T + R \frac{T_T + T_2}{2} \log_e p_T/p_2 \right).$$

This may be rewritten

$$C = -R\left[\tfrac{1}{2}(T_1 - T_2) \log_e p_T/p_2 + \tfrac{1}{2}(T_2 - T_T) \log_e p_1/p_2 \right].$$

With p_1 = 300 mb. and p_2 = 200 mb.,

$$-C \simeq 33.72 (T_1 - T_2) \log_{10} p_T/200 + 6 (T_2 - T_T)$$ in geopotential metres.

The thickness of the layer was then evaluated as $\Delta\phi' + C$.

Charts of 300-200 mb. thickness were first drawn for the five years separately over the area where data were available, i.e. the western sector, and an average chart constructed by reading off grid values and meaning. Charts of 300 mb. temperature were then drawn over the

/whole

whole area of the chart for the five years separately and a chart of average 300 mb. temperature constructed. From this chart, the temperature lapse rates mentioned above and the "correction for tropopause", values of average 300-200 mb. thickness were calculated at a set of grid points covering the eastern sector. These were then plotted on the working chart of average 300-200 mb. thickness. Unfortunately the pattern produced was most irregular and unconvincing.

It was then decided to investigate the average 200 mb. temperature chart. Over the western sector the average chart was constructed from the five charts for the individual years (the climat charts were accepted for 1951, 52 and 53, but charts had to be drawn for 1949 and 50) and the remaining sector completed by use of grid values derived from average 300 mb. temperatures and temperature lapses from 300 to 200 mb. Over the eastern sector the grid values of 200 mb. temperature and 300-200 mb. thickness were then adjusted by a somewhat laborious method of trial and error to obtain the most satisfactory mutually consistent patterns. The resulting average 300-200 mb. thickness chart was then added to the average 300 mb. contour chart to obtain the average 200 mb. contour chart.

(4) 150 mb. charts. A further problem arose at the 150 mb. level. While there were, of course, no data over the eastern sector, even over the western sector, where, at lower levels, the network of data had been adequate, the number of data varied through the period from poor in 1949 to good in 1953. The quality of the data was also more suspect owing to loss of observations with height.

To make the best use of the data available, it was decided to construct charts of 200-150 mb. thickness for the individual years over the western sector. In the first place, all data were ignored and thickness charts for the individual years were computed from the appropriate charts of 200 mb. temperature and the average temperature lapse from 200 to 150 mb. obtained from the charts of average temperature prepared in the Upper Air Climatology Branch. The mean temperature of the layer was assumed to be the 200 mb. temperature less half the temperature lapse from 200 to 150 mb. These computed charts were used in conjunction with the available data to construct the working charts of thickness for the individual years. By reading off grid values and meaning, a chart of average 200-150 mb. thickness was obtained over the western sector. The remaining sector was then completed by computing grid values of average thickness from values of average 200 mb. temperature and temperature lapse from 200 to 150 mb. Minor amendments were made in adjusting the two halves of the chart and in smoothing the pattern. A revised set of grid values was then read off over the whole chart and added to the 200 mb. height grid values to obtain the average 150 mb. contour chart.

(5) 100 mb. charts. The data at this level presented problems similar to those occurring at 150 mb. and a similar technique was employed. The grid values of average 200-150 mb. thickness were converted into grid values of average temperature of the layer and by combining these with grid values of average 200 mb. temperature, a chart of average 150 mb. temperature was produced. Over the western sector, grid values of 150 mb. temperature for the individual years were computed by a similar process applied to the corresponding yearly charts. It was now possible to construct a chart of average 150-100 mb. thickness in a manner exactly analogous to that described above for the 200-150 mb. thickness. Finally this last chart was added to the average 150 mb. contour

/chart

chart to obtain the average 100 mb. contour chart.

(6) Final adjustments to charts. The average charts of contours, temperatures, thicknesses and temperature lapses were now examined as a whole and certain anomalies over northern Russia were apparent. Data of any sort from this area were very sparse and of doubtful interpretation, so it was felt that some adjustment over this area was allowable. By redrawing the chart of average tropopause pressure and altering the temperature lapses above 300 mb. in the light of those over Canada, it was found possible to remove, at the same time, the major anomalies in contour height and temperature lapse. The charts were then redrawn over Russia from the 200 mb. level upwards.

References

(1) Die Grosswetterlagen Mitteleuropas. Deutsche Wetterdienst. Bad Kissingen, Germany.

Average 700mb. Contour heights (gp.d.m.)
JANUARY 1949-53

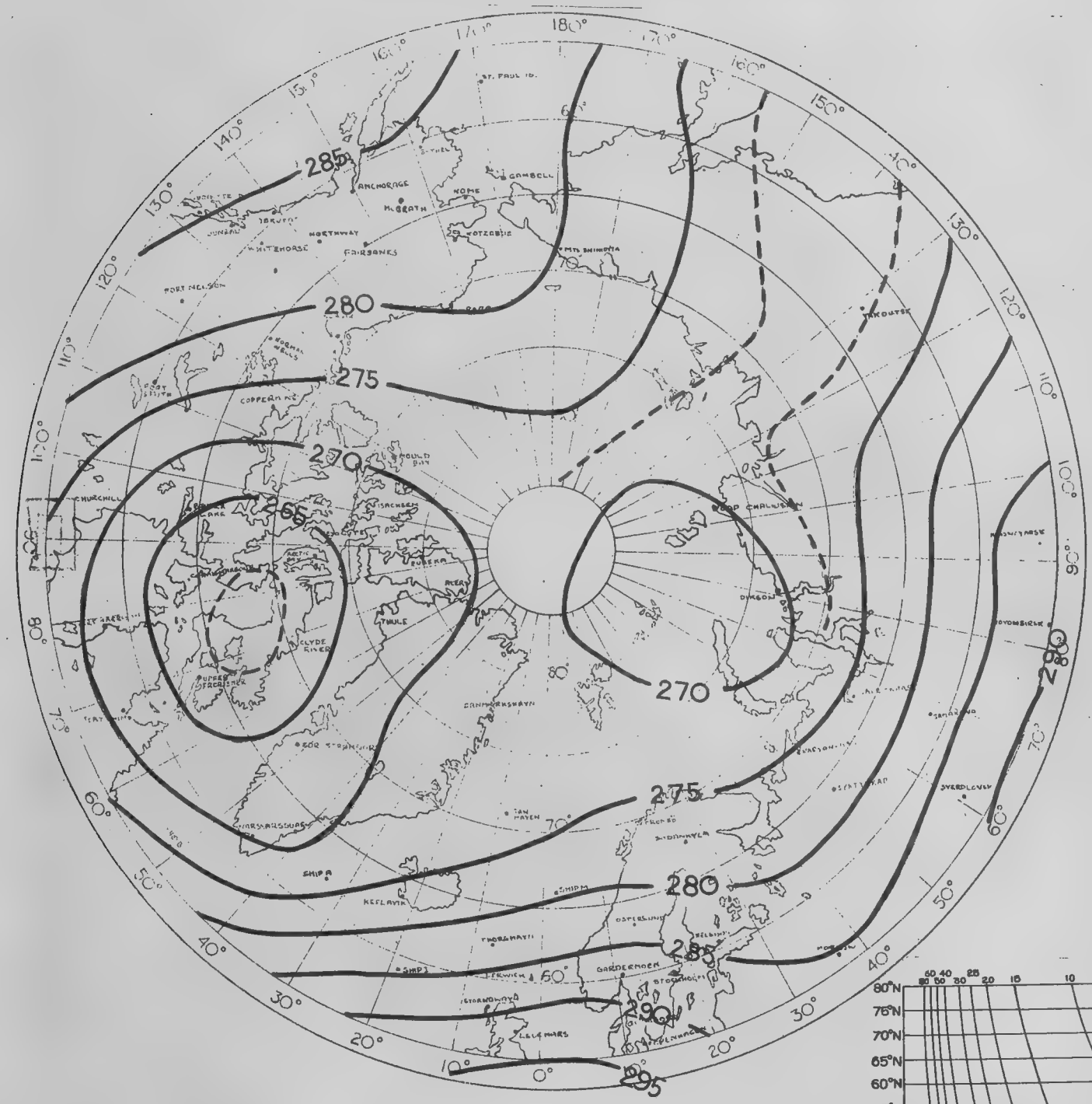

Height in dekametres

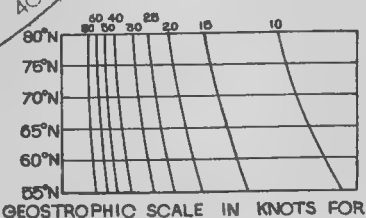

GEOSTROPHIC SCALE IN KNOTS FOR CONTOURS AT 100gp.dm. INTERVALS

Upper Air Branch (M.O.23)

Average 700-500 mb. Thickness g.p.d.m.
JANUARY 1949-53

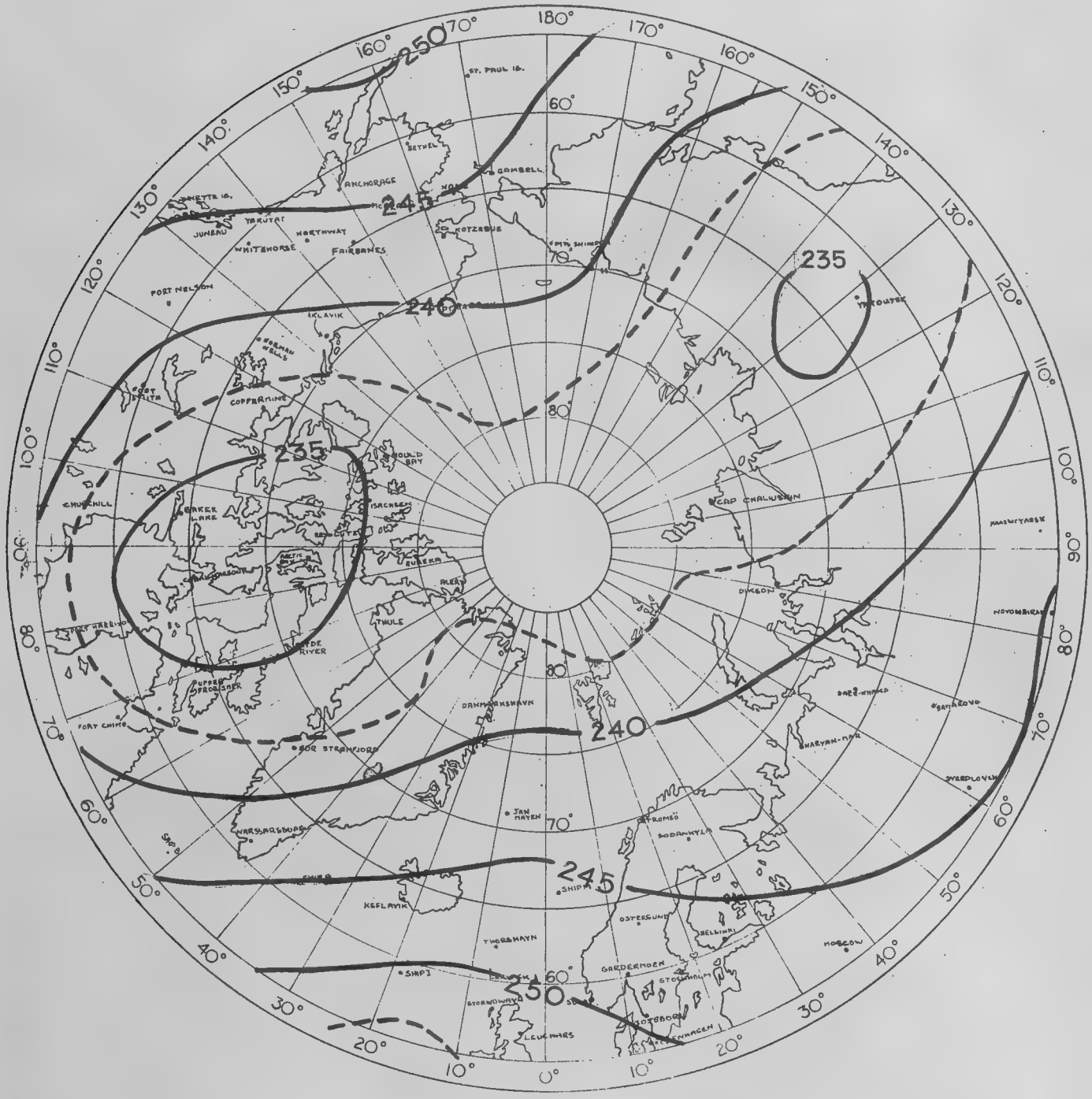

Height in dekametres

Upper Air Branch (M.O.23)

Average 500mb. Contour heights (g.p.d.m.)
JANUARY 1949-53

Height in dekametres

Upper Air Branch (M.O.23)

Average 500-300mb. Thickness (gpdm)
JANUARY 1949-53

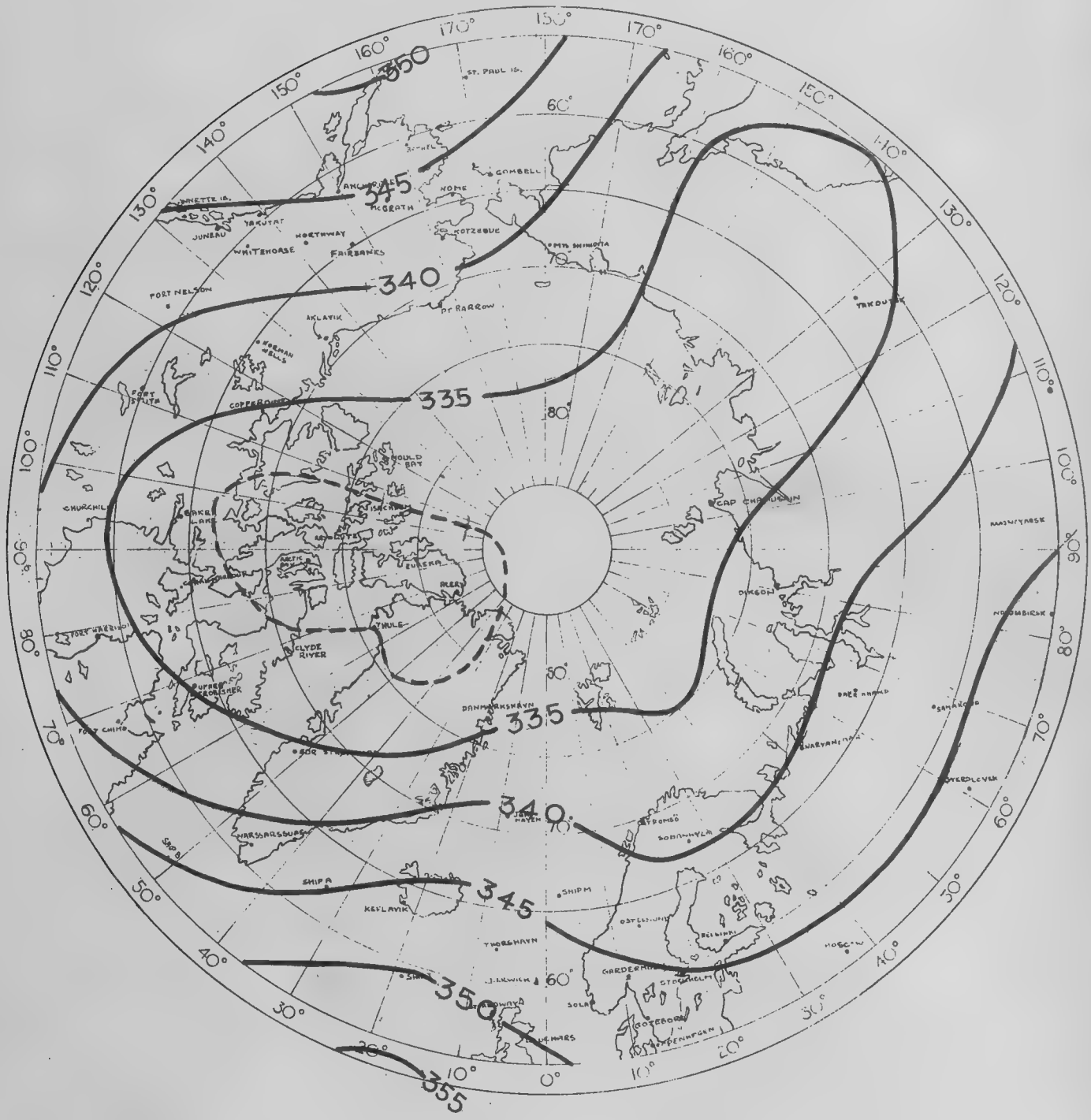

Height in dekametres

Upper Air Branch (M.O.23)

Average 300mb. Contour heights (g.p.d.m.)
JANUARY 1949-53

Height in dekametres

Upper Air Branch (M.O.23)

Average 300-200 mb. Thickness (gp.d.m.)
JANUARY 1949-53

eight in decametres

Upper Air Branch (M.O.23)

Average 200mb. Contour heights (g.p.d.m.)
JANUARY 1949-53

Height in dekametres

Upper Air Branch (M.O.23)

M.R.P. 918

Average 200-150 mb. Thickness (g.p.dm.)
JANUARY 1949-53

Height in dekametres

Upper Air Branch (M.O.23)

Average 150mb. Contour heights (g.p.d.m.)
JANUARY 1949-53

Height in dekametres

Upper Air Branch (M.O.23)

M.R.P. 918

Average 150-100 mb. Thickness (g.p.d.m.)
JANUARY 1949-53

Height in dekametres

Upper Air Branch (M.O.23)

Average 100 mb Contour heights (gp.dm)
JANUARY 1949-53

Height in dekametres

Upper Air Branch (M.O.23)

M.R.P. 919.
S.C. III/186.
31st MAY 1955.

ATMOSPHERIC TURBULENCE IN AVIATION.

by

G. A. CORBY.
(METEOROLOGICAL OFFICE)

METEOROLOGICAL RESEARCH COMMITTEE.
AIR MINISTRY

At the time of issue this report has not been published. Any author desiring to quote this paper should refer to it as "A paper of the Meteorological Research Committee (London).
M.R.P. No. 919 by Mr. G. A. Corby
A copy is available in the library of the Meteorological Office."

M.R.P. 919
S.C.III/186
31st May, 1955.

AIR MINISTRY

METEOROLOGICAL RESEARCH COMMITTEE

Atmospheric turbulence in aviation

by

G.A. Corby (Meteorological Office)

1. The operational requirement

It has been the practice for many years in aviation forecasting for predictions of turbulence to be included in forecasts issued to pilots, and at the M.O. Training School forecasters are taught to do this. A clear requirement for such forecasts is contained in the I.C.A.O. Specifications for Meteorological Services for International Air Navigation. No similar document dealing with meteorological requirements for the R.A.F. exists, but broadly speaking the principles followed for both military and civil flying are much the same. The current I.C.A.O. Specifications require indications of turbulence (with an estimate of intensity) to be given to pilots. The indication is given either by the insertion of appropriate symbols on pictorial cross-section forecasts or in plain language on other forms. Criteria governing the amendment of forecasts on account of changes in the forecaster's expectations regarding turbulence have been prescribed by I.C.A.O. Furthermore, there is a formal requirement for the issue of warnings of turbulence to Air Traffic Control Centres for broadcast to all aircraft in the area, at the discretion of the flying control staff. In practice it is the present Met. Office policy to restrict such clear air turbulence warnings to the re-issue of aircraft reports of severe incidents actually received.

Forecasters, therefore, have an obligation to attempt forecasts of turbulence. Whilst most flying was confined to the lowest few thousand feet of the atmosphere, forecasts of turbulence could be based on subjective estimates derived largely from considerations of instability, wind strength, and surface roughness. Turbulence was (and is) forecast in strong winds, in unstable airmasses and particularly in heavy convective cloud. Moderate success is achieved in forecasting such mechanical and convective turbulence in the lowest few thousand feet and it is probable that there is no great dissatisfaction with the standard attained in this respect. Estimates of intensity are, however, highly subjective, being confined to the descriptions slight, moderate or heavy.

At higher levels, the position is far less satisfactory. At I.C.A.O. Divisional Meetings during recent years, considerable concern has been expressed regarding the lack of understanding of meteorological problems affecting high-level high-speed flight, in particular of high-level clear air turbulence. So far as forecasting is concerned, the obligation to attempt predictions applies at high as well as other levels. At present the forecaster can do little more than exploit the results of synoptic/statistical studies (notably those of Bannon) to indicate preferred locations of turbulence relative to jet streams. Unfortunately such indications are unreliable, since many jet streams contain no significant turbulence at all. It is not known to what extent such forecasts are attempted at M.O. outstations.

It is known that civil aircraft operating over Europe at levels around 400 mb. have suffered a number of disturbing turbulence incidents and that the

/forecasters

forecasters at London Airport are unable to provide satisfactory advice in their flight forecasts. The extent to which high-level turbulence may constitute a hazard to future civil aircraft at higher levels is uncertain. It is likely that the problem will be more acute for civil aircraft than for the R.A.F. Military aircraft are stronger and must be operated in spite of the attendant risks and conditions whereas in civil aviation the safety and comfort of the passengers is a prime consideration.

Apart from the need for a better understanding of high altitude turbulence to assist in the operation of, and forecasting for, high level aircraft, the design of aircraft is also affected by lack of information. It is now well recognised that the behaviour of an aircraft in turbulent air is intimately dependent upon the response characteristics of the particular aircraft, especially of its fundamental frequencies. For example, Canberra pilots commonly report "cobblestone" turbulence having a frequency around 6 c.p.s. with often, in addition, a much slower yawing in the horizontal. According to Zbrozek (of R.A.E., Farnborough), these vibrations correspond with the natural modes of the aircraft about horizontal and vertical axes. Zbrozek is gravely concerned that future aircraft types may be even more seriously affected in this way, because of reduced damping and increased size, which lowers the fundamental frequencies of the aircraft. In the 1954 Report of the Gust Research Committee, the implications of the fact that the natural frequencies of an aircraft can be excited by turbulence, were highlighted as the most noteworthy item. The Committee were disturbed at the lack of knowledge of gusts to enable accurate predictions of the effect of turbulence on future aircraft. In their recommendations, the Committee recorded an urgent need for knowledge of the structure of gusts especially of those gusts which cause high frequency responses in fast aircraft. Concern on similar grounds is recorded in the proceedings of recent I.C.A.O. meetings and recommendations were made calling for continued reporting by transport aircraft, for continued research, for the development of suitable devices for recording turbulence in civil aircraft and for the development of techniques for the investigation of turbulence by the use of additional instruments attached to routine radio-sondes.

It is clear from the foregoing that our knowledge of high altitude turbulence is inadequate:-

(a) for the provision of guidance to aircraft operators for operational planning purposes,

(b) to enable forecasters to provide useful advice in day-to-day flight forecasting (even now and more so in the future),

(c) for the provision of important data bearing on the design of aircraft.

2. What is being done

(a) The scheme under which reports of high altitude turbulence are made by the pilots of R.A.F. aircraft is still in force and a steady supply of such reports continues to be received. In the past these have been sufficient to enable analyses of the distribution of turbulence with altitude and in relation to the jet stream to be carried out (e.g. Bannon, Jones). The nature of the data does not admit of investigations of the structure of the turbulence. Further analyses of similar type could be carried out from the further data accumulated, if desired.

(b) Measurements are being made at East Hill of the movement of smoke puffs at high levels. The direct aim is to assess the variability of wind over periods of the order of a few seconds; indirectly, some information on turbulence should emerge. An alternative method, which avoids the bias towards clear sky conditions, is provided by the radar tracking of small quantities of 'window'. This also makes possible measurements over longer intervals of time than with smoke puffs.

/At

At present no other active research on the topic is actually in progress in the Meteorological Office.

3. What could be done

(a) The large number of aircraft reports supplied by R.A.F. pilots in the past has been invaluable in making it possible to demonstrate the relation between high altitude turbulence and the jet stream, etc. The continuance of these reports is probably worth-while. These reports, however, are almost exclusively confined to the British Isles, and in addition they form an unsatisfactory statistical distribution owing to the unknown irregularities of the flying. It seems highly desirable that a similar fully organised scheme for reporting by civil pilots should be arranged; the advantage would be that information from a much wider geographical area would result and also the data would come from regular flying over known routes. The framework of such a scheme was laid down by I.C.A.O. in 1950 but the response has been negligible. Occasionally incidents come to light at debriefings but there is no organised routine reporting. A suitable form for the purpose was devised by I.C.A.O. and it may be profitable to approach British airlines and appeal to them to make the scheme a reality; a corresponding approach to the meteorological office at London Airport would be necessary. In any event, such data as are available, or which could be obtained from flight logs, should be examined. A study of reports from a much wider area than the British Isles might throw some light on the awkward question as to whether there is any relation between high altitude turbulence and topography. Almost certainly there is some relation, at least in many cases, but the evidence is inconclusive and existing data are inadequate to resolve the question.

(b) Arising from the Gust Research Committee's concern that the natural frequencies of an aircraft might be excited to a dangerous degree by turbulence (analogous to the "flutter" problem), it was recommended that there should be liaison between M.R.F. and the Aerodynamics Dept., R.A.E., with a view to fitting to the M.R.F. Canberra an accelerometer capable of recording high frequency oscillations (2-10 c.p.s.). Other accelerometers used by the M.R.F. do not cover the requisite frequency range. There is understood to be some prospect of a suitable accelerometer being made available and if this were done and the instrument were used as routine on all Canberra flights a useful body of data would be accumulated; certainly the Gust Research Committee's recommendation deserves to be actively followed up. It is understood that R.A.E. might be able to provide data on the response characteristics of the Canberra; this would make it theoretically possible to attempt the determination of the turbulence spectrum from accelerometer records. An indication of the probable behaviour in the same turbulence of any other aircraft whose response characteristics were known would then be possible.

The approach in some American work has been somewhat different. The spectrum of the turbulence in the horizontal has been determined by hot wire anemometry; isotropy has been assumed and thus the spectrum of the vertical components is also determined. If a suitable accelerometer record is also available, the response characteristics of the particular aircraft can be deduced. There are some doubts as to whether this technique can be successful, but experiments with work of this sort are probably justified.

The analysis and interpretation of data of these sorts would no doubt be difficult and highly specialised and it is for consideration whether such work should be attempted within the Meteorological Office, or whether it is more appropriate to an aerodynamicist. An alternative approach might be to try to exploit further the M.R.F. technique by which both vertical and horizontal turbulence velocities are measured by hot wire anemometry. Reliance on accelerometer records or the assumption of

/isotropy

isotropy would not then be necessary, although they might be used as a check. However, the installation of hot wire anemometers in the Canberra might be very difficult. So far as is known, such work of this type as has been undertaken (both here and in America) has been confined to low levels. It should be mentioned also that past experience of the flight investigation of high level turbulence (e.g. Hislop and R.A.E.) suggests that it is an elusive phenomenon, that there would be many abortive flights and that progress would necessarily be slow.

In spite of the difficulties, work on the above lines appears essential if adequate guidance is to be provided to the designers of future aircraft.

(c) The Meteorological Office might with advantage use its influence to try and foster the I.C.A.O. recommendation regarding the fitting of accelerometers to civil aircraft, although it is understood that R.A.E. have already arranged the installation of accelerometers and fatigue meters in selected civil and R.A.F. aircraft and trial installations are now being made at two Bomber Command units.

(d) A few years ago the M.R.F. demonstrated the feasibility of making useful measurements from one aircraft of horizontal and vertical smoke trails laid from another aircraft. The elusiveness of high altitude turbulence would probably make this too ambitious and too expensive a method. It may be mentioned that an American group recently asked for information on this technique as they thought it might be promising for studying the fine structure of wind shear through jet streams.

(e) There are obviously serious difficulties to the I.C.A.O. suggestion regarding the fitting of turbulence measuring devices to routine radio-sondes and this may not be a profitable line to pursue. Nevertheless the possibility might be studied by the Instrument Development Division of the Meteorological Office. Scrase has of course shown that limited information on turbulence may be deduced from radio-sonde radar-wind ascents and the Gust Research Committee recently recommended that the method of following the motion of a balloon-borne target by G.L.VII radar should be pursued.

M.R.P. 922
S.C. 1/100
25th June, 1955

Wind Finding Trials of Radar A. A. No. 3 Mk. V11 (Second Series)

by

C. V. Else
(Meteorological Office)

AIR MINISTRY
METEOROLOGICAL RESEARCH COMMITTEE

At the time of issue this report has not been published. Any author desiring to quote this paper should refer to it as "A paper of the Meteorological Research Committee (London).
M.R.P. No. 922 by Mr. C. V. Else
A copy is available in the Library of the Meteorological Office."

M.R.P. 922
S.C.I/100
25th June, 1955

AIR MINISTRY

METEOROLOGICAL RESEARCH COMMITTEE

Wind Finding Trials of Radar A.A. No. 3 Mk.VII (Second Series)

by

C. V. Else (Meteorological Office)

(1) Introduction

Since the publication of M.R.P. 672, considerable work has been done on the use of Radar A.A. No.3 Mk.7 as an instrument for wind measurement, and it appeared desirable that a further series of comparison flights should be made to re-assess its usefulness, and to obtain information on its performance at longer ranges. To this end a series of nine flights was made comparing readings taken simultaneously from both the Radar A.A. No.3 Mk.2/4 and Radar A.A. No.3 Mk.7 equipments situated at Stanmore.

As a result of these flights some 500 sets of readings were obtained at slant ranges up to about 66,000 yd. From these readings results were calculated for means, mean deviations and R.M.S. deviations of range, azimuth and elevation for individual flights, and for all flights taken together, over the range scales 0-36,000 yd. and 30,000-66,000 yd. The scale change was actually made between 31,000 yd. and 32,000 yd. These results are reproduced in the tables at the end of the report.

(2) Method of Test

The trial flights were made at the beginning of February, 1955. Mesh type corner reflectors were used, being followed by the two equipments simultaneously. Both sets were set up, and adjusted, normally at the beginning of each day's flights, and the settings were checked, and where necessary adjusted, before each subsequent flight.

The G.L.7 (Radar A.A. No.3 Mk.7) was put on target by using automatic scan in azimuth, and manual control of elevation. The signals were fed to the range display via a delay line equivalent to 1,150 yd. of range, which enabled the signal to be observed emerging through the transmitter echo. The signal is normally located at about 600 yd. range with this method, and the set can be "locked-on" at a range of about 950 yd. When the equipment is locked-on, the delay line is switched out of use so that correct ranges are indicated by the ranging magslip indicators. The range tube is still used for locating the target as a satisfactory combination of P.P.I. control settings has not yet been found for displaying the target clearly at these short ranges.

Information concerning the G.L.7 readings was taken from the G.L.7 output socket, and fed to a braked magslip box operating in the G.L.3 (Radar A.A. No.3 Mk.2/4) cabin. This type of magslip box has been devised to allow virtually instantaneous halting of the magslip pointers when readings are required. It eliminates any errors due to inertia of the moving parts of the magslips, and permits the readings to be held until just before the next set is due, if necessary. Before the trials started checks were made to ensure that the readings at the braked magslip box and those inside the G.L.7 were the same at various readings of range, azimuth and elevation. No discrepancies were found.

/During

During these tests the G.L.3 equipment was fitted with the recently developed Head Amplifier Mk.2, which improves signal to noise ratio at long ranges, and with the Error Sensing Unit, which improves discrimination against noise at long ranges.

Four operators were employed throughout the trials. Three of these were in the G.L.3, and the fourth in the G.L.7. Of the operators in the G.L.3, one operated range, a second azimuth and elevation, and the third recorded all readings from both sets, each minute. The operator in the G.L.7 locked the set on, and then remained on watch and informed the recorder in the G.L.3 if anything untoward occurred. He also made the necessary scale changes in the G.L.7 at the appropriate time.

Readings were recorded each minute to the nearest 10 yd. and 0.1°. Intermediate readings of azimuth and elevation were thrown to the nearest odd tenth.

(3) Technical Remarks

Since M.R.P. 672 was written, a reassessment of methods of range extension led to the conclusion that a normal type of time delay scale extension was possible since the automatic following circuits work by cancelling a modulation signal imposed upon the returned echoes when the set is "off-target". The cancellation of this signal is not dependent upon a knowledge of its amplitude and phase at the instant of transmitter pulsing, as had been previously supposed. The construction of a scale trebler for use with the G.L.7 equipment was therefore undertaken. As a result of preliminary trials it was apparent that the G.L.7 requires a trebler unit of considerably greater stability than the G.L.3. This is because any drift is equivalent, to the automatic ranging circuits, to adding algebraically to the range rate of the target, the range rate equivalent to the drift. For meteorological purposes the servo system is adjusted to work with relatively low range rates, and drift in the trebler unit may increase these rates to a point at which the set ceases to follow (when the target is already moving at speeds near the maximum follow rate). For the same reason the trebler unit must be kept free of any small, sudden, variations in its delay time, as these would be equivalent to short bursts of very high range rates. The G.L.7 also requires synchronising pulses of one half microsecond duration, which are negative going, and delivered from a low impedance source. These considerations lead to a scale trebler unit which is rather more complicated than the one at present in use in the G.L.3 equipments. The size of the unit, is, however, no greater, owing to the use of modern components and techniques.

To aid changing range scale, a form of semi-automatic range changing has been developed for use with the G.L.7 equipment. When the echo nears a given range, towards the end of the scale, a key is depressed. The scale trebler then steps in a delay of 30,000 yd., and the strobe spot is automatically wound back by 30,000 yd. During this operation, which takes about ten seconds, the follow rates for azimuth and elevation, which existed immediately prior to the scale change, are maintained by a "follow-through" circuit. As soon as the range potentiometer has wound back, automatic following is again resumed. If the range rate at the time of scale change is high it is possible for the ranging to fall out of lock. In such cases the range may be brought on again manually, and automatic following then resumed. This has been facilitated by modifying the manual ranging generator so that it now gives a smaller output than previously. Hence it is now necessary to turn the handle more rapidly in order to follow at any given rate. This control was previously very coarse.

All the auto-follow circuits have been adjusted for best results with the low rates of follow to be expected with meteorological targets. The performance of these circuits is fairly good with weak yet steady echoes, but the set is prone to lose the target with a beating signal. The set has followed to about 80,000 yd. on several occasions, but this ability depends largely on the character of the signal.

/As

As the signal becomes weaker, and relatively long fades occur, the servo systems idle and the set drifts off target. As a result the amount of drift, or hunting, in the information output becomes alarmingly large. With fades lasting for several seconds the set may exhibit drifting up to about 4° off target. This drifting is always in the direction in which the servos were last correcting, and is due to residual magnetism effects in the amplidyne system which cause the servos to continue to idle in the direction of last error signal. From this point of view a change to a metadyne system, which is dead-beat, would be advantageous for meteorological purposes. This, however, would be a major modification and might prove impracticable from an engineering point of view. This effect also causes ranging errors, which are normally in a positive direction as range is usually increasing.

The braked magslip system affords an excellent method of extracting the readings from the G.L.7. It may be used at relatively large distances from the equipment, and since control of the brakes is available to the operator noting down the readings, the readings may be "held" until just prior to the next reading, if this is necessary. This method also obviates the dangers of erroneous readings, due to inertia of the moving parts, which can occur if the excitation voltage only is cut off. Braking is almost instantaneous (a lag of a few milliseconds), and once the brake is applied the reading is locked against quite large torques. The "flasher" unit developed at R.R.D.E. was investigated for this purpose, but was not found suitable as the decay time of the phosphor was too short to allow readings to be taken accurately.

Due to the high P.R.F. of the G.L.7 the range of (about) 100,000 yd. represents the limit to which the set can be made to follow, since, by the time the time-bases have re-set themselves, the next transmitter pulse is due to be transmitted.

This G.L.7 is a very old one, and many modifications have been issued, and improvements made, since it was manufactured. A number of modifications has been obtained and incorporated, but it is felt that the performance of this set must inevitably be considerably worse than a more recent one. One point of importance is that recent G.L.7 equipments are being fitted with a new type of head amplifier, which improves the signal to noise ratio by about 6db. A set fitted with this type of head amplifier would probably follow to 96,000 yd. regularly.

During the past two years the G.L.7 equipment has been run for a fairly large number of hours, and considerable experience has been gained concerning maintenance and reliability. When first brought into regular use the failure rate of components was excessively high, and this was investigated. The cause appeared to be overheating, and the refrigeration system was suspected. This was overhauled by an Army team who reported that it was considerably out of adjustment. After the overhaul it was possible to keep the cabin cooler, and the incidence of faults was much reduced.

Two or three units have shown themselves to be regular offenders for failures. One of these is the negative 5,000 volt supply, which regularly blows fuses for no apparent reason, and another is the automatic frequency control unit, which should maintain the tuning of the local oscillator Klystron against drifting. The range "putting-on" potentiometer has also been a source of trouble, causing "creeping" of the measured range to a stationary object by up to 500 yd. in 30 min.

Considerable trouble was experienced initially with the main I.F. strip, which would not hold its tuning. Screening of certain wiring, and the fitting of a screening base plate, cured this trouble. The motor oscillator circuits have also given a little trouble, including insulation breakdown in the oscillator output transformer. This put the set out of action for nearly six months whilst replacements were obtained.

/Faults

Faults are fairly easy to clear, once located, owing to the rack method of mounting all units; and extension leads are available for testing purposes. There is a fairly large selection of metering and monitoring points, which assists in fault location, and we understand that R.R.E. are developing a built-in type of performance measuring equipment.

A serious disadvantage of this equipment is the height of the cabin, which makes working cramped and uncomfortable for everyone except pigmies of less than about 4 ft. 6 in. tall.

Since it is only necessary for one person to remain in the cabin of the G.L.7 equipment while it is operating, there is a saving of one person during a flight, providing that readings can be taken by one of the persons in the radiosonde office. If a separate person in required to note the readings each minute then there is no saving of personnel over those needed when a G.L.3 equipment is used.

(4) Results

A summary of the results obtained is given in the tables attached. These indicate, in general, a high standard of observations. No smoothing has been made to these results; only obvious reading errors of thousands of yards or tens of degrees have been corrected. The results therefore include deviations, due to drifting on weak signals, of up to 4°. In practice, a large proportion of these deviations would be smoothed out during the plotting operations.

The range results show a relative error which starts in one direction, passes through zero and then increases in the other direction. The probable cause of this is slight differences in the frequencies of the two calibrating crystals, which would cause a percentage error varying with range. There is also a systematic error which appears on the second range, which is probably due to slight relative errors in setting up the two scale treblers. At long ranges the G.L.7 tends to read higher than the G.L.3 which, as stated above, is probably due to idling effects in the range servo system on a fading echo.

A comparison with the results given in M.R.P. 672 shows that the mean deviation of the present flights is about twice as large as that given for the original trials. This is because the mean deviation for the present series of flights includes a term due to the relative drift of the two ranging systems. The true mean deviation is considerably smaller than that given, and probably compares favourably with the original value. The value of the mean deviation given for the second scale results is also affected by this relative drift, and its true value will be somewhat smaller than that shown.

The mean differences in range for the two scales of flight No. 8 show a value for the second scale which is more positive than that for the first scale. This is the reverse of the results obtained in all the other flights. The effect is believed to be due to slight errors in setting up the two scale treblers.

The azimuth and elevation results show systematic errors of a few tenths of a degree, which would be corrected before the set was brought into routine use at a station. Unfortunately, at Stanmore, there is difficulty in finding suitable objects to use for setting the equipments up.

The mean deviations obtained for azimuth and elevation for the first scale compare with those given in M.R.P. 672. The azimuth mean deviations are, in fact, identical, whilst that for elevation from the present flights is $.05^{\circ}$ larger.

A comparison of the mean differences of azimuth and elevation with those from M.R.P. 672 shows the azimuth result to be now in a negative direction and about three times larger than previously, whilst the elevation result is still positive but only about one-third the magnitude of the previous result.

/The

The last three flights show an increased difference of azimuth mean of 0.3°, for which no explanation can be found. This also occurred during the 1951 flights (vide M.R.P. 672).

The rates of change of the parameters measured during these flights were average. Range rates were of the order of 1,500 yd. per min., which was about twice the rates obtained in 1951. The azimuth rates varied from almost nil to 12° per min., and were on the whole considerably less than the 1951 rates of change. Elevation showed rates of the same order as azimuth, and a comparison with the 1951 results shows that there is little difference between the rates obtained on the two occasions.

With regard to the maximum deviations, it will be seen by comparison with M.R.P. 672 that the first scale deviations for the present series of flights show a positive value much in accordance with the previous results, but the negative value is considerably greater. This is caused by the drift between the two range scales. This drift has therefore developed since 1951, and is almost certainly due to ageing of the master calibrating crystals. On the second scale the value of the negative deviations becomes very large, value of more than 1,000 yd. being recorded. These large values are partly due to the relative drift already mentioned, and partly due to drifting caused by fading echoes.

The values obtained for azimuth and elevation on the first scale are very much in accordance with the values obtained previously: an occasional large figure in the present tests being caused either by a fade or by interfering aircraft echoes. As might be expected, the values for the second scale are somewhat larger, being the result of echo fading at long ranges.

(5) Conclusions

The radar A.A. No. 3 Mk. 7 equipment is capable of producing wind information of the same order of accuracy as the present G.L.3 equipment at slant ranges up to about 40,000 yd. At longer ranges fading echoes produce considerable drifting in the information outputs, but the intervention of an intelligent interpreter of the information can still produce wind information of a high order.

These experiments have been made with a very old set, and a modern equipment might be expected to have a considerably better performance, together with a consequent improvement in the accuracy of the information output at longer ranges.

Although this equipment is considerably more complicated than the G.L.3 equipment servicing is easier due to the form of construction and the provision of metering and monitoring points.

The fault rate of the equipment depends upon the efficiency of the refrigerating system, which must be kept fully serviceable. When this unit is operating at full efficiency it is doubtful if the fault rate is any higher than that of a G.L.3 equipment.

TABLE 1 RESULTS G.L.3 - G.L.7 SCALE 1 (0-32,000 yd.)

FLIGHT NUMBER	NUMBER OF OBSERVATIONS	RANGE				
		MEAN YD.	MEAN DEVIATION YD.	R.M.S. DEVIATION YD.	MAX. DEVIATION YD.	APPROX. MAX. RATE OF CHANGE YD./MIN.
1	21	+ 45	46	72	+160; -210	1600
2	22	- 70	42	49	+ 0; -170	2400
3	26	-140	53	74	+ 60; -270	1800
4	54	- 75	50	60	+ 20; -220	1100
5	54	-112	63	71	+ 30; -240	1000
6	57	- 34	35	42	+ 70; -130	2800
7	31	- 49	42	49	+ 40; -140	2000
8	26	+ 29	19	25	+130; - 50	1500
9	27	+ 54	27	37	+ 80; - 30	1600
MEAN		- 39	42	56		

FLIGHT NUMBER	NUMBER OF OBSERVATIONS	AZIMUTH				
		MEAN °	MEAN DEVIATION °	R.M.S. DEVIATION °	MAX. DEVIATION °	APPROX. MAX. RATE OF CHANGE °/MIN.
1	21	-0.40	0.16	0.23	+0.0; -0.5	8
2	22	-0.30	0.06	0.10	+0.0; -0.5	2
3	26	-0.30	0.10	0.14	+0.0; -0.8	3
4	54	-0.30	0.13	0.17	+0.2; -0.7	9
5	54	-0.30	0.16	0.27	+0.9; -0.6	12
6	57	-0.20	0.13	0.18	+0.3; -0.6	9
7	31	-0.70	0.11	0.18	+0.0; -1.2	2
8	26	-0.60	0.08	0.10	+0.0; -0.8	3.5
9	27	-0.60	0.06	0.11	+0.0; -0.8	2.5
MEAN		-0.41	0.11	0.18		

FLIGHT NUMBER	NUMBER OF OBSERVATIONS	ELEVATION				
		MEAN °	MEAN DEVIATION °	R.M.S. DEVIATION °	MAX. DEVIATION °	APPROX. MAX. RATE OF CHANGE °/MIN.
1	21	+0.40	0.15	0.20	+0.8; -0.3	5
2	22	+0.10	0.12	0.16	+0.4; -0.3	2
3	26	+0.20	0.06	0.09	+0.4; -0.0	2.5
4	54	+0.10	0.12	0.16	+0.5; -0.3	3
5	54	0.00	0.20	0.33	+0.5; -1.9	4
6	57	+0.10	0.15	0.19	+0.7; -0.2	4
7	31	0.00	0.13	0.17	+0.3; -0.3	2
8	26	-0.10	0.11	0.14	+0.2; -0.3	2.5
9	27	0.00	0.10	0.13	+0.2; -0.2	1
MEAN		+0.07	0.13	0.20		

TABLE 2 RESULTS G.L.3 - G.L.7 SCALE 2 (32,000-66,000 yd.)

FLIGHT NUMBER	NUMBER OF OBSERVATIONS	RANGE				
		MEAN YD.	MEAN DEVIATION YD.	R.M.S. DEVIATION YD.	MAX. DEVIATION YD.	APPROX. MAX. RATE OF CHANGE YD./MIN.
1	38	-165	104	127	+ 10; - 360	1400
2	30	-710	250	295	+ 0; - 1,190	1700
3	35	-700	46	101	+ 0; - 1,040	1000
4	12	-251	47	57	+ 0; - 340	500
5			NO RESULTS			
6			NO RESULTS			
7	30	-590	73	90	+ 0; - 780	1000
8	20	+268	90	114	+110; - 110	1100
9	37	+ 17	32	45	+510; - 10	1000
MEAN		-307	92	146		

FLIGHT NUMBER	NUMBER OF OBSERVATIONS	AZIMUTH				
		MEAN °	MEAN DEVIATION °	R.M.S. DEVIATION °	MAX. DEVIATION °	APPROX. MAX. RATE OF CHANGE °/MIN.
1	38	-0.20	0.23	0.46	+2.2; - 1.0	1
2	30	-0.30	0.17	0.22	+0.0; - 0.8	0.5
3	35	-0.30	0.38	0.80	+0.1; - 1.3	1
4	12	-0.60	0.20	0.36	+0.0; - 1.5	2
5			NO RESULTS			
6			NO RESULTS			
7	30	-0.60	0.12	0.19	+0.0; - 1.0	0.5
8	20	-0.50	0.17	0.23	+0.0; - 0.9	1
9	37	-0.60	0.14	0.18	+0.0; - 1.1	0.5
MEAN		-0.44	0.21	0.43		

FLIGHT NUMBER	NUMBER OF OBSERVATIONS	ELEVATION				
		MEAN °	MEAN DEVIATION °	R.M.S. DEVIATION °	MAX. DEVIATION °	APPROX. MAX. RATE OF CHANGE °/MIN.
1	38	+0.40	0.18	0.30	+1.1; - 1.1	1
2	30	+0.20	0.13	0.21	+0.6; - 0.6	1
3	35	+0.20	0.13	0.20	+0.8; - 0.4	1.5
4	12	+0.30	0.51	0.84	+2.8; - 0.7	1.5
5			NO RESULTS			
6			NO RESULTS			
7	30	-0.10	0.25	0.43	+0.4; - 2.1	2
8	20	+0.10	0.28	0.34	+0.6; - 0.3	1.5
9	37	0.00	0.14	0.21	+1.1; - 0.6	1.5
MEAN		+0.16	0.23	0.37		

M.R.P. 923
S.C. 11/192
30th July 1955

Five year means of meteorological observations made at the ocean weather stations Item and India, Jig and Juliett. 1948-52

by

R.F.M. Hay
(Meteorological Office)

AIR MINISTRY
METEOROLOGICAL RESEARCH COMMITTEE

At the time of issue this report has not been published. Any author desiring to quote this paper should refer to it as "A paper of the Meteorological Research Committee (London).
M.R.P. No. 923 by Mr. R.F.M. Hay.
A copy is available in the Library of the Meteorological Office."

M.R.P. 923
S.C.II/192
30th July 1955

AIR MINISTRY

METEOROLOGICAL RESEARCH COMMITTEE

Five year means of meteorological observations made at the ocean weather stations Item and India, Jig and Juliett, 1948-52

by

R.F.M. Hay (Meteorological Office)

1. Introduction

Before regular meteorological observations had been started at ocean weather stations in the N. Atlantic towards the end of 1947, it had not been possible to describe the climate of a fixed point in the open ocean in the same detail and to the same order of accuracy as in the case of a land station. The summary of weather and currents at the original ocean weather station positions I and J by Gordon and Barlow(1) which related to the period August, 1947 to March, 1950 was the first published summary which gave results derived from a continuous series of observations at a fixed point away from land. Since that time the manning of the ocean weather stations has been continued, and this paper contains monthly mean values of the principal meteorological elements based on the five years 1948 to 1952. This period is of course too short to yield means which are quite representative.

2. Ocean weather stations

By international agreement the positions of both ocean weather stations were shifted by approximately 70 nautical miles on 25th March, 1950*. The assumption has been made therefore that the mean values given in Tables 1-13 are the same as those which would have been obtained from positions nearly mid-way between the positions occupied by the ships before and after 25th March, 1950, assuming these mid-way positions had been manned through the same five years. Such an assumption naturally involves errors, but it is considered these will be relatively small in this region where horizontal gradients of temperature are not pronounced. In the next place, on several occasions, the weather ship manning station I has been moved away for special purposes to a position some 150 nautical miles to ENE. (61°N.$14\frac{1}{2}^{\circ}$W.). Data for the few days when this move happened during 1948-52 were excluded in computing the tables. During 1953 removals of the ship on duty at station I to this position were more frequent than in the previous years, so that it was decided that better results would be obtained by omitting this year

* For convenience throughout this paper the ocean weather stations will be referred to as I and J. Their positions and official descriptions during the period 1948-52 were in fact as follows:-

ITEM $60^{\circ}00'$N.$20^{\circ}00'$W. to 0800Z, 25th March, 1950;
INDIA $59^{\circ}00'$N.$19^{\circ}00'$W. after 0800Z, 25th March, 1950;
JIG $53^{\circ}50'$N.$18^{\circ}40'$W. to 0230Z, 25th March, 1950;
JULIETT $52^{\circ}30'$N.$20^{\circ}00'$W. after 0230Z, 25th March, 1950.

from the calculations. Lastly observations are made aboard the ocean weather ships at the eight synoptic hours (00, 03, 06, 09, 12, 15, 18 and 21 G.M.T.), and the tables are based upon these observations except where there is a statement to the contrary.

3. The monthly mean values

Tables 1-11 contain monthly mean values of the principal meteorological elements observed aboard the ocean weather ships. Information about observational procedures is given either in the sub-paragraphs below, or in paragraph 5.

(a) Wind

Mean surface wind speed for the year is slightly higher at J (18.3 kt.) than at I (17.7 kt.). At both stations January is the windiest month, but the quietest months are July at J and August at station I. The mean wind speeds shown in Table 1 have been corrected to the standard height of 33 ft.; in the British ocean weather ships the actual height of the anemometer cups is approximately 55 ft. For the relation of mean wind velocity v to height h, most writers assume a relation of the form:-

$$v = kh^{\alpha}$$

The value of α depends largely upon the kind of surface over which observations are made and is larger over a smooth than a rough surface. Carruthers(2) quotes some figures due to C.E.P. Brooks which give values of α of 0.13 over the open sea and 0.15 over low islands. The nature of the air flow over an ocean weather ship (or any ship) hardly seems comparable to the exposure which would be found over the open sea away from obstructions. Hence the exposure of the anemometers has been assumed to correspond to the conditions on a low island and a value of 0.15 has been assigned to α, in the expression $V_h/V_{10} = (h/10)^{.15}$ where h is in metres. Taking the height of ships' anemometers as 16.8 m. (55 ft.) and the standard height as 10m. (33 ft.) this gives $V_{16.8} = V_{10} \times 1.08$ whence the factor to convert winds at 55 ft. to 33 ft. is found to be 0.93. The figures in Table 1 were obtained by multiplying the mean winds for the ocean weather ships at the anemometer level by this factor.

The windiness of these ocean weather stations is clearly shown by referring to Table 2. Over the year, mean wind speed at station I is nearly 25% greater than the value at Lerwick, the nearest land station lying in the same latitude. Similarly the value for station J is three quarters as large again as the mean wind speed recorded at Valentia. Both ocean weather stations I and J have rather higher wind speeds than Macquarie, Heard and Deception Islands which lie near the most frequented storm tracks of the southern ocean, although they are still far less windy than the coast of Antarctica at Adélie Land as found by the Mawson expedition in 1912-13.

The percentage frequencies of certain ranges of wind force related to direction are given in Tables 3 and 4, which show that winds of force 8-12 were more frequent at station I than at station J in all months except May, June, July, August, October and December. Table 9 shows that the number of gale days was 92 at station I and 117 at station J; the smaller number of gale days at I being due to a marked falling off in the frequency of gale days in the summer months at I as compared with J. A gale day was defined as a day (0-24 G.M.T.) when wind force 8 and above occurred, at one or more of the eight synoptic hours of observation.

Table 5 gives the number of occasions on which winds of force 8-12 occurred from different directions. Storm force winds of force 10 have occurred from all directions at both stations, and force 11 has occurred with winds between east and south as well as from all directions with a westerly component. The second part of the table shows that force 10 has occurred in all months at I except in June, July and August, and at J except in May, June and July.

(b) Pressure

The mean monthly values of pressure, together with the absolute extreme values reported through the five years in each month, are given in Table 6. In this table are also shown the differences between these values and the corresponding values taken from the Monthly Meteorological Charts of the Atlantic Ocean (M.O.483)(3) expressed as the differences (Table 5 - M.O.483) in each case. The large value of the differences in some months is hardly surprising, in view of the shortness of the period used for determining the means.

Interesting features of these tables are the fact that the normal pressure gradient between J and I was reversed in May (1948-52), and that at J pressure reached its highest mean monthly value in July, but at I in May. The highest pressure so far observed at these stations (1046.4 mb. at J in January) is not far short of the absolute extreme recorded for a land station in the British Isles (1054.7 mb. at Aberdeen on 31st January, 1902). Although the lowest values of pressure so far observed at either station have not been lower than the extreme lowest value of 925.5 mb. recorded on land in the British Isles, (at Aberdeen on 26th January, 1884) the monthly absolute extremes for February at I and for October at J during this five years were lower than the corresponding long period figures for the British Isles for these months (4). Lower extreme values of pressure have so far been reported at J than at I in the months of March, May, August, October and December. The range between the absolute extremes of pressure so far recorded at I is 96.6 mb. and at J 105.4 mb.

(c) Temperature

Monthly means of dry bulb temperature and dewpoint, also extreme temperatures, are given in Tables 7 and 8 for the two stations. Mean ranges of average monthly temperatures (11.5°F. at I, 11.2°F. at J) compare with values of 15°F. on the western seaboard of the United Kingdom and 23°F. in East Anglia(4). The ranges of extremes (33.3°F. at I and 30.5°F. at J) are far lower than at land stations in the British Isles. Air temperature has never fallen below freezing point at J, and only on 18 days in five years at I. These days were distributed as follows, December and January 5 each, February 4, March 2, April and November 1 each.

Monthly mean sea temperatures are included in the same table, also mean monthly values of air-minus-sea temperature difference, which are of greater scientific interest. The latter show a fairly regular seasonal variation, at station I they vary between -5·0°F. in January to -0·8°F. in July, and at station J from -3·9°F. in February to -0·2°F. in June. Thus on the average the air is colder than the sea at all seasons through the year. However the mean air-minus-sea temperature difference has a very small negative value during the spring and early summer. In individual years air temperatures exceed sea temperatures at both stations for periods of 2 or 3 weeks in the spring and early summer and very occasionally for a few days in the autumn and winter.

(d) Weather

Table 9 brings out clearly the notably high annual frequency of precipitation at both stations, 323 days at station I and 321 days at station J, although no precise comparison can be made between amounts of rainfall at the ocean weather stations and those at adjacent land stations until a raingauge can be devised which will make accurate measurements of precipitation amounts aboard the weather ships.

The frequency of snow and sleet at station I (54 days per annum) compares with about 35 and 40 days in the Orkneys and Shetlands respectively, similarly at station J the figure of 10 days compares with 5 days at Falmouth and 3 at Scilly. A rather similar parallelism can be found in the hail frequencies (64 days at I and 20 at Orkney, 38 at J and 16 at

Falmouth). The high frequency of hail in the winter months is probably related with the large number of occasions when the air is much colder than the sea at that season. Thunder was heard on 5 days a year at J (average 5 at Falmouth) but on 2 days a year at station I, which compares with 7 at Deerness and 3 at Stornoway.

(e) Visibility

Table 10 shows that the percentage frequency of fog (defined as all occasions when visibility was < 1000 yd.) at station I was greatest in July when it rose to 3.2%. Fog was very infrequent there from October to April; in this particular period there was no fog recorded in November. At station J the frequency of fog was higher, up to 5.4% in June and 3.6% in July; fog was infrequent from October to April and was not observed in January. At both stations there was a high frequency of visibilities above 10 miles (60-70%) which was noteworthy at J in most winter months and at I between July and January.

(f) Height of base of low cloud

Percentage frequencies are given in Table 11. Cloud below 600ft. was slightly more frequent at station J.

4. Comparison with the Monthly Meteorological Charts for the Atlantic Ocean

On the assumption that the mean positions of the stations were 59½°N. 19½°W. and 53°N. 19½°W. the monthly and annual means of pressure and air and sea temperatures given in Tables 6, 7 and 8 were compared with values obtained by interpolation from the charts given in M.O.483 (Monthly Meteorological Charts for the Atlantic Ocean). These charts were based upon readings of air and sea temperatures made by British observing ships during the period 1887-99 and by British selected ships from 1921-38. The results are shown in the last column but one on the right of Table 6 and in the two right hand columns of Tables 7 and 8. The annual values of the differences between Tables 6, 7 and 8, and M.O.483 were:-

	Pressure mb.	Air temp. °F.	Sea temp. °F.
Station I	-0.1	+0.3	+0.4
" J	+0.1	-1.1	-0.3

The results for station I agree with the conclusion that the sea and overlying air in this region have been warming up in recent years, but suggest that slight cooling has occurred at station J.

5. Diurnal variation of surface barometric pressure, wind velocity, air and sea temperature and cloud amount at ocean weather stations I and J

For the sake of completeness a few of the results of an investigation into diurnal variations of certain meteorological elements at the ocean weather stations are included here. In this investigation, which it is intended to publish in full later, surface data for the ocean weather ship stations I and J for the four years 1948-51 were used.

(a) Treatment of the data

Preliminary results obtained for the first two years 1948-49 showed that the magnitudes of the diurnal variations in both elements were in close agreement at the two stations I and J. It was therefore decided to use the data for the four years period 1948-51, ignoring the changes which were made in the positions of I and J in March, 1950, as described earlier.

As in previous work on this subject, data were used for those days only when the ships were within a square grid whose sides at their nearest were 105 miles distant from the station positions given earlier, when the

ship was considered to be "on station". In addition, only days were used on which observations were available at all eight synoptic hours from a ship "on station"; any days on which one or more observations at synoptic hours were missed were rejected. When one ship relieved another "on station", and both ships were making observations within the grid at the same time, the observations of the ship nearer to the grid centre were used.

(b) Accuracy of the observations available

(i) In obtaining results for surface barometric pressure, wind and total cloud amounts data were taken from Hollerith cards. For air and sea temperatures Hollerith cards were not considered sufficiently accurate for this part of the analysis, and therefore all temperatures used were taken from the O.W.S. log books. For the greater part of the period air and sea temperatures have been read to 0.1°F. and entered to this degree of accuracy in the log books.

(ii) Pressure was read to 0.1 mb. and punched on Hollerith cards to the same degree of accuracy.

(iii) Wind velocity was measured from the cup anemometer exposed on the mainmast about 55 ft. above the sea surface, the wind velocity being recorded in the log book and punched on Hollerith cards in Beaufort Force. The punched data have been reconverted to knots in this analysis using the appropriate mean values of Beaufort Force on the international scale.

(iv) All observations of cloud amount used in this analysis have been converted to amounts in tenths.

(v) Air temperatures were read to the nearest 0.1°F. from a thermometer in a Stevenson Screen exposed on the weather side of the ship. Data from the original log books were used.

(vi) Sea temperatures were read to the nearest 0.1°F. using a canvas bucket which aims to catch a sample from the top six inches of the sea. Data from the original log books were used. Most of the entries were made to the nearest 0.1°F. but a few were entered to the nearest 0.5°F. or 1.0°F., and had to be used in this form.

(c) Number of observations available

In the first instance the diurnal variations of the elements were determined for all days which were available after applying the procedure already described. The numbers of days for each station, element and season, which were available at the time when this investigation was begun, are shown below.

Station I

Season	Winter Dec.-Feb.	Spring Mar.-May	Summer June-Aug.	Autumn Sept.-Nov.
Pressure	257	328	319	296
Wind	268	328	318	296
Total cloud	269	327	319	296
Air temp.	269	328	318	295
Sea temp.	257	324	316	283

Station J

Season	Winter Dec.-Feb.	Spring Mar.-May	Summer June-Aug.	Autumn Sept.-Nov.
Pressure	318	359	353	348
Wind	331	360	353	349
Total cloud	331	360	353	349
Air temp.	331	360	349	349
Sea temp.	301	359	351	347

(d) Diurnal variations of sea and air temperatures (all days)

Values of the ranges of the diurnal variation of certain elements obtained from these data are given in Tables 12 and 13.

There is good agreement between the magnitudes of the yearly diurnal ranges of the two stations, and also between most of the seasonal values. There is little difference between the diurnal ranges of sea temperature in autumn and winter, and also between spring and summer.

For air temperature the ranges at both ships are largest in spring and summer and smallest in winter, the largest value for I is 1.36°F. in spring, for J 1.41°F. in summer.

For sea temperature the ranges at both ships are largest in spring and summer (0.36°F. at J in spring, 0.32°F. at I in summer), in autumn and winter the range is very small, being near 0.1°F. at both stations.

In all seasons, but particularly in summer, the range of diurnal variation of air temperature appears greatly to exceed that of sea temperature.

Radiation errors are discussed later.

(e) Diurnal variations of sea and air temperature (classified days)

The reality of these diurnal variations of air temperature is open to doubt since they are subject to errors due to heating of the air as it passes across the ship. Possibly the sea temperatures also are affected by the presence of the ship.

Sufficient data were available to make it worth while to determine separately the magnitude of diurnal variations on days when the heating effect of the ship could be expected to be (a) at a minimum and (b) at a maximum. The smallest heating from the ship would clearly occur on days with strong winds and overcast skies, while the greatest heating would similarly be anticipated on calm, sunny days.

A classification of days which are both "windy" and "cloudy" was readily devised for the ocean weather ship stations, but it proved much harder to select a definition for days which were both "quiet" and "fair" which could be used with the data, since periods as long as twenty four hours with winds of less than force 4 at all eight synoptic hours, and also with cloud amounts less than 4 oktas (5 tenths) at all eight synoptic hours are uncommon on the N.E. Atlantic. After some consideration days were classified as follows:-

Day (0-24 G.M.T.)	Description
"Quiet"	Five observations or more with wind force 0-4.
"Windy"	Five observations or more with wind force 6-12.
"Cloudy"	All eight observations in code figures 4-9. (Applied for both former International Code and present International Code).
"Fair"	Four observations or more in code figures 0-5. (Applied for both former International Code and present International Code).

The inclusion of any observation of force 4 on "quiet" days was open to objection, but was found to be unavoidable, as otherwise the number of "quiet" days would have been too small for satisfactory analysis.

A few days which, according to the definitions above, could have been classified as both "cloudy" and "fair", were excluded from the analysis. Afterwards values of the diurnal variation were computed for the classified days. Henceforward the terms "quiet fair" days and "windy cloudy" days will be used with the meaning given above. Values of the ranges of the diurnal variation as defined earlier are given in Table 13.

(f) Reality of the diurnal variation

The results for both stations I and J for the "windy cloudy" days in winter afford strong proof of the existence of a small diurnal variation of air and sea temperature. The low elevation of the sun in winter, together with the rigid classification of the "windy cloudy" days, imply that heating of the ship by insolation would be negligible, and similarly cooling of the ship by nocturnal radiation in these circumstances would be at a minimum.

At both stations the diurnal variation of air temperature is markedly greater on "quiet fair" than on "windy cloudy" days for all seasons, except in winter, when the reverse is true. For sea temperature the diurnal variation similarly is greater on "quiet fair" than on "windy cloudy" days for all seasons, the exceptions being winter and autumn both at station J when the reverse is true.

The code figures for cloud amount had the following significance:-

Code Fig.	Oktas	Tenths
0	0 oktas	0 tenths
1	1 "	trace
2	2 "	1,2 "
3	3 "	2,3 "
4	4 "	4,5,6 "
5	5 "	7,8 "
6	6 "	9 "
7	7 "	9+ "
8	8 "	10 "
9	sky obscured	sky obscured

The results here are in good agreement with those of earlier values as the table below shows:-

Element whose diurnal variation is shown		Magnitude °F.	Location	Authority and date
Air		0.5-0.8		Geiger
Air		(0.95 (0.85	Station I " J	Gordon 1948-49 " "
Air	All days	(0.90 (1.03	Station I " J	Hay 1948-51 " "
Air	"Windy cloudy" days	(0.63 (0.61	Station I " J	" " " "
Air	"Quiet fair" days	(1.57 (1.93	Station I " J	" " " "
Sea		0.5	Tropics	Geiger
Sea		0.0-3.5	Tropics	Schott
Sea		0.4-0.6	Trades	Sverdrup
Sea		0.4	30°-40°N.	Challenger
Sea		(0.22 (0.12	Station I " J	Gordon 1948-49 " "
Sea		(0.20 (0.20	Station I " J	Hay 1948-51 " "
Sea	"Windy cloudy" days	(0.05 (0.10	Station I " J	" " " "
Sea	"Quiet fair" days	(0.33 (0.55	Station I " J	" " " "

Further work which has been undertaken to investigate the magnitude of the diurnal variation of the meteorological elements at the ocean weather stations I and J, together with a discussion of the errors to which these measurements are subject, will, it is hoped, be published later in another paper.

6. Summary and conclusions

Monthly means of the meteorological elements observed aboard the British ocean weather ships manning stations I and J have been obtained for the period 1948 to 1952. Features of interest which stand out are the very high frequency of precipitation at all seasons, the low frequency of thunder at all seasons and of fog in the winter half year. The high mean wind speeds at these ocean weather stations, previously indicated by means of ships' data, are corroborated in the data presented here. Mean annual range of air temperature is small at both stations: at station J temperature did not fall below 35°F. during the period discussed, and fell below 32°F. on 18 days at station I. At both stations the monthly mean values of air and sea temperature show that the air is colder than the sea in every month; the difference is largest in the winter, 5.0°F. at station I in January, and smallest in the early summer, 0.2°F. at station J in June.

The magnitude of the diurnal variation of certain elements was also obtained from the data. For all days at both stations the value is about 1.0°F. for air and 0.2°F. for the sea. The existence of a real diurnal variation over the ocean in these latitudes can be inferred from the fact that, for days selected as being windy and cloudy, even in winter there is a diurnal variation of both air and sea temperature. In the case of the air temperature the diurnal variation in winter is greater on "windy cloudy" days than on "quiet fair" days in the same season at both ocean weather stations.

References

1. Gordon, A.H. and Barlow, E.W. Summary of weather and currents at the original ocean weather stations "Item" and "Jig", Marine Observer, Vol.XXII, p.91-97, April, 1952.

2. Carruthers, N. 1943. Quart J.R. Met. Soc., London, Vol.69, p.289.

3. M.O. 483. Monthly Meteorological Charts of the Atlantic Ocean, 1948.

4. M.O. 488. Climatological Atlas of the British Isles, Table I, 1952.

Table 1

Mean Wind Velocity in Knots (1948-52)

Month	Station I		Station J	
	Mean	No. of obs.	Mean	No. of obs.
January	(22.9)	717	22.6	1,251
February	21.5	1,026	21.2	1,117
March	21.4	1,160	20.2	1,244
April	20.0	1,179	17.7	1,219
May	14.9	1,190	14.7	1,255
June	14.1	1,173	14.2	1,207
July	13.6	1,175	13.7	1,209
August	13.4	1,160	16.1	1,204
September	15.8	1,019	16.5	1,189
October	18.0	1,013	20.4	1,207
November	19.6	1,188	20.3	1,203
December	(20.3)	846	22.4	1,175
Year	17.7	12,846	18.3	14,480

( ) = 4 year means only

Note. The height of the anemometer cups above the sea surface in the British ocean weather ships is approximately 55 ft. The figures above refer to the standard height of 33 ft. above the sea surface and were obtained by multiplying the original mean wind speeds by 0.93.

Table 2

Mean Wind Velocities for some Windy Locations

Knots

Month	Adélie Land 1912-13	Macquarie Island 1912-15	Macquarie Island 1948	Heard Island 1948	Hope Bay (Grahamland) 1952	Deception Island (S. Shetlands) 1944-45, 1947-50	Lerwick (Shetland) 9 years data	Valentia (Eire) 35 years data	Station I 1948-52	Station J 1948-52
January	24.4	13.9	-	-	-	11.8	19.3	12.7	(22.9)	22.6
February	28.1	12.7	-	10.5	-	12.4	18.2	12.2	21.5	21.2
March	41.5	13.0	-	19.0	-	12.8	14.3	11.4	21.4	20.2
April	40.8	12.8	16.6	17.4	-	16.2	14.3	10.5	20.0	17.7
May	45.7	14.1	11.3	17.0	23.5	14.4	12.9	9.5	14.9	14.7
June	42.5	14.3	18.4	19.1	16.7	16.5	12.6	8.9	14.1	14.2
July	45.8	14.9	13.1	20.3	18.5	15.0	9.9	8.8	13.6	13.7
August	42.0	14.4	15.4	18.4	19.0	13.8	10.2	8.9	13.4	16.1
September	36.6	15.6	19.0	18.1	18.4	16.4	13.0	9.1	15.8	16.5
October	41.9	18.8	13.5	17.8	21.1	16.0	14.6	10.4	18.0	20.4
November	32.2	13.0	15.8	17.3	17.0	14.2	16.7	11.5	19.6	20.3
December	25.6	14.6	17.4	15.7	17.3	11.4	18.2	12.6	(20.3)	22.4
Year	37.3	14.3	-	-	-	14.2	14.4	10.5	17.7	18.3

Position (to nearest whole deg.)

Macquarie Island 55°S. 159°E.

Heard Island 53°S. 73°E.

Adélie Land 67°S. 137°E.

Hope Bay 63°S. 57°W.

Deception Island 63°S. 61°W.

G 22815/MG/6/55/50

Table 3

Percentage Frequencies of Wind Force and Direction

Station I

January

Beaufort Force	N	NE	E	SE	S	SW	W	NW	Calms	Total
Calm									5	0.7
1-3	1.1	0.8	0.8	1.1	1.1	1.6	1.8	2.1		10.4
4	0.7	0.5	0.7	3.4	1.9	3.6	2.2	1.8		14.8
5-6	2.1	0.3	2.7	4.5	6.4	11.1	7.9	4.1		39.1
7	0.5	0.4	0.4	1.0	2.3	4.0	2.5	1.1		12.2
8-12	0.1	0.4	1.6	2.9	4.2	7.7	5.5	0.4		22.8
Total	4.5	2.4	6.2	12.9	15.9	28.0	19.9	9.5	0.7	731 obs.

February

Beaufort Force	N	NE	E	SE	S	SW	W	NW	Calms	Total
Calm									21	2.0
1-3	1.3	1.1	1.1	1.1	0.9	1.7	1.3	2.2		10.7
4	1.0	1.3	1.6	2.4	2.4	2.5	1.9	2.3		15.4
5-6	2.9	2.3	1.4	2.9	8.1	7.5	6.5	5.2		36.8
7	0.8	0.2	0.2	1.3	4.4	6.8	3.3	2.4		19.4
8-12	0.4	0	0.2	1.4	2.2	6.0	4.6	0.9		15.7
Total	6.4	4.9	4.5	9.1	18.0	24.5	17.6	13.0	2.0	1034 obs.

March

Beaufort Force	N	NE	E	SE	S	SW	W	NW	Calms	Total
Calm									16	1.4
1-3	0.8	1.4	0.7	1.1	0.8	1.3	1.0	2.1		9.2
4	1.0	2.7	1.5	3.4	3.8	2.4	1.7	2.7		19.2
5-6	2.4	4.6	3.7	5.8	4.7	6.4	5.4	2.6		35.6
7	0.7	2.0	1.5	1.9	3.3	2.2	3.9	1.1		16.6
8-12	0.9	3.9	3.2	0.8	1.3	3.6	3.6	0.7		18.0
Total	5.8	14.6	10.6	13.0	13.9	15.9	15.6	9.2	1.4	1165 obs.

April

Beaufort Force	N	NE	E	SE	S	SW	W	NW	Calms	Total
Calm									22	1.9
1-3	1.2	1.3	0.1	0.8	1.9	1.7	2.9	2.1		12.0
4	1.1	1.2	0.8	1.3	1.9	2.7	3.1	3.5		15.6
5-6	4.5	2.4	2.8	2.4	5.0	6.9	7.9	10.4		42.3
7	1.2	0.3	1.3	1.4	1.2	2.8	4.2	4.5		16.9
8-12	1.2	0.1	0.3	0.7	0.4	1.9	4.1	2.6		11.3
Total	9.2	5.3	5.3	6.6	10.4	16.0	22.2	23.1	1.9	1186 obs.

May

Beaufort Force	N	NE	E	SE	S	SW	W	NW	Calms	Total
Calm									37	3.1
1-3	2.0	3.2	1.9	2.4	2.2	2.6	2.2	4.5		21.0
4	3.0	4.6	4.6	3.3	2.8	2.8	2.7	2.2		26.0
5-6	2.7	8.6	6.7	5.4	7.7	6.3	3.8	2.0		43.3
7	0.3	0.6	0.6	0.8	1.4	0.1	0.6	0.7		5.1
8-12	0.7	0.3	0.1	0.1	0	0	0.3	0		1.5
Total	8.7	17.3	13.9	12.0	14.1	11.8	9.6	9.4	3.1	1198 obs.

June

Beaufort Force	N	NE	E	SE	S	SW	W	NW	Calms	Total
Calm									26	2.2
1-3	2.3	1.9	1.9	5.2	2.7	2.3	2.1	3.2		21.6
4	3.3	3.6	3.4	8.7	4.0	3.8	4.1	4.2		35.1
5-6	3.0	3.7	6.5	5.9	3.0	5.2	5.0	3.6		35.9
7	0.2	0.8	1.1	0.6	0.3	0.6	0.1	0.4		4.1
8-12	0.1	0.3	0.5	0	0	0	0.2	0		1.1
Total	8.9	10.3	13.4	20.7	10.0	11.9	11.5	11.4	2.2	1180 obs.

Table 3 (contd.)

Station I

July

Beaufort Force	N	NE	E	SE	S	SW	W	NW	Calms	Total
Calm									32	2.7
1-3	2.1	2.3	1.4	1.9	4.7	4.7	5.4	5.4		27.9
4	1.7	0.8	2.1	3.9	5.1	5.7	5.6	4.0		28.9
5-6	1.6	3.0	2.7	2.0	5.1	7.1	7.9	7.0		36.4
7	0	0.1	0	0.2	0.5	0.5	1.1	0.9		3.3
8-12	0.1	0.1	0	0	0.2	0.3	0.1	0		0.8
Total	5.5	6.3	6.2	8.0	15.6	18.3	20.1	17.3	2.7	1185 obs.

August

Beaufort Force	N	NE	E	SE	S	SW	W	NW	Calms	Total
Calm									24	2.1
1-3	3.7	4.5	4.0	3.6	3.7	3.3	3.1	4.5		30.4
4	3.3	3.7	2.4	2.9	3.3	5.0	4.7	3.9		29.2
5-6	5.6	6.2	1.8	3.5	3.1	6.2	3.1	4.0		33.5
7	0.3	1.6	0	0.3	0.2	0.3	0.7	0.1		3.5
8-12	0.2	0.8	0	0	0	0	0.3	0		1.3
Total	13.1	16.8	8.2	10.3	10.3	14.8	11.9	12.5	2.1	1168 obs.

September

Beaufort Force	N	NE	E	SE	S	SW	W	NW	Calms	Total
Calm									44	4.3
1-3	2.5	3.2	2.0	2.4	2.1	3.1	3.2	3.2		21.7
4	2.3	1.8	1.4	3.7	3.7	5.4	4.8	3.9		27.0
5-6	3.1	1.6	2.2	4.0	3.2	5.8	7.2	4.7		31.8
7	0.6	1.1	0.5	0.6	0.4	0.8	2.1	1.4		7.5
8-12	0.8	1.3	0.3	0.5	0.6	1.3	1.9	1.0		7.7
Total	9.3	9.0	6.4	11.2	10.0	16.4	19.2	14.2	4.3	1026 obs.

October

Beaufort Force	N	NE	E	SE	S	SW	W	NW	Calms	Total
Calm									20	2.0
1-3	1.3	1.8	2.0	2.1	1.8	1.9	2.3	2.2		15.4
4	1.0	2.0	1.5	3.6	2.1	3.8	4.2	2.2		20.3
5-6	1.3	2.6	3.6	7.3	7.9	8.9	7.6	3.5		42.7
7	0.4	0.5	0.8	1.7	1.9	1.8	1.8	0.9		9.8
8-12	0.6	0.1	1.6	1.9	1.6	1.1	2.1	0.8		9.8
Total	4.5	7.0	9.5	16.6	15.2	17.5	18.0	9.6	2.0	1024 obs.

November

Beaufort Force	N	NE	E	SE	S	SW	W	NW	Calms	Total
Calm									29	2.4
1-3	1.4	1.6	1.7	2.1	1.2	2.0	2.4	1.9		14.3
4	2.0	3.0	2.4	3.1	1.6	2.4	1.8	3.2		19.5
5-6	2.6	6.7	4.5	5.7	3.5	4.9	6.5	3.1		37.5
7	0.8	2.0	1.6	1.8	0.9	1.2	1.9	1.2		11.4
8-12	0.3	2.3	1.5	1.3	0.9	3.4	4.3	0.9		14.9
Total	7.1	15.6	11.7	14.0	8.1	13.9	16.9	10.3	2.4	1192 obs.

December

Beaufort Force	N	NE	E	SE	S	SW	W	NW	Calms	Total
Calm									11	1.3
1-3	0.7	0.8	0.9	1.5	2.2	1.5	1.1	0.8		9.5
4	1.1	1.1	0.5	2.4	2.8	2.8	3.4	3.3		17.4
5-6	1.5	2.5	2.2	5.8	8.4	8.8	12.7	4.4		46.3
7	0.8	0.6	0.9	0.5	2.7	2.1	2.7	2.1		12.4
8-12	1.9	0	0.7	0.6	1.3	3.2	4.0	1.4		13.1
Total	6.0	5.0	5.2	10.8	17.4	18.3	23.8	12.0	1.3	848 obs.

Table 4

Percentage Frequencies of Wind Force and Direction

Station J

January

Beaufort Force	N	NE	E	SE	S	SW	W	NW	Calms	Total
Calm									17	1.4
1-3	0.5	0.4	0.3	0.6	1.1	1.7	1.4	1.8		7.8
4	0.6	0.4	0.2	0.6	2.1	3.1	1.7	1.7		10.4
5-6	2.0	0.6	0.2	1.5	9.3	11.9	10.6	6.9		43.0
7	0.9	0.2	0	0.6	3.3	5.0	6.1	3.7		19.8
8-12	0.2	0	0	0.6	1.8	3.5	6.7	4.8		17.6
Total	4.2	1.6	0.7	3.9	17.6	25.2	26.5	18.9	1.4	1259 obs.

February

Beaufort Force	N	NE	E	SE	S	SW	W	NW	Calms	Total
Calm									11	1.0
1-3	1.3	0.9	1.1	1.4	1.9	1.6	1.7	1.8		11.7
4	1.5	0.9	1.5	1.9	3.1	3.6	2.9	2.0		17.4
5-6	2.0	2.7	1.9	4.5	6.8	9.9	9.3	4.3		41.4
7	1.0	0.4	1.1	2.0	2.2	3.5	5.5	2.4		18.1
8-12	0.2	0.3	0.2	0.2	0.8	3.0	3.2	2.5		10.4
Total	6.0	5.2	5.8	10.0	14.8	21.6	22.6	13.0	1.0	1130 obs.

March

Beaufort Force	N	NE	E	SE	S	SW	W	NW	Calms	Total
Calm									6	0.5
1-3	0.6	0.7	1.7	1.3	2.4	1.5	1.9	0.7		10.8
4	0.7	1.3	2.4	3.0	2.8	3.1	3.1	1.2		17.6
5-6	2.5	4.5	1.6	5.8	7.0	11.8	8.6	5.5		47.3
7	0.9	1.6	0.9	1.3	2.7	3.9	1.3	1.2		13.8
8-12	1.5	0.8	0.9	1.8	1.4	1.7	1.0	0.9		10.0
Total	6.2	8.9	7.5	13.2	16.3	22.0	15.9	9.5	0.5	1260 obs.

April

Beaufort Force	N	NE	E	SE	S	SW	W	NW	Calms	Total
Calm									17	1.4
1-3	2.2	1.7	1.1	1.5	1.9	2.7	1.8	2.5		15.4
4	3.2	1.9	1.1	2.1	2.8	3.6	3.7	4.9		23.3
5-6	2.8	0.2	0.7	2.5	6.1	9.8	10.6	8.6		41.3
7	0.6	0	0	0.6	1.5	2.6	3.2	3.3		11.8
8-12	0	0	0	0.4	0.5	0.8	3.2	1.9		6.8
Total	8.8	3.8	2.9	7.1	12.8	19.5	22.5	21.2	1.4	1236 obs.

May

Beaufort Force	N	NE	E	SE	S	SW	W	NW	Calms	Total
Calm									31	2.5
1-3	2.5	3.2	2.1	4.0	3.3	2.8	1.6	1.7		21.2
4	3.7	5.1	2.3	4.3	5.6	3.6	3.6	4.4		32.6
5-6	3.2	4.5	1.7	2.8	4.9	2.7	5.1	5.4		30.3
7	1.3	0.7	0.6	0.8	1.1	0.7	0.7	0.9		6.8
8-12	1.8	1.1	0.2	2.1	0.8	0.1	0.2	0.3		6.6
Total	12.5	14.6	6.9	14.0	15.7	9.9	11.2	12.7	2.5	1265 obs.

June

Beaufort Force	N	NE	E	SE	S	SW	W	NW	Calms	Total
Calm									28	2.3
1-3	1.9	1.6	1.6	2.7	3.3	3.7	5.1	4.8		24.7
4	1.7	1.1	1.1	4.2	3.9	7.2	5.6	6.1		30.9
5-6	1.8	0.3	0.9	6.0	4.7	10.1	5.4	6.0		35.2
7	0.2	0.1	0.6	0.7	0.2	2.0	1.1	0.3		5.2
8-12	0.1	0	0	0.1	0	0.7	0.7	0.1		1.7
Total	5.7	3.1	4.2	13.7	12.1	23.7	17.9	17.3	2.3	1224 obs.

Table 4 (contd.)

Station J

July

Beaufort Force	N	NE	E	SE	S	SW	W	NW	Calms	Total
Calm									33	2.7
1-3	2.6	1.5	0.5	2.0	3.2	3.0	4.2	5.2		22.2
4	2.5	0.9	0.4	2.4	5.3	7.0	8.9	6.0		33.4
5-6	1.4	0.6	0.4	1.5	4.2	12.3	12.1	5.7		38.2
7	0.2	0	0	0.2	0.6	0.4	0.7	0.6		2.7
8-12	0.1	0	0	0	0	0	0.2	0.5		0.8
Total	6.8	3.0	1.3	6.1	13.3	22.7	26.1	18.0	2.7	1236 obs.

August

Beaufort Force	N	NE	E	SE	S	SW	W	NW	Calms	Total
Calm									50	4.1
1-3	2.3	1.5	0.6	1.7	2.5	2.7	3.8	4.1		19.2
4	4.0	0.7	0.4	2.3	2.1	3.1	5.6	7.1		25.3
5-6	4.4	0.6	0.5	2.0	3.3	7.6	8.4	10.7		37.5
7	0.3	0.2	0.2	0	0.7	0.9	3.2	1.9		7.4
8-12	0.2	0.2	0.1	0	0.2	1.1	2.5	2.2		6.5
Total	11.2	3.2	1.8	6.0	8.8	15.4	23.5	26.0	4.1	1223 obs.

September

Beaufort Force	N	NE	E	SE	S	SW	W	NW	Calms	Total
Calm									33	2.8
1-3	1.6	2.1	3.1	1.8	2.6	3.5	2.2	1.4		18.3
4	2.1	2.4	2.7	1.7	3.2	4.6	3.9	2.5		23.1
5-6	2.2	1.2	1.7	2.0	5.2	9.4	12.6	7.3		41.6
7	0.3	0	0.1	0.3	1.0	1.8	3.2	2.3		9.0
8-12	0.3	0.1	0	0.1	0.5	1.8	1.4	1.0		5.2
Total	6.5	5.8	7.6	5.9	12.5	21.1	23.3	14.5	2.8	1195 obs.

October

Beaufort Force	N	NE	E	SE	S	SW	W	NW	Calms	Total
Calm									21	1.7
1-3	1.6	1.0	0.7	0.6	0.8	1.6	1.9	2.2		10.4
4	1.5	0.4	1.2	3.2	2.5	3.1	3.8	2.2		17.9
5-6	1.6	2.0	2.3	2.4	7.5	10.3	11.3	5.1		42.5
7	0.4	0.1	0.4	1.2	2.0	3.9	4.3	2.0		14.3
8-12	0	0	0.6	1.0	1.8	2.9	5.3	1.6		12.2
Total	5.1	3.5	5.2	8.4	14.6	21.8	26.6	13.1	1.7	1220 obs.

November

Beaufort Force	N	NE	E	SE	S	SW	W	NW	Calms	Total
Calm									10	0.8
1-3	1.3	1.2	0.6	1.0	1.1	3.1	2.3	1.7		12.3
4	2.5	1.5	1.0	1.5	3.9	2.5	2.6	1.5		17.0
5-6	3.0	3.3	3.1	3.0	4.3	7.8	10.2	7.6		42.3
7	1.5	0.9	0.6	1.8	0.8	2.9	3.4	2.8		14.7
8-12	1.4	0.3	0.7	1.7	1.6	1.7	4.0	1.5		12.9
Total	9.7	7.2	6.0	9.0	11.7	18.0	22.5	15.1	0.8	1242 obs.

December

Beaufort Force	N	NE	E	SE	S	SW	W	NW	Calms	Total
Calm									10	0.8
1-3	0.7	0.5	0.4	0.7	0.8	1.0	0.3	1.2		5.6
4	1.6	0.4	0.3	1.7	2.0	2.2	2.1	3.2		13.5
5-6	2.6	0.5	1.3	3.1	5.5	8.1	13.3	10.1		44.5
7	1.6	0.3	1.0	1.5	1.9	3.5	5.7	5.6		21.1
8-12	0.5	0.1	0.2	1.1	1.4	3.1	5.1	3.0		14.5
Total	7.0	1.8	3.2	8.1	11.6	17.9	26.5	23.1	0.8	1187 obs.

Table 5

Number of Occasions* on which Winds of Beaufort Forces 8 to 12 Occurred Reported for Different Directions During Five Years 1948-1952.

Force	Station I						Station J					
	8	9	10	11	12	8-12	8	9	10	11	12	8-12
Direction (Points)												
1-4	82	20	4	10	0	116	24	5	1	0	0	30
5-8	68	15	5	0	0	88	23	3	1	0	0	27
9-12	75	22	10	1	1	109	51	16	1	0	0	68
13-16	69	27	8	5	0	109	62	18	7	1	2	90
17-20	131	34	19	3	1	188	149	33	10	2	0	194
21-24	241	90	42	13	3	389	202	58	16	3	0	279
25-28	118	18	10	1	0	147	213	67	22	3	2	307
29-32	66	8	5	0	0	79	45	10	4	0	0	59
All (1-32)	850	234	103	33	5	1225	769	210	62	9	4	1054

During 5 years 1948-52 there were two months when there were no reports for station India.

* Based on 8 observations per day.

G 22815/MG/6/55/50

Table 5 (contd.)

Mean No. of Occasions* on which Winds of Forces 8 to 12 Occur each Month
Based on Five Years 1948-52

Month \ Force	Station I						Station J					
	8	9	10	11	12	8-12	8	9	10	11	12	8-12
January	(21)	(12)	(7)	(3)	(1)	(44)	30	12	3	0	0	45
February	22	7	3	0+	0	32	15	6	1	1	0	23
March	29	8	2	2	0	41	19	5	1	0	0+	25
April	21	4	1	0	0	26	12	3	0+	0	0	15
May	2	1	0+	0	0	3	4	0+	0	0	0	4
June	2	0	0	0	0	2	2	2	0	0	0	4
July	2	0	0	0	0	2	0+	0	0	0	0	0+
August	2	1	0	0	0	3	5	1	1	0	0	7
September	11	4	0+	0+	0	15	7	1	1	0+	0	9
October	17	2	1	0+	0+	20	8	2	1	0+	0	11
November	24	7	5	0+	0	36	26	5	1	0	0	32
December	(24)	(5)	(3)	(1)	(1)	34	24	6	3	1	1	35
Year	177	51	22	6	2	258	152	43	12	2	1	210

( ) = 4 years observations only.
* Based on 8 observations per day.

Table 6

Pressure at M.S.L., Means and Extremes (1948-52)

Station I

Month	Mean	No. of obs.	Max.	Hour	Date	Year	Min.	Hour	Date	Year	Difference of Values (Table 6 - M.O.483)	Extremes of Pressure over British Isles Highest mb.	Lowest mb.
Jan.	*(1008.0)	878	1036.5	2100	29	1949	954.7	0900	10	1949	+5.5	1055	925
Feb.	1000.6	1054	1041.9	0001	21	1948	945.3	0600	2	1948	-1.4	1050	951
Mar.	1006.1	1210	1033.0	2100	1	1949	971.2	1500/0900	31	1948	-0.9	1045	948
Apr.	1004.8	1204	1035.0	2100	30	1951	970.3	1800	9	1952	-5.4	1045	953
May	1016.6	1171	1036.4	0900	1	1951	981.6	0600	13	1948	+5.3	1042	968
June	1012.1	1164	1032.5	1200	14	1949	981.3	0300	28	1952	+0.5	1034	977
July	1011.7	1159	1032.7	0001	8	1948	980.1	0900	25	1948	+2.7	1038	976
Aug.	1007.1	1152	1027.3	0001	1	1948	980.6	1500	9	1950	-1.9	1032	968
Sept.	* 1007.4	1004	1035.1	1200	14	1952	963.6	0600	4	1951	-0.7	1039	971
Oct.	998.4	1057	1027.8	2100	21	1951	952.3	0001	9	1951	-8.2	1039	947
Nov.	1004.6	1175	1029.5	0001/2100	16/17	1952	963.6	1200	19	1948	+5.6	1044	940
Dec.	(998.7)	1086	1035.6	0001/1200/2100	2/3	1952	948.9	0600	28	1948	-2.3	1050	927
Year	1005.0	13276									-0.1		

* Less than half possible observations in any one month

( ) = One monthly mean obtained by interpolation from a "NACLI" Chart.

Station J

Month	Mean	No. of obs.	Max.	Hour	Date	Year	Min.	Hour	Date	Year	Difference of Values
January	1007.1	1242	1046.4	2100	8	1949	968.4	0001	12	1951	-0.2
February	1008.7	1091	1037.8	1200	18	1952	951.8	0300	4	1951	+3.2
March	1009.2	1236	1037.4	0001	2	1949	957.6	0900	31	1948	-0.4
April	1012.5	1209	1039.5	1200	26	1948	971.7	2100	30	1952	+0.8
May	1014.8	1236	1036.6	1200	25	1952	974.7	0001	1	1952	+1.4
June	1013.7	1200	1035.4	1800	13	1949	981.5	1800	5	1949	-2.4
July	1017.1	1128	1035.5	1200	8	1948	981.3	0300	15	1950	+2.7
August	1010.8	1191	1029.1	1200/1500	16	1949	977.3	0900	8	1950	-2.6
September	1011.0	1171	1032.9	1500	14	1952	972.0	1800	26	1948	-1.4
October	1009.7	1200	1033.9	1200	22	1951	941.0	2100	27	1952	0.0
November	1006.9	1184	1038.4	1200/2100	6	1952	965.6	0001	26	1952	-0.8
December	1008.3	1155	1036.5	0001	20	1948	945.1	1800	26	1951	+1.5
Year	1010.9	14243									+0.1

Table 7

Air and Sea Temperatures (1948-52)

(Mean Position = 59°29'N. 19°29'W.)

Station I

Month	Temperatures (°F.)																
	Mean Values									Extremes							
	Air Temp.	Dew Point	No. of obs.	Sea Temp.	No. of obs.	Air–Sea Temp. Difference	Mean Daily Max.	Mean Daily Min.	No. of obs.	Extreme Max.	Year & Date	Extreme Min.	Year & Date	Extreme Daily Range	Year	Difference of Values (Table 6 – M.O.483) Air	Sea
January	42.2	36.3	963	47.2	889	-5.0	45.2	40.1	120	51.0	1950 12	28.5	1949 19	13.3	1951	+1.2	-0.3
February	42.5	37.5	1070	47.2	810	-4.7	44.6	40.4	126	52.3	1952 25	31.9	1949 8	14.1	1949	+1.9	+0.5
March	43.3	38.6	1211	47.1	909	-3.8	45.6	41.6	144	51.5	1948 3	29.0	1949 12	11.1	1948	+0.9	+0.5
April	43.3	36.9	1204	47.6	798	-4.3	45.5	41.2	144	52.0	1951 28	31.8	1951 16	12.0	1949	-2.3	0.0
May	47.2	42.2	1170	48.9	794	-1.7	49.1	45.6	144	61.0	1948 18	36.1	1948 2	14.0	1948	-0.3	+0.1
June	50.4	45.9	1163	51.5	779	-1.1	51.6	49.0	141	56.9	1950 28	40.0	1952 2	8.3	1952	+0.1	+0.4
July	52.9	48.8	1159	53.7	827	-0.8	54.4	51.6	142	59.9	1950 31	47.7	1949 15	8.5	1948	-0.8	-0.3
August	53.7	49.1	1152	54.8	810	-1.1	55.2	52.3	140	61.3	1950 2	45.2	1949 15	8.9	1948	+0.4	+0.4
September	52.0	46.8	1004	54.3	740	-2.3	53.8	50.6	128	59.7	1952 9	42.8	1952 30	8.0	1949	0.0	+1.1
October	48.9	44.0	1057	52.0	733	-3.1	50.7	47.1	135	55.1	1951 8	36.2	1951 20	8.2	1952	+0.5	+1.3
November	46.6	41.7	1175	49.7	825	-3.1	48.4	44.9	145	54.7	1952 13	30.2	1950 30	13.4	1949	+0.2	+0.6
December	43.6	38.4	1086	48.5	906	-4.9	45.4	41.0	133	51.9	1948 1,17	28.0	1949 8	11.1	1951	+1.9	+0.3
Year	47.3	42.3	13414	50.3	9820	-3.0	49.0	45.5	1642								

No. of days on station at 60°N. 20°W. = 777
at 59°N. 19°W. = 824

Total = 1601

Table 8

Air and Sea Temperatures (1948–52)

(Mean Position = 53°06'N. 19°25'W.)

Station J

Month	Temperatures (°F.)																
	Mean Values									Extremes							
	Air Temp.	Dew Point	No. of obs.	Sea Temp.	No. of obs.	Air–Sea Temp. Difference	Mean Daily Max.	Mean Daily Min.	No. of obs.	Extreme Max.	Year & Date	Extreme Min.	Year & Date	Extreme Daily Range	Year	Difference of Values (Table 6 – M.O.483) Air	Sea
January	46.7	41.1	1242	50.3	621	-3.6	49.1	43.8	155	54.5	1952 5	34.9	1950 30	11.5	(1948 (1949	-1.7	-0.7
February	46.3	40.3	1091	50.2	544	-3.9	48.4	43.7	137	54.1	1951 1	35.0	1951 17	16.3	1951	-1.4	-0.5
March	48.5	43.5	1236	50.2	617	-1.7	50.1	46.8	154	54.8	1949 28	38.9	1951 12	10.7	1948	+0.3	-0.2
April	48.1	42.0	1209	49.9	604	-1.8	49.9	46.1	150	54.4	1948 12	38.3	1952 9	10.5	1948	-2.1	-1.1
May	51.2	45.8	1240	52.1	620	-0.9	52.8	49.6	155	58.5	1948 16	39.0	1952 6	8.7	1949	-1.1	-0.6
June	54.4	50.0	1200	54.6	600	-0.2	55.7	53.0	150	60.4	1952 29	45.6	1948 4	7.4	1949	-1.1	-0.9
July	57.5	53.2	1127	57.9	564	-0.4	58.7	55.8	152	64.5	1952 21	51.6	1948 14	8.7	1949	-0.5	-0.3
August	57.5	52.6	1191	59.1	595	-1.6	59.0	56.1	148	65.5	1949 26	50.3	1948 21	7.9	1949	-1.4	+0.6
September	56.4	51.5	1171	57.9	585	-1.5	58.0	54.9	146	65.2	1952 21	48.4	1950 16	7.6	1950	-1.0	+0.2
October	53.7	48.0	1200	55.8	600	-2.1	55.5	52.1	152	61.4	1949 7	43.7	1949 23	9.8	1952	-0.8	+0.2
November	50.5	45.1	1184	53.3	592	-2.8	52.3	48.8	146	57.0 57.0	1948 29 1952 1	40.4	1950 18	8.0	1951	-1.7	-0.3
December	47.8	42.9	1155	51.5	575	-3.7	49.9	45.6	144	56.1	1952 6	35.0	1951 31	12.9	1949	-1.2	-0.5
Year	51.5	46.3	14246	53.4	7117	-1.9	53.3	49.7	1789								

No. of days on station at 53°50'N. 18°40'W. = 789
at 52°30'N. 20°W. = 985

Total = 1774

Table 9

Weather

Station I

Month	Mean No. of Days Per Month							No. of days
	Precipitation	Rain	Snow Sleet	Hail	T L R/	Fog	Gale*	
January	28	24	14	13	1	0	15	31
February	27	21	11	11	>0	1	11	28
March	26	24	8	8	>0	0	14	31
April	28	26	7	9	0	1	10	30
May	24	23	2	3	>0	3	1	31
June	24	24	>0	0	0	4	1	30
July	27	27	0	0	0	4	1	31
August	27	27	0	0	0	3	1	31
September	25	25	0	1	0	3	6	30
October	29	29	1	3	>0	1	9	31
November	28	28	2	3	0	>0	10	30
December	30	27	9	13	>0	1	13	31
Year	323	305	54	64	2	22	92	365

"Precipitation" includes rain, hail or snow.
Drizzle is included under "rain".

/ Includes T or L in addition to TLR.

* i.e. Force 8 and above.

The symbol >0 denotes a value of 0.1 to 0.4.

Station J

Month	Mean No. of Days Per Month							No. of days
	Precipitation	Rain	Snow Sleet	Hail	T L R/	Fog	Gale*	
January	30	29	2	9	1	>0	18	31
February	25	24	4	8	1	1	13	28
March	27	27	1	3	>0	2	12	31
April	27	26	1	4	0	1	8	30
May	22	22	>0	2	0	3	5	31
June	25	25	0	0	0	7	3	30
July	27	27	0	0	>0	8	2	31
August	28	28	0	>0	>0	3	7	31
September	26	26	0	1	>0	4	7	30
October	29	29	>0	2	1	2	13	31
November	26	26	>0	2	0	2	13	30
December	29	28	1	7	1	>0	16	31
Year	321	317	10	38	5	33	117	365

Number of days per month denotes the number of days (0-24 GMT) on which the particular type of weather was entered in the "present weather" and/or "past weather" on at least one synoptic hour or occasion.

The figures obtained for the original number of days available for the different months have been converted to the equivalent number of days per month which would have been observed if the observations had been made on every day of the month.

Table 10

Percentage Frequency of Occurrence of Visibility (1948-52)

Station I

Vis. / Month	0-50 yd.	50-200 yd.	200-500 yd.	500-1000 yd.	1000 yd.-1 n.mile	1-2 n. miles	2-5 n. miles	5-10 n. miles	10-25 n. miles	>25 n. miles	No. of obs.
January				0.3	0.5	2.3	10.5	24.2	56.7	5.5	705
February				0.2	2.0	4.0	10.2	27.8	43.4	12.4	1063
March					0.4	3.8	17.2	22.2	49.2	7.2	1181
April				0.2	0.8	3.2	10.0	25.8	56.6	3.4	1202
May			0.2	0.6	0.8	3.6	11.8	23.4	48.0	11.6	1170
June		1.0	0.8	1.0	2.8	6.2	12.4	23.0	40.6	12.2	1166
July		0.2	1.4	1.6	2.8	2.8	9.0	22.8	49.2	10.2	1158
August			0.6	1.0	0.4	2.0	7.4	18.0	55.2	15.4	1150
September		0.2	0.2	0.8	1.8	2.0	9.6	20.2	59.2	6.0	1004
October				0.8	1.2	2.6	9.2	21.8	59.0	5.4	1052
November					0.8	2.8	10.8	24.8	46.0	14.8	1174
December				1.3	1.7	2.7	8.5	28.3	55.0	2.5	838
Year	<0.1	0.1	0.3	0.6	1.3	3.3	10.8	23.8	50.1	9.1	12863
No.of obs.	1	16	38	80	166	423	1385	3062	6524	1168	12863

Station J

Vis. / Month	0-50 yd.	50-200 yd.	200-500 yd.	500-1000 yd.	1000 yd.-1 n.mile	1-2 n. miles	2-5 n. miles	5-10 n. miles	10-25 n. miles	>25 n. miles	No. of obs.
January					0.4	2.6	13.0	28.0	44.6	11.4	1233
February			0.2	0.6	0.8	1.6	9.8	32.4	50.2	4.4	1091
March		0.2	0.2	1.2	1.0	3.2	13.0	29.8	49.2	2.2	1238
April		0.2	0.2	0.4	1.0	2.6	11.8	32.4	47.6	3.8	1210
May		0.6	0.6	1.0	0.6	3.2	11.0	26.8	50.0	6.2	1238
June		0.6	2.4	2.4	1.8	3.8	12.0	29.2	40.2	7.6	1190
July		0.2	2.0	1.4	1.8	4.4	9.4	30.0	45.4	5.4	1119
August		1.2	0.8	0.4	2.0	5.8	12.8	26.0	45.4	5.6	1074
September			1.4	1.0	2.4	4.2	9.4	27.0	46.2	8.4	1159
October	0.2	0.2		1.2	1.8	5.2	14.0	32.0	41.4	4.0	1124
November			0.6	0.4	1.0	3.4	9.2	23.0	55.8	6.6	1154
December		0.2		0.6	0.8	4.6	9.4	23.8	48.6	12.0	1098
Year	<0.1	0.3	0.7	0.9	1.2	3.5	11.0	28.2	47.7	6.5	13928
No.of obs.	1	41	103	126	173	487	1534	3930	6642	889	13928

Table 11

Percentage Frequency of Height of Base Low Cloud (1948-52)

Station I

Month / Height in ft.	0 to 150	150 to 300	300 to 600	600 to 1000	1000 to 2000	2000 to 3000	3000 to 5000	5000 to 6500	6500 to 8000	Above 8000	No. of obs.
January	0	0	0	4	42	39	12	1	>0	2	(686)
February	0	0	2	8	43	33	10	1	>0	3	1042
March	0	0	2	5	37	32	19	2	1	2	1177
April	0	>0	2	8	37	40	11	1	0	1	1194
May	1	1	4	8	26	38	17	2	>0	3	1170
June	1	2	7	6	29	32	15	3	1	4	1160
July	1	1	7	8	30	35	13	2	>0	3	1154
August	1	1	3	7	28	43	12	2	1	2	1145
September	1	>0	4	7	30	40	15	2	0	1	995
October	1	0	5	9	32	40	11	>0	0	2	1046
November	>0	0	2	9	37	39	10	1	0	2	1148
December	1	1	3	5	45	34	9	1	0	1	(829)

( ) = 4 years only

The symbol >0 denotes a value of 0.1 to 0.4.

Station J

Month / Height in ft.	0 to 150	150 to 300	300 to 600	600 to 1000	1000 to 2000	2000 to 3000	3000 to 5000	5000 to 6500	6500 to 8000	Above 8000	No. of obs.
January	0	0	3	8	33	39	12	1	0	4	1193
February	>0	0	2	3	30	41	17	3	>0	3	1091
March	>0	>0	3	7	29	41	15	1	0	3	1241
April	0	1	3	6	25	43	17	1	1	3	1215
May	1	2	4	7	28	34	13	1	1	9	1241
June	3	3	7	11	28	30	15	1	>0	2	1196
July	3	2	9	11	28	27	14	3	0	3	1136
August	1	1	4	9	37	33	11	2	>0	2	1225
September	2	1	6	6	26	40	14	3	>0	2	1165
October	>0	>0	4	8	33	39	12	2	>0	1	1187
November	1	>0	3	7	34	39	12	1	0	4	1186
December	>0	0	2	6	30	50	10	1	0	1	1160

G 22815/MG/6/55/50

Table 12

Diurnal variation of pressure, wind and total cloud (all days)

Element	Station	Winter (Dec.-Feb.)	Spring (Mar.-May)	Summer (June-Aug.)	Autumn (Sept.-Nov.)	Year
Pressure (mb.)	I	1.03	.68	.79	.94	.70
	J	.76	.98	.72	.74	.70
Wind (kt.)	I	.92	1.45	.65	.27	.83
	J	.74	.92	.71	1.28	.69
Total cloud (tenths)	I	1.30	.90	.42	1.02	.76
	J	1.35	.95	.72	.96	.88

The ranges given here were obtained by taking the difference between the highest and lowest among the mean values found for all eight synoptic hours for each of the elements.

Table 13

Diurnal variation of air and sea temperature

All days

Air temp. °F.	I	.43	1.36	1.31	.68	.90
	J	.56	1.30	1.41	.88	1.03
Sea temp. °F.	I	.12	.24	.32	.10	.20
	J	.05	.36	.35	.08	.20

"Windy cloudy" days

Season		Winter (Dec.-Feb.)	Spring (Mar.-May)	Summer (June-Aug.)	Autumn (Sept.-Nov.)	Year
Air °F.	I	.91 (57)	1.05 (72)	.71 (29)	.70 (60)	.63 (218)
	J	1.18 (69)	.88 (48)	.91 (37)	.60 (55)	.61 (209)
Sea °F.	I	.09 (54)	.17 (71)	.26 (27)	.13 (60)	.05 (212)
	J	.20 (66)	.19 (48)	.17 (36)	.22 (55)	.10 (205)

		Spring and Summer (Mar.-Aug.)	Autumn and Winter (Sept.-Feb.)
Wind (kt.)	I	3.17 (101)	4.13 (117)
	J	2.64 (85)	3.43 (123)

"Quiet fair" days

Season		Winter (Dec.-Feb.)	Spring (Mar.-May)	Summer (June-Aug.)	Autumn (Sept.-Nov.)	Year
Air °F.	I	.62 (19)	1.99 (17)	2.09 (38)	1.55 (30)	1.57 (104)
	J	.97 (15)	2.12 (42)	2.43 (35)	1.77 (25)	1.93 (117)
Sea °F.	I	.19 (19)	.26 (17)	.70 (38)	.13 (30)	.33 (104)
	J	.11 (15)	.76 (42)	1.02 (35)	.17 (25)	.55 (117)

		Spring and Summer (Mar.-Aug.)	Autumn and Winter (Sept.-Feb.)
Wind (kt.)	I	2.37 (55)	3.08 (49)
	J	1.63 (77)	4.25 (40)

Figures in brackets denote the number of days used.

M.R.P. 924
S.C. 11/193
28th June, 1955

Canada
Marine
(11)S

AD 143191

The Sub-tropical Jet-stream of the eastern North Pacific in January and April, 1952

by

H. D. Hoyle
(Meteorological Office)

AIR MINISTRY
METEOROLOGICAL RESEARCH COMMITTEE

At the time of issue this report has not been published. Any author desiring to quote this paper should refer to it as "A paper of the Meteorological Research Committee (London).
M.R.P. No. 924 by Mr. H. D. Hoyle
A copy is available in the Library of the Meteorological Office."

M.R.P.924
S.C.II/193
28th June, 1955

AIR MINISTRY

METEOROLOGICAL RESEARCH COMMITTEE

The Sub-tropical Jet-stream of the eastern North Pacific in January and April, 1952

by
H.D. Hoyle (Meteorological Office)

1. Introduction

It has been demonstrated by several writers, e.g. Gilchrist(1), Bannon(2) and Cressman(3), that the belt of strong westerly winds in the upper troposphere, known as the sub-tropical jet-stream, sometimes displays a two core structure. Bannon(2) shows that the eastern North Pacific in January and April is an area especially notable for this. One core is clearly associated with the polar front, but the other, nearer the Equator and at a higher level, is not so clearly associated with features of the surface synoptic weather map. Owing largely to the distribution of upper air reporting stations, most areas in which the high level winds of the sub-tropics have been investigated are ones in which, in winter, the land-sea distribution gives rise to semi-permanent troughs and considerable equatorward penetrations of polar air, making distinction between the two streams more difficult than in the area studied in this note.

The area considered and the observing stations used are shown in Fig.1. During April, 1952 an almost complete set of observations was available from all the stations shown. In January, 1952 observations were less complete and there were none from Ocean Weather Station "Q". Consequently, the analysis of the upper level charts is less trustworthy in January than in April, particularly in the north west portion of the area. To help in the construction of the mean and anomaly charts for January, values of contour height and temperature at a few latitude and longitude "grid" points were interpolated from the isopleths on the daily charts and their means calculated. April is therefore treated in rather greater detail in this note, January being used largely as confirmation.

As Fig.1 shows, the network of observations is very open. Fine methods of analysis are thus inappropriate and this study is therefore restricted to the major features.

2. Classification into types

Daily maps for 0300 G.M.T. were drawn of the contours at 500, 300, 200 and 150 mb. In addition, cross-sections were drawn, one or more per day. The plane of the cross-sections was not meridional but chosen to cut across the main flow, reported speeds being used and not components in any one direction. From these charts and cross-sections it was possible to find with reasonable accuracy the position of jet-stream cores on each day. The simplest method of distinction between the polar front jet and the sub-tropical jet was the pressure at the core. This was about 200 mb. for the sub-tropical jet and 300-350 mb. or even 400 mb. for the polar jet.

Fig. 2 and 3 show the daily positions of both cores. Positions of the polar front are also shown, these positions being taken directly from the analyses

given in published charts in the "Daily Series Synoptic Weather Maps" of the U.S. Weather Bureau.

Study of Fig. 3 suggests classification of the April charts into three types as follows:-

Type 1 - A strong jet-stream roughly W.-E. near Hawaii and a separate polar front jet-stream clearly present to the north (3rd-5th, 11th-15th, 20th-23rd, 26th-30th).

Type 2 - A weaker sub-tropical jet-stream with a northerly wind component near Hawaii (1st, 2nd, 6th, 7th, 16th, 24th, 25th).

Type 3 - A sub-tropical jet-stream well north of its usual position (8th-10th, 17-19th).

The classification is, to some extent, subjective but the main features of Types 1 and 3 are readily recognisable and days not falling naturally into either of these types showed features in keeping with the definition of Type 2. The six days of Type 3 occurred in two spells of three days each and the seventeen days of Type 1 were in four spells of from 3-5 days each. The types occurred in some suggestion of a sequence, in that Type 2 followed Type 1 and preceded Type 3 on both occasions of a change from Type 1 to Type 3.

In order to represent diagrammatically the conditions prevalent in the three types mean cross-sections were drawn for each. The usual practice of plotting zonal wind components at appropriate latitudes on a meridional cross-section was thought to give an unsatisfactory representation of the conditions especially since, as noted previously by Bannon(4), strong northerly winds often exist near the Hawaiian Islands. Consequently, the mean cross-sections for each type were taken perpendicular to the axis of the jet-stream, the observations being grouped according to perpendicular distance from the jet-stream core. Reported wind speed was thus used directly. Where a second (polar front) jet-stream was also present, a separate mean cross-section for the type was drawn in a similar manner relative to this core. The two were then combined into one diagram for each type by using the mean latitude of the surface position of the polar front as a basis of reference and placing the jets at their mean distances from this position.

The resulting cross-sections are shown as Fig. 4(a), (b), (c). It is clear from the method of construction that although the scale of distance is quite precise the latitudes are only approximate, since the cross-sections are not strictly meridional. This does not interfere, however, with the assessment of wind shear.

The January charts (Fig.2) are more complex. There is little doubt that two separate jet-streams exist on the first fifteen days. During these days there is no certain evidence of the conditions classified as Type 3, but the days 2nd-5th show reported winds of 100 kt. or more and clearly can be classified as Type 1. The remainder of the 15 days can be classified as Type 2. Mean cross-sections (Fig. 5(a) and (b)), prepared as before, are very similar to those of equivalent type in April.

From 16th-22nd January, 1952 the synoptic situation is disturbed in the Hawaii area by the formation of a "kona" storm (see, for example, Palmer(5)). As this is a somewhat special situation these days are not analysed in detail. From 23rd-31st January, 1952 the daily maps show only one jet-stream core, the type of flow pattern common in other longitudes. This has been called Type 4 and the appropriate mean cross-section for this type is shown at Fig.5(c).

3. Discussion of the cross-sections

In the types which show two clearly separate jet-stream cores (Types 1 and 2) the following major points are apparent, from Fig. 4 (April):-

/(i)

(i) There seem to be three tropopause levels defined by the temperature field; a tropical tropopause at about 90 mb., a polar tropopause (poleward of the polar front) at about 300 mb. and an intermediate or sub-tropical tropopause at about 200 mb.

(ii) Just as the polar front jet-stream has its core at about the same level as the tropopause poleward of the polar front, so the sub-tropical jet-stream has its core at about the same level as the sub-tropical tropopause on its poleward side.

The following features suggested by the mean cross-sections were more apparent on the cross-sections for individual days:-

(iii) The sub-tropical jet-stream is associated with a baroclinic zone. Unlike the baroclinic zone associated with the polar front this sub-tropical baroclinic zone is most marked between 400 and 200 mb. with virtually barotropic conditions at lower levels.

(iv) It appears that this sub-tropical baroclinic zone is connected with the temperature minimum associated with the sub-tropical tropopause. As pointed out by the writers of "The Jet Stream"(6) the fact that at 200 mb. the temperature is lower at about 30-40°N. than at any other latitude is a feature which calls for some explanation and cannot be dismissed purely in terms of advection from other latitudes. The cross-sections suggest that this temperature minimum may be more clearly defined when the sub-tropical jet-stream is strong (Type 1).

When there is only one jet-stream (Type 4) the intermediate sub-tropical tropopause is absent and there is no sign of any temperature minimum at or near the 200 mb. level (see Fig.5(c)). It seems, therefore, that the existence of this temperature minimum at 200 mb. (and the associated three-tropopause scheme) may be an essential requirement for a sub-tropical jet-stream separate from the polar front jet-stream.

4. The horizontal temperature distribution

It is evident from the foregoing discussion that strong winds are associated with baroclinic zones and this suggests that the geostrophic approximation through the thermal wind relation may be roughly valid even at latitudes as low as 20°N. There is thus some prospect that the variations in position and intensity of the sub-tropical jet-stream may be understood if the variations in horizontal temperature gradient can be demonstrated and explained. The cross-sections show that the 400-200 mb. layer is the significant one as regards the thermal wind contribution. Consequently, attention is directed to the 300 mb. and 250 mb. temperatures. Fig. 6 shows the 300 mb. temperature distribution for April, 1952, Fig. 6(a) being the mean for the month and Fig.6(b), (c) and (d) showing the mean isotherms for Types 1, 2 and 3 respectively. The dotted isopleths on Fig. 6(b), (c) and (d) show the anomaly from the mean for the month. Fig. 7 shows similar charts for the 250 mb. level.

It is at once apparent that whereas Fig.6(a) displays a fairly steady N.-S. temperature gradient at 300 mb., Fig.7(a) shows that the temperature minimum associated with the sub-tropical tropopause is apparent at 250 mb. The sequence of Types (1-2-3-1 etc.) is noticeable, particularly at 250 mb., by the manner in which the coldest air is displaced eastwards (i.e. down-stream) from Fig.7(d) to 7(b) to 7(c). The steep temperature gradient near Hawaii for Type 1 is clearly shown in Fig.6(b). The northerly component characteristic of Type 2 is shown in Fig.6(c) and the belt of thermal contrast at about 40°N. for Type 3 is indicated in Fig.6(d). Fig.6(d) also gives a strong thermal gradient near Hawaii where, as inspection of Fig.3 for 17th, 18th, 19th shows, a residual sub-tropical jet-stream can still exist despite the re-creation of the main sub-tropical jet-stream further north. (Note that to avoid undue complication this

/residual

residual low latitude stream is not shown in Fig.4(c) which does not extend south of about 30°N.)

That the thermal wind relation holds approximately, down to 20°N., is borne out by the daily values in Fig.8(b) and (c). Fig.8(b) shows the maximum reported wind speed in the sub-tropical jet-stream near Hawaii, whilst Fig.8(c) shows the reported temperature difference between Hilo and Lihue. Now a temperature difference of 2.5°C. between these stations at all levels from 500-200 mb. would be equivalent to a geostrophic thermal west wind of about 100 kt. through this layer. There is clearly a rough similarity between the two curves (correlation co-efficient .49) and the mean values of temperature difference and wind speed are approximately equal to those which the geostrophic relation requires.

The temperature anomalies (Fig.6 and 7) show that, in the central portion of the area considered, temperatures are below normal during Type 1 and above normal during Type 3. The broad features of the observed temperature distribution and anomalies would be obtained if a portion of the monthly mean charts were displaced southward in Type 1 and northward in Type 3. Type 2 could be an intermediate stage in which the southward displacement is in the east of the area and the northward displacement in the west of the area. This suggests that horizontal advection may be an important factor in the type transitions.

Fig.9 shows isotherms for January, 1952 at 250 mb. Fig.9(a) shows the mean isotherms for the first 15 days. This is the mean for the days on which there were two separate jet-streams and is thus comparable with the mean for April, 1952. Fig.9(b) shows the mean for Type 1 during January, 1952, the dotted isopleths being the anomaly from the 15-day mean of Fig.9(a). Although based on only 4 days, features similar to all those pointed out for Type 1 during April are readily apparent. As the mean chart Fig.9(a) is almost entirely Type 2 no separate diagram for Type 2 is given.

It is interesting to note the different temperature field during the period January 23rd-31st which was characterised by a single jet-stream, (Type 4). Fig.9(c) gives the mean for the month of January excluding the days affected by the "kona" storm, i.e. a 24-day mean chart. Fig.9(d) gives the mean for Type 4, the dotted isopleths being the anomaly from the 24-day mean. The absence of the area of minimum temperature shown on all other 250 mb. temperature charts is very striking and agrees with the deduction from the cross-section Fig.5(c).

5. Geostrophic advection

Mean contour maps for the 200 mb. level are shown at Fig.10. Fig.10(a) shows the mean chart for the month of April, 1952, whilst Fig.10(b), (c) and (d) show, respectively, the mean contours for Types 1, 2 and 3. The dotted isopleths on these latter charts show the height anomalies from the mean for the month. Fig.11 shows similar charts for the 500 mb. level.

In view of the strong zonal component over most of the area the essential features of meridional geostrophic advection show more clearly in the anomaly patterns. It is clear that in the region of 40°N. 160°W. Type 1 is characterised by a N.-S. flow component and Type 3 by a S.-N. flow component at the levels which contain the sub-tropical baroclinic zone. These appear not only in the mean charts but also in the daily charts.

A simple index of the N.-S. geostrophic flow in this area is given by the contour height difference between 40°N. 150°W. and 40°N. 170°W. The daily values of this index (positive for flow from N.-S.) are shown at Fig.8(d) and (e) for the 500 and 300 mb. levels respectively. This index was measured in hundreds of metres per 20° of longitude (at 40°N.) so that an index value of 1 corresponds to a mean geostrophic flow of about 13 kt. Comparison with

/Fig.8(a)

Fig.8(a) and (b) confirms the suggested association between the N.-S. flow component and the type. It is further suggested that a strong N.-S. flow component is associated with a strong jet-stream and in this connection it may be noted that the correlation co-efficient between N.-S. flow index at 500 mb. and maximum reported speed in the jet-stream near Hawaii was .52.

Following the discussion in the previous section and comparing Fig.7 and 10, the geostrophic advection anomalies for the three types are such as to deform the mean temperature field in roughly the manner which is, in fact, observed.

An attempt was made to assess the advective temperature change directly using a geostrophic scale on the 300 mb. height and temperature isopleths. The process was found to be inaccurate and too easily affected by the subjective judgment of the analyst, and was therefore abandoned. As the usual method of assessing vertical motion is dependent upon an estimate of the temperature change due to horizontal advection no reliable analysis of the vertical motion was possible from the available data.

A more crude, but considerably more objective, method of estimating the advective temperature change at 300 mb. was then tried. If I is the N.-S. index of flow at 300 mb. and Δ_i ($i = 1, 2, 3$) is the N.-S. temperature gradient in this area read from the mean charts for the three types, then $-I\Delta_i$ is of the nature of an advective change of temperature. With I measured as indicated earlier and Δ_i measured in °C. per 10° of latitude, $-(1/2)I\Delta_i$ gives this rate almost exactly in °C. per 24 hours. Daily values of $I\Delta_i$ are shown in Fig.8(j). The dotted curve in Fig.8(j) shows the actual 24-hour temperature change (since 0300 G.M.T. on the previous day) at 300 mb. These latter values are for 35°N. 150°W., roughly the position of maximum temperature anomaly as shown by Fig.6. They were read from the isotherms and may well have an error of 1°C. or so owing to the open network of observations. (It will be noted that in Fig.8(j) the scale for the actual temperature change is on the right and is twice as large as the scale for $I\Delta_i$. Note also that the zero of the observed change (δT) has been plotted to correspond with the mean value of $I\Delta_i$ (equal to 1.5) and not with $I\Delta_i$ equals 0). Close agreement between the two curves cannot be expected since the method ignores temperature changes due to W.-E. advection, but Fig.6 suggests that this may only be important on isolated days, notably during Type 2 conditions. Nevertheless the curves of Fig.8(j) show fair agreement in regard to both the occurrence and the magnitude of points of maximum and minimum.

The data for January show the same broad features of the contour patterns as those observed in April. Fig.12(a) shows the mean contours for the first 15 days of January, 1952 whilst Fig.12(b) shows the mean for Type 1 and its anomaly from the 15-day mean. The stronger jet-stream days are again associated with a marked N.-S. advection anomaly reasonably near to 40°N. 160°W., the slightly different position and orientation of this anomaly being in keeping with the slightly different position of the negative temperature anomaly in Fig.9(b) compared with that of Fig.7(b).

It is interesting to note conditions above the tropical tropopause. Fig.13 shows 60 mb. charts for April, 1952 giving the temperature and contour height means (and anomalies from the mean for the month) for Type 1 and Type 3. The height anomalies are similar in general character to those at lower levels and once again the temperature anomalies are not incompatible with those which might be expected as a result of the advection anomalies.

Although the effects of vertical motion may not be negligible there is thus considerable evidence suggesting that during the existence of two separate jet-stream cores the variations in position and intensity of the sub-tropical jet-stream are largely controlled on a day-to-day basis by geostrophic advection of the temperature field.

6. Related features of the surface synoptic chart

Daily values of some parameters from the surface synoptic charts during

April, 1952 are included in Fig.8. These values were taken directly from the published maps in the "Daily Series Synoptic Weather Maps" of the U.S.W.B. which are for 1230 G.M.T. They are accordingly plotted on the time scale mid-way between the plots of the 0300 G.M.T. values for the other graphs. Fig.8(f) shows the latitude of the polar front at or near 150°W. As the polar front marking successive outbreaks of cold air (compare Palmén(7)) usually advances roughly from NW. to SE., latitudes of the polar fronts were sometimes measured at 160°W. early in a polar outbreak and at 140°W. in the later stages of such an outbreak. Measurements at different longitudes are distinctively marked. It is noticeable that at the beginning of each period of Type 1 there is a cold front in about latitude 40°N. The converse is not however true, i.e. each cold front crossing 40°N. does not coincide with the beginning of a Type 1 period.

Fig.8(g) and (h) show the longitudes of cold and warm anticyclones (situated respectively to north and south of the polar front). These show a remarkable correspondence between cold anticyclones reaching longitude 175°W. and the beginning of Type 1. Serebreny(8) pointed out the importance of an anticyclone in such longitudes to the accurate forecasting of the polar front jet-stream. It would seem to play an equally important role in the formation of a strong sub-tropical jet-stream.

Fig.14 shows mean surface charts (including mean frontal positions) for the month of April, 1952 and for the three types during that month. Mean surface pressure values were computed at 10° latitude and 10° longitude grid points from the surface maps published in the "Daily Series Synoptic Weather Maps". Mean frontal positions were obtained by averaging the longitudes at which the front intersected specified lines of latitude. It will be seen that the features of polar front and anticyclone positions mentioned in the two previous sub-paragraphs as associated with the onset of Type 1 conditions are clearly shown in Fig.14(b). It is noticeable too that the N.-S. advection component near 40°N. 160°W. characteristic of the upper level flow during Type 1 is also evident at the surface, and similarly for the S.-N. advection during Type 3.

A further point of interest is observed if the mean frontal positions for Types 1, 2 and 3 are compared with the horizontal temperature distribution shown in Fig. 6 and 7. The major cold front on each chart of Fig.14 has been denoted by the letter M showing E.-W. progression in the previously noted sequence of Types 3-1-2 etc. It will be seen that the major frontal region coincides with the lowest temperatures at 300 and 250 mb. - the trough in the isotherms being over the frontal zone rather than behind it over the low level cold air mass. This was quite noticeable on the daily charts.

Surface charts for January, 1952 are shown at Fig.15. Fig.15(a) shows the 24-day mean (i.e. mean for the month excluding only the "kona" storm days) whilst Fig.15(b), (c) and (d) show the mean charts for Types 1, 2 and 4 respectively. The positions of the polar front and anticyclone cell for Types 1 and 2 are similar to those for April. The most striking feature of Fig.15, however, is that for Type 4 (the single jet-stream type) there is no sub-tropical high pressure cell. It is also noticeable that polar air has penetrated well south.

7. Relation to the general (meridional) circulation

Fig.16 shows the model of the general meridional circulation proposed by Palmén(7); this is considered as a mean for all longitudes. Such mean meridional flow is therefore essentially ageostrophic, as opposed to the local day-to-day geostrophic meridional motion considered in Section 5. Fig.16 also includes a sketch of the mean temperature distribution for all longitudes. It is apparent that the regions of low temperature associated with the tropical and sub-tropical tropopauses are situated above the regions of tropical and frontal ascent respectively. Whether or not these regions of cold air are the result of adiabatic cooling on ascent is a

/matter

matter for conjecture. The vertical motion associated with the polar front is in the mean largely a result of the dynamically driven ascent in frontal depressions, and adiabatic cooling shown by the mean isotherms thus seems a likely result in this region. The local existence of cold air in the upper troposphere above the polar front has already been pointed out and thus the association of the two can be accepted, even if the causal relation is in doubt.

It will also be seen that the meridional circulation is such as to give confluence and hence a steepening of the horizontal temperature gradient at just the levels and latitudes at which the sub-tropical baroclinic zone exists on occasions of the two-jet structure. It also gives diffluence and hence a slackening of the horizontal temperature gradient in the lower levels of this region where observations suggest that conditions are largely barotropic. It would seem, therefore, that the meridional circulation involved in the usual concept of a sub-tropical high pressure belt to the south of the polar front region may be important in producing the type of temperature distribution associated with a sub-tropical jet-stream separate from the polar front jet-stream. This is borne out by Fig.15(d) which shows a complete breakdown of the usual polar front - sub-tropical anticyclone relationship during the period in which there is only one jet-stream in this region.

8. Conclusions

1. The area of the Pacific considered frequently shows in January and April two separate jet-streams; one associated in conventional manner with the polar front having a core at about 300 mb., the other often a thousand miles or more to the south of the polar front with a core at about 200 mb.

2. Both jet-streams show speeds in excess of 100 kt. on some days with pronounced shear in both the horizontal and vertical. The more southerly of the two streams weakens considerably at times and becomes a very broad stream with speeds of the order of 50-75 kt. and with little shear in the horizontal.

3. The two-jet type of flow is associated with a characteristic temperature distribution with three distinct tropopause levels - a tropical tropopause at about 90 mb., a sub-tropical tropopause at about 200 mb. and a polar tropopause at about 300 mb.

4. Day-to-day variations in the speed of the more southerly of the two jet-streams seem to be dependent, through the geostrophic relation, upon day-to-day changes in the temperature field largely brought about by geostrophic meridional advection.

5. The temperature distribution characteristic of the two-jet type of flow may well be a result of the ageostrophic meridional circulation accompanying the maintenance of a sub-tropical high pressure belt to the south of the general polar front and frontal depression region.

6. From the very limited number of occasions studied the occurrence in this region of a single jet type of flow appears to accompany a breakdown in the sub-tropical high pressure belt with extensive equatorward penetration of polar air. The three tropopause temperature structure also breaks down under these circumstances by the disappearance of the sub-tropical tropopause.

References

1. GILCHRIST, A. 1953, Met. Research Papers, London, No.795.

2. BANNON, J.K. 1953, Proc. of Toronto Met. Conference, page 109.

3. CRESSMAN, G.P. 1950, Journal of Meteorology, 7, page 39.

4. BANNON, J.K. 1954, Met. Mag., 83, page 257.

/5.

5. PALMER, C.E. — 1952, Q.J. 78, No.336, page 126.

6. ALAKA, M.A. / JORDAN, C.L. / RENARD, R.J. — "The Jet Stream" U.S. Navy, Navaer 50-1R-249.

7. PALMÉN, E. — 1951, Q.J. 77, No.333, page 337.

8. SEREBRENY, S.M. — 1954, Pan American World Airways, Met. Dept., Tech. Report, 2.

REPORTING STATIONS

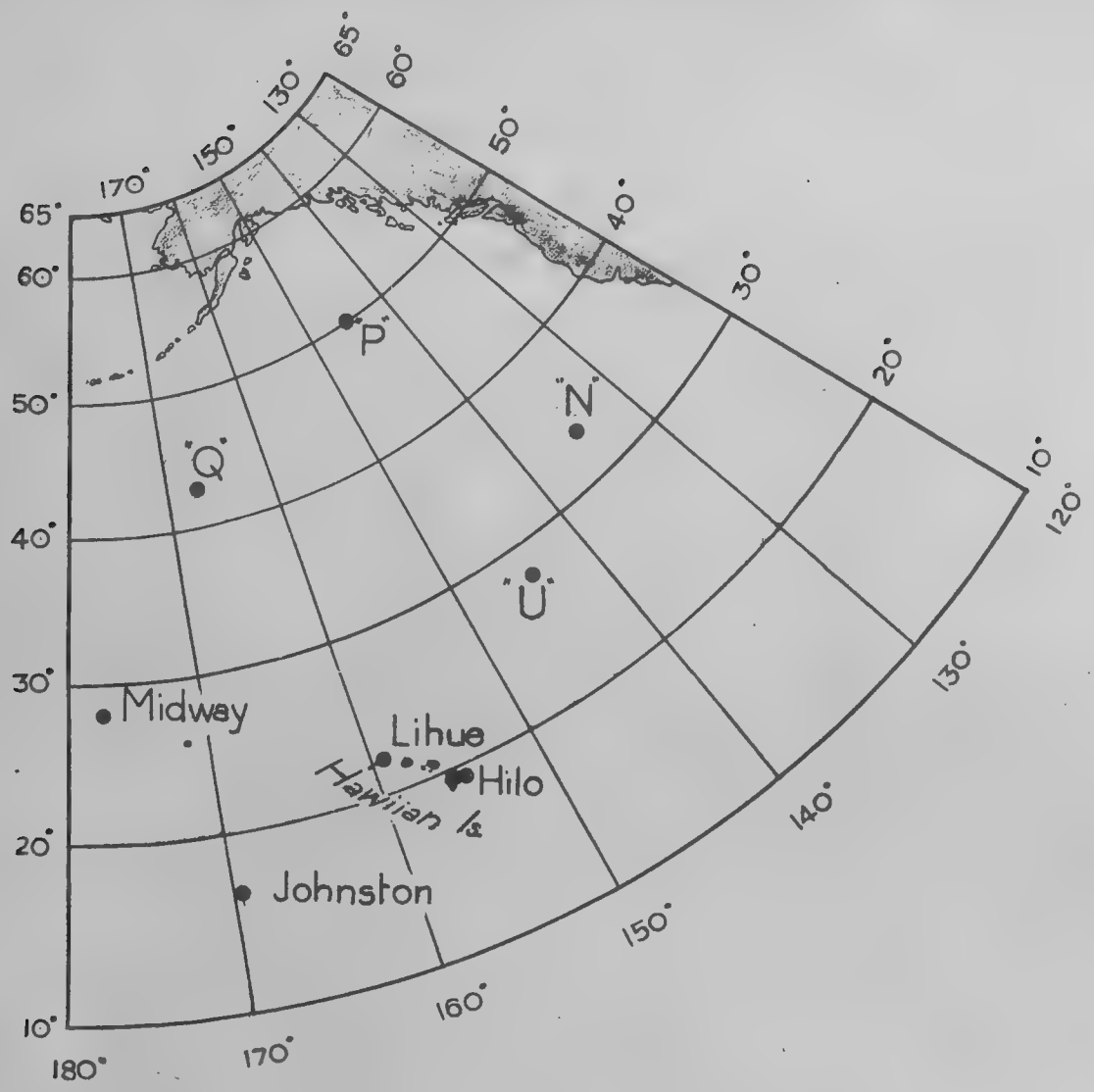

"P", "Q", "U", "N", denote ocean weather ships

Fig. 1

DAILY SCHEMATIC CHARTS 0300 G.M.T. JANUARY, 1952

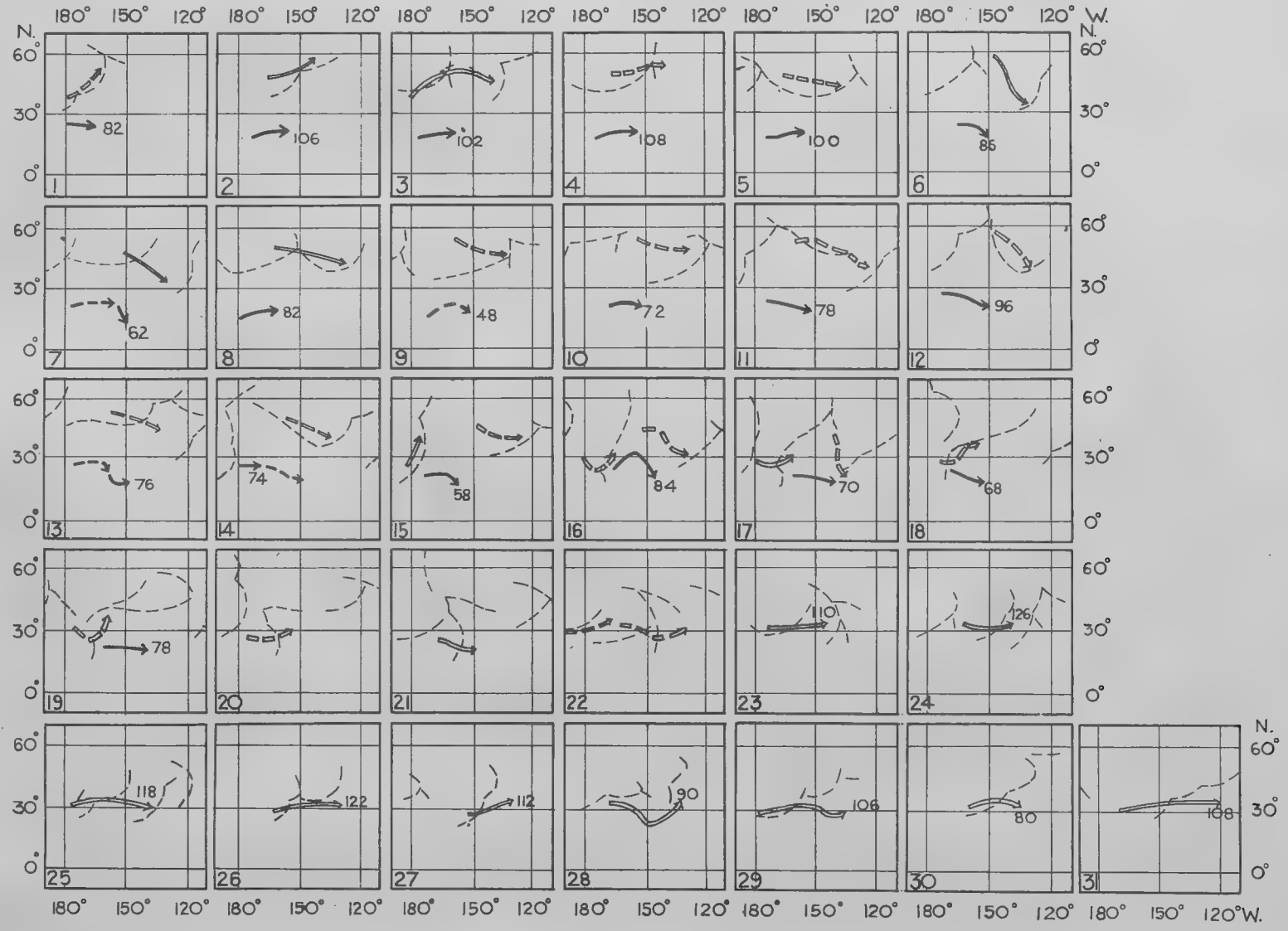

Fig.2

Core of maximum winds at about 200mb. Possible cores with maximum reported speed in kt.

Core of maximum winds at about 300-400 mb. Possible cores. Polar front.

DAILY SCHEMATIC CHARTS 0300 G.M.T. APRIL, 1952

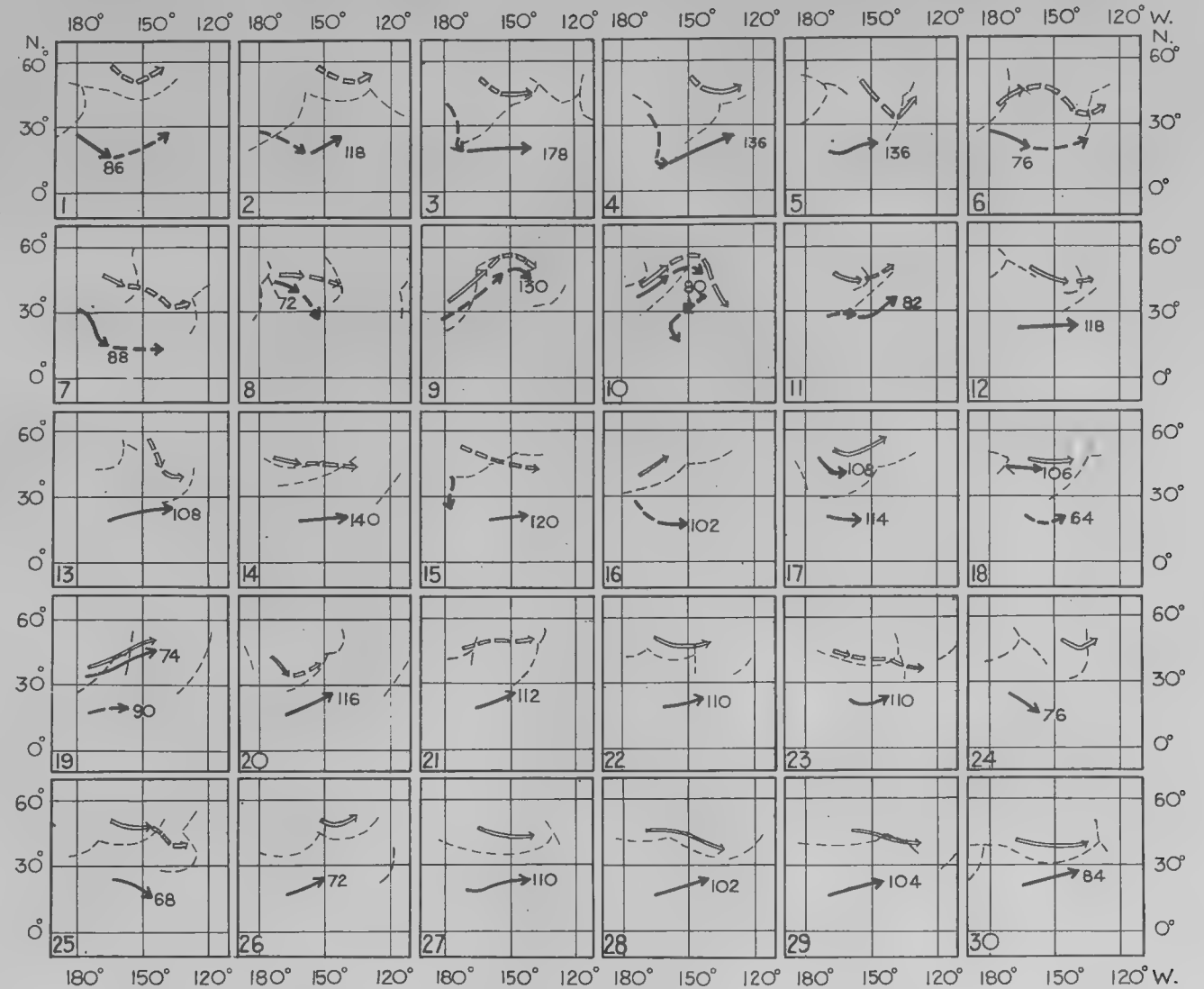

Fig. 3

→ Core of maximum winds at about 200mb. - - - → Possible cores with maximum reported speed in kt.

⇒ Core of maximum winds at about 300-400 mb. ⇢⇢⇢⇢ Possible cores. ------ Polar front

APRIL 1952
VERTICAL CROSS-SECTIONS

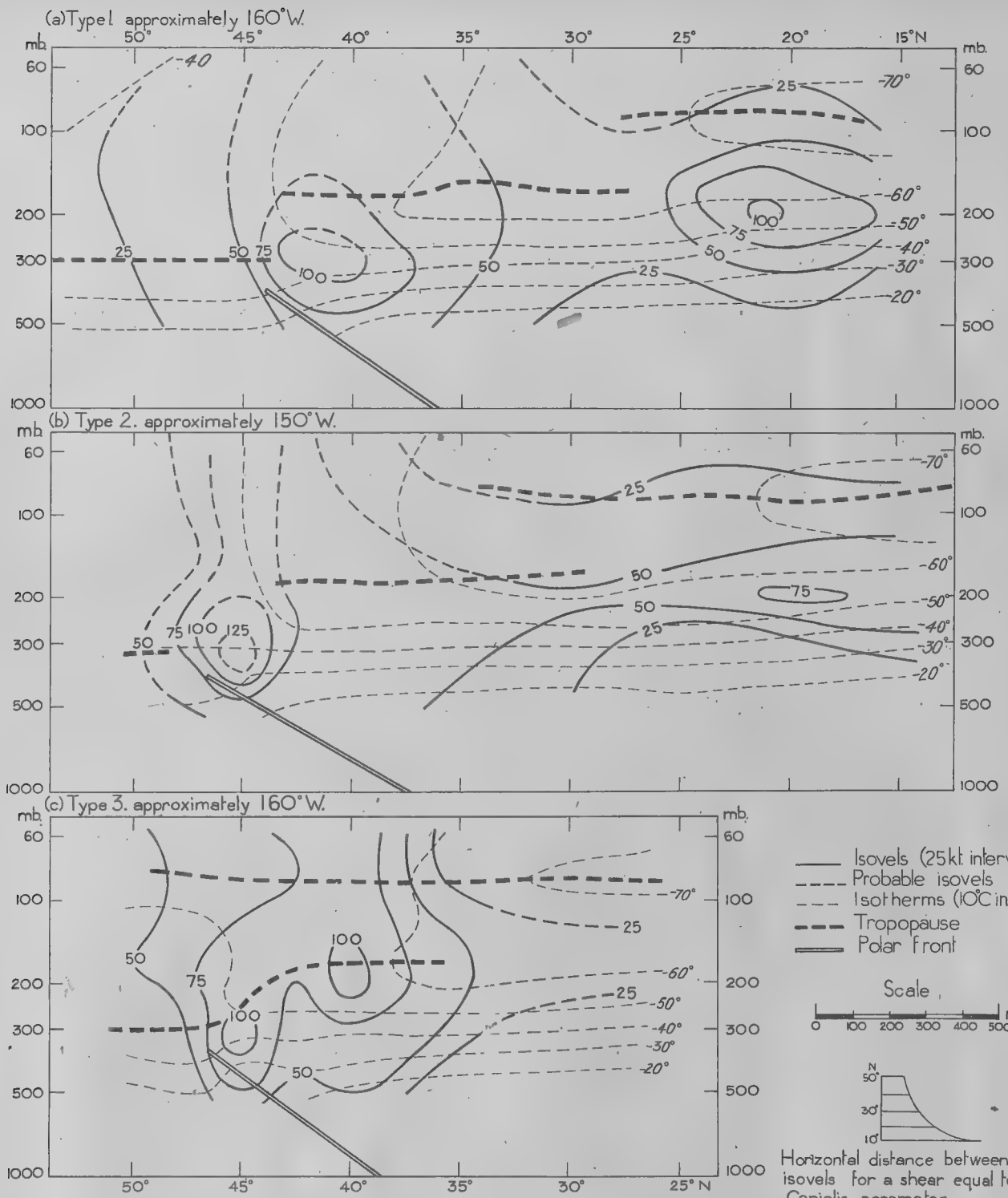

Fig. 4

JANUARY 1952
VERTICAL CROSS-SECTIONS

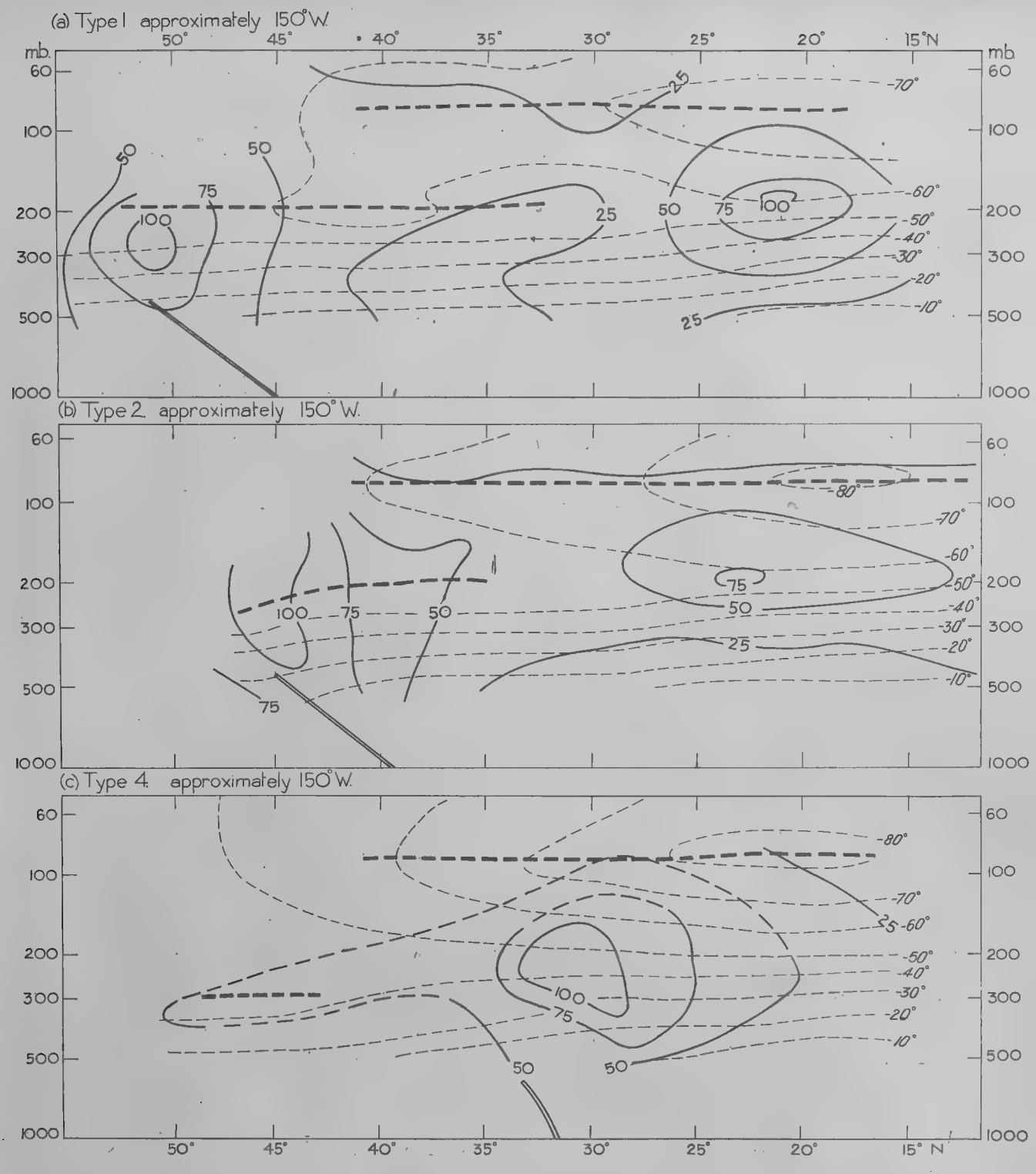

Fig. 5

Isovels (25kt. intervals) — Probable isovels — Isotherms (10°C intervals) — Tropopause — Polar front

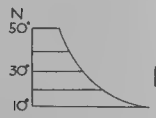

Horizontal distance between 25 kt. isovels for a shear equal to the Coriolis parameter

Scale

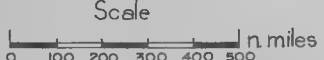

APRIL 1952
300 mb. ISOTHERMS (°C)

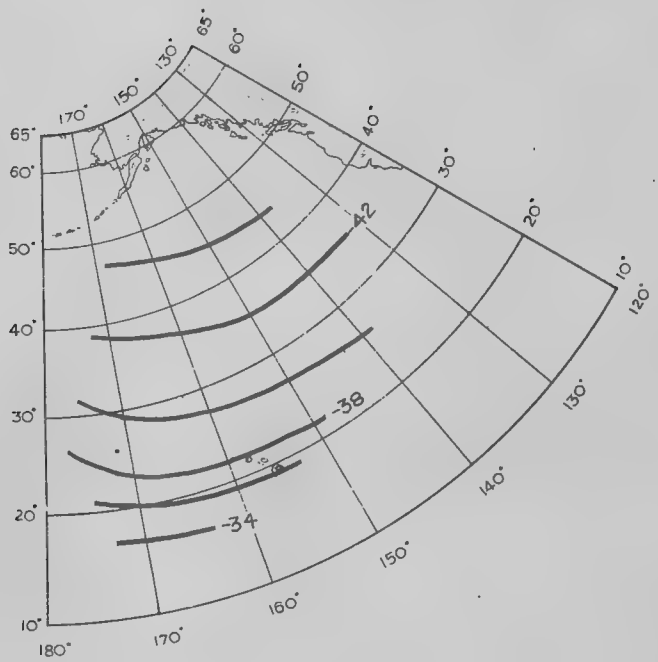

(a) Mean for April

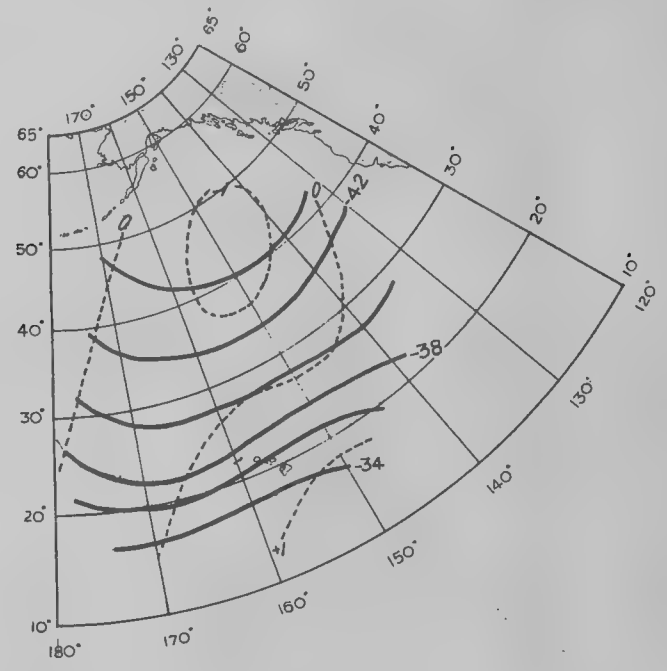

(b) Mean for Type 1.

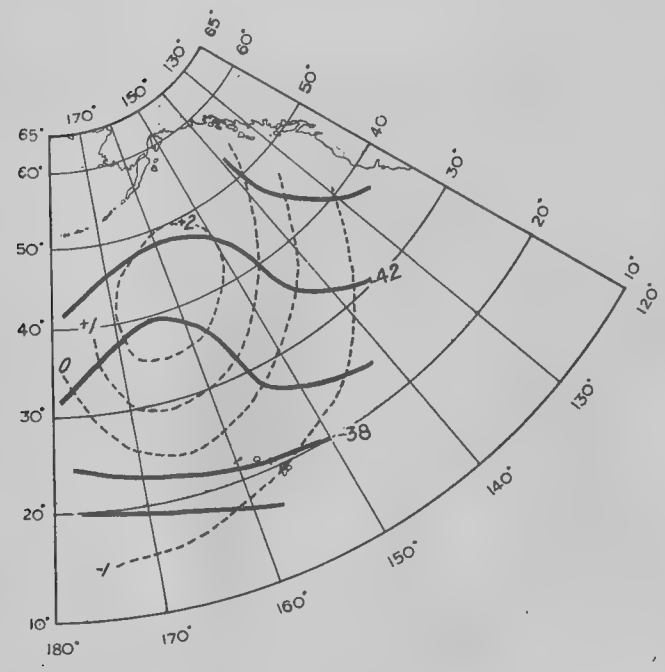

(c) Mean for Type 2

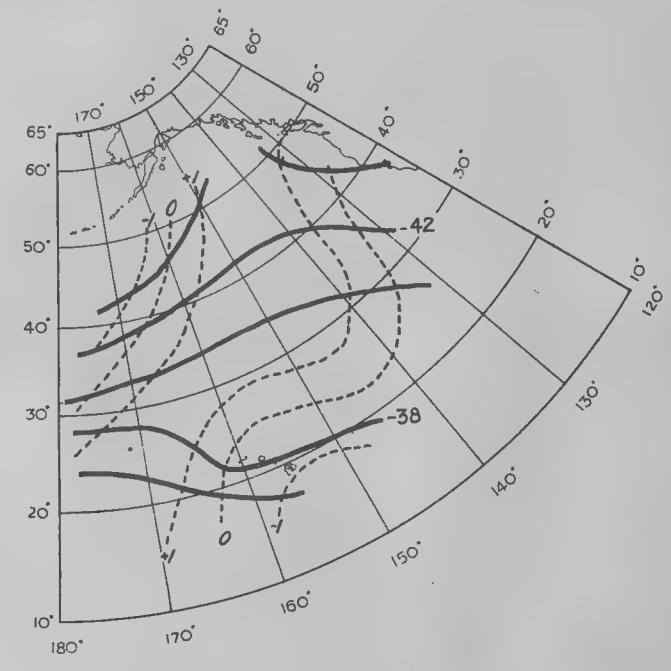

(d) Mean for Type 3.

Fig. 6

_____ Isotherms (2°C intervals)

- - - - - - - Anomalies (1°C intervals)

APRIL 1952

250mb. ISOTHERMS (°C)

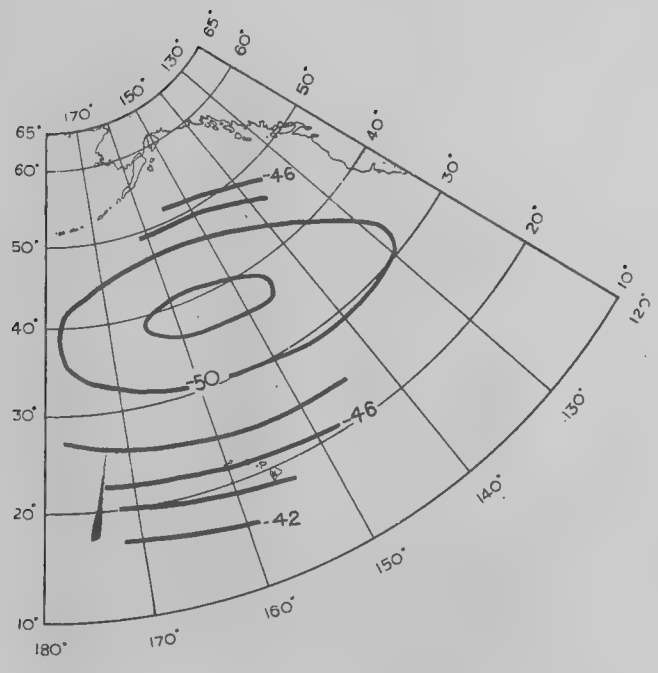

(a) Mean for April

(b) Mean for Type 1

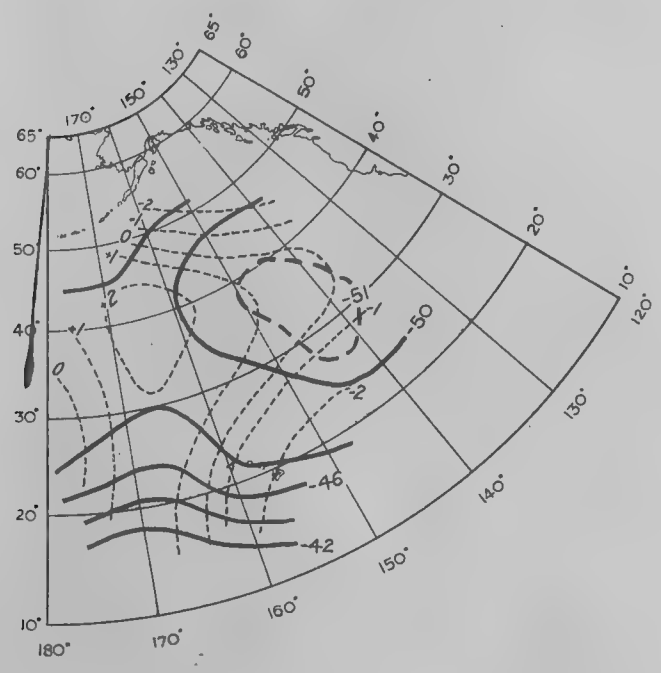

(c) Mean for Type 2

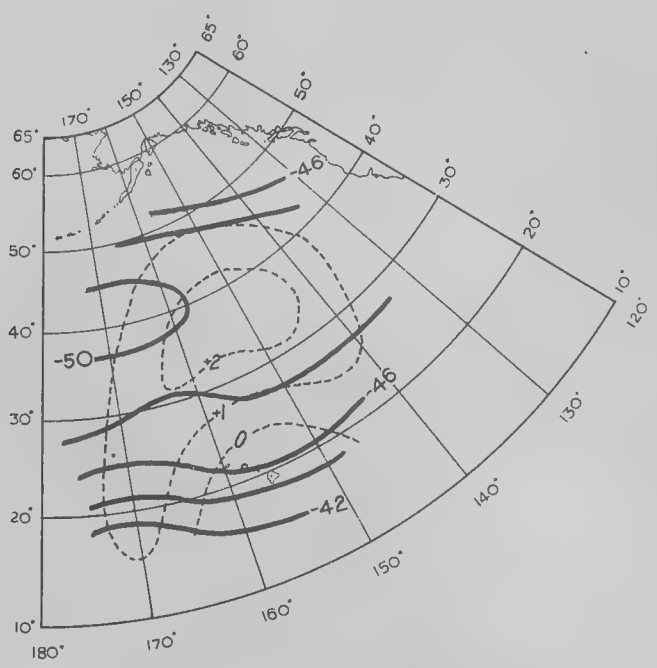

(d) Mean for Type 3

Fig. 7

——— Isotherms (2°C intervals)

- - - - - - - - - Anomalies (1°C intervals)

DAILY VALUES OF VARIOUS PARAMETERS

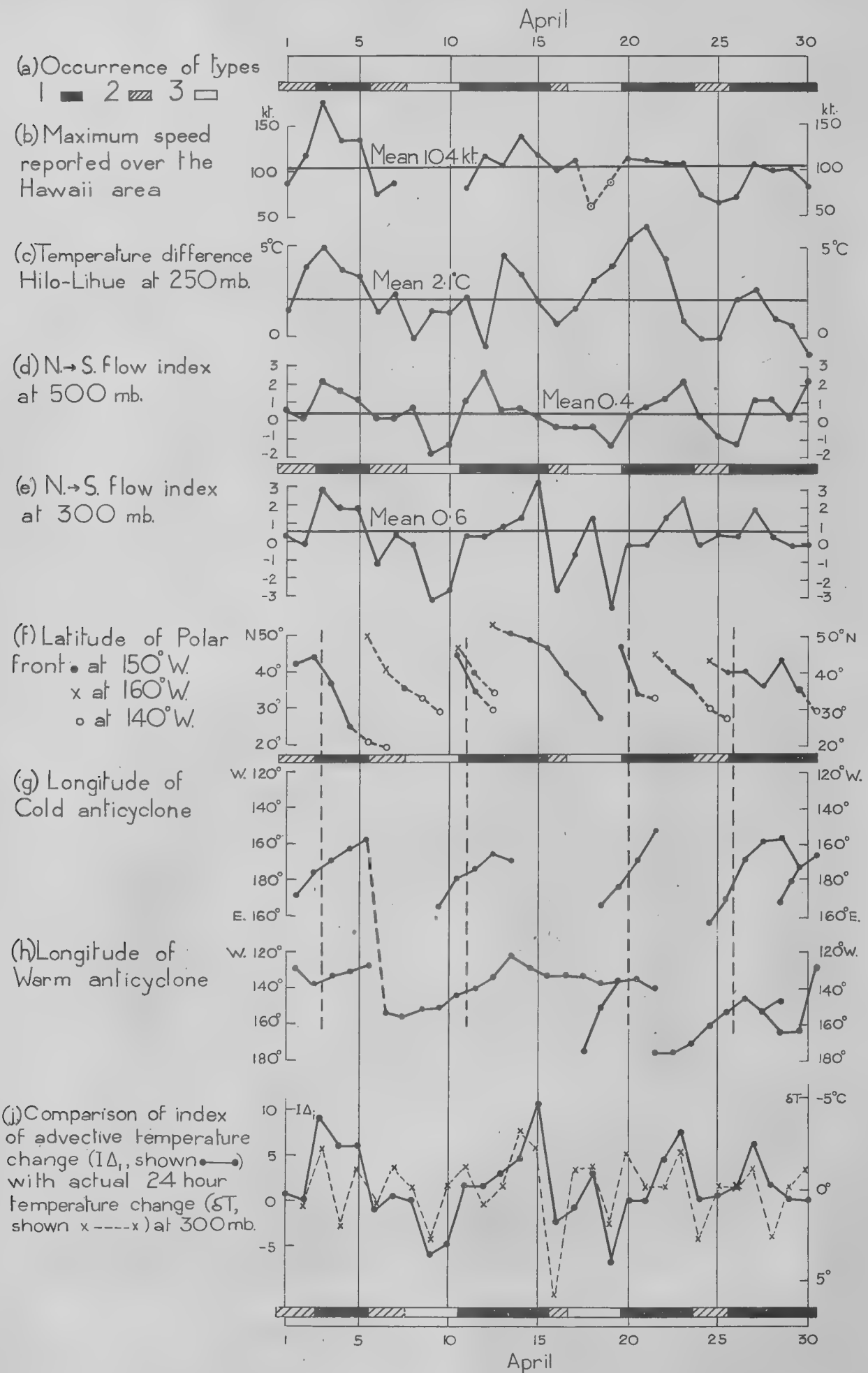

Fig. 8

JANUARY 1952
250mb ISOTHERMS (°C)

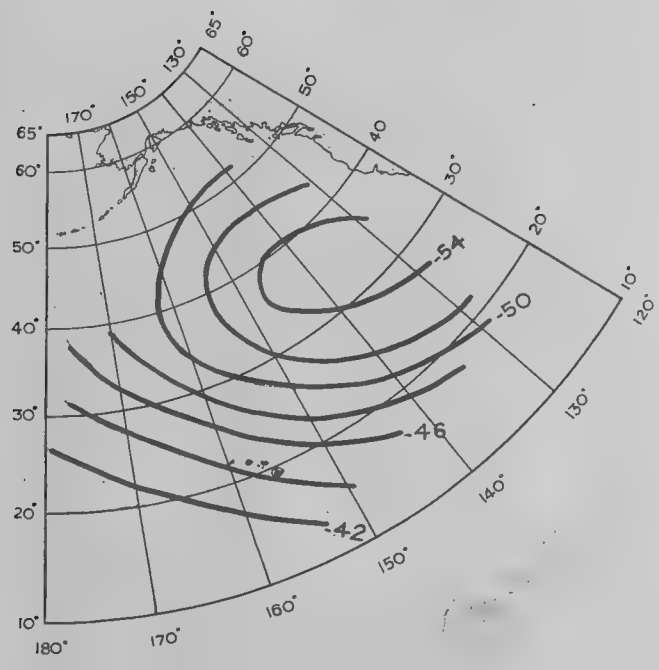

(a) Mean, January 1st-15th

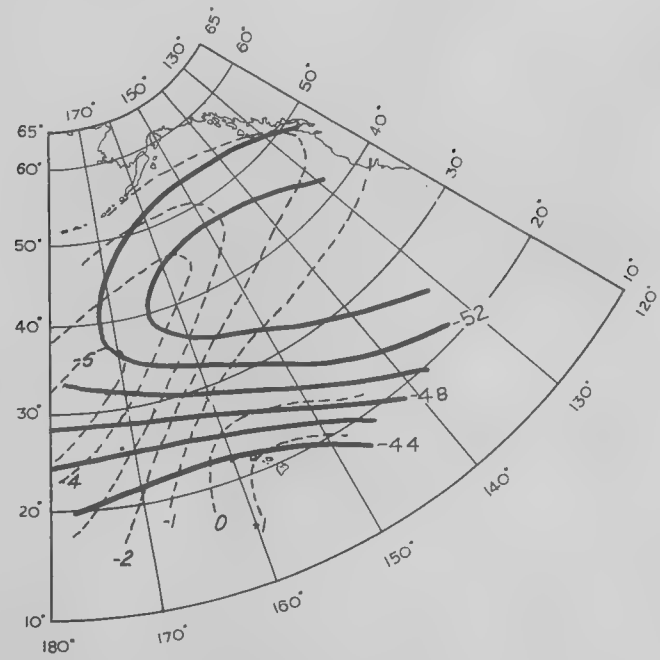

(b) Type1. Mean and anomaly from Fig.9(a)

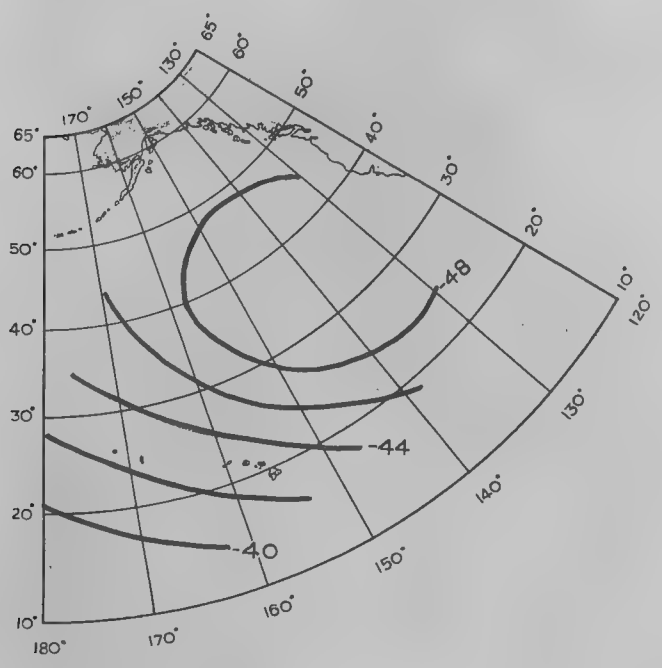

(c) 24 day mean ("kona" storm days omitted)

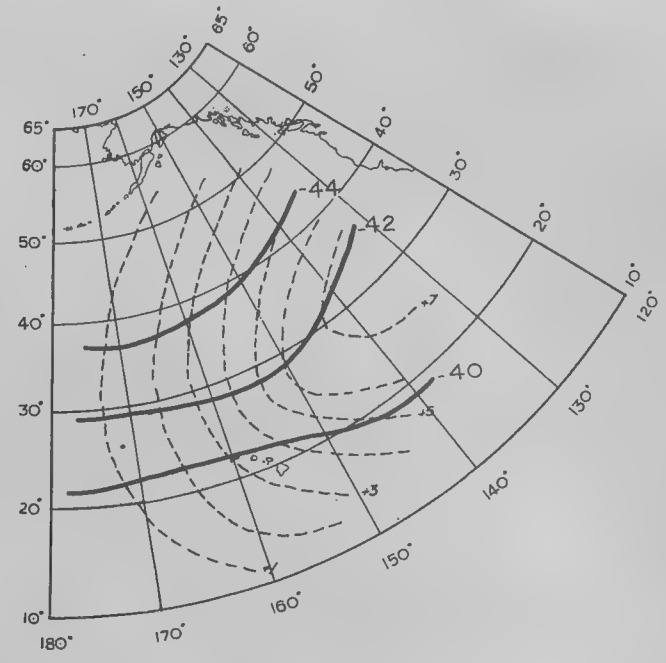

(d) Type 4. Mean and anomaly from Fig.9(c)

Fig. 9

——— Isotherms (2°C intervals)
- - - - - - Anomalies (1°C intervals)

APRIL 1952
200mb. CONTOURS (metres)

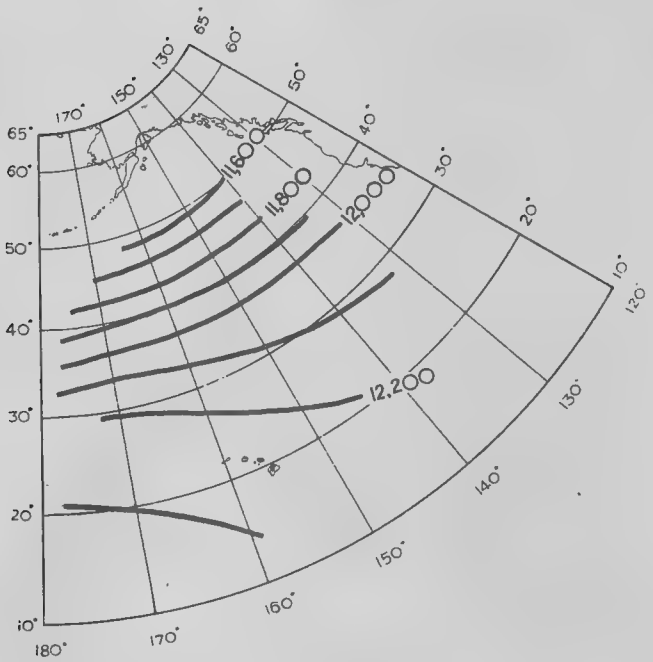

(a) Mean for April

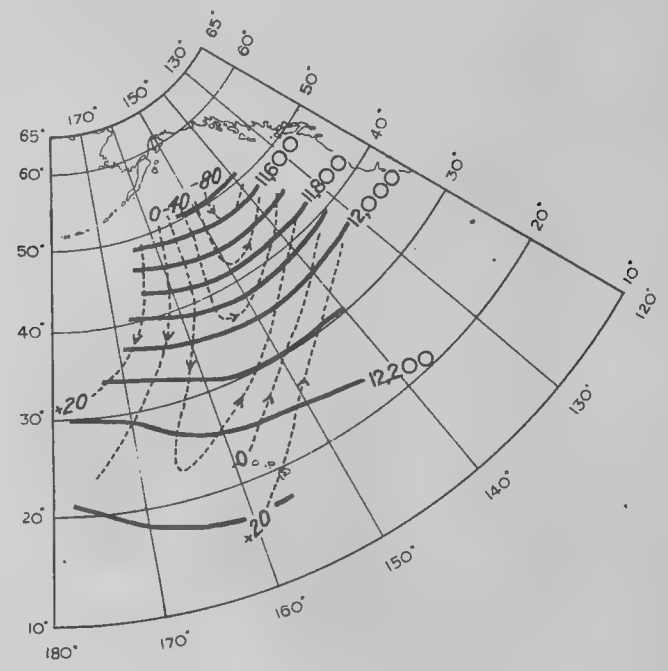

(b) Mean for Type 1.

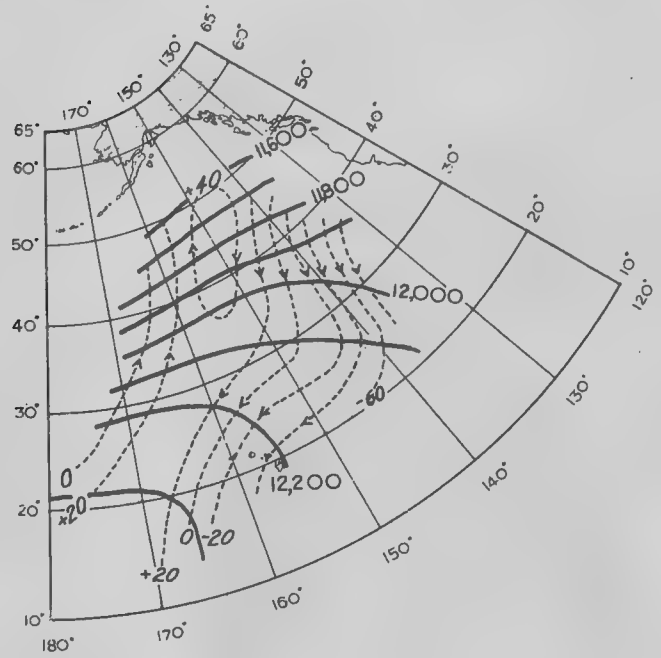

(c) Mean for Type 2.

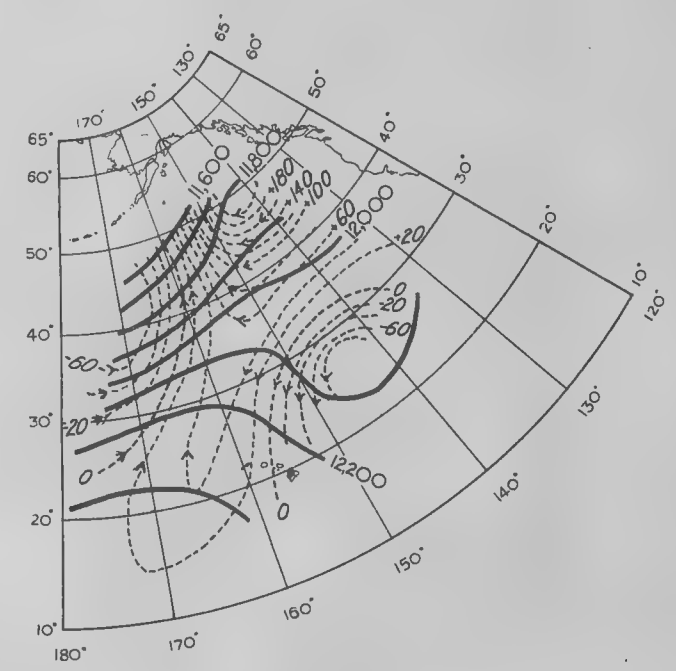

(d) Mean for Type 3.

Fig. 10

——— Contours (100 metre intervals)
- - - - - Anomalies (20 metre intervals)

APRIL 1952

500 mb. CONTOURS (metres)

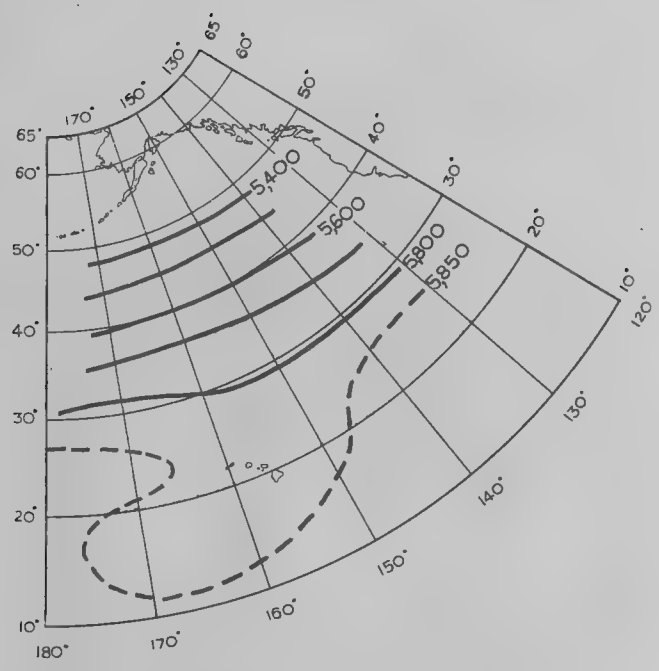

(a) Mean for April

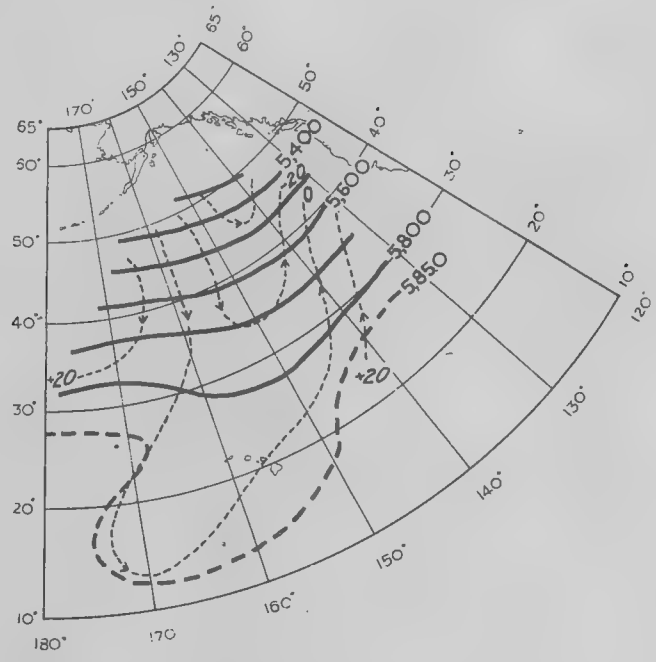

(b) Mean for Type 1

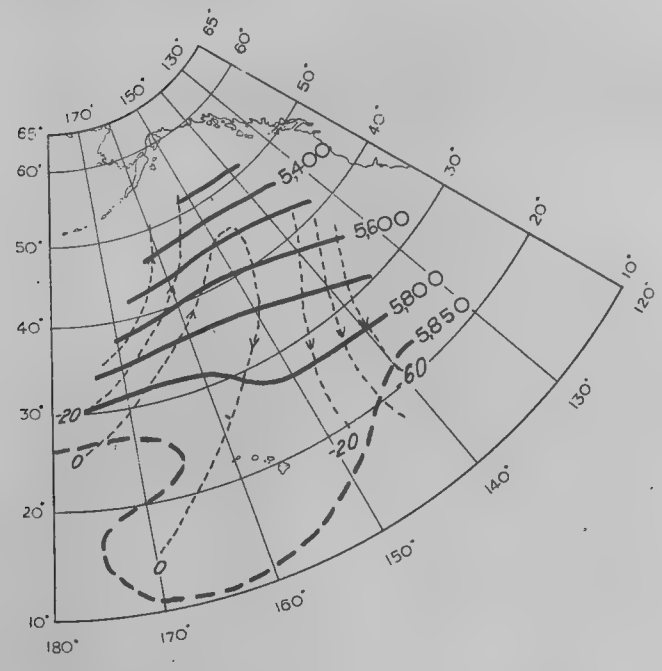

(c) Mean for Type 2.

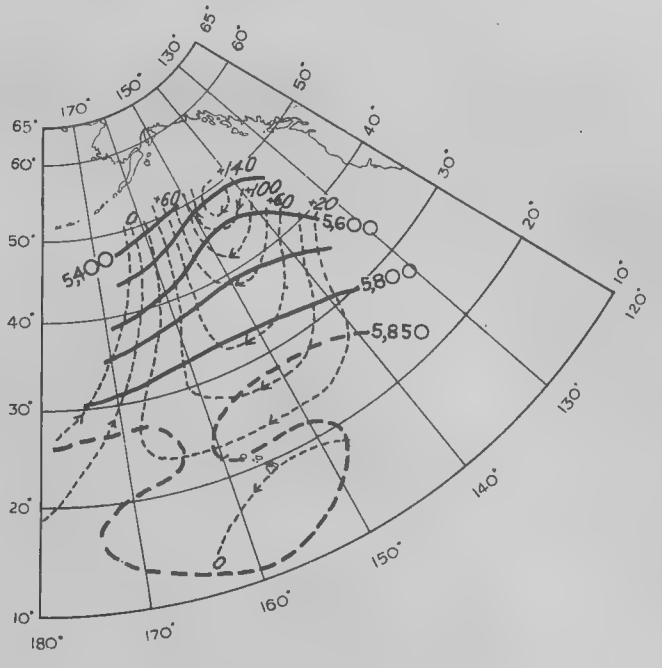

(d) Mean for Type 3.

Fig. 11

——— Contours (100 metre intervals)

---------- Anomalies (20 metre intervals)

JANUARY 1952
300 mb CONTOURS (metres)

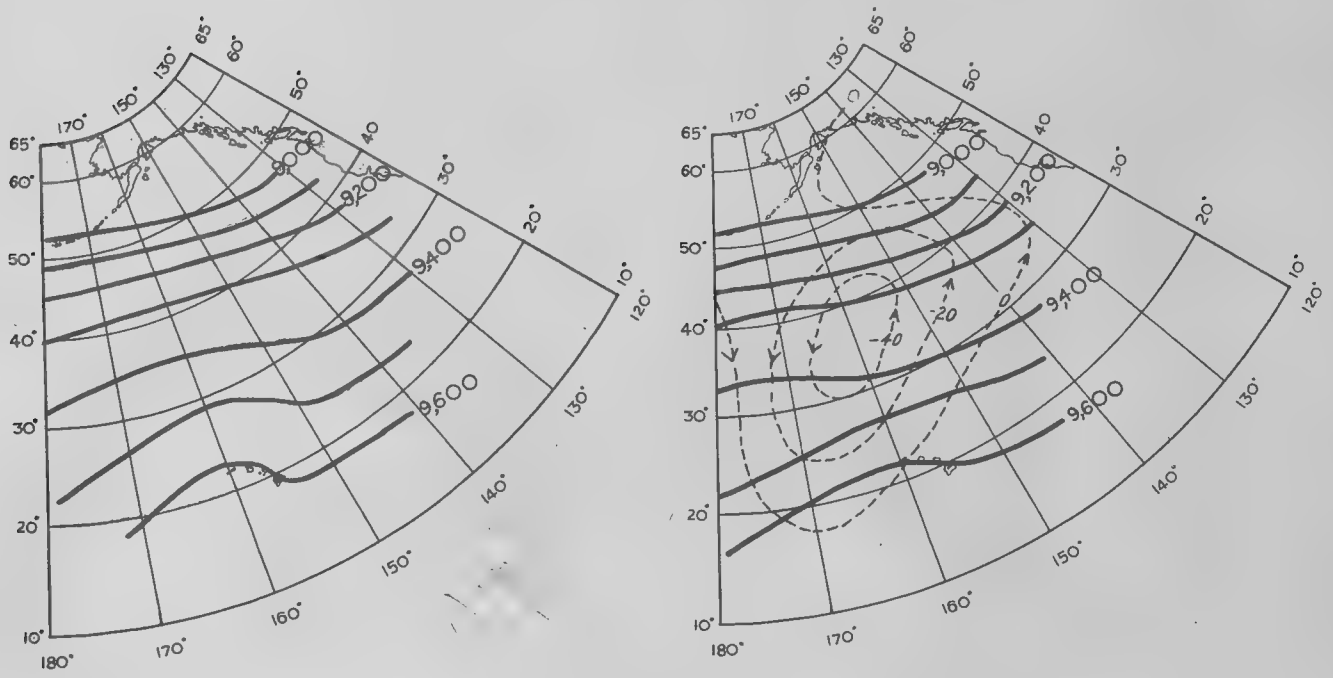

(a) Mean for January 1st - 15th

(b) Mean for Type I.

Fig. 12

——— Mean contours (100 metre intervals)
- - - - Anomalies from Fig. 12 (a) (20 metre intervals)

APRIL 1952
60mb.

ISOTHERMS

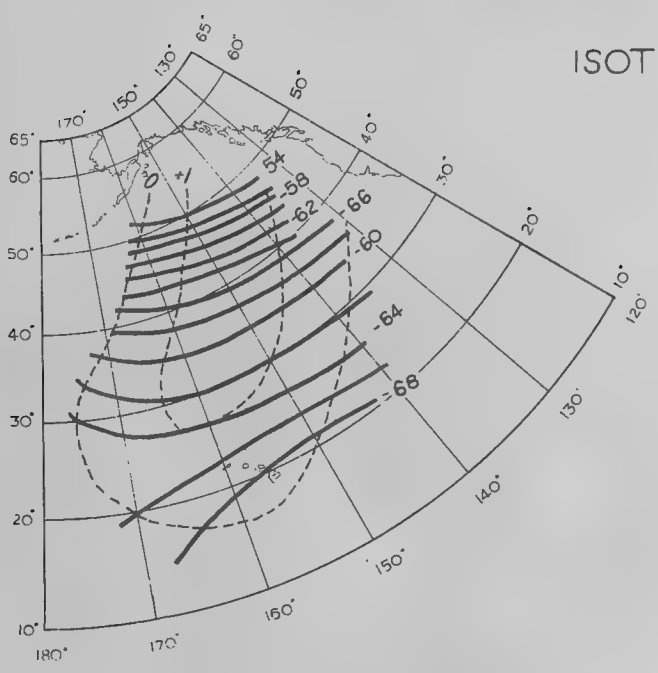

(a) Mean for Type 1

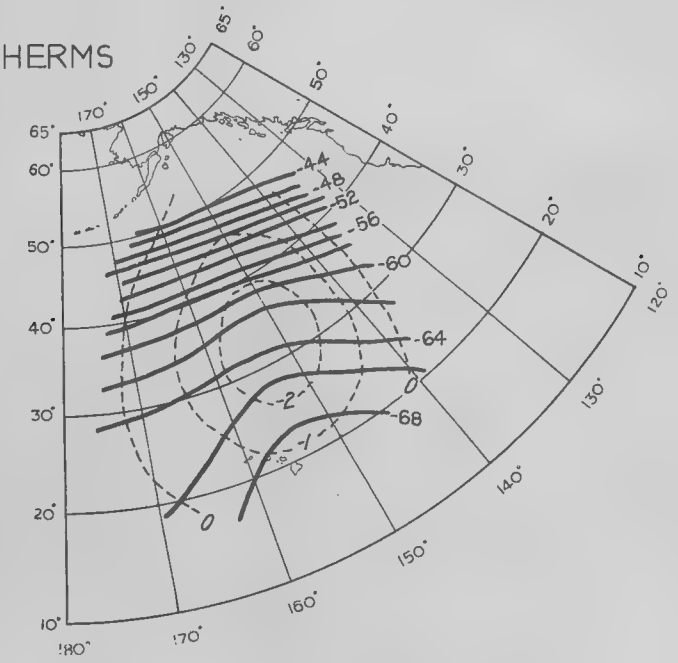

(b) Mean for Type 3

CONTOURS

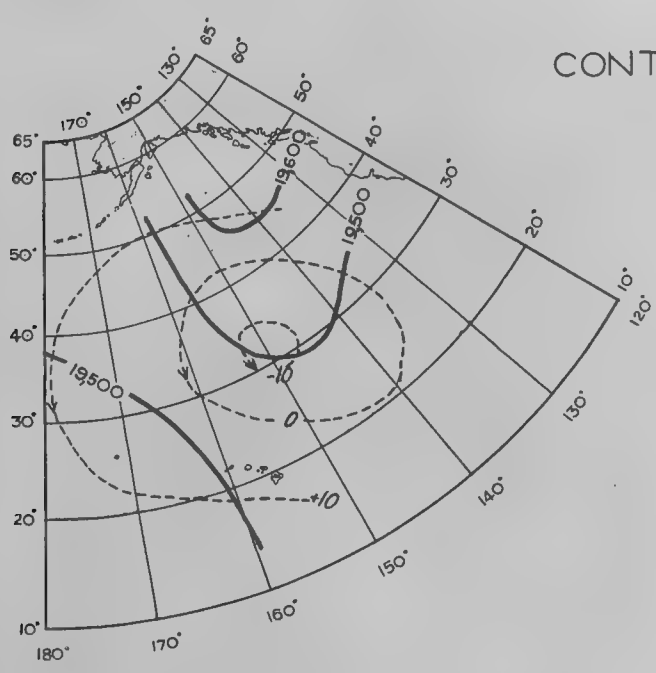

(c) Mean for Type 1

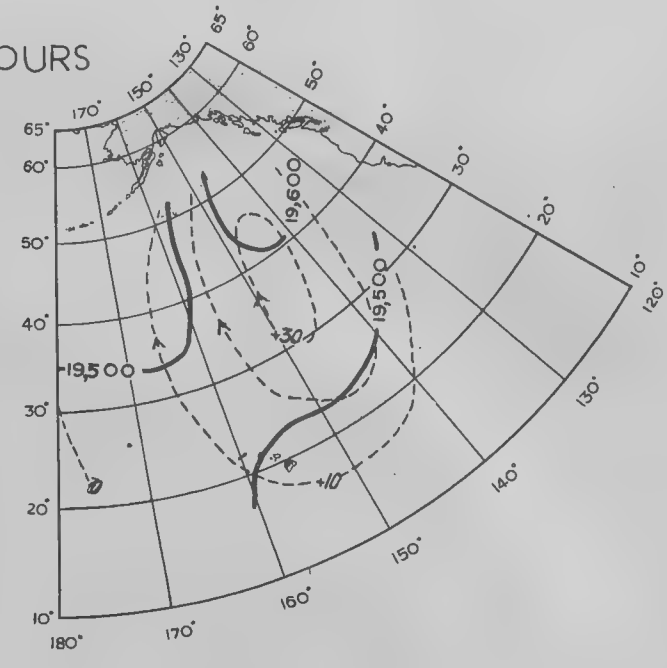

(d) Mean for Type 3

Fig. 13

——— Isotherms (2°C intervals) - - - - - Anomalies (1°C intervals)
——— Mean contours (100metre intervals) - - - - Anomalies (10metre intervals)

APRIL 1952
MEAN SURFACE ISOBARS (mb.)

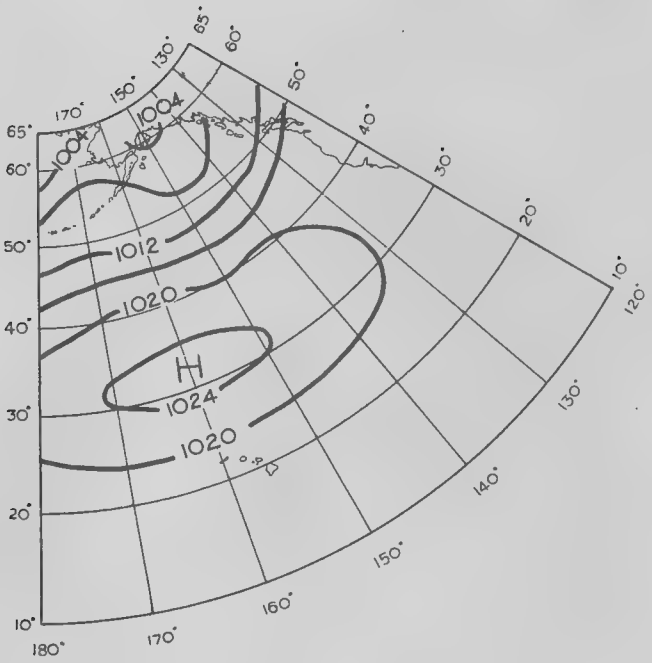

(a) Mean for April 1952

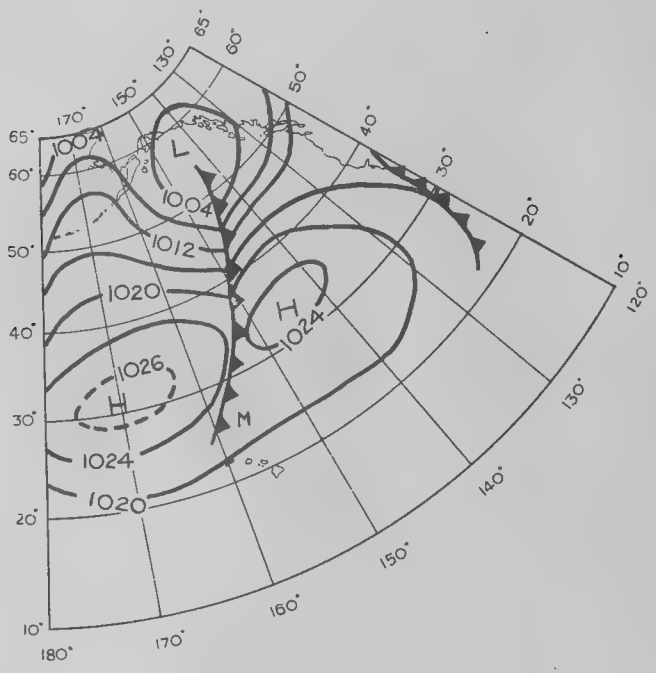

(b) Mean For Type I.

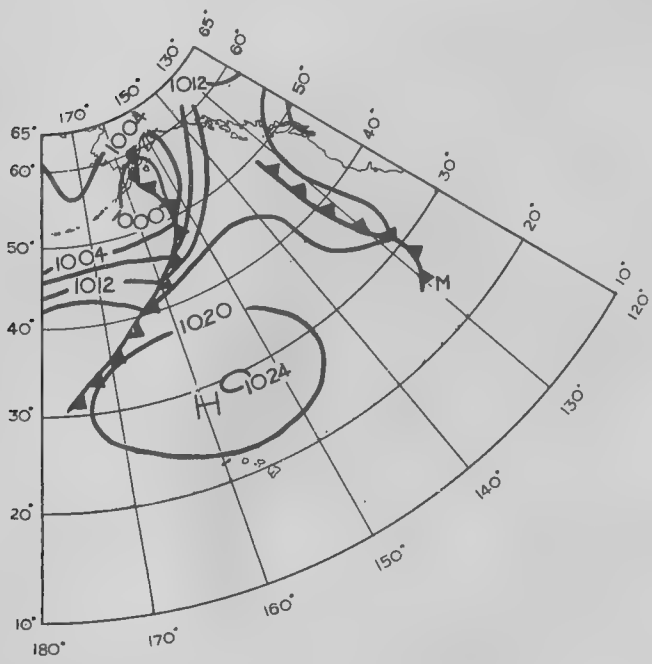

(c) Mean for Type 2

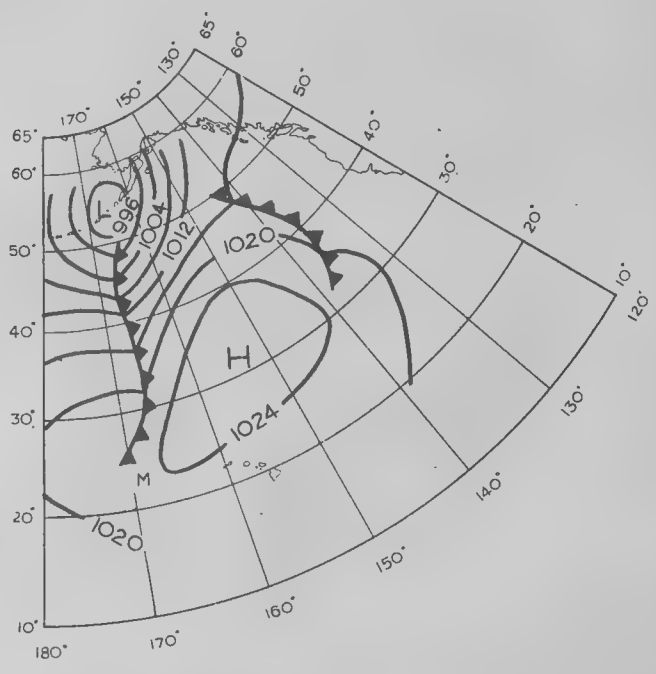

(d) Mean for Type 3

Fig. 14

Isobars. (4 mb. intervals)

Polar fronts

M Major cold front

JANUARY 1952
MEAN SURFACE ISOBARS (mb.)

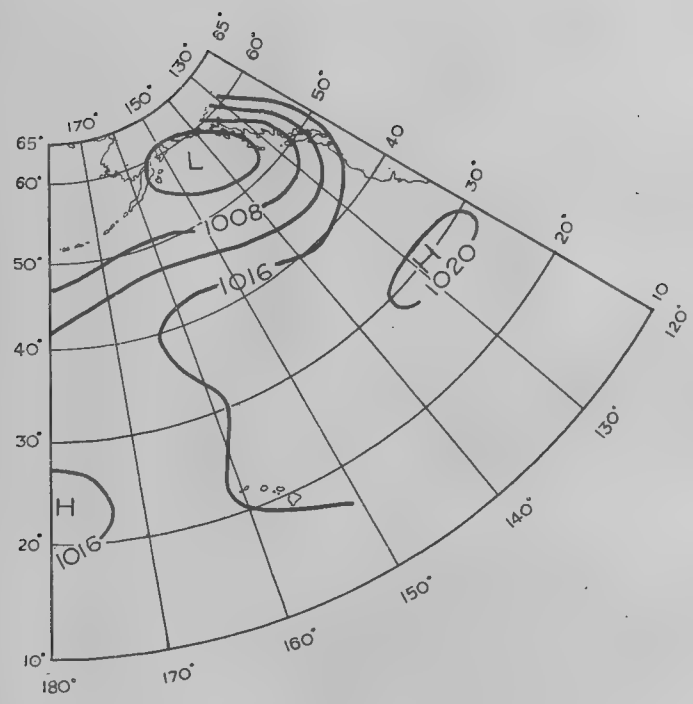

(a) Mean (24 day) for January

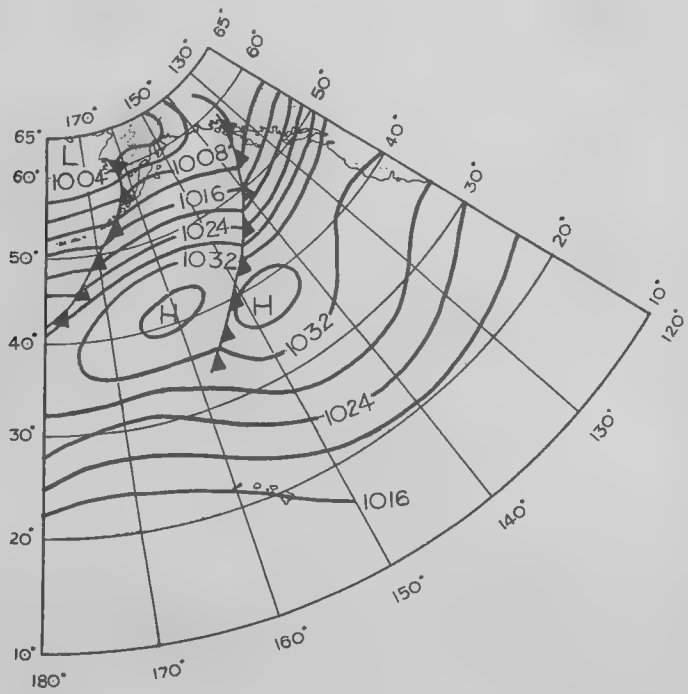

(b) Mean for Type 1.

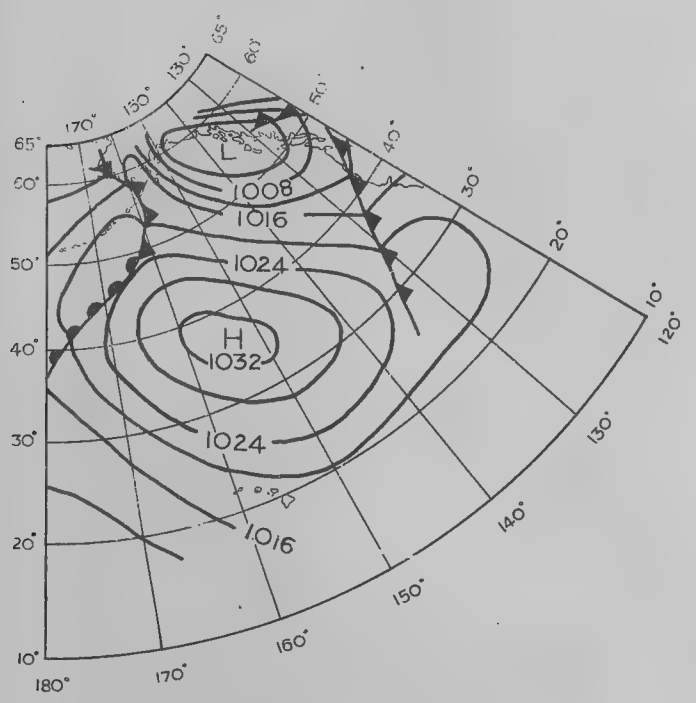

(c) Mean for Type 2

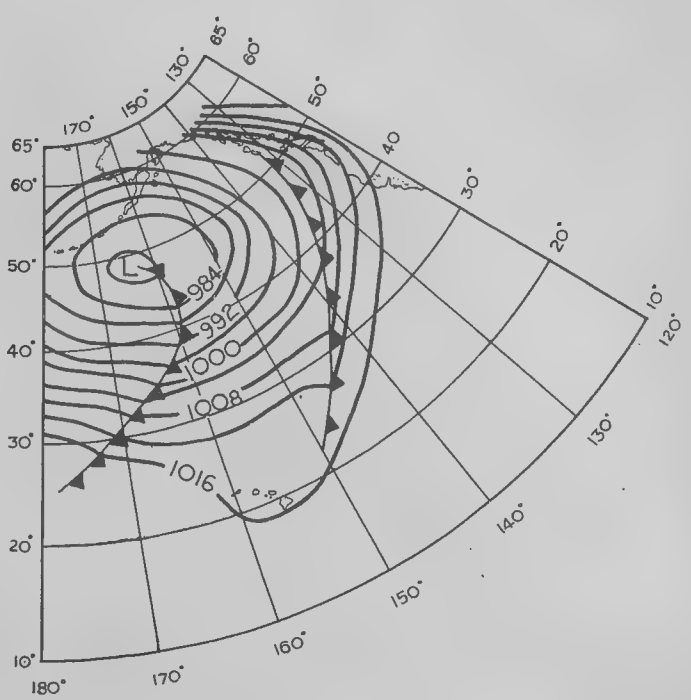

(d) Mean for Type 4

Fig. 15

Isobars (4 mb. intervals)

Polar fronts

General meridional circulation (after Palmén)

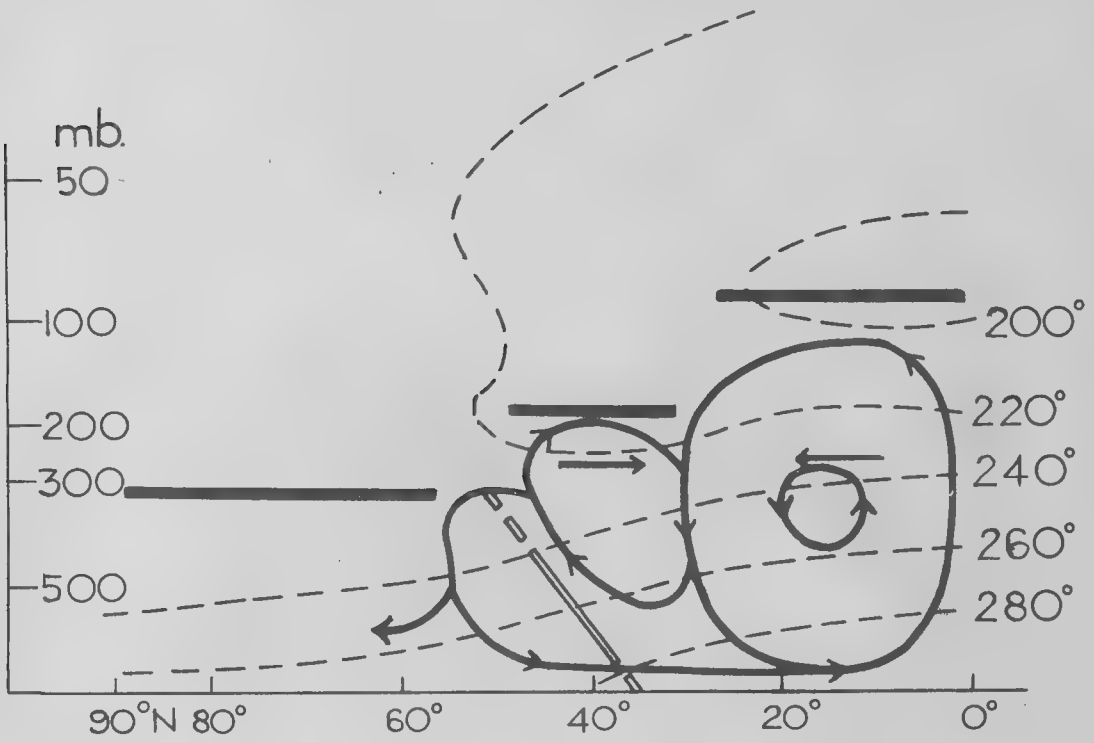

Fig. 16

Tropopause
Polar front
Isotherms (°A)
Streamlines

at the level of

of chart 25[9] is represented by the

chart (1,3) that the

are few the charts can only
curacy of the charts can be

Committee (London).
M.R.P. No. 925 by Mr. J. K. Bannon and R. A. Jones.
A copy is available in the Library of
the Meteorological Office."

24th August, 1955

AD 117 796

AIR MINISTRY

METEOROLOGICAL RESEARCH COMMITTEE

The mean wind at 60 mb.

by

J. K. Bannon and R. A. Jones (Meteorological Office)

Summary

An attempt is made to chart the mean wind over the world at the level of 60 mb. (20 km.) in the mid-season months January, April, July and October. Stream lines and isotachs are shown on Mercator charts for the latitudes 75°N. to 60°S. Mean vector resultants of observed winds at 60 mb. are tabulated; frequencies of wind directions are also listed for a few stations.

1. Introduction

The mean upper winds over the world at levels up to 100 mb. (approximately 54,000 ft.) have been described and mapped by Brooks and others (1) and more recently by Jenkinson (2). An attempt is made here to extend this work to the level of 60 mb. (approximately 65,000 ft. or 20 km.)

The mean flow for latitudes poleward of about 25° is represented by the contour lines of the height of the constant pressure surface. This is the method adopted in the previous studies and it is known (1,3) that the geostrophic winds measured from such charts are an adequate approximation to the true mean wind. Isotachs (lines of equal mean speed) are also drawn; the contour lines are equivalent to mean stream lines. For latitudes less than 25° the mean flow is also shown by isotachs and stream lines which were estimated directly from observed winds.

As data for levels above 100 mb. are few the charts can only give a rough outline of the true mean winds. The accuracy of the charts can be expected to be least over the tropics where observations are few and the geostrophic approximation cannot be invoked as an aid.

2. Wind summaries

Direct observations of wind at 60 mb. are few. Most of the observations are from radio-- or radar - wind soundings. A few pilot-balloon observations are available and there are also a few determinations of wind by acoustic methods. All the data are unfortunately liable to bias. The radio - or radar - winds are necessarily biased towards lighter winds at lower levels and so may not be truly representative of all conditions. This is particularly evident over North America during winter and spring where direct observations are fewer than at other seasons, strong westerly winds in the troposphere causing the balloons to drift out of range of the tracking instrument. Pilot-balloon observations are unlikely to be representative of all conditions; the limitations of this type of data are well known. Acoustic methods of measurement lack precision and the numbers of observations are very small.

/Table

Table I contains the station names, their geographic positions, the period covered by the observations and the type of observation (e.g. radar-wind).

Table II contains the mean vector resultant winds at 60 mb. for all stations at which ten or more observations are available during any one mid-season month. Resultants from less than ten observations are enclosed in brackets. The number of observations and the speed and direction of the maximum observed wind are also given.

Supplementary tables (Table III A, B) give the frequency of wind direction for the following groups of stations:-

A. British home stations and Ocean Weather ships. British stations in the Mediterranean - Middle East region, together with Nairobi and Khartoum. Directions are in 30° intervals centred on the cardinal points.

B. Pacific island stations, Albrook Field and Havana, for the directions of a 16 point compass, centred on the cardinal points.

In the tables the observing stations are first grouped according to latitude, namely north of 60°N., 30° to 60°N., 10° to 30°N. in the Northern Hemisphere. In these separate zonal belts the stations are then arranged latitudinally from north to south in the broad areas America, British Isles area, Mediterranean and Middle East, Japanese Main Islands and Pacific. In the equatorial regions and the Southern Hemisphere two divisions only are used, namely, 10°N. to 10°S. and 10°S. to 60°S.

The form in which the data are available differs from station to station. In summarizing and computing the vector resultants the following methods were used:-

(a) British home and overseas stations, Nairobi, Lagos, Khartoum, Hong Kong, Falkland Islands and Pacific Island stations. Data were extracted in the form of frequency distributions of wind speed and direction for the 60 mb. surface. These frequencies were then compounded vectorially.

(b) American stations (excepting the acoustic results) and the Japanese Main Island stations. Data were already available in the form of monthly vector resultant winds at 20 km. These were compounded for the separate areas.

(c) New Zealand stations and Woomera. Values at 65,000 ft. were interpolated between the values at 60,000 and 70,000 ft. given in the original data. When there was a reversal of direction between the two heights both values are quoted.

3. Charts of the mean wind

The mean flow at the level of 60 mb. is shown by charts of stream lines and isotachs for each of the mid-season months January, April, July and October. (Figs. 1 to 4). The stream lines in temperate and high latitudes are taken as the mean contour lines of the height of the 60 mb. pressure surface.

These contours were constructed as follows: - Charts showing the mean temperatures at standard pressure levels up to 100 mb. are available in the Upper Air Climatology Branch and charts had been computed from these of the mean height of each of the standard pressure surfaces. These contour charts may not be accurate in detail since the method of computation assumed constant lapse rates of temperature between the standard levels. It is believed, however, that they are not much in error except perhaps over Siberia and in

/regions

regions of the Southern Hemisphere where observations are lacking. The above charts of the height of 100 mb. surface were the basis for the construction of the charts for 60 mb. Observations of temperatures in the layer 100 to 60 mb. are few. However, mean lapse rates were obtained for this layer from available data and mean lapse rates were inferred for all regions by interpolation and extrapolation from these. The thickness of the layer 100 to 60 mb. was evaluated from these lapse rates and the mean temperature distribution at 100 mb. This thickness was then added to the height of the 100 mb. surface to obtain the contour of the 60 mb. surface. A grid of points at intervals of 10° latitude and 20° longitude for latitudes polewards of 30° was used in constructing the mean thickness of the layer 100 to 60 mb. and in effecting the addition of this thickness to the 100 mb. chart. Some smoothing was necessary in drawing the final contours of the 60 mb. surface. These contours are given at intervals of 400 geopotential ft. Contour charts of the 100 and 50 mb. surfaces for North America prepared by the U. S. Air Weather Service (6) were consulted and were of assistance in drawing the 60 mb. contours in that region.

Since observations above the level of 100 mb. are so few, these contour charts for temperate latitudes cannot be considered accurate though it is hoped that they show the main features correctly. It should be noted that an error in estimating the lapse rate will have only a small effect on the computed value of the thickness 100 to 60 mb. The mean lapse rate between 100 and 60 mb. seems to vary little for a particular latitude belt for any one month; the greatest variation noted was 5°C. over the layer 100 to 60 mb. between Japan and the corresponding latitude in southern Europe in July. The variation is usually less than 2°C. An error of 2°C. in estimating the mean fall of temperature between 100 and 60 mb. will result in an error of 1°C. in the mean temperature of this layer leading to an error of only 50 ft. in the thickness of the layer. An error of 2°C. in the mean temperature at 100 mb. will result in an error of 100 ft. in the thickness of the layer 100 to 60 mb. The accuracy of the contours of the 60 mb surface thus depends mainly on the accuracy of the contours of the 100 mb. surface and on the accuracy of the charts of mean temperature at 100 mb.; the latter are probably the less well determined.

The wind speeds from which the isotachs were constructed were mainly derived from the charts using the geostrophic relation. Direct observations were used in the few places for which they are available.

In the tropics the stream lines and isotachs were constructed from the wind observations. The principle that the mean flow must be largely without horizontal convergence or divergence was of assistance in the drawing; thus inflow into any particular region must roughly balance outflow. Nevertheless, even the main features of the flow in the tropics may not be adequately described in these charts because of the lack of observations.

The mean resultant winds given in Table II are also plotted on the charts. The number of observations is indicated at the head of the wind arrow. In temperate latitudes greater weight is given to the orientation and spacing of the mean contours than to the observed mean resultant winds.

4. Discussion of charts

(a) January (Fig. 1)

(i) Northern Hemisphere

The predominant feature of the mean flow in January is the general westerly circulation north of about 25°N. Two areas of maximum wind speed are shown, namely, over the Canadian Arctic and southern Greenland with speeds of 70 kt. and to north-east of Japan with speeds of over 90 kt.

/Over

Over the British Isles and the Mediterranean the mean winds are westerly of order 30 kt., but wind speeds of 70 kt. have been reported at most stations.

Darling (7), in an investigation of the mean flow at 40 mb. over the United States in 1952, shows the existence of a mean westerly flow of 25 kt. over the zone 31°N. to 40°N. and a pronounced westerly flow of 30 kt. over the zone 41°N. to 50°N.

The high velocity of 295°/150 kt. was recorded at Ocean Weather Ship V (31°N., 164°E.). Only two observations are available from this station in January, however, so it is impossible to judge whether such speeds are of regular or frequent occurrence.

South of about 20° to 30°N. the winds are generally light and variable. A few pilot-balloon observations over India at 60 mb. (8) show a westerly flow with a tendency to southerly components. The few wind observations at 65,000 ft. over Singapore (9) were moderate west-south-westerly.

Mironovitch (10), who has prepared a meridional cross-section at 150°E., indicates light easterly winds or calm south of 15°N. with westerlies north of this latitude with a maximum mean speed of 60 kt. at 60°N.

(ii) Southern Hemisphere

By analogy with the Northern Hemisphere in July it might be expected that the easterly flow south of the Equator would exceed 20 kt. over a considerable area. Mironovitch (10) shows speeds of 20 to 30 kt. in longitude 150°E. However, as there is no direct evidence of strong easterlies in this belt they are not shown in Fig. 1.

Farkas (11) has recently summarized the observations of upper winds over Canton Island (02°49'S.,171°43'W.) for the period July, 1952 to June, 1953. This information became available after the charts to Figs. 1 to 4 were drawn. In the three months December, January, February, the mean wind at 20 km. (31 observations) was westerly, 12 kt., with a standard vector deviation of 22 kt. Palmer (12) states that a narrow belt of westerlies (what he calls "von Berson Westerlies") is probably to be found at heights from about 18 to 23 km. near the Equator at all seasons. The Canton Island observations and the few (less than 10) from Singapore are the only data known to the authors in support of the existence of this equatorial westerly stream in January. In Figs. 1 to 4 no attempt has been made to chart this westerly flow which is light where it can be found and seems to cover a small area.

The mean flow between 50°and 60°S. appears to be moderate westerly in contrast to the light and variable flow in similar latitudes in the Northern Hemisphere in July. This difference between the flows in the two hemispheres may not be the result of significant differences between the summer stratospheres of the two hemispheres but may be caused by the stronger westerly flow in the troposphere in the Southern Hemisphere in summer.

A wind with an easterly component has never been recorded over the Falkland Islands (52°S., 58°W.) at 60 mb.

/(b)

(b) April (Fig. 2)

(i) Northern Hemisphere

There are two main regimes, the westerly flow north of about 25°N. and the weaker and more variable flow south of 25°N.

The westerly stream is everywhere much weaker than in January and its southernmost limit has moved northwards slightly, the easterly winds having increased in frequency in the south.

The increase in the frequency of easterly wind from January to April in northern temperate latitudes is confirmed by Darling (7) who also shows that the mean flow over the zone 41°N. to 50°N. over America at 50 mb. in April, 1952 was westerly of the order of 10 kt.

In the westerlies mean winds are light or moderate but winds of 70 kt. have been observed over the Japanese Main Islands. The maximum wind reported was again at Ocean Weather Ship V in the Pacific where a wind of 270°/100 kt. was recorded, but the resultant wind for this station (based on 41 observations) is only 270°/10 kt.

At 100 mb. the mean contour map for April shows strong winds in many areas and there is also a strong meridional gradient of temperature at 100 mb. As stated in section 3 the method of obtaining the contours of the 60 mb. surface must necessarily give results that are inaccurate in detail, but since this method correctly indicates the weak flow in April, though computed from strong gradients at lower levels, one may confidently expect that the technique will reproduce the main features of the upper flow in temperate latitudes in other months.

Singapore (1°N., 104°E.) (9) and Batavia (6°S., 107°E.) (13) show south-westerly winds at 60 mb. but few observations are available. (The latter observations were by pilot-balloon, six in number, and therefore may not be representative.) Palmer (12, 14) shows that westerlies also occur in a narrow band near the Equator in the central Pacific in April (see reference to Canton Island below).

(ii) Southern Hemisphere

The mean flow is light variable or easterly from 0° to 25°S. The mean wind at Canton Island (ii) in March to May, 1953, was south-easterly, 3 kt., (62 observations) with a standard vector deviation of 26 kt. The "von Berson Westerlies" were thus not apparent over that station at that time. As in January the belt of easterlies may contain stronger mean winds than are indicated.

South of 30°S. the mean flow is westerly and increases in strength poleward at least as far as 55°S.

(c) July (Fig. 3)

(i) Northern Hemisphere

North of about 40°N. mean winds are generally light and vary in direction. South of 40°N. there is a mean easterly stream.

Darling (7) shows that the mean flow over America at 50 mb. in July, 1952 was 15 kt. from an easterly direction in latitudes 41° to 50°N.

/The

The main area of maximum wind speed greater than 50 kt. is associated with the large Asian land mass and lies along the belt of latitude 15° to 20°N. from Khartoum to Hong Kong. The maximum wind velocity observed was 90 kt. from east at Hong Kong (22°N., 114°E.*) and wind speeds of the order of 40 kt. occurred at most stations south of 40°N.

Mironovitch (10) indicates an easterly flow across the meridian of 150°E. in the tropics with a maximum mean speed of 50 kt. at 20°N.

In equatorial regions Nairobi shows easterly and westerly winds of equal frequency with a resultant calm; the maximum wind recorded there was 070°/66 kt. The few observations from Singapore (9) show south-east winds.

(ii) Southern Hemisphere

Between the Equator and 20°S. the flow is probably light and variable.

The mean flow is strong westerly south of about 25°S. increasing southwards to speeds of the order of 70 kt. at 50°S. The maximum wind reported was 270°/110 kt. over the Falkland Islands.

(d) October (Fig. 4)

(i) Northern Hemisphere

As in April the mean flow can be divided naturally into two broad regimes, an easterly flow in the 10°N. to 30°N. zone and a general westerly flow north of 30°N. Both streams are stronger than the corresponding streams in April.

The mean currents are of moderate strength but maximum individual wind speeds of the order of 50 kt. have been recorded over the British Isles and the Japanese Main Islands.

Darling (7) shows that over the U. S. A. in 1952 there was a mean westerly flow of 15 kt. over the region 41° to 50°N. at 50 mb. and a mean westerly flow of 10 to 15 kt. in the zone 31° to 40°N.

The directions of winds observed at 60 mb. over Nairobi are variable. Hay (9) reports a moderate south-westerly flow over Singapore. Palmer (14) says that at 40 mb. (22 km.) there is a light westerly flow between longitudes 150°and 160°E. in the zone 0° to 7°N. but in the observations summarized in Fig. 4 the "von Berson westerlies" are only locally defined at 60 mb. (see also below).

(ii) Souther Hemisphere

Between the Equator and 20°S. winds are probably light variable or easterly. The mean wind at Canton Island in the autumn of 1952 (ii) was 263°/18 kt. (27 observations) with a standard vector deviation of 18 kt. (see above). Over Nandi (Fiji) (4) the mean wind changes from westerly at 60,000 ft. to easterly at 70,000 ft.

/Westerly

* Few observations are available from this station for 60 mb.

Westerly flow exists south of 30°S. increasing in strength southwards to about 50 kt. at 50°S. A maximum wind of 270°/70 kt. was recorded over the Falkland Islands.

5. Variation from year to year

There is evidence that variations occur in the mean flow at 60 mb. from year to year. The largest variations noted occurred during the Northern Hemisphere winter and summer seasons.

Wind speeds in general showed no marked variation from year to year.

The year 1952 showed a more easterly character in winter and early spring over America and the Pacific Ocean and also at Aden, Lagos and Nairobi than did other years.

Winds appear to be less variable from year to year in the Southern Hemisphere but observations are also fewer. In particular, however, the Falkland Islands observations are remarkably persistent in magnitude and in direction; no wind with an easterly component was reported in any month of any year during the period 1948 to 1953.

BIBLIOGRAPHY

1. BROOKS, C.E.P., DURST, C.S., CARRUTHERS, N., DEWAR, D. and SAWYER, J.S. "Upper winds over the world". Geophysical Memoir No. 85, Met. Off., London, 1950.

2. JENKINSON, A.F. "The average vector wind distribution of the upper air in temperate and tropical latitudes". Met. Off. London, Met. Res. Ctee., M.R.P. 823, 1953.

3. CROSSLEY, A.F. "Significance of mean contour charts". Met. Mag. London, 81, 1952, p.229.

4. PORTER, E.M. "Upper winds over Nandi and Auckland". New Zealand Met. Off., Tech. Note No. 92, 1952.

5. PORTER, E.M. "Upper winds over Invercargill". New Zealand Met. Off., Tech. Note No. 94, 1952.

6. - "Mean monthly maps of pressure surfaces over North America". U.S. Air Weather Service, Tech. Report No. 105-107, 1953.

7. DARLING, E.M. "Winds at 100 mb. and 50 mb. over the United States in 1952". Bul. Am. Met. Soc., 34, 1953, p. 458.

8. VENKITESCHWARAN, S.P. "Winds at 10 km. and above over India and its neighborhood". India Met. Dept., Memoirs 28, Part 2, 1950, p. 55

9. HAY, R.F.M. "Winds at high levels over Singapore (1950-1952)". Met. Off., London, Met. Res. Ctee., M.R.P. 770, 1952.

10. MIRONOVITCH, V. "Essai d'une coupe aerologique verticale a travers les deux hemispheres de 0 a 22 Km.". Annales de Geophysique, Tome 9, No. 4, 1953.

11. FARKAS, E. "Upper winds over Canton Island and Trawe." New Zealand Met. Service, Tech. Note No. 115, 1954.

12. PALMER, C.E. "The general circulation between 200 mb. and 10 mb. over the equatorial Pacific." Weather, 9, 1954, p. 341.

13. VAN HEMMELEN, W. "The atmosphere circulation above Australasia according to the pilot-balloon observations made at Batavia". Akademie van Wetenschaffen te Amsterdam, Proceedings of the Section of Sciences, 20, 1918.

14. PALMER, C.E. "The Central Pacific Project". California University, Institute of Geophysics, Contract AF.19(122)-414, 1st Quarterly Report, Appendix A, Oct., 1951. Ibid. Final Report, March, 1953.

15. BRASEFIELD, C.J. "Winds and temperatures in the lower stratosphere". J. of Met., 7, 1950, p.66.

16. AUSTIN, E.E. And DEWAR, D. "Upper winds over the Middle East and Mediterranean". Met. Off., London, Met. Res. Ctee., M.R.P. 811, 1953.

17. SCRASE, F.J. "Radiosonde and radar wind measurements in the stratosphere over the British Isles". Q. J. Roy Met. Soc., II, 1951, p.483.

18. - Ms. data of wind observations at British Home and Overseas Stations, Met. Off., London. (part published for period 1956-50 in Upper Air Data, Met. Off., London, M.O.555 Pts. 1-6.)

/19.

19. - Ms data supplied by the Directors of the respective meteorological services for:

(a) Khartoum (Sudan Met. Office)
(b) Nairobi (Br. East Africa Met. Service)
(c) Hong Kong (Royal Observatory)
(d) Woomera (Australia Met. Service).

20. - "Aerological data for Japan". Central Meteorological Observatory, Tokyo.

21. - Radio sonde data: microfilm records supplied by U. S. Weather Bureau.

22. - Climatological data, National Summary. U.S. Weather Bureau.

23. - "Meteorological Report on the Main Islands of Japan". Met. Off., London, Aviation Met. Report, 27, 1945, M.C.M. 365/27.

24. HOFMEYR, W.L. "A statistical analysis of radar winds over Pretoria in winter". South African Weather Bureau, Notos 1, 1952, p.186.

25. HOFMEYR, W.L. "A statistical analysis of radar winds over Pretoria in summer". South African Weather Bureau, Notos 2, 1953, p.144.

26. CRARY, A.P. "Stratospheric winds and temperatures in low latitudes from acoustical progagation methods". Cambridge, Mass., Air Force Cambridge Research Center, Geophysics Research Directorate, Geophysics Research Paper No. 5, June, 1950.

27. - "Determination of atmospheric winds and temperatures in the 30 to 60 Km. region by acoustical means". Denver University Institute of Industrial Research. Contract AF19(122) - 252. Quarterly Progress Reports No. 2 and 4, 1951.

28. KENNEDY, W.B., BROGAN, L., SIBLE, N.J. and BROWN, R.A. "Atmospheric winds and temperatures to 55 Km. altitude over south-west New Mexico as determined by acoustical propagation studies." University of Denver Research Institute, Scientific Report No.2. Contract No. AF19 (122) - 252, 1953.

29. RICHARDSON, J.M. and KENNEDY, W.B., "Atmospheric winds and temperatures to 50 KM. altitude as determined by acoustical propagation studies". J. Acoustical Soc. of America, 24, 1952, p.731.

30. - Provisional charts of mean height of 100 mb. surface. Met. Off., London. Unpublished.

31. - Provisional charts of mean temperature at various levels. Met. Off., London. Unpublished.

32. - "Climatological Summary, 1951. Eureka N.W.T. Canada". U.S. Weather Bureau.

33. HUTCHINGS, J.W. "A meridional atmospheric cross-section for an oceanic region". J. of Met., 7, 1950, p.94.

34. - A.N.A.R.E. Reports, Series D, Meteorological Vols II, III, IV, 1949-1951. Heard and Macquarie Is., Commonwealth of Australia, Dept. of External Affairs.

35. EDWARDES, H.N. "Measurements of velocity of high-altitude winds at Sydney, N.W.W.". Bul. Am.Met. Soc., 33, 1952, p.56.

36. GABITES, J.F. "Mean westerly flow in the upper levels over the New Zealand region". New Zealand Met. Off., Tech Note No. 38, 1953.

Appendix

(i) Wind data

The chief sources of data of radio- or radar winds employed are:

(a) Northern Hemisphere

1. MS. data for M.O. stations both at home and overseas. (18)
2. MS. data for Nairobi, Lagos, Khartoum and Hong Kong. (19)
3. Data for stations in Japanese Main Islands. (20)
4. Data for the Pacific islands received in microfilm by courtesy of the Chief of the United States Weather Bureau. (21)
5. Data for the U.S.A. (22)
6. Data for mean winds over zones 31°N.-40°N. and 41°N.-50°N. at 50 mb. over America. (7)
7. Data from Nemuro and Nagasaki. (23)

(b) Southern Hemisphere

1. MS data for the Falkland Islands. (18)
2. New Zealand Technical Notes Nos. 92, 94. (4,5)
3. Mean winds over Pretoria (26°S., 28°E.). (24, 25)
4. Observations at Sydney, N.S.W. (35)
5. Deduced mean winds over New Zealand. (36)
6. MS. data for Woomera (double theodolite observations on pilot-balloons). (19)

Where no radar wind data were available, use was made of:

(i) pilot balloon data
(ii) high altitude winds derived from accustical propagation studies.

Pilot balloon observations are mainly for India and its neighbourhood (8) and for Batavia in Java. (13)

Acoustical propagation results were used for the American stations Canal Zone (9°N., 77°W.), Florida (28°N.,82°W.), Denver (40°N., 105°W.) and Wray (40°N., 102°W.).(26, 27, 28, 29)

(ii) Contour height data

1. Preliminary 100 mb. circumpolar charts north of 55°N., and Mercator charts for the region 70°N. to 50°S. (30)
2. Contour charts over North America (4 year mean values 1947-1951). (6)
3. Stream line and isotach charts given by Jenkinson. (2)

(iii) Temperature data

1. Average temperature charts over the world. (31)
2. MS. data of British home stations.
3. MS. data of British overseas stations and the Falkland Islands
4. Temperature data for North America. (6)
5. Data for Eureka (80°N., 85°W) in Canada. (32)
6. Data for Auckland, Norfolk Is. (28°S., 168°E.) and Hokitika. (33)
7. Data for Heard Is. and Macquarie Island. (34)

Table I Wind observing stations

R = Radio- or radar- wind
P = Pilot-balloon
A = Accoustic determination

Station	Position	Type	Period of available data
North of 60°N.			
Narssarssuak	61°N. 45°W.	R	July, 1941-January 1942.
Lerwick	60°N. 1°W.	"	1948-April, 1953
30°N.-60°N.			
America			
American Zone (1)	31°N.-40°N.	"	1952
" " (2)	41°N.-50°N.	"	1952
Spokane	48°N. 118°W.	"	1950-53.
Caribou	47°N. 68°W.	"	"
Bismark	47°N. 101°W.	"	"
St. Cloud	46°N. 94°W.	"	"
Rapid City	44°N. 103°W.	"	October, 1945-January 1946; 1948-July, 1950.
Omaha (Nebr.)	41°N. 96°W.	"	July, 1938.
Wray (Col.)	40°N. 102°W.	A	July, 1950-April, 1951
Denver	40°N. 105°W	A	January, 1951
Grand Junction	39°N. 109°W.	R	1950-53
Washington	39°N. 77°W.	"	"
Nashville	36°N. 87°W.	"	"
Greenboro'	36°N. 80°W.	"	"
Oklahoma	35°N. 98°W.	"	"
Hatteras	35°N. 76°W.	"	"
Albuquerque	35°N. 107°W.	"	"
Santa Maria	35°N. 120°W.	"	"
Little Rock	35°N. 92°W.	"	"
Charleston	33°N. 80°W.	"	"
Big Spring	32°N. 101°W.	"	"
British Isles Area			
O.W.S. "I"	59°N. 19°W.	"	1951-52
Stornoway	58°N. 6°W.	"	1951-April, 1953
Leuchars	56°N. 3°W.	"	" "
Aldergrove	55°N. 6°W.	"	" "
Hemsby	53°N. 2°E.	"	" "
O.W.S. "J"	53°N. 20°W.	"	1951-52.
Larkhill	51°N. 2°W.	"	1951-April, 1953
Camborne	50°N. 5°W.	"	"
Mediterranean and Middle East			
Gibraltar	36°N. 5°W.	"	1948-April, 1953
Malta	36°N. 14°E.	"	"
Nicosia	35°N. 33°E.	"	"
Habbaniya	33°N. 44°E.	"	"
Benina	32°N. 20°E.	"	"
Japan			
Nemuro	43°N. 146°E.	-	from isopleths of height.
Wajima	37°N. 137°E.	R	1951-53
Tateno	36°N. 140°E.	"	"
Yonago	35°N. 133°E.	"	"
Shionomisaki	33°N. 136°E.	"	"

/Nagasaki

Station	Position	Type	Period of available data
Nagasaki	33°N. 130°E.	-	from isopleths of height
Kagoshima	32°N. 131°E.	R	1951-53
Pacific			
O.W.S. "N"	33°N. 135°W.	"	1951-52
O.W.S. "V"	31°N. 164°E.	"	"
10°N.-30°N.			
America			
San Antonio	30°N. 98°W.	"	1950-53
Burrwood	29°N. 89°W.	"	"
Florida	28°N. 82°W.	A	January, 1951
Brownsville	26°N. 97°W.	R	1950-53
Miami	26°N. 80°W.	"	"
Havana	23°N. 82°W.	"	1951
San Juan	18°N. 66°W.	"	1950-53
Arabia, Sudan			
Bahrain	26°N. 51°E.	"	1948-April 1953.
Khartoum	16°N. 33°E.	"	April, 1953-January, 1954
Aden	13°N. 45°E.	"	1948-April, 1953
Pacific			
Midway Island	28°N. 177°W.	"	1951-52,
O.W.S. "U"	28°N. 145°W.	"	"
Okinawa	26°N. 127°E.	"	"
Iwo Jima	25°N. 141°E.	"	"
Marcus Island	24°N. 154°E.	"	1951-53
Hong Kong	22°N. 114°E.	"	1951-52
Lihue Kauai	22°N. 159°W.	"	"
Hilo	20°N. 155°W.	"	"
Wake Island	19°N. 167°E.	"	"
Johnston Island	17°N. 170°W.	"	July, 1951-52
Clark Field	15°N. 121°E.	"	1951-52
Guam	14°N. 145°E.	"	"
Eniwetok	11°N. 162°E.	"	"
10°N.-10°S.			
Albrook Field	9°N. 80°W.	"	1951.
Canal Zone	9°N. 80°W.	A	January, 1950
Kwajalein	9°N. 168° E.	R	1951-52.
Kusaie	5°N. 163° E.	"	1951-52
Lagos	7°N. 3°E.	"	1952, 1953 (except July), January, 1954.
Nairobi	1°S. 37°E.	"	1948-April, 1953
Singapore	1°N. 104°E.	"	October, 1950-July, 1952.
Batavia	6°S. 107°E.	P	1909-1917
10°S-60°S.			
Pretoria	26°S. 28°E.	R.	April-September 1952; October, 1952-March, 1953.
Nandi	18°S. 177°E.	"	October, 1945-July, 1952.
Woomera	31°S. 138°E.	P(Double)	July, 1950-October, 1954.
Auckland	37°S. 175°E.	R	1943-1951.
Hokitika	43°S. 171°E.	"	October, 1944-1950.
Invercargill	46°S. 168°E.	"	July, 1951-October, 1952
Falkland Is.	52°S. 58°W.	"	1948-April, 1953.

Table 11

Vector mean winds at 60 mb. for mid-season months

Station	January				April				July				October			
	Direction (degrees)	Speed (kt.)	No. of obs.	Max. wind	Direction (degrees)	Speed (kt.)	No. of obs.	Max. Wind	Direction (degrees)	Speed (kt.)	No. of obs.	Max. wind	Direction (degrees)	Speed (kt.)	No. of obs.	Max. wind
North Pacific																
Yakutat					(270)	(20)	(3)		-	Calm	37		(285)	(10)	(8)	
Lorick	270	35	31	270/70	280	15	57	270/50	-	Calm	94	120/15	265	15	78	270/50
Canada																
Alaska																
American Zone (1)*	W.	-	-		-	10	265		E.	20	598		W.	15	435	
American Zone (2)*	W.	-	-		-	10	163		E.	15	151		W.	15	168	
Spokane	-	-	-		-	-	-		-	-	-		295	5	39	
Salem	-	-	-		-	5	13		-	-	-		-	-	-	
Klamath	-	-	-		-	5	10		-	-	-		-	-	-	
Mt. Cloud	-	-	-		-	Calm	37		-	-	-		300	10	18	
Rapid City	(130)	(17)	(3)		-	15	11		110	10	12		335	5	10	
Omaha	-	-	-		-	-	-		050	5	22		-	-	-	
Grand Junction	-	-	-		-	-	-		085	15	23		320	15	11	
Washington	-	-	-		270	10	24		080	15	42		253	10	20	
Ft. Wolde	-	-	-		-	-	-		080	15	23		-	-	-	
Fredericton	-	-	-		-	-	-		085	15	31		265	20	10	
Nitchika	-	-	-		-	-	-		080	20	33		275	5	26	
Yellowknife	-	-	-		-	-	-		075	20	22		280	5	14	
Albuquerque	-	-	-		-	-	-		085	30	35		015	5	22	
El Paso Intnl	-	-	-		270	5	29		090	20	61		045	5	57	
Ft. Worth	-	-	-		-	-	-		085	20	26		-	-	-	
Del Rio	-	-	-		-	-	-		085	20	44		190	5	27	
Big Spring	-	-	-		-	-	-		085	25	31		-	-	-	
North Atlantic																
U.S.N.A.S.	(270)	(25)	(7)	270/30	(270)	(10)	(5)	210/35	255	5	45	270/15	(235)	(15)	(8)	240/25
Stornoway	300	35	16	270/70	270	20	21	270/50	-	(Calm)	(7)	060/15	235	5	11	210/25
Lerwick	295	35	16	290/50	280	20	36	270/50	-	Calm	46	090/25	285	10	48	270/50
Aldergrove	(270)	(20)	(2)	310/25	270	20	52	270/50	-	Calm	30	090/15	265	10	23	270/25
Belfast	295	30	10	290/70	290	15	50	260/50	-	Calm	75	090/25	305	10	70	290/25
U.K.M.O. 161	275	35	28	270/70	265	5	18	270/25	-	Calm	25	300/15	295	10	16	300/25
Larkhill	290	30	33	270/70	290	5	70	270/50	095	5	128	090/25	280	10	98	300/50
Benbecula	(295)	(25)	(6)	300/50	275	10	27	270/35	-	Calm	34	120/25	270	10	34	270/25

Zone 1 mean winds Zone (1) 41-50°N; Zone (2) 31-40°N. Mediterranean -

Station	January				April				July				October			
	Direction (degrees)	Speed (kt.)	No. of obs.	Max. wind	Direction (degrees)	Speed (kt.)	No. of obs.	Max. wind	Direction (degrees)	Speed (kt.)	No. of obs.	Max. wind	Direction (degrees)	Speed (kt.)	No. of obs.	Max. wind
Mediterranean - Middle East																
Gibraltar	295	15	73	270/50	265	10	93	270/35	100	5	91	270/35	285	5	97	090/50
Malta	275	25	33	270/50	270	15	54	240/50	145	5	66	210/35	270	10	30	240/35
Nicosia	265	45	13	270/70	270	15	62	270/50	135	10	69	180/50	245	15	67	270/50
Habbaniya	235	35	15	240/70	260	15	71	240/50	105	15	77	120/35	275	10	37	270/35
Benina	(270)	(30)	(5)	270/50	285	10	21	300/35	110	15	60	090/35	2[illegible]	10	37	270/35
Japan - W. Pacific																
Naha/	260	15	"	"	090	45	"	"	"	"	"	"	"	"	"	"
Iwojima	"	"	"	"	"	(Calm)	(5)	290/15	E.	35	11	090/35	(W)	(15)	(7)	280/30
Tateno	(SW.)	(35)	(3)	265/60	(W.)	(20)	(7)	275/30	E.	20	37	200/30	"	Calm	16	255/60
Yonago	"	"	"	"	(SW.)	(5)	(1)	"	"	Calm	13	070/40	"	Calm	14	270/50
Shionomisaki	(W.)	(30)	(1)		(W.)	(20)	(1)		E.	30	11	065/40	(035)	(10)	(9)	
Nagasaki/	270	50	"	"	270	15	"	"	"	"	"	"	"	"	"	"
Kagoshima	"	"	"	"	(NW.)	(20)	(1)		E.	25	13		(W.)	(35)	(2)	230/40
O.W.S. 'V'	(280)	(139)	(2)	290/150	270	10	41	270/100	(095)	(35)	(4)	110/50	300	5	25	270/50
O.W.S. 'N'	"	"	"	"	259	11	10	340/40	083	17	17	090/30	244	10	24	270/60
10°-30°N. America																
San Antonio	"	"	"	"	"	"	"		085	25	56		025	5	12	
Burrwood	"	"	"	"	"	"	"		080	25	45		065	10	29	
Brownsville	"	"	"	"	"	"	"		095	30	34		090	10	11	
Miami	"	"	"	"	"	"	"		080	35	23		100	15	10	
Havana	280	5	19	360/50	(090)	(10)	(5)	110/20	091	34	25	090/48	093	12	33	090/40
San Juan	280	5	33		100	5	33		080	35	37		085	15	53	
Arabia, Sudan																
Bahrain	(275)	(30)	(4)	270/50	255	5	31	270/35	090	45	71	090/50	-	Calm	44	(090) 270/25
Khartoum	260	5	14	240/35	275	5	11	270/25	075	50	17	090/50	100	15	20	090/35
Aden	-	Calm	30	270/25	250	5	49	090/35	090	50	30	090/70	075	10	45	090/50

/Pacific

/ Computed winds (23)

C.22929(d)/PN/6/55/50

Table II (Cont.)

Station	January				April				July				October			
	Direction (degrees)	Speed (kt.)	No. of obs.	Max. wind	Direction (degrees)	Speed (kt.)	No. of obs.	Max. wind	Direction (degrees)	Speed (kt.)	No. of obs.	Max. wind	Direction (degrees)	Speed (kt.)	No. of obs.	Max. wind
Pacific																
Midway	[illegible]	2	27	130/30	313	5	60	360/44	090	[illegible]	10[illegible]	090/56	[illegible]71	[illegible]	7[illegible]	[illegible]70/[illegible]
[illegible] Is.	"	"	"		292	14	22	250/44	090	19	2[illegible]	250/[illegible]	[illegible]09	[illegible]	[illegible]3	[illegible]4/[illegible]
Okinawa	"	"	"		286	9	15	270/34	087	25	[illegible]	[illegible]10/[illegible]5	2[illegible]	[illegible]	2[illegible]	[illegible]3/[illegible]
Iwo Jima	"	"	"		280	5	10	090/20	(084)	(35)	[illegible]	090/50	"	[illegible]	[illegible]4)	[illegible]5/[illegible]
Marcus Is.	"	(Calm)	(9)	090/20	(050)	(10)	(8)	040/20	(095)	(30)	[illegible]2)	[illegible]0/[illegible]0	[illegible]10	[illegible]6	1[illegible]	060/[illegible]
[illegible]ware Kanal	043	3	20	110/52	345	3	5[illegible]	070/26	090	33	[illegible]6	[illegible]60/[illegible]2	[illegible]57	[illegible]1	[illegible]5[illegible]	[illegible]90/[illegible]2
Hilo	348	6	30	350/36	29[illegible]	5	63	315/40	092	36	96	[illegible]90/[illegible]8	[illegible]09[illegible]	[illegible]6	[illegible]9[illegible]	[illegible]70/[illegible]5
[illegible]	[illegible]5	[illegible]4	[illegible]2	[illegible]40/[illegible]2	[illegible]0[illegible]	[illegible]0[illegible]	[illegible]7[illegible]	[illegible]20/[illegible]6	[illegible]8[illegible]	[illegible]8[illegible]	[illegible]9[illegible]	090/62	086	17	[illegible]6	[illegible]5/[illegible]2
Johnston Is.	065	5	15	110/35	(280)	(10)	(8)	295/70	(095)	(25)	(8)	090/44	093	14	4[illegible]	125/[illegible]3
Guam	081	4	32	070/24	"	"	"		097	37	10	[illegible]30/[illegible]6	[illegible]07	[illegible]1	[illegible]5[illegible]	110/62
Clark Field	260	2	43	090/32	081	7	33	090/32	091	43	22	090/74	094	20	4[illegible]	120/50
Eniwetok	"	"	"		"	"	"		093	41	42	090/70	102	16	1[illegible]	[illegible]10/[illegible]3
[illegible]0°N. - 10°S.																
[illegible]brook Field	[illegible]0[illegible]	[illegible]5	[illegible]7	[illegible]70/[illegible]4	[illegible]0[illegible]	[illegible]	[illegible]3	[illegible]0/[illegible]2	[illegible]0[illegible]	[illegible]7	[illegible]8	090/72	[illegible]0[illegible]	[illegible]3	[illegible]6[illegible]	[illegible]05/[illegible]5
Kwajalein	"	"	"		279	3	20	170/16	"	"	"		[illegible]05	[illegible]5	[illegible]3[illegible]	[illegible]90/[illegible]5
Nusaie	"	"	"		274	9	19	250/38	"	"	"		[illegible]09	[illegible]5	[illegible]3[illegible]	070/60
[illegible]agos	055	5	14	300/35	250	5	11	270/20	k(070)	(30)	[illegible]1)	090/35	075	15	3[illegible]	[illegible]90/[illegible]5
[illegible]ntsal	085	16	53	090/70	"	Calm	31	090/50	"	Calm	49	070/66	[illegible]75	[illegible]3	[illegible]5	080/35
10°S. - 60°S.																
Pretoria[a]	E.	20	64	090/40	"	"	"		Var.	15	30	[illegible]10/[illegible]5	"	"	"	
Wendl	095	15	192		(145	5	99		(245	5	112		(2[illegible]	[illegible]	[illegible]0[illegible]	
					*(095	20	42		("	Calm	41		*([illegible]	[illegible]	2[illegible]	
Woomera	*(280	12	24		*(287	11	20		*(26[illegible]	18	24		*([illegible]	[illegible]	[illegible]7	
	(079	2	24		(211	1	20		(262	5	24		([illegible]	15	[illegible]7	
Auckland	*(270	5	79		*(285	20	55		("	"	"		("	Calm	[illegible]0	
	(090	10	26		(335	5	31		(260	20	73		(090	16	[illegible]8	
Hokitika	E.	5	"		W.	15	"		W.	15	"		W.	[illegible]0	"	
Invercargill	*(290	10	11		280	20	36		270	35	58		*([illegible]7	[illegible]1	[illegible]2	
	(060	5	11		"	"	"		"	"	"		[illegible]	Calm	41	
Falkland Is.	260	20	21	270/50	265	15	17	270/[illegible]	260	7[illegible]	11	270/110	260	[illegible]2	[illegible]7	270/40

a The two values concerned are the mean wind at 60,000 ft. and 70,000 ft. respectively.

k 65,000 ft. wind for July at Lagos.

a Half-yearly mean resultant winds (24, 25)

() Next highest 225/52

Table IIIA

Frequency of wind direction at 60 mb.

	Station	30	60	90	120	150	180	210	240	270	300	330	360	Calm	No. of obs.
								January							
North of 60°N.	Lerwick							2	6	6	4	2	1	4	25
30°- 60°N.															
British Isles Area	O.W.S. 'I'								3	3	1				(7)
	Stornoway								1	8	3	2	2		16
	Leuchars								1	6	4	5			16
	Aldergrove								1		1				(2)
	Kersay								1	4	3	2			10
	O.W.S. 'J'							4	5	11	5	3			28
	Larkhill								4	12	7	8		2	33
	Camborne								1	1	3	1			(6)
Mediterranean - Middle East	Gibraltar						1		1	17	25	12	5	11	73
	Malta								3	17	9	1		3	33
	Nicosia								3	9	1				13
	Habbaniya								3	10	2				15
	Benina								1	3	1				(5)
10°- 30°N.	Bahrain									3	1				(4)
	Khartoum					1		1	1	2		1	1	7	14
	Aden		2	1	1	2	1			3	2		3	15	30
10°N-10°S.	Nairobi	1	9	11	8			2	5	6	3	1	1	3	53
South of 10°S.	Falkland Is.							3	6	8	2	2			21

/April

	Station	30	60	90	120	150	180	210	240	270	300	330	360	Calm	No. of obs.
							April								
North of 60°N.	Lerwick					1		5	4	13	10	4	1	19	57
30°- 60°N.															
British Isles Area	O.W.S. 'I'					1		1		1				2	(5)
	Stornoway							2	1	5	7	3		3	21
	[illegible]							1	5	13	5	6		8	38
	[illegible]								12	13	7	12		6	50
	[illegible]								8	12	6	12	4	15	57
	O.W.S. 'J'									3	3	1	1	10	18
	[illegible]	2	1	1	4	1		1	2	9	4	5	3	37	70
	Cambborne					1		1	4	5	1	3	1	11	27
Mediterranean - Middle East	Gibraltar			1		1	1	3	18	31	19	2	1	16	93
	Malta						1	3	10	13	9	5	1	4	54
	Nicosia							1	14	14	13	4		16	62
	Habbaniya	1						7	17	17	6	3		20	71
	Benina								1	6	3	1		10	21
10°- 30°N.															
	Bahrain		3		1			2	4	4	1			16	31
	Khartoum			1		1				2			1	6	11
	Aden	1	1	12	3	2	2	3		3	3			19	49
10°N-10°S.	Nairobi	1	1	6	4		1		2	5	3	4		4	31
South of 10°S.	Falkland Is.						1	1	7	6	2				17
							July								
North of 60°N.	Lerwick	4	1	3	7		2		1			1	2	73	94

/30°-60°N.

Table IIIA (Cont.)

	Station	30	60	90	120	150	180	210	240	270	300	330	360	Calm	No. of obs.
							July (Cont.)								
30°-60°N.															
British Isles	O.W.S. 'I'						1	1	4	6	2			31	45
Area	Stornoway		1							1				5	(7)
	Devonport	2	1	2	1	1	1	1	1	2	1	1		32	46
	Aldergrove	1	1	4	2	2		1	1	1	1			18	30
	Hemsby		4	10	2				1	1	2	1		54	75
	O.W.S. 'J'	1								2	4	1		17	25
	Lerwick	3	3	15	6	2	1	2	3	2	2		2	87	126
	Camborne		3	4	2		1		1	1				24	34
Mediterranean -	Gibraltar	3	13	20	15	7	3	2	2	4	1	1	1	19	91
Middle East	Malta	1	2	5	10	7	4	8		2	1	2		20	66
	Nicosia		2	15	17	6	5	3	3	1	1			15	69
	Habbaniya	1	6	24	28	5	2	1						9	76
	Bedina		3	16	28	3		1						7	50
10°-30°N.															
	Bahrain			68	3										71
	Khartoum		9	8											17
	Aden			27	2										29
10°N.-10°S.															
	Nairobi		4	10	3	3	2		10	10	2	2	1	3	45
South of 10°S.															
	Falkland Is.							1		10					11
							October								
North of 60°N.															
	Lerwick						1	10	20	19	15	3		10	78

/30°-60°N.

Table IIIA (Cont.)

	Station	30	60	90	120	150	180	210	240	270	300	330	360	Calm	No. of obs.
							October (Cont.)								
30°-60°N.															
British Isles Area	O.W.S. 'I'						1	2	3	1		1			(8)
	Stornoway							2	2			1		1	11
	Leuchars							1	3	11	1	5		1	42
	Aldergrove							3	3	4		1		6	33
	Hemsby	1			1				1	6	4	8	2	12	39
	O.W.S. 'J'								1	1	4	1		3	10
	Lerwick						1	1	15	20	16	11	2	8	75
	Camborne							2	6	5	6	2		15	34
Mediterranean - Middle East	Gibraltar	1	4	3		1		2	6	20	15	4	3	36	97
	Malta							4	17	13	12	4		20	80
	Nicosia	1					1	3	25	12	7	5		9	67
	Habbaniya		1	1	1	1		1	1	12	6	1		12	37
	Sarafand	1	1					1	4	10	2			16	37
10°-30°N.															
	Khartoum		1	9		1		1	1	5	3			22	43
	Khartoum			3	5									7	20
	Aden	2	6	11	1								1	22	45
10°N.-10°S.	Nairobi	5	5	7	3	2	1	1	10	14	8	1	1	14	65
South of 10°S.	Mahé							1	4	10	2				17

Table III.b

Frequency of wind direction at 60 mb.

Directions - 16 point compass

	Station	1	2	3	4	5	6	7	8	9	10	11	12	13	14	15	16	Calm	No. of obs.	Max. velocity	
										January										Dir.	Kt.
30°-60°N.	O.W.S. 'V'												1	1					(2)	290	150
	O.W.S. 'N'										1	2	2					3	(9)	340	30
10°-30°N.	Midway Is.			3	3	2	2	1	1			2	1	2	1	1		8	27	130	30
	O.W.S. 'U'												2	1	1	1	2		(7)	290	40
	Havana			1	1	1		1			1	3	3	2			1	5	19	360	50
	Lihue Kauai	1	1	2		2					1		1	1	1		1	5	20	110	52
	Hilo	2	2	2	1				1			1	4	2	3	5	4	14	39	330	38
	Wake Is.		2	1	2	3		4	5		2		2	1		1		9	32	135	22
	Johnston Is.					1										1	1	12	15	110	35
	Clark Fld.		1	1	2					1	1	3	5	2		1		26	43	090	32
	Guam		1	5	5	3	3	2			2	2		2	2	2	1		32	070	24
	Eniwetok																	2	(2)		
10°N.-10°S.	Albrook Fld.	1	1	1	1		1	1	1	1	1	4	10	10	2	2	1	8	45	270	30
	Kwajelein										1					1	1	1	(6)	360	20
										April											
30°-60°N.	O.W.S. 'V'	2	1							1	2	4	6	3	4	1		17	41	270	100
	O.W.S. 'N'	1					1					2	2	1		1	1	1	10	340	40
10°-30°N.	Midway Is.	4	2		7	5	1	1			4	2	4	12	1	2	8		60	360	34
	O.W.S. 'U'	1										4	3	1	3	3	1	6	22	250	44

/Okinawa

Station	Hr.	0	1	2	3	4	5	6	7	8	9	10	11	12	13	14	15	16	17	18	19	20	21	22	23	Mean Velocity	Mean Dir.
Oroluk																										15	090
Ponape																										(6)	
Kusaie																										50	
Majuro Atoll																										22	070
Palau																										77	315
Wake																										(8)	320
Johnston Is.																										33	247
Clark Fld.																										(4)	310
Guam																											
Enewetak																										11	040
Albrook Fld.																										25	135
Kwajalein																										20	270
Kusaie																										19	250
C.W.S. V'																										(4)	130
O.W.S. N'																										17	070
Midway Is.																										100	090
O.W.S. U'																										26	090
Oroluk																										25	110
Hawaii																										25	090
Lihue Kauai																										76	070
Hilo																										96	090
Wake Is.																										95	090
Johnston Is.																										(9)	090
Clark Fld.																										22	090
Guam																										18	090

Andersen

(C-2229(1)/PW/55/50

Table IIIB(Cont.)

	Station	1	2	3	4	5	6	7	8	9	10	11	12	13	14	15	16	Calm	No. of Obs.	Mean velocity Dir.	Mean velocity Kt.
									July (Cont.)												
10°-30°N.																					
10°N.-10°S.	Eniwetok			3	31	5	1											1	42	090	70
	Albrook Fld.			3	14	6	1											1	24	090	72
	Kwajalein		1		1	1													(3)	050	30
									October												
30°-60°N.																					
	O.W.S. 'V'	2	1	3	1				2		1	1	2	2	1	1	1	7	25	270	50
	O.W.S. 'N'			1		1	1		1	2	1	4	3		2	2		8	24	270	60
10°-30°N.																					
	Midway Is.	3	5	8	5	6	1		2	1		1	2	1	3		1	34	74	270	24
	O.W.S. 'U'		1	1	1										1	1		8	13	315	48
	Okinawa			3	2	2	1		1	1	1	—	2	1		1		10	29	250	96
	Havana	1		4	13	2	2	1	1									9	33	090	40
	Lihue Kauai		3	6	17	5	2				3		1				2	14	55	070	32
	Hilo	1	5	17	33	22	2	1										15	96	110	32
	Wake Is.		4	17	23	12	3	1										6	66	090	42
	Johnston Is.		1	8	11	4	2											15	41	135	50
	Clark Fld.		1	4	25	7	1											6	44	120	56
	Guam		2	11	13	13	3	2	1					1			1	8	55	110	82
	Eniwetok			3	4	3			1									3	14	110	58
10°N.-10°S.	Albrook Fld.		2	7	14	8	3	2	1		1	1	2		1	1		17	60	090	46
	Kwajalein		2	2	14	8	2		1	1	1	1	2			1			35	090	50
	Kusaie	3	7	15	14	4	1											6	50	070	60

Fig 1

MEAN WIND FLOW AT 60 mb JANUARY

N.R.P. 935

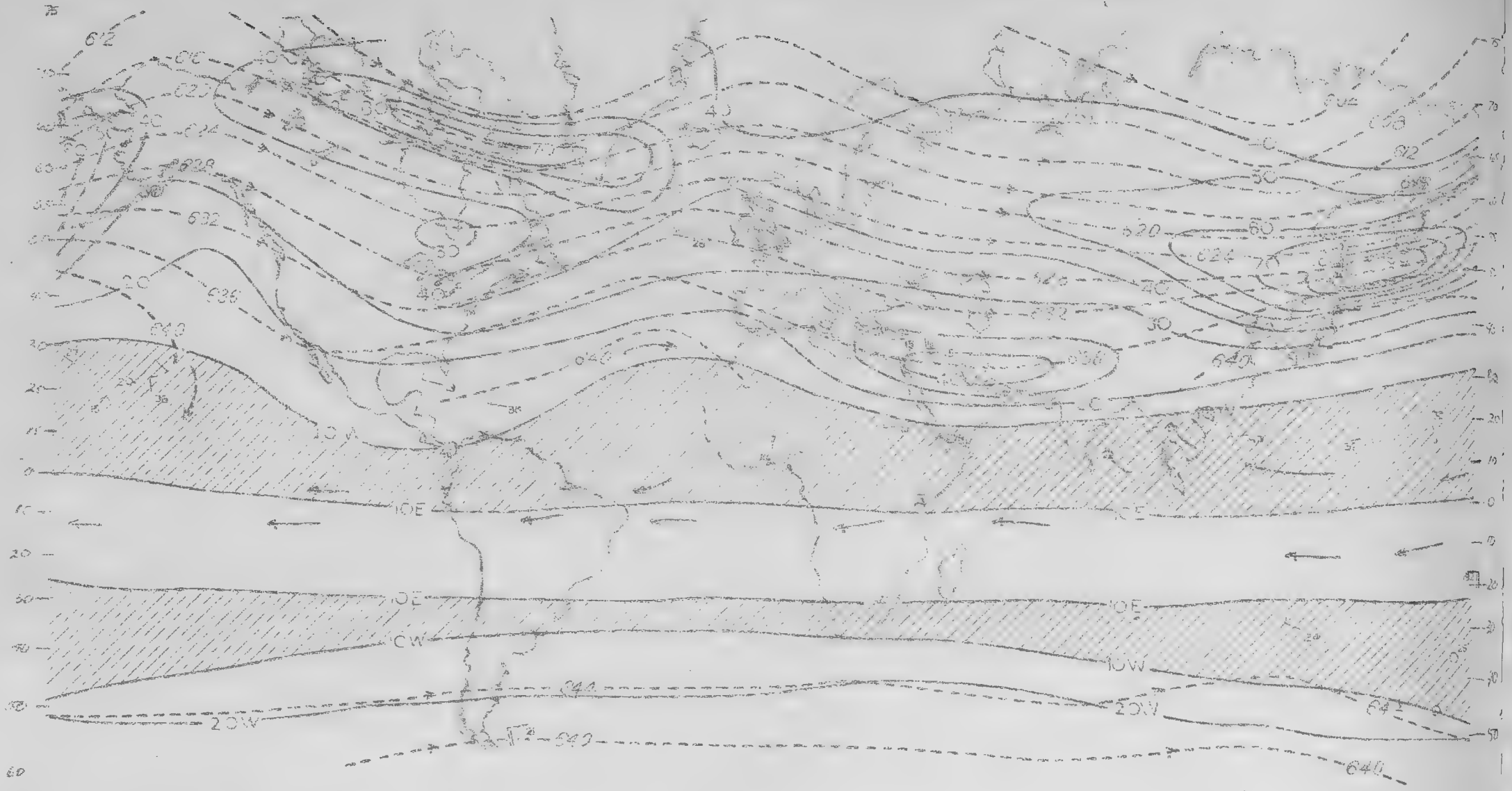

Fig. 2 MEAN WIND FLOW AT 60 mb. APRIL MAP 925

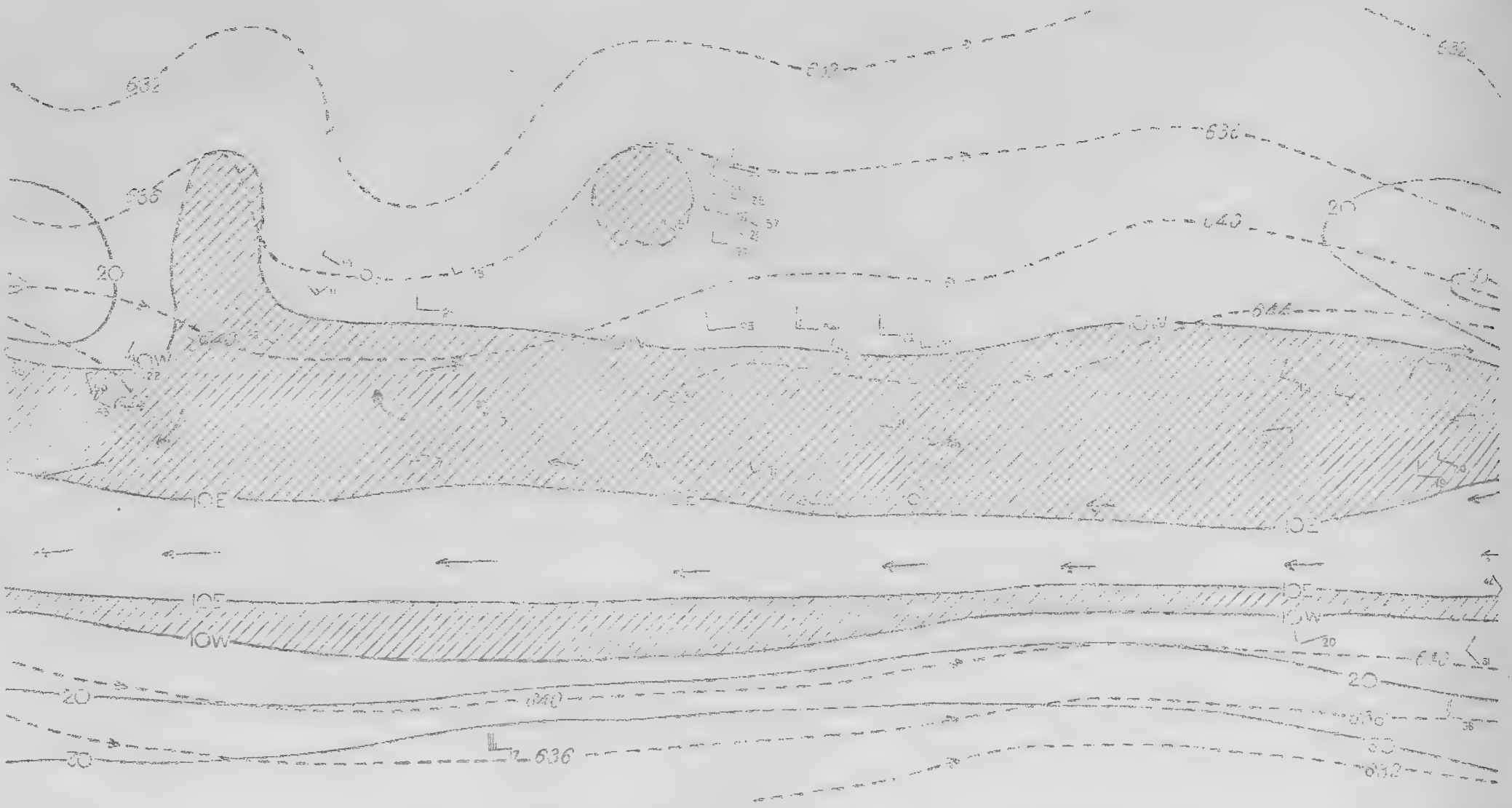

Fig. 3

MEAN WIND FLOW AT 60 mb. JULY

M.R.P. 925

Fig. 4

MEAN WIND FLOW AT 60 mb OCTOBER

M.R.P. 928
S.C. 1/102
8th August 1955

Radar wind comparisons on the Ocean Weather Ships (second series)

by

D. N. HARRISON
(Meteorological Office)

AIR MINISTRY
METEOROLOGICAL RESEARCH COMMITTEE

At the time of issue this report has not been published. Any author desiring to quote this paper should refer to it as "A paper of the Meteorological Research Committee (London).
M.R.P. No. 928 by Dr. D.N. Harrison.
A copy is available in the Library of the Meteorological Office."

M.R.P. 928
S.C. I/102
8th August, 1955

AIR MINISTRY

METEOROLOGICAL RESEARCH COMMITTEE

Radar wind comparisons on the Ocean Weather Ships (second series)

by D.N. Harrison (Meteorological Office)

Summary

A repetition of the trials made in 1949 (MRP 508) shows a small but definite improvement in the systematic and random errors of range and in the mean vector difference of wind measurement between two ships. Azimuth and elevation errors are about the same as before.

1. Introduction

Since MRP 508 was written attempts have been made to improve the accuracy of the radar wind observations in the Ocean Weather Ships. Improvement was sought in three directions, (1) in the observational drill, (2) in the standard of maintenance of the equipment, (3) by modification of the equipment. In the case of (1) and (2) it was realized that there were no obvious defects and that progress could only be made by attention to details. In the case of (3) it was found that appreciable improvement could only be expected from major changes which it was impracticable to make; the only feasible modifications were minor ones relating to the range display, and a list of the modifications made is given in the Appendix.

In order to test the success of these attempts, a second series of comparisons was made at sea. The methods of observation and computation were the same as those described in MRP 508. The results are given in Tables I, III and IV, corresponding to Tables I, III and IV of MRP 508. In Table I, where signs are given they represent, as before, the differences obtained by subtracting the readings of the ship named second from those of the ship named first, e.g. Watcher minus Explorer. The approximate elevation angles near the beginning and end of each ascent have been added. Table II gives the state of the sea, and remarks where observations are missing.

2. Radar readings: systematic differences

Considering first the mean differences (Table I, columns 6-10), it will be seen that whereas in 1949 differences of range up to more than 2,000 yards were found, they are now not more than about 500 yards, while the azimuth and elevation differences are about the same as before. There is a tendency for a given pair of ships to show systematic differences of the same sign on successive occasions. The azimuth differences are naturally reflected in differences of wind direction.

3. Radar readings: random differences

The mean deviations (Table I, cols. 11 and 12) are practically the same as before. These, however, as explained in MRP 508, are not a good measure of the scatter which is chiefly responsible for errors in wind measurement, on account of the existence of long-period changes or drift. A better measure is the average change, without regard to sign, between successive observations, of the difference between the two ships' readings. These are shown in cols.

/13-15.

13-15. The value for range has improved from 190 yds. in 1949 to 100 yds. in the present series, while the values for azimuth and elevation are practically unchanged at 0.9° and 0.5° respectively. If the observational errors are proportional to these figures, the contribution of the angular errors to the vector wind error is considerably greater in general than that of the range error, so that the improvement to be expected in wind measurement is small.

4. Vector differences of wind measurement

Table III should be compared with Table III of MRP 508. There has been a small improvement, the mean of 392 values being 6.8 knots (7.4 kt.in 1949), or, giving equal weight to each ascent, 6.9 kt. (7.3 kt.in 1949). The improvement is found at every level except 1,000 ft. and 2,000 ft., where the mean differences are now much greater than before. The reason for the large values at these low levels is not known. In both series the mean vector difference increases from the lower levels to a maximum at about 30,000 - 40,000 ft., and tends to decrease above this height; this decrease may not, however, be genuine, as the data are far from homogeneous, the number of ascents reaching high levels falling off rapidly. There is no obvious explanation of the very large differences which occur in individual measurements, including one of 50 knots.

The frequency distribution is shown in Table IV, and is practically the same as that given in Table IV of MRP 508. 46 per cent of the differences lie in the range 0-4 kt. (i.e. less than 4.5 kt.) and 89 per cent in the range 0-14 kt. (less than 14.5 kt.). In 1949 the percentages were 46 and 90.

There is no connexion between the mean vector difference for an ascent and the state of the sea. Both the highest and the lowest difference occur on an ascent when the sea was slight, while for sea rough and moderate-rough the differences are quite small. There is a tendency for calm or slight sea to be associated with high elevations in the early stages of an ascent, which may cause loss of observations, since the radar aerials are limited to an elevation of about 70°.

The trials were organized and most of the computation for this paper was done by Mr. R.F.M. Hay and the staff of the Marine Branch of the Meteorological Office. A high standard of care and accuracy is shown in the observations by the staff of the ships; there is a remarkable absence of gross errors of reading of the kind which would be revealed in the computation, and the results probably represent the best that the equipment is capable of giving.

References

Harrison, D.N. 1949 Meteorological Research Papers, Air Ministry, London. No. 508.

Table I. Difference of Radar readings

1 Ascent No.	2 Date	3 No. of obs.	4 Range 1000's yds.	5 Approx. elev. min. 5	5 Approx. elev. end	6 Mean difference Range (yds.) First 5	7 Mean difference Range (yds.) Last 5	8 Mean difference Range (yds.) Mean	9 A 0	10 E 0	11 Mean deviation A 0	12 Mean deviation E 0	13 Mean change between successive obs. R yds.	14 Mean change between successive obs. A 0	15 Mean change between successive obs. E 0
WATCHER - EXPLORER															
2	25. 4.53	31	8-53	41	22	- 50	-910	-460	+1.7	+1.5	1.1	0.5	110	0.4	0.4
20	31. 7.54	44	1-43	34	29	+460	+650	+410	-4.8	-3.1	1.0	0.4	100	0.5	0.3
26	23.10.54	42	4-55	38	19	- 70	-800	-420	-0.3	-2.0	1.9	0.7	150	0.9	0.4
EXPLORER - RECORDER															
7	31.10.53	43	1-28	38	49	-120	+140	+ 30	+3.3	+1.7	3.0	0.7	80	1.2	0.5
10	2. 1.54	40	4-54	27	24	-430	-500	-520	+3.5	+1.5	1.2	0.5	90	1.1	0.5
11	22. 1.54	24	10-38	27	25	-100	-140	- 80	+0.4	+2.1	1.9	0.5	70	0.7	0.3
15	17. 4.54	28	10-48	34	24	- 20	-170	-120	+3.6	-0.7	1.0	0.8	80	0.4	0.5
17	8. 5.54	39	2-45	32	24	+ 70	+100	+110	+7.9	+4.0	2.1	0.9	150	0.8	0.6
23	20. 8.54	28	5-35	62	32	-240	-410	-250	+2.6	+3.8	1.5	0.7	80	0.7	0.6
OBSERVER - WATCHER															
1	5. 4.53	31	3-37	23	24	-340	-390	-165	+0.5	-0.3	1.2	0.4	180	0.5	0.1
12	23. 1.54	36	4-60	33	19	-180	-270	-160	-0.2	-0.8	0.9	0.8	100	0.7	0.4
14	6. 3.54	18	1-10	57	60	-150	-130	-140	+9.1	-2.1	2.0	1.7	70	1.8	1.3
16	17. 4.54	33	2-25	60	53	- 90	-100	- 80	-3.2	+2.4	1.6	1.5	70	1.5	1.0
22	20. 8.54	7 & 14	3-6 & 16-25	41	72	-110	-250	-210	-3.3	+2.8	1.7	2.4	40	1.5	1.4
24	2.10.54	42	1-68	39	17	- 10	+420	+360	-0.1	+3.8	3.3	1.1	130	0.7	0.6
27	13.11.54	36	2-79	30	13	+110	+390	+340	-2.8	+2.7	2.6	1.2	90	0.6	0.5
RECORDER - OBSERVER															
3	21. 6.53	33	6-43	23	27	+120	+560	+350	+1.7	0.0	0.8	0.8	80	0.7	0.3
4	29. 8.53	17	11-28	-	41	-190	- 80	- 75	+0.9	-1.5	1.3	0.6	100	0.9	0.5
21	1. 8.54	34	2-50	24	21	+ 70	-200	-110	+0.7	-3.9	1.6	0.3	90	0.8	0.2
25	23.10.54	33	4-78	26	13	+100	-240	-120	-6.0	+0.3	1.7	0.9	120	0.9	0.4
RECORDER - WATCHER															
5	19. 9.53	47	1-25	70	57	-150	- 90	-110	-4.2	-2.5	1.4	3.1	60	1.1	0.6
6	10.10.53	28	3-83	58	9	-340	-940	-470	-1.6	-1.1	1.4	1.3	210	1.0	0.9
8	13.12.53	26	8-52	40	21	+ 60	- 50	-170	+0.1	-0.2	1.1	1.0	120	1.3	0.5
13	14. 2.54	29	8-64	44	19	+ 50	+ 60	-170	-0.4	0.0	1.3	1.1	210	0.4	0.4
18	28. 5.54	33	2-35	55	33	-190	-130	-350	-1.5	+2.6	2.0	1.0	70	1.5	0.5
19	18. 6.54	39	2-26	31	49	+ 40	+ 30	+ 30	+6.0	-2.0	1.6	1.8	80	0.8	0.5
EXPLORER - OBSERVER															
9	15.12.53	31	4-28	35	41	+ 15	- 20	+ 55	+4.3	-0.6	2.2	0.6	50	1.1	0.5
Mean WEATHER EXPLORER		(10 ascents, equal weight to each)									1.7	0.6	100	0.8	0.5
" WEATHER WATCHER		(16 " " " " " ")									1.6	1.3	110	0.9	0.6
" WEATHER OBSERVER		(12 " " " " " ")									1.7	1.0	90	1.0	0.6
" WEATHER RECORDER		(16 " " " " " ")									1.6	1.0	110	0.9	0.5
Mean of all		(27 " " " " ")									1.6	1.0	100	0.9	0.5

Table II. Notes on ascents

Ascent No.	State of Sea	Remarks
2	mod.	E above 70° at first. 1st obs. min. 12.
20	slight	
26	calm-slight	
7	mod.	
10	slight-mod	
11	mod.	First obs. min. 10
15	slight-mod.	
17	slight-mod.	
23	calm	E above 70° at first. 1st obs. min. 10.
1	rough	
12	mod.	
14	slight	E about 60° throughout. Some obs. lost above 70°.
16	calm	
22	slight	E above 70° and obs. unreliable min. 12-27.
24	slight	
27	slight-mod.	
3	mod.	
4	calm-slight	E above 70° first 18 mins; no obs.
21	mod.	
25	mod.	
5	slight	E 52°-70° throughout. Some obs. lost above 70°.
6	mod.	
8	mod.	No parallax correction before min. 10. Obs. omitted.
13	slight-mod.	
18	slight	
19	mod.	
9	mod-rough	

Table III. Vector Difference of Wind Measurement (knots)

Ascent No.	1	2	3	4	5	6	7	8	9	10	11	12	13	14	15	16	17	18	19	20	21	22	23	24	25	26	27	Mean	No. of obsns.
Height 1000's feet																													
60					2		8			22						2												8.5	4
55		2		8	3		8			3			8			12			5	5								6.0	9
50		3	20	2	0		5	20	6	5		8	9			5	2	11	3	12			15		12	11		8.3	18
45	4	7	6	5	3		12	13	1	7	4	7	11			8	16	2	4	2	7		28	36	10	2	23	9.5	23
40	6	1	3	10	4		5	16	2	7	7	8	3		17	8	24	5	3	15	11		17	27	10	7	32	10.3	24
35	1	7	3	3	2	30	2	5	6	7	5	6	6		11	3	31	12	4	10	11		13	18	16	9	23	9.8	25
30	2	21	10	3	21	6	6	50	15	5	16	5	7		4	3	17	9	11	2	22		3	17	10	7	7	11.2	25
26	15	5	4	8	11	9	1	18	6	12	9	3	6		8	4	12	3	4	9	19		3	24	4	7	21	9.0	25
23	6	1	6		6	20	4	5	4	6	8	2	4	4	6	6	11	3	2	5	10		6	18	14	9	9	7.0	25
20	3	2	4		7	3	5	12	1	5	13	6	7	3	11	9	10	2	5	3	12		4	23	9	7	9	7.0	25
18	1	3	3		4	10	3	8	2	3	4	6	2	6	10	7	7	2	3	3	11		4	14	16	9	2	5.7	25
16	3		6		1	15	2	4	3	1	7	2	2	1	8	2	6	4	7	2	4		2	8	24	2	3	5.0	24
13	4		2		0	9	1	1	2	3		1	1	0	4	1	30	3	4	1	15	3		6	9	2	15	5.1	23
10	3		0		2		1	0	2	4		8	1	1	3	3	11	4	1	1	4	7		11	3	5	2	3.5	22
8	3		3		3		1	3	6	3		2	2	1	11	5	4	4	1	3	2	2		9	6	2	7	3.8	22
6	3		3		2		1	3		4		3	1	5		2	8	2	1	3	6	2		5	3	4	8	3.5	20
4	4		2		2			3				6	1	7		3	5	1	1	3	2	5		3	1	1	5	3.1	18
2	2		1		1			6				12	7	6		6	5	3	2	6	6	1		5	8	5	8	5.0	18
1	6		1		1			13				13	10	8		4		4	3	7	8	2		7	8	9	11	6.8	17
Mean	4.1	5.2	4.5	5.6	3.9	12.7	4.1	10.6	4.3	6.1	8.1	5.8	4.9	3.8	8.5	4.9	12.4	4.4	3.6	5.1	9.3	3.1	9.5	14.4	9.6	5.8	11.6	6.9	392

Table IV. Frequency distribution of Vector Differences

Vector diff. (kt.)	No. of cases	Percent-age	Vector diff. (kt.)	No. of cases	Percent-age	Vector diff. (kt.)	No. of cases	Percent-age
0	5	1.3	12	10	2.6	24	3	0.8
1	37	9.4	13	5	1.3			
2	49	12.5	14	2	0.5	27	1	
3	56	14.3	15	7	1.8	28	1	
4	35	8.9	16	5	1.3	30	2	
5	28	7.1	17	4	1.0	31	1	2.0
6	33	8.4	18	3	0.8	32	1	
7	26	6.6	19	1	0.3	36	1	
8	22	5.6	20	3	0.8	50	1	
9	16	4.1	21	3	0.8			
10	11	2.8	22	2	0.5			
11	15	3.8	23	3	0.8	Total	392	100.1

Appendix

Modifications to radar wind sets

Weather Watcher

Delayed synch and signal generator fitted 4.9.53.

Range expansion unit fitted 1.11.53.

On 1st voyage after fitting, R.E.U. was used intermittently; after that no periods of unserviceability.

G.41 trigger: started on 4.6.54; not used 10.11.54 to 15.11.54.

Weather Recorder

D.S.S.G. fitted 9.10.53

R.E.U. fitted 9.10.53.

R.E.U. unserviceable 24.10.53 to 3.11.53 and 15.4.54 to 19.4.54.

G.41 trigger: Not used.

Weather Explorer

D.S.S.G. fitted 19.12.53

R.E.U. fitted 18.1.54

Unserviceability: None.

G.41 trigger: Not used.

Weather Observer

D.S.S.G.)
) fitted January 1954.
R.E.U.)

Unserviceability: None.

G.41 trigger: Not used.

M.R.P. 929
S.C. 111/189
10th SEPTEMBER, 1955

The energy balance of surface and atmosphere at Kew, May 1953 to April 1954

by

G.D. Robinson

(Meteorological Office)

AIR MINISTRY

METEOROLOGICAL RESEARCH COMMITTEE

At the time of issue this report has not been published. Any author desiring to quote this paper should refer to it as "A paper of the Meteorological Research Committee (London), M.R.P. No. 929 by Dr. G.D. Robinson. A copy is available in the Library of the Meteorological Office."

M.R.P. 929
S.C.III/189
10th September, 1955

AIR MINISTRY
METEOROLOGICAL RESEARCH COMMITTEE

The energy balance of surface and atmosphere at Kew, May 1953 to April 1954

by

G.D. Robinson (Meteorological Office)

SUMMARY

An estimate is made, based mainly on surface measurements, of the net radiation entering or leaving the system atmosphere plus surface layer of earth at Kew during the whole period May 1953 - April 1954, inclusive, and for separate periods of three summer and three winter months. The heat liberated by phase changes of H_2O and the heat conduction from the system to the ground are also estimated. The deduced dynamical and advective heating is compared with the latitude means derived from similar world wide studies, and from published studies of the meridional eddy flux of heat.

In the course of this work new estimates are made of the local albedo of the planet for visual plus ultra-violet, infra-red, and total radiation, and of the photometric albedo.

The bearing of the results on methods of implementing the programme of radiation measurements during the International Geophysical Year 1957-58 is examined.

1. INTRODUCTION

In the programme of meteorological observations planned for the International Geophysical Year 1957-58 it is recommended that certain radiation measurements be made at cooperating stations, as part of a large scale investigation of atmospheric circulation. Ideally measurements are needed of the net flux of radiation over a surface representative of a wide area of the surroundings of the station, and at all heights in the atmosphere. There are at present no techniques for measuring radiation from balloons, and should one be developed it can hardly be used on more than an experimental scale. Measurements of solar radiation from aircraft are possible and methods for measuring terrestrial radiation from aircraft have been tried out, but expense forbids any general use of these. The most that can be expected from all but a few I.G.Y. stations is a record of the flux of total radiation at the ground and perhaps a separate record of solar radiation. Such measurements have been made for a trial period of one year at Kew Observatory (Roach 1955, Blackwell 1954b), and the purpose of the present paper is to show how they can be used to further the I.G.Y. investigation.

The problem is to determine the flux of radiation at any level in the atmosphere from surface measurements; it falls into two parts concerned respectively with solar and terrestrial radiation. No new suggestions will be offered here concerning the latter, and attention will be restricted to the whole depth of the atmosphere, reducing the problem to a determination of the local value of the albedo of the earth and atmosphere at different seasons of the year.

/2.

2. THE ALBEDO OF THE ATMOSPHERE

Direct measurement of the earth's albedo requires observation from outside the atmosphere. The nearest approach to this ideal is the method of Danjon involving photometry of the earthlit part of the moon. Danjon's observations were visual, and give the albedo of the planet at different wavelengths in the visual range. Fritz (1949) has applied Danjon's measurements to an estimate of the albedo of the planet for the whole solar radiation (" total albedo "). To do this he was obliged to consider the absorption of the solar infra-red radiation, and in particular to assume values for the absorption in cloud. H.G. Houghton (1954) has estimated the albedo of the planet from measurements of solar radiation at the ground and assumed atmospheric absorptions. Drummond and van Deventer (1954) have derived a local albedo, that of the South African plateau and its atmosphere, in the same way. The method here applied to the Kew observations is essentially that of Drummond and van Deventer, with the advantage that the continuous record of illumination at the ground allows a separate estimate of the photometric albedo and the splitting of the total albedo into the contribution from the infra-red and visual plus ultra-violet ranges.

It was shown by Blackwell, Eldridge and Robinson (1954) that in cloudless conditions the Kew illumination and radiation records are self-consistent if there is present in the atmosphere a grey absorber, in addition to the known gaseous absorbers, which removes about 10% of the incident radiation, and if at the same time the illumination measurements are about 5% too high. Blackwell (1954a) estimated an accuracy of about ±5% for the long term means of illumination, and there is independent evidence, discussed by Blackwell, Eldridge and Robinson, that the Kew measurements are high. However it has been pointed out to me by Mr. D.B. Lake that the records are also self-consistent if the illumination measurements are correct, grey absorption in the atmosphere is small, and backward scattering from the haze is much greater than previously assumed, as a result of multiple scattering. It is hoped that aircraft observations will resolve this doubt in the near future. In this paper both possibilities are examined. That involving absorption by haze of about 10%, which is considered the more probable, will be called case a; that involving high backward scattering from haze case b.

Making the reasonable assumption that absorption of visible light by cloud droplets is negligible the photometric albedo can be determined directly, since only ozone absorption and haze absorption are concerned, and the extraterrestrial illumination is known. (Appendix 1). The total albedo follows in the same way from the total radiation at the ground, with the additional difficulty of allowing for absorption in cloud. There is very little information on which to base this estimate; the possibilities have been discussed by H.G. Houghton (1954). Practically all cloud absorption must be in the infra-red region, so that it is advantageous to consider separately the albedo in the infra-red and visual + ultra-violet ranges.

Blackwell (1954a,b) has shown that the mean value of the luminous efficiency of daylight, i.e. the mean ratio of illumination to total radiation, is practically the same in cloudless, mean, and overcast conditions at Kew. No large errors will be introduced by extrapolating this result and saying that the ratio of energy at the ground in the ultra-violet + visual range to that in the infra-red range is the same in the mean as in cloudless conditions. No direct measurements of either range are available at Kew, but measurements of solar intensity in the range $\lambda < 0.64\mu$ have been made and discussed by Blackwell, Eldridge and Robinson. Table VII of their paper allows an estimate of the ratio visible + ultra-violet energy to infra-red energy on a number of cloudless occasions. It turns out to be 0.9 ± 0.1 if the division is made at $\lambda = 0.70\mu$. Applying this to the measurements of

/total

total radiation at the ground gives separate estimates of the two ranges. The incoming energy in the two ranges at the limit of the atmosphere is known (Appendix I). If probable and limiting assumptions concerning the various absorptions are now made probable and limiting values of the various albedos follow.

Computations were based on the records for the period May 1953 to April 1954, to allow combination with Roach's results for the heat balance at the ground over this period. It can however be seen from Table I that the solar radiation measurements for this year did not differ appreciably from the mean of the five year period 1947-51 treated by Blackwell. In addition to the whole year, summer conditions - May, June and July -, and winter conditions - November, December and January -, were considered. In view of the expected degree of accuracy it was not thought appropriate to treat the observations hour by hour and integrate over all solar altitudes, so a weighted mean solar altitude $\bar{h}$ ($\sin \bar{h} = \int A \sin h \, dt / \int A \, dt$, where A is the observed radiation or illumination on a horizontal surface at solar altitude h and the integrals are from sunrise to sunset over the period concerned), was derived. The absorptions by O_3 and H_2O in a model cloudless atmosphere containing 2 cm. H_2O and 2 mm. O_3 had been used by Blackwell, Eldridge and Robinson; values appropriate to the present problem are shown in Table II, together with the additional absorption attributed to haze.

Computation of the albedo now proceeds in the following manner. For the photometric albedo the observed illumination at the ground is first corrected to remove that part contributed by reflection from the atmosphere of radiation reflected at the ground. It is necessary to assume albedos for ground and atmosphere to arrive at this correction; 0.1 and 0.6 were used. The corrected illumination, here designated that "reaching the ground direct", is subtracted from the extraterrestrial illumination and expressed as a fraction of the latter. In the tables this fraction appears as "albedo + absorption". Subtraction of an assumed absorption leaves the albedo. A similar procedure is followed for the visual + ultra-violet and infra-red ranges, the observed radiation at the ground being split between the ranges in the manner indicated above. For the re-radiation correction the albedos assumed in the visual + ultra-violet range were the same as for the illumination; in the infra-red range 0.2 was used as surface albedo and 0.4 for the atmosphere. One example will now be given in detail.

Period May 1953 - April 1954 inclusive.

1. <u>Determination of photometric albedo</u>

Extraterrestrial illumination (mean)	29.0 kilolux (kl.)
Illumination recorded at ground	13.8 kl.
Correction for re-reflection	0.7 kl.
Illumination reaching ground direct	13.1 kl.

Albedo + Absorption 0.55 (case b)
If illumination record is 5% too high
Albedo + Absorption 0.58 (case a)

Case a.
1. If absorption is 7% photometric albedo is 0.51
2. If absorption is 12% photometric albedo is 0.46

Case b.
Absorption is 2.5%, photometric albedo is 0.52^5

2. <u>Determination of albedo in visual + ultra-violet range</u>

Extraterrestrial mean radiation 13.6 mw. cm^{-2}
Total radiation recorded at ground 10.4 mw. cm^{-2}
Ratio visual + ultra-violet/infra-red 0.9
Visual + ultra-violet at ground 4.9 mw. cm^{-2}
Re-radiation correction 0.3 mw. cm^{-2}
Visual + ultra-violet radiation reaching ground direct 4.6 mw. cm^{-2}
Albedo + Absorption 0.66

Case a.

1. If absorption is 10% visual + ultra-violet albedo is 0.56
2. If absorption is 15% visual + ultra-violet albedo is 0.51

Case b.

Absorption is 6%, visual + ultra-violet albedo is 0.60

3. Determination of albedo in infra-red range

Extraterrestrial mean radiation 14.3 mw. cm^{-2}
Infra-red radiation at ground 5.5 mw. cm^{-2}
Re-radiation correction 0.5 mw. cm^{-2}
Infra-red radiation reaching ground direct 5.0 mw. cm^{-2}
Albedo + absorption 0.65

Case a.

1. If absorption is 30%, infra-red albedo is 0.35
2. If absorption is 35%, infra-red albedo is 0.30

Case b.

If absorption is 25%, infra-red albedo is 0.40

The same procedure was followed for the periods May, June, July 1953 and Nov., Dec. 1953 Jan. 1954. The results are collected in Table III, which shows the absorptions assumed in the various cases. Values of the total albedo range over about 15% for each period, but the likely limits can be contracted by an examination of probable absorptions. In mean cloud conditions the effects of haze are likely to be less than in the cloudless atmosphere, if only because of greater ventilation of the polluted region; the following estimates allow for this. The estimated cloud absorption is additional to the full absorption for the appropriate amount of water vapour.

Year.

Haze absorption 5% (grey)
Cloud absorption say 5% to 10% of infra-red
Water content between 1 and 2 cm.
Albedos lie between those for case a.1 and case a.2.

Summer.

Haze absorption 5% (grey)
Cloud absorption 5%-10% of infra-red
Water content 2 cm.
Conditions between b.1 and a.2.

Winter.

Haze absorption 5% to 10% (grey)
Cloud absorption 10% to 20% of infra-red
Water content 1 cm.
Conditions between a.1.2 and a.2.2.

The albedos corresponding to these probable conditions are set out in Table IV. They refer to the atmosphere alone. Assuming an albedo of 0.15 for the land surface (this is confirmed by unpublished measurements made extensively over southern England by the Meteorological Research Flight), and allowing for re-reflection by the atmosphere it is found that 0.03 must be added to the albedo of the atmosphere to give the local value of total albedo of earth + atmosphere. The final estimates of this quantity are

Year	0.475
Summer	0.46
Winter	0.525

and it seems likely that the true values for Kew lie within ±0.05 of these. Over southeast England as a whole the effect of haze must be less than at Kew; it seems reasonable to reduce the estimates by about 0.02.

/If

If the mean cloudiness is known the albedo of the cloudy portion of the atmosphere can be obtained from the mean albedo, using the values of Blackwell, Eldridge and Robinson for the albedo of the cloudless atmosphere which are given in Table II. Taking the mean cloudiness as 0.7 the results listed under "Kew mean" in Table V are obtained. Two sources of comparable data are available. Blackwell (1954 a, b) has tabulated the illumination and total radiation at Kew for persistent overcast conditions (i.e. for periods of at least 3 hours without direct sunshine, the end hours of the periods being ignored), and albedos may be determined from these figures in the same way as for mean conditions. This was done for all occasions (more than 100 hours) during the period 1947-51 with solar altitude h in the range $\arcsin 0.5 < h < \arcsin 0.6$, corresponding to $\bar{h}$ for the year, the absorption being assumed to be the same as in the mean condition. The results are shown in Table V; as would be expected they are considerably higher than the corresponding figures for mean cloud. An entirely independent estimate was obtained by slight manipulation of figures quoted by Fritz (1949) in his extension of Danjon's work. The results set out in Table V follow from Fritz's work without further assumption; they are appropriate to his case 1 and a mean cloudiness of 0.54. In view of the doubts as to the true mean cloudiness appropriate to each investigation and the differences in mean solar altitude, the agreement between the Kew mean and the Fritz/Danjon results is remarkable. Another comparison with Fritz's work is available. F.J. Sorase (private communication) has computed the mean albedo for S.E. England, on the basis of Fritz's figures for cloud, atmosphere, and surface, to be 0.47, less than 0.02 higher than the value here suggested. Finally there is H.G. Houghton's (1954) figure for cloud alone of 0.55; the small difference between this and the mean Kew value being due mainly to different assumptions concerning cloud absorption which in Houghton's words are in each study "little more than an educated guess".

3. TERRESTRIAL RADIATION AT THE LIMIT OF THE ATMOSPHERE

Numerous attempts have been made to estimate the radiation of the earth to space. Of the available methods the radiation chart of Elsasser is the best known, and that of Yamamoto probably the least open to objection. All known methods are inadequate at high levels and it is not even possible to estimate the likely degree of error of the results they yield. The only observations at substantial heights are a few very recent ones by J.T. Houghton (1954) made over southern England with the co-operation of the Meteorological Research Flight.

The earliest reasoned survey of the outgoing radiation is that of Simpson (1929) who found a mean annual value of 18.7 mw.cm^{-2} in 50°N. Typical recent estimates are those of Raethjen (1950) using his own radiation chart and H.G. Houghton (1954) with the Elsasser chart. Raethjen's results for the zone 40°-60° are

Summer half-year	21.2 mw. cm^{-2}
Winter half-year	20.6 mw. cm^{-2}
Yearly mean	20.9 mw. cm^{-2}

Houghton gives for 52°N (by interpolation)

Yearly mean	21.3 mw. cm^{-2}.

Increasing cloudiness decreases this figure, and data given by H.G. Houghton suggest that for the mean cloudiness of southern England his yearly mean value would reduce to 21.0 mw. cm^{-2}. H.G. Houghton states specifically that his figure refers to the tropopause, not to the limit of the atmosphere. Simpson, and Raethjen presumably, computed the radiation leaving the earth, though the computations are so uncertain that the difference between the results for this and for the tropopause radiation are hardly significant.

The measurements of J.T. Houghton were made at near-tropopause levels in cloudless or near cloudless conditions. He found for the upward flux a value

/about

about 22 mw. cm^{-2}, and for the downward flux 3 to 4 mw. cm^{-2}. Presence of the mean cloud cover might reduce the former value by 5 to 10 per cent, and have little effect on the latter. J.T. Houghton's measurements therefore suggest a value of about 18 mw. cm^{-2} for the net radiation at the tropopause in mean conditions over southern England. He himself comments "calculations of the mean outgoing radiation will be very dependent on the assumptions made regarding mean cloud amount, and on the emissivity of high level clouds. Since very little is known about the frequency of occurrence of cirrus clouds of different emissivities it is impossible to predict an accurate value for the mean outgoing radiation, and, in fact, Simpson's rough calculation making it about 18 mw. cm^{-2} may not be far wrong".

Two comments seem necessary on J.T. Houghton's work. In the first place the measurements themselves have some disturbing features. The results for the upward flux at 40,000 ft. are rather less, and for the downward flux rather more than was expected. The same remark applies to his low level measurements at about 3000 ft. Here the measured downward flux is greater than that indicated by standard radiation charts, a result contrary to the experience of Robinson (1947, 1950) and Yamamoto and Sasamori (1954) at the surface. However there is no obvious flaw in Houghton's work and his observations must be given more weight than the suspect calculations. The second comment concerns the relation between the tropopause radiation and that at the limit of the atmosphere. Absorption of solar radiation in the stratosphere in this latitude amounts to roughly 2 mw. cm^{-2} in the mean, so that if the stratosphere is locally in overall radiative balance the mean net outward radiation must increase by this amount above the tropopause. How far the stratosphere is from this radiative balance is at present merely a matter for speculation, and the outgoing radiation remains in doubt to this extent.

The most likely value for the radiation to space over southern England will be taken as 20±3 mw. cm^{-2} in the mean over the year, seasonal variation being probably not more than ±1 mw. cm^{-2}.

4. THE RADIATION BUDGET

The energy changes by radiation of the atmosphere and surface layer at Kew follow from Roach's work and the present results. They are shown in Fig. 1. Table VI reproduces the relevant part of Roach's results. There are minor inconsistencies between Fig. 1 and Table VI mainly connected with the surface albedo. This has been taken as 0.15 in the present study, a value appropriate to a wide area of southern England, whereas the figure used by Roach is that measured for the immediate surroundings of the radiometers at Kew, 0.25.

The figures for the net radiation entering the atmosphere are

Year	-5.5 ± 3.5 mw. cm^{-2}
Three summer months	+3.8 ± 3.5 mw. cm^{-2}
Three winter months	-14.3 ± 3.5 mw. cm^{-2}.

Raethjen (1950) and H.G. Houghton (1954), whose studies of the world wide radiation balance have been mentioned, give tables from which may be interpolated the mean for latitude 52° of the net radiation entering the atmosphere. The values are

H.G. Houghton	Year	-5.0 mw. cm^{-2}
Raethjen	Year	-5.5 mw. cm^{-2}
"	Six summer months	+2.5 mw. cm^{-2}
"	Six winter months	-13.0 mw. cm^{-2}.

In comparing the values it should be remembered that the Kew results are for midsummer and midwinter quarters whilst Raethjen's estimates are means for

/the

the half-year. Nevertheless there is a remarkable agreement. There is no obvious reason why a single station should not differ widely from the latitude mean of net radiation received, and it will be interesting to see whether other stations show the same agreement as Kew.

5. THE ENERGY BALANCE

The heat required to balance that radiated to or from the system can be supplied in a number of ways - by temperature changes of the system, by phase changes of water within the system, by conduction between the system and the deeper layers of the ground, by advection from surrounding air, and by conversion to and from gravitational potential energy in vertical currents within the system, (dynamical heating or "transport of potential energy").

The first three methods can be accounted for by direct measurement. On the assumption that systematic change in the liquid water and ice content of air passing through the system is negligible the amount of water vapour condensed in a period is equal to the measured precipitation. Evaporation at the ground has been estimated and the conduction term measured by Roach. Precipitation at Kew during the year considered was about 15 per cent below the mean value, the deficit being concentrated in the winter months. This is not an unusually large deviation, and its effect on the overall energy balance is not large, as may be seen from Fig. 2 which includes all the known terms. The value of 0.5 mw. cm^{-2} used for the heat absorbed or emitted by the atmosphere in the three month periods is a rough estimate of a small term. It corresponds to an overall temperature change of 4°C in three months. The balances, to be accounted for by advective and dynamical heating, are

Year	-5 ± 3.5 mw. cm^{-2}
Three summer months	$+1.8 \pm 3.5$ mw. cm^{-2}
Three winter months	-11.8 ± 3.5 mw. cm^{-2}.

A non zero mean dynamical heating term implies a mean vertical velocity. The possible magnitude of the term may be estimated using some computations of Bannon (1948). The rainfall in the year considered was rather more than 500 mm., a mean rate of 0.055 $mm.hr^{-1}$. According to Bannon an atmosphere defined by the 60°F saturated adiabat requires a vertical velocity of about $+3 cm.sec^{-1}$ between 1000 mb. and 300mb. to produce a rainfall rate of 1 $mm.hr^{-1}$. The mean vertical velocity required to produce the observed rainfall is thus about 0.17 $cm.sec^{-1}$ and the rate of working, $\overline{\omega} \int \alpha dp$, about 12 $mw.cm^{-2}$, i.e. more than twice the rate of release of heat by condensation. This dynamical cooling would normally be approximately balanced by dynamical heating in the descending limbs of the vertical circulations producing the rainfall, but it is clear that the rates of working involved are so large that very small systematic vertical circulations or even random fluctuations about a zero mean vertical velocity might well dominate the energy balance of a single station over a period of a year or less. The vertical velocities involved are of course much too small for direct detection.

Some idea of the size of the advective term may be obtained from studies of heat transport such as those of Priestley (1949), White (1951) and Mintz (1954), some of whose results are shown in Fig. 3. Mintz computed $c_p \overline{\rho v_g' T'}$ for a series of pressure levels where v_g is the poleward component of geostrophic wind, T the temperature, and the primes denote deviations from mean values round a circle of latitude over the period concerned. White's figures are for $c_p \overline{\rho v' T'}$, v now being the observed poleward wind component. His study was restricted to N. American stations. Priestley computed $c_p \overline{\rho v' T'}$ for a single station, Larkhill, so that here the primes indicate deviations from a time mean and heat transport by horizontal standing eddies is not included. Raethjen's estimates of advective transport of heat plus potential energy for the winter and summer half years, derived from estimates of radiation balance, water balance, and storage of heat, are also shown in Fig. 3 which is in terms of the variation with latitude of the poleward energy flux F in mw. cm^{-1}.

/The

The local heating by the process producing F is given, in mw.cm^{-2} by the expression $-(\partial F/\partial\phi - F\tan\phi)/r$ (where ϕ is the latitude and r the radius of the earth); its magnitude at $\phi = 52°$ is approximately:-

Mintz	Two summer months	+1.0 mw. cm^{-2}
	Two winter months	+1.5 mw. cm^{-2}
Raethjen	Year	+0.5 mw. cm^{-2}
	Six summer months	-2.5 mw. cm^{-2}
	Six winter months	+3.5 mw. cm^{-2}.

The close general agreement between the estimates of Raethjen (flux of heat and potential energy), White (flux of heat) and Mintz (heat flux accounted for by geostrophic wind) poleward of 50° indicates that no appreciable mean vertical circulation is active in this region, so that there is no dynamic heating component in the latitude-mean heat balance. There is thus a less close agreement between the Kew regime of advective and dynamical heating and the latitude mean than was found for the radiation balance alone. Comparison with Raethjen's work in detail shows that the water phase change term and the storage term at Kew are much below the latitude average. The low value of the heat transport found by Priestley for southern England, in comparison with the figures of White and Mintz, suggests that horizontal standing eddies are of importance in this region, and non zero mean vertical motion might well be associated with such eddies. This is the type of question which might be elucidated by successful conclusion of the I.G.Y. programme.

6. CONCLUSIONS, WITH PARTICULAR REFERENCE TO THE I.G.Y. PROGRAMME

This study in combination with that of Roach suggests that the programme of radiation measurements proposed for the I.G.Y. can make a useful contribution to solution of the meteorological problem, i.e. that results of useful accuracy can be obtained with apparatus which is available, not unreasonably expensive, robust, and not too difficult to maintain. The minimum requirements are records of net radiative flux at the ground and solar radiation on a horizontal surface. Precipitation should be measured and an estimate of evaporation will be required which should be supported by all possible measurements (though it is hardly possible to recommend a method). A refinement which should be adopted at as many stations as possible is measurement of solar radiation in the infra-red, so that separate estimates of albedo in the infra-red and visible plus ultra-violet can be made. This allows comparison with estimates of the planetary albedo by the method of Danjon, which will almost certainly be confined to the visual and possibly near ultra-violet regions.

It has been shown that the inaccuracy to be expected in estimates of the local net radiation excess of the atmosphere - surface system is rather large in comparison with the seasonal means for the latitude belts. The major source of uncertainty is the value taken for the outward atmospheric radiation, and it is most likely to be reduced by many further measurements on the lines of those of J.T. Houghton combined with theoretical work on radiative transfer aimed at developing a sound substitute for the present radiation charts at high levels. It cannot be expected that this problem will be decisively resolved before or during the I.G.Y., but it will be possible to combine future results with I.G.Y. data. The uncertainty due to errors of the estimated albedo has been assessed as about half that of the long-wave radiation to space. It can be reduced by extensive measurements by Danjon's method. It is believed that an attempt will be made to encourage these during the I.G.Y., but the method is no doubt much simpler in principle than in practice, and the co-operation of astronomical observatories will be required. A more direct check of local estimates of albedo is provided by measurement of the downward and upward flux of solar radiation from aircraft to as high

/levels

levels as possible, comparing the results either individually with simultaneous estimates from ground measurements in the same locality, or in the mass with means such as those derived in this paper. Fritz (1948, 1950) has reported a few aircraft measurements in the U.S.A. and in this country the M.R.F. has begun systematic collection of data. It will be possible to apply the results of such investigations retrospectively to I.G.Y. data.

It also appears that the individual items of the local energy balance over a season or a year may differ very significantly from the long term mean, and this may well be true for a whole circle of latitude. It follows that to realise the full value of the I.G.Y. measurements a few selected stations should maintain the same routine for a period of say five years. This aspect is of course not confined to the radiation measurements. Continuous recording of solar radiation is now widespread and it should not be too difficult to add a record on the lines of that of Roach at a few stations.

In summary the conclusions are

(1) Radiation measurements recommended during the I.G.Y. can be made with a useful degree of accuracy, given care and frequent standardisation.

(2) The accuracy, and therefore the utility, can best be increased by measurements in the air of solar and atmospheric radiation. Such measurements wherever and whenever they are made deserve support as part of the I.G.Y. programme.

(3) The year to year variability of the various meteorological elements is an important factor. To determine this a few stations operating during the I.G.Y. should extend their measurements over a period of at least five years.

Appendix 1

The solar constant and scales of radiation

The value of the solar constant, and the spectral distribution of the extraterrestrial radiation are required before albedos can be estimated by the present method. The data used have been those suggested by Nicolet (1951a, 1951b). Johnson (1954) has recently published a new appreciation of the data on which the solar constant and the spectral distribution of solar energy are based. Nicolet's estimate for the solar constant was 138.0 mw. cm^{-2}, Johnson's 139.4 mw. cm^{-2}. Nicolet considered that his value might be in error by as much as ±5%, Johnson his by ±2%. This very satisfactory agreement does not extend to the details of the spectrum though both authors consider the relative accuracy of their data to be much higher than the absolute accuracy of their solar constant. The energy in certain ranges according to these authors is (in mw. cm^{-2})

Range	$\lambda < 0.3\mu$	$0.3\mu < \lambda < 0.4\mu$	$0.4\mu < \lambda < 0.7\mu$	$0.7\mu < \lambda < 3.0\mu$
Nicolet	0.96	8.2	57.7	70.8
Johnson	1.34	10.5	56.9	70.3

whilst the extraterrestrial illumination computed from their detailed spectra is

Nicolet 142.0 kilolux
Johnson 136.7 " .

Nicolet's relative values in the visual region depend mainly on astrophysical arguments connected with the solar emission, Johnson's on the extrapolation to zero air mass of measurements at the ground. The non specialist has little guidance when choosing between them, indeed he may well be surprised at the confidence expressed by each author in his chosen method. The difference in the extraterrestrial illumination arises mainly from differences in the spectral region $0.56\mu < \lambda < 0.62\mu$, which is very close to the long wave-length limit of the measurements on which Johnson relies. The difference in the extraterrestrial illuminations is large enough to be detected by careful and prolonged photometric measurements at the ground. The Kew record is certainly easier to fit to a value of 142 kl. than to 137 kl., indeed it has been inferred that the Kew measurements are systematically high because the albedo deduced from them assuming 142 kl. outside the atmosphere is low in comparison with that obtained by other methods. The discrepancy is greatly magnified if 137 kl. is used.

The probable errors of the estimated albedos given in the present paper include no allowance for the probable error of the solar constant. If Johnson's figures had been used rather than Nicolet's the derived total and visual plus ultra-violet albedos would have been about 1% higher and the photometric albedos about 4% lower. As far as energy balances are concerned the differences are of no importance in view of other uncertainties. In questions of photometry however, (for example in comparisons with Danjon's method) the difference is quite significant and it is important that it should be resolved.

A second source of systematic error is introduced in standardisation. Two instruments are in general use in meteorological services - the Ångström compensation pyrheliometer and the Smithsonian silver disc pyrheliometer. The Ångström instrument is used at Kew. It is not used absolutely, but is referred to a scale maintained in Sweden. Guild (1937) has shown that the scale as embodied in the Kew instrument in 1936 agreed within 0.5% with that maintained at the National Physical Laboratory. Guild (1937) and Eldridge (1952) have shown that the Ångström scale as embodied in the Kew instrument differs from the scale on which the Kew example of the Smithsonian instrument is calibrated ("Smithsonian scale of 1913") by 2.7%. The generally accepted difference between the Smithsonian 1913 and the Ångström scales is 3.5%, and

/it

it is almost certain that individual instruments, in use in various services as standards, differ from the mean of their type by at least 2%. There is a strong possibility of systematic differences of as much as 5% between the records of different meteorological services, even when these records are carefully maintained in reference to a local standard. Some effort is being made to reduce these differences in Europe and Africa. More extensive intercomparison of local standards could well form part of the I.G.Y. programme.

Table I

Mean values of total radiation and illumination

Period	At ground		Extraterrestrial	
	Radiation mw.cm^{-2}	Illumination kl.	Radiation mw.cm^{-2}	Illumination kl.
Year. May 1953-April 1954	10.4	13.8	27.9	29.0
Mean Year. 1947-1951	10.7	13.4		
May, June, July 1953	18.4	24.5	46.0	47.9
Mean. May, June, July 1947/51	19.1	24.2		
Nov., Dec. 1953 Jan. 1954	2.4	3.3	9.8	10.2
Mean. Nov., Dec., Jan. 1947/51	2.6	3.0		

Table II

Absorption and albedo of the cloudless atmosphere at Kew, expressed as a fraction of the extraterrestrial solar radiation in the range concerned (From MRP.894)

Period	Sin $\bar{h}$	O_3 Absorption		Water Absorption(I.R.)		Haze Absorption	Albedo			Total
		U.V.+Vis.	Illumination	2cm	1cm		$\lambda < 0.64\mu$	$\lambda > 0.64\mu$	Photometric	
Year	0.54	0.06	0.03	0.24	0.18	0.09	0.30	0.08	0.25	0.16
May, June, July	0.71	0.05	0.02^5	0.22	0.15	0.07	0.20	0.05	0.17	0.13
Nov., Dec., Jan.	0.23	0.08	0.07	0.28	0.24	0.15	-	0.11?	0.38	0.20

Table III

Summary of assumed absorptions and derived albedos

Period	Case	Ultra violet + visual		Photometric		Infra-red		Total	
		Abs.	Alb.	Abs.	Alb.	Abs.	Alb.	Abs.	Alb.
May 53	a.1.	.10	.56	.08	.50	.30	.35	.20	.46
to	a.1.1.					.35	.30	.22^5	.43
Apr. 54	a.1.2.					.40	.25	.25	.41
inc.	a.2.	.15	.51	.12	.46	.35	.30	.25	.41
"	a.2.1.					.40	.25	.27^5	.38
"	a.2.2.					.45	.20	.30	.36
"	b.	.06	.60	.03	.52	.25	.40	.15	.50
"	b.1.					.30	.35	.17^5	.48
"	b.2.					.35	.30	.20	.45
May	c.1.	.10	.53	.07	.47	.30	.33	.20	.43
June	a.1.1.					.35	.28	.22^5	.41
July	a.1.2.					.40	.23	.25	.39
1953	a.2.	.15	.48	.12	.42	.35	.28	.25	.38
"	a.2.1.					.40	.23	.27^5	.35
"	a.2.2.					.45	.18	.30	.33
"	b.	.05	.58	.02	.49	.25	.38	.15	.48
"	b.1.					.30	.33	.17^5	.45
"	b.2.					.35	.28	.20	.43
Nov.	a.1.	.13	.66	.12	.60	.30	.48	.21^5	.57
Dec.	a.1.1.					.35	.43	.24	.55
1953	a.1.2.					.40	.38	.27	.52
Jan.	a.2.	.18	.61	.17	.55	.35	.43	.24	.52
1954	a.2.1.					.40	.38	.27	.49
"	a.2.2.					.45	.33	.29	.47
"	b.	.08	.71	.07	.61	.25	.53	.19	.62
"	b.1.					.30	.48	.21	.60
"	b.2.					.35	.43	.24	.57

Table IV

Probable values of the albedo of the mean atmosphere at Kew

Period	Vis + U.V.	Photometric	I.R.	Total
May 1953 - Apr. 1954	.56	.50	.33	.445
May, June, July 1953	.55	.48	.31	.43
Nov., Dec. 1953 Jan. 1954	.63	.57	.35	.495

Table V

Albedo of clouded part of atmosphere

Source of data	Vis + U.V.	Photometric	I.R.	Total
World (Fritz/Danjon case 1)	.63	.56	.39	.52
Kew mean	.67	.61	.44	.56
Kew persistent overcast	.79	.79	.51	.65

G.23465(e)/PN/8/55/50

Some terms in the energy budge
Unit mw.cm

Period	Net Radiation flux		
	Total	Solar	Terre:
May 1953 - Apr. 1954	-4.0±0.5	-7.8±0.2	+3.8±(
May, June, July 1953	-8.8	-13.8	+4.9
Nov., Dec. 1953 Jan. 1954	+0.7	-1.8	+2.5

G.23465(f)/PN/8/55/50

Table VI

Some terms in the energy budget of the surface at Kew (after Roach).
Unit mw.cm^{-2}, positive upwards

Period	Net Radiation flux			Heat flow to ground	Evaporation	Convection	Precipitation
	Total	Solar	Terrestrial				
May 1953 - Apr. 1954	-4.0±0.5	-7.8±0.2	+3.8±0.5	+0.05±0.1	+3.6(±0.5)	+0.5±1.0	4.0
May, June, July 1953	-8.8	-13.8	+4.9	-0.4	+6.8	+1.7	5.6
Nov., Dec. 1953 Jan. 1954	+0.7	-1.8	+2.5	+0.4	+0.7	-1.0	2.3

References

Bannon, J.K. 1948 The estimation of large scale vertical currents from the rate of rainfall. Q.J.R. Met. S., 74, pp.57-66.

Blackwell, M.J. 1954a Meteorological Research Papers, London. No.831.

1954b Meteorological Research Papers, London. No.895.

Blackwell, M.J., Eldridge R.H. and Robinson G.D. 1954 Meteorological Research Papers, London. No.894.

Drummond, A.J. and van Deventer, E.N. 1954 The atmospheric transmission of solar energy over Southern Africa. Notos, 3, pp. 272-284.

Eldridge, R.H. 1952 A comparison of substandard pyrheliometers. Q.J.R. Met. S., 78, pp. 260-264.

Fritz, S. 1948 The albedo of the ground and atmosphere. Bull. Amer. Met. Soc., 29, pp. 303-312.

" 1949 The albedo of the planet earth and of clouds. J. Met., 6, pp. 277-282.

" 1950 Measurements of the albedo of clouds. Bull. Amer. Met. Soc., 31, pp. 25-27.

Guild, J. 1937 Investigations in absolute radiometry. P.R.S., A161, pp. 1-38.

Houghton, H.G. 1954 On the annual heat balance of the northern hemisphere. J. Met., 11, pp. 1-9.

Houghton, J.T. 1954 Dissertation. Oxford.

Johnson, F.S. 1954 The solar constant. J. Met., 11, pp. 431-439.

Mintz, Y. 1954 The mean geostrophic poleward flux of angular momentum and sensible heat in the winter and summer of 1949. Univ. California, Los Angeles, Sci. Rep. No.7, Contract AF19(122)-48.

Nicolet, M. 1951a Sur la problème de la constante Solaire. Ann. Astrophys., 14, pp. 249-265.

1951b Sur la détermination du flux energetique du rayonnement extraterrestre du soleil. Arkiv. Met. Geophys. Bioklimat. 13. 3, pp. 209-219.

Priestley, C.H.B. 1949 Heat transport and zonal stress between latitudes. Q.J.R. Met. S., 75, pp. 28-40.

Raethjen, P. 1950 Kurzer Abriss der Meteorologie dynamisch gesehen II. Wärmeshaushalt der Atmosphäre. Hamburg. Published by the author.

Roach, W.T. 1955 M.S. submitted to M.R.C.

/Robinson,

Robinson, G.D.	1947 1950	Notes on the measurement and estimation of atmospheric radiation, 1 & 2. Q.J.R. Met. S., 73, pp. 127-150 and 76, pp. 37-51.
Simpson, G.C.	1929	The distribution of terrestrial radiation. Mem. R.Met. S., 3, pp.53-78.
White, R.M.	1951	The meridional eddy flux of energy. Q.J.R. Met. S., 77, pp. 188-199.
Yamamoto, G. and Sasamori, T.	1954	Measurement of atmospheric radiation. Sci.Rep., Tohoku Univ. Geophys. Ser. 6, pp. 19-31.

FIG. 1 RADIATION BUDGET OF SURFACE + ATMOSPHERE AT KEW.

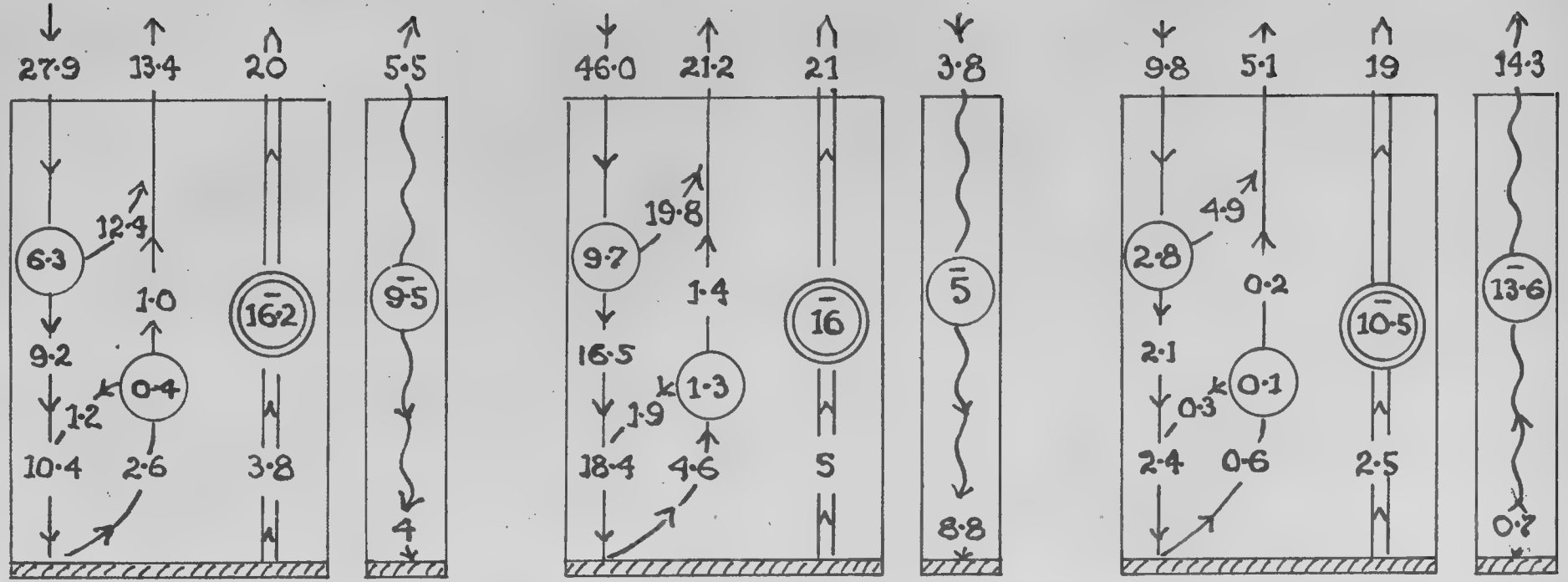

1a YEAR

1b MAY. JUNE. JULY.

1c. NOV. DEC. JAN.

SOLAR RADN. TERRESTRIAL RADN. TOTAL RADN.

RADIATION IN MW.CM.$^{-2}$ ABSORPTION IN CIRCLES

FIG 2. ENERGY BUDGET OF SURFACE + ATMOSPHERE. KEW. UNIT - MW.CM^{-2}.

2a. YEAR

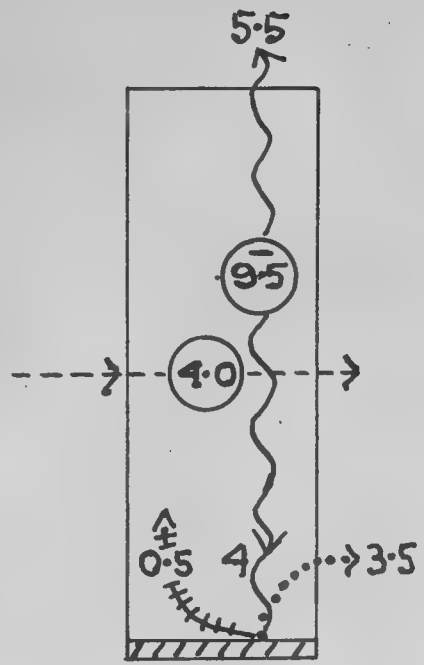

2b. MAY, JUNE. JULY.

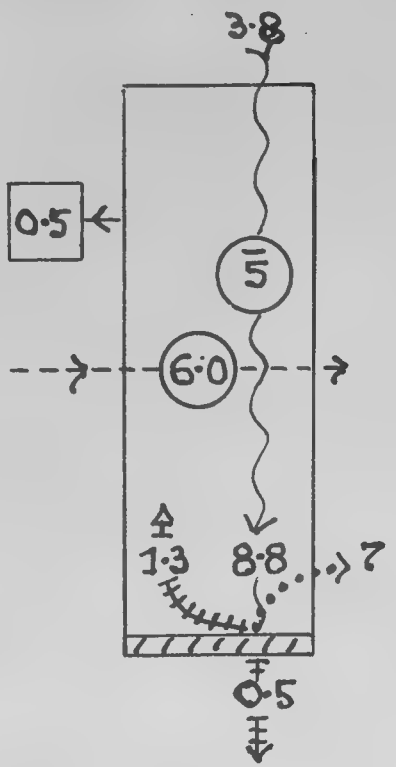

2c. NOV. DEC. JAN.

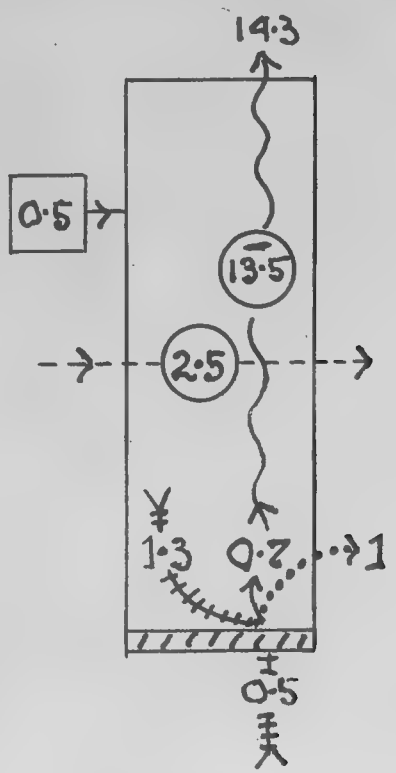

NET GAIN -5

NET GAIN +1·8

NET GAIN -11·8

TOTAL RAD^{N}

PRECIPITATION

EVAPORATION

CONDUCTION / CONVECTION TO AIR AND GROUND

AIR TEMPERATURE CHANGE

FIG 3. POLEWARD ENERGY FLUX DETERMINED BY VARIOUS METHODS.

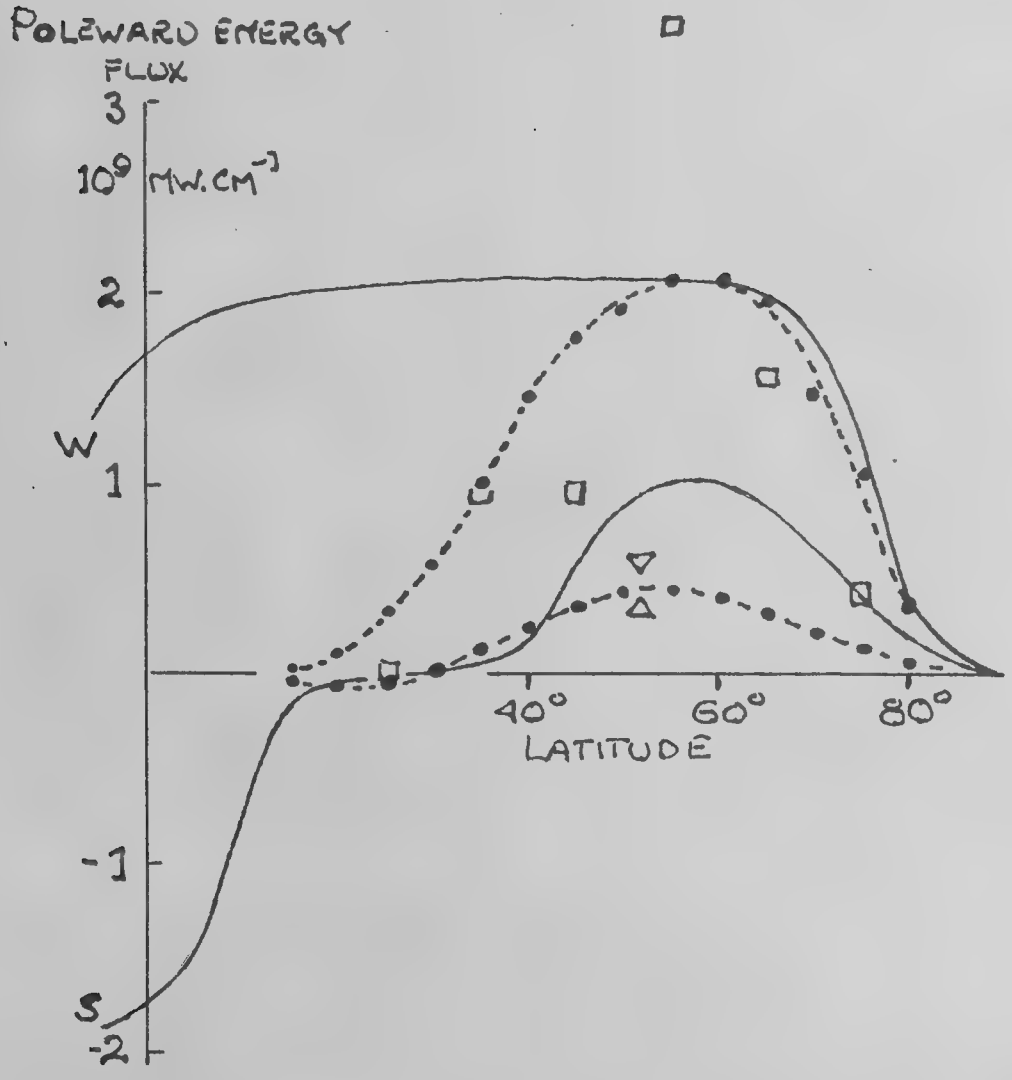

W —— RAETHJEN. HEAT AND POTENTIAL ENERGY. WINTER.
S —— " " " " " SUMMER
- - • - - MINTZ. HEAT BY GEOSTROPHIC WIND N. HEMISPHERE. JAN./FEB. AND JULY/AUG. 1949
□ WHITE. HEAT BY OBSERVED WIND N.AMERICA FEB. 1949
△ PRIESTLEY. HEAT BY OBSERVED WIND LARKHILL MAY/JUNE/JULY/AUG. 1946/47.
▽ " NOV./DEC./JAN./FEB. 1946/47.

M.R.P. 929

M.R.P. 930
S.C. 1/103
8th December, 1956

Some further determinations made by the M.R.F. of the speed correction coefficients of aircraft thermometers

by

W. G. Durbin
(Meteorological Office)

AIR MINISTRY
METEOROLOGICAL RESEARCH COMMITTEE

At the time of issue this report has not been published. Any author desiring to quote this paper should refer to it as "A paper of the Meteorological Research Committee (London). M.R.P. No. 930 by Mr. W.G. Durbin. A copy is available in the Library of the Meteorological Office."

M.R.P. 930
S.C.I/103
8th December, 1955

(A revised version has been issued)

AIR MINISTRY

METEOROLOGICAL RESEARCH COMMITTEE

Some further determinations made by the M.R.F. of the speed correction coefficients of aircraft thermometers

by
W. G. Durbin (Meteorological Office)

Summary

An account is given of recent determinations by the M.R.F. of speed correction coefficients of flat plate and conical head aircraft thermometers on Ashton and Canberra aircraft.

Both series of flights, up to 35,000 ft. in the Ashton aircraft and 40,000 ft. in the Canberra aircraft, showed no consistent variation with height of these coefficients, although there was a large scatter in the determined values.

A thermometer mounted by the manufacturers on the leading edge of the Canberra aircraft's port wing, and indicating on a meter in the navigator's position, showed a large increase with height of its speed correction coefficient.

It is concluded that future work on the improvement of thermometer design should await further investigation of the causes of the random variation of the determined values of speed correction coefficients. Pending such investigation the flat plate or the conical head thermometer is considered to be as good an indicator of free air temperature as any other type of aircraft thermometer now available.

1. Introduction

In M.R.P. 527(1), which gave an account of flight determinations by the M.R.F. of the speed correction coefficients of the M.O. flat plate resistance thermometer and the R.A.E. pitot head thermometer, it was concluded that these coefficients decrease with increasing height. In M.R.P. 822(2) an account is given of attempts to verify this and the results obtained did not support the previous findings. It was thought that with regard to heights and airspeeds outside the limits of the aircraft then available (viz. a Hastings) it might well be that the speed correction coefficients varied with height in some regular manner but that further experimental work by the M.R.F. should await the availability of aircraft with a wide speed range at great heights. Meanwhile a series of flights(3) made in a Meteor VII aircraft at R.A.E. between sea level and 36,000 ft. produced fresh evidence of speed correction coefficients decreasing with height.

This problem came to the fore once again in the latter half of 1953 in connexion with the instrumentation of a Canberra aircraft which had just been allocated to the M.R.F. There happened to be an Ashton aircraft available at the same time, and some calibration trials were also carried out with thermometers fitted to this aircraft, mainly in order to provide a comparison with the data obtained on the Canberra.

/2.

2. Ashton flights

(i) Instrumentation

The thermometers used on the Ashton were

(a) a flat plate thermometer,

(b) a flat plate thermometer with two trip wires arranged ahead of the element to ensure that it was always in their turbulent wake,

(c) a conical head thermometer, made at the M.R.F. and shown in Fig.4.

The flat plate thermometers had elements with resistances of about 120 ohms and the resistance of the element of the conical head thermometer was about 160 ohms.

All three thermometers were mounted underneath and about midway along the starboard wing of the Ashton aircraft. Each thermometer was connected to a ratiometer and these together with altitude and airspeed indicators were mounted in an auto-observer panel. The panel was automatically photographed every 10 sec. by an F.24 camera.

(ii) Flight procedure

The speed runs were made in a manner similar to that described under the heading "Flight Procedure" in part I of M.R.P.822[2] but with increased height and airspeed ranges. The flying on this work was through the courtesy of Mechanical Engineering Dept., R.A.E. who allowed the observations to be made during their own investigations.

In all there were six flights in which it was possible to make speed runs. The flights were made at heights ranging from 5,000 ft. to 35,000 ft. with indicated airspeeds between 108 and 280 kt. The maximum number of levels at which pairs of speed runs were made on any flight was three and the maximum number of pairs of speed runs made at any level on any flight was also three. Each pair of speed runs consisted of one run at high speed and the other at low speed. In the calculations of the speed correction coefficient full position errors (including calibration compressibility errors (see Appendix B)) were allowed for.

3. Canberra flights

(i) Instrumentation

The thermometers used on the Canberra were

(a) a flat plate thermometer,

(b) a conical head thermometer,

(c) a thermometer installed on the port wing by the manufacturers.

(a) and (b) were the same thermometers as those used on the Ashton aircraft flights. (a) and (c) were used on all twelve flights but (b) was used on the first eight flights only.

Thermometers (a) and (b) were mounted under the nose of the Canberra aircraft, the flat plate to starboard and the conical head to port. The thermometer installed by the aircraft manufacturers is of the resistance type, the element of which is contained in a small cylinder, about 3 cm. long and 1 cm. diameter, which juts out from the leading edge of the port wing.

/(ii)

(ii) Flight procedure

On each flight readings of the flat plate and conical head thermometers were obtained from M.O. balanced bridges while the readings of thermometer (c) above were displayed on a ratiometer dial in the navigator's position. The two bridge readings and the height as displayed by a pressure altimeter were made by one member of the crew and the readings of airspeed, height as displayed by a radar altimeter and thermometer (c) were made by another member of the crew.

The lapse rate at the level of the speed runs was obtained by taking readings during one-minute runs 1,000 ft. below and 1,000 ft. above the operating level. By arranging these supplementary runs to be at the same speed the lapse rate was found directly from the difference of the indicated temperatures.

The speed runs themselves consisted of five-minute runs on two reciprocal bearings, one at high speed (about 340 kt. I.A.S. at heights up to 20,000 ft. and 230 kt. I.A.S. at 40,000 ft.) and one at low speed (about 140 kt. I.A.S. at all heights), readings being taken every 30 sec. Runs were made in clear air and at least 2,000 ft. above or below any cloud. Although it was the original intention to confine the speed runs to the levels 5,000, 20,000 and 40,000 ft. the presence of cloud made it necessary to fly at levels other than 5,000 ft. (usually 10,000 ft.) on some occasions and at 25,000 ft. instead of 20,000 ft. on one occasion. The runs were flown at constant radar altimeter height (as far as possible) and the values of the speed correction coefficients were obtained by three methods. The first method allowed for full pressure error correction to both height and airspeed. The second method made no allowance for position (pressure) error but allowed for calibration compressibility error to the airspeed. In the third method an attempt was made to use the readings of a radar altimeter to allow for static pressure errors to the airspeed, calibration compressibility errors having already been allowed for. The method does not provide any correction for static pressure errors in the altimeter readings. It has been shown however in Ref. 2 that the former normally give rise to errors in the speed corrections which are much greater than those produced by the latter. Provided that the radar altimeter gives correct readings this method should give a good indication of the accuracy of the pressure errors used in method 1.

4. Results

The results of the Ashton aircraft flights are given in Table 1 and those of the Canberra aircraft flights in Table 2.

Because of the small number of observations possible at levels up to 20,000 ft. with the Ashton aircraft, the results for 5,000, 10,000, 15,000 and 20,000 ft. were combined and those for 30,000 and 35,000 ft. were also combined.

(a) Flat plate thermometer

There is no evidence of any systematic variation of the speed correction coefficient with height and the mean values for all levels were 1.83 and 1.76 for the Ashton and Canberra aircraft respectively.

(b) Conical head thermometer

There is no evidence of any systematic variation of the speed correction coefficient with height and the mean values for all levels were 2.01 and 1.92 for the Ashton and Canberra aircraft respectively. These values are greater than those for the flat plate thermometer and Student's "t" tests carried out to determine the probabilities for each type of aircraft that these higher values of α could have arisen by chance, gave probabilities of only 4% for the Ashton aircraft and 0.05% for the Canberra aircraft. Combination of these two probabilities by a χ^2 test indicates a combined chance probability of only 0.5%.

/(c)

(c) Navigator's thermometer

There is no evidence of any systematic variation of the speed correction coefficient with height between 5,000 and 20,000 ft. where the mean value is 2.30 but the mean value at 40,000 ft., 2.94, is significantly larger. A "Fisher-Behrens" test carried out to compare these two mean values gave a level of significance of less than 0.1%. This difference between the means results in a large value for the standard deviation for all levels, given in Table 2 as .35.

The value of 2.94 is greater than that which would be realised by full kinetic heating ($\alpha = 2.38$). It is thought that the indicated airspeed values can not be applied directly to the position where this thermometer is mounted and it is doubtful whether the usual law of $\Delta T = \alpha (V/100)^2$ can be correctly applied in this case.

(d) Flat plate thermometer with trip wires

This thermometer, which was used only on the Ashton aircraft, had greatly reduced values of the speed correction coefficient compared with the ordinary flat plate thermometer. Otherwise no effects as regards variation with height through the use of these trip wires were detected.

(e) To test the significance of the larger values of the standard deviations of the speed correction coefficients at 40,000 ft. compared with lower levels, "Variance Ratio" tests were carried out for the flat plate, conical head and navigator's thermometers. These gave significance levels of about 6%, 2½% and 1% respectively. Clearly, some additional effect, most marked in the case of the navigator's thermometer, is in evidence at 40,000 ft.

5. Discussion

It appears from the results obtained that within the speed range of these experiments there is no consistent variation with height of the speed correction coefficients of the flat plate and conical head thermometers. This is in agreement with the findings of M.R.P. 822(2) but not with those of M.R.P. 527(1) or Ref. 3. The results also show a very large scatter.

The immediate purpose of this work was to provide values of the speed correction coefficients of the existing thermometers used by the Meteorological Research Flight and to estimate the accuracy with which temperature measurements can at present be made at high levels. From these results it appears that at levels up to 20,000 ft. the probable error of all the thermometers examined is less than 0.5°F. at speeds up to 200 kt. but increases with speed to about 2°F. at 450 kt. At 40,000 ft. the probable errors are somewhat larger being about 0.7°F. at speeds up to 200 kt. and about 3.5°F. at 450 kt.

In considering these errors, it must be remembered that the accuracy of all work on aircraft thermometry depends on the accuracy of the altimeter and air-speed indicator.

In all three methods of calculation the observed values of α showed considerable random variation which increased at high levels and it is apparent that the reason for it lies in the original observational data rather than in the method of calculation. Provided that calibration compressibility errors are initially allowed for, different methods of allowing for static pressure errors to the airspeed do not appreciably affect the result except at 40,000 ft. At this level values of α calculated by method 3 were significantly less than the corresponding values calculated by method 1. This suggests that at levels up to 20,000 ft. the static pressure errors used in method 1 are correct but that at 40,000 ft. they may be too small. This is contrary to evidence given in M.R.P. 926 which maintained that at 40,000 ft. the pressure errors used were correct. The true explanation of the discrepancy is not known but the consequence is to reduce the mean values of α. In the case of the flat plate thermometer α is reduced from 1.76 to 1.74 which has the effect of increasing the corrected value of the temperature by an amount which increases with speed from a negligible amount at 100 kt. to about 0.5°F. at 500 kt.

/It

It must be stressed however that the main reason for the scatter in the calculated values of α is that the original temperature data have a large scatter and it is not at all evident why this should be so. It was not found, however, that the deviations of individual values of speed correction coefficients from the mean values were associated with the angle at which the speed runs were flown across the thermal gradient. It might be that the scatter is in some measure due to the effect of atmospheric inhomogeneities.

Another possible cause of the scatter is concerned with differences in flow over the thermometer surfaces at different heights and airspeeds. In this respect, it is known that the practice of making speed runs at different levels using the same range of indicated airspeed masks any effects due to changes in Reynold's number. Such changes probably contribute to the variations in α from one level to another but do not provide an explanation of the scatter found at a particular level. The inference is that the scatter at any level and from one level to another are due to some other factor.

It is thought that further work on the causes and elimination of the scatter of the original observations is necessary before further progress can be made in the design of aircraft thermometers. Meanwhile it is considered that either the flat plate thermometer or the conical head thermometer is as good an indicator of free air temperature as any other type of aircraft thermometer now available.

Acknowledgements

Acknowledgements are due to Mr. R. J. Murgatroyd at whose suggestion the work was carried out and to whom the suggested method of using the radar altimeter is due. The author is also indebted to the Mechanical Engineering Dept., R.A.E. for the use of the Ashton aircraft.

References

1. Shellard, H.C. 1949. Variation with altitude of the speed correction coefficient of aircraft thermometers. M.R.P. 527.

2. Murgatroyd, R.J. 1953. A report on the determination of the speed correction coefficients of aircraft thermometers made by M.R.F. in 1951. M.R.P. 822.

3. Allen, R.M., F/Lt. 1953. The experimental determination of the speed correction factor of an outside air temperature thermometer. Tech. Memo No. Aero. 306.

4. Meteorological Air Observer's Handbook. 1945. M.O.470.

5. Charnley and Fleming. 1949. R.A.E. Report No. Aero. 2299.

APPENDIX A

Methods of calculating the speed correction coefficients

Equation (3) of M.R.P. 822 gives as a good approximation the result

$$\alpha = \frac{(T_H - T_L)P}{\frac{1{\cdot}95}{100^2}\left\{V_H^2(T_L+459) - V_L^2(T_H+459)\right\}} \qquad \text{-----(1)}$$

where T = indicated temperatures in degrees Fahrenheit,
V = equivalent airspeed (see Appendix B) in kt.,
P = pressure in mb.

Suffixes "H" and "L" refer to the values at the fast and slow speeds and it is assumed that both runs were made at the same pressure level. This assumption is rarely true however and more accurately

$$\alpha = \frac{T_H - (T_L + dT)}{\frac{1{\cdot}95}{100^2}\left\{\frac{V_H^2}{P_H}(T_L+459) - \frac{V_L^2}{P_L}(T_H+459)\right\}} \qquad \text{-----(2)}$$

where P_H and P_L are the pressures corresponding to indicated altimeter heights for the fast and slow speed runs respectively and where dT is the amount by which the true air temperature at the level at which the fast run was made exceeds that at the level at which the slow run was made.

Equation (2) was used in the first two methods of calculation, the only difference being that in the first method the indicated pressure heights and airspeeds were corrected for full pressure errors (including calibration compressibility errors) and in the second method airspeeds were corrected for calibration compressibility errors only. The latter correction is always necessary in this work.

The correction for position (pressure) error at the static source is necessary whenever the lapse rate departs considerably from the saturated adiabatic value (Ref. 2). Hence it will usually be small in the troposphere except in inversions and large in the stratosphere. The relative accuracies of the above two methods are related to the deviation of the actual lapse rate from the saturated adiabatic value.

In the third method of calculation it is assumed that the static pressure is in error by an amount dP. This can be regarded as giving rise to an error dZ in true pressure height where

$$dZ = -\frac{dP}{g\rho} \qquad \text{.....(3)}$$

where ρ is the density of the ambient air and g is the gravitational constant.

Let P and V' be the true pressure and true airspeed respectively at the level of flight. Then, from Bernouilli's equation for steady flow of an inviscid fluid (viz. $\int \frac{dP}{\rho} + \frac{V'^2}{2} = \text{constant}$) it follows that a pressure error dP can also be regarded as giving rise to an error dV' in true airspeed where

$$dP = -\rho V' dV' \qquad \text{.....(4)}$$

It follows that if dP is <0, dZ and dV' must be >0. In other words, due to a negative static pressure error within the static tube, both airspeed indicator and altimeter read high.

/Furthermore

Furthermore, the pressure height of the aircraft will differ from the true height of the aircraft by an amount that depends on the difference between the actual atmosphere and the standard I.C.A.N. atmosphere.

Combining equations (3) and (4)

$$dZ = V' dV'/g \qquad \text{.....(5)}$$

For the fast and slow speed runs

$$dZ_H = V_H' dV_H'/g \quad \text{and} \quad dZ_L = V_L' dV_L'/g$$

so that $$dZ_H - dZ_L = \frac{1}{g}(V_H' dV_H' - V_L' dV_L') \qquad \text{.....(6)}$$

Fig.1 illustrates the notation and the circumstances in which dP is a negative static pressure error so that dZ_H and dZ_L are errors in indicated height due to the error dP. dZ_H' and dZ_L' are the differences between I.C.A.N. pressure heights and the true heights, and for simplicity of illustration are shown in Fig.1 as arising from an atmosphere that is colder than the standard I.C.A.N. atmosphere.

From Fig.1 it will be seen that

$dZ = Z'' - Z'$ and $dZ' = Z' - Z$ for both high and low speed runs. Hence

$$(dZ_H - dZ_L) = (Z_H'' - Z_L'') - (Z_H - Z_L) - (dZ_H' - dZ_L')$$

Now, $Z_H - Z_L$ is the difference between the radar altimeter readings which are assumed to be correct and $Z_H'' - Z_L''$ is the difference between the indicated pressure heights for the high and low speed runs. $(dZ_H' - dZ_L')$ is the difference between a small height interval (equal to the difference between the mean height at which the high and low speed runs were flown) and the response to it of a pressure altimeter. Assuming no instrument lag, this difference will be small compared with $(Z_H'' - Z_L'') - (Z_H - Z_L)$ and may be ignored. Hence

$$(Z_H'' - Z_L'') - (Z_H - Z_L) = \frac{1}{g}(V_H' dV_H' - V_L' dV_L') \qquad \text{.....(7)}$$

It is shown (4) that the relation between true and indicated airspeeds is given by

$$V' = V\left[1{\cdot}95(T'+459)/P\right]^{1/2}$$

where T' is the true air temperature in $^{\circ}F$, P the true air pressure in mb. and where the true airspeed V' and indicated airspeed V are in knots. At any particular level of flight therefore

$$dV' = dV\left[1{\cdot}95(T'+459)/P\right]^{1/2} \qquad \text{.....(8)}$$

If allowance is made for the static pressure errors to the airspeed, equation (2) becomes

$$\alpha = \frac{T_H - (T_L + dT)}{\frac{1{\cdot}95}{100^2}\left\{\frac{(V_H - dV_H)^2}{P_H}(T_L+459) - \frac{(V_L - dV_L)^2}{P_L}(T_H+459)\right\}}$$

where V_H and V_L are the airspeeds corrected for calibration compressibility only and dV_H and dV_L are the static pressure errors to the airspeed.

The new denominator is less than the denominator of (2) by

$$2\left(\frac{1{\cdot}95}{100^2}\right)\left\{\frac{V_H\, dV_H}{P_H}(T_L+459) - \frac{V_L\, dV_L}{P_L}(T_H+459)\right\}$$

neglecting the terms containing $(dV_H)^2$ and $(dV_L)^2$.

/Using

Using equation (8) this becomes $\frac{2}{100^2}\left(V_H' dV_H' - V_L' dV_L'\right)$ where the approximations

$$\frac{T_H+459}{T_L'+459} = \frac{T_L+459}{T_H'+459} = 1 \qquad \text{are made.}$$

Finally, using equation (7) this expression becomes $\frac{29}{100^2}\left\{(Z_H''-Z_L'')-(Z_H-Z_L)\right\}$ and the modified equation for the third method of calculating the speed correction coefficient becomes

$$\alpha = \frac{T_H-(T_L+\alpha T)}{\frac{1{\cdot}95}{100^2}\left\{\frac{V_H^2(T_L+459)}{P_H} - \frac{V_L^2(T_H+459)}{P_L}\right\} - \frac{2}{100^2}\left\{(Z_H''-Z_L'')-(Z_H-Z_L)\right\}}$$

APPENDIX B

Note on the corrections to be applied to indicated airspeed readings

An airspeed indicator and altimeter do not in general correctly indicate the "free stream" (i.e. away from the pressure field surrounding the aircraft) pressures from which the speed and pressure altitude must be deduced. The calibrations of these instruments are chosen so that the derivation of the free stream pressures from the indicated pressures is a simple process. In the case of the airspeed indicator the scale equation is

$$P_D = \tfrac{1}{2}\rho_0 V_R^2 \left(1 + \tfrac{1}{4}\frac{V_R^2}{a_0^2}\right)$$

where P_D is the dynamic pressure, ρ_0 and a_0 are the density of air and the speed of sound under standard sea level conditions and V_R is the actual reading of the airspeed indicator.

If the free stream conditions were applied to the pitot static system the corresponding equation would be

$$P_d = \tfrac{1}{2}\rho_0 V_r^2 \left(1 + \tfrac{1}{4}\frac{V_r^2}{a_0^2}\right)$$

where P_d is the dynamic pressure in the free stream and V_r is the airspeed indicator reading corresponding to P_d.

Under standard sea level conditions and in the absence of compressible flow, V_r would be the same as the true airspeed V. Compressibility is however always present to some extent and its effect under standard sea level conditions is to introduce a difference between V_r and the true airspeed. This error is small at low speeds but increases with speed and is due to compressibility not being allowed for in the original calibration of the instrument. It is called the Calibration Compressibility error.

When the airspeed indicator is used under conditions of free stream air density ρ (i.e. different from ρ_0) and in the absence of compressibility the true airspeed V is equivalent to an airspeed V_i (which is what the instrument would read) called the "Equivalent Airspeed". V_i is related to V by the equation

$$V_i = V(\rho/\rho_0)^{1/2}$$

Again allowing for compressibility, the indicated airspeed V_r differs from the equivalent airspeed V_i due to the calibration compressibility error.

Conditions of air density and true airspeed (and hence equivalent airspeed) in the free stream differ from those at the static source due to position error so that the actual indicated airspeed V_R depends on the equivalent airspeed at the static source.

It follows that to obtain true airspeed V from indicated airspeed V_R it is necessary first of all to find the equivalent airspeed in the free stream, V_i. This involves knowing the position error and calibration compressibility error and they are obtained by means of the "aneroid method". The values near the surface are found by comparing the aircraft heights as read on the altimeters with those obtained from ground photography as the aircraft flew low over the runway at various speeds. These results are then extrapolated to altitude by the method of Ref. 5. The errors for both the Ashton and Canberra aircraft were obtained in this way and are plotted as combined errors in Figs. 2 and 3.

Table 1

Ashton Aircraft Results

Type of thermometer	Height (ft.)	Number of measurements	Mean α	Standard deviation	Greatest α	Smallest α
Flat plate	5,000, 10,000, 15,000, 20,000 (combined)	6	1.82	.22	2.12	1.58
	30,000, 35,000 (combined)	8	1.83	.18	1.96	1.42
	all levels	14	1.83	.20	2.12	1.42
Flat plate with trip wires	5,000, 10,000, 15,000, 20,000 (combined)	7	0.99	.37	1.51	0.67
	30,000, 35,000 (combined)	8	1.07	.31	1.43	0.41
	all levels	15	1.03	.31	1.53	0.41
Conical head	5,000, 10,000, 15,000, 20,000 (combined)	9	1.94	.17	2.26	1.66
	30,000, 35,000 (combined)	8	2.08	.43	2.84	1.48
	all levels	17	2.01	.32	2.84	1.48

Table 2

Canberra Aircraft Results (all values)

Type of thermometer	Height (ft.)	No. of measurements	Mean α (Method 1)	Mean α (Method 2)	Mean α (Method 3)	Standard deviation	Greatest α Method 1	Smallest α
Flat plate *	5,000	5	1.78	1.80	1.78	.12	1.92	1.60
*	10,000	6	1.80	1.81	1.80	.12	1.93	1.59
*	20,000	9	1.67	1.69	1.68	.11	1.76	1.42
	40,000	11	1.81	1.83	1.73	.20	2.25	1.58
	all levels	31	1.76	1.78	1.74	.15	2.25	1.42
Navigator's *	5,000	5	2.28	2.29	2.27	.14	2.37	2.15
thermometer *	10,000	6	2.28	2.31	2.28	.15	2.53	2.04
*	20,000	9	2.34	2.36	2.35	.11	2.50	2.13
	40,000	11	2.94	2.99	2.84	.23	3.43	2.65
	all levels	31	2.53	2.56	2.50	.35	3.43	2.04
Conical head *	5,000	4	2.01	2.02	1.99	.08	2.08	1.94
*	10,000	3	1.91	1.93	1.92	.15	2.03	1.74
*	20,000	6	1.93	1.94	1.93	.16	2.03	1.61
	40,000	7	1.87	1.89	1.81	.25	2.31	1.54
	all levels	20	1.92	1.94	1.90	.17	2.31	1.54

* includes one value at 3,000 ft. at 5,000 ft. level, one value at each of 8,000 ft. and 9,000 ft. at the 10,000 ft. level and one value at 25,000 ft. at the 20,000 ft. level.

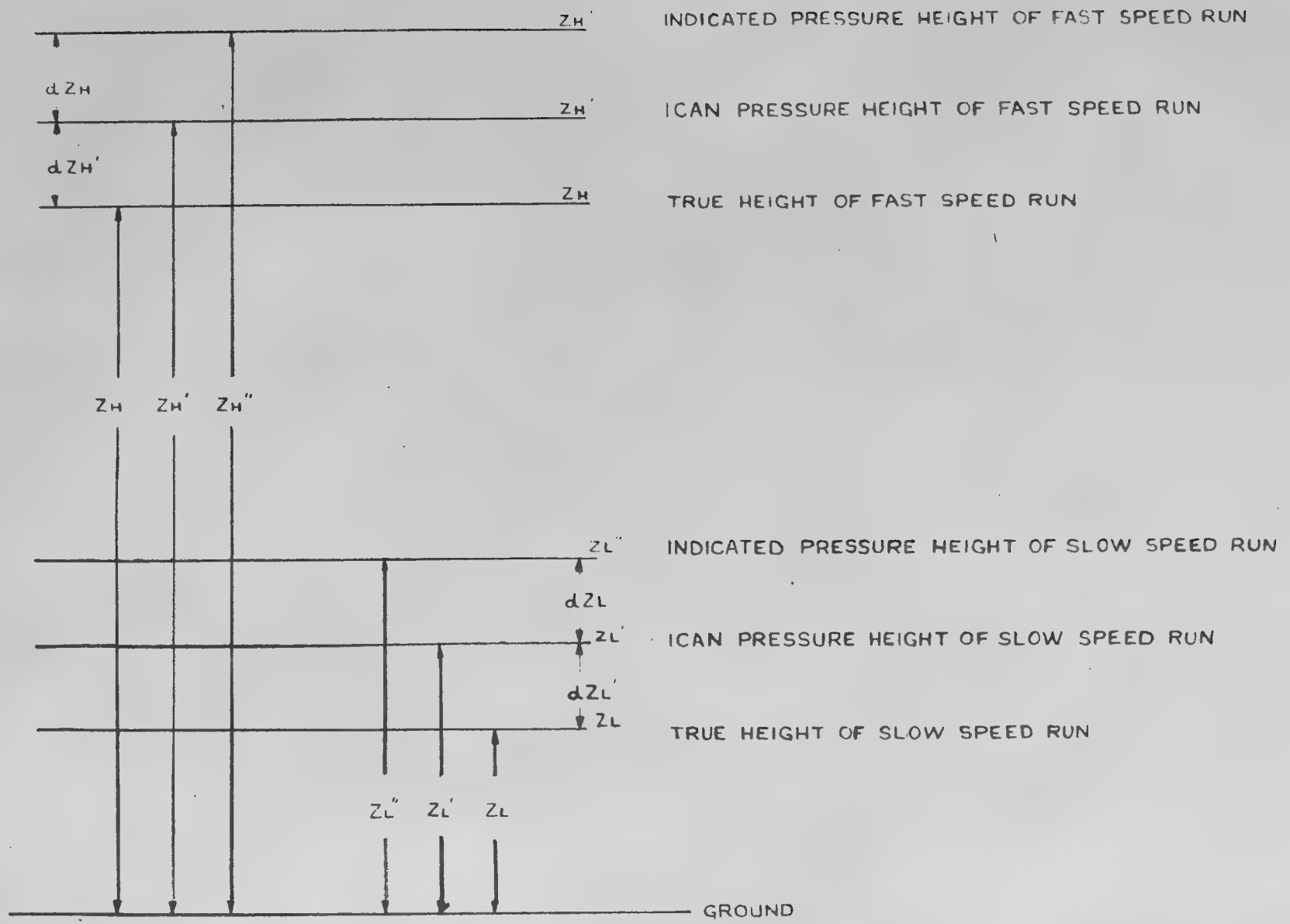

FIG. 1. DIAGRAM OF NOTATION USED IN THE THIRD METHOD FOR CALCULATION OF SPEED CORRECTION COEFFICIENTS.

M.R.P. 930 FIG. 1.

FIG.2.a & b.

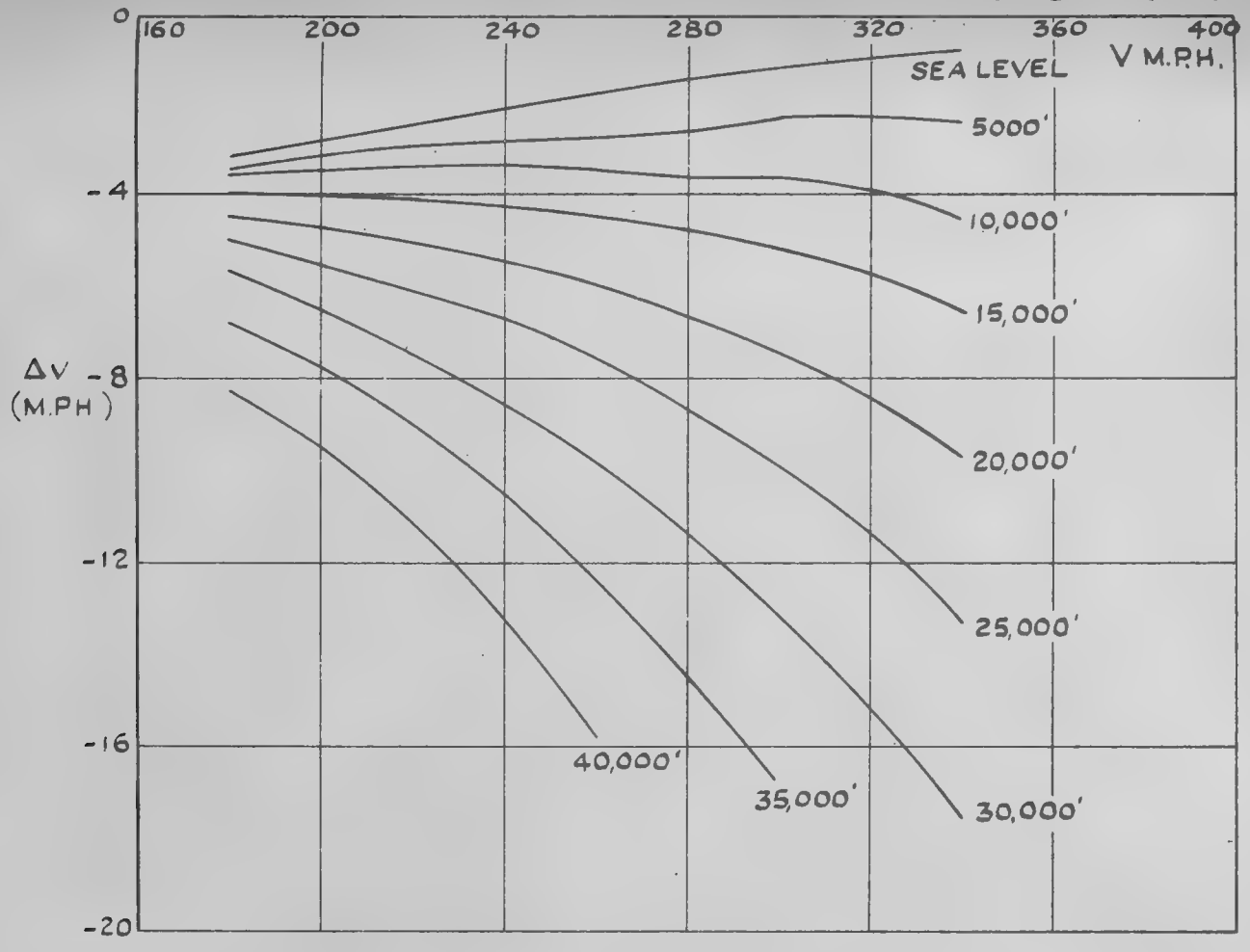

a. INDICATED AIRSPEED.

b. INDICATED PRESSURE HEIGHT.

FIG.2.a & b. COMPLETE ASHTON CORRECTIONS.

FIG. 3. a & b.

a. INDICATED AIRSPEED

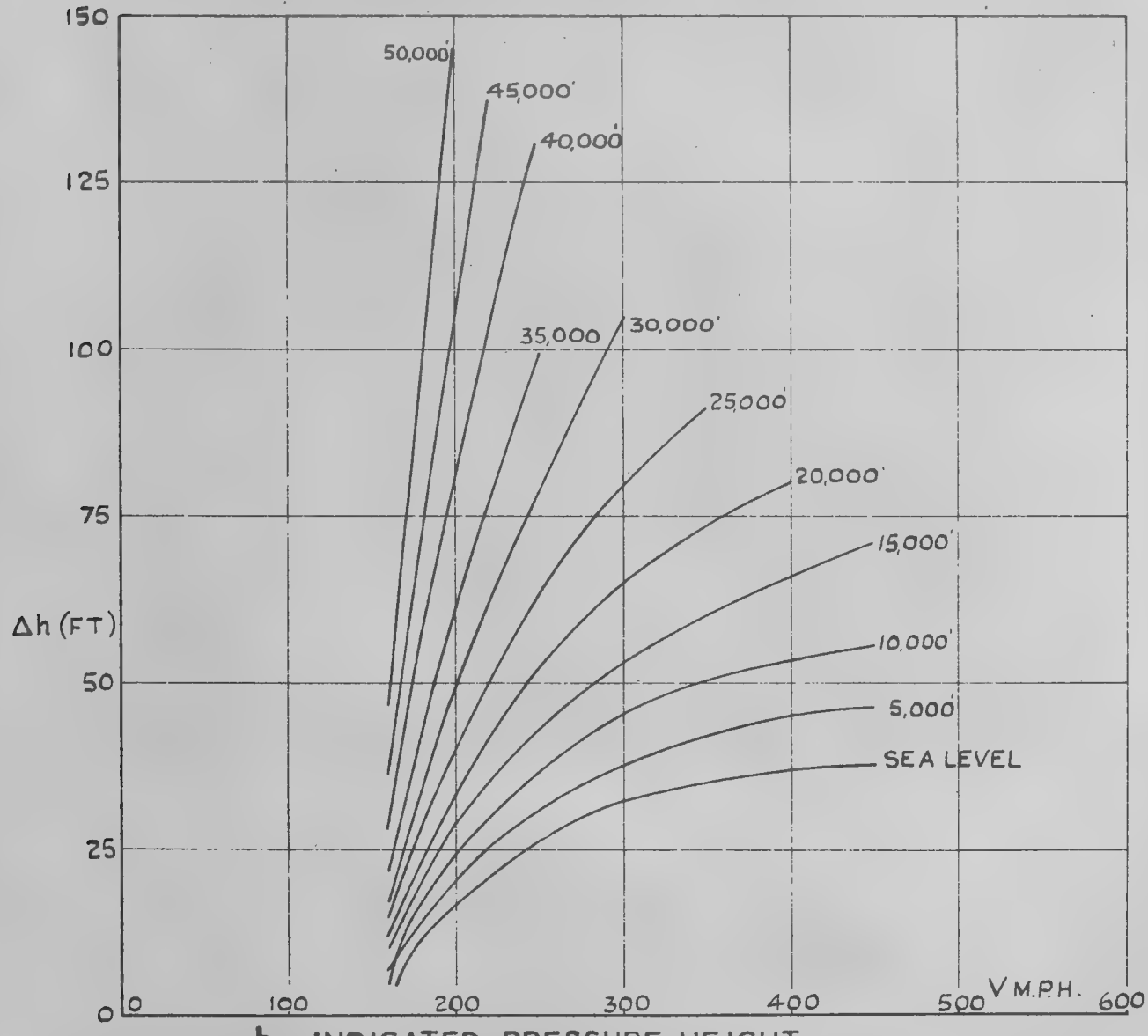

b. INDICATED PRESSURE HEIGHT

FIG 3. a & b. COMPLETE CANBERRA CORRECTIONS.

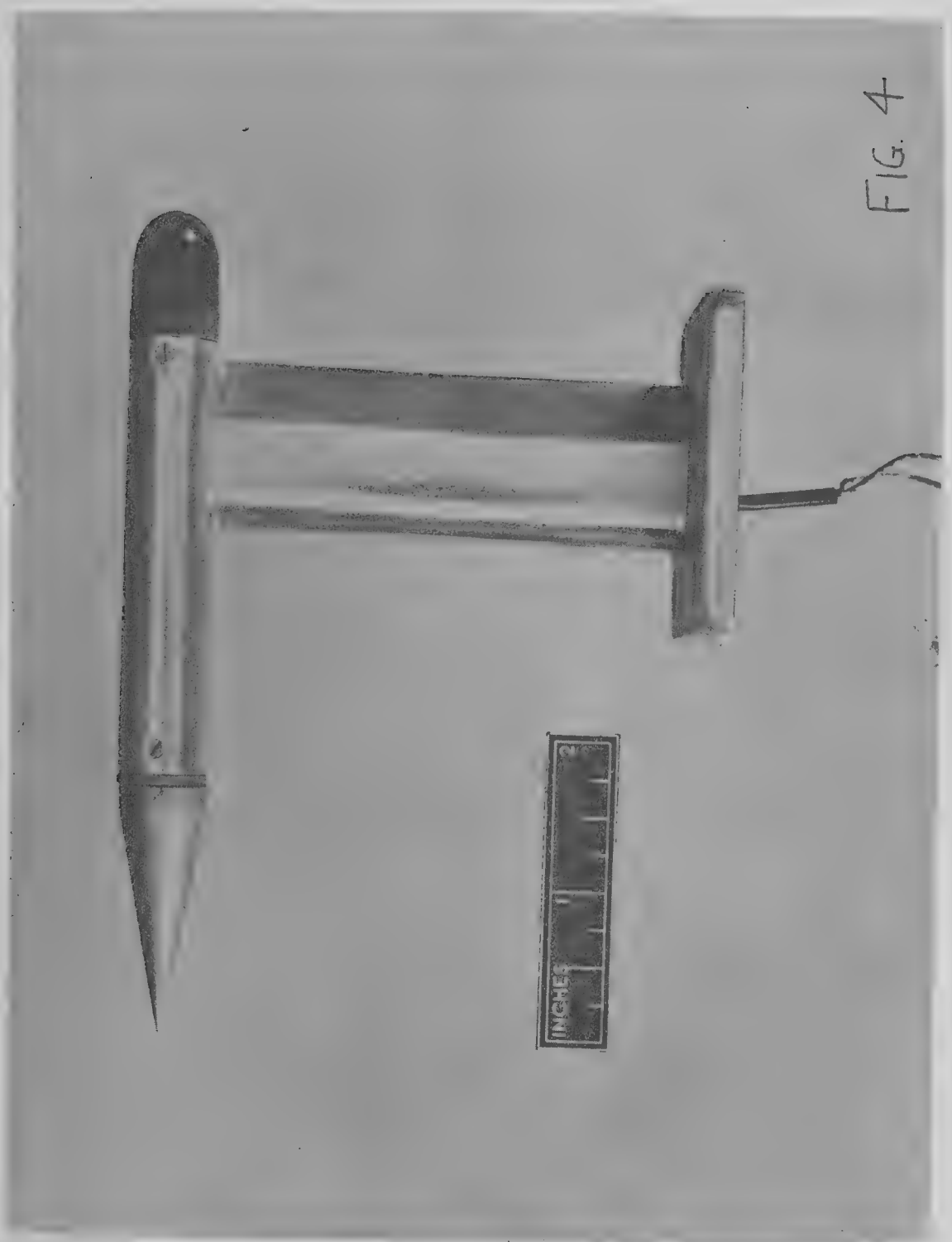

FIG. 4

M.R.P. 931
S.C. 111/190
14th September, 1955

Some statistical aspects of a rain-making experiment

by

A. F. Jenkinson
(Meteorological Office)

AIR MINISTRY
METEOROLOGICAL RESEARCH COMMITTEE

56 322

At the time of issue this report has not been published. Any author desiring to quote this paper should refer to it as "A paper of the Meteorological Research Committee (London).
M.R.P. No. 931 by Mr. A.F. Jenkinson
A copy is available in the Library of the Meteorological Office."

M.R.P. 931
S.C.III/190
14th September, 1955

AIR MINISTRY
METEOROLOGICAL RESEARCH COMMITTEE

Some statistical aspects of a rain-making experiment

by
A. F. Jenkinson (Meteorological Office)

1. Nature of the experiment

The experiment is one which the Meteorological Office proposes to carry out during the next two or three years and is designed to enable us to assess the effects of cloud seeding from ground based silver iodide generators, located in the Salisbury Plain area, in a particular type of weather situation, viz. cloudy (frontal) situations with south-westerly winds.

The variability of rainfall amount in these situations, although of course less than in other situations in which convection may play a considerable part, is nevertheless considerable, and the ratio of the standard deviation S_x to mean rainfall $\bar{x}$ is of the order of 1.5 if occasions with very slight rainfall are included. (This has also been confirmed from data sent to me by J. S. Sawyer. The data were provided by G. A. Corby). Since these light falls are not of importance to the rainfall total, and since also it is difficult to give any meaning to a proportionate increase of rainfall when the rainfall is small, it is better to consider only occasions which give substantial falls of rain.

To make the selection of occasions objective, and to ensure that the ratio $S_x/\bar{x}$ is as low as possible while retaining an adequate number of occasions, the criterion chosen for selection of an occasion is that there should be a broad south-westerly air stream south of the Humber with layered (frontal) cloud which gives 5mm. or more of rain in the Salisbury area (mean rainfall for four stations). In these situations the ratio $S_x/\bar{x}$ is very nearly 0.66 over a large area of England.

2. Locating the silver iodide plume

At the moment little is known about the diffusion of the plume, and in the cloudy conditions we expect during the seeding operations it may not be possible to make effective use of tracer substances. In the light of present knowledge the best method of locating the plume at the "effective" seeding levels, with temperatures between -3°C. and -15°C., is to adopt the suggestion of R. F. Jones (1954), that the plume at those levels has been carried there by the mean vector wind from the surface to those levels. (In a verbal communication, F. Pasquill has said that this approximation is probably fairly reasonable.)

This gives us the direction in which to look for the plume at the effective seeding levels. Formulae given by O.G. Sutton (1947; 1953, p.287) for diffusion from a point source, indicate that the concentration of silver iodide is a maximum at a height H at a distance D where

$$H = C\, D^{\frac{7}{8}}$$

and C is approximately constant (probably varying from 0.5 to 2.0 times the mean of its value under all conditions). For H in thousands of feet and D in miles, the mean value of C is about 0.2 (R.F. Jones, 1954; O.G. Sutton, 1953, p.292). Corresponding values of H and D for a mean C are given in Table 1.

TABLE 1. CORRESPONDING VALUES OF H AND D

$H(10^3$ ft.)	D(mi.)
2.5	20
5.5	50
10.1	100
14.4	150
18.5	200
22.6	250

Thus, without a knowledge of C_S, the value of C for a particular seeding occasion, there is likely to be some doubt about the horizontal distance of the area effectively seeded. R. F. Jones (1954) suggests that location of a succession of balloons, fitted with radar target and having a slow rate of ascent (100 to 200 ft./min.), released at $\frac{1}{2}$ hour to 1 hour intervals might provide data for an assessment of C_S. These balloons would also give regular wind measurements over approximately the same track as the smoke.

Some knowledge of the diffusion of small particles of silver iodide has been gained from experimental work on the diffusion of small particles of "tracer" substances. The tracer substance most commonly used up to the present time has been zinc sulphide. This has the disadvantage that it can only be used in clear air. Sampling has been carried out at levels up to 4,000 feet. (R.R. Braham, B.K. Seely and W.D. Crozier, 1952).

O. Vittori (1954) has suggested that silver nitrate particles can be emitted along with the silver iodide, and detected by a modification of the Liesegang reaction.

Future work with tracer substances will increase our knowledge of the vertical diffusion of small particles of silver iodide, and it may be that values of C_S will be determined on individual occasions.

3. Vertical and horizontal distribution of the effectively seeded clouds

It may be noted that the assumption in this paper that an effect of seeding is to be detected by statistical methods is equivalent to an assumption that silver iodide smoke diffuses vertically to heights of say 20,000 feet, through cloud and probably through rain. With this assumption let us examine the vertical and horizontal distribution of the effectively seeded clouds.

The vertical diffusion of the silver iodide smoke is depicted in Fig. 1. Since in general wind increases with height, the motion of the silver iodide smoke relative to the cloud formations, is like that of the paths AA^1, BB^1, CC^1. The cloud is above the frontal slope A^1C. The two levels -3°C. and -15°C., between which silver iodide is said to be most effective as a seeding agent, are shown. Then the emissions of silver iodide which first reach the medium cloud layers, AA^1, may well be above the -15°C. level. We may first seed in the "effective" layer at X along BB^1 and the last seeding, through cloud and rain from near the surface, may be supposed to be along CC^1.

Now let us suppose for example that the time between the beginning of movement of silver iodide along BB^1 and CC^1 is seven hours. Then during that period the particle paths will have changed due to the variations of vector wind with time. Fig. 2 shows the horizontal projection of the particle paths of the silver iodide (not streamlines). Then the line OA_1 shows the particle path for the ascent AA^1, OB_1 for BB^1, OC_1 for CC^1. The line $A_1X_1Y_1O$ shows where cloud is first met. X_1X_2 and Y_1Y_2 show where the -15°C. and -3°C. levels are reached. Then the area $X_1Y_1Y_2X_2$, together with any additional area due to the plume having definite width, is the "seeded" area.

/On

On occasions the latitudinal movement of the plume due to the vector change of wind with time may be as much as 20 to 30 miles at a distance from the generators of 100 miles; but if we for the moment consider the plume to be very narrow then the areas seeded during each hour will be those marked in Fig. 2 with the words "First hour", "Second hour" etc., corresponding only to the vertical cloud structures marked "First hour" etc. in Fig. 1. The plume width from a single generator, from the analysis of R. F. Jones (1954), is effectively of the order of 5 to 10 miles, and this width is only slightly increased even by large (ten-fold) increases of the rate of production of silver iodide particles by the generator.

If there is no change of vector wind with time, and we have a single generator, then all the vertical cloud structures marked first hour, second hour etc. will pass over the same horizontal plume width of 5 to 10 miles. It will be seen, if we have a single generator, that as the latitudinal distance which the plume moves due to vector variation of wind with time increases, so does the relative efficiency of seeding of any horizontal area decrease, defining efficiency of seeding as the proportion of the cloud structures which pass over the area; and with a latitudinal time-movement of the plume of 30 miles (at a distance of 100 miles) and a single generator with plume width of 10 miles, each part of the horizontal extent of the plume receives one third or less of the cloud structure, while if the multiple generator plume width is 30 miles there will be an area 30 miles wide over which four sevenths or more of the cloud structure passed, and an area 20 miles wide over which five sevenths or more of the cloud structure passed. Fig. 3 shows what parts of the cloud structure would pass over the various horizontal widths for a latitudinal time-movement of the plume of 30 miles, and plume widths of 10, 20 and 30 miles.

It is evident that to ensure a high seeding efficiency over an area 20 miles wide it is necessary to have a line of generators, say five, over a width of 20 to 25 miles, perpendicular to the S.W. direction. This will also greatly increase the probability that, even with some uncertainty in the angular direction of the plume, we would be able to locate a substantial area which has been efficiently seeded.

4. Statistical analysis

If $y = x/\bar{x}$ where x is a random variable with expected value ξ and standard deviation σ such that $\sigma/\xi = \alpha$ and $\bar{x}$ and S_x are the mean value and standard deviation of x determined from N values, then to order $1/N$ the expected value and variance of y are

$$\left.\begin{aligned} \mathcal{E}(y) &\simeq 1+(\alpha^2/N) \\ \sigma^2(y) &\simeq \alpha^2\left[1+\frac{1+3\alpha^2}{N}\right] \end{aligned}\right\} \quad \text{- - - - - -} \qquad (1)$$

(N. L. Johnson and H. Tetley, 1949, Vol. I, 7.38 and 7.39)

If x is the rainfall of a small area for a particular experimental occasion, then if $\bar{x}$ is the mean derived from over 200 occasions, and we note that $\alpha \simeq 0.66$, then

$$\left.\begin{aligned} \mathcal{E}(y) &\simeq 1{\cdot}002 \\ \sigma^2(y) &\simeq 1{\cdot}01\alpha^2 \end{aligned}\right\} \quad \text{- - - - - -} \qquad (2)$$

It is proposed to estimate the mean and standard deviation of the falls of rain in small areas for the selected occasions during the period 1945-54. There are about 20 to 25 occasions a year, and we should have 200 to 250 occasions for our estimate of mean, standard deviation and the ratio α.

/But

But for the purpose of the present preliminary analysis, the rainfall for each of the 92 occasions during the 4-year period 1951-54 has been extracted from the twice-daily readings given in the Daily Weather Report. Rainfalls for West Malling were extracted from M.S. data in the Meteorological Office, M.O.3. The area was divided into 8 sub-areas, A, B, C, D, E, F, G, H. These are shown in Fig. 4. The stations used to give the mean rainfall on each occasion are marked. For each sub-area the mean rainfall for the 92 occasions was computed, and also the ratio $S_x/\bar{x}$, approximately α. The value of $S_x/\bar{x}$ did not vary much from area to area (see Table 5) and we are justified in using a mean value of 0.66 for the whole area. We may be able to assess a more accurate value for α when rainfall for all occasions during 1945-54 is analysed.

Because of the correlation between the rainfall of one sub-area and the rainfall in a neighbouring area, we can estimate the proportion $y = (x/\bar{x})$ received in any area from the proportion $y_1 = (x_1/\bar{x}_1)$ received in a neighbouring area. The estimate y^1 is given by

$$y^1 - \bar{y} = b(y_1 - \bar{y}_1) \qquad (3)$$

where $\bar{y}$, $\bar{y}_1$ are the mean values of y and y_1 in the sample of N, and

$$b = r \frac{S_y}{S_{y_1}} \qquad (4)$$

where r is the correlation coefficient between y and y_1, and S_y, S_{y_1} are the standard deviations of y and y_1, found from the sample. The residual variance S_Y^2 of the differences $Y = y - y^1$ is given by

$$S_Y^2 = S_y^2 (1 - r^2) \qquad (5)$$

It may be noted that r is also the correlation coefficient between x and x_1, and

$$S_y = (S_x/\bar{x}) \qquad S_{y_1} = (S_{x_1}/\bar{x}_1)$$

By using a combination of areas, we can estimate y by a linear regression in terms of the several ratios $y_i (i = 1, 2, 3 \ldots)$ and the residual variance S_Y^2 will be given by

$$S_Y^2 = S_y^2 (1 - R^2) \qquad (6)$$

where R is the multiple correlation coefficient between y and the y_i.

If we contemplate using a ten-year period, with N situations, to estimate the regression, and a three-year period with n situations to test the seeding effects, N and n will be of the order of 230 and 69 respectively.

Then if $\overline{Y_n}$ is the mean value for the n occasions of the differences y and y^1 based on a simple regression, then we can test the null-hypothesis that seeding has not increased rainfall by means of the t-variable

$$\frac{\overline{Y}_n}{\left[S_y^2 (1 - r^2) \left(\frac{1}{n} + \frac{1}{N} + C_{11} \overline{y_{1n}}^2 \right) \right]^{1/2}} \qquad (7)$$

for approximately 300 degrees of freedom.

$/\overline{y_{1n}}$

$\overline{y_{1n}}$ is the mean of the n values of $(y_1 - \overline{y_1})$ and C_{11} is the Gaussian coefficient. The term $C_{11}\overline{y_{1n}}^2$ is unimportant with these sample sizes.

Strictly, the t-test can only be applied if the population of Y's, whose expected value is 0, is normally distributed, but the test can be satisfactorily applied if the Y's are reasonably near normal.

The t-test may be extended to a multiple regression, with multiple correlation coefficient R, replacing r by R in expression (7) and $C_{11}\overline{y_{1n}}^2$ by $\sum_{ij} C_{ij}\overline{y_{in}}\,\overline{y_{jn}}$ where i, j take values 1, 2, ... N. This sum is also unimportant with these sample sizes. Multiple regressions are however not easy to compute, and for the purpose of this assessment we can use a simpler approach.

When using a simple correlation, y estimated from y_1, then the best estimation line for y, taking S_y and S_{y_1} to have the same value, is

$$y = ry_1 + (1 - r) \qquad (8).$$

But if we were to consider the best estimation line for y_1 from y this is

$$y_1 = ry + (1 - r) \qquad (9)$$

So, if a straight line really represents a good fit to the data of y and y_1, that is if r is high, there seems, from the physical aspect, much to be said for using the common estimator $y = y_1$. The variance of $(y - y_1) = 2(1-r)\,S_y^2$ and we see from Table 2 that for $r \geq 0.8$ there is little difference between $\sqrt{1 - r^2}$ and $\sqrt{2(1 - r)}$.

TABLE 2

CORRESPONDING VALUES OF $\sqrt{1 - r^2}$ and $\sqrt{2(1 - r)}$

r	$\sqrt{1 - r^2}$	$\sqrt{2(1 - r)}$
0.80	0.600	0.633
0.85	0.527	0.548
0.90	0.436	0.447

If we extend this method and estimate y by

$$y^1 = \frac{1}{m}(y_1 + y_2 + \cdots y_m)$$

then $$Y = y - \frac{1}{m}(y_1 + y_2 + \cdots y_m)$$

If $S_y^2 = S_{y_1}^2 = S_y^2 = \cdots a^2$ (very nearly equal to a^2)

$$S_Y^2 = a^2\left\{(1 + \frac{1}{m})(1 - \overline{r_{ij}}) - 2(\overline{r_i} - \overline{r_{ij}})\right\} \qquad (10)$$

where r_i is the correlation between y and y_i

r_{ij} is the correlation between y_i and y_j

Figs. 5 to 12 show the correlations between each of the sub-areas and the remainder of the area. It will be apparent from the variation of these correlations that around each seeded area it should be possible to find four neighbouring areas each with a correlation of 0.70 or more with the seeded area, but with a smaller average degree of correlation among themselves if they are chosen two each on opposite sides of the seeded area. Table 3 gives the values of $\sqrt{(1 + \frac{1}{m})(1 - \overline{r_{ij}}) - 2(\overline{r_i} - \overline{r_{ij}})}$

/for

for corresponding values of $\overline{r_i}$ and $\overline{r_{ij}}$.

TABLE 3. VALUES OF $\sqrt{(1 + \frac{1}{m})(1 - \overline{r_{ij}}) - 2(\overline{r_i} - \overline{r_{ij}})}$

$\overline{r_i}$ \ $\overline{r_{ij}}$	0.60	0.65	0.70	0.75
0.70	0.55	0.58		
0.75		0.49	0.52	
0.80			0.41	0.46

A value for $\sqrt{(1 + \frac{1}{m})(1 - \overline{r_{ij}}) - 2(\overline{r_i} - \overline{r_{ij}})}$ of 0.60 or less indicates a multiple regression coefficient of 0.80 or more.

We may thus reasonably expect to be able to find for each seeded area a group of areas which have a multiple correlation coefficient with the seeded area of 0.80 to 0.85, giving a value for S_Y of 0.60 a or less.

Even with the rather widely spaced areas used in this analysis, this estimation is confirmed. In estimating the rainfall of area E from rainfalls of G, F, W and H, $\overline{r_i} = 0.69$, $\overline{r_{ij}} = 0.60$ and $S_Y = 0.56$ a. In estimating the rainfall of area C from rainfalls of A, B, X and W, $\overline{r_i} = 0.71$, $\overline{r_{ij}} = 0.56$, $S_Y = 0.50$ a.

If we take a = 0.66 and we use the (maximum) value $S_Y = 0.60$ a $\simeq 0.40$ for the purpose of this analysis we can ignore the varying locations of the seeded area and its concomitant regression areas, and we can use the t-test (effectively the normal since $n + N \simeq 300$) to test the null hypothesis that there is no increase in rainfall due to seeding. The value of t will be effectively

$$\frac{\overline{Y_n}}{0.40\left(\frac{1}{69} + \frac{1}{230}\right)^{1/2}} = \frac{\overline{Y_n}}{0.055} \qquad (11)$$

Thus, given the answer $\overline{Y_n}$ for the experiment with n seedings, we can give the conclusion:

If $\overline{Y_n} > (2\frac{1}{3} \times 0.055) = 0.13$ then there is a probability of 0.99 that seeding has produced a real increase in rainfall.

So if the experiment reveals that the rainfall in the seeded area is greater by 13 per cent. than would be predicted from the rainfalls of neighbouring non-seeded areas we can say that there is only 1 chance in 100 of this increase having occurred by chance variation of rainfall. If the experiment reveals a 16 per cent. greater value than predicted from neighbouring non-seeded areas we can say that there is only 1 chance in 1000 of this increase having occurred by chance variation of rainfall. If the experiment were to go on for five years instead of three, the respective figures for 0.01 and 0.001 probability levels would be 10 per cent. and 13 per cent.

5. Illustrative example

To make the statistical procedure more clear, a practical analysis was carried out.

For the period 1951-54, the rainfall of every synoptic situation of the

/required

required type was analysed, using the 12-hourly rainfall amounts given in the British D.W.R's. The choice of synoptic situations was objective; the requirement was that there should be a broad south-west stream, south of the Humber, (upper winds from 3,000 feet to the 0°F. level from direction 190°-270°, with some backing of the surface wind permissible) with layered frontal cloud. It was further required that there should have been 5mm. or more of rain at Boscombe Down. (In the actual experiment, of course, this kind of selective choice would be made in retrospect by the analyst. Emission of silver iodide smoke would no doubt be made on doubtful occasions).

The rainfall stations were divided into area groups. These areas, and the rainfall stations, are shown in Fig. 4.

There were 92 selected occasions during the period 1951-54. The seasonal distribution is shown in Table 4.

TABLE 4. DISTRIBUTION OF "SEEDING" OCCASIONS DURING 1951-54

	1951	1952	1953	1954	Total	Mean
November	5	0	2	5	12	3.0
December	3	5	0	2	10	2.5
January	2	4	2	1	9	2.3
February	4	0	2	2	8	2.0
March	1	1	1	2	5	1.3
April	2	1	3	1	7	1.7
May	0	1	1	0	2	0.5
June	0	0	1	1	2	0.5
July	0	0	2	2	4	1.0
August	4	2	3	2	11	2.7
September	3	2	4	3	12	3.0
October	1	2	3	4	10	2.5
November-January	10	9	4	8	31	8.8
February-April	7	2	6	5	20	5.0
May-July	0	1	4	3	8	2.0
August-October	8	6	10	9	33	8.2
Year	25	18	24	25	92	23.0

It will be seen that there is a definite seasonal variation in frequency. The months May-July are least likely to have suitable occasions, and the six months from August to January have nearly three quarters of the total number of occasions.

In the following account, area rainfall will refer to an area mean for a single occasion, and the word "mean" will refer to a mean for a station or area derived from the 92 occasions.

The fall of rain for each station and area were written down for each occasion. From the mean station rainfalls isohyets of average rainfall, representative of low-lying areas, were drawn, and are shown in Fig. 13.

The area rainfalls x_a were then all expressed as ratios of the corresponding mean area rainfalls $\overline{x_a}$, $y_a = (x_a/\overline{x_a})$.

The standard deviation of these ratios is shown in Table 5.

/TABLE 5.

TABLE 5. VALUES OF S_{y_a}

Area	S_{y_a}
A	0.70
B	0.65
C	0.60
D	0.63
E	0.68
F	0.67
G	0.60
H	0.70
Mean value	0.66

There is no evidence to show that there is any real variation from area to area in the value of S_{y_a} and a mean value of 0.66 can be taken.

The correlation coefficients between area rainfalls (ratios of mean) for pair of areas were computed, as also were the serial correlation coefficients for each area of rainfalls on successive occasions. These are shown in Table 6. The serial correlation coefficients run diagonally from top-left to bottom-right.

TABLE 6. CORRELATION AND SERIAL CORRELATION COEFFICIENTS

	A	B	C	D	E	F	G	H
A	-0.12	0.62	0.78	0.42	0.29	0.42	0.26	0.16
B	0.62	0.00	0.74	0.38	0.38	0.52	0.35	0.26
C	0.78	0.74	0.05	0.54	0.39	0.44	0.39	0.17
D	0.42	0.38	0.54	0.11	0.55	0.51	0.51	0.43
E	0.29	0.38	0.39	0.55	0.07	0.68	0.75	0.64
F	0.42	0.52	0.44	0.51	0.68	0.15	0.58	0.59
G	0.26	0.35	0.39	0.51	0.75	0.58	0.04	0.77
H	0.16	0.26	0.17	0.43	0.64	0.59	0.77	0.19

It will be seen that there is little or no serial correlation in any area between successive rainfalls from seeding occasions, and effectively the rainfalls, for any area, may be taken as forming an independent set.

The correlation coefficients between pairs of areas were plotted, a separate map being used for all pairs associated with each area in turn. Isopleths were drawn. The maps are shown as Figs. 5 to 12. They show the way in which the correlation between area rainfalls varies; and they can be used to construct similar maps showing the variation of the correlation coefficient from the centre of any area. To illustrate the method, correlation maps were constructed for the areas V, W, and X (shown in Fig. 4 with pecked lines). For example, for X the correlations of the rainfalls of X with those of the eight standard areas were obtained by interpolation from Figs. 5 - 12. These were plotted on a map for X, and isopleths drawn. Similarly correlation maps were drawn for V and W, and the three estimated maps are given as Figs. 14 to 16.

Estimated correlations of rainfalls for V, X and W with other areas are given in Table 7.

TABLE 7. ESTIMATED CORRELATION COEFFICIENTS

	A	B	C	D	E	F	G	H	V	X	W
V	0.32	0.21	0.29	0.62	0.60	0.52	0.76	0.57	-	0.37	0.63
X	0.57	0.72	0.76	0.53	0.53	0.64	0.42	0.35	0.37	-	0.62
W	0.38	0.46	0.57	0.81	0.70	0.56	0.61	0.47	0.63	0.62	-

Frequency distribution of area rainfalls

The frequency distribution of the ratio y(E) for the area E is given in Table 8.

TABLE 8. FREQUENCY DISTRIBUTION OF y(E)

y(E)	Frequency	y(E)	Frequency
0 - 0.2	4	1.8 - 2.0	2
0.2 - 0.4	10	2.0 - 2.2	1
0.4 - 0.6	16	2.2 - 2.4	2
0.6 - 0.8	17	2.4 - 2.6	2
0.8 - 1.0	12	2.6 - 2.8	2
1.0 - 1.2	8	2.8 - 3.0	1
1.2 - 1.4	5	3.0 - 3.2	0
1.4 - 1.6	3	3.2 - 3.4	1
1.6 - 1.8	6		
		Total	92

The frequency distribution is markedly positive skew. The mode is at about 0.65, and 64 per cent. of the observations have less than the mean value.

The mean values of $x/\bar{x}$ for the separate years 1951, 52, 53, 54 were 0.94, 0.70, 1.18, 1.09.

Regression estimate of y(E)

Let $y = x/\bar{x}$ for the area E, and y_1, y_2, y_3, y_4 be the corresponding ratios for the area G, D, H, F.

Then if $$Y = y - \tfrac{1}{4}(y_1 + y_2 + y_3 + y_4)$$

$$S_Y = \alpha \sqrt{\frac{5}{4}\left(1 - \overline{r_{ij}}\right) - 2\left(\overline{r_i} - \overline{r_{ij}}\right)}$$

Then from Table 6

$\overline{r_{ij}} = 1/6\ (0.51 + 0.77 + 0.58 + 0.43 + 0.51 + 0.59)$
$= 0.565$

$\overline{r_i} = 1/4\ (0.75 + 0.55 + 0.64 + 0.68) = 0.655$

and S_Y should thus be given by

$$S_Y = (0.66)\sqrt{5/4(1 - 0.565) - 2(0.655 - 0.565)}$$

$$= 0.398.$$

It is of interest to check this from actual values of Y, and also to examine the frequency distribution of Y for nearness to normality. The frequency distribution of Y is given in Table 9.

TABLE 9. FREQUENCY DISTRIBUTION OF Y

Y	Frequency	Y	Frequency	Y	Frequency
-1.1	1	-0.2	13	0.7	1
-1.0	1	-0.1	14	0.8	0
-0.9	1	0	10	0.9	1
-0.8	0	0.1	12	1.0	1
-0.7	0	0.2	5	1.1	1
-0.6	0	0.3	6	1.2	0
-0.5	6	0.4	3	1.3	0
-0.4	4	0.5	3	1.4	1
-0.3	7	0.6	1		
				Total	92

/The

The distribution is symmetrical.

S_Y is found to be 0.395, which agrees with the value 0.398 predicted from the correlation formula.

Table 10 shows the comparison of frequencies with those expected from the corresponding fitted normal curve, fitting mean, standard deviation and total.

TABLE 10. COMPARISON OF FREQUENCY DISTRIBUTION OF Y WITH NORMAL DISTRIBUTION

Y		Frequency	Expected Normal Frequency
	-0.45	9	11.9
-0.45	-0.25	11	12.4
-0.25	-0.15	13	8.5
-0.15	-0.05	14	8.8
-0.05	0.05	10	8.8
0.05	0.15	12	8.8
0.15	0.35	11	15.5
0.35	0.55	6	9.8
0.55		6	7.5
Totals		92	92.0

The value of χ^2, for 6 degrees of freedom, is 10.6, giving P = 0.10. The frequency distribution of Y is thus seen to be reasonably near the normal. We can thus with confidence use the t-test with t given in expression (11).

It was noted that the values of $\frac{1}{4}(y_1 + y_2 + y_3 + y_4)$ differed very little from those of

$$\left[x(G) + x(D) + x(H) + x(F)\right] / \left[\bar{x}(G) + \bar{x}(D) + \bar{x}(H) + \bar{x}(F)\right]$$

The mean of the absolute differences was only 0.03, and so the combined area rainfall of the "control" area (expressed as a ratio of the mean) can be used instead of the arithmetic mean of the area rainfall ratios.

Using the regression equation has given us a residual variable normally distributed with a mean of zero, and with standard deviation 0.39, whereas the "percentage of normal" comparison of y with its "normal" value, 1, gives us a residual variable which is markedly skew, with mean zero and with standard deviation 0.66. The efficiency of the regression technique is further shown in Table 11, which gives the mean values for each year of y, (y - 1), and Y.

TABLE 11. MEAN VALUES FOR AREA E OF y, y - 1, Y FOR EACH OF THE YEARS 1951, 52, 53, 54

Year	y	Mean values of y - 1	Y
1951	0.94	-0.06	-0.02
52	0.70	-0.30	-0.04
53	1.18	0.18	0.08
54	1.09	0.09	-0.04

6. Randomisation

It has been suggested (B. J. Mason, 1955) that with a line of silver iodide generators set up roughly perpendicular to the prevailing wind, a control area, whose rainfall has a high correlation with the seeded area, should be chosen upwind of the generators. Then in order to avoid the effects of weather

/trends,

trends, for example, an abnormally long wet period, seeding should be carried out by random selection on only half the suitable occasions. Rainfall in the seeded area could be predicted from the regression with the control area, and the difference between predicted and actual rainfall could be attributed to seeding on the seeded occasions and to random variations on the non-seeded occasions. Comparison of the two sets of differences would enable the true effects of seeding to be evaluated.

We note that the idea of having control areas upwind of the generators would give very poor correlations. Fig. 17 shows the correlation map for a typical seeded area Q. It will be seen that correlations of rainfall (for our choice of situations) would be 0.5 or less, and these would be valueless. Control areas must be chosen on each side of the seeded area.

Assuming however that this has been done, let us now examine the "randomisation" suggestion. Since there is no serial correlation between successive rainfalls, the "randomisation" method simply doubles the variance of the difference of means that we are testing, and so for two test periods of equal length, one employing "randomisation" and the other not, the "randomisation" method would only be capable of detecting seeding effects $\sqrt{2}$ times as great as those detectable without using randomisation. Putting it another way, the randomisation method would take twice as long to detect a given "seeding" increase as would be needed if all possible seeding occasions were used.

When we used a regression to estimate y for the area E from y_1, y_2, y_3, y_4 for the areas G, D, H, F we found the standard deviation of $Y = y - \frac{1}{4}(y_1 + y_2 + y_3 + y_4)$ to be 0.395. If now we consider the set of Y's to be obtained when seeding took place on the 1st., 3rd., 5th., etc. occasions and no seeding on the 2nd., 4th., 6th., etc. occasions, and we now compute the standard deviation of the quantities $Y_1 - Y_2$, $Y_3 - Y_4$, $Y_5 - Y_6$ etc., we find that it has the value 0.587. The ratio 0.587/0.395 = 1.49, slightly greater than $\sqrt{2}$.

There is no doubt that the randomisation technique is very valuable when there is a high serial correlation among the data being examined; but in the present experiment it is inefficient.

It should in addition be noted that the fear that abnormal weather, for example a long wet period, would lead to spurious results is without justification. For high rainfall in the seeded area would be accompanied by high rainfall in the comparison area with which it has a high correlation, and the difference of the rainfalls (ratios of normal) would, as previously explained, be randomly distributed about a mean of zero. We have already noticed in Table 11 that in 1952, an abnormally dry year (for the seeding occasions), although the seeded area received only 70 per cent. of normal rainfall per occasion, the mean value of the difference was -0.04, merely a small sampling deviation from a true population mean of zero.

7. Detection of seeding increases when the seeded area is unknown

If the seeded area is unknown, the detectable increase due to seeding will be much higher than if we know the area seeded. Practical examples will make this clear.

First example

Let us consider the five areas E, G, D, H, F for the 92 seeding occasions during 1951-54. Assume that one, and only one, of the five areas receives a proportionate increase of P (P = 0, 25, 50, 75, 100) per cent. in rainfall (ratio). The addition was given randomly in turn to the different areas. Then Table 12 shows the number of times that at least

/one

one area now has more than twice normal rainfall when one and only one area, randomly selected, has a percentage increase of rainfall ratio of P. (Curve A of Fig. 18).

TABLE 12. NUMBER OF TIMES FOR GIVEN P THAT AN AREA RAINFALL IS > 200 PER CENT. OF NORMAL. (CURVE A OF FIG. 18)

P	0	25	50	75	100
Number of times in 92	21	26	29	35	42

If we take the value 21/92 to be the mean value of a Poisson variable, then in another set of 92 occasions the probability of having 0, 1, 2, 3 ----- occasions when at least one area has more than 200 per cent. of normal rainfall

$$= e^{-21}\left(1, \frac{21}{1!}, \frac{21^2}{2!}, \frac{21^3}{3!} \ldots\ldots\right)$$

Then we find that the probability p is 0.01 that on 33 or more occasions there would be one or more areas with more than 200 per cent. of normal, and p is 0.001 that on 37 or more occasions there would be one or more areas with more than 200 per cent. of normal.

The frequencies from Table 12 are plotted in Fig. 18, and curve A drawn from them. The lines for p = 0.01 and p = 0.001 are pecked.

Then from curve A we read off that there is a probability of 0.01 that a 64 per cent. increase, given to one and only one area on each occasion, might be undistinguishable from random variations, and at the 0.001 probability level increases of over 82 per cent. would be needed for them to be distinguished from random fluctuations.

Second example

Again consider the areas E, G, D, H, F and give one and one only at random on each occasion a proportionate percentage increase in rainfall ratio of P (P = 0, 25, 50). Write down the differences between the highest and second highest rainfalls, and also the range, on each of the 92 occasions. Then the difference that was exceeded on 21 occasions with 0 per cent. increase was 0.41 and the range that was exceeded on 21 occasions was 1.11.

Table 13 shows the frequencies of difference greater than 0.41 and of range greater than 1.11 for percentage increase P (P = 0, 25, 50).

TABLE 13. (CURVE B OF FIG. 18)

P	0	25	50
Frequency of difference > 0.41	21	28	39
Frequency of range > 1.11	21		38

Curve B of Fig. 18 shows the (common) results of these two methods. From the intersections of the curve with the pecked lines of p = 0.01 and p = 0.001 we see that at the 0.01 and 0.001 probability levels respectively more than 36 per cent. and more than 46 per cent. increases would need to be received by one area to be distinguished from random fluctuations.

These increases are much smaller than those of the first example, which gave 64 and 82 per cent.

/Third

Third example

Consider the five stations in order Manchester, Watnall, Cottesmore, Mildenhall and Felixstowe. Give on each occasion to one and one only, selected at random, of the three middle stations a proportionate percentage increase in rainfall ratio of P (P = 0, 50). Then the difference between the highest of the three middle stations and the lower of the two outer stations is greater than 1.16 on 21 occasions in 92 for P = 0, and on 34 occasions for P = 50. These values are plotted as curve C of Fig. 18. We see that the percentage increases detectable at the 0.01 and 0.001 probability levels are 47 and 60 per cent.

As a check on the reliability of the analysis used in these three examples, let us apply the method to seeding of a known area. Let us consider again the areas E, G, D, H, F. Give on each occasion to the area E a proportionate percentage increase of rainfall P (P = 0, 25, 50). Then compute the values of

$$Y = y - \tfrac{1}{4}(y_1 + y_2 + y_3 + y_4)$$

The value of Y exceeded 0.19 on 21 occasions with 0 per cent. increase in y the rainfall of the area E and exceeded 0.19 on 46 and 76 occasions with percentage increases P = 25 and 50.

These values are plotted as curve D of Fig. 18. We see that the percentage increases required by the area E, to be detected at the 0.01 and 0.001 probability levels, are 13 and 17 per cent. These values are in good agreement with those found by the t-test for the regression technique.

Discussion

In each of the three examples it might be argued that we have been unfair to the comparisons of "unknown location" against "known location", in that we could have a closer network of areas or stations for the "unknown location" methods.

It is, however, unlikely that we could get much improvement for the area network. For a group of areas covering 75 by 75 miles the mean correlation between pairs of areas is about 0.71, and for areas covering 50 by 50 miles about 0.76, and we cannot expect to be able to reduce the detectable increase at the 0.01 level to less than 25 to 30 per cent.

The line method appears to be more capable of improvement, due to closer spacing of stations, when the maximum difference between neighbouring stations is analysed as in the third example. Examination of the correlation charts shows that we can make the assumption that correlation coefficient decrease from 0.9 at 10 miles to 0.9^d at 10d miles distance. It can then be shown that, if there is a close even spacing of stations in a line, with correlation ρ between neighbouring stations, the differences of rainfall amounts between neighbouring pairs of stations form a set which is very nearly independent (very small correlation). Thus the detectable increase will be proportional to $\sqrt{2(1-\rho)}$. In the third example, ρ is about 0.67. The correlation coefficient for two stations, London Airport and Kew, distant six miles from each other, is 0.91. It is doubtful whether we could ever hope to have ρ greater than 0.95, especially since we would not expect seeding effects, if they exist, to have a very sharply defined edge across the plume. Even assuming ρ = 0.95, the method of example three would give a detectable increase of 20 per cent. at the 0.01 probability level. We are, of course, in this latter analysis making the assumption that we can look for seeding effects along a line at a given radial distance from the generators. In

/other

other words, we are not strictly assuming an unknown seeding location.

We must revert to a partial area - type analysis by using two lines of stations, arcs of circles at a radial distance apart of say 30 to 40 miles. With the resulting decrease in efficiency, it is unlikely that we can detect, at the 0.01 probability level, proportionate increases of less than about 25 per cent.

Nevertheless it may be necessary, if we cannot locate the silver iodide plume sufficiently accurately to carry out the comparison between a known seeded area and a chosen control area, to use some sort of "unknown location" comparison. In this event a detailed analysis, probably using the two line method, must be made of historical records of rainfall on "seeded" occasions for stations as closely spaced as possible along the lines, in order to provide an accurate figure for the detectable proportionate increase at the 0.01 probability level, instead of the estimated value of 25 per cent. given above.

8. Distribution of rainfall stations

The area in which we are likely to be interested is England, south of the Humber and east of $2\frac{1}{2}^{\circ}$W. In this area there are many hundreds of rainfall stations which provide daily readings. But there are seeding occasions when 24-hour falls of rain do not give representative values of rainfall, and 12-hourly readings are more desirable. There are however only some 120 stations from which 12-hourly falls can at present be obtained, and East Anglia and Kent are very poorly represented. It may be possible, with the co-operation of voluntary observers, to have evening readings made at 9 p.m. on days in which precipitation had fallen between 9 a.m. and 9 p.m. This would mean the observer having, on the average, to read in the evening about twice a week. Perhaps some 50 to 100 additional 12-hourly readings might be obtained. For this set of additional stations there would of course be no historical data of 12-hourly falls, but mean 12-hourly falls could be computed by comparison with 24-hour falls, and variability as we have seen does not change much from one part of the area to another; we have also seen that correlations can be computed from area maps.

So no insuperable difficulty is anticipated in making full statistical use of any additional 12-hourly readings we might obtain. If it should be considered undesirable to ask voluntary observers to make the additional readings then we must rely mainly on 24-hourly readings. This will involve some loss of power in the statistical test for detection of seeding increases in rainfall, and our estimated detectable increase, of 13 per cent. in 69 seedings, at the 0.01 probability level must be changed to the order of 16-18 per cent.

In the event of our having to adopt the "unknown location" method, it will obviously be desirable to have a very close network of rain gauges. A good network would be formed by stations along arcs of circles at radii of say 25, 50, 75, 100, 125, 150 miles. With a spacing of stations at 5 miles apart, this would require some 200 stations. If we use 24-hourly readings, this network will be already available. It may however be desirable, even if the location of the plume is known, to set up this network with recording rain gauges if there are encouraging results from the first year of seeding.

9. Conclusions

(i) Rainfall variation in the type of weather situation in which the cloud seeding will be carried out, viz. cloudy (frontal) situations with south-westerly winds, is reduced to a minimum if we restrict the statistical analysis to those occasions with substantial rainfall, defined objectively by an area mean rainfall for the Salisbury area of 5mm.

(ii) To ensure a high seeding efficiency over a substantially wide area, say 20 miles, it is necessary to have a line of some five silver iodide

/generators

generators over a width of 20 to 25 miles. Having a line of generators instead of one only will also greatly increase the probability that we would be able to locate a substantial area which has been efficiently seeded.

(iii) If we can locate such an area on each seeded occasion over a period of three years, then the detectable increase of rainfall due to seeding, measured by the difference between the rainfall in the seeded area and the rainfall in neighbouring non-seeded areas, will be 13 per cent. (at the 0.01 probability level).

If on each occasion we consider the location of the seeded area to be unknown, the detectable increase will be about 25 to 30 per cent.

The respective estimates of 13 per cent. and 25 to 30 per cent. must be increased slightly if we do not obtain additional 12-hourly rainfall readings in East Anglia and Kent.

References

Braham, R.R., B.K. Seely and W.D. Crozier. Trans. Amer. Geophys. Union, 33, 825, 1952.

Johnson, N.L. and H. Tetley. Statistics. Cambridge University Press, 1949.

Jones, R.F. An experiment to test the efficacy of silver iodide seeding in enhancing precipitation. Air Ministry, London, Meteorological Research Papers, No. 876, 1954.

Mason, B.J. Design and evaluation of large-scale rain-making experiments. Nature, Vol. 175, No. 4454, Mar. 12, 1955.

Sutton, O.G. Q.J.R. Met. Soc., Vol. 73, 1947.

Sutton, O.G. Micrometeorology. McGraw Hill, London. 1953, pp.287, 292.

Vittori, O. Sur la détermination de la distribution dans l'atmosphère des noyaux de condensation et de particles obtenues par sublimation. Rome, 1954. (Reviewed in Bull de l'Obs. du Puy de Dome, 1955, No. 1).

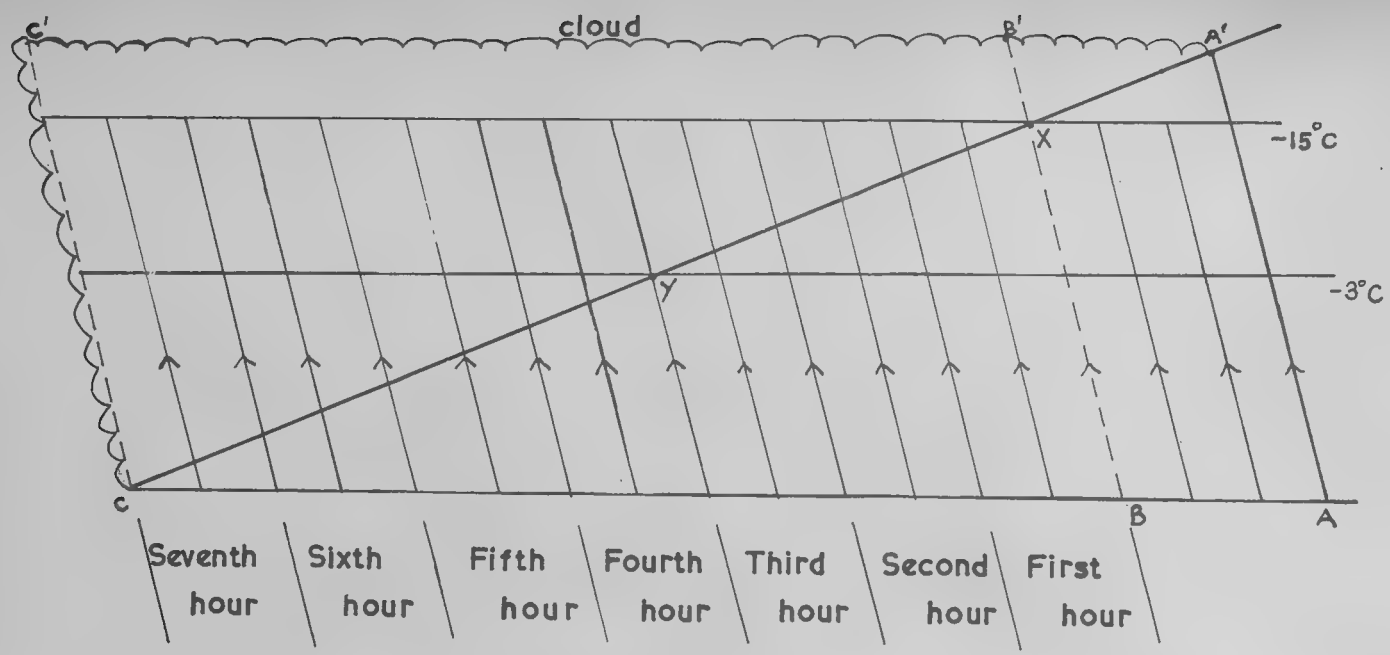

FIG. 1 Vertical diffusion of AgI.

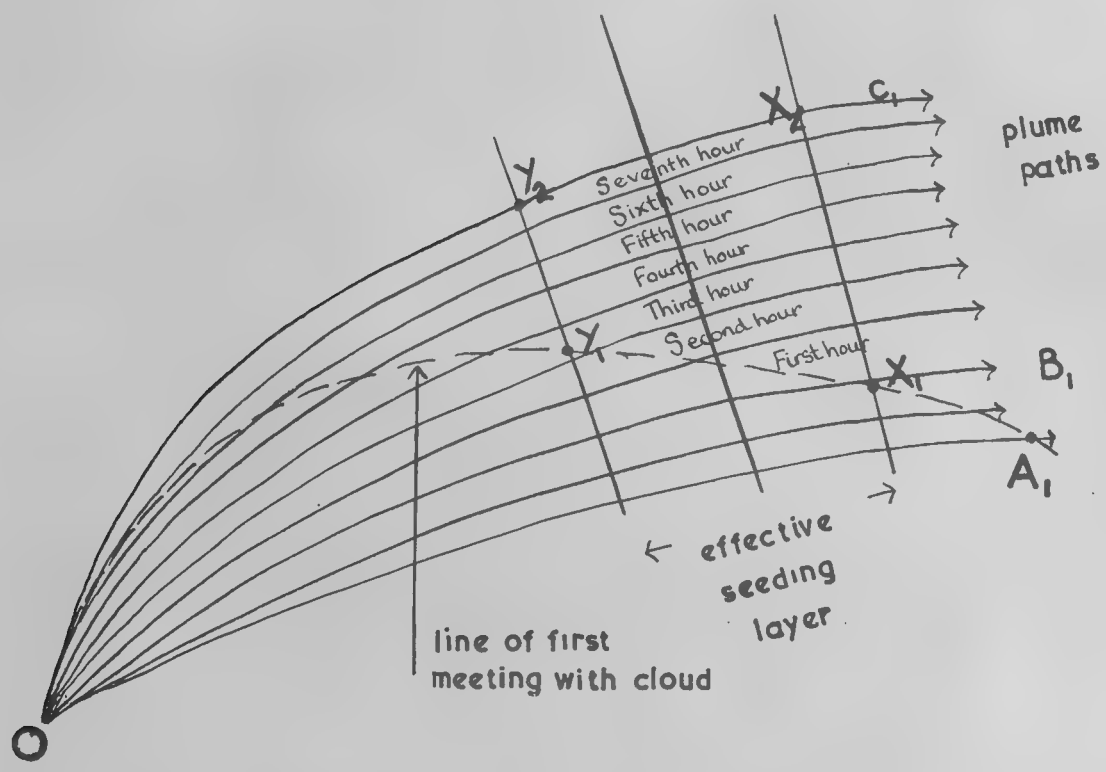

FIG. 2 Horizontal projection of particle paths of AgI

		7
	7	6+7
7	6+7	5+6+7
6+7	5+6+7	4+5+6+7
5+6	4+5+6+7	3+4+5+6+7
4+5	3+4+5+6	2+3+4+5+6+7
3+4	2+3+4+5	1+2+3+4+5+6
2+3	1+2+3+4	1+2+3+4+5
1+2	1+2+3	1+2+3+4
1	1+2	1+2+3
	1	1+2
		1
10 miles	20 miles	30 miles

FIG. 3 30 miles latitudinal movement of plume, with plume widths of 10, 20 and 30 miles

FIG. 4

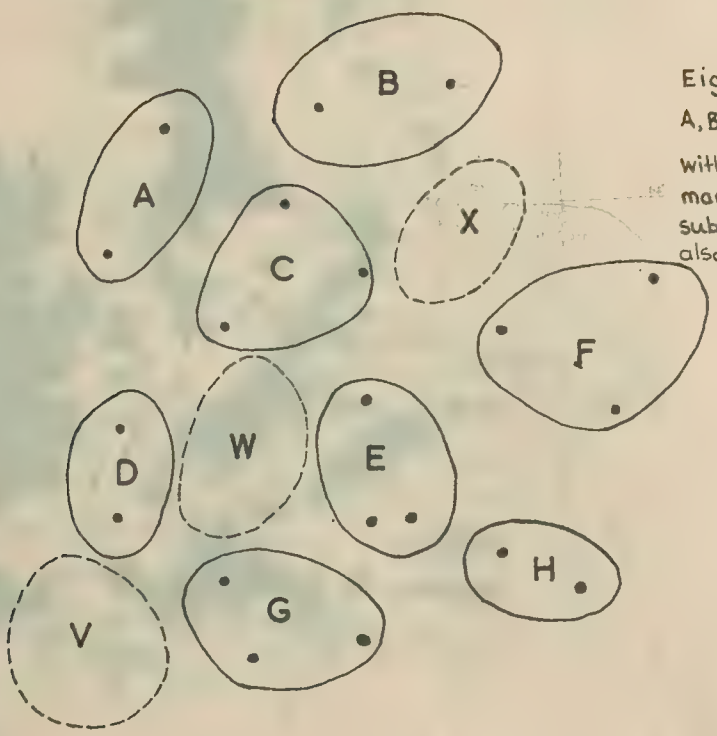

Eight sub-areas
A, B, C, D, E, F, G, H
With rainfall stations marked. Additional sub-areas V, W, X are also marked.

FIG. 5

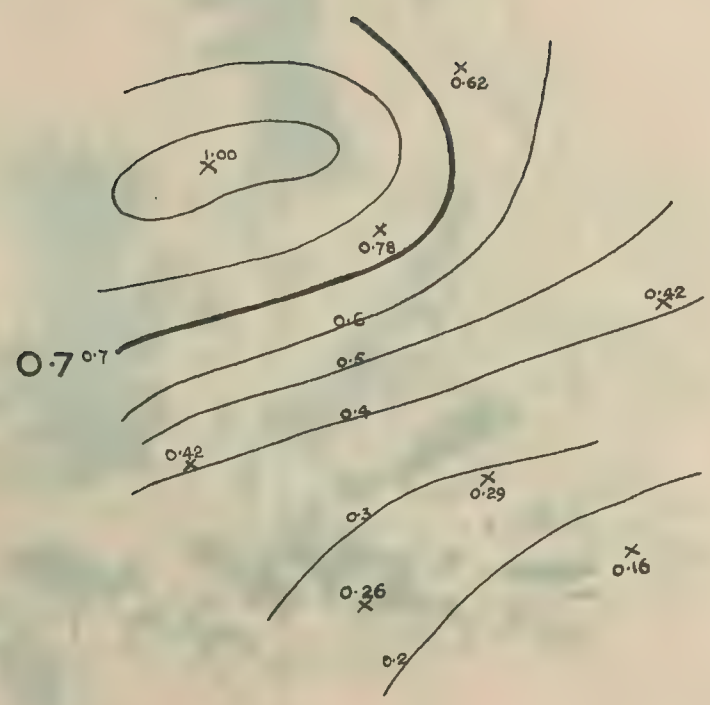

A correlations
With other areas

FIG. 6

B correlations with other areas

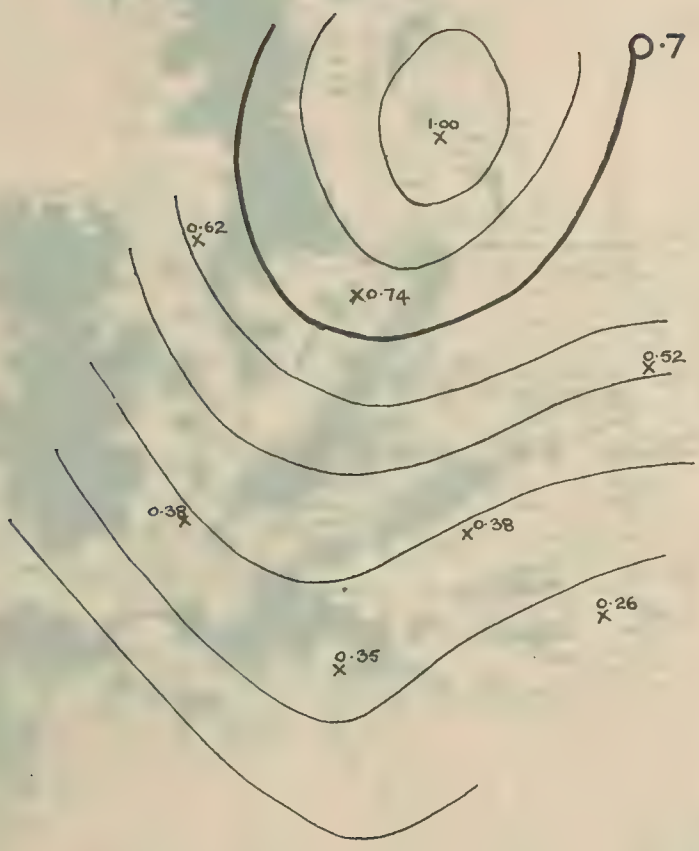

FIG. 7

C correlations with other areas

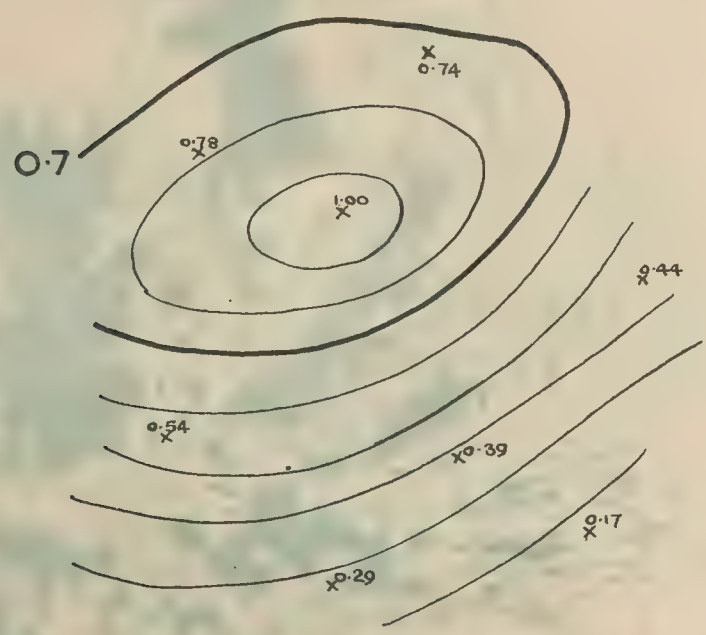

FIG.8

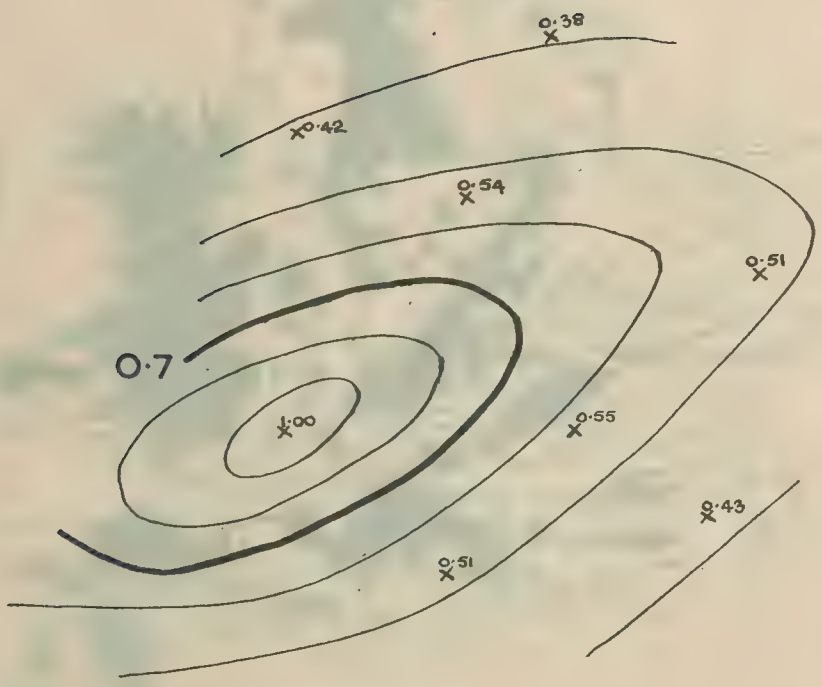

D correlations with other areas

FIG.9

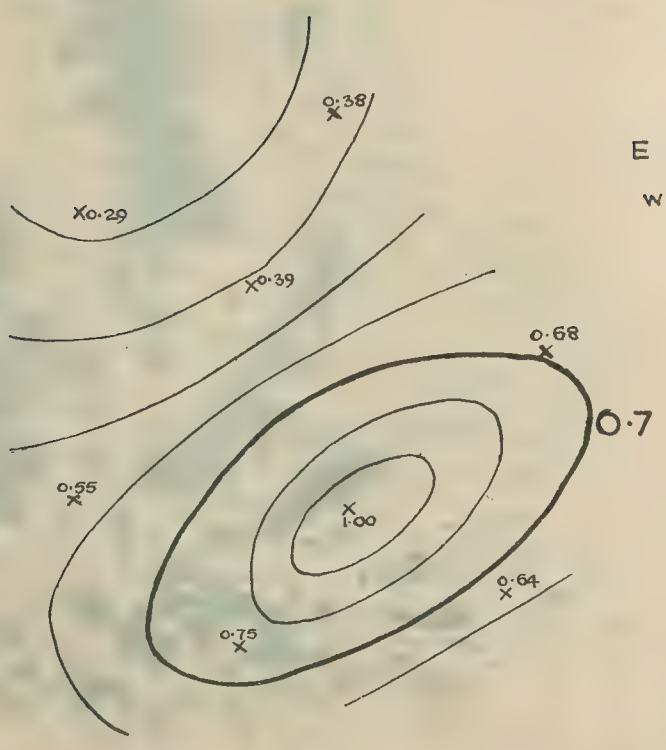

E correlations with other areas

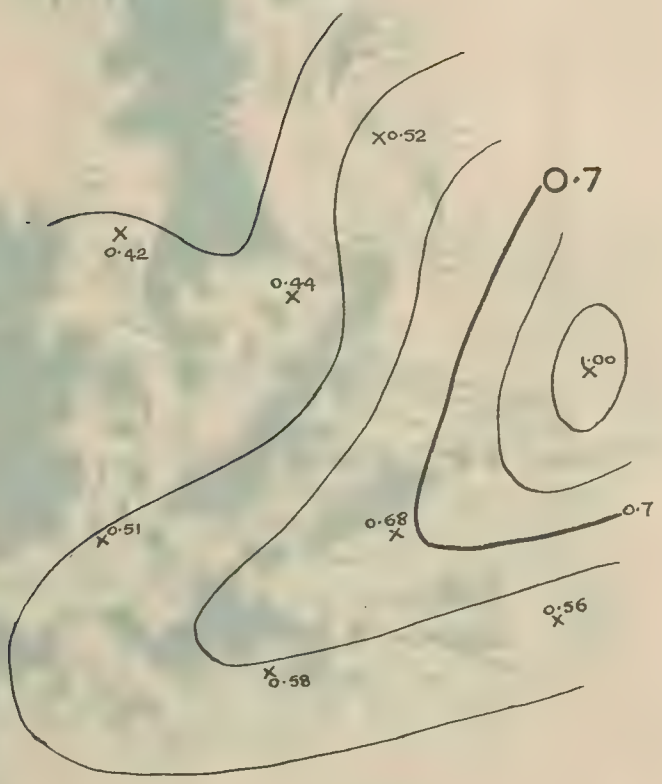

FIG. 10

F correlations with other areas

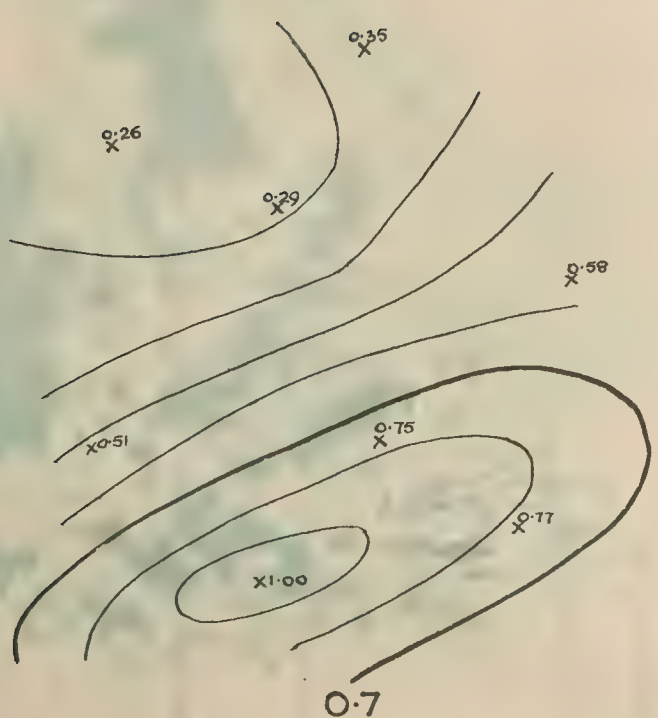

FIG. 11

G correlations with other areas

FIG. 12

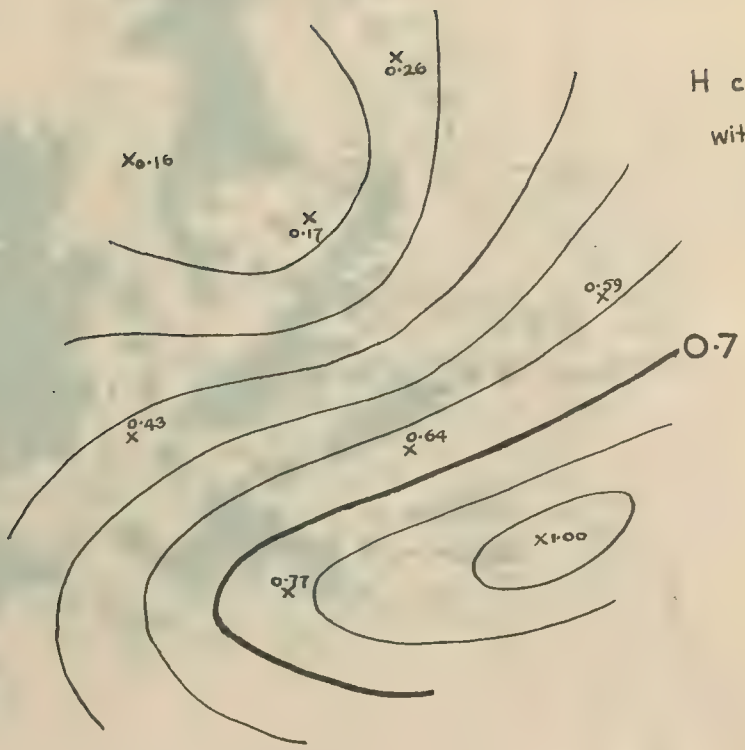

H correlations with other areas

FIG. 13

Average rainfall amount (mm.) from 92 occasions 1951 - 1954

FIG. 14

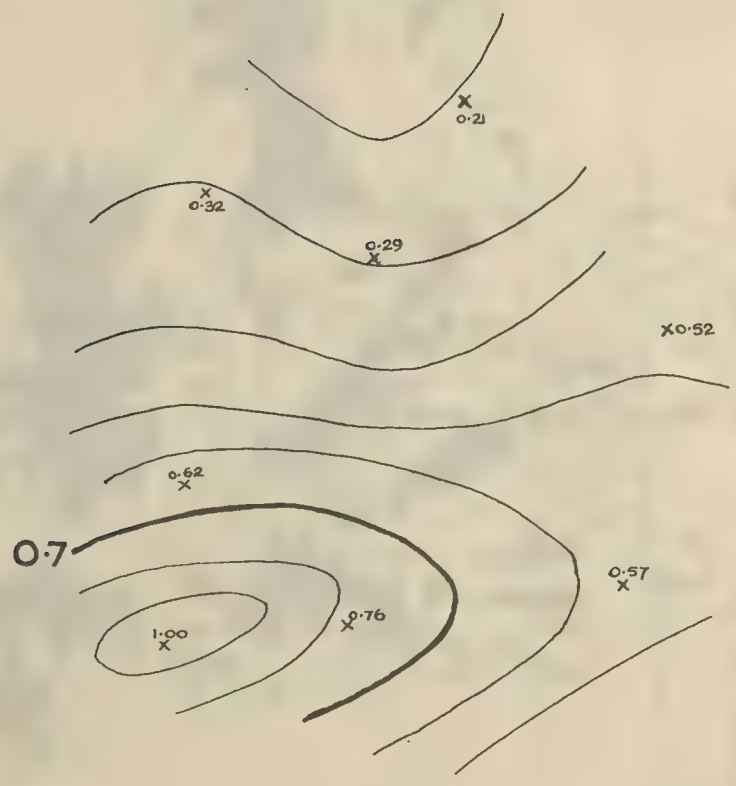

V estimated correlations with other areas

FIG. 15

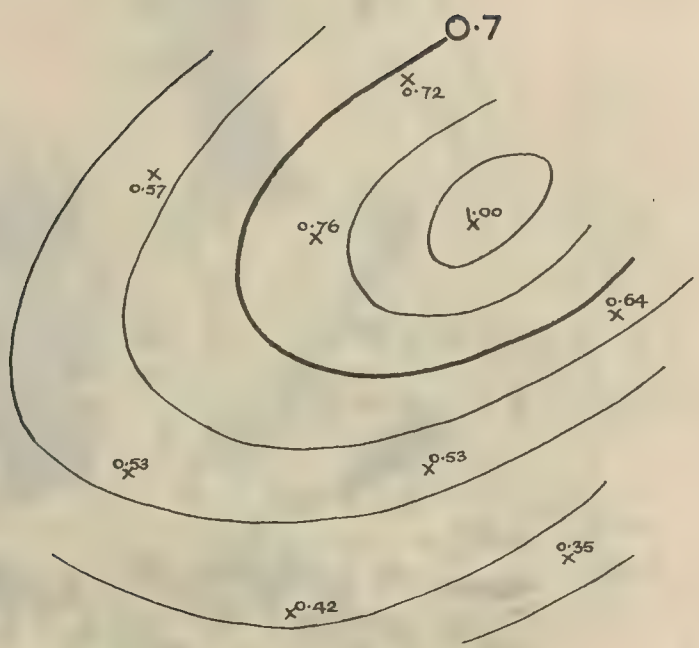

X estimated correlations with other areas

FIG. 16

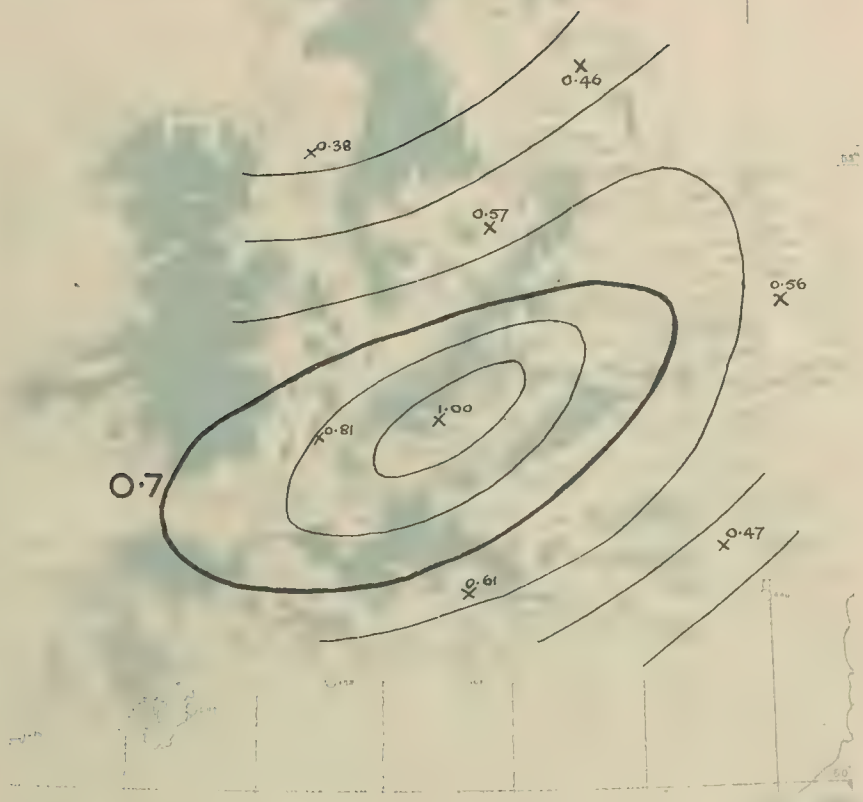

W estimated correlations with other areas

FIG. 17

Typical "seeded" area with correlations

FIG. 18

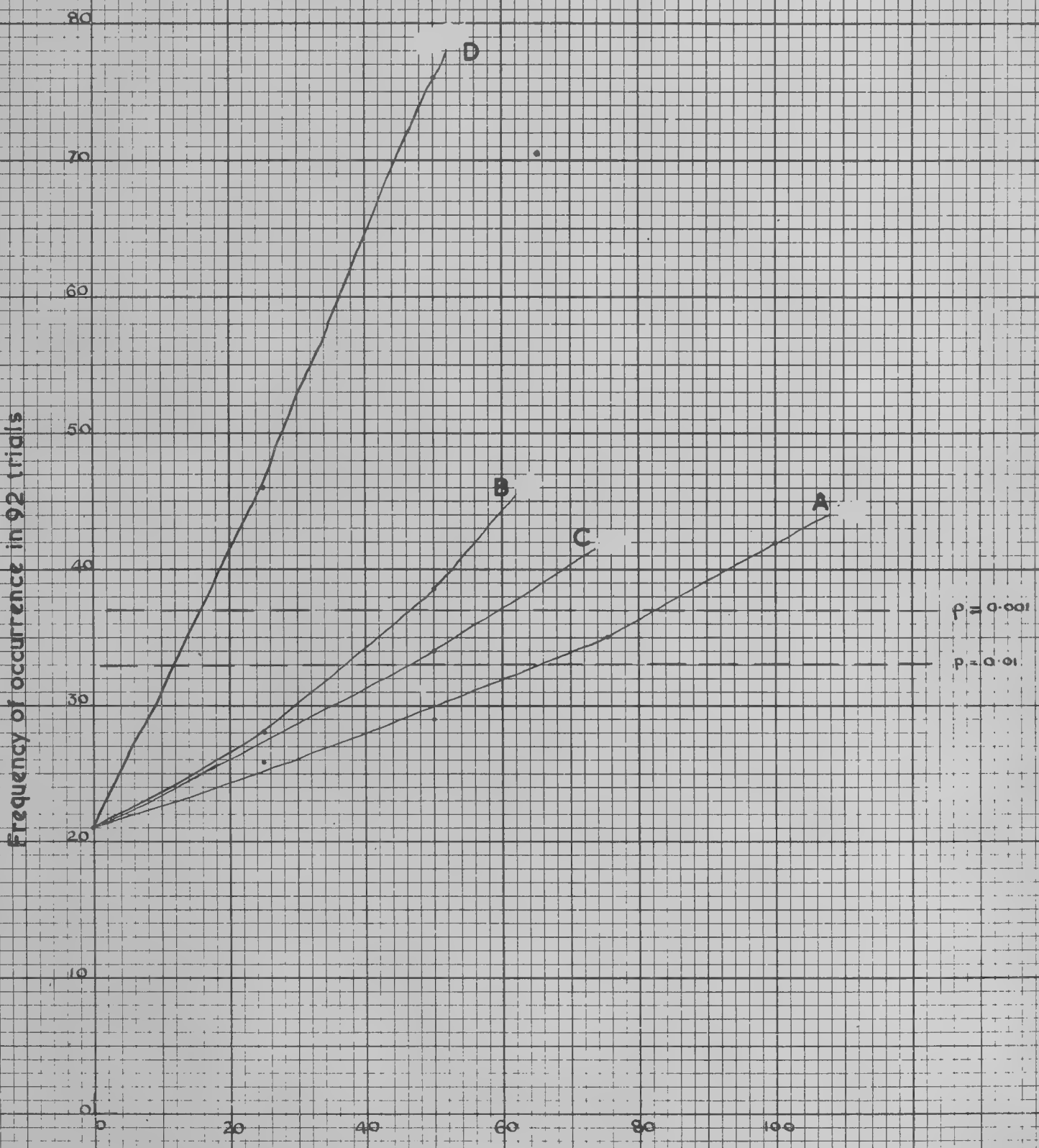
80
70
60
50
40
30
20
10
0
D
B
C
A
P = 0·001
P = 0·01
Frequency of occurrence in 92 trials
0
20
40
60
80
100
Percentage increase of rainfall

M.R.P. 933
S.C. 11/196
1st September, 1955

Investigations relating to cirrus cloud

by

D. G. James
(Meteorological Office)

AIR MINISTRY
METEOROLOGICAL RESEARCH COMMITTEE

At the time of issue this report has not been published. Any author desiring to quote this paper should refer to it as "A paper of the Meteorological Research Committee (London), M.R.P. No. 933 by Dr. D.G. James. A copy is available in the Library of the Meteorological Office."

M.R.P. 933
S.C.II/196
1st September, 1955

AIR MINISTRY

METEOROLOGICAL RESEARCH COMMITTEE

Investigations relating to cirrus cloud

by

D. G. James (Meteorological Office)

1. Introduction

This paper analyses observations of cirrus cloud which were made from aircraft between August, 1952 and December, 1954. In the main, the observations were obtained from aircraft based at West Raynham and at Wyton, the aircraft being on routine navigation flights over the British Isles. Reports were also obtained from aircraft of the Meteorological Research Flight based at Farnborough and were made during their routine high level ascents. It was hoped that any ascent to cirrus levels by aircraft from these stations would yield a report of "Cirrus observed" or "No Cirrus observed", but in the early stages of the investigation a certain reluctance was shown to make a report of the latter type.

In order to facilitate simple analysis of the reports, the reporting stations were issued with proformae which were so designed that an observer was only required to tick whether cirrus cloud had been observed, and if so to give the distribution and type of the cloud, and the heights and temperatures of bases and tops. Amplifying remarks were also invited.

Altogether about 220 reports for 180 separate days were available for analysis by January, 1955. The majority of these cases were reports of the presence or absence of cirrus cloud at a particular place, though several were reports made on long distance navigation flights, sometimes as far as North Africa. There were approximately twice as many reports of "Cirrus observed" as "No Cirrus observed", but it was thought that sufficient observations had been obtained to permit a statistical examination of the reports.

Although a request was made that visibility in and through cirrus cloud should be reported, very few such estimates were made, and no statistical analysis was possible.

2. Analysis of observations

Murgatroyd and Goldsmith (1953) made an analysis of cirrus cloud observations obtained from routine high level ascents by aircraft of the Meteorological Research Flight, and also from several selected synoptic reporting stations. With the greater number of observations available for the present investigation, it was thought worth while repeating some of the histograms presented in the earlier paper.

Fig. 1 shows the distribution of observations of the tops of cirrus cloud relative to the tropopause. It can be seen that a maximum occurs between 2,000 ft. and 3,000 ft. below the tropopause, and that rather more than 50% of the observations of cirrus tops occur from the tropopause down to 6,000 ft. below whilst 29 observations were made of cloud in the stratosphere. Of these latter, 10 were more than 6,000 ft. above the tropopause, the greatest reported height (estimated) being 20,000 ft. above. The occurrence of a maximum just below the tropopause is consistent with the results presented by Murgatroyd and Goldsmith, although a peak of more than 50% was found by those authors to be from 0 to 2,000 ft. below the tropopause.

/Fig. 2

Fig. 2 presents a histogram of the frequency distribution of the depths of bases of the cirrus clouds below the tropopause. No well-marked peak is evident, but more than 50% of the observations give a cloud base between 4,000 ft. and 12,000 ft. below the tropopause.

The frequency distribution of the heights of cirrus cloud bases is shown in Fig. 3, where maxima are evident at about 20,000 ft., 25,000 ft. and 30,000 ft. It was thought that these maxima may well be due to a preference for estimating and reporting heights to the nearest 5,000 ft., though a maximum was also obtained by Murgatroyd and Goldsmith between 25,000 and 30,000 ft. Ten cases were reported when the base of the observed cirrus was above 40,000 ft.

Fig. 4 presents the frequency distribution of the thicknesses of cirrus cloud. About 70% of the cirrus reported had thicknesses in the range from a few hundred feet to 6,000 ft., though thicknesses of up to 17,000 ft. were reported.

3. Analysis of surface charts

It is well known that cirrus cloud is frequently observed in association with a frontal boundary between air masses. However, it is equally apparent from analysis of surface synoptic charts that extensive cirrus cloud is observed in situations other than those exhibiting surface frontal features.

Table 1 presents the frequency distribution of distances of reports of "Cirrus" and "No Cirrus" from surface fronts. It is seen that more than a half of the cirrus reports lie up to 400 mi. ahead of a front and that about a third of the reports lie up to 200 mi. ahead of a front. For observations of "No Cirrus", less than a tenth of the reports lie up to 200 mi. ahead of a front. 38 reports of "Cirrus" and 33 reports of "No Cirrus" were more than 600 mi. distant from any well-marked front.

Table 2 shows the distribution of distances of certain surface pressure features from points of observation of "Cirrus" or "No Cirrus". It will be seen that rather more than half of the "No Cirrus" reports occurred in association with a surface ridge or high cell, while only about 1/3rd of the "Cirrus" reports were found in this region. This table is consistent with Table 1 where a maximum of "Cirrus" reports appear in the region up to 600 mi. ahead of a surface front.

Although Tables 1 and 2 serve to illustrate that the greater part of cirrus cloud reports were made in association with frontal boundaries and with surface troughs, this is already common knowledge among forecasters, and makes no additional contribution to the cirrus forecasting problem.

4. Analysis of upper air soundings

The occurrence of cirrus cloud is undoubtedly associated with moist air in the upper troposphere. Since humidity observations are not normally available at these heights, an examination was made of the dew point depressions at 500, 450 and 400 mb. in the hope that a significant increase in humidity might be apparent below the usual cirrus levels. Table 3 presents the mean depressions of the dew point at 500, 450 and 400 mb. and the significance levels of the differences between the means for occasions of "Cirrus" and "No Cirrus". It can be seen that at all three levels the differences between the means of dew point depression are highly significant.

An analysis was made of cases when the depressions of dew points below temperatures were simultaneously lower at all three levels than the mean depressions for "Cirrus" reports at these levels, and also when the depressions were simultaneously greater at all three levels than the means obtained for "No Cirrus" reports. This included rather more than half of the total cases.

/The

The results are presented in Table 4, from which it is seen that if these criteria had been used as a basis for forecasting, the "useful effort", (Crossley, 1954) and forecast accuracy for forecasts of cirrus cloud would have been 84% and 80% respectively.

This would undoubtedly be of some assistance to a forecaster is assessing the distribution of cirrus cloud from radio-sonde observations.

Kimachi, (1952), suggests that cirrus cloud over Japan is observed only when the 500 mb. temperature falls within discrete limits and has a maximum frequency of occurrence between temperatures from 0°F and -20°F. Analysis of observations in the present investigation showed that the temperatures at 500 mb. when cirrus cloud is reported range from 20°F to -30°F with a flat maximum between +10°F and -15°F. Furthermore, no significant difference was found between the distributions of 500 mb. temperatures for reports of "Cirrus" and "No Cirrus".

Kimachi also suggests that the lapse rate of temperature with height may well be important in the cirrus forecasting problem. This is consistent with the work of Bannon, Frith and Shellard (1951) who obtained a correlation coefficient of 0.80 between the temperature at 500 mb. and the frost point at 300 mb. as measured from aircraft of the Meteorological Research Flight engaged on high level ascents. Table 5 presents the means of the temperature lapse rates at 100 mb. intervals from 500 mb. at times of reports of "Cirrus" and "No Cirrus". The means at each interval are not significantly different, and are of little use for assessing the presence or absence of cirrus cloud.

Murgatroyd and Goldsmith suggest that cirrus cloud is more frequent when the wind at 300 mb. is in the southwest to west sector and least when the wind is in the northeast to east sector. No significant differences were found between the means of the wind strengths at any level up to 200 mb. for reports of "Cirrus" and "No Cirrus". Table 6 presents the frequencies of the winds in various sectors at levels from 500 mb. to 200 mb. for observations of "Cirrus" and "No Cirrus". Considerable variation is observed in the distribution of the winds for these two classes of reports at all levels up to 200 mb., and application of the χ^2 test indicates that the differences are most significant at 400 mb. It can be seen that the large values of χ^2 at most levels result from an excess of "No Cirrus" reports in the E-S sector and an excess of "Cirrus" reports in SW-W sector. These results are in good agreement with those of Murgatroyd and Goldsmith.

It has further been suggested by these authors that warm air advection at cirrus levels is frequently observed when cirrus cloud is reported. This is supported by a report issued by the Washington Air Weather Service, where it is claimed that warm air advection between 700 mb. and 300 mb. may be used as a parameter for forecasting cirrus cloud. Table 7 presents frequencies with which warm or cold air advection are found at times of reports of "Cirrus" and "No Cirrus" at intervals from 500 mb. These frequencies were obtained by examining the winds reported from routine upper air soundings at the times and in the neighbourhoods of the reports. A veering wind with height was taken to indicate warm air advection between the two levels considered and vice versa. In numerous cases the change in direction was slight within the height interval, and all instances where this change was less than 5° were classified as "Neither". Also under this classification were reports of wind strengths less than 5 kt. The distributions of frequencies in these classes were significantly different for reports of "Cirrus" and "No Cirrus" at the 0.1% level or better for all intervals considered except 500-400 mb. Reports of clouds in the stratosphere were not included in these analyses. The association between the occurrence of cirrus cloud and warm air advection in the upper troposphere is thus confirmed.

5. Analysis of 1000-500 mb. thickness charts

Although time differences of up to six hours occurred between the times of observation and the times of the thickness chart used in this analysis, for the purpose of comparison with the thickness charts it was thought justifiable to

neglect the changes in the thermal pattern in this interval. In fact, most of the reports were made on afternoon flights and the average time interval was probably of the order of 1 to 2 hours.

No significant difference was found between the means of the thickness values for the two classes "Cirrus observed" and "No Cirrus observed", though significant differences were evident in the means of the thickness gradients. This is shown in Table 8, where the means of the thermal winds are given for cases of "Cirrus" and "No Cirrus". The means are 21 kt. and 16 kt. respectively, and application of "Student's 't'" test indicates that they are significantly different at the 0.5% level.

An attempt was made to relate the point from which an observation was made to a trough - ridge pattern in the 1000 - 500 mb. thickness field. To allow simple classification, an idealised wavelength was divided into six equal parts along its axis, and the frequencies obtained for each class of reports of "Cirrus" or "No Cirrus". Only about half of the observations allowed of a reasonable degree of confidence in this classification. Fig. 5 presents the ratios of the percentages of the frequency of observations of "Cirrus" to "No Cirrus" in each section of the ideal wavelength. It is clear that this ratio is greatest in and near a thermal ridge and least near a thermal trough, and is consistent with surface observations of the association of cirrus clouds with warm fronts.

Since only about half of the observations were used in the above analysis, an attempt was made to classify types of thickness pattern over the area from which reports were obtained, in terms of the curvature of the thickness lines. The thickness patterns were labelled as cyclonic or anticyclonic according to the sign of the curvature of the thickness lines. If these were straight, or the gradients very weak, the observation was assumed to belong to a third class, neither cyclonic nor anticyclonic. Table 9 presents the frequencies of these observations in these three classes. A χ^2 test applied to the distributions showed that they were significantly different at a level which was better than 0.1%, and the individual χ^2 values indicate that there is a tendency for cirrus cloud to be most frequent when the curvature of the isotherms is anticyclonic.

6. Cirrus cloud and vorticity advection at 300 mb.

French and Johannessen (1953) attempted to relate the presence of extensive layers of cirrus cloud to patterns on the 300 mb. contour chart. For their analysis observations were obtained from high flying aircraft engaged in routine navigation flights over extensive areas of the United States. Their observations were classified according to the sign of the advection of cyclonic vorticity at 300 mb.

Theoretical considerations indicated that if the vertical motion at the tropopause was zero or very small compared with the vertical motions at lower levels then the sign of the vorticity advection at 300 mb. gave the direction of the mean vertical motion through a layer which had its top at the tropopause and its base somewhere below 300 mb.

The authors found that 86% of the mileage flown through extensive cirrus by the aircraft corresponded with a positive sign of the vorticity advection at 300 mb. at the same time, implying on the above assumption upward vertical motion at 300 mb. Further, cirrus cloud sheets were always to be found when the absolute vorticity at 300 mb. was negative.

Using a finite difference approximation to the geostrophic wind it is possible to express the vorticity and also the advection of vorticity at a point in terms of (1) known contour heights at a set of points on a grid centred on the given point, (2) the Coriolis parameter and (3) the magnification factor of the grid. Although the preparation of vorticity

/and

and vorticity advection charts is possible by hand computation, with a large number of cases considerable time and labour is saved by using an electronic computer.

A grid of 12 by 11 points was adopted covering an area bounded approximately by longitudes 40°N and 60°N and latitudes 15°E and 35°W. To conform with the limited capacity of the machine - the M E G computer at Manchester University was used - mean values along a line of latitude of the Coriolis parameter and the magnification factor of the grid were used. These were shown to be justifiable approximations by comparison of several charts analysed fully by hand with and without these limitations. A total of 180 charts was subjected to analysis by the computer, and the field of vorticity advection at 300 mb. obtained for the times of the charts. The distribution of absolute vorticity at the same level was also evaluated for some 40 charts.

Sixteen charts were analysed for occasions when the reporting aircraft were engaged on long distance flights generally at altitudes in excess of 40,000 ft. On two of these flights the cirrus cloud was reported as being well above the aircraft and consequently well into the lower stratosphere. These were not included in the statistical analysis at this stage.

Considering first these observations made during long distance flights, points were taken every 100 mi. of the aircraft track and Table 10 presents the frequencies of the sign of the vorticity advection at 300 mb. for cases of "Cirrus" and "No Cirrus". The cirrus observations have been further divided into two classes, namely thick and patchy. The former includes all observations of cloud sheets thicker than 1,000 ft., whilst the latter includes all observations of wisps, bands and tufts, generally believed to be 3-6 eighths. Reports of anvil cirrus alone were not included. Table 10 shows that 77% of all thick cirrus cloud reported on long range flights were in areas where the vorticity advection at 300 mb. was positive, indicating upward vertical motion in the upper troposphere.

Table 11 presents corresponding figures obtained from the remaining 164 cases, viz., point observations, the cases of cirrus cloud in the stratosphere again being excluded. Several observations were made independently on individual days, and all have been included in Table 11.

Table 12 is obtained by combining Tables 10 and 11, i.e. assuming that an observation every 100 mi. of aircraft track is equivalent to a spot observation. Thus 76% of the observations of thick cirrus cloud were found in areas where the advection of cyclonic vorticity at 300 mb. was positive, whilst 66% of the cases of "No Cirrus" were found in areas where the term was negative.

Little significant difference was found between the means of the absolute vorticities for the two classes "Cirrus" and "No Cirrus", although the number of cases available for analysis was not sufficient to give any statistical accuracy. French and Johannessen state that extensive sheets of cirrus cloud were found in areas where the absolute vorticity at 300 mb. is negative. Since this implies dynamical instability at 300 mb., a phenomenon which is thought to be rare, and in any case confined to small areas only, it is not surprising that no cases were found in the charts analysed when the absolute vorticity was negative. Hence no additional evidence is available for comparison with the claims of the above authors.

7. Analysis of 300 mb. contour charts

Sawyer and Illett (1951) described an investigation into the frequency distribution of type and amount of cirrus cloud in relation to the jet stream at 300 mb. Later, Murray (1953) in an analysis of flights through jet streams made by aircraft of the Meteorological Research Flight drew similar conclusions concerning the distribution

of high and medium layer cloud with respect to the jet stream. Fig. 6(a) shows the frequency distribution of cirrus reports of the present series with distance from the jet stream axis at 300 mb. In spite of the difficulty in placing the jet axis to within ± 100 mi. it is clearly seen that the majority of cirrus reports lie on the high pressure side of the axis, very few being more than 200 mi. on the low pressure side. The division of reports of "No Cirrus" shown at 5(b) is not so well marked, but even so about 2/3 of the reports occur on the low pressure side. These figures show good agreement with the conclusions of the above authors, although many reports of "Cirrus" or "No Cirrus" were rejected as having no apparent association with a jet stream at 300 mb.

It has been shown in Section 6 that there is a significant connection between the presence of cirrus cloud in the upper troposphere and the sign of the vorticity advection at 300 mb. Considering only the curvature of the contours, the advection term $(-V\,\partial\zeta/\partial s)_{300}$ is positive to the rear of a ridge and forward of a trough in the contour pattern. Fig. 7 shows the ratios of the percentages of observations of "Cirrus" to "No Cirrus" in relation to an idealised wave pattern in the 300 mb. flow. It is clearly seen that this ratio is a maximum in and to the rear of a ridge and a minimum in and to the rear of a trough. At first sight this does not appear fully consistent with the conclusion of Section 6, since we should expect upward vertical motion in the layer immediately below the tropopause to be taking place through the region forward of the trough line and to the rear of the ridge line at 300 mb. However, it is thought that although the air may commence to ascend immediately forward of the trough, some little time must elapse before the rising air becomes saturated, and hence before the appearance of cirrus clouds. Thus it is not surprising that the maximum frequency of reports should occur just in and to the rear of the ridge, as shown in Fig. 7.

8. Cirrus clouds in the stratosphere

Some 30 cases were reported when the bases or tops of cirrus cloud were above the tropopause obtained from analysis of neighbouring upper air ascents. In eight of these cases, the clouds had been definitely below the tropopause reported from neighbouring stations, and extended upwards above the tropopause. These cases are not surprising since local variations in the height of the tropopause could permit reported tops of cloud to extend above the tropopause height reported by the nearest radio-sonde ascent.

Some of the remaining reports were discussed by Jacobs (1954), who concluded that the extensive layer clouds observed over Southern England on 27 - 29th July, 1953 were in fact dust clouds, which originated from a volcanic eruption in Alaska on July 9th, 1953. The clouds reported in this case were estimated to be at heights in excess of 50,000 ft. at times.

It seems highly improbable that the remaining 18 cases could be attributed to similar disturbances, and in all probability these were genuine ice crystal cloud, at times as much as 10,000 ft. above the tropopause.

Little can be said concerning the existence of these very high clouds; the sample is too small to permit a statistical investigation, even if the relevant parameters were known at these heights. However, vorticity advection charts at 300 mb. were constructed for these occasions, and the results were remarkable in that for all cases of extensive cirrus sheets in the stratosphere, the sign of the advection of cyclonic vorticity at 300 mb. was negative (Table 13). The theory postulated by French and Johannessen associates upward vertical motion in the upper troposphere with a positive value of vorticity advection at 300 mb. assuming little or no vertical motion at the tropopause. A negative value of the vorticity advection would imply downward vertical motion below the tropopause, which would thus be a region of horizontal convergence. If this is so then it is possible that upward

/vertical

vertical motion was occurring in the lower stratosphere, and hence if the air were sufficiently moist at these levels the formation of cirrus cloud might result. Obviously, this is far from being anything but a tentative suggestion, and considerably more cases need to be reported of these high clouds which undoubtedly do exist in the stratosphere.

9. Conclusions

1. The observations confirm the work of earlier writers on the association of cirrus cloud in the troposphere with the area ahead of surface fronts, the high pressure side of the jet stream at 300 mb., and with thermal ridges. Considerable agreement is obtained with the statistical results presented by Murgatroyd and Goldsmith regarding the distribution of bases and tops of cirrus cloud in relation to the tropopause.

2. A strong association is found between the presence of cirrus cloud and the humidities at 500, 450 and 400 mb. Some assistance to the forecaster is possible in assessing the distribution of cirrus cloud from radio-sonde ascents if the humidities at all three levels are taken into consideration.

3. At all levels from 500 mb. to 300 mb. the winds between south and west were most frequently accompanied by cirrus cloud and winds between south and east had the lowest frequency of cirrus reports.

4. Consideration of the winds at 500 and 300 mb. confirms that cirrus cloud is associated with warm air advection at these levels. Also, cirrus cloud has an association with strong thermal contrasts as indicated by the 1000-500 mb. thickness pattern.

5. Cirrus cloud in the troposphere is associated with positive values of the advection of cyclonic vorticity at 300 mb., implying upward vertical motion in the upper troposphere.

6. Reports of cirrus cloud in the stratosphere were comparatively few, but are sufficient to confirm that high clouds at these levels do exist.

References

1. Murgatroyd, R. J. and P. Goldsmith. 1953. Meteorological Research Papers, Air Ministry, London. No. 833.

2. Kimachi, T. 1952. J. Met. Soc., Japan. Vol. 30, 9.

3. Bannon, J. K., R. Frith and H. C. Shellard. 1952. Geo.Mem. No. 88.

4. French, J. E. and K. R. Johannessen. 1953. Proc. Toronto Met. Conf.

5. Sawyer, J. S. and Betty Illett. 1951. Meteorological Research Papers, Air Ministry, London. No. 633.

6. Murray, R. 1953. Meteorological Research Papers, Air Ministry, London. No. 813.

7. Washington, A. W. S. T.R. 105/81. "The Cirrus Forecasting Problem".

8. Jacobs, L. 1954. Met. Mag., 83, pp. 115-119.

9. Crossley, A. F. 1954. Met. Mag., 83, pp. 66-73.

Table 1

Number of observations of "Cirrus" and "No Cirrus" at various distances from surface fronts

	Dist. ahead of front (x 10^2 mi.)			Dist. behind front (x 10^2 mi.)			No marked front	
	0-2	2-4	4-6	0-2	2-4	4-6		
Warm (Cirrus	33	21	8	13	2	1	Cirrus	38
Warm (No Cirrus	2	7	8	0	3	3	No Cirrus	33
Cold (Cirrus	18	12	4	10	3	1		
Cold (No Cirrus	6	3	0	6	2	0		
Occlusion (Cirrus	12	3	0	3	5	1		
Occlusion (No Cirrus	0	5	1	1	3	2		

Table 2

Number of reports of "Cirrus" and "No Cirrus" at specified distances from features of the surface pressure chart

	Dist. from low or trough (x 10^2 mi.)				Dist. from ridge or high (x 10^2 mi.)				Totals
	0-2	2-4	4-6	>6	0-2	2-4	4-6	>6	
Cirrus	11	24	28	48	17	13	18	13	172
No Cirrus	4	8	3	18	9	12	4	11	69

Table 3

Dryness of air in association with reports of "Cirrus" and "No Cirrus". Parameter used is depression of dew point below temperature in °F

	500 mb.			450 mb.			400 mb.		
	Mean	No. of obs.	Sig^{ce}	Mean	No. of obs.	Sig^{ce}	Mean	No. of obs.	Sig^{ce}
Cirrus	18	164	Better than 0.1%	18	152	Better than 0.1%	17	156	Better than 0.1%
No Cirrus	26	80		26	74		25	72	

Table 4

Number of reports of "Cirrus" and "No Cirrus" when the depressions of frost points at 500, 450 and 400 mb. were simultaneously (a) less than the means for "Cirrus" reports (humidity favourable) and (b) greater than the means for "No Cirrus" reports (humidity unfavourable)

	Cirrus	No Cirrus	Totals
Humidity favourable	70	18	88
Humidity unfavourable	13	32	45
Totals	83	50	133

/Table 5

Table 5

Means in °F/1000 ft. of temperature lapse rate in 100 mb. intervals

	500 - 400 mb.	400 - 300 mb.	300 - 200 mb.
Cirrus	3.90	4.06	2.07
No Cirrus	4.02	4.02	1.47
"Student's 't'"	1.86	0.06	1.00

Table 6

Distribution of wind directions at various pressure levels for reports of "Cirrus" and "No Cirrus"

		N-NE	NE-E	E-SE	SE-S	S-SW	SW-W	W-NW	NW-N	Total	χ^2	Sig$^{ce.}$ (%)
500	Cirrus	17	11	6	5	19	30	40	19	147)	23.3	0.3
	No Cirrus	11	5	7	2	8	8	13	12	66)		
400	Cirrus	15	13	3	4	22	31	36	22	146)	45.7	< 0.1
	No Cirrus	8	4	7	5	11	6	12	13	66)		
300	Cirrus	17	13	2	7	14	35	29	26	143)	24.0	0.1
	No Cirrus	7	6	4	4	11	11	10	14	68)		
200	Cirrus	13	17	0	5	11	39	34	29	148)	36.1	< 0.1
	No Cirrus	9	4	2	3	9	8	16	12	63)		

Table 7

Number of occasions of cirrus associated with advection of warm or cold air

		Warm advection	Cold advection	Neither	χ^2	Significance
500-400 mb.	Cirrus	52	41	42)	3.92	≏ 20%
	No Cirrus	20	23	22)		
400-300 mb.	Cirrus	53	31	48)	13.67	≏ 0.1%
	No Cirrus	20	26	21)		
300-200 mb.	Cirrus	50	42	42)	15.46	< 0.1%
	No Cirrus	16	30	18)		
500-300 mb.	Cirrus	70	37	35)	21.40	< 0.1%
	No Cirrus	23	30	14)		

Table 8

Association of cirrus with the thermal wind speed

	Cirrus	No Cirrus
Mean thermal wind (kt.)	21	16
No. of obs.	174	79
Std. deviation	11.4	12.3
Std. error of mean	0.9	1.4

/Table 9

Table 9

Association of cirrus with curvature of thickness lines

(No. of cases)

	Cyclonic	Anticyclonic	Neither	Totals
Cirrus	59	54	49	162
No Cirrus	31	15	35	81

Table 10

Association of cirrus with sign of vorticity advection at 300 mb. for points at 100 mi. intervals along aircraft track

Sign of advection
(No. of cases)

Cirrus	+	-	0	Total
Thick	23	7	0	30
Patchy	18	16	0	34
Nil	19	39	3	61

Table 11

Association of cirrus with sign of vorticity advection at 300 mb. for spot reports

Sign of advection
(No. of cases)

Cirrus	+	-	0	Total
Thick	69	19	3	91
Patchy	27	28	5	60
Nil	18	40	2	60

Table 12

Sign of vorticity advection at 300 mb. combining Tables 10 and 11

Sign of advection
(No. of cases)

Cirrus	+	-	0	Total
Thick	92	26	3	121
Patchy	45	44	5	94
Nil	37	79	5	121

Table 13

Sign of vorticity advection at 300 mb. for cirrus cloud certainly in the stratosphere (Route flights and spot observations included)

Sign of advection
(No. of cases)

Cirrus	+	-	0	Total obs.
Thick	0	17	1	18
Patchy	3	5	0	8

DISTRIBUTION OF CIRRUS TOPS BELOW THE TROPOPAUSE

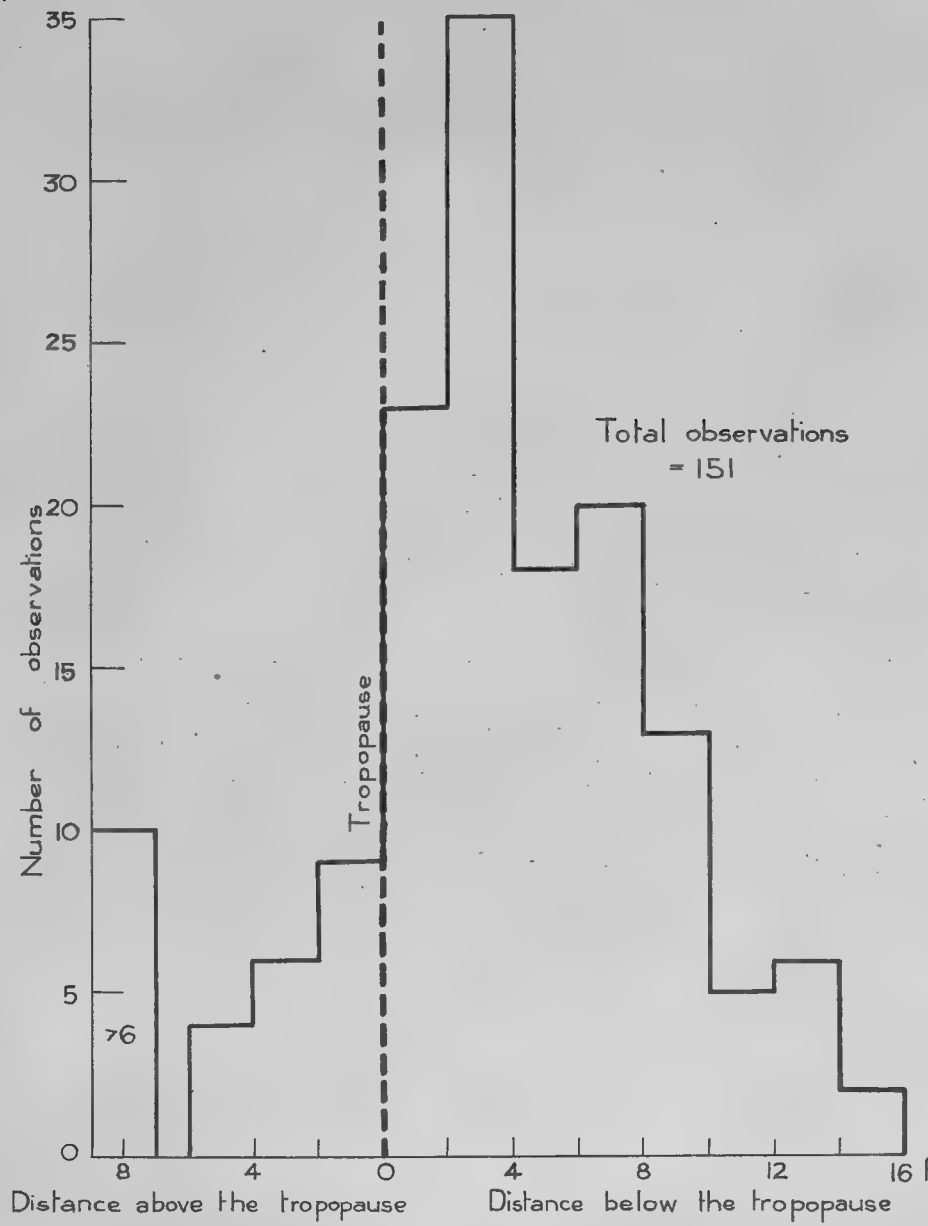

Fig. 1

DISTRIBUTION OF CIRRUS BASES BELOW THE TROPOPAUSE

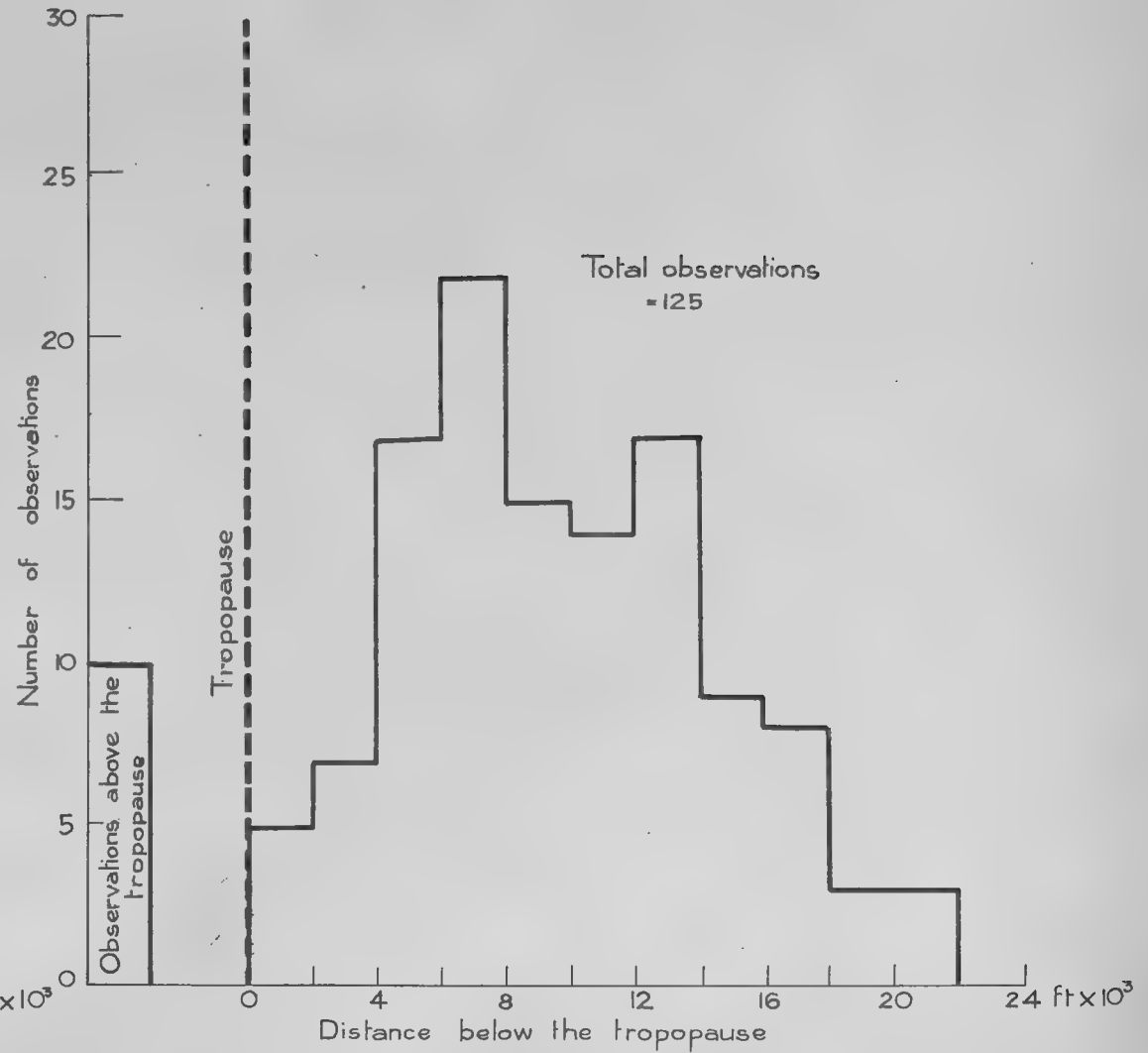

Fig. 2

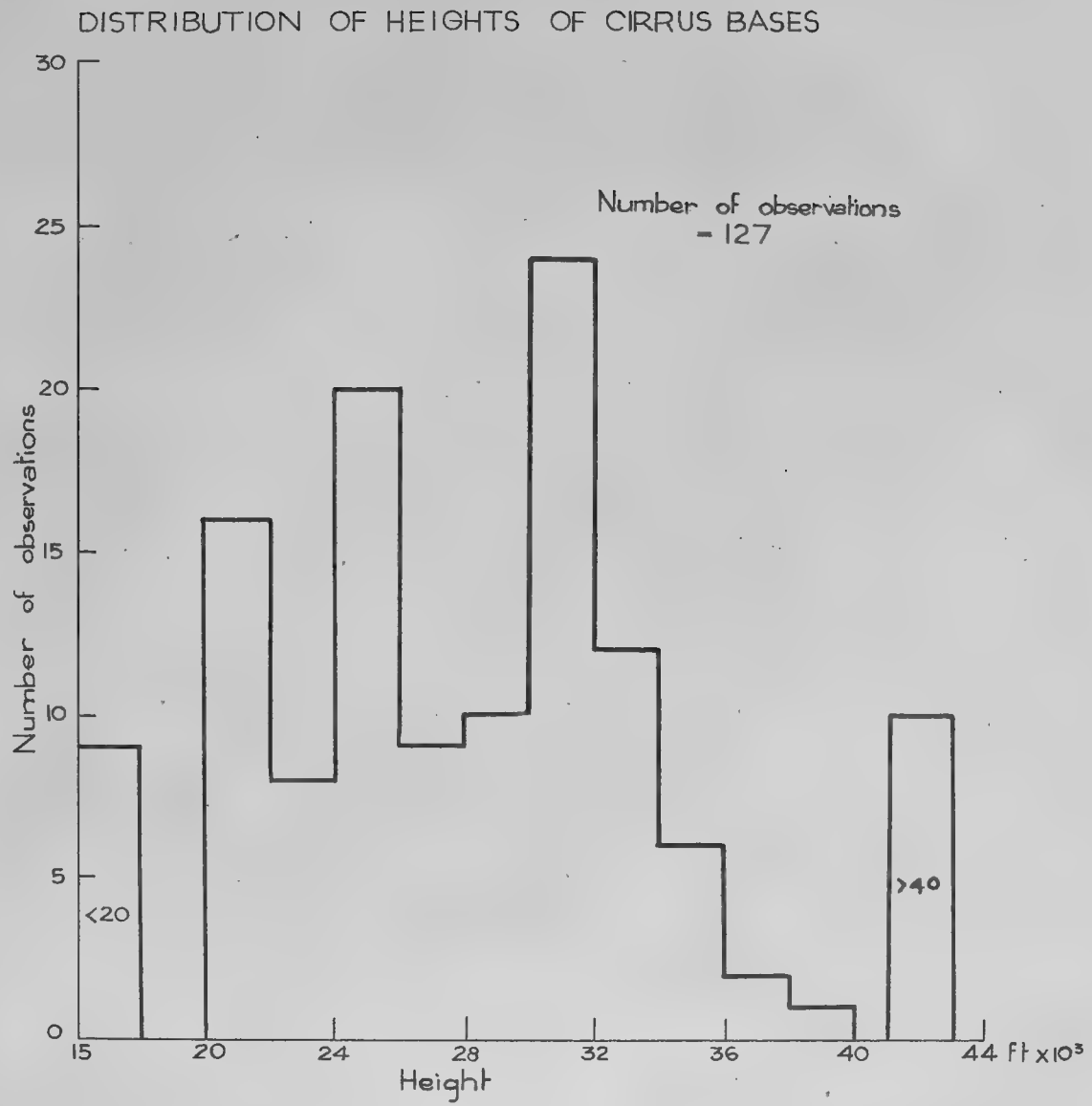
DISTRIBUTION OF HEIGHTS OF CIRRUS BASES
Number of observations
= 127
Number of observations
30
25
20
15
10
5
0
<20
>40
15
20
24
28
32
36
40
44 ft x10³
Height

Fig. 3

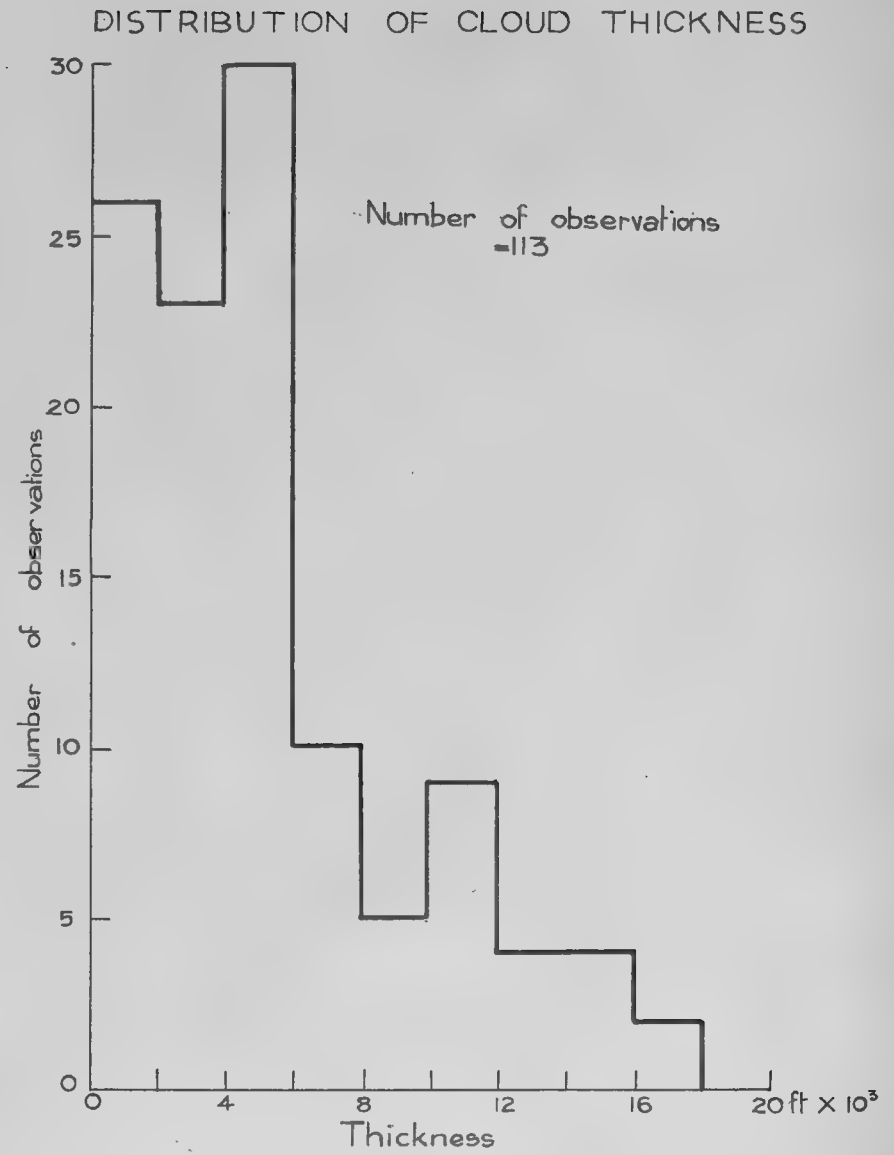
DISTRIBUTION OF CLOUD THICKNESS
Number of observations
=113
Number of observations
30
25
20
15
10
5
0
0
4
8
12
16
20 ft x 10³
Thickness

Fig. 4

Ratios of the percentages of number of observations of "cirrus" to "no cirrus" in relation to an assumed wave-form in the total thickness pattern.

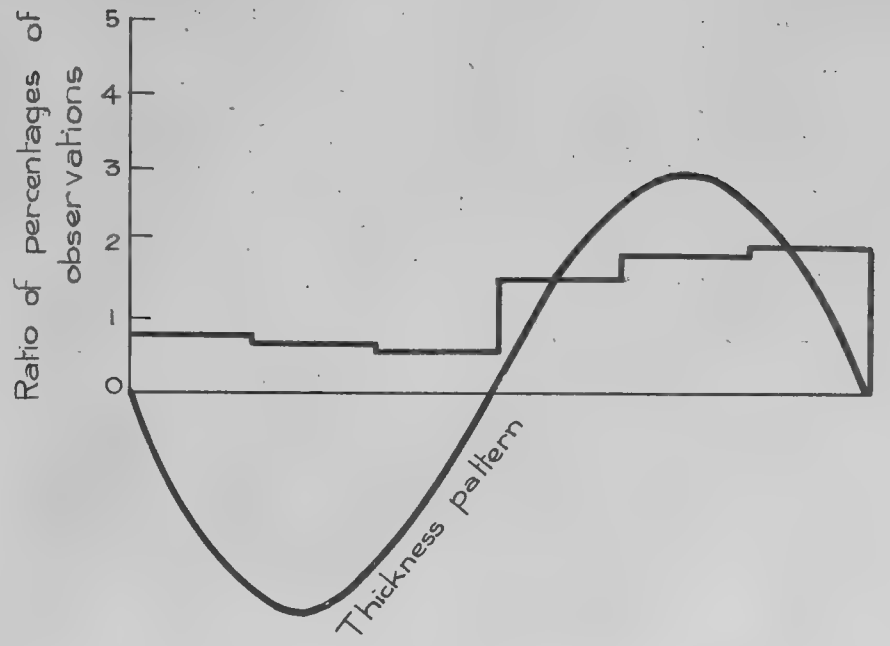

Fig. 5

Ratios of the percentages of number of observations of cirrus" to "no cirrus" in relation to an assumed wave-form in 300mb. contour pattern

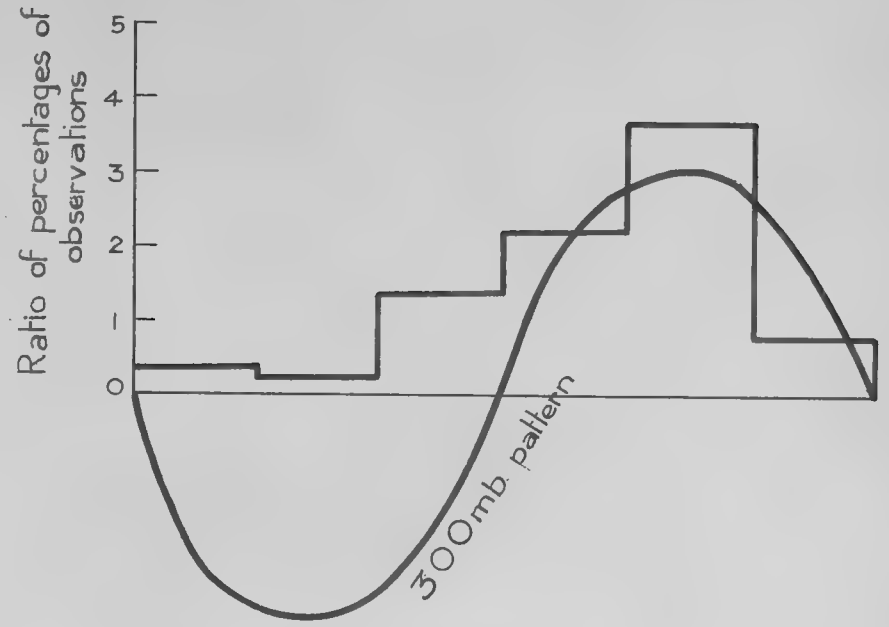

Fig. 7

FREQUENCY OF REPORTS IN RELATION TO DISTANCES FROM AXIS OF JET STREAM AT 300 mb.

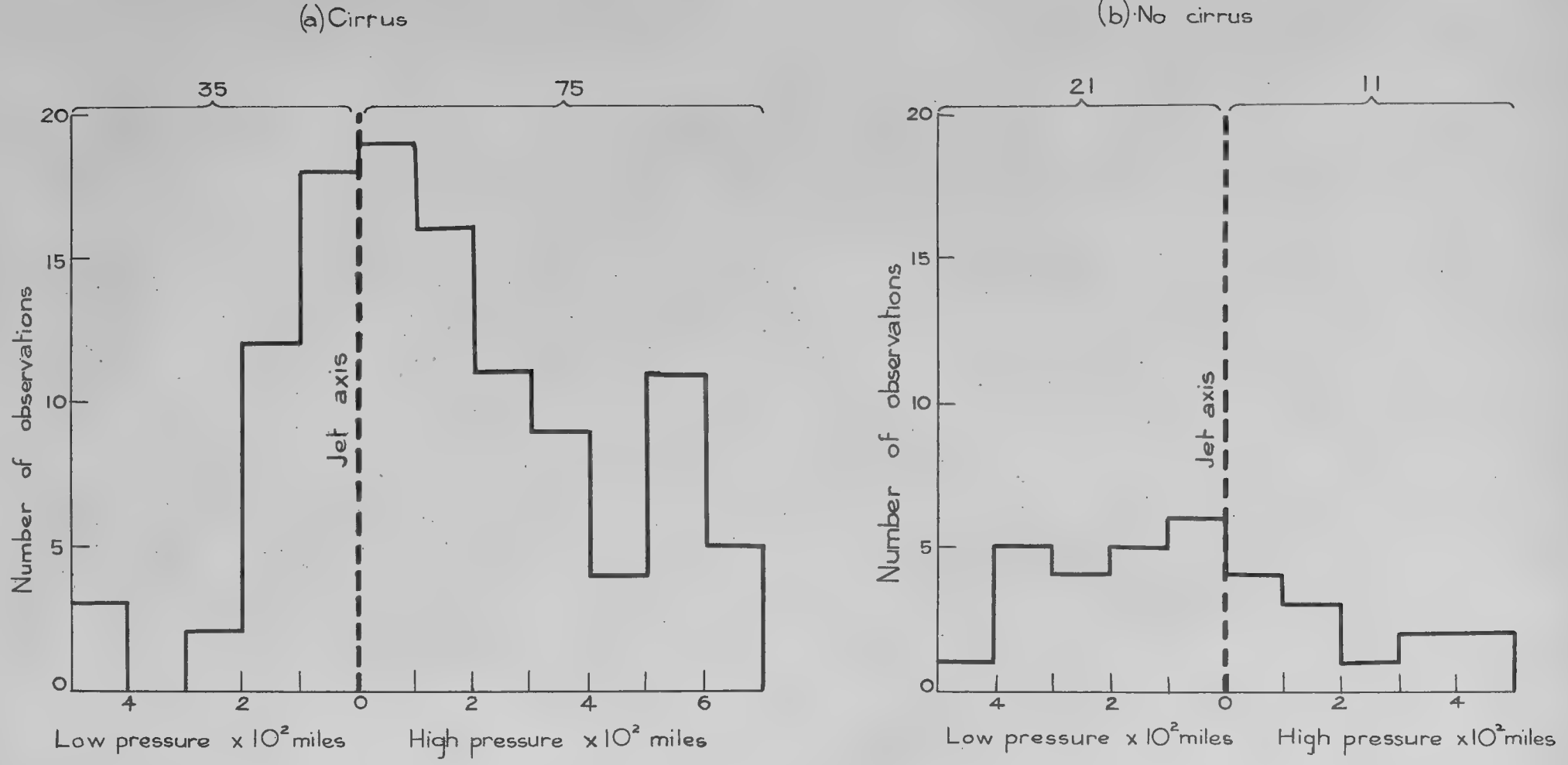

Fig. 6

M.R.P. 935
S.C. 111/191
S.C. 11/198
16th September, 1955

Dynamical similarity in an incompressible fluid model of two-dimensional airflow over a ridge

by

J. S. Sawyer
(Meteorological Office)

AIR MINISTRY
METEOROLOGICAL RESEARCH COMMITTEE

At the time of issue this report has not been published. Any author desiring to quote this paper should refer to it as "A paper of the Meteorological Research Committee (London), M.R.P. No. 935 by Mr. J.S. Sawyer. A copy is available in the Library of the Meteorological Office."

M.R.P. 935
S.C.III/191
S.C.II/198
16th September, 1955

AIR MINISTRY

METEOROLOGICAL RESEARCH COMMITTEE

Dynamical similarity in an incompressible fluid model of two-dimensional airflow over a ridge

by
J.S. Sawyer (Meteorological Office)

Introduction

In order that the flow in any laboratory model should be of value in interpreting or predicting the observed flow in the atmosphere, it is essential that the two systems should be dynamically similar. This means that it must be possible to describe the flow in the two systems by the same equations after appropriate adjustment of the units of length, time etc. has been made.

One of the difficulties which arise in attempting to devise a model which will be dynamically similar to the atmosphere is that air is a compressible fluid, and that in the adiabatic motion with which we are concerned the density changes with pressure so that

$$D/Dt\,(p/\rho^{\gamma}) = 0 .$$

Any model which is to be strictly similar must therefore use a compressible fluid with the same value of γ, and this restricts the models to those using air as a working fluid. Unfortunately, if the model is to be scaled down to laboratory size the similarity requirements lead to the need to use strong temperature gradients and very low velocities of a few centimetres per sec.; conditions which are impractical for useful experiment. The present note is intended to examine whether adequate similarity can be achieved using an incompressible fluid, and simulating the effects of atmospheric compressibility by modification of the shape of the model.

Extensive experiments have been carried out by Long (1954) on the flow of stably stratified liquids over obstacles in channels, although he has not attempted to simulate the important effects of wind shear. His results show vertical oscillations of the fluid closely analogous to those observed in the atmosphere and he has discussed the requirements for similarity between the flow in the atmosphere and the model. However, recent Meteorological Research Papers (M.R.P. 842 and 892) have tended to emphasise the limitations of model experiments and it seems desirable to restate the degree of similarity which may be achieved, in order that the possibilities of model experiments should not be overlooked.

The governing equations

The requirements for dynamical similarity in atmospheric motions have been discussed by Batchelor (1953) and his treatment can be followed here. The equations which govern atmospheric motion are assumed to be those which are applicable to the frictionless motion of a perfect gas under adiabatic conditions.

/They

They are the vector equation of motion

$$\frac{D\tilde{u}}{Dt} = \tilde{g} - \frac{1}{\rho}\tilde{\nabla}p, \qquad (1)$$

the equation of continuity

$$\frac{1}{\rho}\frac{D\rho}{Dt} = -\nabla.\tilde{u}, \qquad (2)$$

and the relation between p and ρ for a perfect gas under adiabatic conditions, namely:-

$$\frac{D}{Dt}\left(p/\rho^{\gamma}\right) = 0. \qquad (3)$$

An essential feature of the type of motion with which we are concerned in the flow of air over mountains is that the pressure field is very nearly in hydrostatic equilibrium, and differs little from the pressure field in undisturbed flow. The density field also differs little from the density field of a fluid in adiabatic equilibrium. Batchelor has shown that these conditions lead to a simplification of the requirements for dynamical similarity and his treatment is followed here.

We write ρ_a and p_a for the density and pressure in an atmosphere with an adiabatic lapse rate at the same level z at which the true density and pressure are ρ and p. Under the circumstances outlined in the preceding paragraph any change in density of the moving air parcel arises almost entirely from the changes of pressure due to its change of level and these can be regarded as the same as those in the equilibrium atmosphere. Thus from (3)

$$\frac{1}{\rho}\frac{D\rho}{Dt} = \frac{1}{\gamma}\frac{1}{p}\frac{Dp}{Dt}$$

$$\simeq \frac{1}{\gamma}\frac{1}{p}w\frac{\partial p}{\partial z}$$

$$\simeq -\frac{g\rho_a}{\gamma p_a}w$$

Equation (2) thus becomes

$$\nabla.\tilde{u} = \frac{g\rho_a}{\gamma p_a}w \qquad (4)$$

Also

$$\frac{1}{\rho}\frac{D\rho}{Dt} = \frac{1}{\gamma p}\frac{Dp}{Dt} \simeq \frac{1}{\gamma p_a}\frac{Dp_a}{Dt} = \frac{1}{\rho_a}\frac{D\rho_a}{Dt}.$$

Changing the variables in (1), (3) and (4) to $p-p_a$ and $\rho-\rho_a$ and making use of the fact that $\tilde{\nabla} p_a \to \rho_a \tilde{g}$, these equations may be rewritten:-

$$\left(\frac{\rho-\rho_a}{\rho_a}+1\right)\frac{D\tilde{u}}{Dt} = \tilde{g}\left(\frac{\rho-\rho_a}{\rho_a}\right) - \frac{\tilde{\nabla}(p-p_a)}{\rho_a}, \tag{5}$$

$$\nabla.\tilde{u} = \frac{g\rho_a}{\gamma p_a} w, \tag{6}$$

$$\frac{D}{Dt}\left(\frac{\rho-\rho_a}{\rho_a}\right) = 0 . \tag{7}$$

In order to write the equations in non-dimensional form, we introduce a unit length x_0, a unit velocity u_0, unit density ρ_0 and unit pressure p_0. The unit of time t_0 must then be given by $t_0 = x_0/u_0$.

Equations (5), (6) and (7) can then be written in non-dimensional form in terms of new variables, $u' = u/u_0$, etc., giving

$$\frac{D\tilde{u}'}{Dt'} = \frac{x_0\rho_0}{u_0^2}\left(\frac{\rho'-\rho_a'}{\rho_a}\right)\tilde{g} - \frac{x_0 p_0}{u_0^2\rho_a}\tilde{\nabla}(p'-p_a') \tag{8}$$

$$\nabla.\tilde{u}' = \frac{g\rho_a x_0}{\gamma p_a} w' \tag{9}$$

$$\frac{D}{Dt}\left(\frac{\rho'-\rho_a'}{\rho_a'}\right) = 0 \tag{10}$$

Here $\frac{\rho-\rho_a}{\rho_a}$ has been ignored compared with unity in equation (8).

An incompressible model of variable width

The essential difference between equations (8) - (10) which describe the atmosphere, and the equations which describe an incompressible fluid model arises from the equation of continuity (9). If, however, our study is restricted to two-dimensional motion in the atmosphere, it may be possible by using a narrow tank of variable width to bring the equation for the two-dimensional divergence to the form (9) but at the same time to retain the essentially two-dimensional character of the motion.

Thus if the width of the tank is $a = a(z)$ and the motion can still be regarded as essentially two-dimensional, the equation of continuity of an incompressible fluid becomes

$$\frac{\partial}{\partial x}(au) + \frac{\partial}{\partial z}(aw) = 0 ,$$

or

$$\frac{\partial u}{\partial x} + \frac{\partial w}{\partial z} = -\frac{w}{a}\frac{da}{dz} . \tag{11}$$

This is of a similar form to equation (9) provided the latter is treated as referring to two-dimensional motion, i.e.,

$$\nabla . u' = \frac{\partial w'}{\partial x'} + \frac{\partial w'}{\partial z'} .$$

The equations of motion for the two-dimensional motion of an incompressible fluid are:-

$$\frac{D\tilde{u}}{Dt} = \tilde{g} - \frac{1}{\rho} \nabla p , \tag{12}$$

and the equation corresponding to the equation of state (3) is

$$\frac{D\rho}{Dt} = 0 \tag{13}$$

If we write ρ_{am} and p_{am} as the density and pressure in a model with uniform density in hydrostatic equilibrium, the three equations (11), (12) and (13) become

$$\left(\frac{\rho - \rho_{am}}{\rho_{am}} + 1 \right) \frac{D\tilde{u}}{Dt} = \frac{\rho - \rho_{am}}{\rho_{am}} \tilde{g} - \frac{\nabla (p - p_{am})}{\rho_{am}} , \tag{14}$$

$$\nabla_2 . \tilde{u} = - \frac{w}{a} \frac{da}{dz} , \tag{15}$$

$$\frac{D}{Dt} \left(\frac{\rho - \rho_{am}}{\rho_{am}} \right) = 0 , \tag{16}$$

where $\nabla_2 .$ is the two-dimensional divergence.

/If

If again we neglect $(\rho - \rho_{am})/\rho_{am}$ compared with unity and express the equations in terms of non-dimensional variables by means of unit lengths, velocities etc. x_m, u_m, we have

$$\frac{D\tilde{u}'}{Dt'} = \frac{x_m \rho_m}{u_m^2 \rho_{am}} (\rho' - \rho'_{am}) \tilde{g} - \frac{x_m p_m}{u_m^2 \rho_{am}} \nabla (p' - p_{am}) \qquad (17)$$

$$\nabla_2 . \tilde{u}' = - \frac{x_m}{a} \frac{da}{dz} w' \qquad (18)$$

$$\frac{D}{Dt} \left(\frac{\rho' - \rho'_{am}}{\rho'_{am}} \right) = 0 \qquad (19)$$

Conditions for dynamical similarity

The equations (17), (18) and (19) can be made identical with (8), (9) and (10) provided the following conditions are satisfied.

$$\frac{g \rho_a x_o}{\gamma p_a} = - \frac{x_m}{a} \frac{da}{dz} , \qquad (20)$$

$$\frac{x_o \rho_o}{u_o^2 \rho_a} = \frac{x_m}{u_m^2} \frac{\rho_m}{\rho_{am}} , \qquad (21)$$

$$\frac{x_o p_o}{u_o^2 \rho_a} = \frac{x_m}{u_m^2} \frac{p_m}{\rho_{am}} . \qquad (22)$$

It should be noted that both ρ_o and ρ_a are functions of z but equations (21) and (22) ensure that $\rho' = \rho_o / \rho_a$ is a constant and that the coefficients in equation (8) are also constants.

The third relation determines the ratio between the pressure units but as pressure will not be specified in the initial or boundary conditions (being given adequately by the hydrostatic condition) this need not concern us here.

Equation (20) shows that

$$\frac{da}{a} = - \frac{g \rho_a x_o}{\gamma p_a x_m} dz ,$$

where dz is a height increment in the model.

If dz^* is a corresponding height increment in the atmosphere

$$dz^* = \frac{x_o}{x_m} dz \quad .$$

Thus $$\int \frac{da}{a} = -\int \frac{g\rho_a}{\gamma p_a} dz = \frac{1}{\gamma}\int \frac{dp}{p_a} \simeq \frac{1}{\gamma}\int \frac{dp_a}{p_a} ,$$

or $$a \simeq A p_a^{1/\gamma} = B\rho_a \quad .$$

Thus equation (20) implies that the width of the model shall be proportional to the density at the corresponding level in the atmosphere. Equation (21) is the only remaining condition to be satisfied namely

$$\frac{x_o \rho_o}{u_o^2 \rho_a} = \frac{x_m \rho_m}{u_m^2 \rho_{am}} . \qquad (21)$$

ρ_o/ρ_a and ρ_m/ρ_{am} measure the ratio of the density unit (or density gradient) to the density itself in the atmosphere and the model respectively. If these proportional gradients are the same and $x_o/u_o^2 = x_m/u_m^2$ the neglect of $(\rho-\rho_a)/\rho_a$ in (5) and the similar approximation in deriving (17) from (14) are unnecessary. Equation (21) expresses the equality of the Froude number in the model and the atmosphere (see Long, 1954).

The physical requirements of a fluid model of two-dimensional flow over a ridge

In the atmosphere a typical range of potential temperature from the 1000 mb. to the 500 mb. level is around 12% so the change in $(\rho-\rho_a)/\rho_a$ is about 12% through the layer. If ρ_o/ρ_a is to equal ρ_m/ρ_{am} a similar proportional change in density is required through the model. Such a density gradient might be achieved with salt solution of varying concentration but only about a quarter of the change could conveniently be achieved in a liquid model using temperature gradients. In which case we should have

$$\rho_o/\rho_a = 4\rho_m/\rho_{am} .$$

Thus the restrictions on the dimensions and velocities are

$$\frac{x_o}{x_m}\frac{u_m^2}{u_o^2} = 1 \text{ for a salt solution model}$$

$$= \tfrac{1}{4} \text{ for a temperature gradient model.}$$

If a model about 2 ft. high is contemplated, $x_o/x_m = 10^4$

and $u_m/u_o = 10^{-2}$ for a salt solution model

$= 0{\cdot}5 \times 10^{-2}$ for a temperature gradient model.

/Taking

Taking u_0 in the atmosphere in the range 5 to 50 m/s this requires flow velocities in the models of 2·5 to 50 cm./sec. Other requirements already considered are that the flow should take place in a deep narrow channel with a width proportional to the density at a corresponding level in a standard atmosphere.

Boundary conditions

In constructing a model of the type described the lower boundary presents no difficulty. Similarity in shape between the model and the hill on the appropriate scale is all that is required. It can also be assumed that if the flow is constrained to be horizontal at a distance upstream from the model ridge the lateral boundary conditions will be similar to those in the atmosphere.

The upper boundary of the model cannot however satisfactorily reproduce conditions in the atmosphere; to be truly similar the model would need to be of infinite depth, tapering continuously with increasing height. However, it seems unlikely that the conditions in the upper atmosphere strongly influence the flow at low levels, and it may be possible to demonstrate this experimentally in a model. The atmospheric flow might be expected to be intermediate between that appropriate to a model with a rigid lid and one with a free surface, and if these showed little difference in the lower sections of the model it might reasonably be inferred that the upper boundary condition was not important.

Viscosity

Neither in the model nor in the atmosphere is it expected that viscous effects are of primary importance except in a shallow boundary layer. In the model, the shears to be expected in the body of the fluid are of the order of 50 cm./sec. in 60 cm. and with viscosity of ·013 c.g.s. units appropriate to water, the tangential stresses would be of the order of ·01 dynes/cm.^{2}. If this changes to zero over a distance of 10 cm. the net acceleration of the fluid would be 10^{-3} cm./sec.^{2}. However the accelerations, Du/Dt , are likely to be of the order of 1-100 cm./sec.^{2} so that viscous effects should be unimportant away from the boundary layer.

Since the kinematic viscosity has dimensions l^2t^{-1} or lu the value of ·013 appropriate to water would correspond to a value of $1{\cdot}3 \times 10^4$ in the atmosphere if the salt solution model considered earlier were used, or $2{\cdot}6 \times 10^4$ if the temperature gradient model were used. These values are of much the same order as the atmospheric eddy viscosity in the boundary layer and the effect of molecular viscosity in the model may be somewhat like that of eddy viscosity in the atmosphere.

Summary and recommendation

From the preceding analysis it appears that a useful degree of similarity can be achieved between the flow of liquid in a channel and the flow of air over a ridge of hills and that experiments with fluid models would be valuable. It is essential that the fluid should contain a density and velocity gradient because these have been shown by R.S. Scorer (1949) and others to be the primary factors which determine the nature of the flow. The effect of compressibility in the atmosphere might be simulated by making the channel taper upwards, the width being proportional to the density at a corresponding level in the atmosphere.

References

Batchelor, G.K.	1953	Quart. J.R. Met. Soc., 79, p.224.
Long, R.R.	1954	Tellus, Stockholm, 6, p.97.
Scorer, R.S.	1949	Quart. J.R. Met. Soc., 75, p.41.

M.R.P. 936
S.C. 111/192
18th October, 1955

AD [illegible]

Measurements of atmospheric radiation and the heat balance at the ground at Kew May, 1953 - May, 1954

by
W. T. Roach
(formerly at Kew Observatory)

AIR MINISTRY
METEOROLOGICAL RESEARCH COMMITTEE

At the time of issue this report has not been published. Any author desiring to quote this paper should refer to it as "A paper of the Meteorological Research Committee (London), M.R.P. No. 936 by Mr. W.T. Roach. A copy is available in the Library of the Meteorological Office."

M.R.P. 936
S.C.III/192
18th October, 1955

AD 223101

AIR MINISTRY

METEOROLOGICAL RESEARCH COMMITTEE

Measurements of atmospheric radiation and the heat balance at the ground at Kew May, 1953 - May, 1954

by
W.T. Roach (formerly at Kew Observatory)

1. Introduction

It was decided early in 1953 to use the ventilated flux radiometer advocated by Mörikofer (1951), Gier and Dunkle (1949) and others to obtain a continuous record of total net flux of radiation into the ground over a period of one year.

This project came into operation on 1st May, 1953 and continued until 12th May, 1954, during which period continuous photographic records of the following elements were obtained:-

(i) Surface temperature - measured by a fine copper-constantan thermojunction immersed in a small glass bulb containing ethylene glycol. The reference junction was maintained thermostatically at a temperature of 44.3 ± 0.1°C over the whole period.

(ii) Total net flux of radiation - measured by the ventilated flux radiometer, hereafter referred to as the VFR.

(iii) Flux of heat in soil at a depth of 6 cm. - measured by a flux plate constructed and operated on the same principle as the VFR, except that it was not sandwiched between two metal guard plates as are the elements of the VFR.

The calibration of instruments is discussed in Appendix I, and the setting up of a standard source of long-wave radiation in Appendix II.

2. Symbols

As far as possible, these follow the symbols and conventions used by Rider and Robinson (1951). We repeat the relevant symbols here.

z = Height above surface (cm.).

$T(z)$ = Temperature at height z (°K unless otherwise stated).

T_r = Radiative temperature.

$R_L(z)$ = Net vertical flux of long-wave radiation at z.

$R_s(z)$ = Net vertical flux of short-wave radiation at z.

$\downarrow,\uparrow$ = Direction of radiative fluxes through a horizontal plane.

$R_L(z)\downarrow + R_L(z)\uparrow = R_L(z)$; $R_s(z)\downarrow + R_s(z)\uparrow = R_s(z)$.

/R(z)

$R(z)$ = Total net vertical flux of radiation at height z.

= $R_L(z) + R_s(z)$.

$C(z)$ = Flux of heat by convection at height z.

$G(-z)$ = Flux of heat into ground at a depth of z cm.

$E(z)$ = Flux of water vapour at height z ($g.cm^{-2}sec^{-1}$).

$F(z)$ = Total net vertical flux of heat at z.

λ = Latent heat of evaporation of water.

$\bar{x} = \frac{1}{t}\int_0^t x\,dt$ where x is the instantaneous value of any physical quantity, and t - which may vary from 10^4 to 10^7 sec. - is defined in the context.

All fluxes of heat are in units of $mw.cm^{-2}$ unless otherwise stated.

Conventions

(i) All fluxes are considered as passing through a horizontal plane.

(ii) All fluxes are reckoned positive if directed upwards.

3. Theory

3.1. Surface temperatures

It has been shown experimentally by Robinson (1947) that T(0) - as measured by a thermometer laid directly on a short grass surface - agrees very well with $T_r(0)$ as measured by a Linke-Feussner radiometer. For instantaneous values, he found:-

$$\left|T_r(0) - T(0)\right| < \begin{cases} 3°C \text{ in conditions of strong insolation,} \\ 2°C \text{ in all other conditions.} \end{cases}$$

The standard deviations given were 1.5°C and 0.7°C respectively.

The mean value of a number of readings gave

$$\frac{1}{n}\sum_n \left[T_r(0) - T(0)\right]_n = \begin{cases} -0.5°C \pm 1.2°C \text{ in strong insolation} \\ +0.25°C \pm 0.6°C \text{ in other conditions.} \end{cases}$$

For the purposes of this investigation, therefore, it is assumed that $\overline{T_r(0)} = \overline{T(0)}$ over any period greater than an hour.

Hence we may write

$$R_L(0)\uparrow = \sigma T(0)^4 \pm 1 \text{ mw.cm}^{-2}$$

and

$$\overline{R_L(0)\uparrow} = \sigma \overline{T(0)}^4 \pm 0.2 \text{ mw.cm}^{-2} \qquad (1)$$

3.2. Ventilated flux radiometer

This measures R(z) directly. It was operated at a height of one metre above short grass, so that if R(z) is split into its components, the relevant equation is

$$R(100) = \left[R_s(100)\uparrow + R_s(100)\downarrow + R_L(100)\uparrow + R_L(100)\downarrow\right] \qquad (2)$$

/3.3.

3.3 Solar radiation

We are justified in assuming that absorption of solar radiation in the lowest metre is quite negligible, so we can write

$$R_s(100) = R_s(0)$$

Since we are interested mainly in the heat balance at the surface, it is convenient to be able to reduce the terms in eq. 2 to ground level.

$R_s(0)$ can be separated from eq.2 and split into its components which are obtained as follows:- $R_s\downarrow$ is obtained from Kew records. $R_s\uparrow$ is the solar radiation reflected diffusely from the grass, and is not normally a routine measurement. However, one month's continuous record of this quantity was obtained during summer 1953 by M.J. Blackwell at Kew using an inverted solarimeter. His final result was

$$\overline{R_s}\uparrow = (0.25 \pm 0.01)\overline{R_s}\downarrow \text{ for short grass over one month.}$$

This figure has been adopted in the reduction of the results discussed in this paper.

Instantaneous values of the albedo of short grass can vary over quite a wide range under varying conditions, and we reproduce a table of these for interest.

Conditions	Albedo
Clear sky with high sun	0.22
Overcast sky	0.25
Low sun - altitude about 10°	0.3 - 0.4
Low sun and heavy dew on grass	$\sim$ 0.5
Overcast sky and heavy rain	0.1 - 0.2

In general, the heavier the rain, the lower the albedo, but whether this is a real or instrumental effect has apparently not been tested.

3.4. Long-wave radiation

$$R_L(100) = R_L(0) + \int_0^{100} \frac{\partial R_L(z)}{\partial z}\, dz \qquad (3)$$

The integral term usually assumes an appreciable value under clear skies - especially under a hot sun, when it may be of the order of 1 mw.cm^{-2} for short periods. When averaged over a day or more, it becomes negligible. Hence we assume

$$\overline{R_L(100)} = \overline{R_L(0)}$$

and

$$\overline{R_L(100)}\uparrow = \overline{R_L(0)}\uparrow = \sigma\,\overline{T(0)}^4 \qquad (4)$$

It follows from this and 3.3 that

$$\overline{R(100)} = \overline{R(0)}$$

From the foregoing, eq.2 can be rewritten

$$\overline{R(0)} = 0.75\,\overline{R_s}\downarrow + \overline{R_L}\downarrow + \sigma\,\overline{T(0)}^4 \qquad (5)$$

This is the equation used in reducing the results, and represents the radiative heat balance at the ground.

/3.5.

3.5. Earth flux plate

This gives a measure of the heat flow by conduction through the soil at a depth of 6 cm. The equation of heat conduction is

$$G(-z) = k_s(-z)\left(\frac{\partial T}{\partial z}\right)_z \equiv \alpha V \qquad (6)$$

where k_s = thermal conductivity of soil ($mw.cm^{-1}\ deg^{-1}$)

α = calibration constant of the flux plate ($mw.cm^{-2}/\mu V$ output)

V = output from flux plate in μV.

It has been found that α has a slight dependence on the ratio of k_s to the thermal conductivity of the material of the flux plate former - in this case paxolin. Experimental work shows that an increase in k_s of 40 to 1 results in an increase in α of only 1.6 to 1. This may be expressed as an approximate power law $\alpha \propto k_s^{1/8}$. Since k_s varies by a factor of about 3 over the year, α varies less than 10% on either side of a mean value.

3.6. Energy balance equation

We can now write down the equation for the energy balance in the top 6 cm. of soil. First we have the expression for flux of heat across the surface.

$$F(0) = C(0) + \lambda E(0) + R(0) = G(0)$$

since energy flow across the surface is continuous. The divergence of heat energy in the layer considered is

$$F(0) - F(-6) = C(0) + \lambda E(0) + R(0) - G(-6) \qquad (7)$$

on the assumption that flow of heat in the soil is practically all conductive; i.e., that transfer of heat by processes involving the movement of water or water vapour is negligible.

Over a period of one year, we can write

$$\overline{F(0)} - \overline{F(-6)} = 0,$$

and even after a few days

$$\left|\overline{F(0)} - \overline{F(-6)}\right| \ll \left|\overline{C(0)} + \lambda\overline{E(0)} + \overline{R(0)}\right|$$

Hence we can write eq.7

$$-\left[\overline{R(0)} - \overline{G(-6)}\right] = \overline{C(0)} + \lambda\overline{E(0)} \qquad (8)$$

The L.H.S. of eq.8 consists of measurable terms, and if $\lambda\overline{E(0)}$ can be estimated from evaporation tank readings or by other methods (Penman (1950)), a value for $\overline{C(0)}$ can be obtained.

Finally, we should expect that over a period of one year

$$\overline{G(-6)} = 0. \qquad (9)$$

So that over this period, eq.8 becomes

$$-\overline{R(0)} = \overline{C(0)} + \lambda\overline{E(0)} \qquad (10)$$

/4.

4. Discussion of records

4.1. Reduction of records

There is available a complete year's record of surface temperature, and so $R_L(0)\uparrow$, and flux of heat into the soil, $G(-6)$. Hourly means have been tabulated for about the first six months and daily means for the whole year.

With total radiation, $R(0)$, a difficulty arises. Tests by the N.P.L. on the paint used to blacken the surfaces of the VFR showed that while the paint had a very high absorptivity (0.98 for radiation from a black body source at 473°K), it was rather susceptible to damage - the mattness of the paint surface is easily ruined. Hence for most of the year, it was the practice to cover the radiometer plates whenever rain occurred or was forecast, so that half the total possible record of $R(0)$ was lost.

The main difficulty arises from the fact that the recorded half of $R(0)$ will not be representative of the unrecorded half, and if it is desired to extract monthly or even daily means of $R(0)$, some method has to be found of estimating R over the blank periods. Returning to eq.5, we see that, since continuous records of $R_s\downarrow$ and $T(0)$ are available, the problem reduces itself to estimating $R_L\downarrow$ in order to obtain R.

4.1.1. Estimation of $R_L\downarrow$

There now exists a large amount of literature on the estimation of $R_L\downarrow$ by empirical formulae and by radiation charts; the formulae involving surface parameters only, and the charts taking some account of the vertical distribution of temperature and humidity in the lower troposphere. The latter method, if practicable, is to be preferred, since it is based on the equation of radiative transfer and experimental results.

The normal procedure in drawing a radiation chart for a given situation is to obtain vertical soundings of temperature, pressure and dew-point from the relevant Daily Aerological Record. From these data, a profile of temperature against precipitable water vapour is obtained, and hence, using experimental data, of $\sigma T(p)^4$ against emissivity of the column of precipitable water vapour between the ground and height corresponding to pressure p. In practice, this would be an impossibly laborious process for our purposes, so that drastic cuts had to be made in the programme of work.

The procedure adopted was to draw curves on the Kew Radiation Chart representing the humidity-temperature profiles in an atmosphere having a lapse rate of 6.5°C/Km. for five different values of screen temperature over a range of about 273°K to 300°K. For each screen temperature two curves were drawn, one for a saturated atmosphere, and one for a relative humidity throughout of 50%; ten curves in all.

It was then found sufficiently accurate to draw any actual curve from a D.A.R. sounding using the arbitrary curves as guidance, and making allowance for conditions of inversion or steep lapse near the ground.

4.1.2. Cloud cover

The radiation chart can only take account of a completely clear sky, or a completely overcast sky if the height and temperature of the cloud base are known - the latter then being considered to radiate as a black body at cloud base temperature.

For intermediate cloud cover, we have adopted the following intuitive expression:-

$$\overline{R_L(c)\downarrow} = \overline{cR_L(1)\downarrow} + \overline{(1-c)R_L(0)\downarrow} \qquad (11)$$

/where

where c is the fraction of sky covered (the bracketed quantity after $R_L\downarrow$ represents cloud amount and not height for this short section only). Eq.11 is similar to, but less restricted than Ångström's expression, which, using the notation above, is

$$R_L(c) = (1 - 0.9c)R_L(0)$$

The constant 0.9 restricts the use of the expression to rather low cloud bases.

Neither expression is valid for instantaneous values of $R_L\downarrow$ or R_L, since c as measured by climatological stations is represented by an expression of the form

$$c = \frac{1}{2\pi}\int_{cloud} d\Omega$$

where $d\Omega$ is an element of the total solid angle of sky obscured by cloud. From the point of view of radiation, however, an expression of the form

$$c_r = \frac{1}{\pi}\int_{cloud} \cos\theta . d\Omega$$

is relevant, and it follows that R_L is strongly dependent on cloud distribution as can soon be seen on working out one or two arbitrary examples. Over a period of an hour or more, however, the effects of distribution would be expected to average out and become negligible, so that we assume that $\bar{c} = \overline{c_r}$, and eq.11 is probably as reasonable as can be expected. It has been found practically impossible to check eq.11 against actual records. Cloud amount observations given in the Daily Weather Report are instantaneous values tabulated every six hours, and these readings, coupled with a survey of the general weather conditions prevailing, form the only direct method of obtaining $\bar{c}$, and any comparison of the observed value of $\overline{R_L\downarrow}$ over this period with the value of $\overline{R_L\downarrow}$ obtained by substituting the relevant value of $\bar{c}$ in eq.11 will certainly not be any more reliable than the direct use of this equation.

Indirect estimates of $\bar{c}$ can be obtained from sunshine records and night sky camera records. For instance, the quantity $(1-\bar{c})$ will be roughly correlated to the ratio of actual to total possible hours of sunshine, but the correlation depends upon time of year, altitude of sun, and type of cloud to name but a few variables. A comparison of the quantity $(1-\bar{c})$ - which we shall call A - and actual/total possible number of hours of sunshine - which we shall call B - was made for the months June and December 1953, and the values of A/B were about $\frac{3}{4}$ and 1.6 respectively. The values of A/B for individual days showed a wild scatter over a range of as much as 3 to 1, and it appears that this method of estimating $\bar{c}$ is of not much use over periods less than a month.

Cloud amount estimation at night is more difficult and therefore less reliable; in any case, these observations are not made at Kew between 2100 and 0600, so that no comparison with night sky camera records is possible.

4.2. Summary of results and comparison with estimates

Table I summarises the monthly and annual means of the various quantities contributing to the heat balance, and Fig.1 (a) and (b) illustrates the annual variation of the more important terms. Table II summarises the readings of the surface thermometer, which are thought to have some climatological interest.

4.2.1. Surface temperatures (Table II)

The quantitative and qualitative variations of surface temperature on short grass throughout the year were much as expected in all types of

weather. In particular, the marked discontinuity of rate of temperature change about dusk under clear skies reported by several observers was never observed at Kew.

As expected, the monthly and annual mean temperatures are not appreciably different from the monthly and annual mean screen temperatures. The diurnal range is just about twice that of screen temperature all the year round. In summer, diurnal ranges of 30°C were not uncommon, and although the greatest range recorded was 31.2°C it is considered that ranges up to 40°C are quite possible - especially in periods of summer drought - and would be most likely to occur between about mid-May and mid-June. Extreme values for the year were 312°K and 261°K. Probable absolute extremes at Kew are 320°K (325°K over parched brown turf) and 255°K.

The mean times of occurrence of daily maxima and minima are substantially earlier than those of screen temperature: the maxima are about $2\frac{1}{2}$ hr. earlier in summer and 1 hr. in winter, while the minima are about $1\frac{1}{2}$ hr. earlier in summer and 2 hr. in winter.

4.2.2. Total radiation

The monthly value of $\overline{R(0)}$ varies from about -10 mw.cm^{-2} in midsummer to about +1 mw.cm^{-2} in midwinter, so that the ground becomes a heat sink by radiation from about mid-November to mid-February. (See Table I).

The annual mean of -4.0 mw.cm^{-2} is probably numerically a little below normal due mainly to rather poor summer weather when increased cloudiness has the greatest effect on incoming solar radiation.

Extreme values of R(0) numerically exceeding -80 mw.cm^{-2} occurred during June and July, and a peak value of -91 mw.cm^{-2} was recorded soon after midday on 20th June. From eq.5, we find that $R_S\downarrow$ simultaneously reached an extreme value of -135 mw.cm^{-2}, which compares with the Solar Constant (-138 mw.cm^{-2}). This was a day of brilliant sunshine, with large Cu and Cb typical of a polar maritime air mass in summer. This record has been reproduced in the series of charts included as specimens later in this paper.

Considering the probable error of R(0) we see from eq.5 that the main uncertainty arises from errors in $R_L\downarrow$. While it may be as large as ±2 mw.cm^{-2} if estimated for a few hours, it is thought that it is not likely to exceed ±0.5 mw.cm^{-2} over a month, and we feel fairly safe in quoting the mean for the year with this error. It is noted that there will be an error of estimation for the unrecorded half of $\overline{R(0)}$ - and therefore of $\overline{R_L\downarrow}$ - and instrumental errors for the recorded half which are not likely to be substantially less than the first type. Furthermore, the value of $\overline{R_L\downarrow}$ over a month is found to lie for most of the time within a range of 5 mw.cm^{-2}, which automatically sets limits to the magnitude of possible errors.

4.2.3. Long-wave radiation

The mean value of $\overline{R_L}$ for the year was 3.8 mw.cm^{-2}. This is substantially less than one is led to expect from estimates based on empirical and scanty observational data found scattered in the literature. The discrepancy may be partly due to the presence of thin layers of tenuous high cloud which is now known to be present in much greater quantity than was thought until recently; it may also be due to the imperfections inherent in the construction of radiation charts. Robinson (1947) found that there was nearly always an additional downward component of long-wave radiation when observations were compared with estimates given by radiation charts. There were about half-a-dozen occasions when good agreement was obtained - occasions of "minimum radiation" as called by Robinson - which suggests that these were rare occasions when the sky was exceptionally clear and free from high cloud.

/The

The presence of this cloud was borne in mind when estimating $\overline{R_L\downarrow}$ as described earlier, and it was noticed that a good indication of its presence was given by the difference between screen and ground temperatures. On a clear night, this can reach 5°C (and more over snow), but was more often 2-3°C. On a hot day in June, the difference is usually around 10°C, but may reach 15°C.

R_L can vary from zero, or even slightly negative (-0.2 mw.cm^{-2}) to about +10 mw.cm^{-2} on clear nights before the development of a large inversion near the ground, and to upwards of +15 mw.cm^{-2} on very hot days - especially in May and June.

$R_L\downarrow$ averaged about -33 mw.cm^{-2} over the year, and ranged between extreme values of -41 mw.cm^{-2} during the heat-wave of the first week in August to -21.5 mw.cm^{-2} during the very severe spell of easterly winds early in 1954.

4.2.4. Earth flux plate

The numerical magnitudes of the fluxes involved here are an order of magnitude less than those associated with R(0). The monthly values of $\overline{G(-6)}$ varied from about -0.6 mw.cm^{-2} in May to about +0.6 mw.cm^{-2} in January. Normally, one expects the phase of the curve of ground heat flow to lead that of air temperature by about 90°, but the extreme of heat flow occurring in January - about 2 months late - is due to the exceptional mildness of November and December 1953.

$\overline{G(-6)}$ over the year was expected to be practically zero. In fact, it came to +0.05 mw.cm^{-2} which corresponds to a total heat loss by the ground below 6 cm. of 350 cal.cm^{-2}yr^{-1}. Now the temperatures at depths of 1 ft. and 4 ft. increased between May 1953 and May 1954 by 0.4°C and 0.3°C respectively, which corresponds to a flux of the order -50 cal.cm^{-2}yr^{-1}. These figures are to be compared with a total change of heat content of the ground of the order 2000 cal.cm^{-2} between winter and summer. These results made the reliability of the flux plate records suspect, and when the flux plate was unearthed in July 1954, it was found to have sunk 2 cm. and to have acquired a tilt of about 15° to the horizontal. The discrepancy may however be a measure of the extent to which heat is transferred through the 6 cm. level by processes involving the evaporation and condensation of water within the soil, though this suggestion implies the downward movement of water vapour. Rough calculation shows that it is much too large to be explained by mass movement of liquid water. While little significance can be attached to the annual mean, this is in any case very small compared to the other fluxes considered, and the discrepancy does not invalidate the records as a means of estimating $\overline{G(-6)}$ over shorter periods. Values of G(-6) are not likely to be in error anywhere by more than 20%.

As expected, there is a high correlation between the diurnal range of temperature at the ground and heat flux at -6 cm. (0.89 for May 1953) but with an annual variation in their ratio. This ratio decreased from 0.29 mw.cm^{-2}/°C in May 1953 to about 0.18 in January 1954, and had risen again to 0.25 by April 1954. Heat conduction in the soil is dependent on thermal diffusivity $k_s/\rho c$. The thermal capacity, ρc, is 2 to 3 times greater in winter than in summer due to much greater average moisture content, so that changes in heat flow in the soil will respond less to changes in surface temperature, whereas there is an increase in k_s in winter which partly offsets this effect, and the net result is an increase in the above-mentioned ratio of about 1.6 to 1 from winter to summer, with maxima and minima in May and November.

4.2.5. Heat balance

We refer back to eq.8,

$$-\left[\overline{R(0)} - \overline{G(-6)}\right] = \overline{C(0)} + \lambda\,\overline{E(0)}$$

/The

The work of Penman (1950) and others on evaporation estimation enables us to obtain a fairly reliable estimate of monthly means of $\overline{\lambda E(0)}$ using the available records at Kew.

Penman derives an expression for the rate of evaporation, E_o, from an open water surface in terms of net radiation, mean vapour pressure, temperature, and wind speed at 2 m. He converts the energy terms to evaporation equivalents ($1 \text{ mw.cm}^{-2} \text{ day} \equiv 0.35 \text{ mm.day}^{-1}$) and the final value of E_o is multiplied by an empirical factor f to allow for the surface under consideration. For short, moist turf, he finds that f varies from about 0.6 in winter to 0.8 in summer.

Since records of R(0) are available, the monthly values were substituted straight into Penman's expression, and the final value of E_o compared with the measured value given by the Kew evaporation tank. Finally, values of fE_o - i.e. $\overline{\lambda E(0)}$ - were tabulated (both the measured and calculated values), and monthly values of $\overline{C(0)}$ thus obtained. (See Table I). It was found that the Kew evaporimeter read lower in summer and higher in winter than the estimates. The value of $\overline{\lambda E(0)}$ for the year was $+4.2 \text{ mw.cm}^{-2}$ from Penman's formula and $+3.6 \text{ mw.cm}^{-2}$ from the tank record. The rainfall for the period (P) was 513 mm., the corresponding rate of supply of energy $(\overline{\lambda P})$ being roughly 4.0 mw.cm^{-2}. Since it is difficult to visualize a year with a negative run-off of rainfall, the tank figure (when corrected by the factor f) is almost certainly the more reliable. Even then, a run-off amounting to only 10% of the rainfall seems too small. The year 1953 was notably dry, and it might be expected that there must have been periods when the turf was affected by drought, and hence modification of the factor f necessary. However, most of the deficit occurred in the winter months, and at no time did the grass appear other than bright green.

This method of estimation only gives us monthly means of $\overline{C(0)}$ which show a small annual variation with an amplitude and an annual mean of the same order of magnitude as the probable error.

4.3. Specimens of photographic records

These are reproduced in chronological order at the end of this paper. We confine ourselves to brief comments on each of them here.

a. 4 June 1953

A day of brilliant sunshine, cold NNE winds and large cumulus typical of a polar maritime air mass in early summer. The air is very dry - relative humidity less than 50% - and fluctuations of surface temperature are enormous - approaching 20°C.

b. 9 June 1953

A rare example of a perfect summer day. The sky was perfectly clear for at least 24 hours apart from small, scattered cumulus in the afternoon. The temperature was not too high - max. 69°F (294°K) at Kew. The synoptic charts show that S. and E. districts of England were situated in a col on this day.

c. 20 June 1953

It is interesting to compare the trace of R(0) with that in chart b. In 20 June, large white cumulus enormously increase the diffuse component of solar radiation reaching the VFR, and, in sunny intervals, give a resultant R(0) at times not far short of twice that recorded on a perfectly clear day at the same time of year.

d. 16-17 November 1953

The main feature of interest here is the sudden arrival of fog at about 0110 on the 17th. When fog forms in situ, the net flux of radiation (at night)

/gradually

gradually approaches zero over a period of 2 or 3 hours. Here, the fog has already formed, and is drifting about. An occlusion from a deep depression was lying almost stationary ENE-WSW across N. England, with widespread fog developing in S. districts.

e. 29-30 November 1953

This shows the effect of the arrival of a warm sector on earth flux at a depth of 6 cm., and the levelling out of T(0) as the sky clouds over.

f. 27-28 January 1954

A day during, and typical of, the severe easterly spell persisting at this time.

Surface temperature rose just above 273°K for about an hour in the early afternoon, and dropped to about 263°K at night. The day was mainly cloudy - $\frac{5}{8}$ to $\frac{7}{8}$ of Sc - decreasing to small amounts at night. The top layer of soil is already frozen, but not yet to the depth of the flux plate. Note how the fluctuations of G(-6) have been ironed out. This is the subject of a short note later in this paper.

g. 7 February 1954

Note the effect on G(-6) of the commencement of the thaw.

h. 15 February 1954

An example of an exceptionally dull, murky day, with very heavy cloud and intermittent drizzle. At this time, Kew was in the vicinity of a slow moving occlusion marking the boundary of the cold continental air experienced recently. On this occasion, it did not reach us.

j. 31 March 1954

This short record indicates what happens to the record of R(0) when rain does get on the top surface of the radiometer plate. This was a day of heavy showers and bright intervals. Rapid evaporation of rain from the top surface of the VFR by its blower causes the wet bulb effect shown. This shower was the first of several, culminating in a thunderstorm about 1700.

4.4. The effect of freezing in the soil upon G(-6)

When the moisture in the soil begins to freeze, the temperature of the layer in process of freezing at any given time will be locked at 0°C for some time while its latent heat is being conducted away through the already frozen layer above. The presence of this freezing layer has the effect of stabilising the temperature profile beneath it, i.e., fluctuations in T(0) have no effect on the temperature gradient below the freezing level, and hence upon the heat flow. The latter does decrease very slowly as heat is drained from the lower layers, and the gradient slackens somewhat. For instance, at Kew during the last week of January, the temperature at 6 cm. remained very near 0°C all the time, while the temperature decreased from about 4°C to 3°C at 1 ft., causing G(-6) to decrease in proportion.

When the freezing level reaches and passes below the level of the flux plate, G(-6) resumes its normal variations in sympathy with T(0) until the thaw sets in. When this occurs, the temperature of the whole of the frozen layer rises to melting point, and remains there for a day or two, during which time the flux plate (being enclosed in an isothermal layer) records zero net flux of heat.

/All

All this sequence of events in fact occurred between 24th January and 7th February 1954. Freezing commenced on the 24th, and after just thawing out under the midday sun on the 25th, continued until the 6th February. Freezing reached the flux plate depth after a week, and eventually extended to about 10 cm. depth.

4.5. Conclusion

The emphasis of this paper has been on the presentation of results of measurements of some meteorological elements not hitherto recorded continuously over a comparable period of time, and preliminary interpretation has shown the results to be, in the mean, much as expected.

The only previous work of this nature that we could find is due to Falckenberg and Bolz (1950), who made $\frac{1}{2}$ to 1 hourly measurements of $R_L\downarrow$ and $R_S\downarrow$ - the latter being the sum of the direct and diffuse components of solar radiation as measured by them - over the period 1.4.1947 to 31.3.1948 using a vibration pyranometer, which employs the same principle as the VFR. These measurements were made in Lat. 54°11'N., Long. 12°5'E., and they obtained a value for $R_L\downarrow$ for the year of -32 mw.cm^{-2}. Their results were expressed as mean values every ten days, and these ranged from -26 to -38 mw.cm^{-2} for $R_L\downarrow$ during the year.

The main use of records of total radiation has been so far simply to provide direct measurements of a major term in the heat balance equation for the surface. If these records are to be used to interpret more transient phenomena in the atmosphere - and especially near the surface - they need to be supplemented by continuous records of many more elements than surface temperature and earth flux. Furthermore, it seems that little further information about radiative processes in the atmosphere can be obtained by measurements of total fluxes of atmospheric radiation near the surface unless these are supplemented by spectral analysis of the long-wave radiation.

Acknowledgments

I should like to express my indebtedness to Dr. G. D. Robinson and Mr. M. J. Blackwell for many useful discussions and help during this work, and to Mr. J. Gordon and Mr. A.J. Lander who installed the apparatus on site and made the initial measurements.

REFERENCES

Deacon, E.L.	1950	Q.J.R. Met. Soc., 76, 479.
Falckenberg, G. and Bolz, H.M.	1950	Zeit. Met. 4, 65.
Hatfield, H.S. and Wilkins, F.J.	1950	J. Sci. Inst., 27, 1.
Gier, J.T. et al.	1949	University of California, Thermal Radiation Project Report.
MacDowall, J.	1954	Meteorological Research Papers, Air Ministry, London, No. 858.
Mörikofer, W.	1951	Proc. of U.G.G.I., Brussels, Compte rendu du Symposium sur le Rayonnement, 207.
Penman, H.L.	1950	Q.J.R. Met. Soc., 76, 372.
Robinson, G.D.	1947 1950	Ibid., 73, 127. Ibid., 76, 479.
Goody, R.M. Robinson, G.D.	1951	Ibid., 77, 151.
Rider, N.E. Robinson, G.D.	1951	Ibid., 77, 375.

APPENDIX I

Calibration of instruments

1. Surface temperature

It is probably sufficiently accurate to use tables of thermo-emfs for copper-constantan junctions in order to convert the galvanometer deflections into temperatures, but the calibration was checked by a conventional method.

2. Earth flux plate

The method used at Kew was that advocated by Hatfield and Wilkins (1950), and need not be discussed here.

3. Ventilated flux radiometer

Four methods of calibration - two in the laboratory and two on site - have been described by MacDowall (1954).

Briefly, these were:-

(i) Comparison of outputs of VFR and Ångström pyrheliometer using a voltage-controlled 2 Kw. tungsten lamp.

(ii) Exposure of one side of radiometer plate to a black body source through an aperture of known size.

(iii) Comparison of direct reading of R(0) on site with value of R(0) obtained by measuring $R_S\uparrow$ and $R_S\downarrow$ with solarimeters, and $R_L\uparrow$ and $R_L\downarrow$ with the surface thermometer and Linke-Feussner radiometer.

(iv) Direct side-by-side comparison on site of outputs of a laboratory calibrated VFR and the VFR on site.

The continuously recording radiometers on site could not be calibrated in the laboratory directly because the ventilation supply was a permanent fixture on site, and could not be transferred to the laboratory.

It was found that (i) provided the most manageable and reliable method of calibration, so that we shall discuss it in some more detail with emphasis on precautions and possible sources of error.

3.1. Short-wave calibration of VFR

Comparison is made between outputs of the Ångström pyrheliometer or the calibrated Linke-Feussner radiometer - which are directional radiometers, their solid angle of acceptance being of the order 0.05 steradians - and the VFR, which receives radiation from a hemisphere on each side and records the difference.

Hence the main problem is to account for all stray sources of long-and short-wave radiation not "seen" by the directional instruments, but which contribute to the output of the VFR.

3.1.1. Extraneous sources of short-wave radiation

These include light from unmasked windows, other lights in the laboratory, reflections from walls of light from the tungsten lamp escaping round the sides of the VFR.

In practice, the laboratory is blacked out for this calibration, but enough light to see what one is doing with comfort is permissible. It must be

/remembered

remembered that the human eye's response to light is logarithmic, whereas the radiometer response is linear, and it requires a surprising amount of light to affect the readings by as much as 1%. For example, imagine replacing the 2 Kw. lamp by a 20 watt bulb.

3.1.2. Extraneous sources of long-wave radiation

These are far more troublesome. They are:-

(i) Emission from heated lamp housing. This is remedied by the interposition of a sheet of glass which is opaque to wavelengths beyond about 3μ. The placing of a second sheet behind the radiometer thus completes a fairly effective shield to all long-wave radiation.

(ii) The heat given out by the tungsten lamp is dissipated with the help of a blower with the result that a vigorous column of hot air rises to the ceiling where it spreads out and steadily warms the ceiling, providing a steadily increasing source of long-wave radiation of which an appreciable part can pass over the top of glass sheets direct to the radiometer plates. During normal calibrations, the angle of incidence of this radiation is not less than 60°, and the effect is small, but becomes very appreciable when cosine law tests are made by rotating the radiometer about a horizontal axis, and may amount to 15% of the total flux if a third glass sheet is not placed above the VFR.

(iii) The sheet of glass between the radiometer and source will be absorbing much more long-wave radiation than the sheet behind the radiometer, and will heat up after a few minutes' exposure to a hot lamp, thus causing a steady drift output from the radiometer, and since these sheets occupy 0.8 to 0.9 of the radiometer's field of view, a temperature difference of 1°K between the sheets is sufficient to cause a drift of some 5% in output. Hence careful and frequent zeroing by screening the lamp is necessary. In practice, it was found necessary to zero before and after each reading.

The only criticism of this method as a complete one is that we employ a short-wave source in the calibration of an instrument that is primarily intended to measure both short- and long-wave radiation. We use, as our basis for justification, the results of the N.P.L. tests on the absorptivity of the paint used to coat the radiometer surfaces. They found this to vary by less than 1% from 0.98 for radiation from black-body sources ranging from 2850°K to 470°K.

We conclude that providing the comparison sub-standard radiometer is well calibrated, it should be possible to rely on a VFR calibration to $\pm$1%; certainly within $\pm$2%.

3.2. Performance and applications of the VFR

It has already been noted that the radiometer is well suited to field work. It works much better and more reliably than is usually expected at first sight. It is robust, easily made portable, and is simple and inexpensive to build. It should give instantaneous values of R under most conditions to $\pm$ 5%, providing it is calibrated carefully and reasonably often, and repainted when the surfaces show signs of marked deterioration.

As a result of weathering tests made in April 1954, it was decided that the radiometer can be left exposed at all times, provided allowance be made for the decrease of absorptivity which becomes more important in the visible wavelengths - especially at large angles of incidence. This is most important for direct radiation coming from a low sun.

Rain has little harmful effect, and, in fact, serves to wash the top surface free of the grey dust deposit which otherwise appears to form -

/probably

probably due to inadequate filtering of the blast of air. Unfortunately, if one attempts to introduce finer filters, the speed of the air blast is inevitably reduced.

In routine use, it is recommended that the radiometer be reversed to ensure washing of both sides, or better, that the under surface be sprayed with water when it appears necessary.

3.2.1. Corrections to records of R(0) for prevailing wind-speed.

The effect on the calibration constant of the VFR of wind of various speeds and directions relative to the orientation of the VFR on site was investigated thoroughly by MacDowall (1954), who found that for wind-speeds less than about 20 mph the change in calibration never amounted to more than ±2% for any wind direction. At the level of the radiometer on site, the wind-speed rarely reached this value, and the mean wind-speed at this level at Kew is probably of the order 2-3 mph throughout the year. The correction for this speed is quite negligible, and no attempt has been made to correct the monthly values of R(0) for wind-speed.

APPENDIX II

A standard source of long-wave radiation

It is proposed to discuss the setting up of a black body cavity radiator as the ultimate standard of long-wave radiation at Kew, concluding with a brief reference to the long-wave calibration of the Linke-Feussner radiometer against the black body. This sets up the Linke-Feussner radiometer as a substandard for calibration of other types of radiometer, or for directional observations of atmospheric radiation.

One of the main reasons for including this section in this paper is because there seems a tendency among workers in this field to refer to calibration of their radiometers against black bodies with little or no mention of the precautions and corrections necessary in such measurements beyond the usual statement that the radiation emerging from the cavity is black-body emission to better than 99% at the temperature of the black body with no mention of how this temperature is measured.

The black body cavity radiator in use at Kew until recently was constructed by Dines in 1920, and had the following main disadvantages:-

(i) Inadequate stirring of water in jacket

(ii) No internal source of heating in water jacket

(iii) No temperature control

(iv) No provision for measuring temperature differences between the cavity walls and the water jacket

(v) Inadequate lagging - partly a function of age

(vi) No convenient form of mounting.

A new black body cavity radiator was designed and built at Kew this year in which these disadvantages have been eliminated as follows:-

(i) Efficient stirring is achieved by a pump which draws water from the bottom of the water jacket into two vertical channels which throw the water out at the top. The rate of pumping is of the order of 30 litres min^{-1}, so that the entire volume of water is pumped through in less than a minute. Circulation of the water is promoted by the shape of the cavity, which is an upright cone instead of the inverted cone used in the Dines' black body (see Fig. 2).

(ii) Internal heating is achieved with a 2 Kw. immersion heater which heats the water from 10° to 50°C in about 30 minutes.

(iii) Temperature control at any desired temperature is obtained by passing enough current through the heater to balance the small loss of heat by cooling. This amounts to about 30 watts for a temperature difference of about 30°C between room and water jacket.

Temperature is read by an N.P.L. calibrated thermometer, and it is possible to keep this constant at any desired value, with supervision, to within ±0.01°C over any desired period; this is scarcely possible by any other method.

The rate of supply of heat caused by the viscous dissipation of the kinetic energy imparted to the water by the pump appears to be of the order of 10 watts, which decreases as the temperature increases. The pump motor is rated at 80 watts.

(iv) For accurate work, it is necessary to know the temperature field within the cavity, and the difference between the temperatures of the water and the

/cavity

cavity walls. This has been achieved by installing suitably placed thermo-junctions in the cavity; they can be compared in turn with a reference thermojunction placed adjacent to the thermometer bulb in the water jacket. A floating junction is also provided as a probe; it can also be immersed in a Dewar flask of ice if it is desired to cross-check temperature readings of the reference junction with the thermometer.

(v) The jacket is surrounded by a thick layer of felt and cotton wool, and the whole contained in a wooden box. The efficiency of the lagging is nearly an order of magnitude better than the Dines' black body.

(vi) The black body is mounted with its cavity looking vertically downwards, but with enough space to insert the Linke-Feussner radiometer below looking vertically up into it.

Cardboard masks are provided to limit the aperture of the black body if desired, and an outlet is provided for the water in the jacket in case it is desired to drop the temperature quickly by replacing some of the hot water by cold.

With careful work, it should be possible to obtain the radiation temperature of the cavity walls reliable to within $\pm 0.05°C$ - i.e. σT^4 to about ± 0.03 mw.cm^{-2}, which is about 1 part in 1000. However, σ itself is not known to this degree of accuracy.

Disadvantages of the new black body

(i) Excessive weight - well over 1 cwt. when water jacket is full. This does not matter unless it becomes inconvenient to have the black body in one position permanently.

(ii) Rather small temperature range - room temperature up to 50°C, although it could be adapted to work up to 100°C.

(iii) No cooling system. Since radiometers looking at the sky are generally losing energy to it, it would be useful if a cold black body were available.

(iv) The water jacket does not extend down to level of aperture, which requires that the temperature field within the aperture be measured carefully.

Calibration of the Linke-Feussner radiometer

This has been described by Robinson (1947), but the following remarks refer to precautions taken and corrections made in a recent calibration.

The Linke-Feussner thermometer - which measures the temperature of the thermopile - was calibrated against an N.P.L. calibrated thermometer in a stirred water bath. Correction was made for stem exposure of the latter; the former was completely immersed as its stem and bulb are practically at a uniform temperature in use.

The output of the Linke-Feussner is of the order 10 μV for a temperature difference of about 20°K between the black body and the thermopile of the Linke-Feussner, so that stray thermo-emfs can be a source of trouble if not accounted for by suitably placed copper reversing switches in the output circuit.

Measurement of the temperature profile between the Linke-Feussner thermopile and the cavity walls was made, and the humidity measured with an Assmann psychrometer, and the correction for absorption of radiation by water vapour and CO_2 computed by constructing a radiation chart. The final calibration obtained was estimated to be reliable to about $\pm$ 1%.

Table I

Summary of Results

MONTH	$\overline{R(0)}$	$\overline{R_s(0)}$	$\overline{R_L(0)}$	$\sigma\overline{T(0)^4}$	$\overline{R_L(0)}\downarrow$	$\overline{G(-6)}$	$-\overline{(R-G)}$	$\lambda\overline{E(0)}$ calc.	$\lambda\overline{E(0)}$ Kew Tank	P	$\lambda\overline{P}$	$\overline{C(0)}$ calc.	$\overline{C(0)}$ Tank	$\overline{h}$
1953														
MAY	-8.6	-14.4	+5.8	+39.2	-33.4	-0.6	+8.0	+8.6	+7.1	39.5	3.7	-0.6	+0.9	11.7
JUN.	-8.4	-12.9	+4.5	+39.9	-35.4	-0.4	+8.0	+7.9	+6.6	46.6	4.4	+0.1	+1.4	11.9
JUL.	-9.6	-14.1	+4.5	+40.4	-35.9	-0.1	+9.5	+9.2	+6.8	91.8	8.6	+0.3	+2.7	8.8
AUG.	-9.0	-13.0	+4.0	+40.8	-36.8	-0.2	+8.8	+8.3	+7.0	43.9	4.1	+0.5	+1.8	14.6
SEP.	-5.5	-9.7	+4.2	+38.7	-34.5	+0.2	+5.7	+5.0	+4.3	50.9	4.8	+0.7	+1.4	13.3
OCT.	-1.6	-4.2	+2.6	+36.7	-34.1	+0.4	+2.0	+1.6	+1.6	58.2	5.5	+0.4	+0.4	12.5
NOV.	+0.2	-2.1	+2.3	+35.7	-33.4	+0.3	+0.2	+0.6	+0.8	37.6	3.5	-0.4	-0.6	12.1
DEC.	+0.7	-1.2	+1.9	+34.8	-32.9	+0.4	-0.3	+0.2	+0.7	12.8	1.2	-0.5	-1.0	10.1
1954														
JAN.	+1.3	-2.0	+3.3	+32.6	-29.3	+0.6	-0.7	+0.8	+0.7	23.4	2.2	-1.5	-1.4	12.3
FEB.	-0.3	-3.0	+2.7	+33.0	-30.3	+0.2	+0.5	+1.2	+1.3	49.6	4.7	-0.7	-0.8	7.9
MAR.	-2.5	-5.7	+3.2	+34.9	-31.7	0.0	+2.5	+2.4	+1.8	49.0	4.6	+0.1	+0.7	11.4
APR.	-4.9	-10.7	+5.8	+35.8	-30.0	-0.1	+4.8	+4.4	+4.2	9.7	0.9	+0.4	+0.6	20.0
YEAR	-4.0	-7.8	+3.8	+36.9	-33.2	+0.05	+4.1	+4.2	+3.6	513.0	4.0	-0.1	+0.5	12.2
P.E. ±	0.5	0.2	0.5	0.2	0.5	0.1	0.5	0.3	-	-	-	1.0	1.0	-

All units are in mw.cm^{-2} except for h which represents the mean number of hours per day that the radiometer was recording, and P, which denotes monthly rainfall in mm. $\lambda\overline{P}$ is the evaporation equivalent.

+ denotes flux or net flux directed upwards.
− " " " " " " " downwards.

G.27181/PC/9/55/50

Table II

Surface Temperature: degrees Kelvin

MONTH 1953	Mean Max.	Mean Min.	Abs. Max.	Abs. Min.	Mean Diurnal Range	Abs. Range	Lowest Max.	Highest Min.	Max. Diurnal Range	Min. Diurnal Range	Time of Diurnal Max.	Time of Diurnal Min.
MAY	299.2	279.7	311.2	271.7	19.5	39.5	283.5	287.8	30.2	3.7	1251	0229
JUN.	301.5	282.0	309.2	276.3	19.5	32.9	288.0	288.9	27.1	7.4	1247	0217
JUL.	302.5	283.2	311.7	279.8	19.3	31.9	292.9	288.3	31.2	7.5	1308	0228
AUG.	303.5	282.9	310.5	277.3	20.6	33.2	292.8	289.9	29.9	4.5	1237	0242
SEP.	299.0	279.7	305.7	274.6	19.3	31.1	291.9	286.1	29.3	7.7	1231	0249
OCT.	291.3	278.3	301.9	271.9	13.0	30.0	284.3	286.4	25.5	1.6	1242	0123
NOV.	285.5	277.7	(290)	270.7	7.8	(19.3)	281.2	285.9	15.5	0.9	1207	0117
DEC.	283.1	276.3	289.3	269.6	6.8	19.7	278.8	282.7	14.6	1.6	1300	0201
1954												
JAN.	280.0	272.1	288.3	263.6	7.9	24.7	271.8	283.8	17.0	0.3	1259	0230
FEB.	282.4	271.4	290.8	261.2	11.0	29.6	275.4	281.1	20.3	1.9	1300	0004
MAR.	289.2	274.7	299.5	(263)	14.5	(36)	274.1	281.1	26.2	1.2	1308	0141
APR.	293.4	273.6	298.9	268.5	19.8	30.4	286.6	282.6	28.5	6.2	1240	0311
YEAR	292.6	277.6	-	-	14.9	-	-	-	-	-	1248	0204

The figures for YEAR are all annual means. Bracketed figures are estimated; this had to be done occasionally when the record was defective for some reason.

BLACK BODY CAVITY RADIATOR

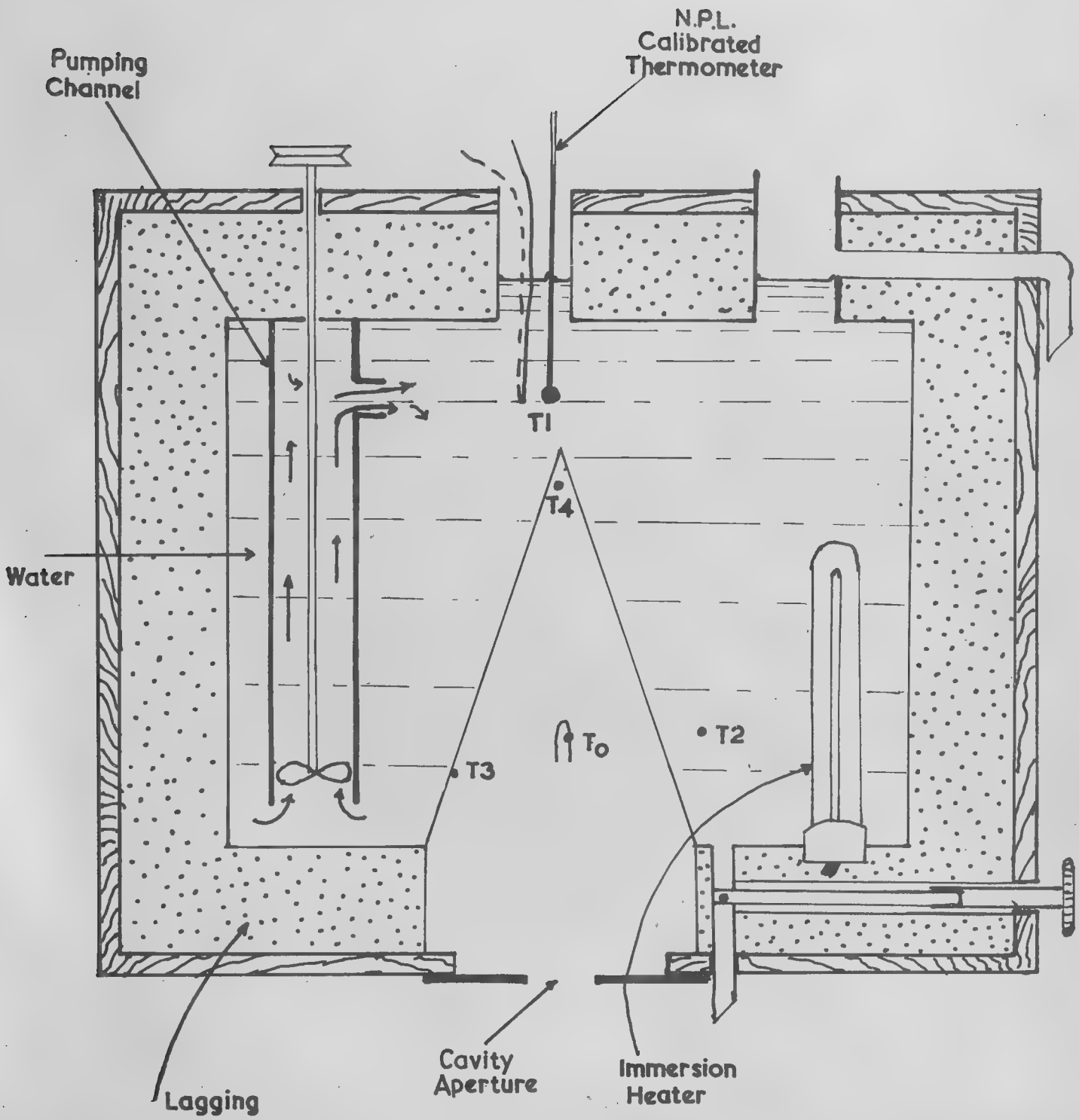

T 1,2,3,4 denote the approximate positions of fixed thermojunctions

To is a movable junction for probing the temperature field within the cavity

N.B. For a diagram of the Dines' Black Body, see MacDowall (1954).

FIG. 1A

M.R.P. 936

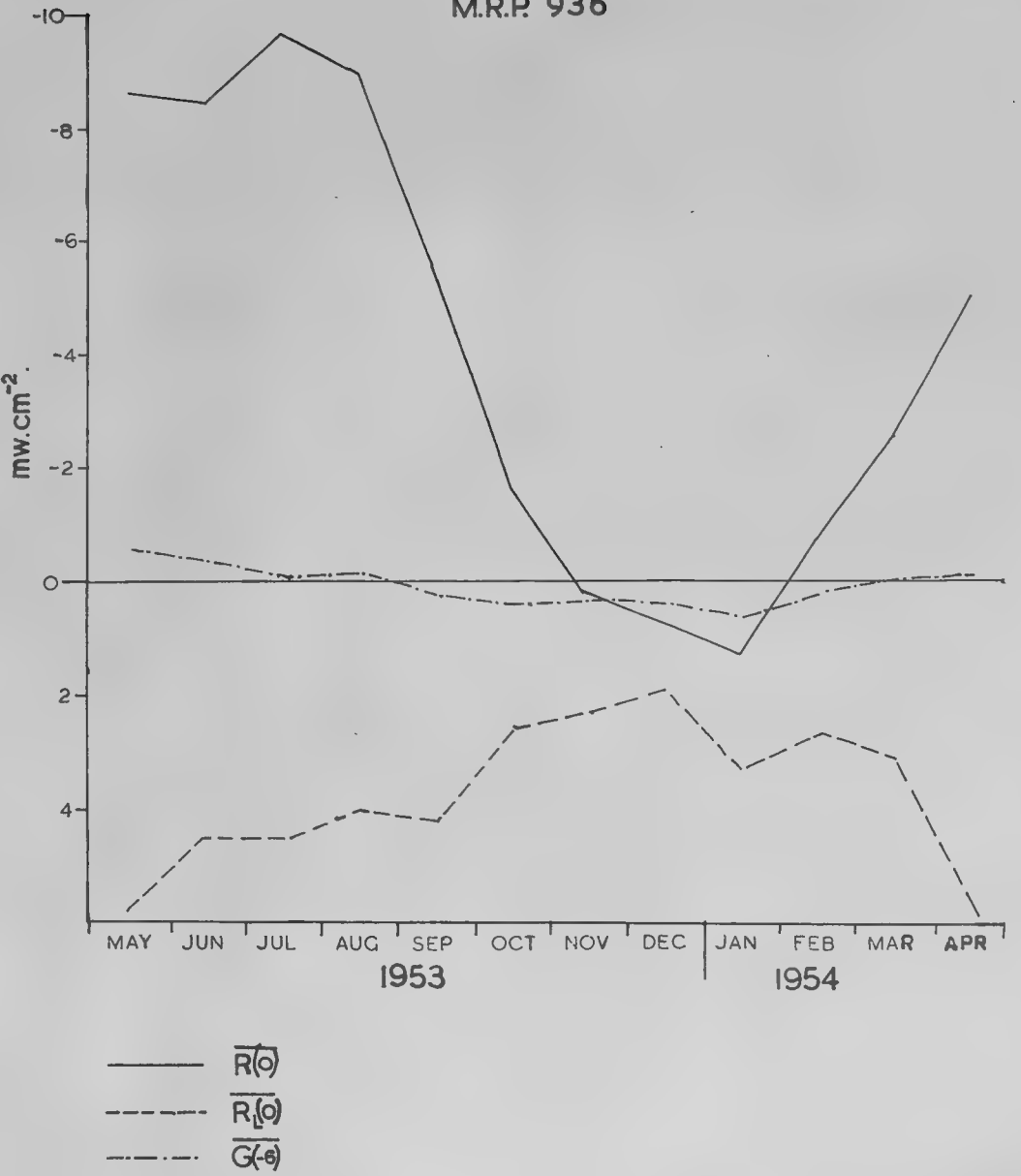

MONTHLY MEANS

FIG. 1B

MONTHLY MEANS

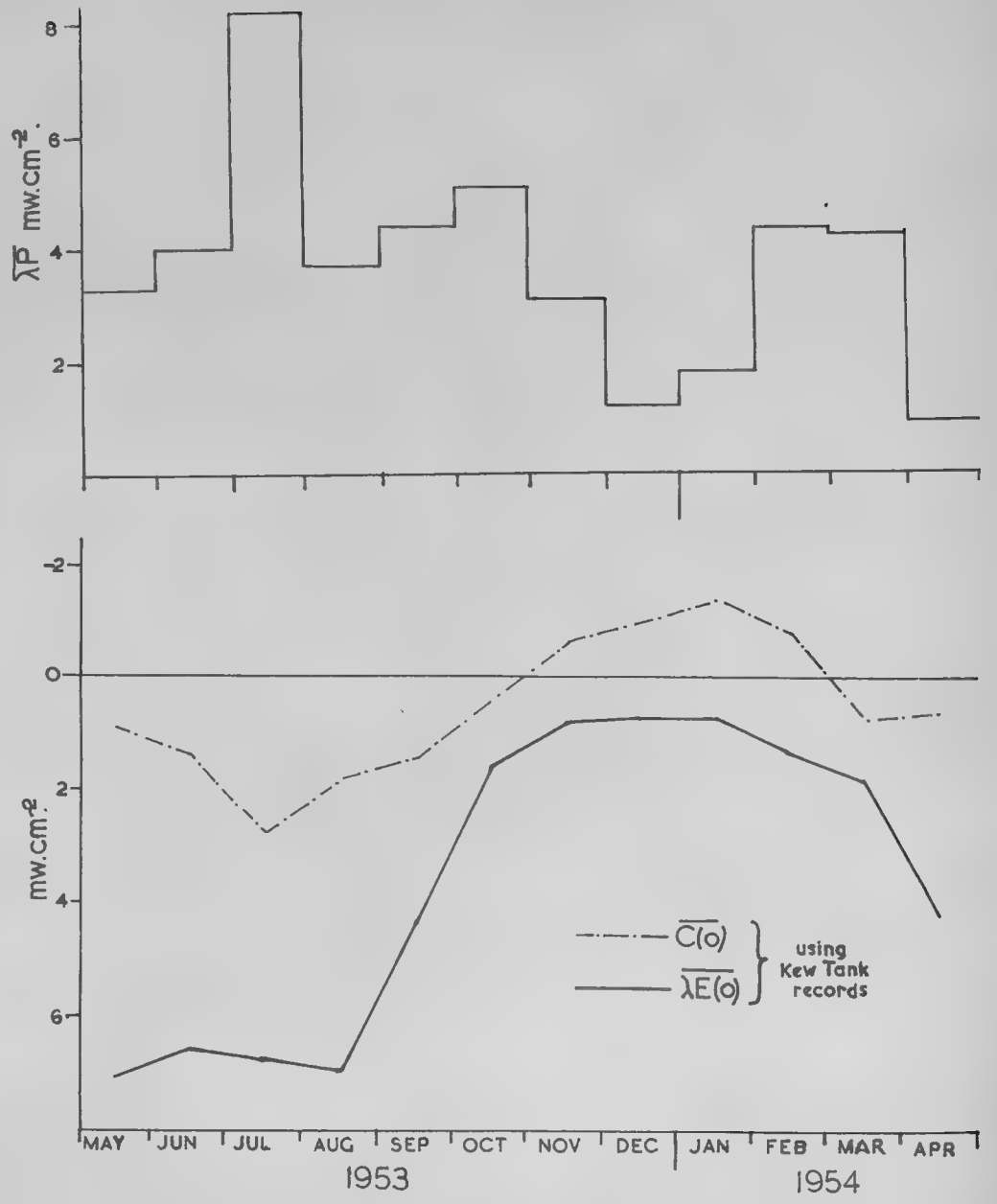

M.R.P. 936

Chart a

4 June 1953

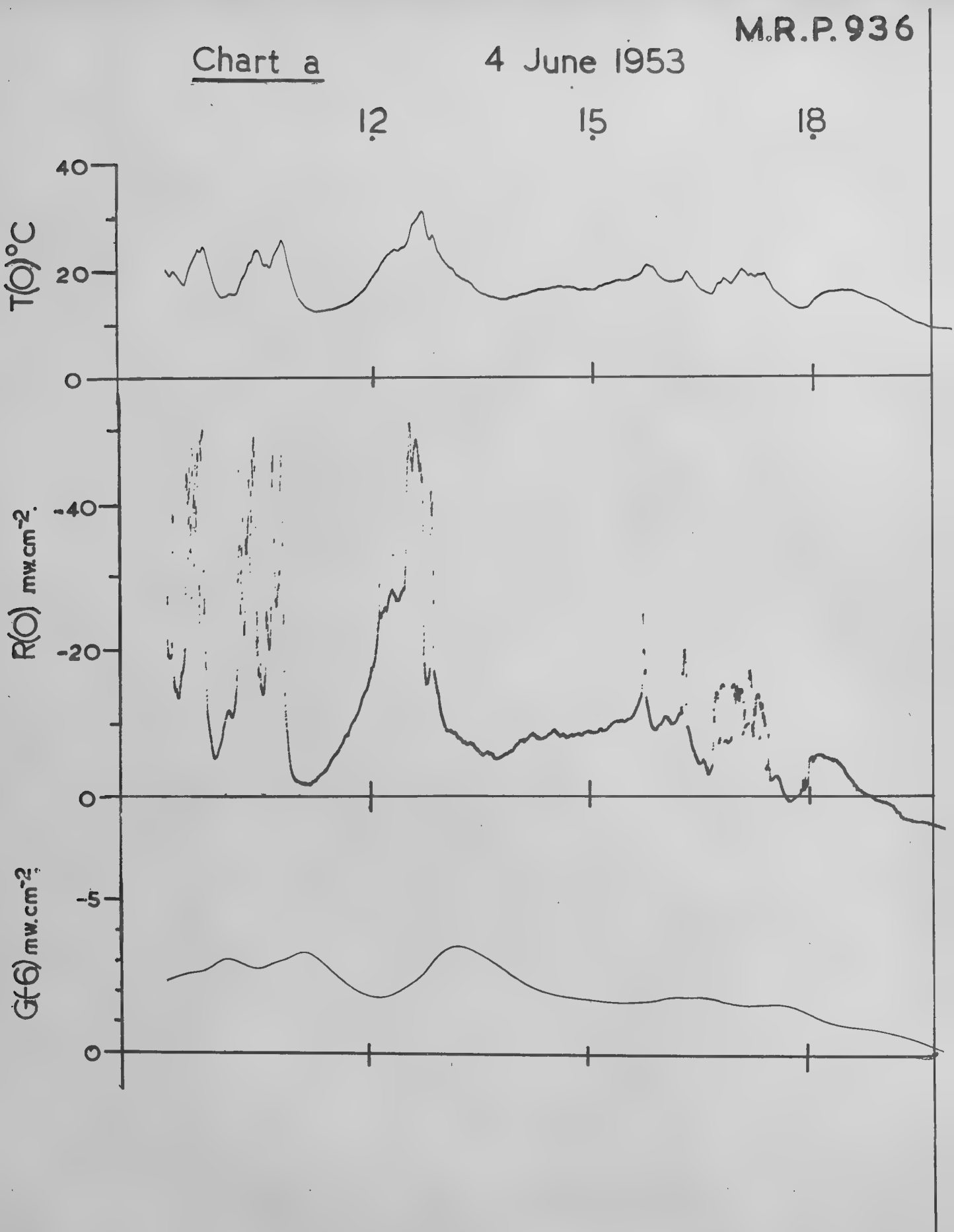

M.R.P. 936

Chart b

9 June 1953

10 June 1953

12 15 18 21 24 3 6 9

T(0)°C

40
20
0

R(0) mw.cm.$^{-2}$

40
20
0

G(-6) mw.cm.$^{-2}$

5
0
+2

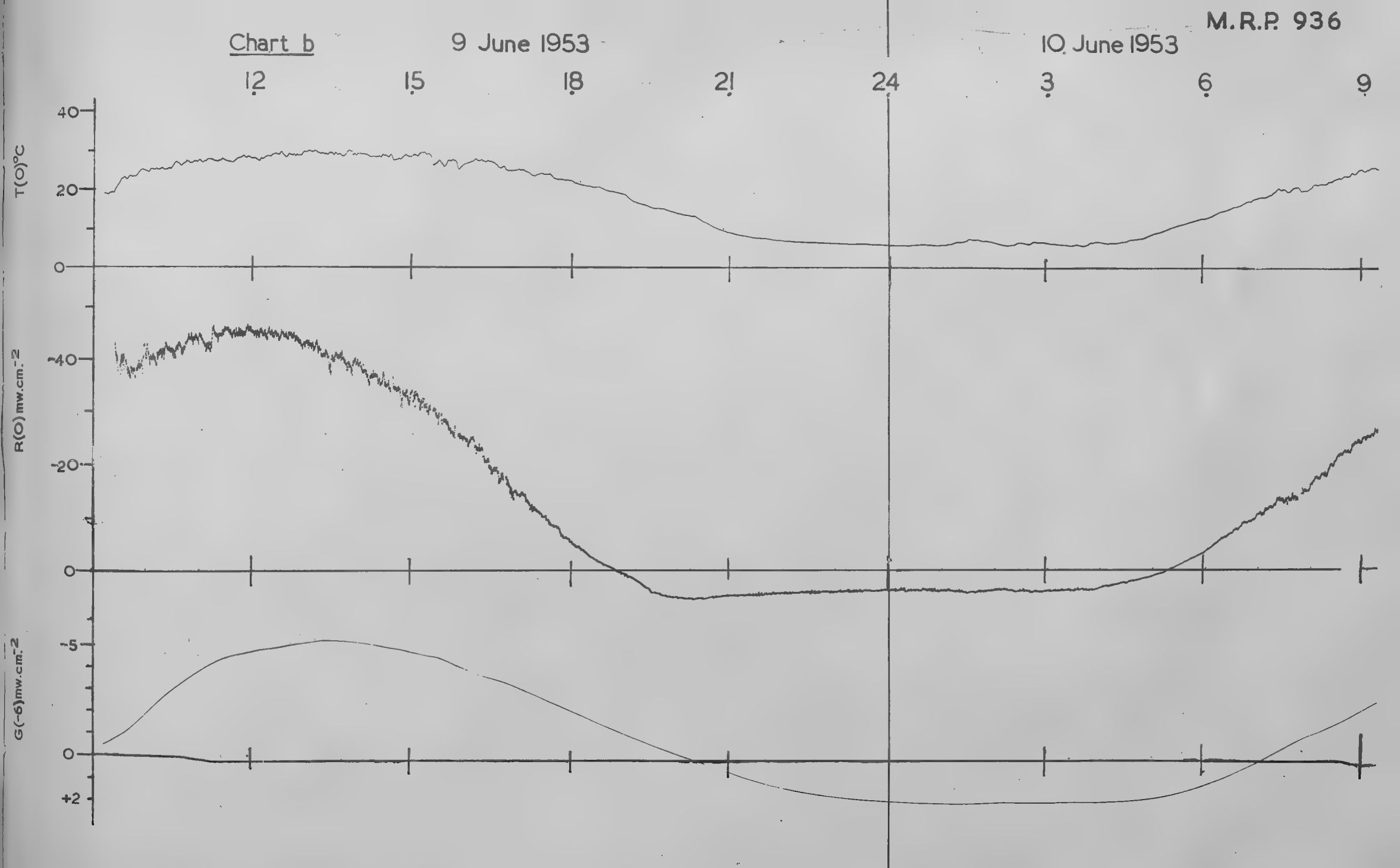

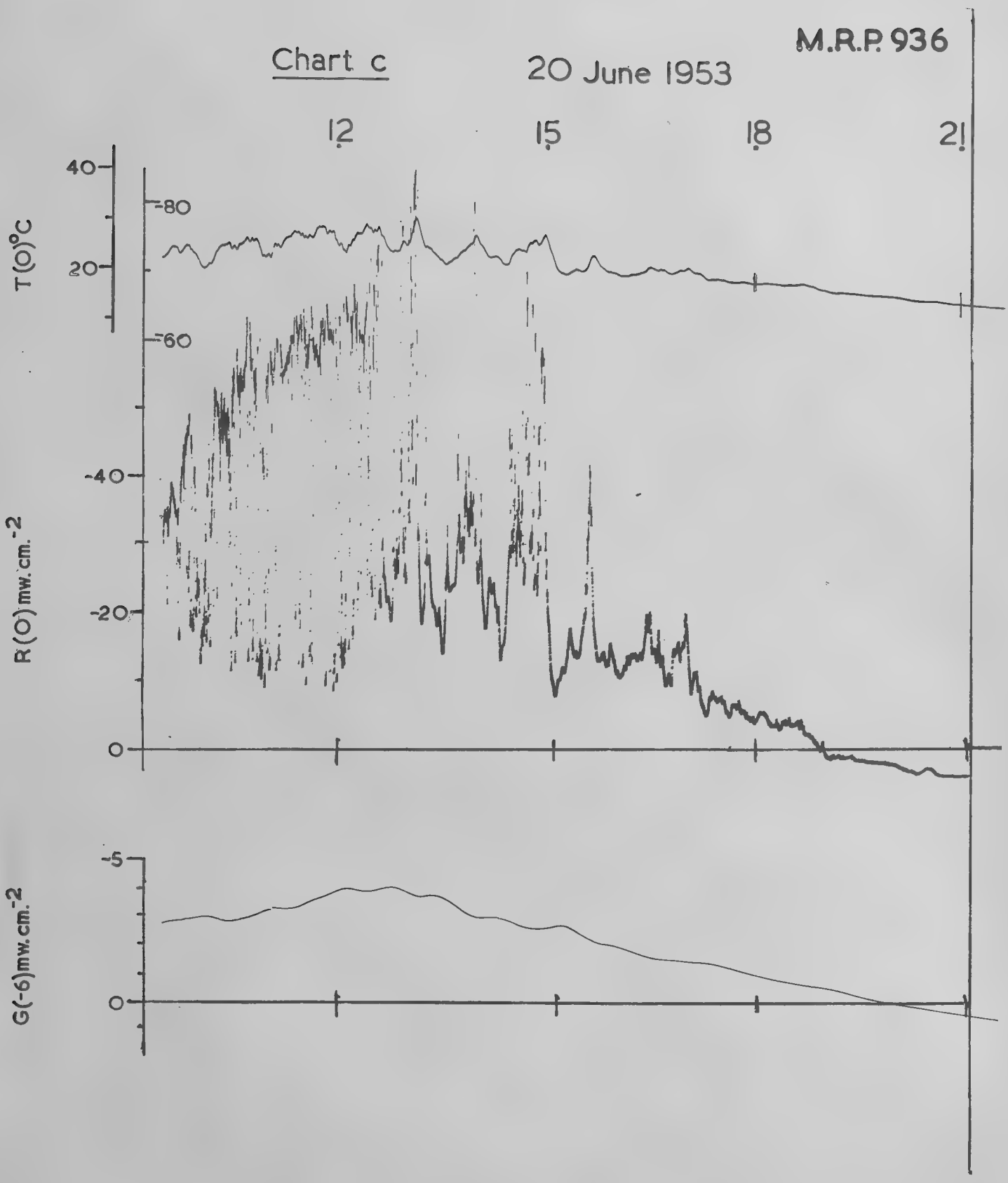
M.R.P. 936
Chart c
20 June 1953
12
15
18
21
40
20
T(0)°C
-80
-60
-40
-20
0
R(0) mw.cm.-2
-5
0
G(-6) mw.cm.-2

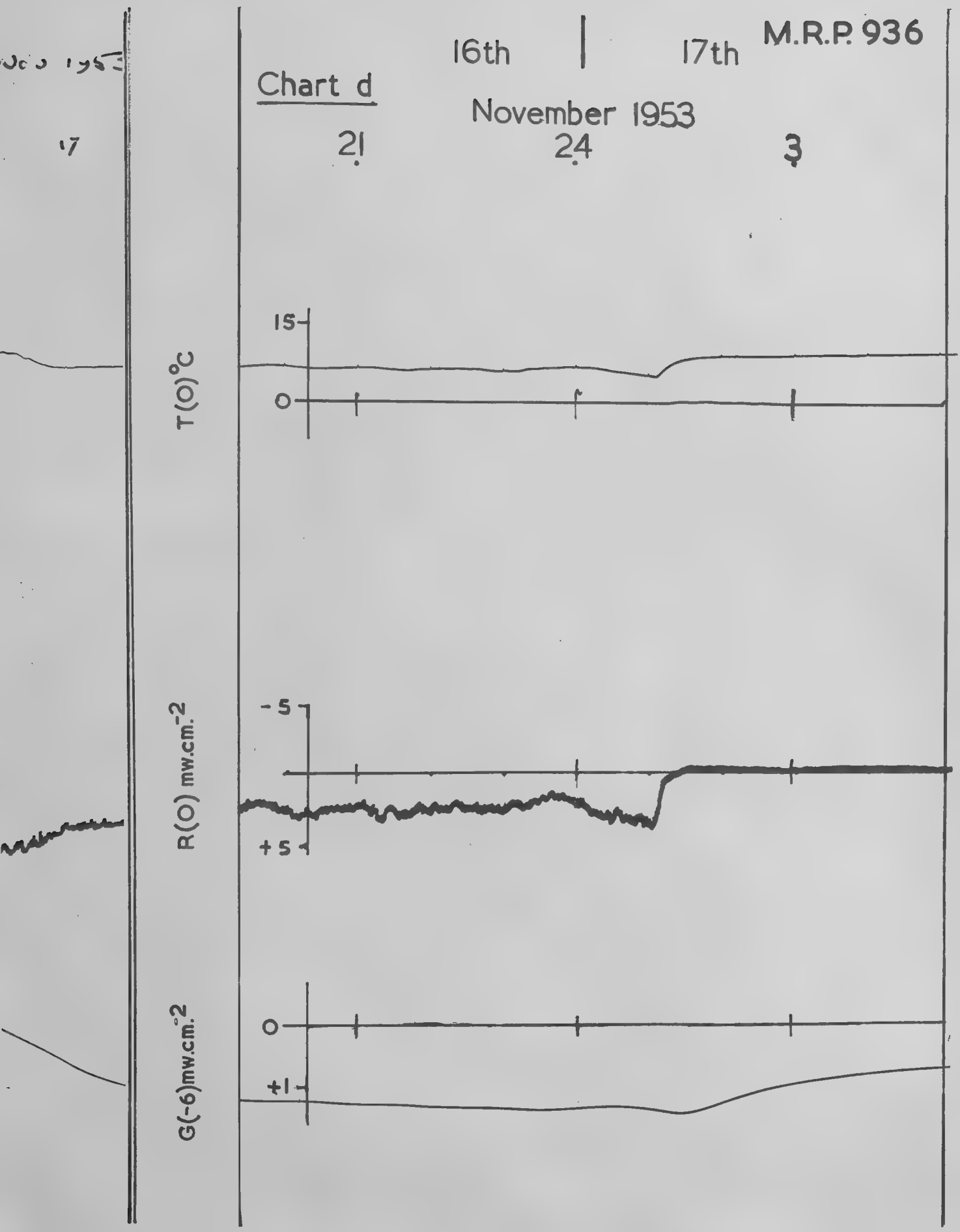
M.R.P. 936
16th
17th
Chart d
November 1953
21
24
3
T(0)°C
15
0
R(0) mw.cm.-2
-5
+5
G(-6)mw.cm.-2
0
+1

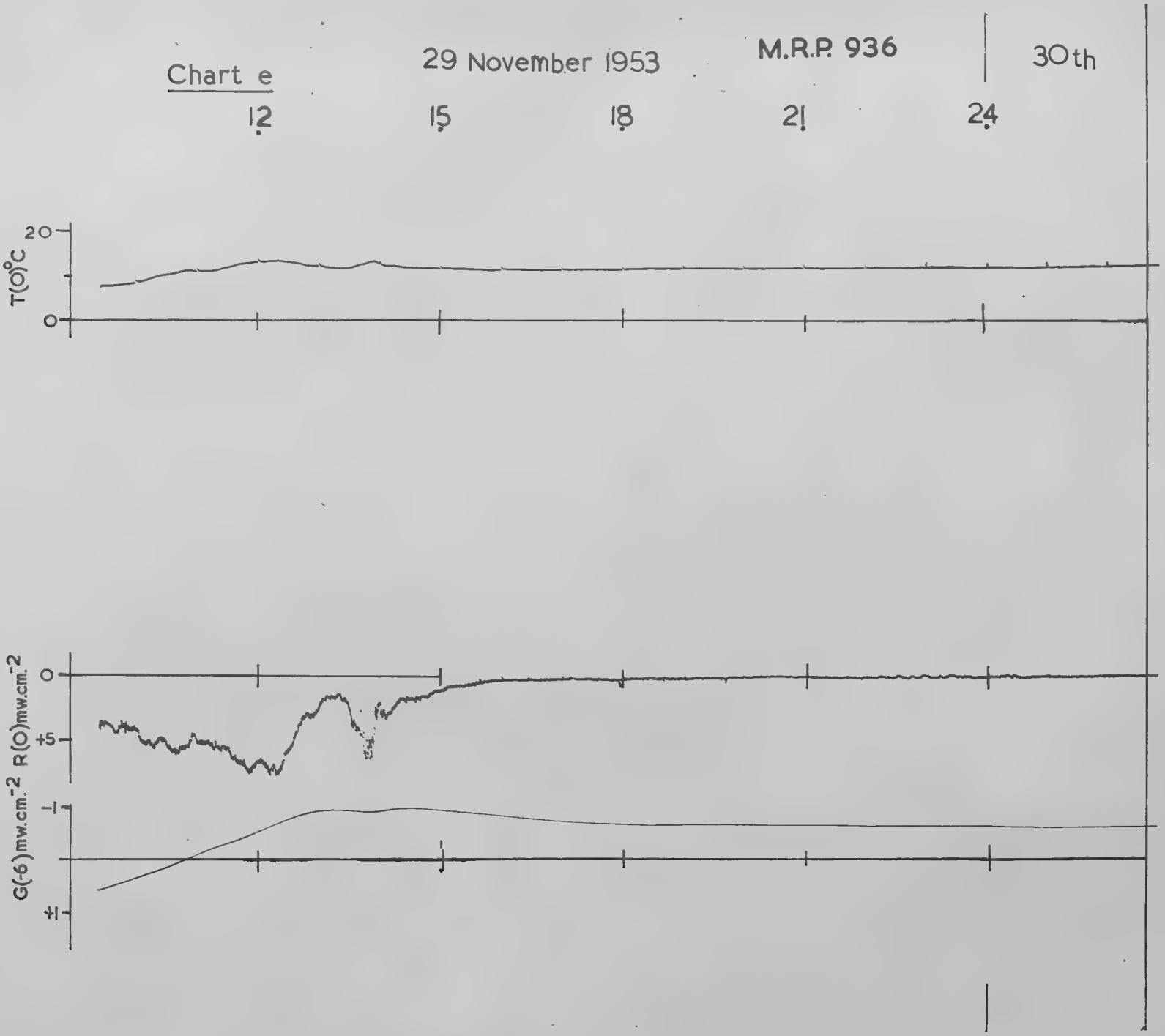
Chart e
29 November 1953
M.R.P. 936
30th
12
15
18
21
24
T(0)°C
20
0
G(-6)mw.cm.-2
R(0)mw.cm.-2
0
+5
-1
+1

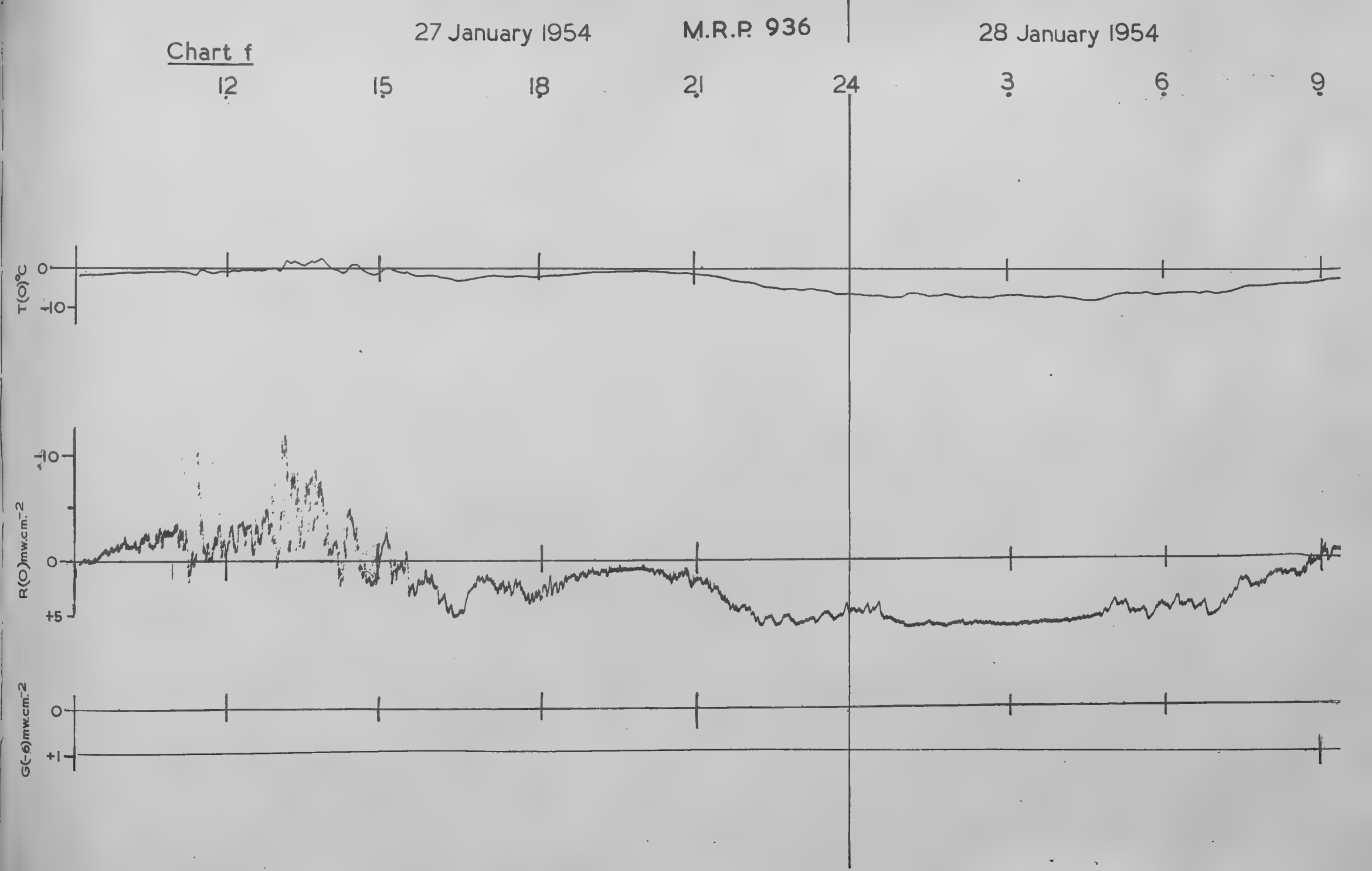
Chart f
27 January 1954
M.R.P. 936
28 January 1954
12
15
18
21
24
3
6
9
T(O)°C
0
-10
R(O)mw.cm.-2
+10
0
+5
G(-6)mw.cm.-2
0
+1

Chart g

7 February 1954

M.R.P. 936

3 6 9 12 15 18 21

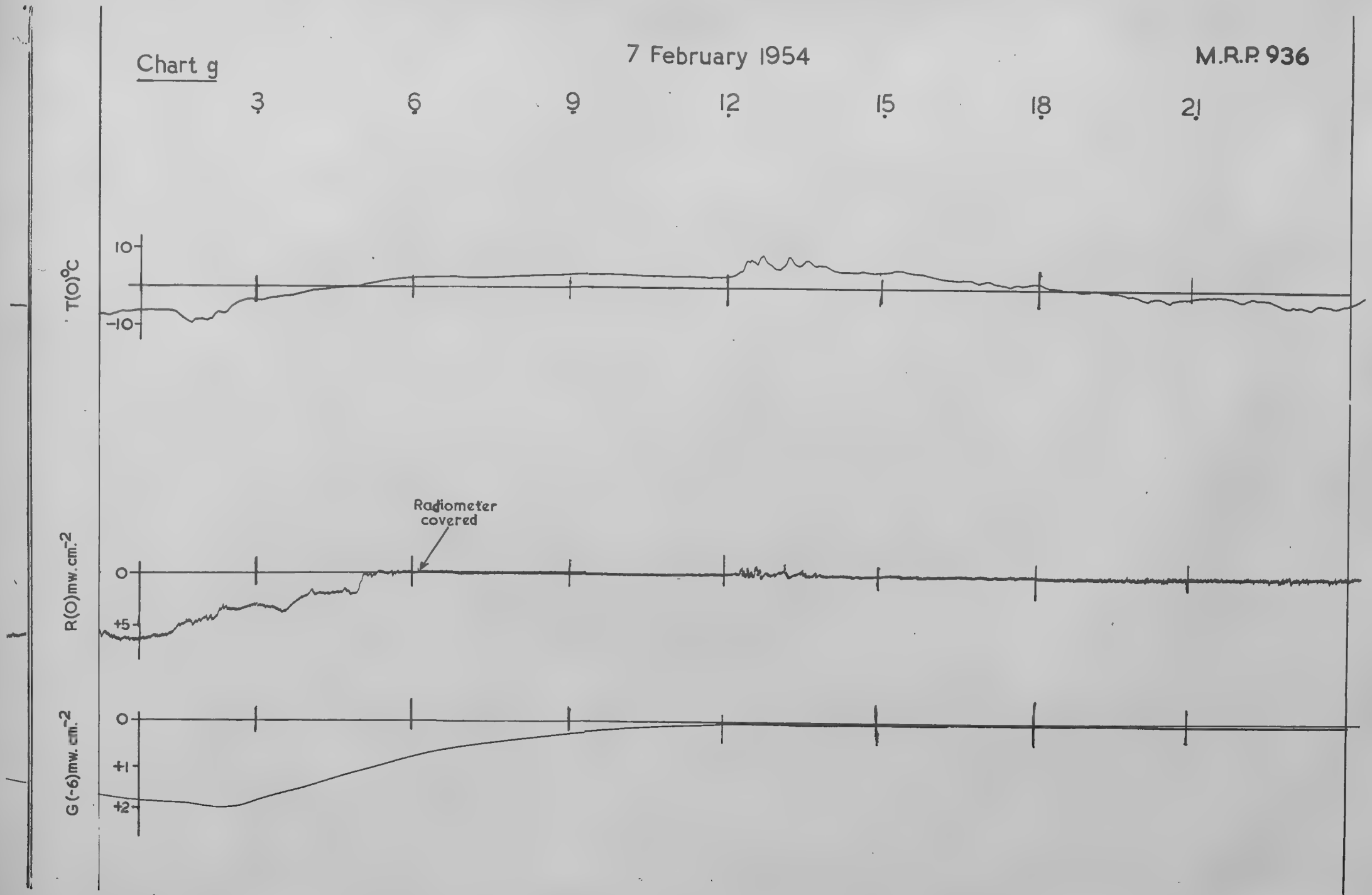

M.R.P. 936

Chart h

15 February 1954

3 6 9 12 15 18

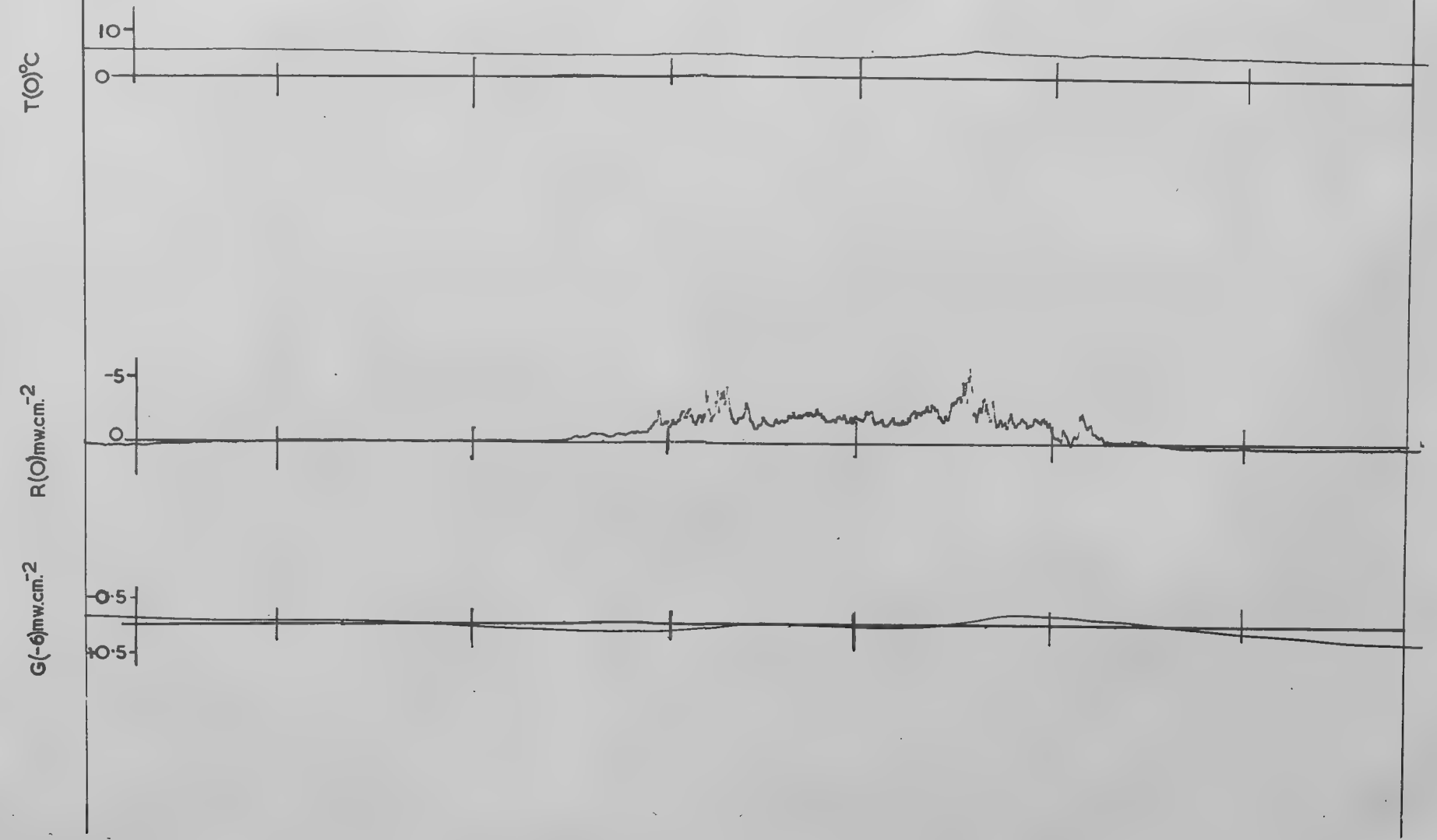

M.R.P. 936

Chart j

31 March 1954

12 15

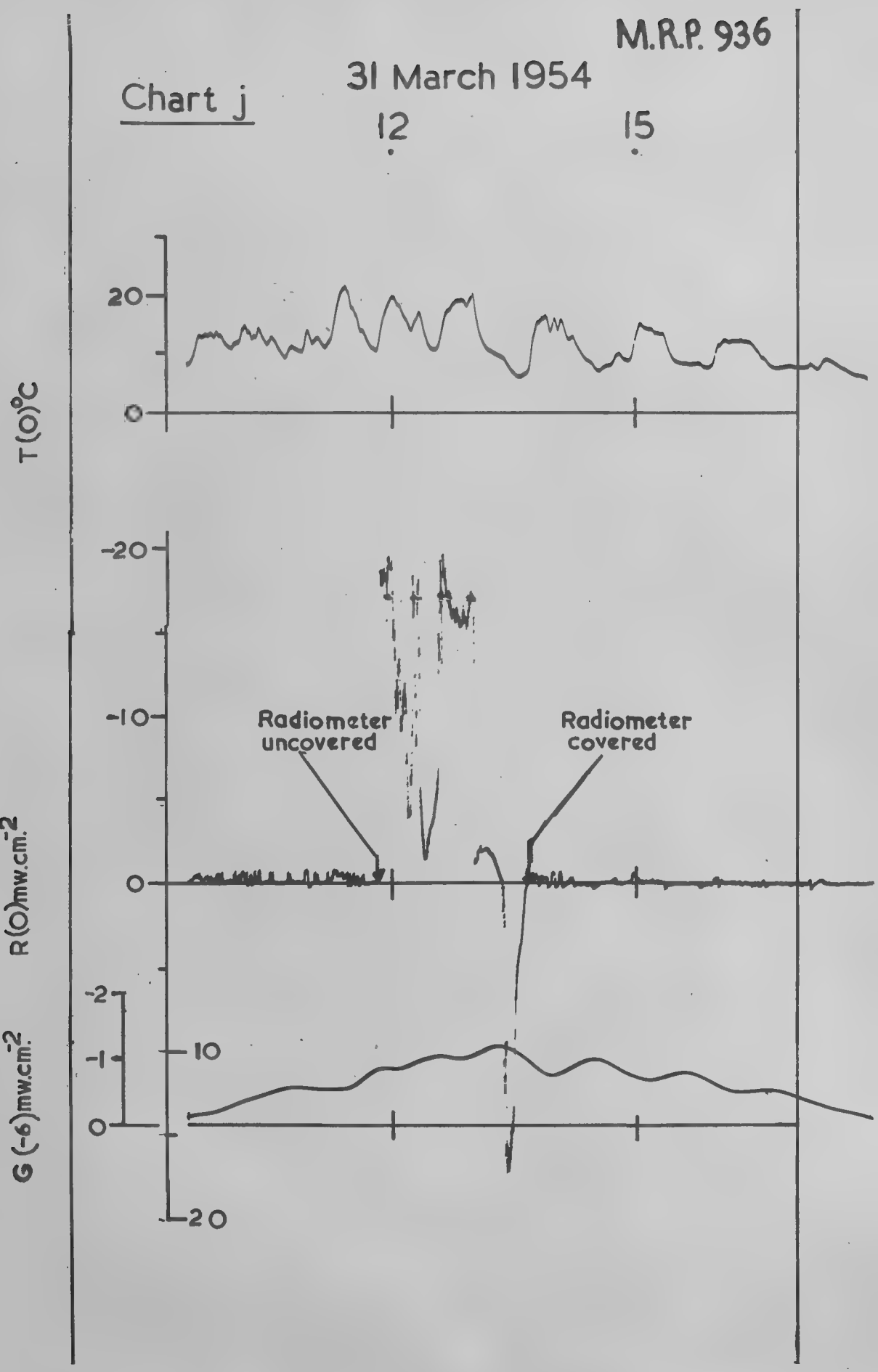

M.R.P. 939
S.C. 11/199
19th September, 1955

Airflow over mountains - the lee wave amplitude

by

G.A. Corby and C.E. Wallington
(Meteorological Office)

AIR MINISTRY
METEOROLOGICAL RESEARCH COMMITTEE

At the time of issue this report has not been published. Any author desiring to quote this paper should refer to it as "A paper of the Meteorological Research Committee (London), M.R.P. No. 939 by Messrs. G.A. Corby and C.E. Wallington. A copy is available in the Library of the Meteorological Office."

M.R.P. 939
S.C.II/199
19th September, 1955

AIR MINISTRY

METEOROLOGICAL RESEARCH COMMITTEE

Airflow over mountains - the lee wave amplitude

by

G.A. Corby and C.E. Wallington (Meteorological Office)

Summary

Although orographic lee waves are probably common over the British Isles, their amplitude is so critically dependent on airstream characteristics and on the scale of local topography that they are likely to be insignificant unless a variety of conditions are satisfied. Precise criteria for large amplitude waves cannot be formulated for airstreams in general, but simplification of the general problem illustrates the pronounced effect of mountain size and shape, stability and wind speed on the lee wave amplitude.

1. Introduction

In theoretical studies of airflow over mountains a good deal of attention has been given to formulating and discussing conditions under which a system of atmospheric lee waves will form in an airstream downwind of hills or mountain ranges (see, for example, Scorer, 1949 and 1953). These conditions involve the vertical variation of a parameter usually denoted by l^2 and given by

$$l^2 = g\beta/u^2 - (1/u)(\partial^2 u/\partial z^2)$$

where g = acceleration due to gravity
β = stability factor defined as $(1/\theta)(d\theta/dz)$, θ being the potential temperature
u = component of wind across the mountain ridge
z = height.

Theoretical study has shown that an airstream can contain lee waves only if l^2 decreases sufficiently with height. In practice such a simple criterion is often difficult to exploit owing to the complex, irregular vertical distributions of l^2 usually found in real airstreams. It does appear, however, that lee wave conditions are frequently satisfied over the British Isles, especially during winter. But familiarity with aircraft reports has given us the impression that only a few of these theoretically possible waves have substantial effects on powered aircraft. This suggests that, although waves may be very common, their amplitude may often be so small that pilots scarcely notice their effects during flight. On some occasions, however, pilots have encountered waves of distinctly troublesome magnitudes.

Accordingly, a preliminary study of the factors controlling the lee wave amplitude has been made and this paper reveals the extreme sensitivity of such amplitude to the stability characteristics of the general airstream and to the local scale of mountain ranges in relation to the wavelength of the free oscillations of the airstream.

/2.

2. Factors determining the lee wave amplitude

Scorer (1949) has derived expressions for the flow over an idealised two-dimensional ridge whose height, ζ, at a horizontal distance x from the crest is given by

$$\zeta = hb^2/(b^2 + x^2) \qquad (1)$$

where h is the height of the ridge and b is the "half-width" parameter. The flow pattern through lee waves induced by such a ridge is indicated by the term

$$\zeta_z = -2\pi h b e^{-kb}(u_1/u_z)\psi_{z,k}\left(\partial\psi_{1,k}/\partial k\right)^{-1}\sin kx \qquad (2)$$

where ζ_z = displacement of a streamline from its undisturbed level at height z
k = the lee wave number
u = horizontal wind speed
ψ = satisfies the equation

$$\partial^2\psi/\partial z^2 + (l^2 - k^2)\psi = 0 \qquad (3)$$

and the suffix 1 refers to ground level.

Thus the lee wave amplitude varies as

$$hbe^{-kb}, \quad u_1/u_z \quad \text{and} \quad \psi_{z,k}\left(\partial\psi_{1,k}/\partial k\right)^{-1}$$

It is convenient to consider these three factors separately.

3. The effect of mountain size and shape

So far as the mountain is concerned, the lee wave amplitude is proportional to hbe^{-kb}. A linear variation with mountain height is to be expected since the results are based on perturbation theory. The expression be^{-kb} has a maximum when $b = k^{-1}$; this means that if the mountain height remains constant the lee wave amplitude attains its greatest value when the mountain width is suitably adjusted to the natural wavelength of the airstream. The variation of lee wave amplitude with mountain width is illustrated by the dashed curve in Fig. 1. In this diagram k has been taken as 1 km^{-1}, i.e. the wavelength of the airstream is 2π km. The maximum at $b = k^{-1}$ is pronounced, and the amplitude falls off sharply for narrower or broader mountains. We may liken this effect to resonance; the natural wavelength is a function of the l^2 profile, i.e. of the airstream's stability and wind profiles, but the lee wave amplitude is likely to be small if the width of the mountain does not match the wavelength of the airstream.

We next enquire how the lee wave amplitude varies if we vary the mountain size while preserving its shape, i.e. the height and width are varied in the same proportion. On this basis the variation of lee wave amplitude has the same form as previously but the maximum amplitude now occurs when $b = 2k^{-1}$; the appropriate curve is drawn as a full line in Fig. 1. Thus we can regard the mountain for which $b = k^{-1}$ as having the optimum width for any specified height; if we then increase the overall mountain size the lee wave amplitude tends to increase with the height factor, h, and to decrease as the width departs from the optimum value. Keeping the ratio h:b constant allows the increasing height to dominate the amplitude tendency until $b = 2k^{-1}$; any further increase in overall mountain size produces a sharp decline in lee wave amplitude. Indeed we see, for example, that if a given airstream produces lee waves of a certain amplitude downstream of a mountain for which

/$b = 2k^{-1}$

$b = 2k^{-1}$ then the same airstream would only produce waves about 1/27 of that amplitude downstream of a mountain four times larger. Clearly this "resonance" effect is of considerable importance.

We infer that any large amplitude lee waves which happen to occur in an airstream will not necessarily be associated with the largest of the mountain ridges or hills in the underlying terrain. Thus an airstream which is favourable for significant waves over, say, the Cotswolds or the Chilterns will not necessarily produce even bigger waves over the Scottish Highlands or the Welsh Mountains. It is true that typical irregular terrain contains orographic features on all scales, but in any given region the dominant features tend to have a common scale.

In view of these conslusions it would be an advantage if the natural wavelength of an airstream could be calculated readily. But, although a system of equations determining the wavelength may formally be set up, the necessary computations are too laborious for routine work on real airstreams. We know, however, that the wavelength lies somewhere between the maximum and minimum values of $2\pi\ l^{-1}$ and we may say that in general if the winds are light at all levels the wavelength will be short, while strong winds will be associated with a long wavelength. Thus we deduce that the larger the mountains, the stronger are the wind speeds necessary for large amplitude lee waves, and such a deduction is supported by Förchtgott's observational studies made in Czechoslovakia (1949). The powerful "Bishop" wave of the Sierra Nevada in California develops only in strong winds approaching jet stream intensity; in this case the mountain ridge is a large feature requiring an airstream with a long natural wavelength for the maximum effect to be achieved.

4. Effect of the wind profile

The lee wave amplitude varies as u_1/u_z where u_1 is the surface wind speed and u_z the wind at height z. Consideration of this factor alone may give the impression that a decrease of wind with height would favour large amplitude lee waves. But we know that for waves to be possible at all l^2 must decrease with height. Such a decrease can be achieved by an increase of wind speed or by a decrease of stability with height, or by some combination of wind and stability distributions. We conclude that if we have two airstreams which, although having different wind and stability profiles, nevertheless have the same l^2 profiles, then the airstream in which u_1/u_z is larger will have the greater amplitude lee waves. Another way of looking at this is to note that, although an airstream with very light winds near the surface and much stronger winds higher up can contain lee waves, the amplitude of the waves would probably be small; other things being equal, larger amplitude waves would occur if the airstream satisfies the conditions for waves partly or mainly by stability variations, so that moderate or strong surface winds can be present without the necessary variation of l^2 with height being destroyed.

This viewpoint is consistent with the observational evidence from aircraft reports collected at Northolt Airport and discussed by Pilsbury (1955). In these reported waves marked stability was always present at middle levels while the low level wind speeds were usually more than 20 kt. and never less than 15 kt.

5. Effect of the l^2 profile

The lee wave amplitude also varies as $\psi_{z,k}\left(\partial\psi_{1,k}/\partial k\right)^{-1}$, which is a function of height and the parameter l^2. At one or more levels this amplitude factor attains some maximum value and we shall focus our attention on this maximum as a basis for studying the general effect of the l^2 profile. Variations in the l^2 profile will of course modify the lee wave number k and also, therefore, the factor be^{-kb}. However, in the present section we confine ourselves to examining the factor $\psi_{z,k}\left(\partial\psi_{1,k}/\partial k\right)^{-1}$ alone. For a given mountain the simultaneous variations of be^{-kb} would intensify the characteristics which emerge.

/For

For ease of mathematical manipulation we follow Scorer by considering the atmosphere to comprise:-

(a) an adiabatic layer ($l = 0$) from the ground to a height h_a.

(b) an intermediate layer in which $l = l_i$ between the levels h_a and $(h_a + h_i)$.

(c) an upper layer in which $l = l_s$ ($< l_i$) extending upwards from the level $(h_a + h_i)$.

Although this three layer structure is a compromise between reality and simplicity it is broadly in accordance with the type of airstream structure which obtains on occasions when aircraft report marked waves. In the first part of this discussion we carry the simplification further by putting $h_a = 0$. Then, taking the top of the intermediate layer as the zero of the height scale (i.e. the ground at $z = -h_i$) and assuming that waves must die out at high levels, the appropriate solutions of eq. (3) are

$$\left.\begin{aligned} \psi_s &= A \exp(-\mu_s z) \\ \psi_i &= A\{\cos \mu_i z - (\mu_s/\mu_i) \sin \mu_i z\} \end{aligned}\right\} \quad (4)$$

where $\mu = \left\{|l^2 - k^2|\right\}^{\frac{1}{2}}$, the suffixes i and s refer to the lower and upper layers respectively, and A is a constant.

If we apply the condition that ψ_i must vanish at the ground downwind of an obstacle we obtain an equation determining the lee wave number, k. The equation may have a number of solutions, but, as Scorer (1949) has pointed out, the smallest root (corresponding to the longest wavelength) will dominate the flow. If the wave equation has n solutions we find that, at the n heights above the ground given by $h_n = \pi/2\mu_i, 3\pi/2\mu_i, \ldots\ldots (2n-1)\pi/2\mu_i$, the amplitude factor $\psi_{z,k}\left(\partial \psi_{i,k}/\partial k\right)^{-1}$ assumes a maximum value, a_n, given by

$$a_n = (\mu_i/k)(h_i + 1/\mu_s)^{-1} \quad (5)$$

Mere inspection of this equation does not easily reveal how a_n varies with the airstream parameters l_i, l_s and h_i; this is because it is not possible to express k explicitly in terms of those parameters. It is simpler to study graphical representations of the equation and for this purpose the introduction of an additional dependent variable is helpful. Thus as k must lie between l_i and l_s we may write

$$k^2 = l_s^2 + L^2 \cos^2\theta \quad (6)$$

$$L^2 = l_i^2 - l_s^2 \quad (7)$$

where $0 \leq \theta \leq \pi/2$

We shall then have

$$\left.\begin{aligned} \mu_i &= L \sin\theta \\ \mu_s &= L \cos\theta \end{aligned}\right\} \quad (8)$$

and the equation for the lee wavelength reduces to

$$(n\pi - \theta)/\sin\theta = Lh_i \quad (9)$$

With this notation the lee wave amplitude factor at the levels where it is a maximum becomes

$$a_n = L^2(l_s^2 + L^2\cos^2\theta)^{-\frac{1}{2}}(n\pi - \theta + \tan\theta)^{-1}\sin^2\theta \quad (10)$$

/This

This equation may be used to calculate the maximum amplitude for various values of l_s, L and Θ, the corresponding values of h_i being determined by eq.(9). Fig. 2 shows an isometric sketch in which the family of curves delineates a surface illustrating the way in which the maximum lee wave amplitude varies with l_s and h_i for a constant value of L ($=5$ km^{-1} in this figure). For values of h_i below the plane ABCD the condition for lee waves is not satisfied. A striking feature of the diagram is that as h_i is increased beyond this critical value we pass very rapidly from a condition in which there can be no lee waves to one in which they will have large amplitudes. It can also be demonstrated that if h_i were kept constant as L varied, the lee wave amplitude would behave similarly as a limiting value of L were crossed. It has been stated that the greater the decrease of l^2 with height, the more likely are lee waves because one can then be more confident that the condition for them is satisfied. Although this statement is correct it is liable to imply that the greater the decrease in l^2, the larger will be the amplitude of lee waves; casual interpretation of the perturbation restrictions may also suggest that deep layers having high values of l favour large amplitude waves. However, it appears that the optimum conditions, when the airstream is most sensitive, are very close to the critical conditions for waves, and that if conditions are made "more favourable" for waves to occur the amplitude falls off sharply. We also note that as l_s increases this sensitivity decreases somewhat (but remains important) and the amplitude falls off.

The variations illustrated in Fig. 2 are for a constant value of L of 5 km^{-1}. We next examine the effect of varying L, which is a measure of the decrease of l^2 with height. Fig. 3 shows curves for the lee wave amplitude (once again for the level at which it is a maximum) for L = 2,5 and 10 km^{-1}. For these curves the other variable is h_i; l_s is kept constant at 0.2 km^{-1} throughout. The corresponding wavelengths are depicted in the left hand section of the diagram. Full curves refer to n = 1, and dashed curves to n = 2; curves for higher values of n are not shown, but the tendency for the wave amplitudes to decrease as k acquires more possible values is maintained, and unless l_s is extremely small this decrease is a rapid one.

We see again the great sensitivity of the airstream near the critical values of the parameters for waves to occur; it is also apparent that the maximum amplitude becomes potentially greater as L is made larger. Indeed, it appears that the more the lower layer tends towards a sharp inversion, the greater does the maximum possible amplitude become. However, since the boundary conditions used at the interface between the two layers assume continuity of density we cannot extend our conclusions to an ideally sharp inversion without modifying these boundary conditions. Nevertheless the conclusion remains valid that greater amplitudes are possible if there is considerable static stability through a shallow layer than with smaller stability through a deep layer.

The variation of amplitude with L illustrated in Fig. 3 enables us to visualise a set of surfaces, one of which is given in Fig. 2,for a single value of L. We may then summarise the principal conclusions of Figs. 2 and 3 by saying that the largest amplitude lee waves will be possible when

(a) conditions are slightly more favourable for waves than the limiting conditions for them to occur at all. By "slightly more favourable" we mean that the stability or depth of the layer having the large l^2 should be a little greater than the limiting combination for waves.

(b) L should be large.

(c) l_s should be small.

We next consider briefly the maximum vertical velocity in these lee waves; its variation with the airstream parameters will not follow exactly that of the

/amplitude

amplitude because of the wavelength changes. Well away from the mountain the displacement of the streamline at the level where $\psi_{2,K}(\partial\psi_{1,K}/\partial K)^{-1}$ has a maximum will be given by putting $z = h_n$ in the equation

$$\zeta_z = -2\pi h_b e^{-Kb}(u_1/u_2)a_n \sin kx \qquad (11)$$

so that if w is the magnitude of the maximum vertical velocity,

$$w = \left[u_z(\partial\zeta_z/\partial x)\right]_{max} = 2\pi h_b e^{-Kb} u_1 a_n k \qquad (12)$$

Thus $$w \propto \mu_i(h_i + 1/\mu_s)^{-1}$$

$$\propto L^2(n\pi - \theta + \tan\theta)^{-1}\sin^2\theta \qquad (13)$$

We note that eq. (13) is independent of l_s so that a family of curves is sufficient to illustrate the variation of vertical velocity with the three parameters defining the airstream. Such curves are drawn in Fig. 4 for $L = 1, 2, 3, 4, 5, 7$ and $10\ km^{-1}$ and for $n = 1$. These curves exhibit features which are similar to the amplitude curves, the main differences being that sensitivity is somewhat less critical near the optimum combination of h_i and L.

It is impracticable to extend the graphical representation of the maximum amplitude factor to deal with a three layer atmosphere fully, but we can study such a model to a limited extent. The addition of an adiabatically mixed layer, that is, a layer with neutral static stability, (denoted by suffix a) at the bottom requires an additional solution of eq. (3) having the form

$$\psi_a = B\cosh kz + C\sinh kz \qquad (14)$$

where B and C are constants. Further application of the boundary conditions leads to the following expression for the lee wave amplitude factor at the level where it is a maximum:

$$a_n = (\mu_i^2 - l_i^2\sin^2\nu)^{\frac{1}{2}}\left[k(h_i + 1/\mu_s) + \tfrac{1}{2}(l_i^2/Lk)\sin 2\nu\ \mathrm{cosec}\,\theta - (\mu_i^2 - l_i^2\sin^2\nu)h_a/k\right]^{-1} \qquad (15)$$

where

$$\tan\nu = (\mu_i/k)\tanh(kh_a) \qquad (16)$$

and

$$\nu = n\pi - \theta - Lh_i\sin\theta \qquad (17)$$

The condition for these equations to yield n real solutions for k can be derived as

$$Lh_i > \tfrac{1}{2}(2n-1)\pi - \alpha \qquad (18)$$

where

$$\alpha = \tan^{-1}\left[(L/l_s)\tanh(l_s h_a)\right] \qquad (19)$$

and

$$0 \geqslant \alpha \geqslant \pi/2$$

Eq. (18) may be regarded as the condition for lee waves to be possible in this three layer model and it corresponds to $Lh_i > \frac{1}{2}(2n-1)\pi$ for the two layer model; indeed as $h_a \to 0$ the former condition tends to the latter. We note that it is possible for the addition of an adiabatically mixed surface

/layer

layer to make lee waves possible when they would not occur otherwise, provided the adiabatic layer is not added at the expense of the intermediate layer. The effect on the maximum amplitude of the additional layer can be seen in Fig. 5 which contains amplitude and wavelength curves for $L = 2\ km^{-1}$ and $l_s = 0.2\ km^{-1}$. This figure contains dashed curves computed for an airstream with a low level adiabatic layer of depth 0.5 km and full curves applicable when the adiabatic layer is absent. The general conclusions reached for the two layer model are seen to be equally applicable if there is an additional layer at the surface having an adiabatic lapse rate, the only differences being a limited reduction in amplitude and an increase of wavelength throughout the range of values.

6. Conclusion

Over the British Isles airstreams which formally satisfy the theoretical conditions for lee waves are probably very common, especially in winter. However, the amplitude of such waves will be subject to very wide variations even amongst airstreams having very similar profiles of l^2 because of the critical way in which the amplitude depends on the airstream characteristics. The largest amplitude waves occur when the airstream satisfies the condition for waves by only a small margin, and in this region very large changes of amplitude may result from very small changes in the airstream characteristics. Apart from the question of this sensitive region, it may be said that larger amplitude waves are theoretically more likely in airstreams containing a shallow layer of great stability than in conditions of slight stability through a deep layer. The main effect of an adiabatically mixed layer near the ground is to reduce the amplitude and increase the wavelength.

Quite apart from the variations which depend on the airstream characteristics it appears that a given airstream is sensitive to the scale of the disturbing mountain. If the mountain is made broader or narrower than the optimum width for the prevailing airstream a considerable reduction of wave amplitude is to be expected.

References

Förchtgott, J.	1949	Bull. Met. tchécosl. Prague, 3, p.49.
Pilsbury, R.K.	1955	Met. Mag. (in press).
Scorer, R.S.	1949	Quart. J.R. Met. Soc., 75, p.41.
	1953	Ibid., 79, p.70.

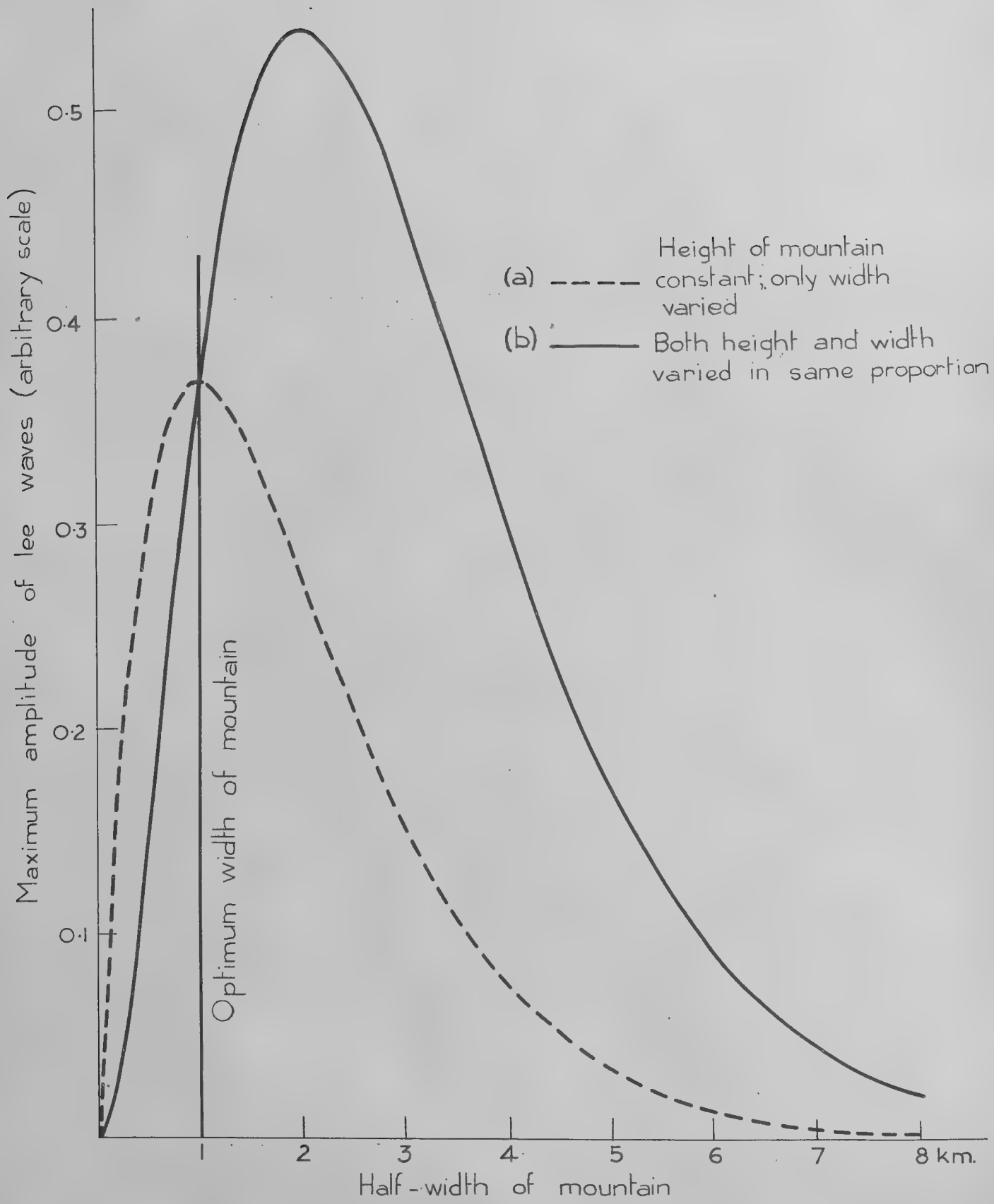

Fig.1 Variation of lee wave amplitude with size of mountain
$k = 1\ km^{-1}$

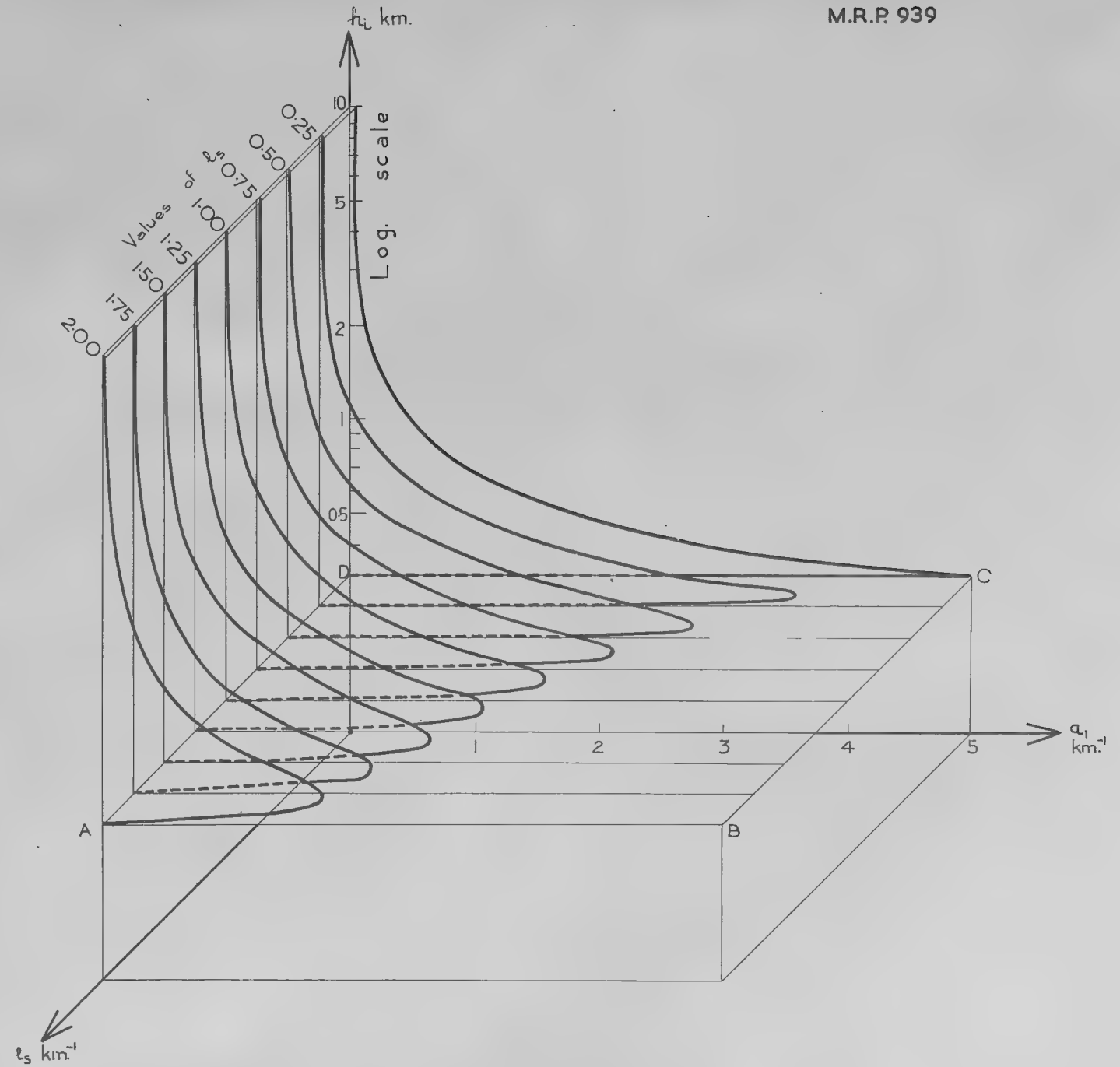

Fig.2 Variation of lee wave amplitude (a_1) with airstream characteristics
L = constant = 5 km.$^{-1}$

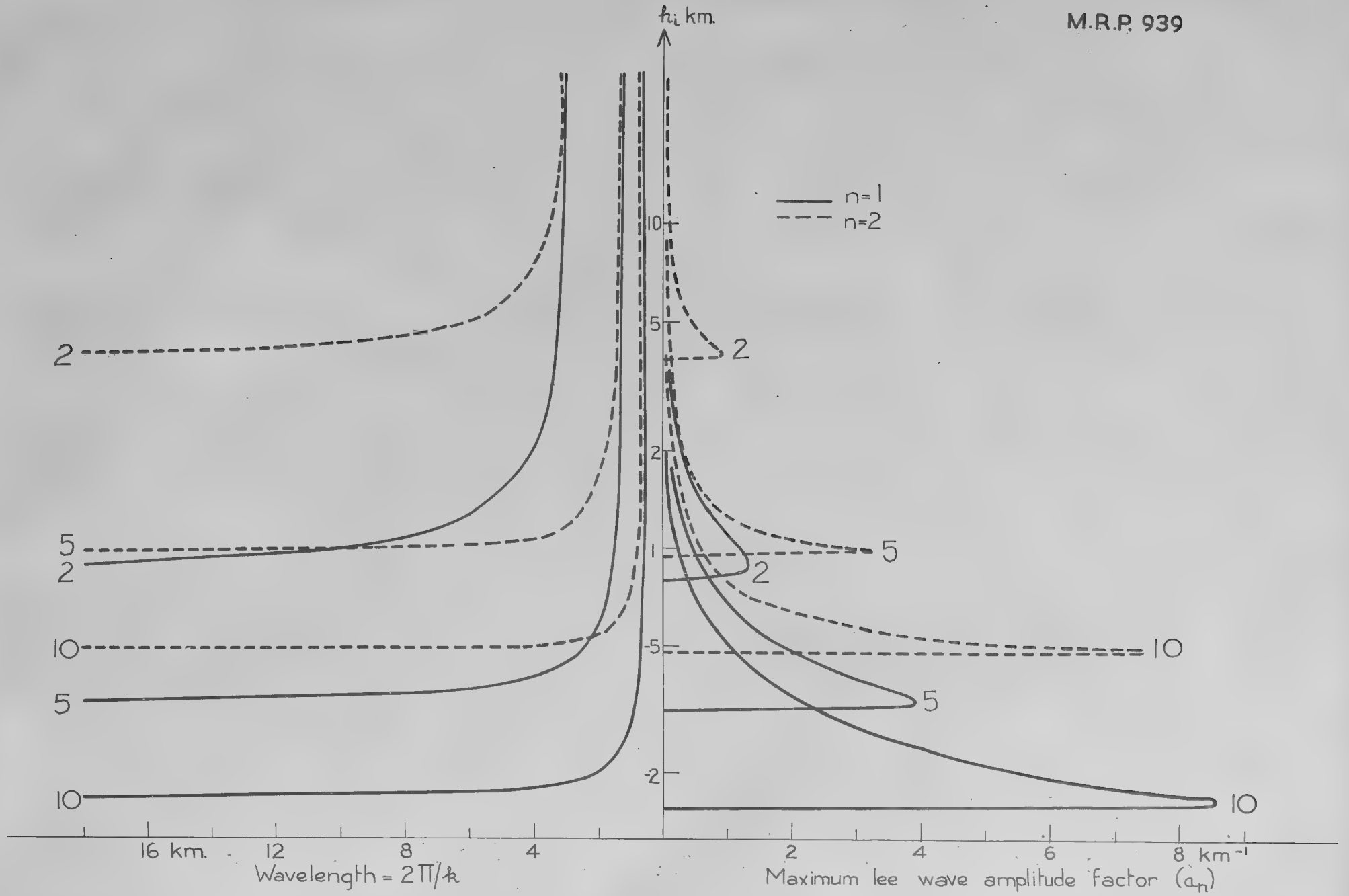

Fig.3 Variation of lee wave amplitude and wavelength with airstream characteristics
l_s = constant = 0·2 km^{-1} Values of L (2, 5, 10 km^{-1}) marked against curves

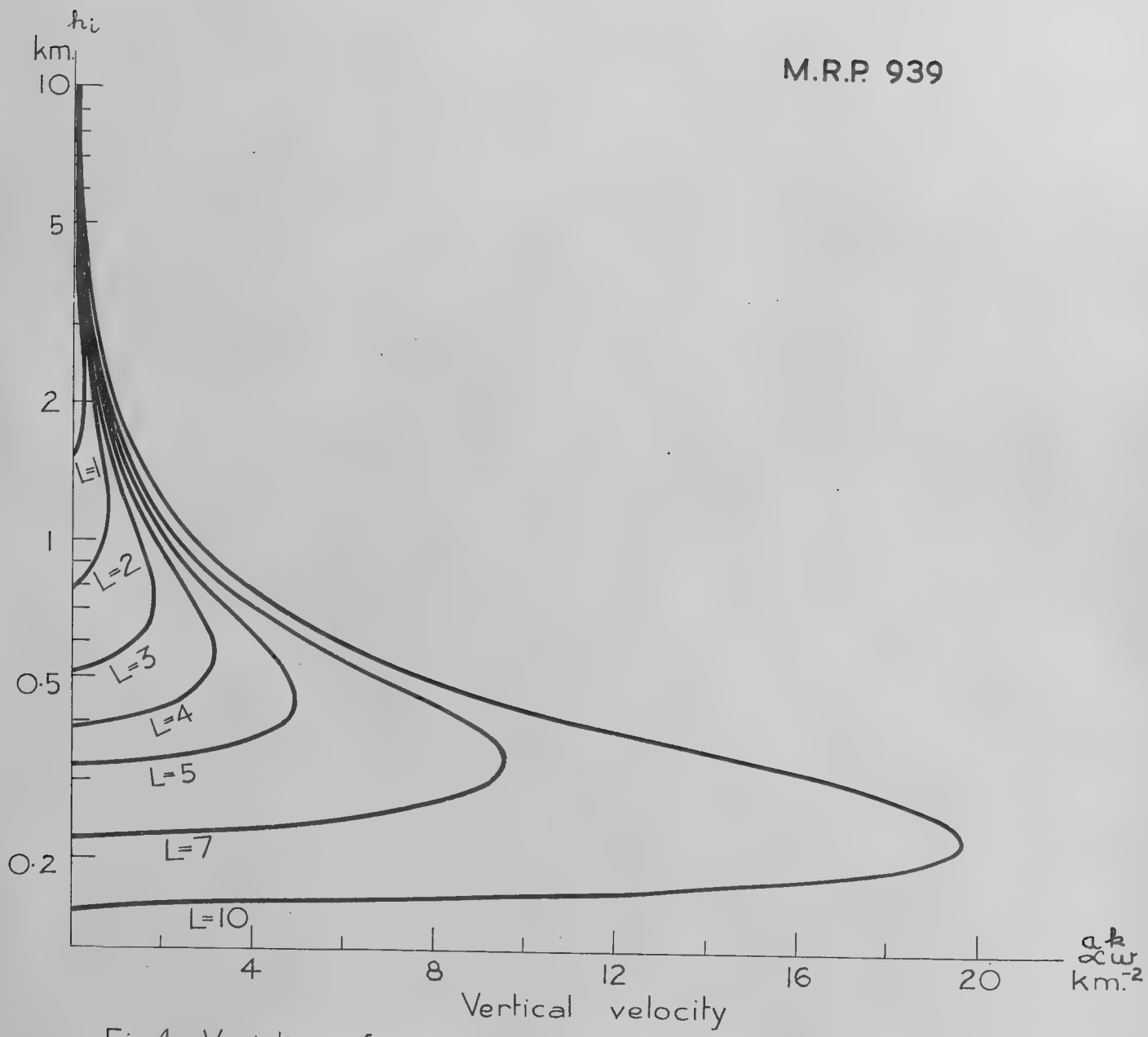

Fig.4 Variation of maximum vertical velocity in lee waves with airstream characteristics. Values of L are indicated. Results are independent of l_s

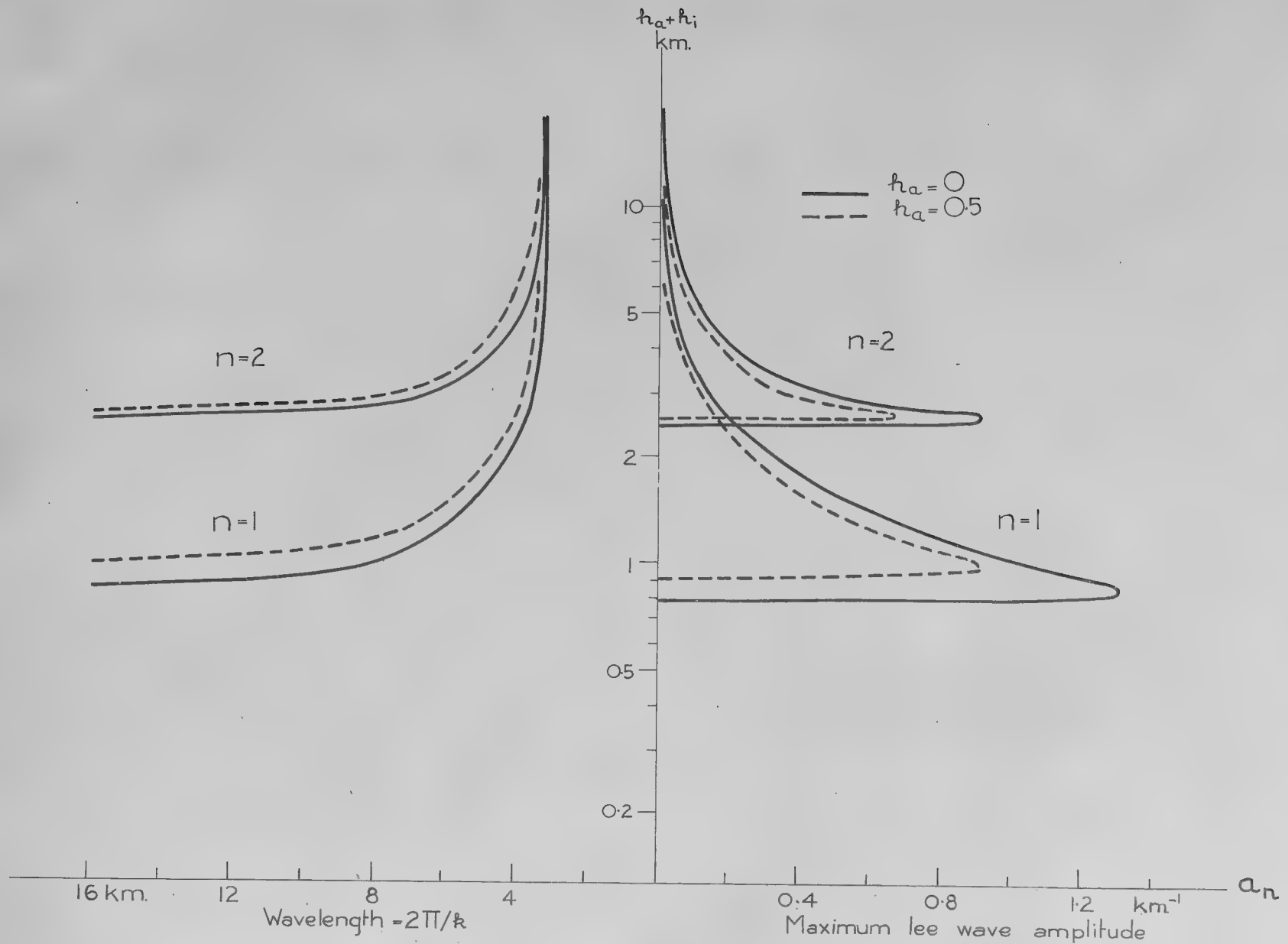

Fig 5. Variation of lee wave amplitude and wavelength for 3-layer airstream
$L=2$ km^{-1} $l_s=0.2$ km^{-1}

AD No. 117797
ASTIA FILE COPY

M.R.P. 941
S.C. 1/106
1st October, 195

Attic

11797

FC

An experimental pulsed-light cloud-base meter

by

R. Almond
(Meteorological Office)

-6. MAR 1956 08 45 Z
IN

AIR MINISTRY
METEOROLOGICAL RESEARCH COMMITTEE

At the time of issue this report has not been published. Any author desiring to quote this paper should refer to it as "A paper of the Meteorological Research Committee (London).
M.R.P. No. 941 by Mr. R. Almond
A copy is available in the Library of the Meteorological Office."

M.R.P. 941
S.C.I/106
1st October, 1955.

AIR MINISTRY

METEOROLOGICAL RESEARCH COMMITTEE

An experimental pulsed-light cloud-base meter

by

R. Almond (Meteorological Office)

CONTENTS:

Summary

1. Introduction

2. Details of present experimental model
   - 2.1. System and layout
   - 2.2. Optical alignment
   - 2.3. Transmitter, receiver and display unit

3. Performance
   - 3.1. General
   - 3.2. Maximum range
   - 3.3. Minimum range
   - 3.4. Operation in precipitation

4. Recommendations for improvements

5. Conclusions

Appendix 1. Some aspects of transmission and reflection theory applicable to the pulsed-light problem

Appendix 2. Summary of Northolt trials reports

Diagrams: fig. 1 and 2

Photographs: Instrument fig. 3-5
Clouds etc. fig. 6-18

Summary

In 1950 the Meteorological Office obtained an experimental cloud-base meter from the Telecommunications Research Establishment. Trials proved unsatisfactory until a 25 ft. separation of transmitter and receiver units was adopted. The report covers the trials and modifications carried out by the Meteorological Office. Electronic and optical features of the instrument are discussed, together with the permanent outdoor housing system evolved. Performance details over the range surface to 15,000 ft. are given, including operation in haze and precipitation. Limitations of the present instrument are discussed and improvements suggested. A selection of photographs of the display covers a wide variety of echoes from cloud, fog, haze and precipitation.

Appendix 1 deals theoretically with the reflection and transmission of light by cloud and fog, and explains the low level working of the instrument.

Appendix 2 covers the two operational trial periods at Northolt and stresses the advantage of the pulsed-light meter over present observing aids.

1. INTRODUCTION

Development work on a cloud-base meter using the pulsed-light technique was carried out at the Telecommunications Research Establishment during the period 1945-49.(1) After the disappointing performance of two prototype models, a final model (2), employing earlier design techniques, was constructed and delivered to the Instruments Division of the Meteorological Office in 1950. After familiarisation trials in 1950, during which period certain minor modifications were made, the equipment was given a routine trial at Northolt aerodrome. The trial report emphasised the limitations of the meter in the range 0-1000 ft. due to the blanking effect of a permanent atmospheric scatter pattern on the height display.

Proximity of the transmitter and receiver optical assemblies was considered responsible for this failure to measure low cloud heights. Separation of these assemblies did not at first produce any improvement, due to optical alignment errors. Eventually with a 25 ft. separation and correct optical alignment the atmospheric scatter pattern was eliminated and cloud heights became measurable from surface to about 15,000 ft.

Further trials at Northolt in 1954 have included extensive photography of the cathode-ray tube display for many cloud types, and indicate the usefulness of the equipment in its present form.

2. DETAILS OF PRESENT EXPERIMENTAL MODEL

2.1. System and layout

Light pulses of very short duration but of high peak power are produced by discharging a condenser across an air gap. They are beamed as narrowly as possible by a paraboloidal mirror with its optical axis vertical. The pulse repetition frequency can be varied from about 1 to 20 per sec. A small proportion of the emitted light energy is collected by a similarly aligned receiver mirror after diffuse reflection and scattering mainly by cloud droplets. This energy is focussed through a small aperture on to a rapid response photocell and the burst of current produced yields a voltage pulse which can be amplified and displayed on the range time-base of a cathode-ray tube.

Synchronised triggering of the light pulse and the range time-base enables the delay between emitted and received pulses to be measured. A range scale calibrated directly in feet expresses the delay as a cloud height. The commencement of the displayed cloud-echo indicates the cloud-base height.

In the original equipment the 20 in. diameter mirrors were arranged with optical centres 2 ft. apart on a heavy cast metal base-plate. Beneath this assembly was housed the remainder of the equipment, with the exception of the display unit, which was placed 15 ft. from the main assembly and so could be operated from an indoor position if necessary. At this stage the apparatus was fully exposed and could not be operated in precipitation.

For the initial trials at Northolt a small outbuilding was erected for the main assembly, a hinged opaque roof being withdrawn during observation periods.

There were originally three supporting arms associated with each mirror(2) in order to locate the transmitter spark gap assembly and the receiver photocell unit. The extreme rigidity thought necessary at the time of design, to give critical optical setting, has not been justified. One support only is now used with each mirror (fig. 5), thus increasing considerably the available working surface.

For the second trial period the transmitter and receiver were separated successively 12 ft. and 25 ft. on a horizontal base-line. Successful optical alignment was eventually achieved with the greater separation, but no further work has since been undertaken with other base-line distances. This separation required the removal and re-assembly of all the associated receiver components on a separate base-plate. A separate housing was provided for the new assembly and could be opened

/ to

to expose the mirror during observation periods. The display unit was now placed in the main assembly housing next to the transmitter mirror (fig. 4). Finally both housings were fitted with optical plate glass roofs set at a suitable run-off angle, and these could be covered with opaque shutters during non-observational periods. This enabled the equipment to be tested for the first time during periods of precipitation. This present layout of the meter is shown in fig. 3-5.

A cathode-ray tube camera, adapted to fit the display unit, could be rapidly interchanged for the normal vizor to obtain permanent records of a representative range of cloud echoes, and other phenomena. A small representative selection of the photographs obtained is shown in fig. 6-18.

2.2. Optical alignment

It was considered that extremely critical optical alignment would be necessary. With the compact assembly of both mirrors on a single base-plate a horizontal light path was used and focus and axis adjustments were made with respect to a point light source at 500 yd.

The next method proved somewhat easier, and consisted of placing a point light source in the aperture position of the receiver, and so viewing two light beams at night. (The transmitter beam is easily visible at night). This new method could also be used for the separated type of meter assembly, but proved unsatisfactory at Northolt due mainly to the high artificial light factor obtaining during the night period.

On the separated assembly, recourse to direct measurement, spirit levelling and plumb-line methods eventually proved a satisfactory method of obtaining vertical beaming for both mirror systems. This setting gave a range trace which contained no permanent atmospheric scatter pattern but was found to display good cloud echoes over a wide range of heights.

Finally the mirror carriages were orientated so that the receiver beam could be swept in the vertical plane passing through the two mirror centres, whilst a vertical plane at right angles to this could be swept by the transmitter beam. This considerably simplified the optimum optical alignment procedure.

2.3. Transmitter, receiver and display units

2.3.1. Transmitter

The transmitter spark requirements are essentially:

(1) The light should reach maximum intensity in a fraction of a microsecond, to give sufficient discrimination at low cloud heights.

(2) The duration of the light pulse must be kept short, in order to keep the ratio of peak to mean energy high for efficient working.

(3) The light produced should have high intrinsic brightness, and luminous efficiency, and should match the spectral response characteristics of the photocell detector.

The light pulse should also be beamed as narrowly as possible to give maximum intensity at the cloud base and hence maximum contrast with daylight illumination.

Requirements (1) to (3) are met by a high frequency open spark discharge almost critically damped. An 0.05 microfarad condenser with terminals connected to a spark gap assembly, such that the total loop inductance is a minimum, is used in the present equipment. Duration of each half cycle of discharge is:

$\frac{2\pi L}{\beta}$ where L = total inductance

$$\beta = \sqrt{\frac{4L}{C} - R^2}$$

and β is positive for oscillatory discharge

R = resistance of spark gap

C = capacity of condenser

For maximum intensity and almost critical damping β and R must be small.

For minimum half cycle period L must be small compared with β. L probably increases approximately proportionally with C so that β is little changed, and therefore increase of L will widen the pulse, which is undesirable. In the present spark gap unit:

$C = 0.05\mu F$, $R = 2.5$ ohms

and $L = 0.11\ \mu H$

giving a half cycle period of 0.43μ sec. Power in the second half cycle expressed as a fraction of the power in the first half cycle is:

$$\frac{1}{18400}$$

Power in the first half cycle is 10 megawatts approximately and assuming a conversion efficiency of 2 lumens/watt this gives 2×10^7 lumens for the light intensity of the spark.

A trigger spark, produced between the inner rod and outer shell of the positive spark gap electrode, provides an ionisation burst which fires the main spark. The electrode structure is shown diagrammatically in fig. 1. The back edge of a 25 μ sec. multivibrator pulse fires a ringing circuit which produces almost all its power in the first half cycle and is effectively a single pulse with a peak voltage of five kilovolts and width of two microseconds. This is the pulse which produces the trigger spark. See A and B of fig. 2.

To minimise electrode erosion the solid negative electrode is tipped with tungsten and the hollow positive electrode has a tungsten-nickel alloy cap with a central rod of tungsten. The only appreciable wear is in the rod and cap. This is because the rod is only 1mm. diameter and the cap thickness must not exceed 1mm. in order to keep the trigger spark close to the main spark gap. The tungsten rod can be fed forward as it wears, and the caps are replaced approximately every 50 hr. of running time. The spark gap unit is supported above the transmitter mirror and adjusted to give the narrowest pulsed beam possible with a vertical axis.

2.3.2. Receiver

This is a resistance capacity coupled video frequency amplifier capable of undistorted amplification of the light pulse detected by a photocell. It is divided into two sections of which the first is mounted above the receiver mirror with the photocell. This gives sufficient pre-amplification for cathode follower low impedance coupling to the second section, and helps to minimise the mirror blanking effect. The maximum gain is about 80,000. This can be increased and manually controlled by a further video stage in the display unit. The photocell is of the vacuum type with a caesium-antimony cathode. It has a very rapid response characteristic and peak sensitivity at a wavelength of about 0.45 microns. The circular photocell aperture is 8 mm. in diameter and is placed horizontally with its centre at the focal point of the receiver mirror which is adjusted so that its optical axis is vertical. The focal lengths of transmitter and receiver mirrors are respectively $8\frac{5}{8}$ in. and 12 in.

2.3.3 Display unit

This produces a range trace on a 3 in. cathode-ray tube possessing a fast writing characteristic. Three time-bases are available with sweep times of 7, 20 and 40 μ sec. corresponding to height ranges 3,500, 10,000, and 20,000 ft. respectively.

The waveforms controlling the time-base triggering and positioning of cloud echoes on the trace are lettered C to H in fig. 2. The 25 μ sec. multivibrator pulse C is differentiated and inverted yielding a 5 μ sec. negative triggering pulse which fires a phantastron circuit. This circuit produces a variable width square wave F with leading edge time coincident with the primary pulse C. The back edge of F can be adjusted by fine and coarse manual controls to occur anywhere in the range 15 to 60 μ sec. after the leading edge. This back edge controls the triggering of the brightening waveform G and the time-base waveform H. The brightening waveform produces the necessary trace intensity for visual observation at the low recurrence frequencies (1 to 20 pulses per second) and fast time-base speeds concerned.

The back edge of waveform C is displayed on the range trace, and forms a step marker indicating th commencement of the trigger spark pulse B. At some definite time interval after this commencement the main spark fires. By deflecting a small fraction of the transmitter light pulse over a minimum path between transmitter and receiver, a correct zero cloud height position can be obtained relative to the displayed step marker (see fig. 6). This zero setting eliminates the errors due to the 25 ft. separation of transmitter and receiver, build-up time of trigger pulse and any delay in the emission of the main light pulse. The remaining absolute error of about 15 ft. due to the height of the small diffuse reflectors used to obtain the minimum light path, together with the height of the transmitter and receiver mirror assemblies, can be eliminated as a standard correction. This is not justified in the present equipment as 15 ft. only represents 0.015 μ sec. light time and the present stability is not better than 0.1 μ sec.

Height is measured on perspex scales mounted immediately in front of the cathode-ray tube face. These scales are ruled with respect to 500 ft. markers, supplied by a crystal controlled calibrator, and take account of any slight non-linearity in the time-base. Subsequent positioning of the zero error setting signal by the phantastron controls, ensures that range measurements obtained from the perspex scales are always correct. This would not be so if the whole time-base was moved laterally to produce such a positioning, unless it was perfectly linear, a condition very difficult to attain at the speeds involved. The fine phantastron control is calibrated directly in feet and facilitates rapid zero setting, i.e. the step marker can quickly be set on the scale zero and then moved back a distance equal to the zero setting error. This error is about 800 ft.

The mounting of the display unit next to the transmitter is convenient, since all the switches and variable controls are to hand. However, the noise of the transmitter spark is a little disturbing, but quite tolerable.

3. PERFORMANCE

3.1. General

The successful alignment of the meter with a separated assembly, has undoubtedly greatly enhanced its usefulness, by making possible the measurements of low cloud heights in the range excluded by the original assembly.

The calculated rise time of the electrical pulse producing the main spark is about 0.2 μ sec. The rise time of the light pulse is only about 1.2 μ sec. This broadening is undesirable and is mainly due to the finite build-up time of the light pulse and speed of response of the photocell. Further broadening in the receiver amplifier sections is very small. Stability of the back edges of waveforms C and F (fig. 2) and of the delay which represents the zero setting error, are the limiting factors governing the accuracy of range measurement. An average figure for this error in terms of cloud height is 100 ft.

3.2. Maximum range

This at present is about 15,000 ft. On one occasion only a persistent small echo was received from cloud at 18,000 ft. Position persistence is an important factor in considering maximum range, for small echoes can be detected down to and even below noise level, by discrimination between haphazard variation of noise amplitude at any given position on the range trace, and the persistence at a fixed position of the small cloud echo.

A greater maximum range could of course be obtained by certain changes which include: using better quality mirrors of larger diameter, and perhaps shorter focal length, together with an increased spark intensity.

3.3. Minimum range

This is limited only by the stability factors mentioned in 3.1. and the rapidity of leading edge build up of the cloud echo. It is clear from an examination of the photographs of low cloud and zero check echoes that the initial portion of the leading edge is very similar in both cases, and does not seem to be dependent on the nature of the cloud. From a study of the shape of the zero check echo, it is possible to fix a point which can be accepted as the commencement of the leading edge. By fixing a similar point on a surface fog echo, it was found to give zero range. However, when the same fog began to lift it was difficult to assess the height of the base until it had reached 200 ft. It is clear that by producing a more rapidly rising leading edge for the received light pulse, cloud height measurement over the range 0-600 ft. would be much improved. Above 600 ft. the present discrimination is reasonable.

3.4. Operation in precipitation

Operation during precipitation from cloud bases in the range 600-5,000 ft. has presented no difficulties. Experience outside this range is lacking at present. On one occasion of heavy precipitation a considerable "bump" was noted prior to the cloud echo leading edge. All precipitation, above a certain density, produces a lifting of the range trace before the commencement of the cloud echo. There is however no difficulty in defining the section of the displayed echo associated with the cloud base. Experience in snow is very limited, but echoes have been received. The main problem is the rapid clearing of housing roof windows for which some automatic sweeping mechanism would be required. All types of precipitation give rise to a certain degree of attenuation of the cloud echo, due to scattering by the particles concerned and effective destruction of the plane optical surface of the glass roof sections by the water or snow which reaches them. This results mainly in a reduction of maximum range performance.

4. RECOMMENDATIONS FOR IMPROVEMENTS

(1) A decrease in the width of the transmitter electrical pulse could probably shorten the rise time of the light pulse, and so give the desired increase in discrimination at low cloud heights. A narrower light pulse would also yield more cloud type and thickness information from the shape and width of the displayed echo. However, the finite time required for the build-up of the transmitter light pulse, and the response of the receiver photocell, may be the limiting factor preventing sharpening of the cloud echo leading edge. Nevertheless, if a spark gap condenser with lower self inductance than the present one becomes available, it would indicate whether the probable limiting factors were indeed real ones. Reduction in the condenser capacity should also be favourable, but the working voltage may have to be increased to maintain the same peak intensity in the light pulse.

(2) Provision should be made for rapid zero range error checking. Two small diffuse reflecting plane surfaces attached permanently to the mirror assemblies, and presenting only a small blanking effect would suffice. One could be permanently orientated correctly, and the other when necessary, in order to reflect fractional transmitter pulse energy over a minimum path into the receiver.

(3) A simple optical device to indicate when cloud is within the field of view of the meter should be available near the display unit.

(4) A single phantastron display shift control with a full range of 1000 ft. calibrated at 50 ft. intervals could replace the two existing controls.

(5) An iris mechanism fitted at the receiver aperture would enable optimum conditions for maximum signal to noise ratio to be attained.

(6) Better matching of pulse handling feeders would help in preserving pulse edges.

(7) Thermal delay switching, associated with a preset main spark voltage, could eliminate three switching operations. Push-button control of main spark firing could be available at the display unit.

(8) Many of the manual controls now available on the experimental model could be replaced by preset controls. (7) and (8) would result in the present meter being put into operation by two switches and one push-button. A single manual control would then fix zero range before a reading.

5. CONCLUSIONS

The present experimental cloud-base meter has given sufficient evidence to indicate that the pulsed-light principle will give satisfactory height data. The only important limitation is that the cloud must be directly above the meter. The range covered is from surface to middle medium cloud. This range can be extended upwards by increasing and concentrating the spark pulse energy. To cover large cloud height ranges it would probably be necessary to have two or more transmitter units of different power outputs. As the optical system need not possess the critical rigidity once considered essential, it should be possible to design a mobile equipment capable of alignment in a period of not more than one hour. In its present form an operator is required to switch on and take readings from the display unit. Automatic strobing of the cloud echo might now be possible as the permanent scatter pattern has been removed from the display. This would in turn make distant recording feasible. Alternatively it would be possible to have the display unit and all switch controls within the forecasting or other appropriate room, with the transmitter and receiver situated in the open, each unit not more than about 30 ft. from the display. It is interesting to note that the present type of transmitter and receiver could be used on a fixed base-line to give heights by altitude-angle determination as with the modulated cloud searchlight.

APPENDIX I

SOME ASPECTS OF TRANSMISSION AND REFLECTION THEORY APPLICABLE TO THE PULSED-LIGHT PROBLEM

The theoretical reasons for choosing radiation in the visible light region are explained in a T.R.E. Report (1) but two further points concerning the transmission, reflection, and absorption by water droplets at visible light frequencies are worthy of mention.

The diffuse reflection of short wave radiation by clouds or fog is practically constant for the wavelength range 0.1 to 1.0 micron (μ) (4) and the greater part of all the energy in the pulsed light spark is concentrated within this band. The percentage of the incident short wave radiation reflected from a cloud-base is dependent on cloud droplet size, liquid water content, and cloud thickness. In the T.R.E. report (1) reflection of 10% was assumed, but from theoretical data prepared by Hewson (3) it is seen that this figure can vary from about 1 to 95%. Hewson was considering solar radiation, but as its spectral distribution of energy is reasonably similar to that given by the transmitter spark, his data is equally applicable.

For a cloud 200 m. thick of medium density 1.0 gm./m.^{3} and drop radius 5 μ, the reflection is about 80%. Hewson gives a figure of 20 μ for typical fog droplets and shows that about 85% of incident light would be transmitted and emerge from the top of a fog 200m. thick of density 0.1 gm./m.^{3} whilst 38% would get through if the density were 1.0 gm/m.^{3}. This explains why two cloud echoes are possible from a single emitted light pulse. If penetration of the cloud or fog can be assumed to be complete, then the resulting effective widening of the displayed echo can be expected to yield cloud or fog thickness information.

The diffuse penetration of cloud by light must give rise to halation of the spark image at the cloud-base. The effective diameter of the image will depend on the nature of the cloud as indicated by the transmission and reflection data given above. Even in very thick cloud this halation will be appreciable, e.g. Hewson gives a transmission figure of 24% after 20 m. penetration of cloud of water content 5.0 gm./m.^{3} with drop radius 5 μ. It is this property which accounts for the operation of the meter at low cloud heights. Below about 700 ft. with a 25 ft. separation between transmitter and receiver, there is no intersection of the transmitter beam and receiver acceptance zone even after making allowance for the divergence due to the finite size of the spark and receiver aperture. It is also this effect which must account for the less critical alignment required for the optical system than was at first thought necessary.

Beam divergence is important when maximum range is considered. The acceptance zone of the receiver should be as narrow as possible, in order to collect minimum permanent light factor (i.e. day or night natural illumination) and so keep the receiver noise at a minimum level. This suggests a spark approaching point source dimensions in order to concentrate the transmitter beam and thus make possible a reduction of the receiver aperture. A compromise must be made in order to maintain sufficient energy in the spark. As small spark gap working implies lower voltages, a much larger capacity would be required in order to maintain the same energy, and the loop inductance in the spark gap circuit would have to be reduced to keep the pulse width narrow, and so maintain a satisfactory peak pulse power. Latest condenser manufacturing techniques together with new dielectric materials may make this improvement a possibility.

APPENDIX 2

SUMMARY OF NORTHOLT TRIALS REPORTS

Phase 1 trial was carried out with the compact version of the meter and Phase 2 with the present separated assembly. The summary of Phase 2 trial is treated in detail.

Phase 1 covered a period July 1951 to January 1952 and the report was prepared by Mr. G.A. Corby. During a period of routine comparison observations, made at standard observing times, no readings were obtainable on slightly more than half the occasions, mainly due to inability to operate in fog and precipitation, the serious masking effect of the permanent low level scatter pattern and absence of cloud directly above the meter. The serviceability of the equipment was of a high standard and extreme heights recorded were 9,000ft. and 500ft. Difficulties were experienced in reading the display accurately, and the controls and switches were considered to be too complex.

Phase 2 covered a period March to October 1954 and the report was prepared by Mr. G. Needham. Certain performance details obtained during the trial period, which have been included in the main report, have been omitted from this summary.

1. INVESTIGATION

The main aims of this trial were:

(1) investigation of very low cloud and fog echoes which was found impracticable during Phase 1.

(2) investigation of cloud echoes during precipitation.

(3) photographic recording of cloud echoes to facilitate investigations of echo characteristics under different weather conditions and for different cloud types.

(4) collection of further display data to serve as a check on or to develop further appropriate sections of Phase 1 work.

(5) a re-assessment of the operational usefulness of the apparatus following the modifications carried out.

About 500 observations were logged and over 350 photographs taken during the period. The observations were analysed and compared with official observations taken about a mile away. The comparisons were not considered a satisfactory basis for the assessment of height accuracy because of the time distance separation involved.

2. RESULTS

2.1. Accuracy

Absolute height accuracy has not yet been assessed. It is considered that only very accurate altimeter information from an aircraft operating directly above the meter would be satisfactory, in the absence of a recognised standard cloud height meter. Reading errors are assessed at 100ft. on the 2,500ft. time-base, 200ft. on the 10,000ft. time-base, and 300ft. on the 20,000ft. time-base. These inaccuracies are due to the slight instability of the cathode-ray tube trace, smallness of the cathode-ray tube, and coarseness of height scales.

2.2. Range

The effective range can be said to be 0 - 9,000ft. with a good chance of receiving some echoes from higher medium levels, particularly from altocumulus. The chances of obtaining a return of sizeable amplitude from thin medium cloud are remote.

2.3. Scatter from intervening medium

In smoke haze, "bumps" on the display trace are sometimes pronounced, particularly at close ranges. A tendency has been noted for these "bumps" to coincide roughly with the estimated level of low inversions. With cloud above thick haze, a clearly defined echo is still received and height measurement presents no difficulties.

2.4. Multi-layer cloud

Part of the transmitted beam has often penetrated through thin parts of, or gaps in, the lower cloud layer, to higher layer(s). On one occasion three echoes were picked up on a single trace. On several occasions there were two echoes but more frequently echoes from different levels appear singly on any given range trace.

2.5. Interpretation of cloud echoes

There is a general feeling that echoes with the most definite commencement to their leading edge, are associated with cloud of high density, such as cumulus and stratocumulus. The width of the echo is probably a function of depth of penetration. Fairly sharp echoes of large amplitude and narrow width are usually found with cumulus and stratocumulus type clouds. Variations in the height of a cloud with a ragged or undulating base is easily recognised on the display trace. When observing individual clouds (e.g. cumulus) echoes are sometimes obtained from the overhang and from patches of fractus cloud at levels above the real cloud base. On these occasions it is necessary to report the minimum return if the base of the cloud did in fact pass overhead.

3. USEFULNESS OF THE PRESENT PULSED-LIGHT METER

Reliability of operation, reasonably close limits of accuracy, and an effective range of 0 - 9,000ft. with a chance of receiving echoes from higher levels make the meter a very valuable observing aid. The pulsed-light method of cloud height determination has distinct advantages over all other methods at present used by the Meteorological Office. Naturally the pulsed-light reading cannot always be included in the official observation; the reported cloud height(s) are required to be representative of the local area, whereas the height(s) indicated by the meter relate only to the cloud directly overhead at the time; interesting pieces of cloud often by-pass the meter or take a considerable time in arriving overhead.

Increased observing accuracy is of importance to the forecaster. Significant information which the meter can provide includes the height of cloud base up to medium levels and the character of variation of low cloud base. Some observers' doubts regarding the character of the night sky can be removed by intelligent use of the meter display.

The usefulness of the meter has not yet been fully exploited owing to limitations in the existing equipment. Useful confirmation of the height accuracy would be obtained by the assistance of aircraft.

4. LIMITATIONS AND SUGGESTIONS FOR IMPROVEMENT OF THE PRESENT METER

An improvement in the signal to noise ratio might increase the information obtainable from the display. A higher cathode-ray tube resolving power is desirable, with a tube of say 9in. diameter. Higher positional stability of the range zero is required. The calibration scale requires further subdivision, which would be possible with a larger cathode-ray tube. Suggestions are:

divisions at 100ft. intervals on the 2,500 ft. time-base

divisions at 200 ft. intervals to 5,000 ft. and thereafter at 500ft. intervals on the 10,000 ft. time-base.

divisions at 1,000ft. on the 20,000 ft. time-base.

Although the range is limited to 9,000 ft. for consistent cloud echoes, this is more than adequate for operational use at aerodromes. The full range is however required for reporting and forecasting purposes. Any improvement in maximum range must not be at the expense of the precision of base measurements on low cloud.

The complexity of switching and manual control setting of the meter is considered too great. Some simplification is strongly urged.

It is recommended that the power supply of 80 volts at 1600 c/sec. be replaced by standard mains supply, 230 volts at 50 c/sec.

The noise of the main spark is somewhat disconcerting and sound proofing or removal from proximity with the display unit would be to advantage.

Automatic recording is desirable, particularly at busy aerodromes. Continuous recording would be a boon during spells of marginal weather. This involves strobe-locking and hence a difficulty in deciding at what signal level locking is to take place. The signal level should be high enough to prevent locking on a precipitation or haze scatter "bump". This would necessitate a correction to the base height corresponding to the distance up the echo leading edge at which locking takes place. Experience with an improved display would help in assessing the problem of automatic recording more thoroughly.

5. USEFULNESS OF THE PULSED-LIGHT METER IN MEETING THE OPERATIONAL REQUIREMENT FOR LANDING AND TAKE-OFF OF AIRCRAFT

As the measurement of slant visual range is still not possible, the immediate concern of Operators is the accurate reporting of cloud-base for assessing the landing critical height.

Runway visual range and visual range of obstacles in the exit path are the important factors for assessing safe take-off conditions. The cloud height should be representative of conditions along the glide-path. For the great majority of aerodromes the critical height will be 600 ft. or less.

Pulsed-light meter readings apply only to clouds directly overhead and, so to comply fully with the operational requirement, the meter must be situated on the approach path and, even so, cloud heights at more than one position on this path may be required. Different runways would require the installation of several sets, so that a mobile meter would be the only economical approach to the problem. Continuous operation of the meter in conditions of low cloud is very desirable.

The pulsed-light meter in its present form would not fit into this instrumentation pattern, but, if it could be made mobile and capable of continuously recording cloud heights when necessary, it would go far in helping to solve the operational problem.

To get the most out of the information displayed, operation by a meteorological observer, in addition to self recording, is recommended. It may be possible to obtain slant visual range with the meter, if the mirrors can be lowered to the appropriate angle, and their beams made to intersect over the whole length of the visibility path considered. This possibility should be investigated. Success will depend on true absorption being negligible, compared with reflection and transmission, and that the path concerned traverses a fairly homogeneous medium. Comparisons would have to be made with air to ground slant visibilities, to assess the change imposed by the different backgrounds.

Regardless of the difficulties in meeting the full operational requirement, the value of the pulsed-light meter as an observing aid has been proved, and this is in itself sufficient justification for the development of a production model. Increased reporting accuracy is a step in the right direction towards reduction in the number of aircraft accidents, and an improved economy of aircraft operation.

Acknowledgements are gratefully offered to Mr. G.A. Corby and Mr. G. Needham for the patience, enthusiasm and helpful criticism given during the respective trial periods of the meter at Northolt, and for preparing very useful reports on these trials.

Mr.R.K. Pilsbury is to be especially thanked for his patient work in obtaining the excellent photographic records of the meter display, covering all types of cloud within the range of the meter, fog, haze and zero error checks.

References

1. Whitehead, J.R. and Fance, D.F.;
An introduction to pulsed-light technique.
T.R.E. Report No. T 2063, March 1947.

2. Hooper, J.E.N. and Dunn, R.F.H.;
A pulsed-light cloud-base indicator.
T.R.E. Report No. T.2133 August 1950.

3. Hewson, E.W.;
The reflection absorption and transmission of solar radiation by fog and cloud.
Quart. J.R. Met. Soc., London, Vol. 69, No. 298, Jan. 1943.

4. Olbers, W.;
Grundlagen der objectiven Wolkenhohenmessung.
Technische Mitteilungen des Instrumentwesens des deutschen Wetterdienstes. Deutscher Wetterdienst, Hamburg, 1955.

Figure references of photographs.

Fig. 3. General view of cloud-base meter showing the transmitter and display housing on the right, and the receiver housing on the left.

Fig. 4. Transmitter and display unit housing. The transmitter chimney shield has been lifted to reveal the mirror and spark gap assembly.

Fig. 5. Receiver unit with housing removed.

Fig. 6. Zero check echo showing separation between step marker and commencement of echo (upper scale).

Fig. 7. Surface fog indicating zero height. (upper scale)

Fig. 8. Lifted fog at 200 ft.
Compare with fig. 6. Height obtained from the calibrated scale (upper) includes the zero error.

Fig. 9. Stratus at 500 ft. received through moderate rain. (lower scale)

Fig. 10. Fractostratus at 800 ft. (upper scale)

Fig. 11. Cumulonimbus at 2,100 ft. received through moderate shower showing effect of precipitation before main echo.

Fig. 12. Cumulus at 3,100 ft. (lower scale)

Fig. 13. Cumulus at 4,000 ft. with stratocumulus above at 5,600 ft. (lower scale)

Fig. 14. Stratocumulus at 4,500 ft. (lower scale)

Fig. 15. Altostratus-altocumulus at 6,700 ft. with evidence of second echo at 8,000 ft. (lower scale)

Fig. 16. Altocumulus at 9,600 ft. double trace. (lower scale)

Fig. 17. Altocumulus at 14,000 ft.

Fig. 18. Four separate traces showing effect of smoke haze on evening of November 5, 1954. No cloud overhead at time. (lower scale)

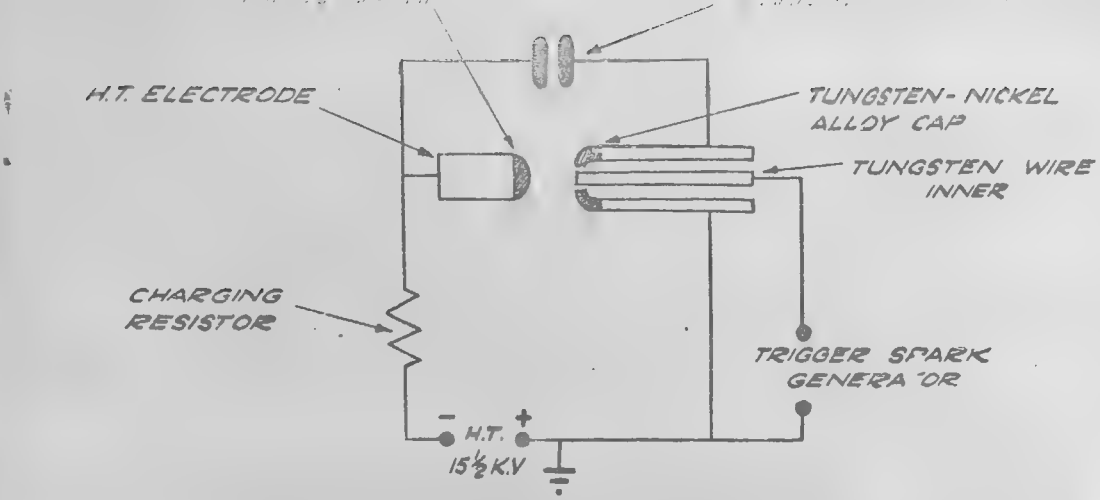

FIG. 1

BASIC ARRANGEMENT OF SPARK GAP CIRCUIT

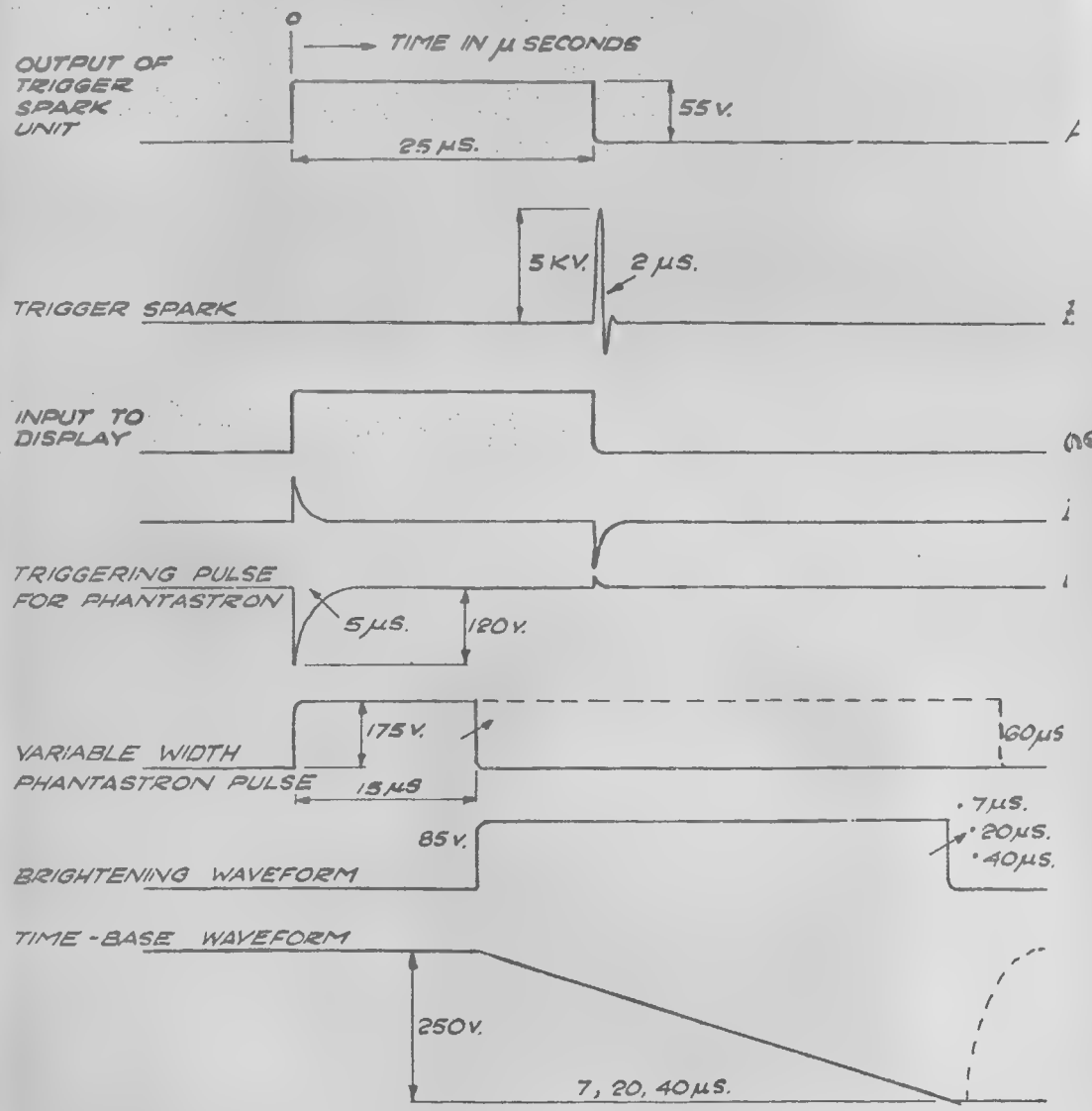

FIG. 2

DISPLAY UNIT WAVEFORMS

Fig. 3. General view of cloud-base meter.

Fig. 9. Stratus at 500 ft.

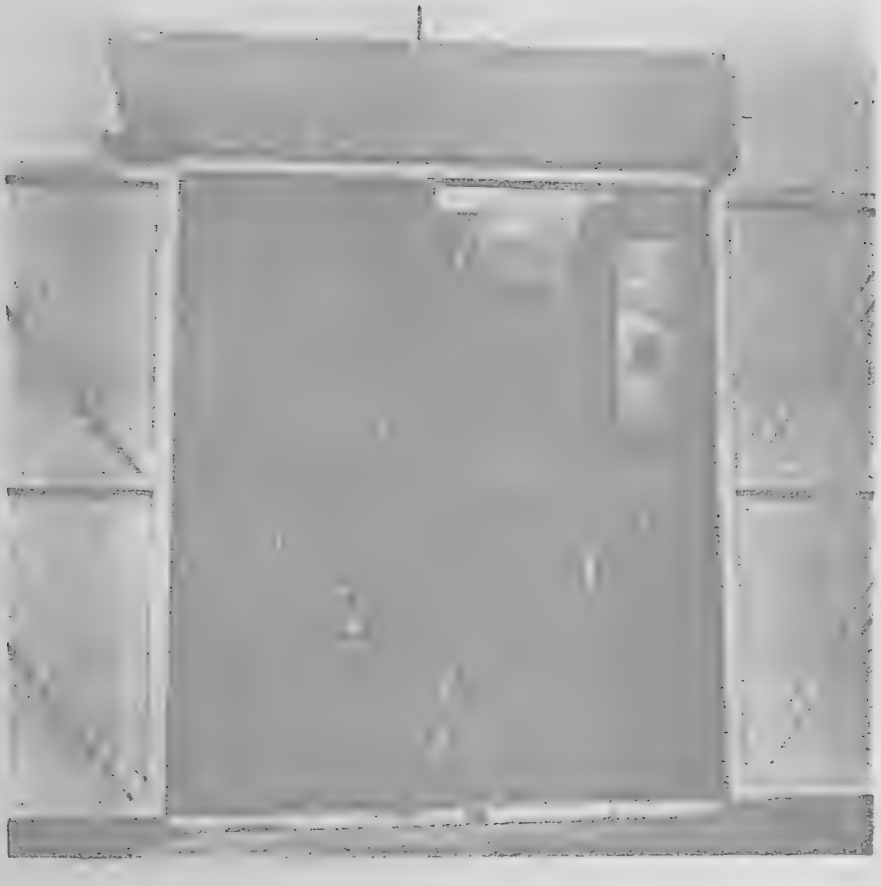

Fig. 4. Transmitter and display unit.

Fig. 10. Fractostratus at 800 ft.

Fig. 5. Receiver unit.

Fig. 11. Cumulonimbus at 2,100 ft.

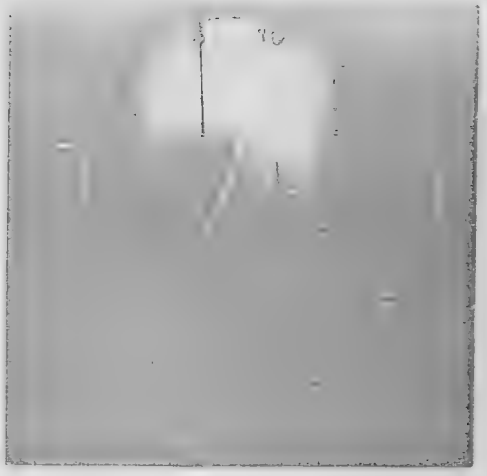

Fig. 6.
Zero check
echo.

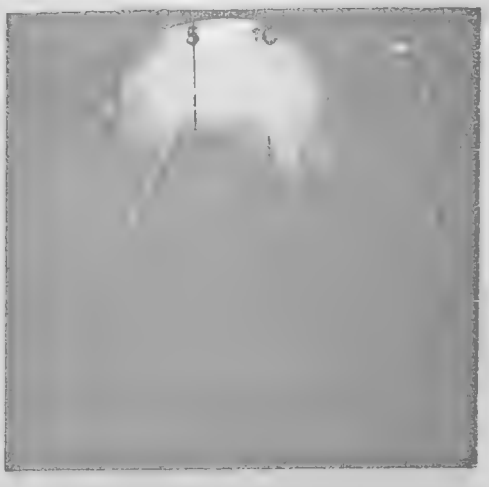

Fig. 7.
Fog

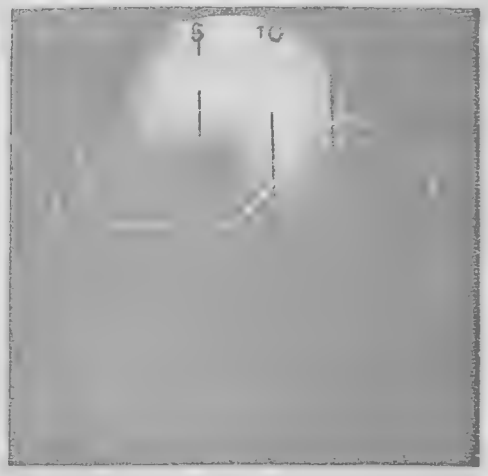

Fig. 8.
Lifted fog
at 200 ft.

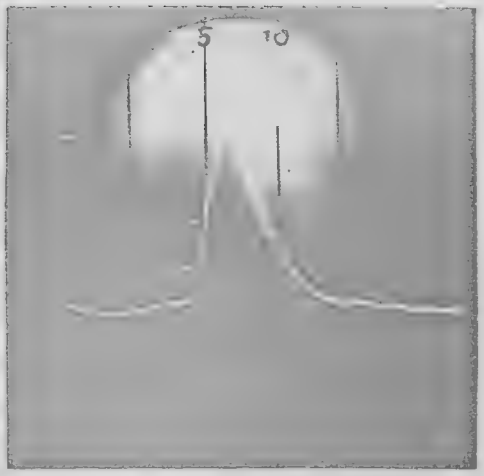

Fig. 12.
Cumulus at
3,100 ft..

Fig. 13.
Cumulus at 4000 ft.
stratocumulus
at 5,600 ft.

Fig. 14.
Stratocumulus
at 4,500 ft.

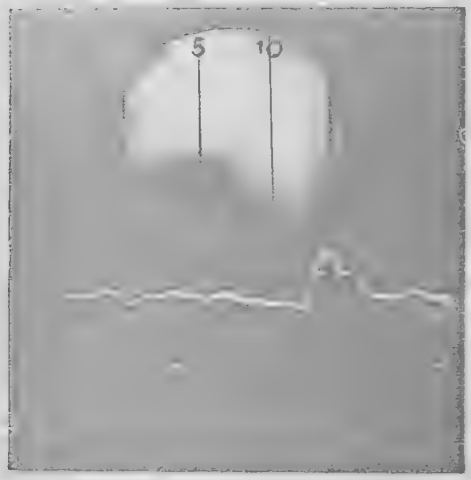

Fig. 15.
Altostratus
altocumulus
at 6,700 and 8,000 ft.

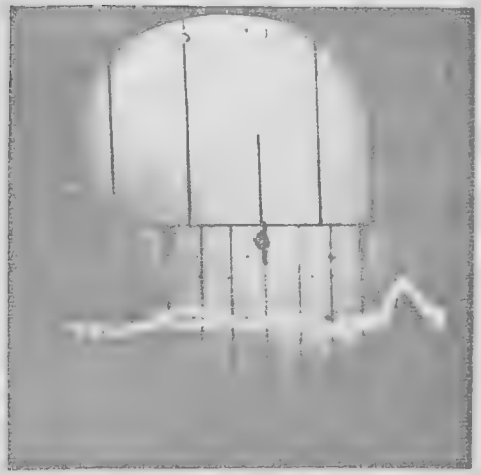

Fig. 16.
Altocumulus
at 9,600 ft.

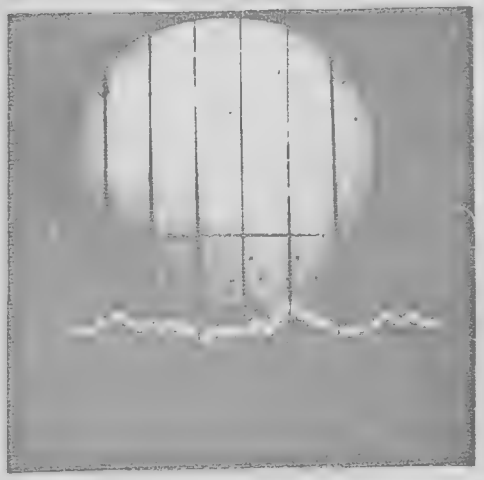

Fig. 17.
Altocumulus
at 14,000 ft.

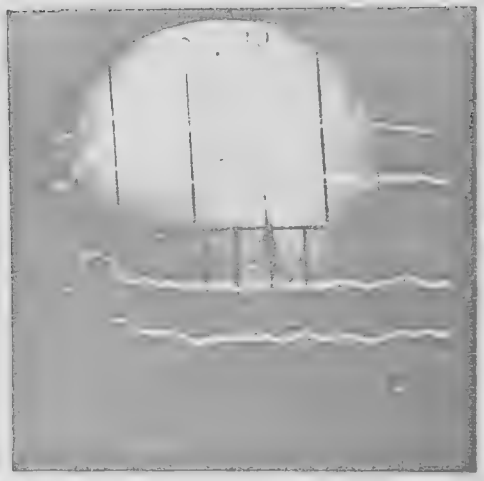

Fig. 18.
Smoke haze
(four traces)

UNCLASSIFIED

UNCLASSIFIED

M.R.P. 943
S.C. 1/108
28th September, 1955

Fog Density Indicator

by

J. R. Bibby
(Meteorological Office)

AIR MINISTRY
METEOROLOGICAL RESEARCH COMMITTEE

At the time of issue this report has not been published. Any author desiring to quote this paper should refer to it as "A paper of the Meteorological Research Committee (London).
M.R.P. No. 943 by Mr. J.R. Bibby.
A copy is available in the Library of the Meteorological Office".

M.R.P.943.
S.C.I./108
28th September, 1955

AIR MINISTRY

METEOROLOGICAL RESEARCH COMMITTEE

Fog Density Indicator

by

J.R. Bibby (Meteorological Office)

Historical

Development started in 1950 with a request by the Ministry of Civil Aviation for a method of measuring the depth of a fog layer, and preferably also the variation of visibility with height, up to at least 500 ft. The most practicable method appeared to be to measure the scattering of light in the air by an instrument carried on a tethered balloon.

At first it was hoped to make an instrument which could be used in daylight as well as darkness. A model was made, using a series of baffles to exclude daylight, but it proved too heavy for the radio-sonde balloons it was proposed to use. Also it appeared that there would always be doubt whether the air inside was representative of that outside. A much simplified instrument was therefore designed for use in darkness only. It weighs (without batteries) about 750 grams.

2. Description

A simplified drawing of the instrument is shown in Fig. 1. A "sandwich" is formed from two sheets of perspex $9\frac{1}{2}$ in. x $7\frac{1}{2}$ in. x $^1/10$ in. thick, each with a rectangular hole $3\frac{1}{2}$ in. x $2\frac{1}{2}$ in. in the centre. Between them, 24 barrier layer photocells 2 in. x $1\frac{1}{2}$ in. are arranged in a double layer facing outwards with a strip of rubber separating the two layers, and strips of copper foil making connection with the cells. The inner and outer edges of the sheets are then cemented together with strips of perspex and the whole made waterproof with a solution of perspex in chloroform. A pair of leads is fitted to allow connection to the photocells (which are all in parallel). In the central hole are placed three filament lamps (6 volts 12 watt). No lamp holders are used (for lack of space) the lamps being fixed in a wire frame with soldered electrical connections. Around the lamps is a metal strip, just wide enough to prevent any light reaching the photocells directly.

Provided the instrument is mounted so that there are no objects within about 50 ft. of it (except in its own plane) and there is no fog or mist, no light can reach the photocells from the lamps, and the current from the cells is very low (less than 0.2 microamp). If fog is present, however, light from the lamps is reflected by the fog particles and a current is generated by the photocells. This current should be roughly proportional to the scattering coefficient of the air, i.e. inversely proportional to the visibility.

3. Method of use

As stated above, it can only be used in darkness, and must be mounted well away from any other object, which implies, for best results, at least 50 ft. above the ground. Normally it is fixed at one edge to the flying cable of a tethered balloon, at least 20 ft. below the balloon.

/An

An accumulator to supply the lamps (6 amp. at 6 volts) must also be carried, though for restricted heights a transformer fed by a length of mains cable could possibly be used. In any case some means of switching the lamps on and off is needed, not only to reduce the drain on the battery, but to check any photocell current due to moonlight or artificial lights. If a remotely controlled switch presents difficulties, an automatic switch controlled by clockwork (or a heated bimetal system) can be used to switch the lamps on for, perhaps, five seconds every thirty seconds.

The galvanometer should have a full scale deflection of about 5 microamp. Its resistance (plus that of the cable to the photocells) should not exceed a few hundred ohms, and a mirror type is therefore necessary. The cable to the photocells can be fairly light, but must be very well insulated in view of the very small currents it carries, and the damp conditions in which it is used.

4. Results obtained

Tests at Cardington have confirmed the expectation that the photocell current would be inversely proportional to the visibility, the approximate relationship being:

Current x visibility = 300 microamp. yards.

For comparison, the following figures may be quoted:

Instrument in moonlight with lights off: current = 0.5 microamp.
Instrument in darkness, clear air, with lights on: current less than 0.2 microamp (but more if leads to lamps and cells are not kept carefully in the plane of the instrument).

Instrument 7 ft. from the ground with lights on: current = 3 microamp.

5. Conclusions

The instrument has been chiefly useful in finding the height of the base or top of a clearly defined layer of cloud or fog. It also gives a rough indication of the fog density, but its accuracy is likely to be limited by sampling errors, for most of the light reaching the photocells comes from the fog within one or two feet of them.

Its chief disadvantage is that it cannot be used in daylight. Other disadvantages which may restrict its use in some cases are: it cannot be used near the ground, or near other objects; its power requirements are rather large for a tethered balloon to carry; it needs rather a delicate galvanometer.

M.R.P. 943

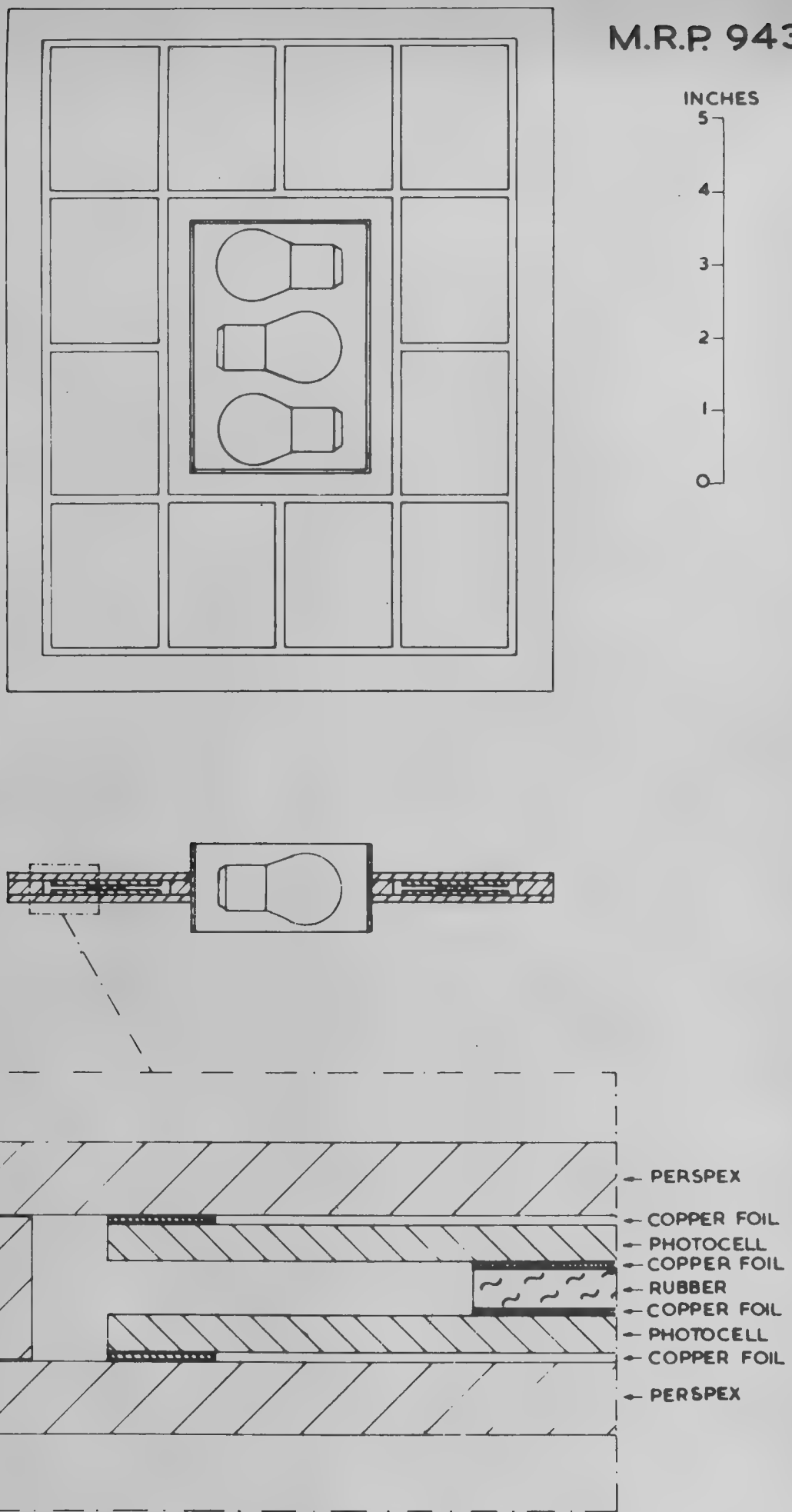
INCHES
5
4
3
2
1
0
PERSPEX
COPPER FOIL
PHOTOCELL
COPPER FOIL
RUBBER
COPPER FOIL
PHOTOCELL
COPPER FOIL
PERSPEX

FIG.1

M.R.P. 946
S.C. 111/195
22nd November, 1955

Ozone concentration measurements from an aircraft in N. Norway

by

A. W. Brewer.
(Clarendon Laboratory Oxford)

AIR MINISTRY
METEOROLOGICAL RESEARCH COMMITTEE

At the time of issue this report has not been published. Any author desiring to quote this paper should refer to it as "A paper of the Meteorological Research Committee (London), M.R.P. No. 946 by Dr. A.W. Brewer. A copy is available in the Library of the Meteorological Office."

M.R.P. 946
S.C.III/195
22nd November, 1955

AIR MINISTRY

METEOROLOGICAL RESEARCH COMMITTEE

Ozone concentration measurements from an aircraft in N. Norway

by
A. W. Brewer (Clarendon Laboratory, Oxford)

Introduction

As a result of a suggestion of D. Tönsberg of the Nordlys Observatoriet at Tromsö, that the Norwegian Air Force would, if suitably approached, provide us with aircraft facilities, a visit was made to N. Norway from April to July of 1955 to make measurements of the vertical distribution of ozone and water vapour. The work was part of a general programme to determine the world wide distribution of ozone and represents an extension of the work of Kay (with Brewer and Dobson) in S. England. (Kay, 1953). The expedition was supported by the Royal Society. There is especial interest in N. Norway because of its high geographical latitude (Tromsö is at 70°N) and the Nordlys Observatory has made a long series of total ozone measurements there, and also "Umkehr" curves, from which some information about the vertical distribution of ozone can be obtained.

Equipment used

The meteorological equipment taken was:-

1. A standard M.O. pattern balanced bridge aircraft air temperature thermometer.

2. An automatic dew-point hygrometer with pressurised test chamber, so that compressed air from the jet engine could be used.

3. The ozone sampler which was used by Kay and was loaned back to us by the Meteorological Research Flight for the expedition. The sampler had been in the possession of the M.R.F. for some time. It had been modified by the M.R.F. for electric instead of mechanical operation; this improvement proved very valuable.

The thermometer and the hygrometer were carried to provide simultaneous data so that the ozone concentration could be correlated with the temperature and humidity structure.

Installation in aircraft

The instruments were installed in a Vampire trainer (two seater) the only suitable aircraft available. The installation, which was made as simple as possible, was completed by R.N.A.F. ground staff in two weeks and in early May the aircraft and crews were moved from Trondheim, where the installation work was done, to Bardufoss near Tromsö for the operational flights.

Early flights

During May four ascents were made to 40,000 feet but after some early doubts it became clear on the fourth ascent that the ozone sampler was not in fact working satisfactorily and that from the ozone point of view these ascents were abortive. Careful tests showed that ozone was being absorbed in the pipes in the sampler leading to the analysing tubes, and on dismantling the apparatus it was found that these were encrusted internally with what appeared to be dried solutions and the products of corrosion of brass and copper. Attempts to clean the apparatus at Bardufoss occupied about two

weeks but failed, and it was decided to return to Trondheim.

At Trondheim, after repeated attempts to get the apparatus to work correctly, it was decided to rebuild all necessary parts of gold, glass or anodised aluminium. Anodised aluminium seemed, on consulting the available literature, to be the most suitable base metal. This took about ten more days. In carrying out this work Professor Westin of the National Technical High School at Trondheim gave substantial assistance.

With these modifications all the tests which could be made at Trondheim suggested that the sampler was now working satisfactorily, and measurements of the ozone concentration made in flight at 1500 feet gave substantially the same value as that obtained near the ground as measured by the techniques tested in the Westmorland experiments described by Kay (1953). The aircraft and men then returned to Bardufoss.

Final flights

Four ascents were then made between 24th June and 12th July. The results of these four ascents are given graphically in Figs. 1, 2, 3 and 4.

It will be seen that except for the ascent of 28.6.55 the ascents show approximately constant concentration (cm./Km. or $\mu g/\rho^3$) up to the tropopause, corresponding to about a 3-1 increase in mixing ratio. On 28.6.55 the concentration approximately doubled between 15,000 feet and the tropopause. All the ascents, but particularly those of the 27th and 28th of June, show a large increase in ozone concentration at the tropopause but the increase is much smaller on 11th July when the ascent was in an air stream of tropical maritime origin.

These results are to be compared with those of Kay (1953), who found that on the average there is no marked change in the ozone concentration at the tropopause. It is possible that this is a real geographical difference or it may be that Kay's results were affected by ozone absorption in the pipes, and this point must be investigated. It is also possible that the accumulation of dirt in the pipes is responsible for the smaller amount of ozone recorded in the stratosphere in the last two flights when compared with the first and second.

The general feature of an increase in ozone concentration at the tropopause is of course a reasonable one and the increase observed is of about the correct amount to account for the observed correlation between total ozone amount and tropopause height. A very variable lower stratosphere concentration would account for the rather low correlation coefficients which are sometimes obtained.

Further work

In view of these results it is very desirable to carry out a considerable amount of further work and it is hoped that this may be possible with the assistance of the Meteorological Office.

1. It is essential that further tests be made with the sampler to ascertain whether the risk of absorption of ozone in the piping is still serious or whether it can be eliminated completely. Fortunately the Vampire used in N. Norway has now been sold to the R.A.F. and arrangements have been made for the aircraft to be available at the M.R.F. for a short time to carry out tests on the actual installation.

2. Sufficient ascents must be made in S. England with a thoroughly tested apparatus to check Kay's results.

/3.

3. If the changes of stratospheric ozone observed in these ascents in N. Norway are real it may be associated with either different air masses or with the annual variation of ozone or both, and it would be most desirable to learn more about the mechanisms involved. Observations in S. England may show something of the former but the annual effect could be best investigated in N. Norway where the total ozone has a large annual variation. In particular during December and January there is a very rapid increase in total ozone, and observations from an aircraft made at that time would show whether the increase is occurring in the lower stratosphere. Simultaneous temperature and humidity measurements would also form a useful investigation of the polar tropopause structure, about which we know so little.

Acknowledgements

The British Council and the British Air Attaché in Oslo made the arrangements for the visit and were most helpful in many ways during the course of the work. The Royal Norwegian Air Force provided the aircraft, carried out all the installation work, and provided all flying facilities, and helped in every way possible. It is a great pleasure to acknowledge the generous assistance which I received in every way and from everyone concerned in the R.N.A.F. It is also a pleasure to acknowledge the help I received from Professor Westin, National Technical High School, Trondheim and from Ing. Gisle Dyvik also of the N.T.H., when I was in difficulties with the sampler. The Gassiot Committee of the Royal Society paid personal travelling expenses.

Reference

Kay, R. H. 1953 Meteorological Research Papers, Air Ministry, London. No. 817.

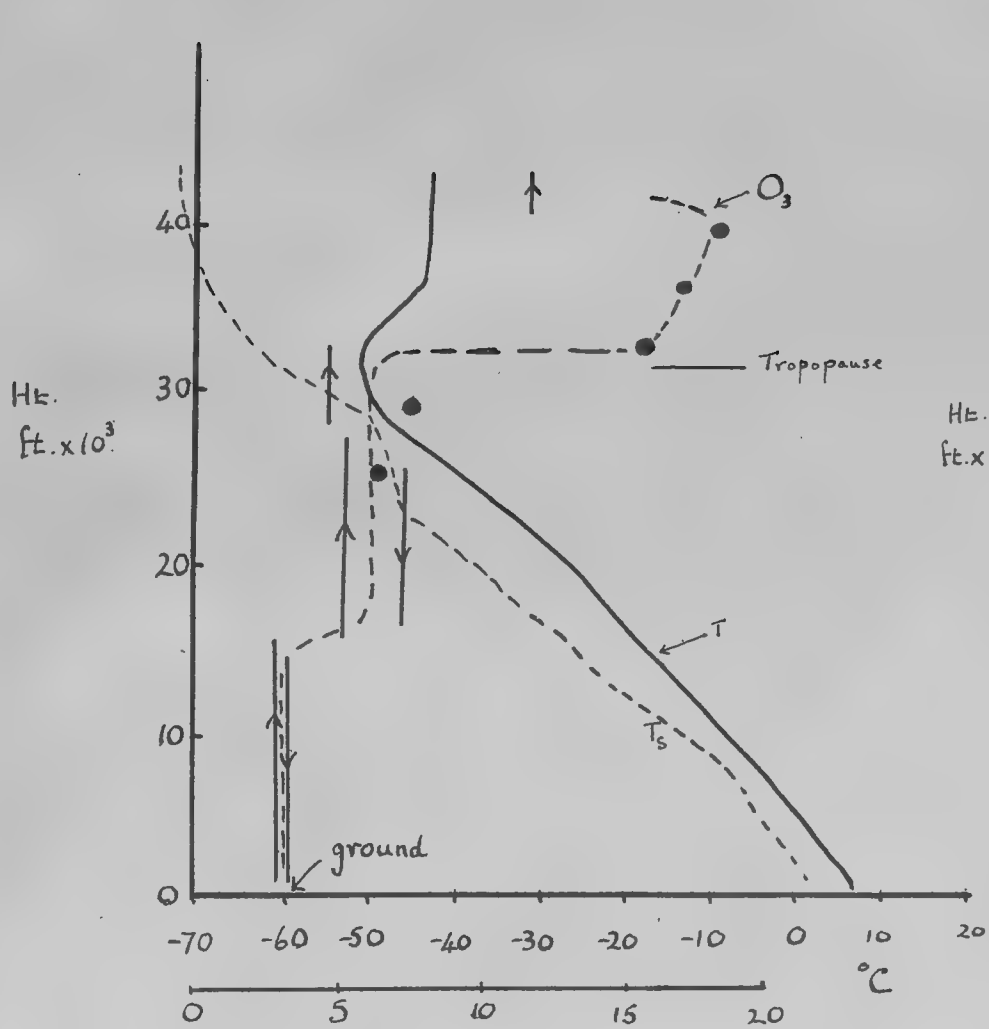

28.-6.-55. total O_3 = 0·248 cm.

Fig. 2.

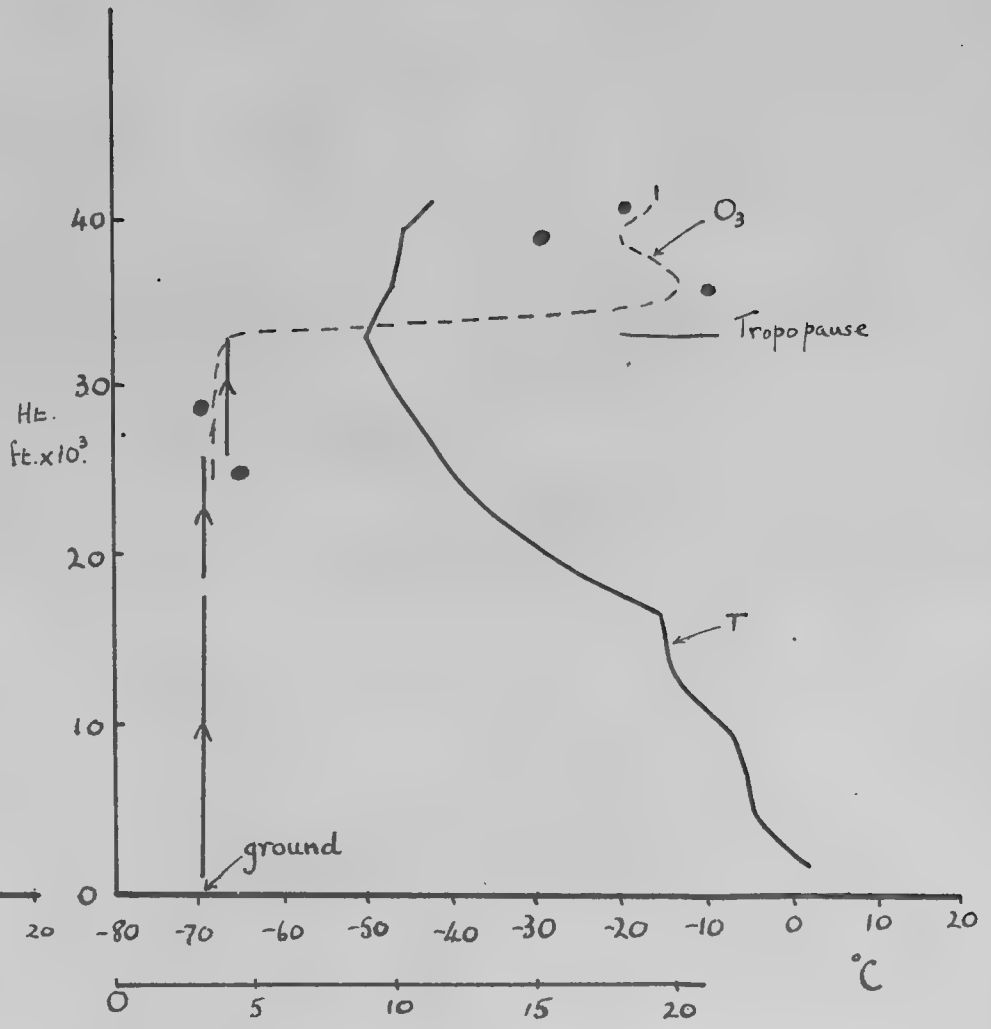

27.6.55. total O_3 = 0·256 cm.

O_3 concentration ●---●

O_3 concentration, measured while climbing or descending ↑ or ↓

Fig. 1.

M.R P. 949
S.C. 11/201
14th February, 1956

Some aspects of variations of air and sea surface temperature in short periods at ocean weather stations I and J of significance to the synoptic climatologist

by

R. F. M. Hay

(Meteorological Office)

AIR MINISTRY

METEOROLOGICAL RESEARCH COMMITTEE

At the time of issue this report has not been published. Any author desiring to quote this paper should refer to it as "A paper of the Meteorological Research Committee (London).
M.R.P. No.949 by Mr. R.F.M. Hay.
A copy is available in the Library of the Meteorological Office".

M.R.P. 949
S.C.II/201
14th February, 1956

AIR MINISTRY

METEOROLOGICAL RESEARCH COMMITTEE

Some aspects of variations of air and sea surface temperature in short periods at ocean weather stations I and J of significance to the synoptic climatologist

by

R.F.M. Hay (Meteorological Office)

CONTENTS

1. Summary
2. Introduction
3. Analysis of the data
4. Sequences of five day mean air and sea temperature values
5. Air and sea temperature differences between stations I and J
6. The magnitude of air-minus-sea temperature differences in cyclonic and anticyclonic situations
7. Air and sea temperature anomaly changes in cyclonic and anticyclonic situations
8. Air and sea anomaly changes with persistent winds
9. Serial correlation between air and sea temperature anomalies
10. Advection of sea surface temperature by surface currents
11. Sea surface temperature changes in five-day periods related to the energy exchange between sea and atmosphere
12. Advection of heat by ocean currents
13. The synoptic-climatological significance of short period variations of air and sea temperatures in the N.E. Atlantic
14. Conclusions

/1. Summary

G.37837/JEK/12/55/50

1. Summary

The almost continuous manning of the ocean weather stations I and J in the North Atlantic* by British and Netherlands ocean weather ships during 1948-52 has provided a series of records which for the first time are sufficiently detailed to enable short period fluctuations of meteorological elements at fixed points over the open sea to be studied in detail. The present study first deals with the seasonal distribution of air-minus-sea temperature differences and then with short period changes of air and sea surface temperature anomalies related to cyclonic and anticyclonic conditions and predominating spells of wind from various directions.

The influence of these factors upon the rates of change of the anomalies is found to be small though not without features of interest. Serial correlation coefficients were then determined between air and sea temperature anomalies, the effect of persistence being taken into account. A significant correlation between simultaneous air and sea temperature anomalies was found for summer but not for winter. Some evidence has been obtained which strongly suggests that sea temperature changes are largely imposed by air temperature changes. Changes in sea surface temperature which could be effected possibly by advection of surface water due to ocean currents (assuming no change in temperature from any other cause) were evaluated for a limited number of occasions in summer, when complete ocean current data were available. It was found that temperature changes resulting from this cause alone would have been very small in comparison with short period fluctuations of sea surface temperature brought about by energy exchange through the sea surface. The net energy exchange through the sea surface was computed for a number of five-day periods in summer and winter, and the results were used to make a comparison between the magnitude of the sea surface temperature changes actually observed in certain five-day periods, and the corresponding values of the changes derived by computing them from the figures for the net energy exchange. In accordance with the physical conditions of the problem, the agreement between actual and calculated values of sea surface temperature change was found to be much better in summer than in winter. Lastly, evidence is produced in support of the argument that short period variations of air and sea temperature are closely inter-related with the distribution of sea temperature through the topmost layers of the sea at various seasons, and with the behaviour of the 1000-500 mb. thickness lines during meridional movements of air masses over the region.

2. Introduction

The surface data for the ocean weather ship stations I and J for the five years 1948-52 have been analysed to investigate the magnitudes of air and sea surface temperature variations over periods of 1, 5 and 10 days or longer in relation to other meteorological elements.

3. Analysis of the data

A period of five days was judged to be the most suitable interval of time for use in the work having regard to the conservative nature of sea temperature. Accordingly the first step was to evaluate five-day means of air and sea temperature, pressure, mean vector wind and total cloud amount. The results are given in Table 10.

The procedure adopted in preparing these data was as follows. In each year 1948-51 the same days of the month were used for corresponding pentads e.g. January 1-5, 6-10, up to December 27-31, the extra day of

/29th February,

*For convenience throughout this paper these ocean weather stations will be referred to as I and J. Their positions and official descriptions during the period 1948-52 were as follows:-

ITEM 60°00'N. 20°00'W. to 0800 G.M.T., 25th March, 1950;

INDIA 59°00'N. 19°00'W. after 0800 G.M.T., 25th March, 1950;

JIG 53° 50'N. 18°40'W. to 0230 G.M.T., 25th March, 1950;

JULIETT 52°30'N. 20°00'W. after 0230 G.M.T., 25th March, 1950

29th February, 1948 being omitted from the pentad 25th February to 1st March. 8 observations in each day were used so that, as a rule, the mean value of an element through a pentad is based upon 40 observations. In the case of mean vector winds, observations for 0000, 0600, 1200, and 1800 G.M.T. were used to reduce the work of computation so the corresponding mean values are based upon 20 observations. Observations used were those when the ships were "on station", that is to say within a square grid whose sides at their nearest were 105 miles distant from the station positions I and J. (A check made for a different purpose upon 3 years' data for station J showed that over 90% of the observations were made within 60 nautical miles of the station position.) The position of I was 60°00'N. 20°00'W. and of J was 53°50'N. 18°40'W. from 1st January, 1948 to 25th March, 1950; for the remainder of 1950 and throughout 1951 and 1952 the position of I was by international agreement 59°00'N. 19°00'W. and of J was 52°30'N. 20°00'W. These changes of station position made in March, 1950 introduced complications which are dealt with at a later stage.

The period 1948-51 was selected for study in this part of the work because the number of pentads for which observations are completely missing at one or both ocean weather stations was quite small*. It was also necessary to take account of the fact that some data were missing in a number of other pentads. The criterion adopted was that a pentad which only contained 36 observations or less (out of a possible total of 40 observations) was excluded from discussion. In the case of mean vector winds where the number of observations used through a pentad was 20, the same rule was followed for pentads containing less than 16 observations.

4. Sequences of five-day mean air and sea temperature values

The variations of air and sea temperature at both stations for all available pentads during 1948-51 were first studied by means of graphs. Figs. 1 and 2 reproduce the data for 1948 and 1949; the other years differ only in detail. The main features shown are:-

(i) Although the magnitude of the variation of air temperature through several pentads greatly exceeds that of the sea temperature change through a corresponding period, the curves showing variations of air and sea temperature usually run fairly parallel, indicating some positive correlation between them. Changes of sea temperature usually occur during the same pentad as changes of air temperature, occasionally there is a delay of one pentad. The magnitudes of changes of sea temperature between consecutive pentads are much smaller than the corresponding changes of air temperature. Koizumi[1] has recently published similar diagrams for the Pacific ocean weather station E.

(ii) The magnitude of air temperature changes between one or more successive pentads is markedly greater between October and April than in the summer months. At station I five-day mean values sometimes varied by 8-12°F. within 15 days between December and March, associated with outbreaks of Arctic air.

(iii) At both stations the air was colder than the sea at the same

./time

*Although material for 1952 was available, it was not included in the period studied in this part of the work because in that year the vessel on duty at station I was displaced from the normal position of the station for special purposes, during rather lengthy periods.

The numbers of pentads for which data were completely missing at the stations I and J during 1948-51 were as follows:-

	I	J		I	J
1948	4	3	1951	9	0
1949	2	0			
1950	7	1			

time during most of the pentads considered. There were few pentads when the air was warmer than the sea at station J, and even fewer at station I during 1948-51. The pentads when the air was warmer than the sea mostly fall in the months May to August; May and June having the largest number. Exceptionally, mean air temperature rose above mean sea temperature at I from November 22-26, 1948 and at J from January 31 - February 4, 1949. Strong southerly pressure gradients persisted in the area of the ocean weather stations during both these periods. They were associated with pronounced blocking anticyclones (and upper warm pools or warm ridges) which formed initially over or just to west of the British Isles and drifted slowly eastwards during the periods considered.

(iv) The fall of sea temperature in autumn was largely independent of air temperature changes. This was well shown at station I during October and November, 1949 (Fig.2). In these months the rate of fall of sea temperature was much greater (even through succesive five-day periods when air temperatures showed little change) than the corresponding falls observed in most winter months during outbreaks of Arctic air. This effect appears to be largely due to mixing of surface water warmed in summer with cooler layers below, but part of it may be ascribed to seasonal radiation loss.

(v) The seasonal variations of sea surface temperature shown by the data for the pentads in individual years (Table 10), as well as when expressed as thirty-day running means (Fig.3), also include the same features as are shown by monthly data. They also bring out how small are the variations which occur in sea surface temperature between January and March in these localities. In most years they are $< 2°F.$ and the warming of the sea surface begins fairly abruptly at a date which may vary from mid-March to mid-April. The coldest pentad of the year occurred as late as April at station J in 1950 and at I in 1951. In the summer months two nearly equal maxima sometimes occurred. Usually the warmest pentad was found in August, but it occurred in September at station I in 1949.

5. Air and sea temperature differences between stations I and J

Air temperature differences, station I minus station J, and the simultaneous sea temperature differences were examined for corresponding pentads through the four years. The sea temperature difference values for 1948, when the data were most complete, (Fig.4), show a considerable degree of persistence, with changes of magnitude of the same sign maintained more or less uniformly over 35 to 40 days. In 1950, as far as can be determined from incomplete data (see Table 10), (I - J) for sea temperature decreased from -3.8°F. in mid-June to +0.1°F. from 24-28 August. In Fig.4 these variations are shown from April to September, 1950, and it can be seen that for part of this period there was an unusually small difference between sea (and air) temperatures at I and J which persisted through several weeks. Corresponding with this period, sea (and air) temperatures at I were above normal and at J below normal. The two stations were $7\frac{1}{2}°$ of latitude apart all through that time. Mean differences (I - J) for sea and air temperatures for each pentad have been computed using the 1948-51 data, although this period is scarcely long enough to provide reliable values. Sea temperature differences (I - J) appear to reach a minimum in late December (about -2.6°F.) and thereafter slowly increase to a maximum in late September when the value is around -4.8°F. For air temperature differences (I - J) the corresponding values are -3.0 to -3.5°F. in summer increasing to -5.5 to -6.5°F. in late winter and early spring.

6. The magnitude of air-minus-sea temperature differences in cyclonic and anticyclonic situations

For the purpose of obtaining auto-correlation coefficients between air and sea temperature anomalies as described later in the first paragraph of Section 9, it was

/decided

decided to compute one-day mean values of pressure and of air and sea temperatures together with anomalies for station J only for the years 1948-52, each mean being based upon 8 observations a day. (This procedure could not be followed for station I since the data were less complete.) These data were in a form suitable for investigating the magnitudes of air-minus-sea temperature difference in relation to the prevailing pressure distribution. The simplest means of doing this appeared to be to select markedly cyclonic and anticyclonic occasions by picking out the five days in each separate month having the largest negative and positive pressure anomalies respectively; then to combine the results for individual months into seasons and thus obtain the seasonal means of air-minus-sea temperature differences on days of low and high pressure. Table 1 gives the results.

Table 1 — Means of air-minus-sea temperature difference (°F.) related to surface pressure, for Station J (1948-52)

Season	Winter (Dec.-Feb.)	Spring (Mar.-May)	Summer (June-Aug.)	Autumn (Sept.-Nov.)
Pressure type				
Low*	$-4.58_{(55)}$	$-1.99_{(75)}$	$-0.67_{(60)}$	$-2.45_{(55)}$
High **	$-2.57_{(55)}$	$-1.10_{(75)}$	$-1.05_{(60)}$	$-1.96_{(55)}$
All days	$-3.41_{(327)}$	$-1.60_{(460)}$	$-0.67_{(367)}$	$-1.82_{(334)}$

Figures in brackets denote the number of days used with low and high pressure respectively.

* Includes the five days in every month which showed the largest negative pressure anomalies.

** Includes the five days in every month which showed the largest positive pressure anomalies.

(N.B. Pressure anomalies for each day are based on 8 observations.)

It is evident that days with low pressure in winter are associated with much colder air than days of high pressure. The same is true to a less extent in autumn and spring. In summer the air still remains colder than the sea on the average, but the differences are small (about 1°F.) and smaller for days of low than of high pressure. The large negative values found during low pressure in winter agree with the fact that a large proportion of depressions passing station J have already reached an advanced stage of occlusion.

7. Air and sea temperature anomaly changes in cyclonic and anticyclonic situations

The data extracted in the previous paragraph were used to obtain mean rates of change of air and sea temperature anomalies during cyclonic and anticyclonic situations lasting for 48 hours or longer using as many as possible of these occasions of low and high pressure. Only cases where at least three consecutive days were included among the five cases of lowest/highest daily mean pressures for the months given above could be considered. so that the rates of change of anomalies given below strictly refer to a period of 48 hours. See Tables 2 and 3.

/Table 2

Table 2 A. Mean values of the initial air-minus-sea temperature differences (°F.) for selected cases of cyclonic and anticyclonic situations

Station J (1948-52)	Winter (Dec.-Feb.)	Spring (Mar.-May)	Summer (June-Aug.)	Autumn (Sept.-Nov.)
Pressure	°F.	°F.	°F.	°F.
Low	-4.45 (8)	-2.42 (11)	+0.83 (6)	-1.76 (7)
High	-2.74 (7)	-0.72 (11)	-0.86 (8)	-2.21 (7)

B. Mean rates of change of air and sea temperature anomalies (°F./day) for the same cases

Station J (1948-52)	Winter (Dec.-Feb.)	Spring (Mar.-May)	Summer (June-Aug.)	Autumn (Sept.-Nov.)
Pressure	°F./day	°F./day	°F./day	°F./day
Air	-0.67 (8)	+0.17 (11)	-0.15 (6)	-0.38 (7)
Sea	-0.16 (8)	-0.15 (11)	-0.13 (6)	-0.06 (7)
Air	+0.58 (7)	-0.37 (10)	-0.01 (8)	+0.71 (7)
Sea	+0.05 (7)	+0.07 (10)	-0.08 (8)	+0.15 (7)

(Number of cases in brackets)

		Winter °F.	Spring °F.	Summer °F.	Autumn °F.
Standard deviation of change of temperature anomalies through 2 days	Air	3.71	0.91	1.45	2.66
	Sea	0.58	0.69	0.82	0.54

Table 3 Frequency distribution of two-day changes of air and sea temperature anomalies in cyclonic and anticyclonic situations at O.W.S. J

Air temperature anomaly changes (°F.)

Season	Pressure type	-8.0 to -6.1	-6.0 to -4.1	-4.0 to -2.1	-2.0 to -0.1	0.0 to +2.0	+2.1 to +4.0	+4.1 to +6.0	+6.1 to +8.0	No. of occasions
Autumn) Winter) (Sept.-Feb.)	Low	0	2	2	7	3	1	0	0	15
	High	0	0	1	4	5	0	1	2	13
Spring) Summer) (Mar.-Aug.)	Low	0	0	1	8	3	2	0	1	15
	High	0	0	3	7	6	2	0	0	18

/Sea

Table 3 (continued)

Sea temperature anomaly changes (°F.)

Season	Pressure type	-2.0 to -1.6	-1.5 to -1.1	-1.0 to -0.6	-0.5 to -0.1	0.0 to +0.5	+0.6 to +1.0	+1.1 to +1.5	+1.6 to +2.0	No. of occasions
Autumn) Winter)	Low	0	1	2	5	6	1	0	0	15
(Sept.-Feb.)	High	0	0	1	3	6	2	1	0	13
Spring) Summer)	Low	1	1	2	2	9	0	0	0	15
(Mar.-Aug.)	High	0	1	4	4	3	5	0	1	18

In Table 3 the data in the previous table are shown in the form of a contingency table.

The warming of the air and sea during anticyclonic conditions in winter is evident from both forms of presentation of the data. There seems little doubt that this is in part due to the warming effect of the sea upon air which originated from high latitudes, and subsequently spent some time in the central regions of the anticyclones. Subsidence probably also plays some part. The slight warming of the sea (0.05°F. per day) is probably because in anticyclonic situations in winter the sea surface is no longer being cooled by rapid advection of colder air; in fact the surface is warmed to some extent by advection of warmer water in the North Atlantic drift; and, after an outbreak of cold air has terminated, by convection of warmer water from a short distance below the surface. The corresponding figure for autumn (0.15°F. per day) suggests the warming effect is even more marked at that season. A calculation made using data set out later which relates to the advection of sea surface isotherms by ocean currents near stations I and J, showed that this slight warming of the sea in anticyclonic (i.e. quiet) conditions in autumn and winter (when the NE. set of the Gulf Stream would be most effective) is certainly due in part to this factor.

The effect of cyclonic situations in winter could hardly be expected to show up strikingly in anomalies since these conditions prevail through such a large proportion of the winter.

The slight cooling of the air and sea during summer anticyclonic situations at J is rather surprising and suggests that other factors such as wind direction or cloudiness are more significant for warming the sea.

The figures in Table 2 are considered to show the temperature changes which occur in cyclonic and anticyclonic situations when the seasonal change has been eliminated. They represent the average temperature changes which occur in these conditions under the influence of advection of heat by the wind, advection by ocean currents, and losses or gains due to radiation. They clearly contain a bias due to wind direction, and so cannot be considered to represent cyclonic and anticyclonic situations for a period which, on trial, would be found sufficiently long to yield closed isobars of mean pressure centred over the stations, although their order of magnitude is probably substantially correct.

8. Air and sea temperature anomaly changes with persistent winds

Periods of 10 days were selected from the four years' data at O.W.S. J for the reason that they had the highest values of mean wind components (a) from a northerly direction and (b) from a southerly direction during that period. The mean values of the daily rate of change of air and sea temperature anomalies for all these cases, grouped into the four seasons, are given in Table 4 below.

/Table 4

Table 4 Mean daily rate of change of air and sea temperature anomalies at ocean weather station J during ten-day periods showing:
(a) largest northerly wind components and
(b) largest southerly wind components

Wind component	Winter				Summer			
	Mean vector wind components (kt.) N.	E.	Air °F./day	Sea °F./day	Mean vector wind components (kt.) N.	E.	Air °F./day	Sea °F./day
Northerly	+9.3	-13.4	+0.25 (6)	+0.00 (6)	+7.2	-7.9	-0.07 (9)	-0.04 (9)
Southerly	-12.8	-10.1	-0.20 (8)	-0.01 (8)	-8.5	-4.3	+0.01 (12)	+0.04 (12)

Bracketed figures show number of ten-day periods used to obtain mean values.

This table shows that the magnitudes of these daily rates of change of air and sea temperature anomalies, in extreme conditions of meridional transport of air, are no larger than the maximum seasonal rates of change of air and sea temperature. (Fig. 3 shows the largest values of daily rate of change of normal values of air and sea temperature at the ocean weather stations to be 0.07 to 0.10°F.) This is true even for periods selected as in Table 4 to bring out the effects of predominating winds. Some data obtained for both stations for winds from the four main quadrants for longer periods of 15, 20 and 40 days, which are not published here, tentatively confirm this conclusion. They also show that the only well-marked cooling effect due to any wind over such long periods is produced by spells of NE. wind at J in summer, and that a warming effect is apparently produced at both stations by spells of wind from the SE. quadrant in both summer and winter. This last is an interesting result since prolonged spells of SE. winds are most likely to occur in association with periods of meridional circulation due to "blocking action". Rex[2] has shown recently that blocking action in the N. Atlantic most frequently occurs in the vicinity of long. 20°W. where ocean weather stations I and J are located. On account of the very small number of cases available for each wind direction these last results should be treated with caution at this stage.

9. Serial correlation between air and sea temperature anomalies

In attempting to correlate variations of anomalies of air and sea temperature using the short intervals under investigation here it was necessary to take the persistence of temperature into account, particularly in the case of sea temperature. (This persistence effect is at once evident from an inspection of Figs. 1 and 2). It was therefore decided to form anomalies of air and sea temperature based this time upon the departures of one-day means of temperature (as described earlier) from 29-day running means. The various interruptions in the record at station I which have already been mentioned restricted the application of this method to station J. The period 1948-52 was used here*. On account of the fact that data were missing on a few days, and that the ocean weather ships were not within close range of the station position on a few other days, it was possible to find only four separate homogeneous periods which were sufficiently long to allow computation of reliable auto-correlation coefficients. Fortunately two of these periods occurred in the summer half-year and two in the winter half-year.

One-day anomalies of air and sea temperature obtained from 8 daily observations as described earlier were used to form auto-correlation coefficients r_1, r_2 ---- up to r_7 and hence to find $\mathcal{E}(n) \equiv n/n' \equiv n\sigma_n^2/\sigma^2$ where $\mathcal{E}(n)$ is the equivalent number of repetitions of n consecutive terms considered as being equivalent to n' random terms each repeated n/n' times. The notation is that used by Waldo Lewis and McIntosh[3] and σ_n and σ have the usual meaning.

Data for the periods used together with the auto-correlation coefficients obtained are given in Table 5 below:-

/Table 5

*The data prepared for this part of the work were too extensive to include in the tables. Copies are available in the Marine Division of the Meteorological Office at Harrow for use as required.

Table 5

Period	1		2		3		4	
	1950 Oct. 22 to 1951 Jan. 3		1949 Nov. 12 to Dec. 31		1952 Apr. 23 to Aug. 23		1951 Apr. 29 to Aug. 24	
No. of days included	74		50		123		118	
	Air	Sea	Air	Sea	Air	Sea	Air	Sea
r_1	+0.531	+0.290	+0.335	+0.416	+0.678	+0.713	+0.653	+0.722
r_2	+0.141	-0.168	-0.043	+0.421	+0.372	+0.518	+0.411	+0.594
r_3	-0.042	-0.087	-0.214	-0.004	+0.280	+0.348	+0.368	+0.481
r_4	-0.108	+0.247	-0.168	+0.044	+0.126	+0.170	+0.264	+0.287
r_5	-0.083	-0.013	-0.284	-0.121	+0.005	+0.068	+0.150	+0.125
r_6	-0.147	-0.118	-0.203	-0.077	-0.068	-0.018	-0.003	-0.090
r_7	-0.105	+0.005	-0.133	-0.131	-0.236	-0.129	-0.151	-0.225

Making use of the expression for the equivalent number of repetitions

$$\mathcal{E}(n) = 1 + \frac{2}{n}\{(n-1)r_1 + (n-2)r_2 + \cdots + r_{n-1}\}$$

and using only the few terms of the same sign (up to the 5th term) which therefore yield the largest values of $\mathcal{E}(n)$ (i.e. those most unfavourable for applying a significance test) as can be seen by inspection, the following values for $\mathcal{E}(n)$ were obtained:-

Period	1		2		3		4	
	Air	Sea	Air	Sea	Air	Sea	Air	Sea
$\mathcal{E}(n)$	2.32	1.57	1.66	2.62	3.88	4.58	4.62	5.32

The next step was to compute correlation coefficients for each period between anomalies of air and sea temperature. Coefficients were computed between the following pairs of related variables.

(a) Air temperature anomalies with the corresponding anomalies of sea temperature for the previous day. (Air/Sea D-1).

(b) Simultaneous anomalies of air and sea temperature. (Air/Sea D).

(c) Air temperature anomalies with sea temperature anomalies one day later. (Air/Sea D+1).

(d) Air temperature anomalies with sea temperature anomalies two days later. (Air/Sea D+2).

(e) Air temperature anomalies with sea temperature anomalies three days later. (Air/Sea D+3).

The magnitudes of the correlation coefficients obtained are shown in Table 6 together with the equivalent number of independent terms. These last were obtained by dividing the actual number of days available (determined by the length of each of the four periods) by the appropriate value of $\mathcal{E}(n)$. In general $\mathcal{E}(n)$ had a different value for air and sea anomalies and the procedure used to obtain the equivalent number of independent terms was to divide N (the actual days available) by the larger of the two values of $\mathcal{E}(n)$. In this way a more severe test of the significance of the correlation coefficients was applied.

/Table 6

Table 6 Correlation coefficients between mean daily anomalies of air and sea temperature at O.W.S. J

Period	Air: Sea (D-1)	Air: Sea (D)	Air: Sea (D+1)	Air: Sea (D+2)	Air: Sea (D+3)	No. of terms used N.	Value of $\varepsilon(n)$ used	Equivalent number of terms $N/\varepsilon(n)$
1950 Oct. 22 -1951 Jan. 3	+.08	+.11	+.05	-.09	-.03	74	2.32	32
1949 Nov. 12 - Dec. 31	+.15	+.44	+.04	+.08	-.06	50	2.62	19
1952 April 23 - Aug. 23	+.20	+.41	+.40	+.34	+.36	123	4.58	27
1951 April 29 - Aug. 24	+.42	+.57	+.49	+.42	+.36	118	5.32	22

The values which are underlined denote correlation coefficients which are significant at the 5% level, using the equivalent numbers of terms shown in the right hand column. This allows for the effect of coherence in each time series.

Table 6 shows that, though there is a small positive correlation between simultaneous air and sea temperature anomalies in winter, it fails to reach the 5% level of significance, while there is little or no correlation between pairs of air and sea anomalies for a day or more apart. This is not altogether surprising since evidence given elsewhere (Figs. 1 and 2) suggests that occasionally in winter and spring sea temperatures were partly or largely independent of air temperature. Both series of data for the summer period show positive values of r exceeding the 5% level of significance between simultaneous anomalies and between pairs of anomalies a day apart. Inspection of the table shows that the coefficients decrease more slowly between pairs of anomalies for sea temperature anomalies a day or more later than the air anomalies, than for sea anomalies a day earlier than the air anomalies. This affords some proof that the temperature changes in the sea in short periods follow the temperature changes in the air, and agrees with similar evidence adduced in an earlier part of the paper.

10. Advection of sea surface temperature by surface currents

Mean components of surface drift of water at stations I and J were evaluated for 1949 for the same five-day periods used for air and sea temperatures. As the drift of the ship does not give a true estimate of the water movement in strong winds, measurements of surface drift of water are not made in these circumstances. Hence the results which follow only refer to occasions when winds did not exceed force 5.

/Table 7

Table 7

Advection of sea surface temperature by surface currents in light and moderate winds

			Station I					Station J				
Year	Month	Days	N. component of drift in 5 days n.m.	Mean sea temp. gradient °F./n.m.	Mean advected temp. change* °F.	Mean sea temp. °F.	Actual sea temp. change* °F.	N. component of drift in 5 days n.m.	Mean sea temp. gradient °F./n.m.	Mean advected temp. change* °F.	Mean sea temp. °F.	Actual sea temp. change* °F.
1949	Mar.	22-26	+25(5)	.011	+.59	46.38	+.67	+23(3)	.011	+.19	50.55	+.52
	Mar.	27-31	+73(5)	.011		47.05		+13(4)	.011		51.07	
	May	1-5	-40(4)	.009	-.31	48.60	+.55	+61(3)	.009	+.44	51.80	+.43
	May	6-10	-31(4)	.008	-.35	49.15	-.96	+41(5)	.008	+.06	52.23	-.17
	May	11-15	-41(5)	.011		48.19		-19(5)	.011		52.06	
	July	15-19	-48(4)	.009	-.39	54.33	-.40	-26(4)	.009	-.05	57.70	+.50
	July	20-24	-29(4)	.012	-.38	53.93	+.24	+11(5)	.012	-.09	58.20	+.51
	July	25-29	-34(5)	.012		54.17		-26(4)	.012		58.71	
	Aug.	19-23	+14(5)	.015	+.35	53.80	+.33	- 6(5)	.015	-.03	59.23	+1.75
	Aug.	24-28	+26(5)	.019	-.01	54.13	+.04	+ 1(5)	.019	-.14	60.98	-1.11
	Aug.29-Sept.2		-35(5)	.015		54.17		-20(5)	.015		59.87	
	Sept.	3-7	-26(5)	.013	-.43	54.57	+.40	-11(3)	.013	-.22	59.27	-.60
	Sept.	8-12	-28(4)	.014	-.37	53.65	-.92	- 1(4)	.014	-.07	58.87	-.40
	Sept.	13-17	-31(5)	.013	-.39	53.91	+.26	+26(5)	.013	+.17	58.60	-.27
	Sept.	18-22	+38(5)	.012	+.03	54.54	+.63	+31(5)	.012	+.35	58.76	+.16
	Sept.	23-27	+ 2(5)	.012	+.24	54.26	-.28	+69(5)	.012	+.60	58.92	+.16
	Oct.	3-7	- 6(5)	.013	+.05	53.93	+.17	+51(5)	.013	+.37	58.77	-.49
	Oct.	8-12	+17(5)	.011		54.10		+ 8(4)	.011		58.28	
1950	June	25-29	- 1(3)	.008	+.23	53.55	+.37	-19(4)	.008	-.14	56.73	+.04
	June 30-July 4		+67(5)	.007	(+.44)	53.92	+1.21	-19(4)	.007	(-.09)	56.77	+.29

Figures in brackets in columns 4 and 9 denote number of days on which separate determinations of drift were made.

*Between successive 5-day periods.

G.37837/JEK/1/56/50

Altogether there were 14 occasions when current sets for two consecutive pentads, together with mean sea surface temperatures, were available at both stations. For each of these occasions an estimate of the temperature change due to the meridional component of the surface current was made for each station, on the assumption that the meridional temperature gradient near both stations was the same as it would have been if a uniform sea surface temperature gradient had existed between both ships, corresponding with the sea temperatures observed at the stations. This assumption is clearly unjustifiable for the individual occasion but can reasonably be applied when considering the mean of temperature changes statistically for all these occasions. Values of sea temperature gradient I to J were already available, and are included in Table 7.

The correlation coefficients between the advected sea temperature change and the actual sea temperature change were found to be 0.41 for station I and 0.13 for station J. In order to be significant at the 5% level it is found that r must equal or exceed 0.53 when 14 pairs of observations are available[4]. It thus appears doubtful whether in these cases, mostly selected from summer months, the influence of advection was significant by comparison with that of solar heating and evaporation in situ.

The fact that the correlation coefficient (r) at both stations is not significant is hardly surprising, since the magnitudes of the sea surface temperature changes computed to have resulted from advection by ocean currents alone (and shown at Table 7, Columns 6 and 11, also 8 and 13) are seen to be quite small compared with the normal sea surface temperature changes in cyclonic and anticyclonic situations as given by Table 2.

11. Sea surface temperature changes in five-day periods related to the energy exchange between sea and atmosphere

The data in Tables 8 and 9 have been used to compare the actual sea surface temperature changes between successive five-day periods, with the sea surface temperature changes in the same periods derived from computations of the energy exchanges through the sea surface. As the computations are lengthy they have been carried out only for a limited number of occasions through the different seasons. The occasions in Tables 8 and 9 were selected so that points of particular interest could be examined, such as the magnitude of energy exchanges during the occasional five-day periods in summer when mean air temperature exceeded (or nearly equalled) mean sea temperature, and during periods in winter when outbreaks of arctic air masses occurred.

The following factors were taken into account in making the computations.

(a) Variation of insolation (Q) on the outer limit of the atmosphere due to season and latitude

The values of Q were found by interpolation from data due to Angot[12].

(b) Depletion of solar radiation incident on the outer limit of the atmosphere, due to scattering and absorption by dust, water vapour and cloud, and by reflection from cloud

In computing the insolation reaching the sea surface (Q_s), use was made of the empirical formula $Q_s = Q_{s_o}(1-0.71C)$ where Q_{s_o} is the insolation

/reaching

reaching the sea surface with a cloudless sky, and C is the total cloudiness in tenths. Q_{s_o} was obtained by allowing for the depletion of the insolation Q at the outer limit of the atmosphere by a factor α, to allow for loss due to both scattering and absorption. In computing α, allowance was made for the variation of the scattering coefficient with the solar elevation, in accordance with the latest available data. The data used for solar elevation was the same as that used in computing the proportions of insolation reflected from the sea surface in paragraph (c) below. Absorption was assumed to be constant at 10% for water vapour and 2% for ozone at all except the lowest solar elevations. The relations used were thus:-

$$Q_{s_o} = Q\ (1-\alpha)$$

and

$$Q_s = Q\ (1-\alpha)\ (1-0.71C).$$

In deriving an expression for the depletion of solar radiation due to reflection from cloud, Houghton[5] gave these figures below for the albedo of various cloud forms,

low	0.69	high	0.21
middle	0.48	cumuliform	0.70.

For the two ocean weather stations for 1950-52 the mean cloud amounts (in tenths) were

low cloud 6.39 total cloud 7.76.

Making an allowance for the great thickness of cumuliform cloud at the ocean weather stations the mean albedo can readily be estimated as 0.65 which compares well with the figures of 0.71 used for depletion in the expression given earlier.

(c) Reflection from sea surface (F)

The fraction of the solar radiation incident on the sea surface which was reflected upwards was obtained from data due to Sverdrup[6]. The data were used to draw graphs giving the amounts of radiation reflected at various solar elevations and values of cloudiness. In order to allow for the roughness of the sea surface the figures for the amounts of reflected radiation were all increased by 25% before preparing the graphs. The mean value of F, the fraction of radiation reflected, was in every case taken from the mean of several measurements of F, made at equal intervals through the day on either side of the sun's meridional position. The solar elevations were all obtained from altazimuth tables.

(d) Effective back radiation (R_D, R_N)

The difference between the amount of energy emitted as long wave radiation at the sea surface and the long wave radiation received from the atmosphere is known as the "effective back radiation". It has been evaluated using Angstrom's data as quoted by Sverdrup. Cloudiness has been allowed for, by day and night separately, by means of the empirical formula $R_D = R_o\ (1-0.083C)$ where R_o is the back radiation for clear sky, and R_D is the back radiation with cloud amount C, in tenths.

(e) Term for evaporation and convection (Q_A)

Using Jacobs'[7] nomenclature the following expression can be readily derived by substitution:-

$$Q_A = 0.0143(e_w - e_a)\ W_a\ L_t \left\{1 + \frac{0.65(t_w - t_a)}{(e_w - e_a)}\right\}$$

/where

where Q_A is the total energy exchanged between sea and atmosphere, e_w, e_a are the vapour pressures in millibars at the sea surface and at the ship's screen respectively, W_a is wind speed in metres/second and $L_t = 596-0.52t$ (where t is in degrees C.). In substituting, the value for R, the Bowen Ratio, has been eliminated, the factor of 0.65 in the bracket follows from the assumption that t is 12°C. and the surface pressure p is 1008 mb., both representative values at the ocean weather stations.

In Tables 8 and 9 the data used in computing energy exchanges and the amounts of energy exchanged (in g.cal.cm.$^{-2}$day^{-1}) are shown under the various headings described earlier. In computing the energy reaching the sea surface the cloud amount used is the mean cloud amount for the observations made during daylight in each five-day period. Back radiation was computed separately for day and night using the appropriate values for relative humidity and cloud amount from the table. In computing the evaporation and convection term, Q_A, five-day means were used of air and sea temperature (t_a, t_w), vapour pressure at the sea surface and at bridge level (e_w, e_a), and wind speed.

Starting with the net energy exchange (Table 9, Column 14) it is at once evident how seldom there is a net gain of sensible heat by the surface layers of the ocean at these ocean weather stations. The cases of net gain of sensible heat by the surface layers of the ocean appear to be limited to five-day periods when the mean wind speed was low, the mean air temperature was above (or only a little below) the mean sea temperature, and the mean cloud amount was lower than usual. Even in early April large net losses can occur and, on the two occasions which showed net gains (both in the summer half year), these were comparatively small. Very large net losses can occur in winter months; in all the cases considered here they exceeded the largest insolation amount which penetrated the sea surface in summer. The evaporation term Q_A is much the largest of the terms involved during the winter, when its value sometimes exceeded 500 g.cal.cm.$^{-2}$day^{-1}. During one of the five-day periods Q_A averaged 784 g.cal.cm.$^{-2}$day^{-1}, which compares with the value of 1128 g. cal.cm.$^{-2}$day^{-1} which Craddock[10] found to be typical for a period of 24 to 48 hours in the same locality and synoptic situation. In summer the losses by scattering, and by absorption and reflection from cloud were, on all occasions, greater than the losses by evaporation.

The actual changes of sea surface temperature which occurred during each of these five-day periods are listed in Column 15 of Table 9. According to data by Sverdrup the penetration of the surface of "average oceanic water" by 1000 g.cal.cm.$^{-2}$ would result in the temperature of the top 1 m. of water being raised by 11.66°F. as a result of the absorption of this radiation, and assuming that no mixing took place with the underlying water. In the cases of the two periods (1948 May 16-20 and 1949 June 20-24) when a net gain of energy occurred in the surface layer of the sea, this result of Sverdrup's was used to determine the theoretical rise of sea temperature in the topmost 1 m. during each period. The ratios of the actual to the theoretical rises of sea surface temperature were found to be 0.73 and 1.55 in these two periods respectively. The influence of mixing in the surface layers of the sea is clearly very important in determining the magnitude of this ratio. In reality all values of the ratio are probably rather less than those given in the table since the comparison in the table is made between sea temperatures measured by means of a canvas bucket, which are considered to be representative of the temperature of the top few cm., whereas the theoretical values refer to a depth of 1 m. Variations of temperature in the top few cm. would normally be larger than through a depth of 1 m. Sverdrup's data cannot be used to investigate the other periods when a net loss of energy took place, since the efforts of long wave radiation outwards and evaporation and convection of sensible heat, take place at the surface and are not distributed through a depth of the sea as with the absorbed solar radiation.

A reference to Table 9, Column 15, shows that the actual changes of sea surface temperature in the winter cases shown therein are very small for the most part. This small response of the sea surface temperature to very large net losses of sensible heat in winter has already been mentioned earlier in this paper. Mixing in the surface layers of the sea is undoubtedly very important in this connection, as is shown by the fact that during the later part of the winter at least, the topmost 100-200 m. of the sea at ocean weather stations I and J comprise a practically isothermal layer. This is known to be the case from numerous bathythermograph observations made from the ocean weather stations in the past two winters. As a result any cooling of the topmost layers sets up convection currents leading to an interchange with warmer water which rises from lower levels, while the cooled water sinks through its environment. The stability is also influenced by density variations brought about by differences in salinity as well as in temperature between the different layers of sub

surface water. However, the influence of salinity will not be discussed any further in this paper. In the summer half year, on the other hand, sea temperature increases sharply upwards through the thermocline, and more slowly, upwards from the thermocline to the surface. Increments of sensible heat received in quiet weather will then be stored in the layers nearest the surface. It would be reasonable to assume therefore that in the five-day periods falling in the summer half year, the rises in sea surface temperature would correspond more closely with the net gains of sensible heat in their respective five-day periods, than would the falls of sea temperature associated with net losses of sensible heat. (This is even more true for those periods of net loss of sensible heat which fall in the winter half year.) This expectation is borne out by the data for 1948 May 16/20, 1949 June 20/24 and 1951 July 20/24.

Some workers have suggested[8] there may be an abrupt change in the stability of the sea surface from stability to instability as the wind increases through a speed of about 13.8 kt. (7.4 m/s). It is possibly significant that, besides the three periods above in which the 24 hours mean wind speeds were 4.12, 5.40 and 5.43 m/s respectively, there was only one other period in which this critical value was exceeded. Although the wind may have exceeded 7.4 m/s at times it can reasonably be assumed that for most of these periods the stability of the surface layers of the sea was not upset by the wind. In most of the other cases considered here the mean wind speed was well in excess of this critical figure. The very small values of many of the ratios of the actual to the computed change of sea surface temperature suggest that disturbance of the sea surface by the agency of wind was a factor responsible for this state of affairs, in addition to the operation of convection currents.

12. Advection of heat by ocean currents

A factor which has been neglected in the foregoing considerations is the transport of heat by ocean currents during each of the five-day periods used in the energy exchange computations. Complete ocean current data for stations I and J are available only for the single five-day period 1949 June 20/24; for the other periods the monthly vector mean values of surface ocean currents at the ocean weather stations were the only data available.

During the period 1949 June 20/24 the ocean weather station I was positioned on a bearing of 358° true from station J, at a distance of 680 Km. The mean sea temperature difference was 1.6°C. (2.9°F.), the five-day vector mean current was 063°/3.2 n.m./day at J and 061°/3.6 n.m./day at I. For the purpose of the present calculations, which refer to J, the former value was used.

From these data an estimate was made of the rate of northwards advection of the sea surface isotherms near J during this period. Assuming the same current prevailed throughout the layer and taking the figure for the net gain of heat by the sea as 86 g.cal.cm.$^{-2}$day^{-1} it can readily be shown from the above figures that the same net gain of heat (assumed shared throughout the layer) could have been brought about by a vector mean current of 063°/3.2 n.m./day only if it had prevailed to a depth of 295 m. Invoking Ekman's[9] theory of the wind driven surface currents of the sea it is unlikely that such a current existed in reality, and more probable that at a short distance below the surface the water layers were moving with an E. or a SE. set. In any case there is no need in this case to invoke the existence of such a deep surface ocean current, since the observed rise of 1.55°F. in the sea surface temperature is in good agreement with the rise of temperature computed on the assumption that 86 g.cal.cm.$^{-2}$ day^{-1} was being absorbed in the topmost 1 m. of the sea. Also in the middle of the summer the temperature stratification of the topmost layers of the sea is stable, and the implications of this state of affairs have been discussed.

In the absence of detailed current data it was pointless to consider the

/remaining

remaining cases in detail. However it seemed worth while to take the single case of 1949 February 20/24, when the greatest net loss of heat from the sea surface occurred while the sea surface temperature actually rose by 0.15°F., and to consider whether surface ocean currents could have played any part in making good this loss. (It was necessary to assume that the monthly value of the vector mean current, (081°/8.2 n.m./day), was the same as the vector mean current for the period February 20/24) From the facts that the difference in mean sea surface temperature between stations J and I was 1.5°C. (2.7°F.) and that their positions were the same as for June 20/24 it was computed that the heat loss of 803 g.cal.cm.$^{-2}$ day^{-1} could only have been provided by a vector mean current of 081°/8.2 n.m./day if it had existed down to a depth of 1966 m. The arguments given earlier[9] show that it is highly improbable that the surface current could have prevailed through so great a depth without a marked change of direction.

Since recent bathythermograph observations at station J have shown that the distribution of the sea surface temperature there is nearly isothermal to a considerable depth in the late winter, it is more realistic to estimate the depth of water through which a uniform cooling of (say) 0.02°F. (0.01°C.) is necessary to compensate for a net heat loss of 803 g.cal.cm.$^{-2}$ day^{-1}. The choice of 0.02°F. is appropriate, since the data in Table 9 show that this is the order of magnitude of the change of sea temperature between successive five-day periods at J and I in winter. The necessary depth is readily shown to be about 803 m. This result shows that the maximum rates of supply of sensible heat to the atmosphere, which have been observed during outbreaks of Arctic air by Craddock[10] and others, can readily be supplied from the upper layers of the sea by means of falls of sea temperature having the same magnitudes as those observed, so long as the distribution of sea temperature in these layers is isothermal. As was mentioned earlier the existence of an isothermal layer in the surface layers of the sea in the late winter has been confirmed by means of bathythermograph observations made recently at the ocean weather stations I and J. The small amount of data for the layer surface to 450 ft. so far available suggests that at station J the thermocline is found at a depth of 150-250 ft. in August and the temperature of the water between the thermocline and the surface is about 3-4°F. above that of the underlying water. The data available for J for a short period in early winter (December, 1953) suggest that, while the temperature distribution is on the average not far from being isothermal down to a depth of 450 ft., it shows some dependence on the sign of the air-minus-sea temperature difference. During periods when this difference has a small negative, or positive, value the surface layers of the sea are warmer than the layers at 300-450 ft., but when the air is much colder than the sea surface, the surface layers of the sea become colder than the layer 300-450 ft. in sympathy. No such effect is apparent at station I where, during the short period examined, the topmost 50 ft. of the sea averaged 0.5°F. warmer than the layer at 450 ft., despite a mean air-minus-sea temperature difference of 6.4°F. Evidently the advection of heat by the surface layers of the sea at I during the period examined (1954 January 26 - February 5) was very considerably larger than the corresponding advection at J during the period 1953 December 2 - 13.

13. The synoptic-climatological significance of short period variations of air and sea temperatures in the NE. Atlantic

Studies by Craddock, Lamb[11] and others have shown that the magnitude of the 1000-500 mb. thickness is quite closely related with the surface air temperature. The small correlations found between air and sea surface temperatures during short periods and described in this work, suggest that any correlation between 1000-500 mb. thickness as at the ocean weather stations and simultaneous sea surface temperatures at any particular time is also likely to be small. However, when consideration is given to longer periods, of the order of one or two months or longer, it is evident that the sea surface must have some influence upon the mean 1000-500 mb. thickness values over short periods. More important, since the sea surface temperature

/imposes

imposes (as shown by Craddock) a limit to the equatorward displacement of a thickness line, the differing values of actual sea surface temperatures at the ocean weather stations and latitudinal gradients of sea surface temperatures between stations such as I and J, from one corresponding season to another, will clearly impose very different limits upon the possible transgressions of isopleths in various cases. For instance attention was directed earlier to the considerable differences between values of the latitudinal gradient of sea surface temperature (I - J) in the summers of 1948 and 1950 (Fig.4); and to the fact that in the latter year the normal sea surface temperature gradient between I and J was even reversed for a short time in the late summer. On the other hand in the summer of 1949 the normal gradient of sea temperature (I - J) was considerably steepened. These differences would certainly impose very different limits in the two different seasons upon the possible transgressions of thickness isopleths during outbreaks of cold air; they may also possibly exert effects in other situations (e.g. during polewards advection of tropical air), though these effects will be harder to define and recognize, and not readily distinguished from the effects of other agencies such as subsidence and radiation. In general the results given earlier show that any influence exerted by the gradient of sea surface temperature upon thickness isopleths over periods of a month or two will be more important in limiting transgressions of isopleths during the winter months when outbreaks of cold air are most frequent.

The brief discussion of the bathythermograph observations at the ocean weather stations I and J given earlier, suggests some ways in which the distribution of sea temperature in the topmost 500-1000 m. may exert a significant influence upon the temperature of the overlying air, and hence upon the thickness isopleths, during a period of a month or two. It is convenient to start with the end of the winter, when the sea temperature is isothermal in the vicinity of the ocean weather stations I and J to a depth which is known to be at least 150 m.; and probably approaches 1000 m. on many occasions, though confirmation of this is lacking. The amount of solar heat penetrating the surface of the sea differs considerably between corresponding seasons in different years, on account of variations of cloud amount, of wind speed and direction and of air-sea temperature differences, among other meteorological factors. Sea surface temperatures experienced in a given locality will be influenced by all these variables. The depth of the thermocline, and its intensity, that is the difference between the sea temperatures above and below the thermocline, are also factors of some significance for the meteorologist. For instance in a given locality there may well be two summers in which the amounts of heat penetrating the sea surface are equal, but one of these summers is relatively quiet, and the other windy. In the former summer, at the end of the season, one would expect to find a shallow and intense thermocline; in the latter summer, more vigorous stirring of the surface waters would ensure that the thermocline was deeper and less intense than in the former case. In the quiet summer the sea surface temperature would rise higher than in the windy summer.

The intensity and depth of the thermocline must clearly exert an important effect upon the rate of cooling of the sea in the autumn and early winter. The effect of each outbreak of cold air at the end of the summer and in early autumn is to destroy the strong positive gradient of sea temperature near the surface, and to replace it by an isothermal layer, whose depth is gradually increased after each successive outbreak of cold air. After summers in which an intense and deep thermocline has been established, there must be a much larger fall of sea temperature at the surface during the autumn than in other years. This fact probably has a synoptic significance. It implies that, in an autumn following such a season, the limit of extreme equatorwards transgressions of the thickness isopleths is pushed towards the equator more rapidly than in a season when the thermocline is weak and shallow at the end of the summer, when isothermal conditions are established in the sea down to a considerable depth early in the autumn. However the significance of this effect should not be exaggerated. Towards the end of a warm summer when an intense and deep thermocline has been established, a particular thickness line will be further from the equator than at a similar period of a cool and windy summer.

/In

In general after a warm summer a given thickness isopleth would retreat more rapidly than after a cool summer, with the result that, during the autumns following, the differences between the positions of the extreme equatorwards transgressions of a particular thickness isopleth will become progressively smaller.

By late in the autumn or early in the winter, depending upon the intensity and depth of the thermocline established during the previous summer, and upon the frequency and intensity of outbreaks of polar air in the autumn, isothermal conditions will become established to a depth of some hundreds of metres. Thereafter the sea surface cools at a much slower rate (i.e. thermodynamically speaking the sea acts as a good "source") and the limits of transgressions of thickness lines toward the warmer regions become almost fixed. While it is still difficult to assess the magnitude of these effects, they appear to merit closer attention than they have received up to the present.

The present study suggests that in short periods of a day, or of a few days, in the summer half year sea temperatures follow air temperatures fairly closely with a lag of a day or two, but in the winter half year the relationship is much less close. In both cases the amplitudes of the sea temperature changes are much smaller than those of the air. For longer periods of a month or more, recent work - e.g. on anomalies of air and sea temperature over the N. Atlantic during the summer of 1954 - suggests that mean sea temperature anomalies tend to follow mean air temperature anomalies in the same locality. However, when the effect of the sea is considered upon the temperatures at various levels of the air masses advected over it, the problem is seen to be less simple. Consideration of the widely differing patterns of sea surface temperature, as shown by the time series of sea surface temperature gradients between stations I and J in 1948 and 1950 already described, suggests that the variations of the sea surface temperatures and the corresponding horizontal temperature gradients between stations such as I and J, the thickness isopleths and the seasonal variations of the intensity and depth of the thermocline, are very likely to be interrelated; though a great deal more evidence will have to be provided before this supposition can be firmly established or otherwise.

14. Conclusions

(a) At station J in winter the air-minus-sea temperature difference in cyclonic situations is large, -4.6°F., i.e. the air is colder than the sea; in anticyclonic situations it is much smaller, about -2.6°F. In summer at station J the air-minus-sea temperature difference is much smaller, -0.7°F. in cyclonic situations, and -1.1°F. in anticyclonic situations.

(b) During the great majority of five-day periods the air was colder than the sea at both stations I and J. However there was a moderate number of five-day periods at both stations during the months from May to August when the air was warmer than the sea, although their occurrence was exceptional during the remainder of the year.

(c) In anticyclonic situations in winter there is warming of the air amounting to a change in the anomaly of 0.58°F. per day at J, also a warming of the sea of 0.05°F. per day at J. The corresponding figures for autumn are +0.71°F. per day for the air and +0.15°F. for the sea. These results are based upon anomalies of one-day means of air and sea temperature.

(d) The effect of persistent winds from a given direction upon daily rates of change of air and sea temperature anomalies is mostly small compared with the maximum seasonal rates of change of actual air and sea temperature. Persistent southeasterly winds appear to produce a warming effect on air and sea temperatures in summer and winter, which is noteworthy in relation to the fact that "blocking action" is most frequent in the N. Atlantic near long. 20°W.

/(e)

(e) Significant serial correlation coefficients are found between simultaneous daily anomalies of air and sea temperature at station J for periods in the summer half year. The correlations are also significant with the anomalies of sea temperature one day earlier or one or more days later than the air anomalies. The values afford some proof that changes in sea temperature are to some extent imposed by changes in air temperature. The serial correlation coefficients for the winter half year were not significant.

(f) The correlation coefficients between advected sea temperature change (due to surface ocean currents) and the actual sea temperature change, were determined from the only data available relating to surface ocean currents, for some occasions of light and moderate winds in summer at ocean weather stations I and J. The values of r were below the 5% level of significance at both stations, though not far below at station I. The influence of advection (due to surface ocean currents) on sea temperatures in summer thus appears to be small in comparison with that of solar heating and evaporation in situ. This fact is not surprising when a comparison is made between the magnitude of the sea surface temperature changes in cyclonic and anticyclonic situations and the corresponding magnitudes of the actual sea temperature changes (Table 7, Columns 8 and 13) computed to have been produced by ocean currents alone (Table 7, Columns 6 and 11).

(g) The net energy exchange through the sea surface was computed for sixteen selected five-day periods. In the seven cases which occurred in the summer half year, there was a net gain of sensible heat by the surface layers of the sea in only two cases. For a net gain of heat to occur in this way necessary conditions in order of importance appear to have been: light winds, mean air temperature above (or only slightly below) mean sea temperature, and a mean cloud amount below average.

(h) Large net losses of sensible heat occurred during all the five-day periods during the winter half year; in some periods the losses were very large. In winter the evaporation term Q_A was responsible for the largest losses; its value sometimes exceeded 500 g.cal.cm.$^{-2}$day^{-1}. In summer the losses due to scattering, and by absorption and reflection from cloud, were greater than losses by evaporation.

(i) Using figures due to Sverdrup computations were made of the rise (or fall) of sea temperature to be expected from the net gain (or loss) of sensible heat in the surface of the sea, and the results compared with the actual changes found in each period. As would be expected it was found that there was a closer relationship between the actual rises of sea surface temperature and the net gains of sensible heat in the surface layers of the sea during the summer months, than there was between actual falls in sea surface temperature and net losses of sensible heat in the sea surface layer on the various occasions in the winter months. This agrees with the known vertical distributions of sea temperature in which there is usually a shallow warm layer close to the surface in summer, but an isothermal layer extending downwards several hundreds of metres from the surface in the winter.

(j) In general it seems unlikely that surface ocean currents in the vicinity of station J are a major factor in transporting heat polewards in summer. The occurrence of very large heat losses from the sea to the air in association with very small variations of sea surface temperature during some of the five-day periods in winter could be explained by a simple calculation, if the distribution of temperature in the sea were nearly isothermal to a depth of 500-1000 m. The existence of this isothermal layer later in the winter has been recently demonstrated by bathythermograph observations made at the ocean weather stations. Evidence of the part played by ocean currents in the poleward transfer of heat in the vicinity of J in autumn and winter is found in the mean daily values of sea temperature anomaly change in anticyclonic situations (+0.15°F./day in autumn and +0.05°F./day in winter) which were quoted under para. (c) above. In anticyclonic (i.e. relatively 'quiet') conditions the northeasterly set of the Gulf Stream would be more effective than at other times.

/(k)

(k) The synoptic-climatological significance of short period variations of air and sea temperatures is considered, in relation to the limits imposed by the sea surface temperature upon the possible transgressions of thickness isopleths in the vicinity of the ocean weather stations; and to variations in the depth and intensity of the thermocline between corresponding seasons in different years. Information contained in this paper is considered to afford some evidence that variations in these parameters are to some extent interrelated, though decisive proof is wanting at this stage.

References

1. KOIZUMI, M. "On the oceanographic and meteorological conditions at the fixed station "Extra" in the Pacific Ocean (Part I)". Record of oceanographic works in Japan, Vol. I, No. 2, p. 13. New Series, December 1953.

2. REX, D.F. "Blocking action in the middle troposphere and its effect upon regional climate". Tellus, Vol. 2, No. 3, and Vol. 2, No. 4.

3. WALDO LEWIS, R.P. and McINTOSH, D.H. "Some effects of the coherence of meteorological time series". Meteorological Magazine, Vol. 81, August 1952, p. 242.

4. BROOKS, C.E.P. and CARRUTHERS, N. "Handbook of statistical methods in meteorology". M.O. 538, p.221.

5. HOUGHTON, H.G. J.Met.(II)1, 1954, p.5.

6. SVERDRUP, H.U. "Oceanography for Meteorologists", Chapter 4.

7. JACOBS, W.C. "On the energy exchange between sea and atmosphere". Jour. Marine Research, La Jolla, Calif., 5, 1942, pp.37-66. (Scripps Inst. Oceanography).

8. MUNK, W.H. "A critical wind speed for air-sea boundary processes". Jour. Marine Research, La Jolla, Calif., 6, 1947, pp.203-218.

9. HAY, R.F.M. "A verification of Ekman's theory relating wind and ocean current directions using ocean weather ships' data". Marine Observer, XXIV, October 1954, p.226.

10. CRADDOCK, J.M. "The warming of arctic air masses over the eastern North Atlantic". Q.J.R. Met. Soc., London, 77, July 1951, p.355.

11. LAMB, H.H. "Two-way relationship between the snow or ice limit and 1000-500 mb. thicknesses in the overlying atmosphere". Q.J.R. Met. Soc., London, 81, April 1955.

12. BRUNT, D. "Physical and Dynamical Meteorology", 2nd edition, p.112.

Table 8

Data used in computing energy exchanged through the sea surface during certain five-day periods at the ocean weather stations I and J

Date	Station	Five-day mean values								
		Temperature		Relative humidity		Vapour pressure		Wind speed (m/s)	Cloud amount (tenths)	
		Air t_a °F.	Sea t_w °F.	Day %	Night %	Sea Surface e_w mb.	Ship's bridge level e_a mb.		Day tenths	Night tenths
Summer half year										
1948 May 16/20	J	54.1	53.2	89	89	13.80	12.69	4.12	4.4	4.5
49 May 1/5	J	50.1	51.8	81	84	13.10	10.13	7.49	8.3	7.0
49 June 20/24	J	55.7	55.2	96	97	14.90	14.55	5.40	9.1	9.6
50 Apr. 6/10	J	46.3	48.9	73	77	11.76	8.08	12.34	8.5	7.3
51 July 20/24	J	59.2	60.4	78	80	17.94	13.57	5.43	7.9	8.3
51 July 25/29	J	60.3	61.0	83	85	18.30	15.02	6.71	6.9	5.5
1951 July 30/Aug. 3	J	58.6	60.1	82	87	17.76	14.13	10.98	8.1	6.7
Winter half year										
1948 Oct. 8/12	J	55.5	56.6	80	87	15.66	12.72	10.73	8.0	7.1
49 Feb. 15/19	J	47.5	49.8	85	87	12.20	9.61	10.60	9.1	8.5
49 Feb. 20/24	J	44.2	49.9	75	72	12.25	7.25	13.07	8.3	6.4
49 Feb. 25/Mar. 1	J	48.4	50.0	76	82	12.30	9.25	8.22	8.0	6.6
49 Mar. 7/11	J	48.0	50.3	79	83	12.42	9.28	10.11	6.9	6.0
49 Oct. 13/17	J	54.4	57.6	86	85	16.26	12.30	11.49	9.4	6.9
51 Nov. 27/Dec. 1	J	49.7	51.7	74	76	13.05	9.14	8.21	7.7	6.9
50 Feb. 10/14	I	39.0	47.1	81	79	11.04	6.49	8.20	7.1	5.7
1950 Feb. 15/19	I	39.9	47.1	78	80	11.04	6.63	9.25	7.2	4.9

Table 9

Energy exchanged through the sea surface during certain five-day periods at ocean weather stations I and J

Unit - g.cal.cm.$^{-2}$.day^{-1}.

Date	Station	Insolation at outer limit of atmosphere (Q)	Proportion of insolation depleted in a clear atmosphere (due to scattering and absorption) (α)	Insolation reaching sea surface (Q_{s_o}) (Cloudless skies) $Q_{s_o}=Q_o(1-\alpha)$	Insolation reaching sea surface (Q_s) with cloudiness (C) $Q_s=Q(1-\alpha)(1-0.71C)$	Proportion of insolation reflected from sea surface (F)	Energy lost by reflection from sea surface (Q_R) $Q_R=Q_S \times F$	Energy lost by back radiation (allowing for cloudiness) Day (R_D)	Night (R_N)	Total (R_B) $R_B=R_D+R_N$	Net insolation penetrating* sea surface (Q_P) $Q_P=Q_S(1-F)-R_B$	Total heat exchanged between sea and air* by convection and evaporation (Q_A)	Net energy* exchange (Q_{AB}) $Q_{AB}=Q_P+Q_A$		Sea temperature change observed (°F)		Sea temperature change** Actual computed	
													+	-	+	-	+	-
(1)	(2)	(3)	(4)	(5)	(6)	(7)	(8)	(9)	(10)	(11)	(12)	(13)	(14)		(15)		(16)	
Summer half-year																		
1948 May 16/20	J	906	0.28	652	447	0.122	55	104	53	157	235	-27	208		1.8		0.73	
1949 May 1/5	J	832	0.28	599	245	0.103	25	50	40	90	130	-225		95		0.6	0.54	
1949 June 20/24	J	992	0.28	715	253	0.103	26	41	14	55	172	-86	86		1.55		1.55	
1950 April 6/10	J	702	0.28	505	201	0.107	22	44	46	90	89	-485		396		0.4	0.09	
1951 July 20/24	J	889	0.28	640	281	0.107	30	58	25	83	168	-220		52	1.2			1.97
1951 July 25/29	J	866	0.28	624	318	0.117	37	70	45	115	166	-200		34	0.25			0.63
1951 July 30/Aug. 3	J	848	0.28	610	259	0.107	28	53	38	91	140	-383		243		1.45	0.56	
Winter half-year																		
1948 October 8/12	J	370	0.34	244	106	0.116	13	38	56	94	-1	-301		302		0.8	0.23	
1949 February 15/19	J	342	0.36	219	77	0.110	8	25	44	69	0	-307		307		0.1	0.03	
1949 February 20/24	J	377	0.35	245	101	0.118	12	35	73	108	-19	-784		803	0.15			0.02
1949 February 25/ March 1	J	415	0.35	270	116	0.122	14	38	66	104	-2	-253		255	0.4			0.13
1949 March 7/11	J	459	0.32	312	159	0.125	20	52	69	121	+18	-340		322	0.25			0.07
1949 October 13/17	J	338	0.35	220	73	0.105	8	24	61	85	-20	-490		510		1.80	0.30	
1951 Nov.27/Dec. 1	J	145	0.45	80	36	0.154	5	30	76	106	-75	-321		396		3.0	0.65	
1950 February 10/14	I	220	0.42	128	63	0.162	10	39	88	127	-74	-520		594		1.6	0.23	
1950 February 15/19	I	251	0.41	148	73	0.155	11	40	94	134	-72	-549		621	0.3			0.04

* Negative values denote a loss of energy by the sea surface.

** Sverdrup "Oceanography for Meteorologists", p.58, for data relating to "average oceanic water".

Table 10

Five-day mean values at ocean weather ship station I

1948	No.	Bar. (mb.)	No. of obs.	Dry bulb (°F.)	No. of obs.	Wet bulb (°F.)	No. of obs.	Sea temp. (°F.)	No. of obs.	Total cloud amount (oktas)	No. of obs.	Mean vector wind components (kt.) E	N	No. of obs.
	1-4			Data not available for January 1st - 20th										
	1-4							47.6	39	5.5	39	+5.3	-6.3	20
Jan. 21-25	5	987.6	39	42.5	39	39.0	39	47.6	35	6.4	40	+20.4	-8.1	20
26-30	6	971.4	40	45.3	40	43.1	40	47.6	26	6.3	40	-10.1	-11.7	20
31-Feb. 4	7	973.4	40	44.8	40	43.2	40	46.7	12	5.8	12			
Feb. 5-9	8	1007.2	12	40.7	12	39.4	12	46.5	40	4.9	40	-14.7	-18.3	20
10-14	9	997.4	40	41.1	40	38.9	40	46.9	40	6.5	40	+2.1	-18.7	20
15-19	10	1017.2	40	46.3	40	44.6	40	47.5	28	6.7	28	+4.9	-3.5	16
20-24	11	1039.4	28	45.8	28	43.7	28	48.0	35	6.3	35	+1.3	-20.3	16
25 Mar. 1	12	1013.4	35	47.1	35	44.9	35	48.0	40	6.5	40	-0.7	-17.2	20
Mar. 2-6	13	1015.3	40	47.9	40	46.6	40	48.6	7	7.6	7			
7-11	14	997.9	7	48.7	7	48.0	7	48.9	23	6.5	23	-21.6	-16.5	12
12-16	15	997.3	23	41.8	23	40.2	23	46.7	41	6.4	41	-30.7	-16.6	20
17-21	16	990.0	41	38.9	41	36.9	41	47.5	39	7.3	39	-1.9	-15.1	20
22-26	17	1006.8	39	47.4	39	46.2	39	47.3	40	5.4	40	+6.9	-12.7	20
27-31	18	992.4	40	46.1	40	44.6	40	46.9	40	5.6	40	-17.5	+13.0	20
Apr. 1-5	19	986.5	40	39.3	40	37.9	40	47.4	31	6.4	31	-11.5	+3.7	16
6-10	20	997.2	31	41.8	31	39.0	31	48.0	23	7.2	23	-21.6	-10.5	12
11-15	21	1010.2	23	44.8	23	43.0	23	48.0	40	6.2	40	+4.7	+8.9	20
16-20	22	1020.2	40	42.5	40	39.3	40	47.5	40	6.6	40	+0.6	-9.7	20
21-25	23	1011.1	40	45.7	40	43.6	40	47.1	39	6.3	39	-2.9	-9.7	20
26-30	24	1014.5	39	41.9	39	37.9	39	48.1	49	5.0	49	-1.3	-0.4	20
May 1-5	25	1009.0	49	42.3	49	38.2	49	48.1	40	6.2	40	-6.5	-11.4	20
6-10	26	1010.5	40	45.6	40	42.9	40	48.3	40	6.8	40	-2.1	-7.1	20
11-15	27	999.9	40	46.4	40	44.1	40	49.1	32	7.0	34	+3.7	-4.1	16
16-20	28	1026.4	35	49.6	35	48.4	35	48.7	46	6.0	46	+1.5	+6.5	20
21-25	29	1022.1	46	43.9	46	39.9	46	48.7	40	6.2	40	+2.3	+2.1	20
26-30	30	1013.0	40	46.6	40	43.1	40							
May 31-June 4	31	1000.9	40	48.2	40	45.4	40	49.3	40	6.2	40	-0.9	+1.7	20
June 5-9	32	1006.6	40	47.9	40	45.6	40	49.6	40	7.0	40	+9.3	+7.2	20
10-14	33	1009.0	49	50.7	49	49.9	49	50.9	49	7.4	49	+18.5	-5.5	20
15-19	34	1005.9	39	49.2	39	47.3	39	50.9	39	7.3	39	+8.6	+4.3	20
20-24	35	1013.0	40	49.6	40	47.2	40	51.5	40	6.4	40	+9.2	+1.5	20
25-29	36	1015.6	34	51.1	34	49.3	34	52.8	34	7.0	34	-4.4	-1.2	20
June 30-July 4	37	1015.8	37	50.6	37	47.6	37	52.5	37	6.6	37	-13.4	-2.1	16
July 5-9	38	1023.2	44	51.5	44	49.3	44	52.4	44	7.4	44	-8.1	-1.2	20
10-14	39	1013.3	40	51.3	40	49.8	40	52.9	40	7.0	40	-10.9	+3.9	20
15-19	40	1005.8	40	51.3	40	49.4	40	52.7	40	7.3	40	+9.5	+9.1	20
20-24	41	1003.0	48	53.2	48	50.6	48	53.5	48	6.5	48	-3.1	+1.8	20
25-29	42	997.7	43	54.2	43	52.3	43	53.1	43	7.0	43	-6.3	-17.9	20
30-Aug. 3	43	1022.5	39	53.2	39	50.4	39	53.9	39	7.4	39	+2.8	+6.5	20
Aug. 4-8	44	1011.1	40	54.0	40	51.9	40	54.5	40	7.3	40	+9.7	+1.4	20
9-13	45	1008.1	41	54.2	41	51.6	41	55.0	41	6.0	41	-7.8	-3.0	20
14-18	46	1015.3	49	54.5	49	51.2	49	55.3	48	5.0	49	+0.9	-1.7	20
19-23	47	1000.4	40	52.7	40	50.2	40	54.5	27	6.4	40	+12.5	+7.7	20
24-28	48	1008.5	40	53.3	40	51.7	40	53.9	40	6.9	40	+6.3	-4.1	20
Aug. 29-Sept. 2	49	1001.7	40	53.0	40	50.5	40	54.7	40	7.0	40	-4.9	+1.9	20
Sept. 3-7	50	1005.2	43	53.2	43	50.0	43	55.0	43	6.0	43	-4.5	+2.8	20
8-12	51	1000.1	39	51.1	39	47.5	39	55.0	39	5.8	39	-7.5	+14.4	20
13-17	52	1002.0	40	51.1	40	48.9	40	54.3	40	6.3	40	-17.1	-6.7	20
18-22	53	1019.9	40	49.1	40	46.1	40	53.2	40	6.5	40	-6.1	-1.5	20
23-27	54	995.7	51	50.9	51	50.0	51	52.5	51	7.6	51	+15.7	+3.9	20
28-Oct. 2	55	998.9	34	49.7	34	48.4	34	51.4	34	6.6	34	+0.3	-3.1	20
Oct. 3-7	56	1017.5	40	49.5	40	47.2	40	51.1	40	6.6	40	-9.4	-2.9	20
8-12	57	993.1	40	50.6	40	48.8	40	51.0	40	6.1	40	+0.5	-17.7	20
13-17	58	988.1	38	45.8	38	43.3	37	50.7	38	5.8	38	-10.5	+1.9	20
18-22	59	1002.0	27	48.2	27	47.2	27	50.4	27	7.2	27	-23.7	+5.9	12
23-27	60	1012.1	17	44.4	17	41.7	17	49.3	17	6.9	17			
Oct. 28-Nov. 1	61	1001.4	40	46.5	40	43.9	40	49.1	40	5.3	40	-6.6	-16.9	20
Nov. 2-6	62	1001.2	40	43.1	40	40.1	40	48.9	40	5.7	40	+12.5	+8.2	20
7-11	63	1011.4	48	46.5	48	44.6	48	48.1	48	6.5	48	+11.7	-5.7	20
12-16	64	997.1	42	48.5	42	47.1	42	48.7	42	5.8	42	+0.8	-16.1	20
17-21	65	995.3	40	44.7	40	42.2	40	47.9	40	6.4	40	-6.9	+0.9	20
22-26	66	1003.4	40	49.9	40	48.7	40	48.0	40	6.6	40	+10.9	-18.1	20
27-Dec. 1	67	998.6	44	48.1	44	46.8	44	48.7	44	6.6	44	-0.9	-10.3	20
Dec. 2-6	68	984.8	40	43.9	40	42.2	40	48.7	40	5.2	40	-7.7	-10.9	20
7-11	69	996.3	40	44.8	40	43.1	40	48.3	40	5.9	40	+15.5	+10.9	20
12-16	70	986.2	39	43.3	39	41.5	39	47.9	39	6.2	39	-6.7	-1.1	20
17-21	71	1018.6	47	47.9	47	46.1	47	48.1	47	6.6	47	-0.9	-15.2	20
22-26	72	1007.5	40	47.5	40	45.4	40	47.9	40	6.6	40	+6.9	-14.9	20
27-31	73	976.9	40	39.8	40	38.1	37	47.9	40	5.7	40	-15.9	-7.1	20

Five-day mean values at ocean weather ship station J

JIG 1948

1948	No.	Bar. (mb.)	No. of obs.	Dry bulb (°F.)	No. of obs.	Wet bulb (°F.)	No. of obs.	Sea temp. (°F.)	No. of obs.	Total cloud amount (oktas)	No. of obs.	Mean vector wind components (kt.) E	N	No. of obs.
Jan. 1-5	1	997.9	40	47.9	40			51.2	40	5.0	40	-15.0	-11.1	20
6-10	2	990.8	42	45.0	42			51.0	42	4.9	42	-12.9	-2.2	20
11-15	3	995.1	46	47.5	46			51.0	46	5.0	46	-24.1	-2.1	20
16-20	4	1000.2	17	44.4	39			49.9	39	6.6	39	-27.8	+6.1	20
21-25	5	-	-	44.0	40			49.6	40	5.9	40	-12.7	-0.9	20
26-30	6	-	-	45.6	40			50.4	40	5.8	40	-8.7	-16.3	20
Jan. 31-Feb. 4	7	-	-	47.4	7			50.0	7	6.7	7			
Feb. 5-9	8	1003.0	35	46.4	35			49.0	35	5.8	35	-21.1	-15.1	16
10-14	9	1007.8	39	44.7	39			49.8	39	5.9	39	-9.5	-4.9	20
15-19	10	1018.7	40	48.4	40			51.0	40	5.8	40	+6.9	-10.1	20
20-24	11	1031.0	40	46.4	40			51.0	40	5.2	40	+13.3	+5.4	20
Feb. 25-Mar. 1	12	1015.8	46	47.9	46			50.1	46	6.5	46	+9.2	-4.7	20
Mar. 2-6	13	1021.8	40	50.3	40			50.2	40	6.4	40	+2.1	-14.9	20
7-11	14	1018.5	40	51.3	40			50.6	40	5.4	40	-6.9	-22.6	20
12-16	15	1019.9	40	48.1	40			50.3	40	5.9	40	-7.5	-7.9	20
17-21	16	1009.5	48	46.5	48			50.5	48	7.1	48	-18.7	-10.9	20
22-26	17	1012.2	41	50.8	41			51.0	41	7.2	41	+6.1	-20.1	20
27-31	18	994.3	40	47.4	40			50.7	40	6.0	40	-8.9	-10.4	20
Apr. 1-5	19	996.3	41	43.7	41			50.7	41	4.7	41	-24.1	+6.1	20
6-10	20	1007.6	48	47.3	48			50.9	48	6.0	48	-17.9	-1.5	20
11-15	21	1024.5	40	50.9	40			51.1	40	6.6	40	-12.7	-5.1	20
16-20	22	1014.3	39	48.1	39			50.8	39	6.9	39	+2.4	+9.9	20
21-25	23	1015.4	40	48.7	40			50.8	40	6.1	40	-5.1	-3.6	20
26-30	24	1016.6	42	47.9	42			51.2	42	6.4	42	-11.3	+3.8	20
May 1-5	25	1008.1	47	49.0	47			51.2	47	4.7	47	-3.5	-0.9	20
6-10	26	1019.5	40	50.3	40			51.9	40	6.5	40	-9.0	-7.4	20
11-15	27	1008.0	40	50.5	40			51.3	40	6.9	40	-4.3	-19.3	20
16-20	28	1021.9	41	54.1	41			53.2	41	3.8	41	+8.9	+0.1	20
21-25	29	1022.5	47	49.7	47			53.3	47	6.5	47	+4.1	+10.9	20
26-30	30	1012.4	40	49.9	40			52.4	40	5.8	40	-4.9	+4.7	20
May 31-June 4	31	1003.4	40	50.1	40			52.3	39	6.6	40	-14.3	0.0	20
June 5-9	32	1006.7	40	50.9	40			52.[illegible]	34	6.2	40	-10.7	+0.8	20
10-14	33	1004.8	47	53.6	47			52.9	47	5.4	47	+2.3	-14.5	20
15-19	34	1006.1	40	53.0	40			53.4	40	5.8	40	-11.1	-1.3	20
20-24	35	1014.6	40	53.2	40			53.6	40	7.1	40	-9.5	-6.0	20
25-29	36	1024.5	40	54.1	40			53.5	40	7.3	40	-14.5	-3.9	20
June 30-July 4	37	1024.6	49	54.7	49			54.0	49	7.6	49	-10.7	-3.3	20
July 5-9	38	1031.7	40	55.2	40			55.4	40	7.4	40	-7.5	+3.9	20
10-14	39	1021.5	40	54.6	40			55.5	40	7.6	40	-8.7	+8.8	20
15-19	40	1007.4	40	54.3	40			56.1	40	7.1	40	-11.7	-1.9	20
20-24	41	1004.9	48	56.2	48			56.7	48	6.6	48	-1.9	-1.5	20
25-29	42	1008.5	40	57.7	40			57.3	40	6.9	40	-6.0	-13.8	20
July 30-Aug. 3	43	1017.1	40	57.2	40			59.2	40	7.4	40	+2.5	+5.8	20
Aug. 4-8	44	1002.3	40	59.0	40			60.3	40	7.1	40	+6.0	+5.7	20
9-13	45	1014.5	43	58.1	43			60.2	43	6.3	43	-6.5	+2.1	20
14-18	46	1013.3	50	56.7	50			59.3	50	7.0	50	-3.3	+6.1	20
19-23	47	1002.9	40	56.2	40			59.7	40	5.4	40	-18.7	-2.7	20
24-28	48	1009.1	40	56.9	40			57.9	40	5.7	40	-4.6	-7.5	20
Aug. 29-Sept. 2	49	1005.1	40	56.6	40			57.5	40	6.4	40	-12.8	-5.5	20
Sept. 3-7	50	1010.9	48	55.3	48			56.6	48	5.8	48	-15.7	-4.9	20
8-12	51	1005.3	40	54.1	40			56.1	40	5.5	40	-11.4	+0.1	20
13-17	52	1017.7	40	54.8	40			55.8	40	6.9	40	-13.7	-3.9	20
18-22	53	1022.5	40	54.9	40			55.9	40	7.4	40	+1.8	-2.5	20
23-27	54	998.4	49	57.0	49			57.1	49	6.9	49	-9.5	-19.0	20
Sept. 28-Oct. 2	55	1009.1	40	56.9	40			58.0	40	5.5	40	-14.5	-13.5	20
Oct. 3-7	56	1021.1	40	53.7	40			57.1	40	4.4	40	+6.5	+2.3	20
8-12	57	1003.1	42	55.5	42			56.6	42	5.7	42	-9.1	-14.7	20
13-17	58	998.7	47	52.8	47			55.6	47	6.7	47	-20.6	+1.9	20
18-22	59	1017.2	40	53.3	40			55.0	40	6.6	40	-17.3	+2.8	20
23-27	60	1011.9	40	50.5	40			55.1	40	6.2	40	-8.9	-2.1	20
Oct. 28-Nov. 1	61	1009.5	40	52.5	40			54.7	40	6.3	40	+0.7	-6.3	20
Nov. 2-6	62	1000.3	49	50.2	49			53.9	49	6.2	49	-4.6	-3.9	20
7-11	63	1007.2	43	53.7	43			53.3	43	5.9	43	+8.9	-13.4	20
12-16	64	1008.4	38	52.9	38			53.8	38	5.4	38	-7.7	-14.4	20
17-21	65	1006.7	38	50.3	38			53.4	36	6.2	38	-10.3	-11.8	20
22-26	66	1003.7	39	54.4	39			53.0	39	7.2	39	+12.7	-20.9	20
Nov. 27-Dec. 1	67	1003.6	48	52.7	48			53.2	48	5.6	48	+3.3	-22.0	20
Dec. 2-6	68	991.1	40	48.7	40			52.4	40	4.6	40	-6.3	-13.7	20
7-11	69	986.4	39	47.2	39			52.1	39	4.8	39	-4.1	-5.9	20
12-16	70	994.2	40	48.3	40			52.0	40	6.3	40	-14.1	-3.5	20
17-21	71	1025.0	49	52.2	49			52.2	49	7.1	49	+3.1	-17.1	20
22-26	72	1005.9	39	51.7	39			51.9	39	6.6	39	+8.5	-15.7	20
27-31	73	1002.3	28	44.8	28			51.6	28	5.7	28	-28.1	-8.3	15

G.37837(h)/JEK/1/56/50

1949	No.	Bar. (mb.)	No. of obs.	Dry bulb (°F.)	No. of obs.	Wet bulb (°F.)	No. of obs.	Sea temp. (°F.)	No. of obs.	Total cloud amount (oktas)	No. of obs.	Mean vector wind components (kt.) E	N	No. of obs.
Jan. 1-5	1	993.2	40	35.7	40	34.2	40	46.9	40	6.2	40	-2.5	+6.3	20
6-10	2	1017.7	44	42.7	44	40.5	44	48.3	44	6.2	44	-22.6	-4.0	20
11-15	3	1003.9	38	42.5	38	40.6	38	47.7	38	6.7	38	-23.3	-8.9	20
16-20	4	990.8	40	38.4	40	37.0	40	46.7	40	6.5	40	-38.3	-7.4	20
21-25	5	996.4	40	41.5	40	40.1	40	46.9	40	6.4	40	-17.8	-21.6	20
26-30	6	1017.6	23	43.7	23	41.8	23	48.0	23	5.1	23	-7.6	-8.9	12
31-Feb.4	7	1017.2	40	46.9	40	45.9	40	47.7	40	7.4	40	-1.8	-16.4	20
Feb. 5-9	8	986.5	40	43.0	40	41.4	40	47.2	40	6.4	40	-4.7	-14.4	20
10-14	9	990.2	39	42.9	39	41.4	39	47.3	39	6.5	39	-20.5	-18.1	20
15-19	10	989.3	34	41.3	34	38.8	34	47.3	34	6.4	34	-12.8	-20.5	18
20-24	11	996.1	38	37.4	38	35.4	38	47.2	38	5.4	38	-31.0	-13.1	20
25-Mar.1	12	1015.5	40	40.7	40	38.7	40	46.9	40	6.5	40	-19.7	-5.1	20
Mar. 2-6	13	1011.0	40	45.1	40	42.9	40	46.7	40	6.9	40	-10.3	-13.1	20
7-11	14	1014.5	41	42.7	41	39.6	41	47.0	41	6.4	41	-5.9	-1.1	20
12-16	15	1004.4	44	38.7	44	37.4	44	46.5	44	7.0	44	-17.5	-1.7	20
17-21	16	1012.6	40	44.4	40	43.4	40	46.6	40	6.4	40	-15.3	-8.3	20
22-26	17	1020.8	39	41.1	39	39.6	39	46.4	39	5.8	39	-12.6	-7.7	20
27-31	18	1020.3	40	46.9	40	45.5	40	47.1	40	7.1	40	+7.1	-6.0	20
Apr. 1-5	19	992.0	47	44.8	47	42.9	47	48.0	47	7.4	47	+5.5	+8.5	20
6-10	20	1007.7	40	42.2	40	38.8	40	47.6	40	6.5	40	-3.6	-0.4	20
11-15	21	989.4	25	45.0	25	41.6	25	48.7	25	6.4	25	-9.2	-3.4	12
16-20	22	1000.8	30	41.1	30	39.1	30	47.7	30	6.6	30	-9.7	-5.0	16
21-25	23	1000.4	40	42.1	40	39.2	40	47.7	40	6.1	40	-12.3	-2.3	20
26-30	24	1006.8	40	44.6	40	42.5	40	48.5	40	6.9	40	-17.7	-7.3	20
May 1-5	25	1014.8	40	44.7	40	41.8	40	48.6	40	7.2	40	-8.3	-0.1	20
6-10	26	1018.7	40	46.1	40	44.2	40	49.1	40	7.4	40	-4.7	-8.0	20
11-15	27	1013.4	47	45.0	47	41.9	47	48.2	47	5.7	47	-8.3	-4.1	20
16-20	28	1017.0	40	44.8	40	41.9	40	48.4	40	6.2	40	+12.6	+5.7	20
21-25	29	1007.3	32	47.0	32	45.5	32	49.0	32	7.3	32	+19.3	+5.8	16
26-30	30													
May 31-June 4	31													
June 5-9	32	1013.5	5	50.8	5	48.8	5	50.2	5	7.6	5			
10-14	33	1018.2	40	49.3	40	47.1	40	50.9	40	7.5	40	-5.5	-2.3	20
15-19	34	1018.5	40	51.2	40	50.1	40	50.9	40	6.9	40	+13.1	-11.6	20
20-24	35	1020.4	39	52.9	39	51.7	39	52.3	39	6.5	39	+7.7	-7.7	20
25-29	36	1011.3	48	52.9	48	51.6	48	52.9	48	7.1	48	+2.9	-12.9	20
June 30-July 4	37	1009.5	37	50.4	37	48.3	37	52.0	37	6.9	37	-10.2	-13.1	20
July 5-9	38	1023.7	40	51.5	40	51.1	40	52.5	40	7.9	40	-5.3	-8.9	20
10-14	39	1025.4	40	51.1	40	48.0	40	53.0	40	7.5	40	-2.7	-0.1	20
15-19	40	1021.7	49	51.0	49	48.6	49	54.3	49	7.3	49	-4.1	+1.7	20
20-24	41	1006.1	40	53.9	40	52.5	40	55.9	40	7.3	40	+1.4	-10.5	20
25-29	42	1005.7	40	53.5	40	52.0	40	54.2	40	7.6	40	-9.8	-3.7	20
30-Aug.3	43	1006.9	40	51.9	40	48.9	40	53.9	40	6.1	40	+2.2	+7.4	20
Aug. 4-8	44	994.7	42	52.5	42	50.6	42	54.1	42	7.1	42	+8.1	+12.3	20
9-13	45	1014.7	41	53.1	41	50.5	41	53.5	41	5.5	41	-8.1	-8.2	20
14-18	46	1019.4	40	52.2	40	49.4	40	53.8	40	6.5	40	-8.7	-3.5	20
19-23	47	1014.9	40	53.1	40	52.1	40	53.8	40	7.6	40	-9.9	-6.9	20
24-28	48	1011.1	46	54.7	46	53.5	46	54.1	46	6.2	46	-3.7	-11.5	20
29-Sept.2	49	993.4	40	53.1	40	51.5	40	54.2	40	6.1	40	+4.1	-2.3	20
Sept.3-7	50	997.6	40	53.1	40	51.4	40	54.6	40	6.2	40	-1.9	+1.1	20
8-12	51	1018.4	40	51.3	39	47.9	39	53.7	40	6.4	40	-6.1	-2.5	20
13-17	52	1015.7	43	52.2	43	49.8	43	53.9	43	6.9	43	+0.9	-1.9	20
18-22	53	1016.7	41	53.8	41	52.9	41	54.5	41	7.1	41	+6.1	-7.3	20
23-27	54	1010.6	39	53.1	39	51.0	39	54.3	39	7.4	39	-4.1	-9.3	20
28-Oct.2	55	1008.1	40	50.9	40	48.1	40	53.8	40	7.1	40	16.8	-8.5	20
Oct. 3-7	56	1011.8	40	51.2	40	50.3	40	53.9	40	7.9	40	12.2	+3.4	20
8-12	57	1000.3	49	53.5	49	52.9	49	54.1	49	7.2	49	+9.5	-5.0	20
13-17	58	981.4	40	51.2	40	49.2	40	53.7	40	6.2	40	-6.9	-10.9	20
18-22	59	983.6	39	46.7	39	43.8	39	52.8	39	5.2	39	+1.7	+0.1	20
23-27	60	1013.4	40	44.3	40	40.9	40	52.2	40	5.4	40	+6.3	+1.9	20
28-Nov.1	61	1008.8	41	48.6	41	45.7	41	51.9	41	5.5	41	-5.6	-11.7	20
Nov. 2-6	62	986.5	40	45.1	40	42.1	40	51.1	40	6.3	40	-24.5	-7.0	20
7-11	63	991.1	40	46.2	40	43.6	40	50.7	40	5.7	40	+2.1	+7.7	20
12-16	64	995.7	40	47.3	40	45.5	40	50.1	40	6.5	40	+4.7	-15.9	20
17-21	65	982.7	45	45.7	45	42.9	45	50.0	45	4.6	45	+6.1	-1.7	20
22-26	66	1005.6	39	47.8	39	45.7	39	50.0	39	5.4	39	+3.7	+9.1	20
27-Dec.1	67	1006.2	40	44.3	40	41.6	40	49.6	40	5.7	40	-20.7	+2.9	20
Dec. 2-6	68	991.0	40	41.0	40	38.3	40	49.2	40	5.1	40	-19.0	+0.6	20
7-11	69	1015.8	41	37.5	41	35.4	41	48.3	41	7.0	41	-8.4	+12.3	20
12-16	70	993.2	40	40.8	40	37.7	40	49.1	40	5.1	40	-15.3	+0.5	20
17-21	71	989.5	39	41.7	39	38.8	39	49.0	39	5.3	39	-1.3	+7.5	20
22-26	72	988.4	38	42.6	38	40.3	38	48.8	38	5.5	38	-8.0	-9.5	20
27-31	73	995.6	40	42.7	40	39.7	40	48.9	40	6.0	40	-2.9	-11.4	20

1949	No.	Bar. (mb.)	No. of obs.	Dry bulb (°F.)	No. of obs.	Wet bulb (°F.)	No. of obs.	Sea temp. (°F.)	No. of obs.	Total cloud amount (oktas)	No. of obs.	Mean vector wind components (kt.) E	N	No. of obs.
Jan. 1-5	1	998.6	37	46.0	37			51.0	37	6.8	37	-13.8	+5.1	20
6-10	2	1027.3	42	47.9	42			51.0	42	6.7	42	-14.3	+1.5	20
11-15	3	1021.5	40	49.9	40			51.0	40	7.1	40	-16.9	-10.9	20
16-20	4	1015.8	40	48.3	40			51.1	40	7.3	40	-22.1	-11.9	20
21-25	5	1013.1	39	46.6	39			50.9	39	6.9	39	-8.7	-17.4	20
26-30	6	1017.2	42	49.0	42			50.9	42	7.0	42	-0.1	-11.9	20
Jan. 31-Feb. 4	7	1025.0	40	51.1	40			51.9	40	6.8	40	+2.1	-20.1	20
Feb. 5-9	8	999.4	40	44.9	40			50.5	40	6.5	40	-9.9	-12.7	20
10-14	9	1012.9	40	48.1	40			50.0	40	7.1	40	-17.7	-13.2	20
15-19	10	1001.1	46	47.5	46			49.8	46	7.0	46	-13.5	-15.2	20
20-24	11	1014.4	40	44.2	40			49.9	40	5.9	40	-25.6	-11.3	20
Feb. 25-Mar. 1	12	1030.4	40	48.4	40			50.0	40	5.7	40	-16.0	-3.9	20
Mar. 2-6	13	1021.9	40	49.5	40			50.2	40	7.5	40	-8.3	-14.0	20
7-11	14	1015.7	48	48.0	48			50.3	48	5.5	48	-4.5	+11.5	20
12-16	15	1017.7	41	49.1	41			50.4	41	7.3	41	-15.3	-0.2	20
17-21	16	1027.4	40	50.0	40			50.6	40	7.1	40	-13.9	-3.1	20
22-26	17	1025.1	40	48.3	40			50.5	40	6.7	40	+2.9	+1.5	20
27-31	18	1014.6	40	51.0	40			51.1	40	5.3	40	+11.9	-6.0	20
Apr. 1-5	19	992.1	48	50.2	48			51.8	48	6.3	48	-4.3	-4.7	20
6-10	20	1012.1	40	47.9	40			51.3	40	6.4	40	-0.9	-7.1	20
11-15	21	1000.5	40	50.4	40			51.4	40	7.1	40	-11.4	-13.4	20
16-20	22	1013.4	40	47.4	40			51.3	40	6.3	40	-11.3	-4.3	20
21-25	23	1011.6	47	48.2	47			50.9	47	6.9	47	-19.9	-2.9	20
26-30	24	1023.5	40	49.6	40			50.8	40	7.0	40	-12.3	-5.2	20
May 1-5	25	1024.6	40	50.1	40			51.8	40	6.4	40	-9.1	-3.6	20
6-10	26	1025.4	40	52.2	40			52.2	40	6.1	40	-3.7	-6.3	20
11-15	27	1020.6	50	49.0	50			52.1	50	6.5	50	-8.1	-6.1	20
16-20	28	1010.8	40	49.2	40			52.0	40	5.5	40	+3.5	+1.0	20
21-25	29	1000.7	40	50.8	40			52.5	40	5.1	40	-5.4	-0.5	20
26-30	30	1001.3	40	48.2	40			52.4	40	5.4	40	-13.9	+8.4	20
May 31-June 4	31	1001.9	48	50.6	48			52.7	48	5.2	48	-6.9	+4.1	20
June 5-9	32	1008.1	39	51.9	39			53.2	39	6.4	39	-3.5	-3.5	20
10-14	33	1026.3	40	53.1	40			54.0	40	7.4	40	-6.7	-1.7	20
15-19	34	1013.8	40	54.9	40			54.1	40	7.9	40	+12.7	-16.1	20
20-24	35	1018.2	42	55.7	42			55.2	42	7.6	42	+6.8	-8.7	20
25-29	36	1016.4	47	57.0	47			57.0	47	6.7	47	-1.7	-8.4	20
June 30-July 4	37	1022.7	40	55.5	40			56.1	40	7.4	40	-10.5	-7.3	20
July 5-9	38	1029.9	40	57.2	40			57.5	40	7.7	40	-4.3	-4.1	20
10-14	39	1018.8	16	58.8	16			61.0	16	7.9	16			
15-19	40	1021.4	44	56.1	44			57.7	44	7.3	44	+1.3	+3.9	20
20-24	41	1012.3	41	57.9	41			58.2	41	7.1	41	-5.9	-9.7	20
25-29	42	1016.1	38	58.2	38			58.7	38	6.9	38	-9.8	-5.6	20
July 30-Aug. 3	43	1007.3	40	57.0	40			58.1	40	7.0	40	-11.5	+2.1	20
Aug. 4-8	44	999.9	47	55.9	47			57.4	47	5.2	47	-15.8	-6.1	20
9-13	45	1021.5	18	57.2	18			58.1	18	7.0	18			
14-18	46	1024.4	36	57.9	36			58.9	36	7.2	36	-1.9	-6.6	20
19-23	47	1019.7	40	59.7	40			59.2	40	6.7	40	+0.9	-3.9	20
24-28	48	1017.6	49	60.5	49			61.0	49	5.2	49	-3.8	-6.9	20
Aug. 29-Sept. 2	49	1001.9	40	56.0	40			59.9	40	6.3	40	-14.3	-0.3	20
Sept. 3-7	50	1001.0	40	57.1	40			59.3	40	6.3	40	-9.1	-5.5	20
8-12	51	1019.0	40	56.8	40			58.9	40	6.8	40	-2.1	+1.1	20
13-17	52	1012.6	48	58.2	48			58.6	48	7.7	48	+5.9	-2.2	20
18-22	53	1013.0	42	59.1	42			58.8	42	6.5	42	+10.0	-0.9	20
23-27	54	1013.8	39	58.7	39			58.9	39	4.9	39	-1.5	-2.3	20
Sept. 28-Oct. 2	55	1022.7	39	56.4	39			58.3	39	6.9	39	-10.3	-2.9	20
Oct. 3-7	56	1010.7	43	59.6	43			58.8	43	6.2	43	+5.8	-8.8	20
8-12	57	997.7	39	58.3	39			58.3	39	6.5	39	-4.8	-7.9	20
13-17	58	991.7	40	54.4	40			57.6	40	6.3	40	-13.7	-13.4	20
18-22	59	990.1	40	48.5	40			56.0	40	4.9	40	-22.5	+1.7	20
23-27	60	1005.6	25	49.6	25			55.0	25	3.8	25	-1.3	+14.5	12
Oct. 28-Nov. 1	61	1019.5	32	51.8	32			54.5	32	5.1	32	-7.7	-9.6	16
Nov. 2-6	62	1005.1	38	49.5	39			54.4	39	6.1	39	-23.5	-7.1	20
7-11	63	997.7	41	50.0	41			53.7	41	6.4	41	-16.3	-8.1	20
12-16	64	1006.9	38	50.5	38			53.5	38	6.2	38	-17.8	-15.2	20
17-21	65	987.9	48	46.8	48			52.9	48	5.0	48	-16.3	+0.7	20
22-26	66	1005.8	41	50.0	41			52.3	41	6.2	41	-9.8	+13.3	20
Nov. 27-Dec. 1	67	1019.5	40	48.3	40			52.2	40	6.4	40	-13.5	+6.5	20
Dec. 2-6	68	1004.9	40	48.7	40			52.3	40	7.0	40	-19.5	-5.5	20
7-11	69	1021.9	49	45.1	49			51.5	49	6.9	49	-9.3	+12.1	20
12-16	70	1006.7	40	48.1	40			51.6	40	6.5	40	-25.5	+2.4	20
17-21	71	999.3	40	43.0	40			51.2	40	5.9	40	-27.1	-1.3	20
22-26	72	1003.3	40	48.7	40			50.6	40	6.4	40	-16.9	-17.1	20
27-31	73	1003.9	42	47.1	42			50.7	42	5.7	42	-8.6	-10.1	20

1950	No.	Bar. (mb.)	No. of obs.	Dry bulb (°F.)	No. of obs.	Wet bulb (°F.)	No. of obs.	Sea temp. (°F.)	No. of obs.	Total cloud amount (oktas)	No. of obs.	Mean vector wind components (kt.) E	N	No. of obs.
Jan. 1-5	1	1000.5	43	45.2	43	43.1	43	48.2	43	6.2	43	-7.3	-8.0	20
6-10	2	979.3	39	45.8	39	44.5	39	47.8	39	6.7	39	+9.2	-11.8	20
11-15	3	992.1	38	44.5	38	42.1	38	47.4	34	5.3	38	-17.2	-14.8	20
16-20	4	1011.9	39	45.9	39	44.3	39	47.1	39	6.8	39	-3.2	-13.1	20
21-25	5	1008.3	44	41.1	44	38.2	44	47.3	44	6.4	44	-7.3	-19.3	20
26-30	6	988.9	39	41.8	39	40.1	39	47.4	39	6.2	39	+8.5	-20.7	20
Jan.31-Feb.4	7	973.0	40	41.7	40	38.5	40	47.0	40	5.9	40	-1.7	-15.9	20
Feb. 5-9	8	980.0	40	40.8	40	38.6	40	47.1	40	6.0	40	-16.9	-14.4	20
10-14	9	990.0	43	39.0	43	36.9	43	47.1	43	5.0	43	+1.7	+6.4	20
15-19	10	987.6	40	39.9	40	37.6	40	47.1	39	4.6	40	-11.7	-4.7	20
20-24	11	1012.1	40	41.1	40	38.2	40	47.1	40	5.9	40	-7.4	+2.1	20
25-Mar.1	12	998.6	39	43.0	39	40.2	39	47.2	39	6.1	39	-2.1	-14.2	20
Mar. 2-6	13	1003.2	38	42.9	38	40.3	38	47.4	37	6.7	38	-17.9	-8.2	20
7-11	14	1022.3	37	45.6	37	44.4	37	47.5	37	6.6	37	-4.7	-0.5	20
12-16	15	1004.5	40	41.5	40	39.1	40	47.0	40	7.3	40	+20.7	+6.9	20
17-21	16	992.3	40	42.9	40	40.9	40	47.1	40	4.8	40	+7.4	+0.5	20
22-26	17	1002.7	45	44.2	45	42.0	45	47.5	45	6.0	45	-8.8	-9.3	20
27-31	18	1031.2	7	46.3	7	41.7	7	48.0	7	6.1	7			
Apr. 1-5	19	996.8	42	43.2	42	41.4	42	47.3	36	6.5	42	-21.5	+0.9	20
6-10	20	988.7	40	41.5	40	39.1	40	47.2	36	5.6	40	-17.3	+6.9	20
11-15	21	1006.3	45	42.8	45	39.4	45	47.8	45	6.6	45	-8.4	+7.0	20
16-20	22	1003.3	39	44.9	39	42.3	39	47.6	39	6.5	39	-13.7	-0.9	20
21-25	23	1017.5	40	44.1	40	40.4	40	47.9	40	4.8	40	-15.7	+12.1	20
26-30	24	1009.5	39	45.8	39	43.3	39	48.2	39	6.1	39	+7.9	-4.5	20
May 1-5	25	1009.2	44	50.0	44	48.3	44	49.2	44	5.7	44	+2.1	-14.6	20
6-10	26	1024.3	42	49.1	42	47.3	42	49.5	42	6.8	42	+5.1	-7.2	20
11-15	27	1028.1	40	51.1	40	49.4	40	50.4	40	7.2	40	+6.0	-2.0	20
16-20	28	1019.3	40	45.3	40	42.5	40	50.1	40	6.2	40	+5.1	+9.9	20
21-25	29	1025.8	40	48.1	40	44.3	40	50.1	40	5.9	40	+5.1	+9.3	20
26-30	30	1008.2	42	48.3	42	46.5	42	50.4	42	6.5	42	-11.8	-2.7	20
May 31-June 4	31	999.6	40	50.7	39	49.4	39	51.2	40	6.5	40	+1.7	-17.7	20
June 5-9	32	1010.3	40	50.0	40	48.7	40	51.7	40	7.2	40	-10.1	-10.1	20
10-14	33	1018.5	40	49.8	40	48.3	40	51.6	40	6.9	40	-5.1	-1.5	20
15-19	34	1009.3	49	50.3	49	48.9	49	52.6	49	6.9	49	-6.4	+6.3	20
20-24	35	1008.9	40	50.6	40	48.7	40	52.5	40	6.4	40	+3.3	+11.0	20
25-29	36	1001.0	40	52.1	40	50.5	40	53.5	40	6.5	40	+1.4	-1.3	20
June 30-July 4	37	1014.3	39	53.5	39	50.4	39	53.9	39	5.5	39	-1.0	-4.7	20
July 5-9	38	1003.8	45	54.8	45	53.9	45	55.1	45	7.1	45	+11.6	-2.3	20
10-14	39	999.2	40	53.8	40	51.7	40	55.4	40	6.1	40	-3.9	-5.2	20
15-19	40	999.4	40	55.3	40	54.5	40	56.1	40	6.5	40	+7.7	+5.5	20
20-24	41	1002.3	8	50.6	8	55.4	8	57.3	8	5.9	8			
25-29	42	998.5	3	56.3	3	55.0	3	54.3	3	8.0	3			
July 30-Aug.3	43	1001.5	40	56.6	40	52.9	40	57.3	40	4.8	40	+0.5	-4.7	20
Aug. 4-8	44	995.9	40	56.1	40	52.9	40	56.7	40	6.2	40	-2.5	-5.3	20
9-13	45	994.9	41	54.9	41	52.2	41	56.7	41	6.7	41	-11.8	-1.9	20
14-18	46	995.5	40	53.9	40	51.9	40	55.9	40	5.9	40	-9.5	+4.5	20
19-23	47	999.5	46	55.3	46	53.6	46	56.1	46	6.0	46	+8.0	+3.2	20
24-28	48	1001.5	39	54.4	39	52.1	39	56.4	39	6.0	39	+0.7	+4.2	20
Aug.29-Sept.2	49	1009.8	40	54.5	40	51.5	40	55.9	40	5.4	40	-4.8	-5.5	20
Sept. 3-7	50	990.5	40	51.7	40	48.7	40	54.3	40	5.7	40	-18.7	-9.8	20
8-12	51	999.3	42	52.8	42	50.5	42	53.7	42	5.5	42	-5.5	-6.3	20
13-17	52	979.9	21	51.2	21	48.8	21	53.3	21	6.2	21	-9.9	+1.3	12
18-22	53													
23-27	54	1011.2	39	51.2	39	48.0	39	52.8	39	6.5	39	-3.0	+3.7	20
Sept.28-Oct.2	55	998.5	45	47.3	45	43.3	45	52.2	45	5.5	45	-6.1	+2.1	20
Oct. 3-7	56	985.0	40	47.5	40	45.3	40	51.0	40	7.1	40	+5.3	-2.9	20
8-12	57	993.5	40	45.9	40	42.7	40	50.5	40	6.0	40	-0.8	0.0	20
13-17	58	989.5	17	49.4	17	47.5	17	50.1	17	4.6	17			
18-22	59	1023.8	4	51.3	4	48.3	4	52.3	4	3.0	4			
23-27	60	1011.2	5	46.4	5	43.0	5	49.8	5	3.8	5			
Oct.28-Nov.1	61	998.5	40	47.1	40	44.1	40	50.1	40	5.3	40	-0.9	-12.5	20
Nov. 2-6	62	1015.2	39	48.3	39	45.8	39	49.5	39	5.8	39	+9.7	-10.7	20
7-11	63	980.6	40	43.6	40	41.3	40	48.9	40	6.3	40	-20.6	-9.9	20
12-16	64	992.8	45	42.1	45	39.4	45	49.2	41	4.7	45	-2.5	+4.4	20
17-21	65	997.7	40	44.0	40	42.2	40	49.0	35	6.1	40	+10.4	+12.7	20
22-26	66	1018.4	32	44.1	32	42.1	32	48.6	27	5.2	32	0.0	+10.4	16
Nov.27-Dec.1	67	976.6	13	36.6	13	35.3	13	48.5	13	6.6	13			
Dec. 2-6	68													
7-11	69													
12-16	70													
17-21	71													
22-26	72													
27-31	73													

1950	No.	Bar. (mb.)	No. of obs.	Dry bulb (°F.)	No. of obs.	Wet bulb (°F.)	No. of obs.	Sea temp. (°F.)	No. of obs.	Total cloud amount (oktas)	No. of obs.	Mean vector wind components (kt.) E	N	No. of obs.
Jan. 1-5	1	1009.4	41	49.3	41			50.9	41	7.0	41	-17.3	-14.1	20
6-10	2	984.7	40	49.9	40			50.9	40	6.5	40	-9.5	-19.4	20
11-15	3	1010.4	42	48.1	42			50.6	42	5.5	42	-16.5	-16.9	20
16-20	4	1021.3	44	49.1	44			50.3	44	7.0	44	-3.1	-12.6	20
21-25	5	1014.6	42	47.1	42			50.8	42	6.5	42	-0.9	-6.8	20
26-30	6	994.3	41	43.1	41					6.7	41	-6.0	-4.3	20
Jan. 31-Feb. 4	7	980.1	41	41.7	41					6.2	41	-13.4	-11.7	20
Feb. 5-9	8	993.3	39	43.8	40					6.9	40	-12.6	-7.7	20
10-14	9	989.8	49	44.3	49			50.2	37	5.7	49	-12.3	-0.3	20
15-19	10	997.6	40	46.6	40			50.9	40	5.5	40	-10.5	-10.6	20
20-24	11	1006.4	40	47.3	40			51.0	40	6.1	40	+8.3	+6.9	20
Feb. 25-Mar. 1	12	1003.7	39	47.3	39			50.6	39	6.1	39	-7.9	-6.7	20
Mar. 2-6	13	1018.6	43	50.0	43			50.7	43	6.7	43	-15.5	-14.0	20
7-11	14	1020.5	40	49.2	40			50.3	40	5.4	40	+12.3	-1.3	20
12-16	15	993.1	40	50.1	40			50.4	40	5.8	40	+9.7	-14.3	20
17-21	16	990.9	40	48.5	40			50.0	40	5.2	40	-13.3	-6.7	20
22-26	17	1008.9	47	49.6	47			50.4	47	6.1	47	-3.7	-14.6	20
27-31	18	1026.7	40	50.4	40			50.0	40	7.1	40	+1.6	-2.5	20
Apr. 1-5	19	1012.5	40	46.3	40			49.4	40	7.1	40	-17.7	-0.5	20
6-10	20	1004.9	40	46.3	40			48.9	40	6.1	40	-23.7	-4.0	20
11-15	21	1013.7	40	46.1	40			49.2	40	5.1	40	-6.6	+3.3	20
16-20	22	1012.7	40	49.9	40			49.5	40	7.1	41	-10.1	-0.1	20
21-25	23	1023.6	40	50.5	40			49.9	40	6.7	40	-3.3	+2.0	20
26-30	24	1009.1	40	52.2	40			50.5	40	6.4	40	-4.1	-10.1	20
May 1-5	25	1011.9	40	52.4	40			50.7	40	5.6	40	-7.7	-8.1	20
6-10	26	1022.6	40	52.6	40			52.3	40	6.9	40	+4.3	-5.1	20
11-15	27	1020.8	40	54.3	40			53.5	40	3.6	40	+10.8	+3.9	20
16-20	28	1014.5	40	50.0	40			53.3	40	5.1	40	+4.2	+10.4	20
21-25	29	1014.1	40	51.8	40			51.9	40	4.9	40	+9.4	+13.3	20
26-30	30	1020.6	47	53.7	47			52.0	47	7.6	47	-12.1	-4.5	20
May 31-June 4	31	1006.9	41	54.9	41			52.3	41	6.0	41	-6.3	-15.2	20
June 5-9	32	1020.1	41	55.2	41			53.6	41	7.8	41	-6.7	-3.7	20
10-14	33	1017.7	40	56.7	40			55.4	40	6.9	40	+5.1	-1.2	20
15-19	34	1015.9	38	55.0	38			55.4	38	7.3	38	-3.3	+5.4	20
20-24	35	1010.2	40	55.1	40			55.7	40	7.3	40	-5.3	+1.0	20
25-29	36	1006.8	40	57.2	40			56.7	40	6.1	40	-9.9	-9.8	20
June 30-July 4	37	1014.8	39	56.5	39			56.8	39	6.8	39	+1.7	-4.1	20
July 5-9	38	1006.4	31	56.5	31			57.1	31	6.8	31	-7.7	-5.8	16
10-14	39	1005.7	40	57.6	40			57.0	40	5.4	40	-9.0	-3.1	20
15-19	40	1000.4	43	57.8	43			56.7	43	6.1	43	-13.0	+2.5	20
20-24	41	1007.1	39	56.9	39			58.4	39	5.3	39	-13.5	-1.9	20
25-29	42	1012.4	40	57.1	39			57.5	40	6.4	40	-13.9	-7.1	20
July 30-Aug. 3	43	1009.3	40	56.8	40			57.9	40	6.9	40	-17.1	+0.9	20
Aug. 4-8	44	999.8	38	57.2	38			57.9	38	6.2	38	-13.1	-3.0	20
9-13	45	992.1	5	56.2	5			57.4	5	6.8	5			
14-18	46	1009.2	40	55.6	40			56.7	40	6.4	40	-23.3	+7.6	20
19-23	47	999.9	40	55.2	40			56.3	40	5.4	40	-7.7	+1.0	20
24-28	48	1004.8	40	55.4	40			56.3	40	5.7	40	-8.5	+8.5	20
Aug. 29-Sept. 2	49	1013.3	40	55.9	40			56.7	40	6.3	40	-9.9	+2.5	20
Sept. 3-7	50	1006.0	40	55.6	40			56.1	40	7.0	40	-23.5	-4.2	20
8-12	51	1006.3	37	55.4	37			56.5	37	5.9	37	-7.3	-6.1	20
13-17	52	995.4	40	52.6	40			56.2	40	5.5	40	-14.9	+8.1	20
18-22	53	1014.7	40	53.3	40			55.1	40	5.9	40	-12.3	+1.1	20
23-27	54	1017.5	40	55.5	40			55.6	40	6.6	40	-12.3	-1.5	20
Sept. 28-Oct. 2	55	1008.4	22	52.4	22			56.5	22	6.0	22	-18.1	+3.9	20
Oct. 3-7	56	1000.3	40	54.1	40			55.3	40	6.5	40	-22.6	-10.7	20
8-12	57	1006.1	39	51.6	39			54.0	39	6.3	39	-18.5	-13.9	20
13-17	58											-17.7	+1.3	20
18-22	59	1021.7	12	53.7	12			54.7	12	3.3	12	-6.4	-8.9	20
23-27	60	1014.1	40	51.1	40			54.3	40	6.3	40	-12.5	-6.9	20
Oct. 28-Nov. 1	61	1004.6	40	51.7	40			53.4	40	6.4	40	-13.3	-8.7	20
Nov. 2-6	62	1008.5	40	54.6	40			53.6	40	7.9	40	+7.6	-12.7	20
7-11	63	1002.1	40	47.9	40			53.1	40	5.6	40	-26.5	+2.8	20
12-16	64	1004.7	40	47.5	40			52.3	40	6.4	40	-16.7	+1.1	20
17-21	65	1001.9	39	46.8	39			51.5	39	5.3	39	-18.2	+11.1	20
22-26	66	1018.0	40	48.1	40			51.3	40	5.3	40	+4.4	+15.7	20
Nov. 27-Dec. 1	67	1009.4	40	48.1	40			51.3	40	5.9	40	-8.0	+6.7	20
Dec. 2-6	68	1023.7	44	44.2	44			51.0	44	4.7	44	-5.8	+12.4	20
7-11	69	1010.6	40	47.7	40			50.9	40	5.9	40	-15.5	-0.1	20
12-16	70	1017.8	40	46.7	40			50.5	40	5.8	40	-12.7	+11.9	20
17-21	71	1007.0	43	48.3	43			50.2	43	5.8	43	-4.5	-3.7	20
22-26	72	1011.7	40	46.9	40			50.1	36	6.0	40	-6.6	+4.0	20
27-31	73	1010.4	39	45.7	39			50.0	35	5.9	39	-6.1	-0.6	20

1951	No.	Bar. (mb.)	No. of obs.	Dry bulb (°F.)	No. of obs.	Wet bulb (°F.)	No. of obs.	Sea temp. (°F.)	No. of obs.	Total cloud amount (oktas)	No. of obs.	Mean vector wind components (kt.) E	N	No. of obs.
Jan. 1-5	1													
6-10	2	987.8	26	42.5	26	38.5	26	47.8	26	4.7	26	-2.7	-7.2	12
11-15	3	976.4	37	40.1	37	37.2	37	47.3	37	5.4	37	-13.4	+5.9	16
16-20	4			41.6	27	39.8	27	47.5	27	6.6	27	-14.1	-11.4	12
21-25	5			40.2	40	37.6	40	47.1	40	5.7	40	-10.1	-4.1	20
26-30	6			37.0	47	34.9	47	47.5	47	5.1	47	-12.5	-6.3	20
Jan. 31-Feb. 4	7	978.2	22	39.7	40	38.5	40	47.7	40	5.1	40	-11.5	+14.4	20
Feb. 5-9	8	983.8	40	42.3	40	39.5	40	47.4	40	5.0	40	-1.9	+6.7	20
10-14	9	1016.5	40	39.9	40	38.2	40	47.2	40	5.2	40	-2.1	-2.9	20
15-19	10	984.7	40	40.0	49	38.2	49	47.0	49	5.8	49	-7.9	+16.3	20
20-24	11	1000.3	49	45.0	41	43.2	41	47.2	41	6.5	41	-14.9	-3.2	20
25-Mar. 1	12	1011.7	41	41.5	40	39.4	40	46.8	40	5.2	40	-19.8	-5.1	20
Mar. 2-6	13	1004.8	40	40.2	40	38.0	40	46.3	40	5.2	40	+18.1	+25.7	20
7-11	14	1015.6	40	41.1	40	38.5	40	46.4	40	6.5	40	+25.6	+4.7	20
12-16	15	994.2	40	42.2	33	39.6	33	47.1	33	6.2	33	+23.3	+3.9	16
17-21	16	1000.9	33	39.9	41	37.5	41	47.1	41	6.8	41	-0.7	+9.1	20
22-26	17	1011.8	41	42.7	40	40.8	40	46.8	40	6.8	40	-9.1	+11.9	20
27-31	18	1010.6	40	41.7	40	39.1	40	46.3	40	5.4	40	-15.0	+0.5	20
Apr. 1-5	19	1003.5	40	41.9	47	38.9	47	46.7	47	6.7	47	-4.4	+8.0	20
6-10	20	1008.4	47	38.3	40	35.7	40	46.1	40	6.6	40	-15.1	+12.9	20
11-15	21	998.7	40	40.4	40	37.2	40	46.5	40	5.4	40	-5.7	+2.3	20
16-20	22	1015.7	40	44.8	40	42.5	40	46.5	40	6.2	40	-14.1	-6.8	20
21-25	23	1006.0	40	45.9	45	42.9	45	47.5	45	6.3	45	-4.9	+5.7	20
26-30	24	1032.1	45	46.4	40	44.8	40	48.0	40	6.1	40	-9.7	+5.7	20
May 1-5	25	1024.2	40	46.3	40	44.3	40	48.1	40	7.1	40	-2.3	-8.5	20
6-10	26	1025.6	40	47.3	40	46.9	40	48.3	40	7.6	40	-11.6	-3.2	20
11-15	27	1025.7	40	49.5	41	48.4	41	48.8	41	5.7	41	-7.6	-10.7	20
16-20	28	1011.8	41	49.8	40	48.8	40	49.2	40	5.8	40	+13.1	+0.3	20
21-25	29	1006.4	40	49.7	40	47.5	40	49.7	40	6.9	40	+9.4	-8.3	20
26-30	30	1019.5	40	51.4	40	50.4	40	50.9	40	6.3	40	+3.9	-8.7	20
May 31-June 4	31	1016.5	40	51.1	45	49.3	45	51.8	45	6.1	45	+19.3	-4.1	20
June 5-9	32	1016.9	45	49.0	40	45.7	40	52.0	40	6.5	40	+7.5	+4.3	20
10-14	33	1004.9	40	50.6	40	46.9	40	52.8	40	5.1	40	-2.7	+1.7	20
15-19	34	1010.1	40	51.3	40	48.7	39	53.3	40	6.4	40	-4.9	+2.3	20
20-24	35	1012.6	40	53.7	44	50.5	44	55.0	44	6.3	44	+4.4	-5.8	20
25-29	36	1019.4	44	52.9	42	50.3	42	54.2	42	6.9	42	-12.0	-2.9	20
June 30-July 4	37	1017.5	42	54.9	40	52.9	40	55.1	40	6.5	40	+0.7	-0.1	20
July 5-9	38	1004.5	40	54.2	40	50.9	40	55.5	40	5.3	40	-3.8	-0.4	20
10-14	39	1013.8	40	54.7	40	52.9	40	55.5	40	6.6	40	-14.7	-4.0	20
15-19	40	1017.0	40	54.3	36	52.0	36	56.0	36	7.0	36	-13.1	+1.1	16
20-24	41	1014.5	36	53.8	18	50.3	18	56.3	18	7.1	18			
25-29	42	1015.3	18	55.3	39	53.4	39	56.4	39	6.2	39	+1.1	-2.7	20
July 30-Aug. 3	43	999.7	39	55.0	40	51.8	40	57.6	40	5.7	40	+0.1	+7.2	20
Aug. 4-8	44	1010.5	40	52.8	39	49.0	39	55.9	39	5.7	39	-3.3	+9.0	20
9-13	45	1012.7	39	53.2	8	50.4	8	55.9	8	5.6	8			
14-18	46	1014.9	8											
19-23	47													
24-28	48													
Aug. 29-Sept. 2	49	998.9	36	54.3	36	52.3	36	55.6	36	6.1	36	-5.1	+9.1	16
Sept. 3-7	50	1002.2	40	53.3	40	51.5	40	54.7	40	6.5	40	-5.6	-9.2	20
8-12	51	995.3	39	54.0	39	52.3	39	54.9	39	6.8	39	+7.7	-23.7	20
13-17	52													
18-22	53													
23-27	54													
Sept. 28-Oct. 2	55	1021.7	6	52.0	6	51.2	6	53.0	6	6.3	6			
Oct. 3-7	56	1007.3	40	51.7	40	49.9	40	53.1	40	5.9	40	-2.3	-13.7	20
8-12	57	990.9	40	49.8	40	48.0	40	52.0	40	5.7	40	-9.5	-17.3	20
13-17	58	999.8	28	50.2	28	47.3	28	51.8	28	6.1	28	-15.1	-21.8	12
18-22	59	1008.6	36	43.4	36	41.1	36	53.5	36	6.2	36	-15.6	+7.1	16
23-27	60	999.7	40	50.6	40	49.9	40	51.3	40	6.9	40	+0.7	-14.3	20
Oct. 28-Nov. 1	61	1008.2	40	46.7	40	45.3	40	50.3	40	4.7	40	-9.9	-2.1	20
Nov. 2-6	62	996.8	43	48.1	43	47.0	43	50.3	43	6.7	43	+16.3	+9.9	20
7-11	63	995.0	40	49.3	40	47.9	40	50.2	40	6.8	40	+13.7	+7.3	20
12-16	64	989.3	40	49.0	40	47.9	40	50.0	40	7.1	40	+12.3	-0.9	20
17-21	65	984.8	40	47.0	40	44.9	40	49.9	40	6.5	40	+7.3	+15.8	20
22-26	66	1000.8	39	44.1	39	41.3	39	50.0	39	6.2	39	-1.2	-0.1	20
Nov. 27-Dec. 1	67	1008.1	40	45.0	40	42.7	40	49.5	40	5.9	40	-21.6	-5.1	20
Dec. 2-6	68	997.5	40	44.3	40	41.3	40	49.1	40	6.6	40	-22.9	-4.3	20
7-11	69	996.2	40	43.4	40	41.1	40	48.8	40	6.6	40	-13.1	-7.3	20
12-16	70	999.9	32	48.3	32	46.4	32	49.1	32	6.9	32	-10.1	-17.4	16
17-21	71	980.6	19	44.6	19	41.3	18	48.6	18	5.5	19			
22-26	72	977.0	34	39.9	34	38.1	34	47.7	21	6.4	34	-13.8	-3.6	16
27-31	73	989.8	40	38.3	40	35.7	40	47.4	40	5.7	40	-12.7	+3.3	20

1951	No.	Bar. (mb.)	No. of obs.	Dry bulb (°F.)	No. of obs.	Wet bulb (°F.)	No. of obs.	Sea temp. (°F.)	No. of obs.	Total cloud amount (oktas)	No. of obs.	Mean vector wind components (kt.) E	N	No. of obs.
Jan. 1-5	1	994.5	40	45.5	40			50.0	38	4.7	40	-15.6	+1.5	20
6-10	2	999.9	38	44.4	38			49.8	34	5.1	38	-13.1	-2.0	20
11-15	3	993.0	40	43.6	40			49.7	40	5.5	40	-21.1	+3.1	20
16-20	4	1013.8	40	51.1	40			49.6	40	7.5	40	-14.7	+13.0	20
21-25	5	1009.4	40	44.9	40			49.6	40	6.7	40	-17.7	+2.3	20
26-30	6	1005.9	40	45.3	40			49.5	40	6.1	40	-18.2	+2.9	20
Jan. 31-Feb. 4	7	991.4	39	43.2	39			49.5	39	5.6	39	-22.5	+4.9	20
Feb. 5-9	8	993.1	40	42.1	40			49.4	40	6.3	40	-22.0	+13.5	20
10-14	9	1014.2	40	44.7	40			49.3	40	4.7	40	-1.5	+11.9	20
15-19	10	994.4	40	42.2	40			49.5	40	6.4	40	-21.2	-0.3	20
20-24	11	1007.0	45	42.6	45			49.5	45	5.4	45	-14.4	+13.1	20
Feb. 25-Mar. 1	12	1021.1	36	48.2	36			48.9	36	7.3	36	-11.7	-1.8	20
Mar. 2-6	13	1018.6	40	46.1	40			50.4	40	6.6	40	-14.7	+2.2	20
7-11	14	1004.8	40	44.9	40			49.4	40	5.6	40	+5.5	+24.1	20
12-16	15	986.9	40	44.6	40			48.8	40	5.7	40	-9.7	-0.7	20
17-21	16	996.9	40	47.6	40			49.9	40	6.5	40	-3.3	-5.3	20
22-26	17	1019.0	34	48.1	34			50.7	34	7.4	34	-8.4	-2.0	16
27-31	18	1020.6	31	46.9	31			50.6	31	6.7	31	-14.1	+16.5	16
Apr. 1-5	19	1015.2	40	46.0	40			50.7	40	6.4	40	-10.7	+4.0	20
6-10	20	1016.3	46	46.4	46			49.4	44	5.9	46	-18.7	+14.3	20
11-15	21	1014.5	41	46.0	41			49.1	40	6.6	41	-13.3	+2.1	20
16-20	22	1014.1	45	48.6	45			49.3	45	7.6	45	+8.5	-4.4	20
21-25	23	1017.8	45	48.0	45			49.4	45	6.1	45	-2.3	+1.5	20
26-30	24	1032.7	21	48.3	21			51.2	21	6.5	21	+4.0	+5.3	20
May 1-5	25	1014.3	34	48.5	38			50.5	38	6.0	38	+2.3	+14.9	20
6-10	26	1028.1	37	50.0	37			51.9	37	6.6	37	+6.1	-6.4	16
11-15	27	1028.2	40	52.8	40			53.7	40	6.0	40	+3.1	-6.3	20
16-20	28	1010.6	42	52.3	42			53.6	42	5.4	42	+0.3	-8.4	20
21-25	29	993.6	50	53.3	50			53.1	50	6.1	50	+12.8	+3.1	20
26-30	30	1015.5	50	54.0	50			53.7	50	6.2	50	+2.8	+4.2	20
May 31-June 4	31	1012.6	50	55.4	50			55.1	50	5.6	50	+6.3	-7.0	20
June 5-9	32	1004.6	48	56.3	48			55.0	48	6.9	48	+17.5	-7.2	20
10-14	33	995.5	40	55.1	40			56.0	40	6.5	40	-1.1	-3.6	20
15-19	34	1015.1	40	52.9	40			55.4	40	6.1	40	-13.9	+2.3	20
20-24	35	1018.8	40	54.1	40			55.7	40	5.7	40	-9.9	+7.1	20
25-29	36	1019.3	40	56.4	40			56.7	40	6.9	40	-4.1	-4.7	20
June 30-July 4	37	1021.2	48	58.3	48			57.6	48	7.8	48	-7.3	-9.4	20
July 5-9	38	1008.0	50	57.8	50			57.4	50	7.1	50	-10.3	-4.3	20
10-14	39	1014.7	50	57.5	50			57.8	50	6.3	50	-0.3	-0.8	20
15-19	40	1028.8	50	59.1	50			59.3	50	7.0	50	-12.3	-1.7	20
20-24	41	1022.0	27	59.2	37			60.4	37	6.2	37	-0.9	-3.2	20
25-29	42	1019.5	40	60.3	40			61.0	40	5.1	40	-10.7	-5.8	20
July 30-Aug. 3	43	1008.1	37	58.6	37			60.1	37	6.0	37	-16.8	+3.5	16
Aug. 4-8	44	1013.3	40	57.9	40			59.7	40	6.9	40	-9.9	+11.3	20
9-13	45	1018.9	23	58.1	39			60.2	39	6.3	39	-5.9	+6.6	20
14-18	46	1009.6	40	58.7	40			59.2	40	6.1	40	-11.5	-10.6	20
19-23	47	1014.7	40	56.7	40			58.0	40	7.3	40	-20.0	+5.1	20
24-28	48	1001.7	40	54.9	40			57.1	40	6.7	40	-24.0	+7.4	20
Aug. 29-Sept. 2	49	1003.0	41	56.3	41			58.1	41	5.6	41	-6.5	+2.2	20
Sept. 3-7	50	1009.7	40	57.3	40			58.6	40	6.2	40	-8.5	-11.5	20
8-12	51	1002.3	40	57.2	40			58.9	40	5.5	40	-13.4	-13.5	20
13-17	52	1012.9	40	56.1	40			58.3	40	5.6	40	-11.8	+1.5	20
18-22	53	1013.3	40	58.2	40			58.9	40	7.7	40	-2.9	-11.1	20
23-27	54	996.2	50	55.1	50			57.2	50	6.1	50	-21.9	+4.3	20
Sept. 28-Oct. 2	55	1005.6	50	56.1	50			57.3	49	5.6	50	-6.4	-7.1	20
Oct. 3-7	56	1012.1	50	55.7	50			56.7	50	6.2	50	-1.4	-10.1	20
8-12	57	1000.2	50	54.0	50			55.7	50	5.6	50	-10.6	-11.1	20
13-17	58	1015.4	40	54.8	40			55.7	40	7.0	40	-12.1	-10.5	20
18-22	59	1021.6	40	50.0	40			55.1	40	5.1	40	-18.0	+12.6	20
23-27	60	1000.9	40	53.6	40			54.7	40	5.9	40	+0.6	-16.1	20
Oct. 28-Nov. 1	61	1016.5	40	52.1	40			54.4	40	5.4	40	-11.3	+3.7	20
Nov. 2-6	62	994.3	43	49.8	43			54.1	43	5.8	43	-8.4	+13.9	20
7-11	63	993.0	40	51.7	40			52.3	40	6.5	40	+0.1	+17.3	20
12-16	64	991.1	35	49.8	35			53.4	35	5.1	35	-10.6	-0.2	16
17-21	65	1002.4	16	49.7	16			53.4	16	5.5	16			
22-26	66	1006.2	47	49.7	47			53.4	47	6.3	47	-9.9	+1.7	20
Nov. 27-Dec. 1	67	1030.8	40	49.7	40			51.7	40	5.7	40	-14.5	-3.8	20
Dec. 2-6	68	1017.6	40	49.3	40			51.2	40	6.6	40	-19.9	-5.1	20
7-11	69	1011.1	7	50.6	7			51.6	7	7.6	7			
12-16	70	1003.9	4	50.3	4			52.7	4	4.7	4			
17-21	71	1006.3	40	46.9	40			51.2	40	5.6	40	-21.6	-9.1	20
22-26	72	993.3	40	44.2	40			50.8	39	5.9	40	-19.3	+0.5	20
27-31	73	1002.6	40	43.5	40			50.1	32	5.5	40	-27.4	+12.1	20

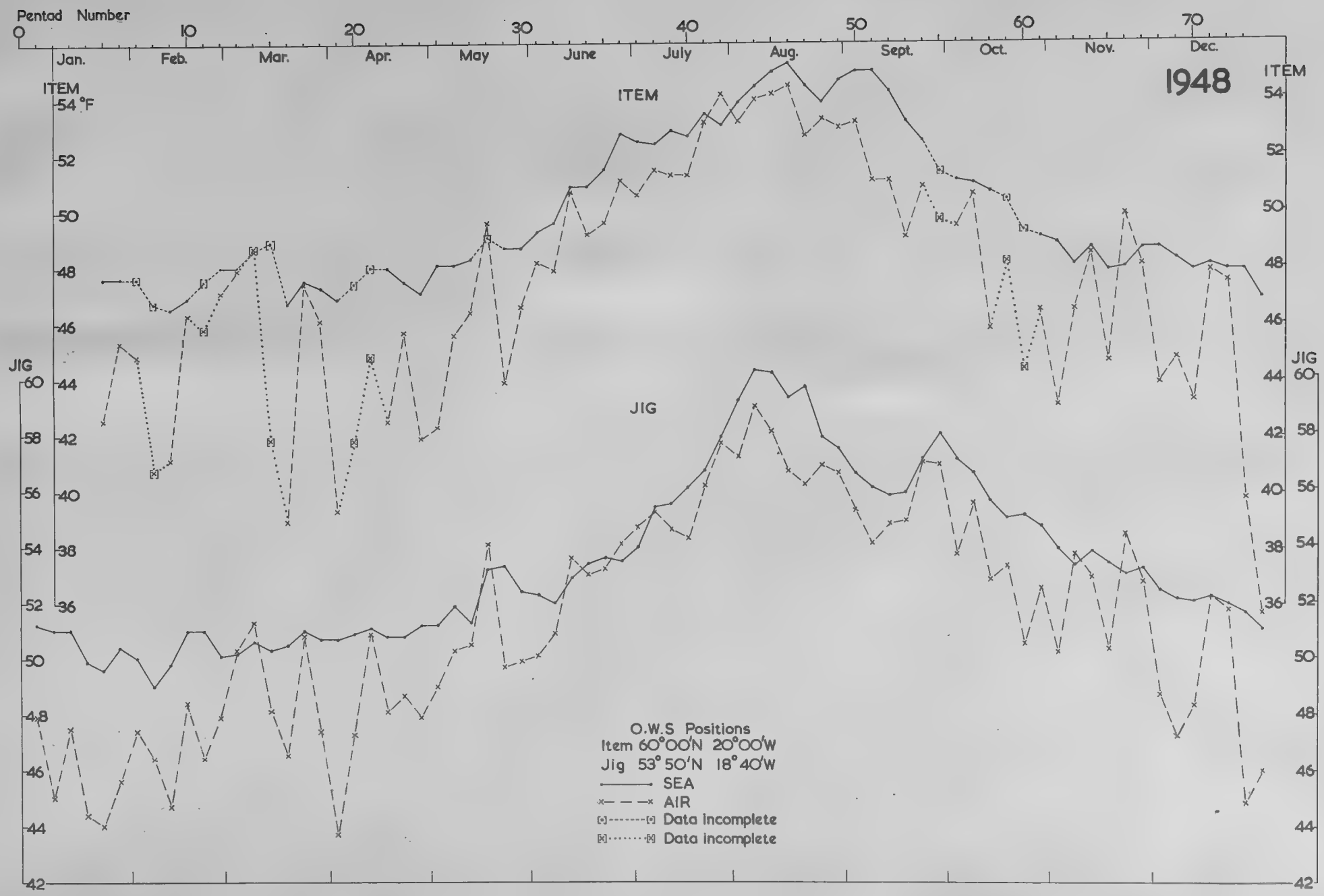

FIG. 1. FIVE DAY MEANS OF AIR AND SEA TEMPERATURE DURING 1948.

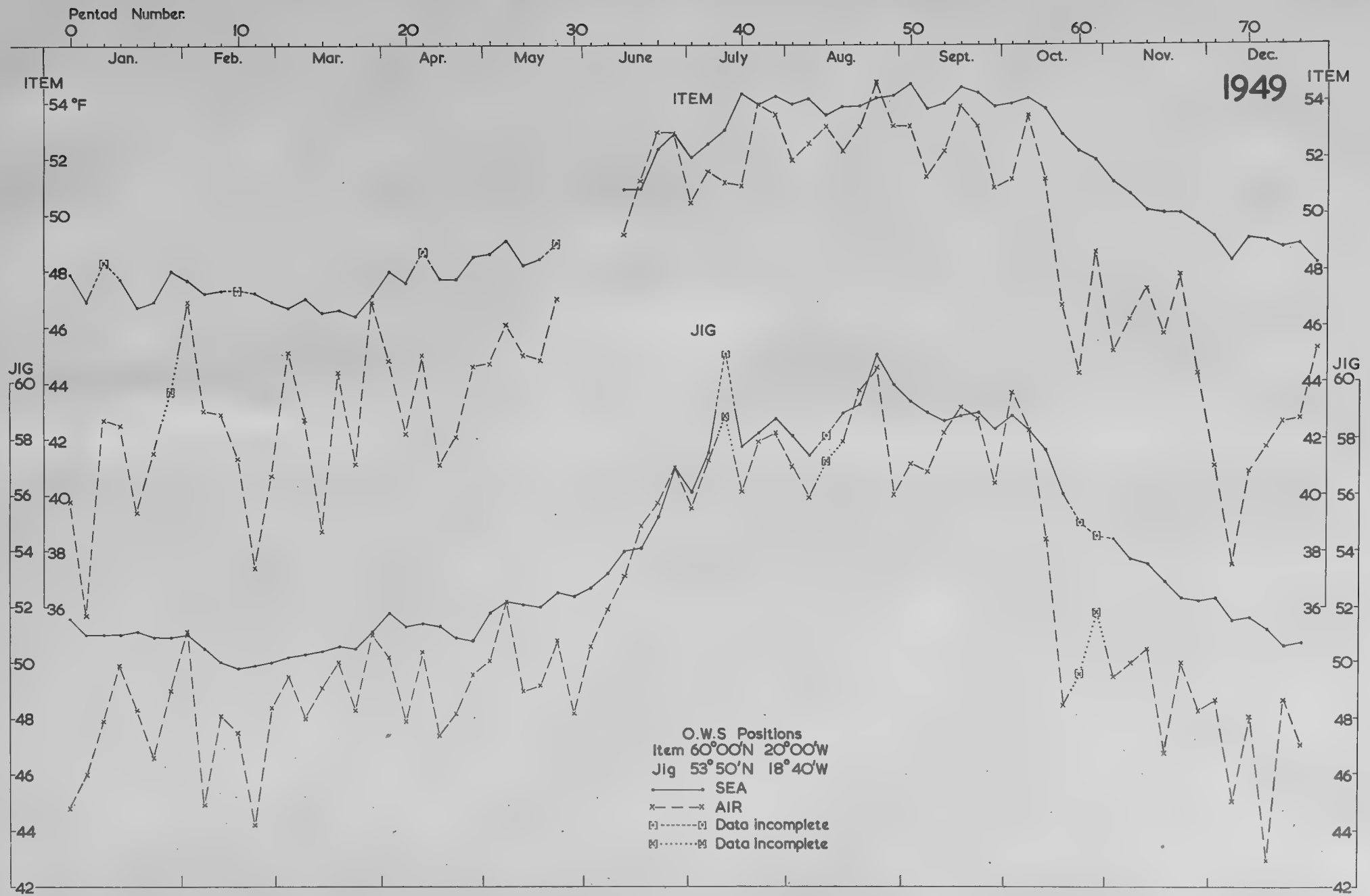

FIG. 2. FIVE DAY MEANS OF AIR AND SEA TEMPERATURE DURING 1949.

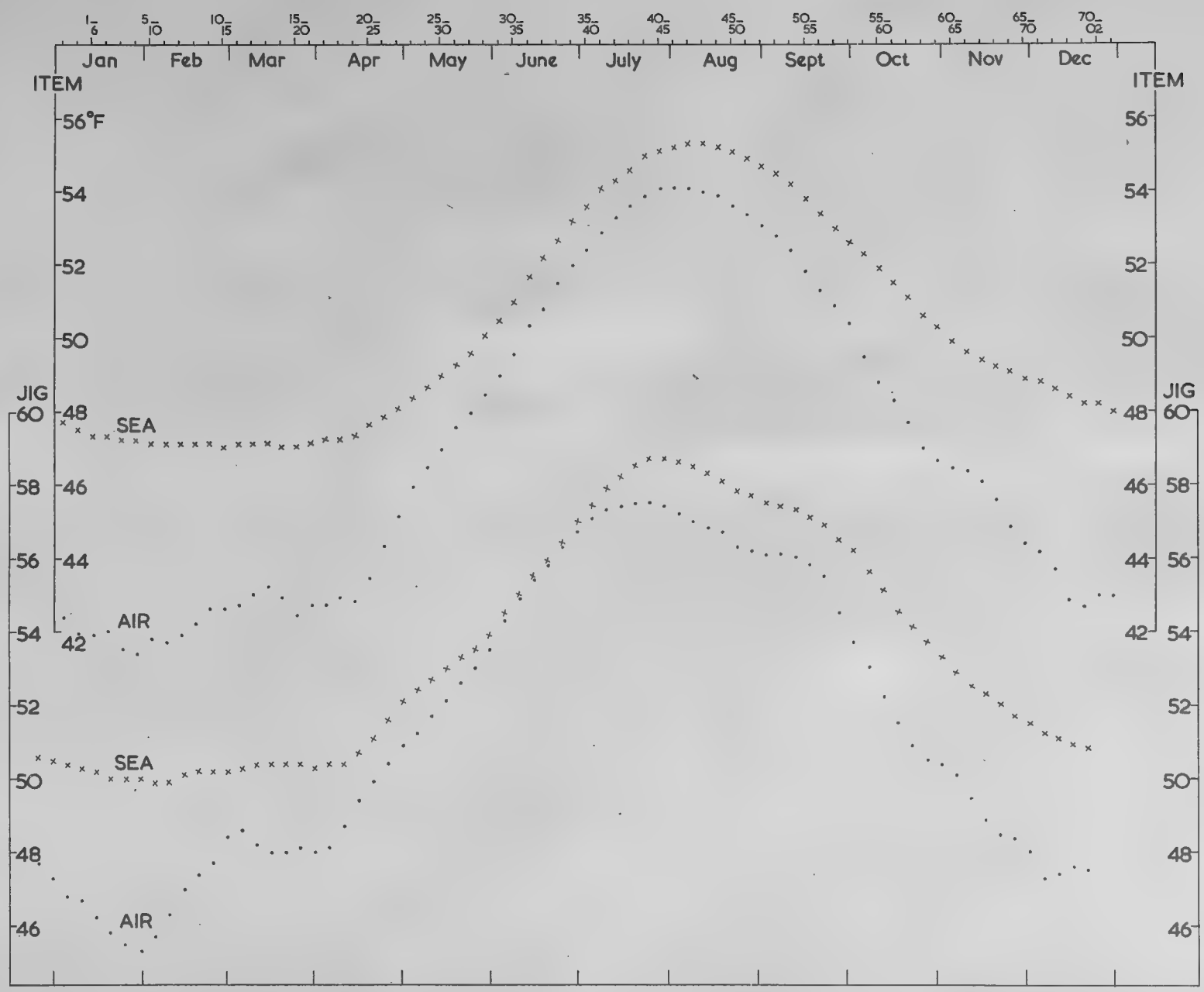

FIG. 3. 30 DAY RUNNING MEANS OF AIR AND SEA TEMPERATURE AT O.W.S "I" AND "J" 1948–51

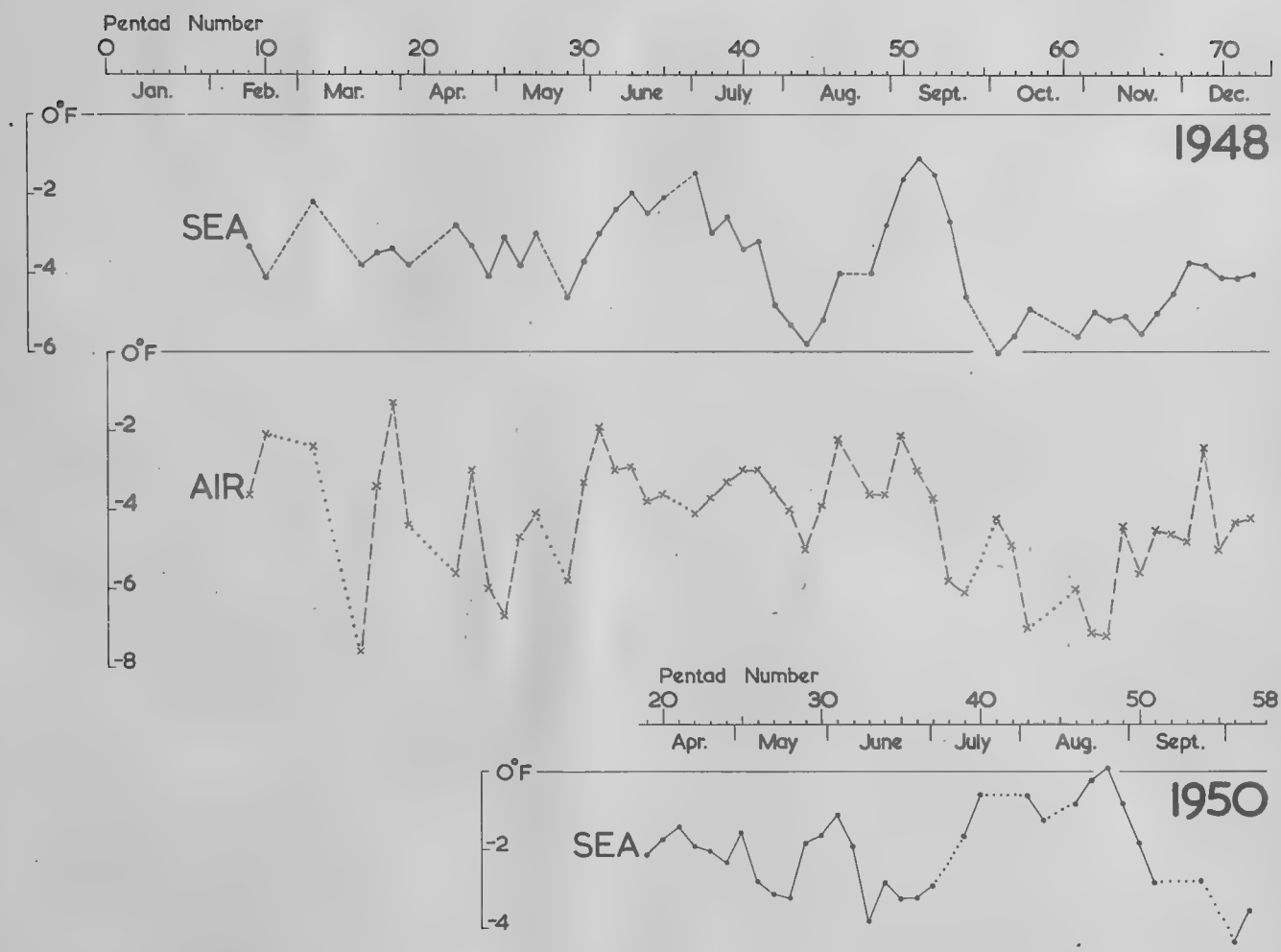

FIVE DAY MEANS OF TEMPERATURE DIFFERENCES (STATION I MINUS STATION J)

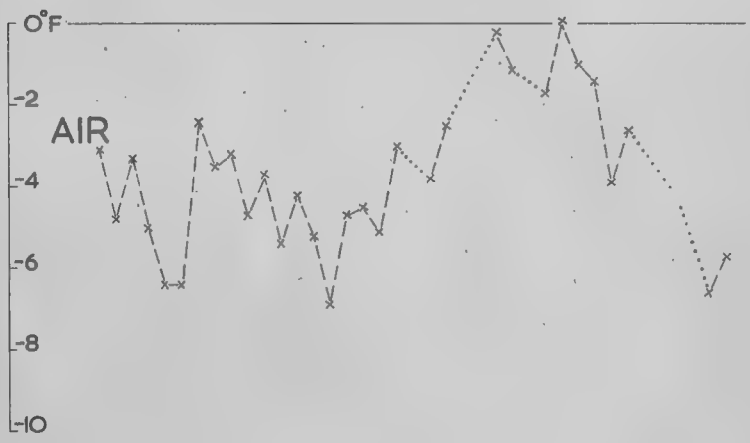

FIG. 4.

M.R.P. 951
12th January, 1956

INDEX OF M.R.Ps.
APPROVED FOR GENERAL DISTRIBUTION

Appendix 15 of M.R.P. 200

AIR MINISTRY
METEOROLOGICAL RESEARCH COMMITTEE

Addendum to M.R.P. 931

M.R.P.	TITLE	AUTHOR
930 (revised version)	Some further determinations made by the M.R.F. of the speed correction coefficients of aircraft thermometers	W.G. Durbin
943	Fog Density Indicator	J.R. Bibby
949	Some aspects of variations of air and sea surface temperature in short periods at ocean weather stations I and J of significance to the synoptic climatologist	R.F.M. Hay

G.5233(a)/JEK/1/57/340

	harmonic form	J.M. Craddock
916	A refrigerated disc icing meter	G.J. Day
917	The variation of the normal air temperature over the Northern Hemisphere during the year	J.M. Craddock
918	Average height of the standard isobaric surfaces over the area from the North Pole to 55° N. in January	H. Heastie
919	Atmospheric turbulence in aviation	G.A. Corby
922	Wind finding trials of Radar A.A. No.3 Mk.VII (second series)	C.V. Else
923	Five year means of meteorological observations made at the ocean weather stations Item and India, Jig and Juliett 1948-52	R.F.M. Hay
924	The sub-tropical jet-stream of the eastern North Pacific in January and April, 1952	H.D. Hoyle
925	The mean wind at 60 mb.	J.K. Bannon and R.A. Jones
928	Radar wind comparisons on the Ocean Weather Ships (second series)	D.N. Harrison
929	The energy balance of surface and atmosphere at Kew, May 1953 to April 1954	G.D. Robinson
931	Some statistical aspects of a rain-making experiment	A.F. Jenkinson
932	The profile of jet-streams in the Middle East	J. Harding

/933

G.37911(a)/MFW/1/56/340

At the time of issue this report has not been published. Any author desiring to quote this paper should refer to it as "A paper of the Meteorological Research Committee (London), M.R.P. No._____ by Mr. _____ A copy is available in the Library of the Meteorological Office."

M.R.P. 951
12th January, 1956

AIR MINISTRY
METEOROLOGICAL RESEARCH COMMITTEE

INDEX OF M.R.Ps. APPROVED FOR GENERAL DISTRIBUTION
Appendix 15 of M.R.P. 200

M.R.P.	TITLE	AUTHOR
901	Index of M.R.Ps. approved for general distribution (Appendix 14 of M.R.P. 200)	-
908	Transportable anemometer for use with mobile meteorological unit	G.E.W. Hartley
912	Radiation fog: investigations at Cardington, 1951-54	K.H. Stewart
913	The nocturnal dissipation of strato-cumulus cloud	D.G. James
914	Measurements of the flux of long wave radiation in the upper air 1953-54	J.T. Houghton and A.W. Brewer
915	The representation of the annual temperature variation over Central and Northern Europe by a two term harmonic form	J.M. Craddock
916	A refrigerated disc icing meter	G.J. Day
917	The variation of the normal air temperature over the Northern Hemisphere during the year	J.M. Craddock
918	Average height of the standard isobaric surfaces over the area from the North Pole to 55° N. in January	H. Heastie
919	Atmospheric turbulence in aviation	G.A. Corby
922	Wind finding trials of Radar A.A. No.3 Mk.VII (second series)	C.V. Else
923	Five year means of meteorological observations made at the ocean weather stations Item and India, Jig and Juliett 1948-52	R.F.M. Hay
924	The sub-tropical jet-stream of the eastern North Pacific in January and April, 1952	H.D. Hoyle
925	The mean wind at 60 mb.	J.K. Bannon and R.A. Jones
928	Radar wind comparisons on the Ocean Weather Ships (second series)	D.N. Harrison
929	The energy balance of surface and atmosphere at Kew, May 1953 to April 1954	G.D. Robinson
931	Some statistical aspects of a rain-making experiment	A.F. Jenkinson
932	The profile of jet-streams in the Middle East	J. Harding

/933

G.37911(a)/MFW/1/56/340

M.R.P.	TITLE	AUTHOR
933	Investigations relating to cirrus cloud	D.G. James
935	Dynamical similarity in an incompressible fluid model of two-dimensional airflow over a ridge	J.S. Sawyer
936	Measurements of atmospheric radiation and the heat balance at the ground at Kew, May, 1953 - May, 1954	W.T. Roach
938	AD 223100	
939	Airflow over mountains - the lee wave amplitude	G.A. Corby and C.E. Wallington
941	An experimental pulsed-light cloud-base meter	R. Almond
946	Ozone concentration measurements from an aircraft in N. Norway	A.W. Brewer